JAEA-Research
2010-068

Horonobe Underground Research Laboratory Project
Synthesis of Phase I Investigations 2001 - 2005
Volume "Geoscientific Research"

(Eds.) Kunio OTA, Hironobu ABE and Takanori KUNIMARU

Horonobe Underground Research Unit
Geological Isolation Research and Development Directorate

March 2011
Japan Atomic Energy Agency
日本原子力研究開発機構

JAEA-Research

本レポートは独立行政法人日本原子力研究開発機構が不定期に発行する成果報告書です。
本レポートの入手並びに著作権利用に関するお問い合わせは、下記あてにお問い合わせ下さい。
なお、本レポートの全文は日本原子力研究開発機構ホームページ（http://www.jaea.go.jp）
より発信されています。

独立行政法人日本原子力研究開発機構　研究技術情報部　研究技術情報課
〒319-1195　茨城県那珂郡東海村白方白根 2 番地 4
電話 029-282-6387, Fax 029-282-5920, E-mail:ird-support@jaea.go.jp

This report is issued irregularly by Japan Atomic Energy Agency
Inquiries about availability and/or copyright of this report should be addressed to
Intellectual Resources Section, Intellectual Resources Department,
Japan Atomic Energy Agency
2-4 Shirakata Shirane, Tokai-mura, Naka-gun, Ibaraki-ken 319-1195 Japan
Tel +81-29-282-6387, Fax +81-29-282-5920, E-mail:ird-support@jaea.go.jp

© Japan Atomic Energy Agency, 2011

JAEA-Research 2010-068

Horonobe Underground Research Laboratory Project
Synthesis of Phase I Investigations 2001 – 2005
Volume “Geoscientific Research”

(Eds.) Kunio OTA[+1], Hironobu ABE and Takanori KUNIMARU[+2]

Horonobe Underground Research Unit
Geological Isolation Research and Development Directorate
Japan Atomic Energy Agency
Horonobe-cho, Teshio-gun, Hokkaido

(Received December 20, 2010)

The Horonobe Underground Research Laboratory (URL) Project is being pursued by the Japan Atomic Energy Agency (JAEA) to enhance the reliability of relevant disposal technologies through investigations of the deep geological environment within the host sedimentary formations at Horonobe in Hokkaido, northern Japan. The project consists of two major research areas, “Geoscientific Research” and “R&D on Geological Disposal”, and proceeds in three overlapping phases, “Phase I: Surface-based investigation”, “Phase II: Construction” and “Phase III: Operation”, over a period of 20 years.

The present report summarises the results of the Phase I geoscientific research carried out from March 2001 to March 2005. Integration of the results from different disciplines ensures that the Phase I goals have been successfully achieved and identifies key issues that need to be addressed in Phases II and III. More importantly, efforts are made to summarise as many lessons learnt from the Phase I investigations and other technical achievements as possible to form a ‘knowledge base’ that will reinforce the technical basis for both implementation and the formulation of safety regulations.

Based on experiences of selecting the URL area and site in Horonobe Town, important factors that should be taken into consideration in such selection processes and their rationale are demonstrated. In the course of stepwise surface-based investigations, a number of achievements have been made, which can eventually provide examples of integrated methodologies for characterising the sedimentary formations. The relevant surface-based investigation techniques have thus been further developed. The Horonobe URL has been designed based on geoscientific information accumulated during the surface-based investigations and the plans for safe construction and operation of the URL have been defined in a feasible manner. In addition, a variety of environmental measures taken during Phase I have proved to be effective on minimising the environmental impact induced by URL construction.

Keywords: Horonobe URL Project, Phase I, Surface-based Investigations, Sedimentary Formation, Geoscientific Research, Synthesis

---

+1 Research and Development Integration Unit

+2 Tono Geoscientific Research Unit

JAEA-Research 2010-068

幌延深地層研究計画における地上からの調査研究段階（第 1 段階）研究成果報告書
分冊「深地層の科学的研究」

日本原子力研究開発機構 地層処分研究開発部門 幌延深地層研究ユニット
（編）太田 久仁雄[+1]、阿部 寛信、國丸 貴紀[+2]

（2010 年 12 月 20 日受理）

幌延深地層研究計画は、原子力政策大綱に示された深地層の研究施設計画の一つであり、堆積岩を対象として、独立行政法人日本原子力研究開発機構が北海道幌延町で進めているプロジェクトである。この計画では、「深地層の科学的研究」と「地層処分研究開発」を、第 1 段階「地上からの調査研究段階」、第 2 段階「坑道掘削（地下施設建設）時の調査研究段階」、第 3 段階「地下施設での調査研究段階」の 3 段階で 20 年程度をかけて進める。

第 1 段階における調査研究は、2001 年 3 月に開始し、2006 年 3 月までの約 5 年間にわたって実施してきた。本報告書は、第 1 段階における調査研究によって得られた成果を網羅的に取りまとめたものである。この取りまとめは、第 1 段階における調査研究の目標に対する達成度を評価し、第 2 段階以降における調査研究の課題や方向性を具体化するうえで重要な意味を持っている。さらに、ここで取りまとめた成果は、処分事業と安全規制の両面を支える地層処分技術の知識基盤として有効に活用されるものである。

第 1 段階における深地層の科学的研究では、「研究所設置地区及び研究所設置場所の選定」、「地上からの地質環境の調査研究」、「深地層における工学技術の基礎の開発」、「地下施設建設に伴う周辺環境への影響調査」を実施し、当初の目標どおり、坑道掘削前の深部地質環境を把握するとともに地下施設の設計・施工計画を策定し、第 2 段階以降における調査研究の課題や方向性を具体化した。「研究所設置地区及び研究所設置場所の選定」では、その実経験を通じて確認した、地区・用地の選定上の要件や考慮すべき条件とその重要性を示した。「地上からの地質環境の調査研究」では、調査結果の解釈とモデル化を通じて、地層処分にとって重要な地質環境の特性・プロセスを把握し、その過程で得られた技術的知見を踏まえて統合化データフローダイアグラムを構築した。また、地上からの調査研究における主要な調査技術の有効性や技術課題などを整理し、堆積岩を対象とした地上からの調査・評価技術の整備を図った。「深地層における工学技術の基礎の開発」では、堆積岩（軟岩）中での地下施設の仕様・レイアウトを決定し、地下施設を安全に建設・維持するための設計・施工計画を策定した。「地下施設建設に伴う周辺環境への影響調査」では、環境調査などを継続し、地上及び地下施設の建設に伴う影響の低減を図る措置が適切であることを確認した。

幌延深地層研究センター（駐在）：〒098-3224 北海道天塩郡幌延町北進 432-2
+1 研究開発統括ユニット
+2 東濃地科学研究ユニット

Contents

目　次

List of Authors

Koichi ASAMORI, Tono Geoscientific Research Unit, Geological Isolation Research and Development Directorate, JAEA ······ Section 4.7

Katsuhiro HAMA, Tono Geoscientific Research Unit, Geological Isolation Research and Development Directorate, JAEA ······ Sections 4.3, 4.7 and 4.8

Takanori KUNIMARU, Tono Geoscientific Research Unit, Geological Isolation Research and Development Directorate, JAEA ······ Chapter 3; Sections 4.3, 4.6, 4.7 and 4.8

Hiroshi KURIKAMI, Horonobe Underground Research Unit, Geological Isolation Research and Development Directorate, JAEA ······ Sections 4.2, 4.6, 4.7 and 4.8

Keisuke MAEKAWA, Geological Isolation Research Unit, Geological Isolation Research and Development Directorate, JAEA ······ Sections 4.2 and 4.6

Hiroya MATSUI, Tono Geoscientific Research Unit, Geological Isolation Research and Development Directorate, JAEA ······ Sections 4.4, 4.6, 4.7 and 4.8

Tadafumi NIIZATO, Horonobe Underground Research Unit, Geological Isolation Research and Development Directorate, JAEA ······ Sections 4.5, 4.7 and 4.8

Kunio OTA, Research and Development Integration Unit, Geological Isolation Research and Development Directorate, JAEA ······ Chapters 1, 2 and 7; Sections 4.6, 4.7 and 4.8

Yutaka SUGITA, Horonobe Underground Research Unit, Geological Isolation Research and Development Directorate, JAEA ······ Sections 4.4, 4.6, 4.7 and 4.8

Hironori FUNAKI, on secondment to Cabinet Office, Government of Japan ······ Section 4.6

Eiichi ISHII, on secondment to Nuclear Waste Management Organization of Japan ······ Sections 4.1, 4.7 and 4.8

Hiroshi MORIOKA, Tokyo Electric Power Services Co. Ltd. ······ Chapters 5 and 6

Sumio NIUNOYA, Obayashi Corporation ······ Section 4.7

Hidefumi OHARA, Kumagai Gumi Co. Ltd. ······ Section 4.7

Kazunori SHIBANO, Tokyu Construction Co. Ltd. ······ Section 4.2

Kazuharu TAKAHASHI, Nittetsu Mining Co. Ltd. ······ Section 4.7

Goji TOMURA, Sumitomo Mitsui Construction Co. Ltd. ······ Sections 4.2 and 4.7

Takehiro YAMAGUCHI, Hazama Corporation ······ Chapters 5 and 6

Masanao YAMASAKI, Tokyo Electric Power Co., Inc. ······ Chapters 5 and 6

著者一覧

浅森 浩一，東濃地科学研究ユニット ……………………………………………………………4.7 節

太田 久仁雄，研究開発統括ユニット …………………………………1 章，2 章，7 章，4.6～4.8 節

國丸 貴紀，東濃地科学研究ユニット ………………………………………3 章，4.3 節，4.6～4.8 節

操上 広志，幌延深地層研究ユニット ……………………………………………4.2 節，4.6～4.8 節

杉田 裕，幌延深地層研究ユニット ………………………………………………4.4 節，4.6～4.8 節

新里 忠史，幌延深地層研究ユニット …………………………………………4.5 節，4.7 節，4.8 節

濱 克宏，東濃地科学研究ユニット ……………………………………………4.3 節，4.7 節，4.8 節

前川 恵輔，地層処分基盤研究開発ユニット ……………………………………………4.2 節，4.6 節

松井 裕哉，東濃地科学研究ユニット ……………………………………………4.4 節，4.6～4.8 節

石井 英一，原子力発電環境整備機構（出向中） ………………………………4.1 節，4.7 節，4.8 節

舟木 泰智，内閣府原子力安全委員会事務局（出向中） ……………………………………………4.6 節

大原 英史，株式会社熊谷組 ……………………………………………………………………4.7 節

柴野 一則，東急建設株式会社 …………………………………………………………………4.2 節

高橋 一晴，日鉄鉱業株式会社 …………………………………………………………………4.7 節

戸村 豪治，三井住友建設株式会社 ……………………………………………………4.2 節，4.7 節

丹生屋 純夫，株式会社大林組 …………………………………………………………………4.7 節

森岡 宏之，東電設計株式会社 ……………………………………………………………5 章，6 章

山口 雄大，株式会社間組 …………………………………………………………………5 章，6 章

山崎 雅直，東京電力株式会社 ……………………………………………………………5 章，6 章

1. Introduction

The Horonobe Underground Research Laboratory (URL) Project is a comprehensive research and development (R&D) project aimed at studying the sedimentary formations in the region of Horonobe Town in Hokkaido, northern Japan. The URL project, which is managed by the Japan Atomic Energy Agency (JAEA; formerly the Japan Nuclear Cycle Development Institute – JNC), is one of two deep URL projects prescribed in "Long-Term Program on Research, Development and Utilization of Nuclear Energy" (Long-Term Program)[1] and "Framework for Nuclear Energy Policy" (Framework)[2], both of which were issued by the Atomic Energy Commission of Japan (AEC). The URL project consists of two research areas: 'geoscientific research' and 'research and development on geological disposal technologies'. This report describes the geoscientific research, synthesising the results of investigations carried out during the surface-based investigation phase – Phase I of the Horonobe URL project.

Section 1.1 provides an overview of the URL project within the context of the Japanese geological disposal programme; Section 1.2 describes the R&D programme of the project and Section 1.3 outlines the strategy for synthesising the results of the Phase I investigations.

1.1 General background

1.1.1 URL projects

Building on the technical basis provided by JNC's report "H12: Project to Establish the Scientific and Technical Basis for HLW Disposal in Japan" (H12 report)[3], the geological disposal programme for high-level radioactive waste (HLW) in Japan has moved from the stage where only R&D is performed to the implementation stage, in which a geological disposal project and safety regulations will be implemented. Necessary R&D activities will be continued in parallel. In June 2000, the Specified Radioactive Waste Final Disposal Act (the Act) was promulgated and, based on this legislation, the Nuclear Waste Management Organization of Japan (NUMO) was established as the implementation body for the geological disposal of HLW in October of the same year. The Nuclear Safety Commission of Japan (NSC) issued the "Basic Concept of Safety Regulation on HLW Disposal" First Report[4]. Thus, the preliminary framework for the geological disposal project and the associated safety regulations has been established.

AEC then specified a new national programme framework in its Long-Term Program[1], which outlined the activities leading up to final disposal of HLW and who would be responsible for performing these. NUMO *"...should take charge of developing those consistent with the safe implementation of the final disposal project and with the improvement of its economic performance and efficiently"*. The government and related organisations *"...should actively push forward with research and development projects necessary for safety regulation and safety assessment of the final disposal, with fundamental research and development activities, including scientific studies of the deep geological environment, and with development of technologies to enhance the reliability of geological disposal technology"*. In particular, JNC was assigned responsibility to *"...steadily carry on research and development activities to verify the reliability of geological disposal technologies and to establish a safety assessment method, using research facilities for deep geological environments and the Quantitative Assessment Radionuclide Migration Experiment Facility in Tokai village"*.

In accordance with the responsibilities assigned to it in the Long-Term Program[1], JNC formulated an R&D programme for the stages following submission of the H12 report. This was published as the "Generic Programme for R&D on Geological Disposal of HLW" (Generic Programme)[5]. In the Generic Programme and within the context of improving 'the technical reliability of geological disposal in Japan', demonstrated in H12 report, and enhancing the technical basis supporting the disposal project and the associated safety regulations, two goals were set for the R&D programme: 'confirmation of the applicability of disposal technologies to specific geological environment' and 'understanding of the long-term behaviour of the geological disposal system' (Figure 1.1.1-1). The aim of the former was to confirm the reliability and practicability of technologies developed to date by applying them to specific geological environments; the latter was intended to improve the reliability of the evaluation by increasing the understanding of various phenomena that affect the disposal system and to improve the associated models and databases. The URLs were focal points for achieving the first goal. In the Generic Programme, the R&D programme was divided into two areas: 'R&D on geological disposal technology' and 'geoscientific research'. The former involves improving the reliability of the disposal technologies and developing advanced safety assessment methodologies, while the latter forms the necessary basis for the former. Specific R&D items were set for each area. Since JNC was merged with the Japan Atomic Energy Research Institute (JAERI) to form JAEA, R&D has continued in line with the above two R&D goals. A new fundamental policy report of JAEA entitled "Plan for Meeting the Midterm Goal – Midterm Plan (October 1, 2005 to March 31, 2010)" (Midterm Plan)[6] states that JAEA will pursue R&D in the fields of geoscientific research and geological disposal technologies. The URL projects at Horonobe in Hokkaido, northern Japan and Mizunami in Gifu, central Japan are mentioned specifically in the Midterm Plan.

The R&D activities summarised in the H12 report were carried out to demonstrate the basic technical feasibility of geological disposal in Japan, without specifying any particular geological environment. In order to improve the technical reliability of geological disposal and enhance the technical basis for the disposal project, it was important that the practicability and reliability of the technologies used in the H12 report should be demonstrated by applying them to specific geological environments; URLs can be used for this purpose.

It was proposed that *"two or more URLs should be constructed, considering the range of characteristics and distribution of the geology of Japan"*[7]. JNC therefore set up the Horonobe URL project[8] for investigating sedimentary rock with saline groundwater and the Mizunami URL project[9] for crystalline rock with fresh groundwater (Figure 1.1.1-2). Both projects consist of three phases that will extend over a period of around 20 years[10]: surface-based investigations (Phase I), investigations during tunnel excavation (Phase II) and investigations in the underground facilities (Phase III). It should be noted that the investigations for repository site selection, which will be carried out by NUMO, will also proceed stepwise, with literature surveys, preliminary investigations and detailed investigations (surface-based investigations in the early stages and those in underground facilities in the later stages) over a period of around 20 years, as specified in the Act. Phase I of the Horonobe URL project corresponds to the preliminary investigations and the first half of the detailed investigations in the NUMO programme and Phases II and III to the detailed investigations using underground facilities. The technical basis for the preliminary investigations has been developed by synthesising the results in the H12 report and investigations carried out during Phase I of the URL projects. It is of importance that the reliability of surface-based investigations and associated modelling techniques should be improved during Phase II investigations; for instance, geological environment models developed during Phase I should be tested using geological data obtained during Phase II. This is defined also in the national "R&D Programme for the Geological Disposal of HLW"[11]; the goal of the fundamental R&D in Phase 2 (2006–2010) will be to establish the technical basis for surface-based investigations and that in Phase 3 (after 2011) to establish the technical basis for investigations using underground facilities.

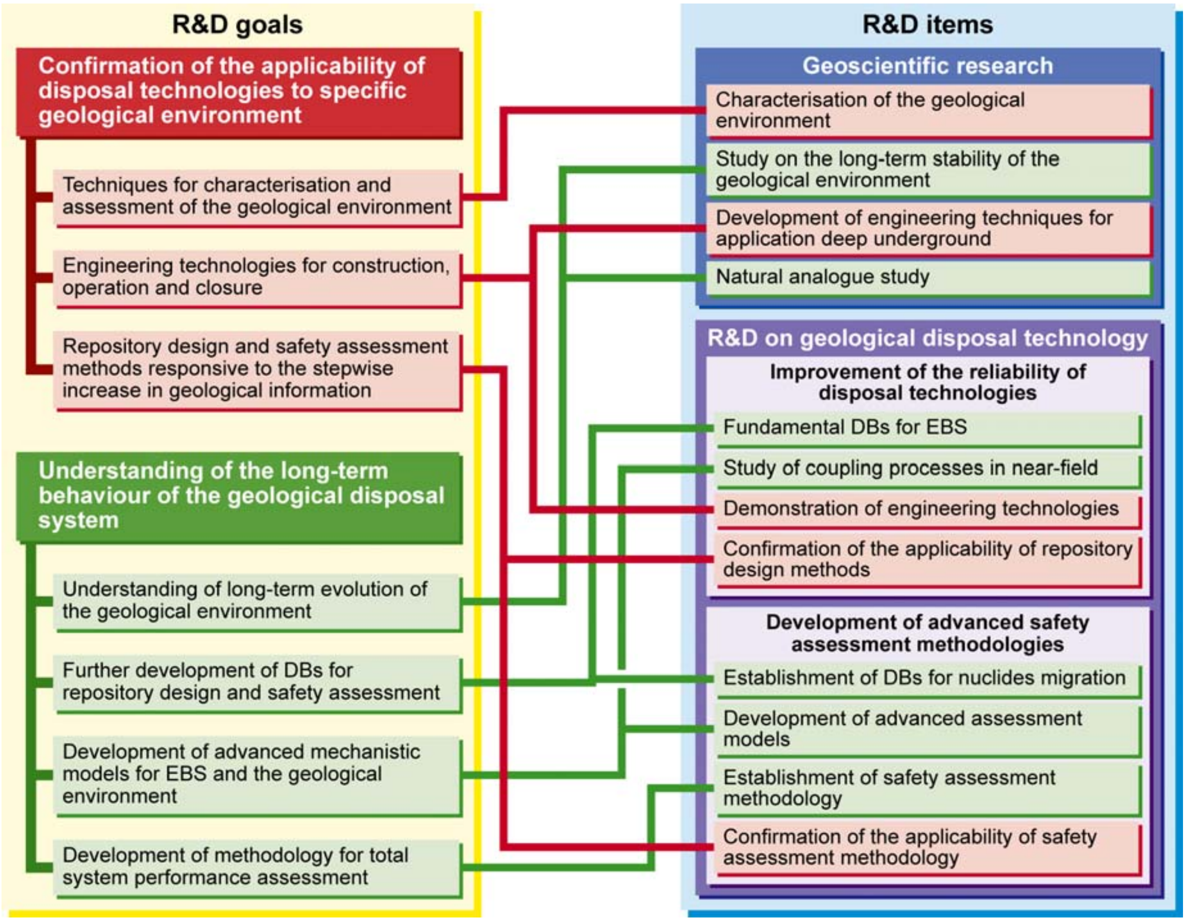

Figure 1.1.1-1 Goals of the R&D plan (2001–2005) mapped onto specific work areas

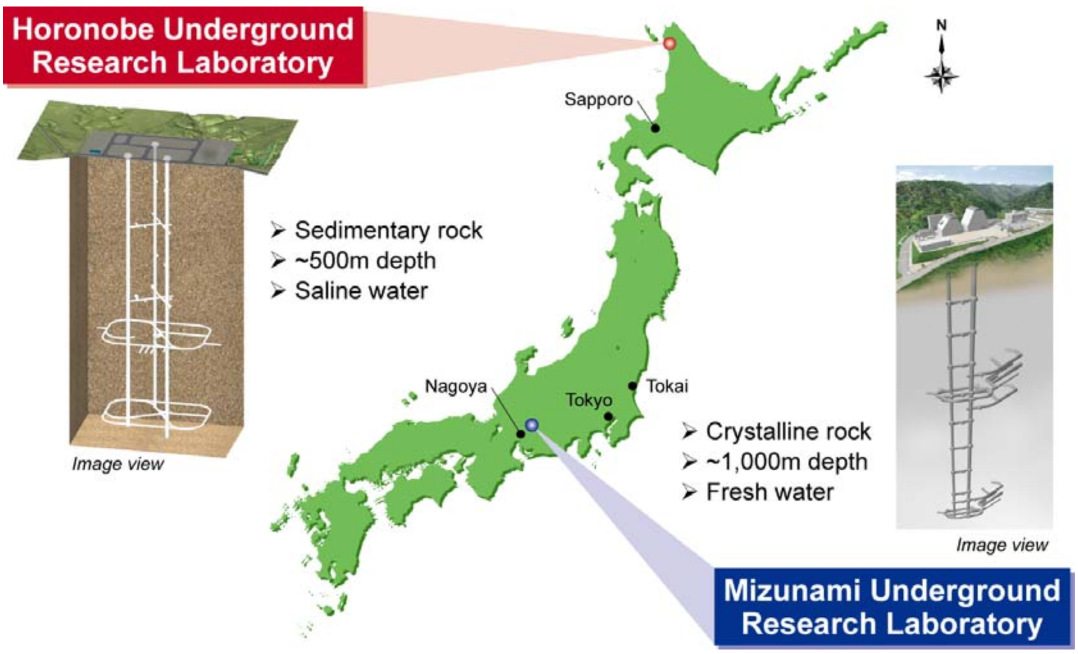

Figure 1.1.1-2 Two URL projects in Japan

1.1.2 R&D goals of the URL projects

The primary goal of the R&D in the URL project is to improve the reliability of geological disposal technologies by applying them to specific geological environments. In the H12 report, techniques and methods for characterising the geological environment were developed based on studies carried out in existing tunnels in the Tono mine (sedimentary rock) and the Kamaishi mine (granitic rock), as well as joint research projects in overseas URLs. After comparing and reviewing the information acquired in these studies and from key literature, it was demonstrated that a safe repository could be designed and constructed economically based on current engineering technologies or if necessary future developments thereof and that the long-term safety of geological disposal could be assessed by current modelling and simulation techniques. It can be concluded that the H12 report successfully demonstrated the feasibility of geological disposal in principle combining information from various fields.

The reliability of geological disposal technologies will be evaluated based on information on the geological environment accumulated with the progress of the URL project, with investigations advancing stepwise starting from undisturbed conditions. A stepwise approach helps in enhancing and ensuring the depth of understanding of the deep geological environment and eventually developing a sound technical basis for systematically characterising the deep geological environment. Design and construction of URLs based on the geological information acquired will result in developing engineering technologies relevant to geological disposal programmes. A key technical challenge for the geoscientific research in the URL project will thus be to establish the basis for techniques for characterising the geological environment and engineering technologies for use in the deep subsurface. In addition, in the Horonobe URL project, techniques for systematically investigating historical records of natural phenomena, such as seismic activity, uplift, erosion etc., and acquiring information on the evolution of the geological environment up to the present will be developed as a case study.

The information and knowledge acquired through geoscientific research will be used as key input for R&D aimed at improving the reliability of repository engineering technologies and developing advanced safety assessment methodologies. In addition, rock and groundwater samples obtained in the geoscientific research will be utilised in the R&D. At the same time as enhancing confidence in the reliability of the underlying engineering technologies for an engineered barrier system (EBS) and the applicability of design and safety assessment methodologies, as shown in the H12 report, it will be important to iterate such developments based on the increasingly detailed geological information accumulated. In this way, the applicability of geological disposal technologies can be confirmed. Consequently the relationship between the degree of understanding of the geological environment and the sensitivity of the characteristics of the geological environment in a safety assessment or the required volume of investigations can be reviewed by feeding the confirmed results back into geoscientific research. Key issues for the planning and/or evaluation of repository design and construction can be identified and compiled as a knowledge base, depending on the progress of the stepwise investigations and the depth of understanding of the geological environment. Laboratory and engineering-scale experiments under controlled conditions or experiments using radionuclides also provide an understanding of various phenomena relevant to the geological disposal system. In the Horonobe URL project, R&D on geological disposal technology is conducted in parallel with geoscientific research, which, particularly in the phases subsequent to Phase II of the project, will involve using drifts for experiments to confirm EBS construction technologies and their performance in sedimentary rock and in situ experiments for improving the reliability of safety assessment models[12)].

1.1.3 Role of the URL projects in Japan

The role of the URL projects in Japan is to develop and confirm the relevant technologies that will be applied in a real geological environment. This is achieved by maintaining an awareness of the overall goal – accurate understanding of the geological environment – while setting tasks such as data acquisition and evaluation of the applicability of the technologies. This will lead to optimisation and improvement of the technologies, as well as an understanding of the adequacy and limitation of technologies. Understanding the limitations of the technologies will form a basis for the detailed planning of repository implementation and the formulation of realistic safety regulations. Since the waste disposal project will proceed stepwise, as specified in the Act, and safety regulations will be developed in accordance with the progress of the waste disposal project, these activities should be preceded by R&D that will provide a sound technical basis for them. It is of particular importance that the results from each URL investigation phase should be synthesised and reported with an appropriate lead-time for the site selection process. This is also essential for reviewing the design and safety assessment methodologies for the geological disposal system using information on the specific geological environments, which will be acquired through the URL programme. This will thus ensure adequate techniques for characterising the geological environment efficiently and an efficient approach to reviewing the design and safety assessment methodologies for the geological disposal system based on limited stepwise information on the geological environment.

When designing a disposal system and evaluating its safety based on the results of characterisation of the geological environment, major challenges include understanding the spatial heterogeneities of the actual geological environment and addressing the uncertainties associated with these heterogeneities. This involves frequent trial and error and repeated feedback. In general, the depth of understanding will increase in proportion to the extent of investigations. However, the further the investigations progress, the less the increase in understanding and cost effectiveness of the efforts become. Detailed investigations of the geological environment generally involve high costs and no investigations, however detailed, will result in complete understanding. The geological disposal system is inherently associated with various degrees of uncertainty and the degree of conservativeness to be taken into consideration in the repository design will vary depending on the level of uncertainty associated with the understanding of the geological environment. For the actual disposal project, this will be reflected in the degree of conservativeness in the repository design and, subsequently, in the construction costs. Understanding the geological environment and reflecting the remaining uncertainties in the margins included in the design and safety assessment is thus a complex issue and the investigations have to reduce the uncertainties to an acceptable level. Hence, in each investigation in the stepwise site selection process, it will be important to examine the objectives and content of the investigations by assessing the level of understanding to be achieved and the requirements to be considered, as well as identifying issues and uncertainties to be carried over to the next stage. Even for investigations of a similar scale, the accuracy of the results and the depth of understanding obtained will vary depending on the geological and geomorphic conditions and the social environment at the site. In order to reflect such realistic conditions, it is important not only to prepare catalogues of investigation techniques and equipment, but also to accumulate experience at the site and to learn from actual case studies. The experience and knowledge gained in the URL projects should support methodologies for investigations for repository site selection and be used to establish safety regulations. For the URL projects, efforts should be made to build a knowledge base and to systematise multidisciplinary results and technological successes as well as experience with failures, recognising that the latter are also important aspects of the ongoing R&D. The approach to the investigations in the URL projects is thus not linear, but involves a process in which planning, execution and evaluation are iterated in each phase. Recognising the relationship between the progress of investigations and the depth of understanding and reduction of uncertainties will result in optimisation of the investigation programme as a whole, with the findings of preceding phases being reflected in subsequent phases.

It is stated in the Long-Term Program[1)] that *"The research facility for deep geological environment will serve not only as a place for scientific investigation, but also as a place for deepening public understanding of research and development activities related to the geological disposal of waste. Accordingly, this research facility project should be clearly distinguished from the disposal facility".* It is worth noting in this respect that an agreement between JAEA and the local government restricts JAEA's activities in the sense that *"JAEA will never bring or use HLW in the URLs and JAEA will never lend or transfer the URL facilities to the implementing entity"*. Collaborative research with domestic and overseas organisations and experts will also be pursued intensively in the URL projects. The public will have the opportunity, in the URLs, to experience the deep geological environment first-hand and to increase their awareness of geological disposal and the associated R&D activities. The investigation programme and results of the URL projects will be open to the local and national public.

1.2 The Horonobe URL project

1.2.1 R&D goals and items

As described in the Generic Programme (Figure 1.1.1-1), the Horonobe URL project involves geoscientific research and R&D on geological disposal technology for sedimentary formations, with three major goals:

- to establish the basis for techniques for characterising the deep geological environment;
- to develop the basis for engineering technologies for use in the deep underground;
- to confirm the applicability of geological disposal technologies in specific geological environment.

With regard to geoscientific research, the R&D item 'characterisation of the geological environment' prescribed in the Generic Programme can be divided into two sub-items: 'development of techniques for investigating the geological environment' and 'development of techniques for long-term monitoring of the geological environment'. Coupled with 'studies on the long-term stability of the geological environment' and 'development of engineering techniques for application deep underground', this constitutes four R&D items. R&D on improving the reliability of disposal technologies consists of three areas: 'study of coupling processes in near-field', 'demonstration of engineering technologies' and 'confirmation of the applicability of repository design methods'. Development of advanced safety assessment methodologies consists of two areas, viz. 'development of advanced assessment models' and 'confirmation of the applicability of safety assessment methodology'. These areas will be addressed in three, partially overlapping, phases extending over around 20 years from the period before construction of the URL up to the phase after completion of construction of the underground facilities (Figure 1.2.1-1). The Phase I surfaced-based investigations will cover seven R&D items, other than 'study of coupling processes in near-field' and 'development of advanced assessment models'. The Phase II investigations during construction of the underground facilities will involve eight R&D items and Phase III will address all nine R&D items.

Figure 1.2.1-1 Timetable of the Horonobe URL project

The outline geological setup of the region of Horonobe Town consists of Palaeogene to Early Pleistocene sedimentary sequences, terrace sediments after the Middle Pleistocene and Holocene sediments (sand dunes and alluvium), which are underlain by a Cretaceous basement[13)] (see Appendix 1). Two large-scale faults and a fold structure with an NNW strike have been identified[14),15)] and active Quaternary structures such as faults and flexures have also been identified to the east and west of the town[16)]. It is also known that the Neogene sedimentary sequences to be characterised (the Wakkanai and Koetoi Formations) have generally low permeability and contain two types of groundwater, saline and fresh, which dissolve gases.

1.2.2 Progress to date

Under an agreement between the Horonobe Town, Hokkaido Prefecture and JNC (now JAEA), with the participation of the Science and Technology Agency (now the Ministry of Education, Culture, Sports, Science and Technology), dated November 2000 on 'Geoscientific Research in Horonobe', Phase I of the Horonobe URL project was initiated in March 2001. The agreement specified that JNC would never bring or use HLW in the area covered by the project and would never lend or transfer the URL facilities to the implementing entity. JNC was also obliged to close the surface facilities and backfill the underground facilities after completion of the project. The area is also excluded from being a site for a radioactive waste repository or an interim storage facility for radioactive waste. In July 2002, based on surveys of existing information and aerial and ground reconnaissance surveys on a regional scale in the previous year and taking into consideration preliminary requirements on the geological environment and safety, as well as social and environmental constraints, an area of 3 km × 3 km square in the Hokushin district in the north-central part of Horonobe Town was selected as the main area for the surface-based investigations (URL area). A site for constructing the underground and surface facilities (URL site) was subsequently selected in the URL area, 3 km from central Horonobe. The selection was based on social conditions and the availability of infrastructure, including roads and land use restrictions, in addition to available geological and hydrogeological information. JNC purchased the site in March 2003 (Figure 1.2.2-1). In June 2003, preparation of the land started and, in April 2005, construction of the underground facilities was initiated, as were the Phase II investigations[17)]. Excavation of the Ventilation Shaft began in November 2005. Phase I investigations continued for approximately five years up to the end of March 2006, during which time aerial geophysical surveys and various surface-based investigations were conducted and supporting laboratory investigations using field information and rock and groundwater samples taken.

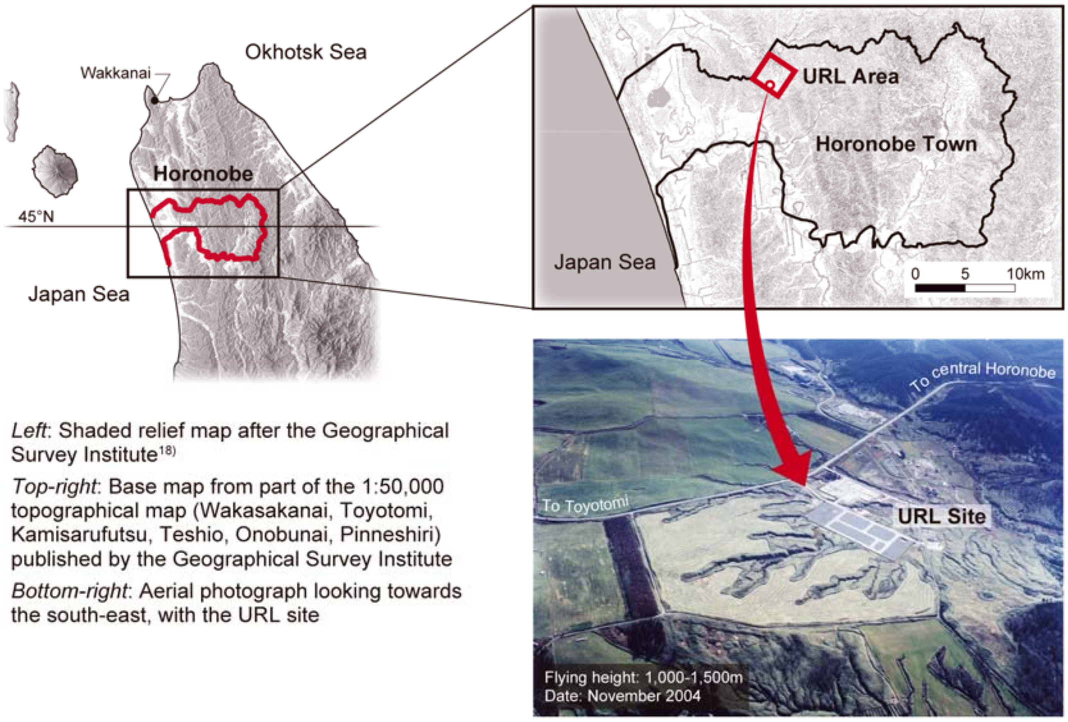

Figure 1.2.2-1 Location of the URL area and URL site in Horonobe Town, northern Hokkaido

1.3 Synthesis of the Phase I investigations

1.3.1 Aims and scope

Synthesis of the results from the Phase I investigations involved systematically compiling the results and knowledge from surface-based investigations up to the end of March 2006. This synthesis is important for evaluating the Phase I goals for which the investigations have been carried and for identifying issues to be addressed in the future, as well as providing guidelines for the investigations in Phase II and subsequent phases. The results of the synthesis should be used as a knowledge base that supports both NUMO's repository implementation (e.g. preliminary investigations and detailed surface-based investigations for site selection) and the formulation of safety regulations by national agencies (e.g. establishing siting factors for the selection of detailed investigation areas and guidelines for the safety review). The results of the Phase I investigations were incorporated into supporting reports 1–3 of the project "H17: Development and Management of the Technical Knowledge Base for the Geological Disposal of HLW" (H17 report)[19)–21)] published in September 2005.

The strategy for the synthesis of Phase I was specified as compiling the results of the investigations and associated knowledge in accordance with the goals of Phase I and defining the investigation needs in Phase II and subsequent phases. More specifically, all the results obtained during Phase I, including those obtained after publication of the H17 report, will be compiled and synthesised and, based on future issues identified in the H17 report and comments provided on the H17 report, the techniques for characterising the geological environment and engineering technologies for deep underground application, developed during Phase I, will be reviewed. Also, from the viewpoint of establishing a knowledge base for geological disposal technologies, it is important to document the full spectrum of experience, including both successes and failures.

The report on the Phase I synthesis of the Horonobe URL project consists of two volumes: “Geoscientific Research” and “Geological Disposal Research”. The present report, Volume “Geoscientific Research”, documents the results of the following R&D items: ‘development of techniques for investigating the geological environment’, ‘development of techniques for long-term monitoring of the geological environment’, ‘studies on the long-term stability of geological environment’ and ‘development of engineering techniques for application deep underground’, while the report, Volume “Geological Disposal Research”, presents the results of ‘demonstration of engineering technologies’, ‘confirmation of the applicability of repository design methods’ and ‘confirmation of applicability of safety assessment methodology’.

1.3.2 Structure of the report on geoscientific research

This report describes the synthesis of geoscientific research conducted in Phase I of the Horonobe URL project in seven chapters. Chapter 2 provides an overview of the goals of the geoscientific research in Phase I and outlines how the investigations were conducted. Chapter 3 presents selection of the URL area and the URL site, the basic site selection policy in each phase, selection factors and results of the selection, as well as the importance of factors for selection and requirements as confirmed by experience with the selection process for the URL area and the URL site. Chapter 4 compiles the results obtained from intensive characterisation of the geological environment in the light of geological properties and processes of relevance for geological disposal; surface-based investigation techniques for sedimentary formations are also presented. The content of Chapter 4 corresponds to three R&D items: ‘development of techniques for investigating the geological environment’, ‘development of techniques for long-term monitoring of the geological environment’ and ‘studies on the long-term stability of the geological environment’ as specified in the Generic Programme[6]. Chapter 5 on development of engineering techniques for application deep underground describes design and construction technologies for underground facilities in sedimentary formations (soft rock) developed through discussion of the specifications and layout of the repository, as well as methods for ensuring safety in the underground facilities. Chapter 6 presents the results of an environmental impact assessment for surface and underground facilities. Finally, Chapter 7 summarises the results of the Phase I geoscientific research and discusses future perspectives.

Note that this report is based on an original Japanese document (JAEA-Research 2007-044), but does not represent a direct translation as the content has been modified (and partly corrected) in an appropriate manner to make it more straightforward for an international audience.

References

1) Atomic Energy Commission of Japan: "Long-Term Program on Research, Development and Utilization of Nuclear Energy", 24th Nov. 2000 (2000). (in Japanese)
2) Atomic Energy Commission of Japan: "Framework for Nuclear Energy Policy", 11th Oct. 2005 (2005). (in Japanese)
3) Japan Nuclear Cycle Development Institute: "H12: Project to Establish the Scientific and Technical Basis for HLW Disposal in Japan", Project Overview Report, JNC TN1410 2000-001 (2000).
4) Nuclear Safety Commission of Japan: "Basic Concept of Safety Regulation on High-Level Radioactive Waste Disposal", First Report, Special Committee on Safety Regulation of Radioactive Waste, 6th Nov. 2000 (2000). (in Japanese)
5) Evaluation Committee of Research and Development Activities, Japan Nuclear Cycle Development Institute: "Assessment Report of Research and Development Activities in FY2001 – Generic Programme for Research and Development on Geological Disposal of High-Level Radioactive Waste", Interim Report, JNC TN1440 2001-008 (2001). (in Japanese)
6) Japan Atomic Energy Agency: "Plan for Meeting the Midterm Goal – Midterm Plan (October 1, 2005 to March 31, 2010)", 3rd Nov. 2005 (2005). (in Japanese)
7) Atomic Energy Commission of Japan: "Long-Term Program on Research, Development and Utilization of Nuclear Energy", 24th Jun. 1994 (1994). (in Japanese)
8) Japan Nuclear Cycle Development Institute: "Deep Geological Research Laboratory (Tentative Name) Project – Plan of Surface-Based Investigation (Phase I)", JNC TN1410 2001-001 (2001). (in Japanese)
9) Japan Nuclear Cycle Development Institute: "Master Plan of the Mizunami Underground Research Laboratory Project", JNC TN7410 2003-001 (2002).
10) Nuclear Waste Management Organization of Japan: "Basic Strategy for Selection Procedures for Preliminary Investigation Areas for the Disposal of HLW" Official Gazette, Extra No. 238, 8th Nov. 2001 (2001). (in Japanese)
11) Agency for Natural Resources and Energy and Japan Atomic Energy Agency: "Research and Development Programme for the Geological Disposal of HLW", Dec. 2006 (2006). (in Japanese)
12) Evaluation Committee of Research and Development Activities, Japan Nuclear Cycle Development Institute: "Assessment Report of Research and Development Activities in FY2004 – Horonobe Underground Research Laboratory Project", Interim Report, JNC TN1440 2005-002 (2005). (in Japanese)
13) T. Oka and Y. Igarashi: "Latest Cenozoic formations in the northern part of Teshio Plain, Hokkaido – Sedimentary facies and pollen stratigraphy", In: M. Kawamura, T. Oka and T. Kondo (Eds.) Commem. Vol. Prof. M. Kato, pp. 341-365 (1997). (in Japanese with English abstract)
14) T. Oka: "Distribution and tectonic evolution of Late Cenozoic basins in Hokkaido", Monogr. Assoc. Geol. Collab. Jpn., No. 31, pp. 295-320 (1986). (in Japanese with English abstract)
15) M. Akiyama and K. Hoyanagi: "Neogene, Tenpoku Area", Regional geology of Japan part 1: Hokkaido, Kyoritsu Shuppan, pp. 105-106 (1990). (in Japanese)
16) T. Nakata and T. Imaizumi (Eds.): "Digital Active Fault Map of Japan", Univ. Tokyo Press (2002). (in Japanese)
17) H. Matsui, T. Niizato and T. Yamaguchi (Eds.): "Horonobe Underground Research Laboratory Project Investigation Report for the 2005 Fiscal Year", JAEA-Research 2006-073 (2006). (in Japanese with English abstract)

18) Geographical Survey Institute: “Digital Map 50 m Grid (Elevation): NIPPON-I” (2001). (in Japanese)
19) Japan Nuclear Cycle Development Institute: “H17: Development and Management of the Technical Knowledge Base for the Geological Disposal of HLW”, Supporting Report 1: Geoscience study, JNC TN1400 2005-014 (2005). (in Japanese)
20) Japan Nuclear Cycle Development Institute: “H17: Development and Management of the Technical Knowledge Base for the Geological Disposal of HLW”, Supporting Report 2: Repository engineering technology, JNC TN1400 2005-015 (2005). (in Japanese)
21) Japan Nuclear Cycle Development Institute: “H17: Development and Management of the Technical Knowledge Base for the Geological Disposal of HLW” Supporting Report 3: Safety assessment method, JNC TN1400 2005-016 (2005). (in Japanese)

2. Overview of the Phase I geoscientific research

Multidisciplinary geoscientific research was conducted during Phase I of the Horonobe URL project, including stepwise investigations and preparation of a design and construction plan for the underground facilities, in accordance with the specific goals established as part of the two major goals of the project. In the early stage of Phase I, investigations were conducted for the whole area of Horonobe Town in order to select a URL area (where surface-based investigations will be focussed) and the URL site (where the surface and underground facilities will be constructed) and extensive investigations were then conducted in and around the selected URL area. Investigation and monitoring of the surrounding geological environment were also conducted continually throughout Phase I, considering the potential environmental impact associated with the construction of the URL.

This chapter describes the goals of the investigations and the basic approach for implementing the investigations in Phase I.

2.1 Goals in Phase I

The geoscientific research during Phase I of the Horonobe URL project has two specific goals based on the major goals[1)] described in Subsection 1.2.1:

a) development of conceptual models of the geological environment and enhancing understanding of the undisturbed deep geological environment before tunnel excavation;
b) detailed design of the underground facilities and formulation of a construction plan.

The former (a) involves acquiring information on the deep geological environment throughout the surface-based investigations, with the aim of improving understanding of the undisturbed conditions before construction of the underground facilities, particularly on properties and processes that would be relevant for geological disposal. It also involved stepwise modelling and analysis of the geological environment (geological structure, hydrogeology, hydrochemistry and rock mechanics) through integration and interpretation of the information obtained. This is expected to lead to establishing systematic techniques for characterising sedimentary formations.

The latter (b) involves formulation of specifications for, and designing the layout of, the underground facilities and preparation of a design and construction plan for the facilities, based on information on the geological environment obtained through the surface-based investigations, the plans for investigations in the underground facilities and conventional construction techniques, with the main aims being ensuring the safe construction and operation of the underground facilities and securing the environment for the investigations in situ. When formulating the construction plan, one consideration is minimising the impact on the surrounding environment associated with the construction of the underground facilities.

2.2 Basic strategy

Of the Phase I geoscientific research, ‘characterisation of a specific geological environment’ aimed at achieving goal (a) will be a key aspect of establishing systematic techniques for characterising the geological environment, including three R&D items: ‘development of techniques for investigating the geological environment’, ‘development of techniques for long-term monitoring of the geological environment’ and ‘studies on the long-term stability of the geological environment’. They also serve as a basis of the selection of the URL area and the URL site and provide input for formulating the design and construction plan of the underground facilities under (b) above.

This section describes the key properties and processes of the geological environment to be investigated in the surface-based investigations.

2.2.1 Key properties and processes of the geological environment

The main safety functions to be served by the geological environment in a geological disposal system will include physically isolating the waste for a sufficiently long period of time, maintaining conditions favourable for the EBS and preventing or attenuating potential release of radioactivity[1),2)]. The requirements on the geological environment in terms of long-term physical isolation of waste have been formulated as 'environmental requirements to be considered at the selection of the Preliminary Investigation Areas (PIAs)[3)]. The geological environment of interest is expected to have the following properties and features in order to meet these requirements and to ensure the feasibility and applicability of geological disposal technologies:

- occurrence at both an appropriate location and adequate depth with sufficient spatial extent for the construction of a repository;
- almost homogeneous stress conditions and low ground temperatures with a view to ensuring safe design and construction and maintaining the integrity of the engineered barriers and the disposal facilities;
- low groundwater fluxes, moderately alkaline groundwater chemistry and reducing conditions, with the aim of restricting erosion of the buffer material, corrosion of overpack and dissolution of the waste glass matrix;
- slow and long groundwater flow paths, ensuring sufficient retardation of radionuclide migration;
- dilution and dispersion of radionuclides migrating in groundwater in the context of reducing radionuclide concentrations.

The geological formations of interest would also be required to maintain a suitable environment for the engineered barriers and to act as a natural safety barrier for a long period of time. For the surface-based investigations, the key geological properties and functions were identified and listed as properties and processes of the geological environment to be investigated in relation to safety assessment of the geological disposal system, with reference to a generic FEP (Features, Events and Processes) list[4)] developed by international collaboration and FEP lists[5),6)] developed for sedimentary formations being investigated in Europe; in particular the Opalinus Clay in Switzerland, and investigation items and methods listed for preliminary investigations[1),7)] (Figure 2.2.1-1).

In the Horonobe URL project, design and construction will be conducted based on information on the geological environment obtained through surface-based investigations (see Chapter 5 for details). The properties and processes of the geological environment to be investigated therefore need to be reviewed from the viewpoint of design and construction of the underground facilities. The current trend in geological disposal projects highlights[8)–10)] the importance of evaluating not only the impact on the safety of the human environment but also societal and environmental impacts, as is the case for large-scale projects such as construction of tunnels and dams. For the URL project, investigations will be conducted in parallel with the construction of the underground facilities and it will thus be possible to evaluate the specific impacts of construction of the surface and underground facilities on the surrounding environment (groundwater levels, water chemistry etc.). With this unique feature of the project in mind, the properties and processes to be investigated were identified from the viewpoint of design and construction of the underground facilities and the environmental impact assessment (Figure 2.2.1-1).

A more specific aim during the surface-based investigations of the geological environment would be to clarify the identified key properties and processes of the geological environment with special emphasis on the safety assessment. In each discipline, it would be necessary to develop adequate characterisation techniques and consequently to establish systematic techniques for investigating, modelling, evaluating the geological environment through synthesising the results obtained in the different disciplines.

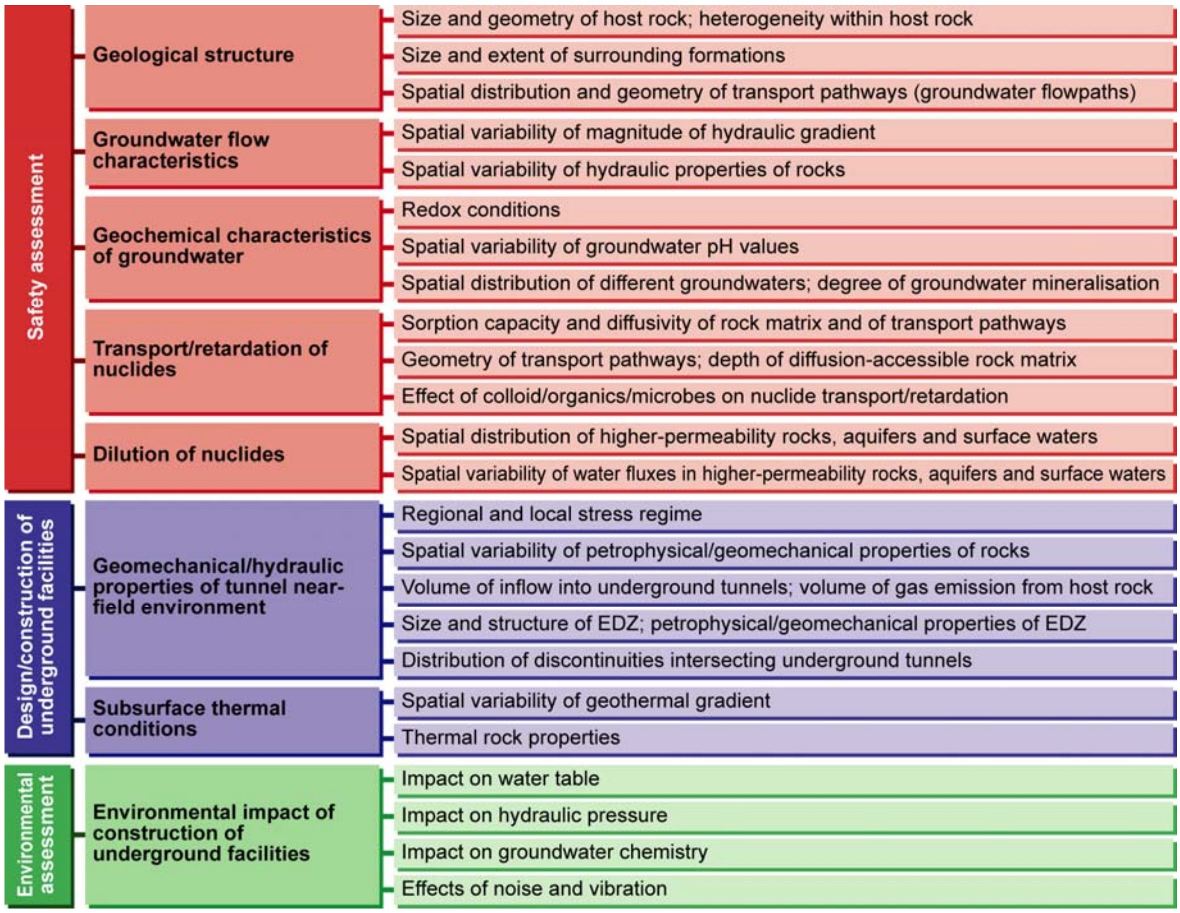

Figure 2.2.1-1 Key properties and processes of the geological environment for safety assessment, design and construction of the underground facilities and environmental impact assessment

2.2.2 Stepwise surface-based investigations

In Phase I of the Horonobe URL project, all surfaced-based investigations were conducted under a restriction that limits the investigation area to within the region of Horonobe Town. The surface-based investigations are divided into two stages: those ‘in the whole Horonobe Town’ area and those ‘in and around the URL area’ (Figure 2.2.2-1).

(1) Investigations in the whole area of Horonobe Town

During the investigations in the whole area of Horonobe Town (the first two years of Phase I), as discussed in Chapter 3, a URL area and a URL site were selected by focussing in stepwise on areas of interest[11),12)]. Along with the progress of the selection process, investigations evolved stepwise from those using existing information through aerial reconnaissance surveys and ground exploration to borehole investigations

(HDB-1 and HDB-2); they also moved from regional to site-specific surveys in order to obtain more detailed information on the geological environment[12].

(2) Investigations in and around the URL area

The investigations in and around the URL area can be divided into three types: investigations using existing information, ground exploration and borehole investigations. The investigations using existing information involve integration and interpretation of information obtained during the investigations covering the whole area of Horonobe Town and identifying issues not addressed in this stage. Based on the results and focussing on determining the spatial distribution of the Omagari Fault and the characteristics of the geological environment and acquiring geological information for the URL site, the latter two types of investigation were conducted. More specifically, ground exploration and borehole investigations were conducted iteratively in parallel in and around the URL area[13)–16)] (see Appendices 2 and 3), as shown in Figure 2.2.2-1. The aim of this approach is to identify any problems associated with the investigation techniques used for certain investigation targets and to improve these techniques by iterative application. Examples include ground geophysical surveys for determining the distribution of large-scale discontinuities (e.g. the Omagari Fault), one of the key features to be characterised for geological disposal, and excavation techniques for oil- or gas-bearing sedimentary formations (soft rock). The basic approach employed in each of the investigations was an iteration of planning, execution of exploration and evaluation of exploration results.

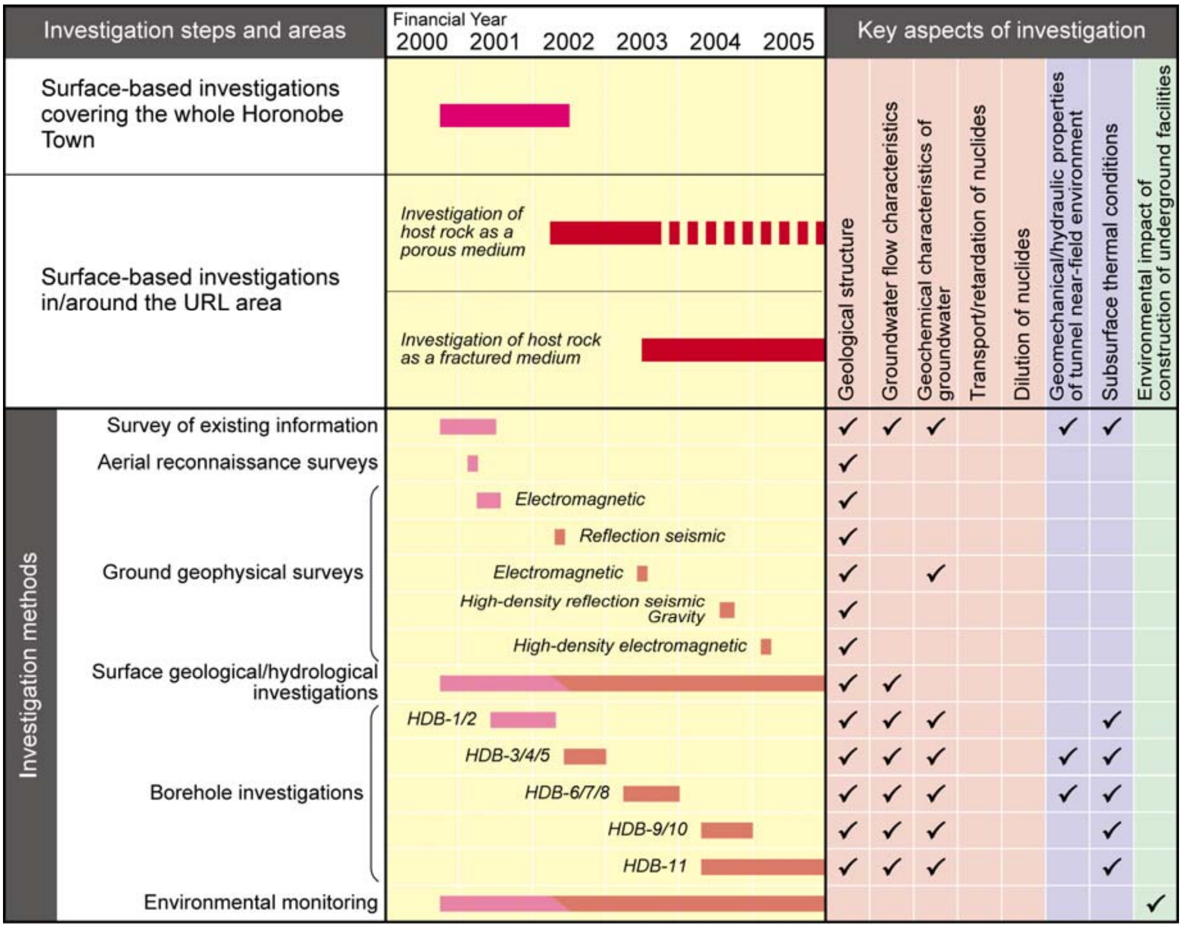

Figure 2.2.2-1 Characterisation of the subsurface geological environment at Horonobe

1) Investigations based on existing information

Literature information collected for selecting the URL area (open literature) and data obtained by regional surveys (aerial and ground geophysical surveys, surface geological surveys and HDB-1 and HDB-2 deep borehole investigations) were used to overview the characteristics of the geological environment in and around the URL area. Plans for the surface-based investigations and borehole investigations were also formulated based on the results.

2) Ground exploration

Ground exploration, aimed mainly at acquiring information on the location and properties of large-scale discontinuities such as the Omagari Fault, include surface geological surveys, gas analyses using shallow boreholes and regional reflection seismic and electromagnetic surveys[13)–16)]. Shallow subsurface hydrological investigations were also conducted for drainage basins around the URL area in order to calculate the groundwater recharge volume used for setting the upper boundary conditions in the groundwater flow analysis; surface water chemistry was also analysed to acquire data for surface waters (river water and shallow groundwater) for hydrochemical modelling[13)–16)].

3) Borehole investigations

Shallow and deep borehole investigations were conducted from the ground surface. As the former are included in the surface-based investigations, only the deep borehole investigations are described here.

The objectives of the deep borehole investigations include determining the geological setting in and around the URL area, particularly the distribution and geometry of the Omagari Fault and the detailed characteristics of the geological environment, acquiring information required for designing the underground facilities and obtaining information on the geological environment surrounding the boundaries of URL area required for modelling and analysis purposes. Since the HDB-1 borehole had been drilled in the URL area during the URL area selection stage, drilling locations were selected so as to be distributed evenly over the area of interest, taking into consideration the data obtained in the HDB-1 borehole and the identified investigation objectives (see Appendix 4). An additional nine deep boreholes (HDB-3 to HDB-11) were drilled with lengths between 470 m and 1,020 m[13)–16)]. In these boreholes, investigations were conducted for the Wakkanai and Koetoi Formations to acquire accurate data on the 3D distribution of geological structures, discontinuities, the hydraulic and mechanical properties of the target formations as well as groundwater chemistry. This included core logging, geophysical logging, fluid logging, hydraulic testing, groundwater sampling and rock mechanical testing. After these investigations had been completed, long-term monitoring systems were installed in the boreholes to monitor groundwater level, pressure and chemistry (see Appendix 3). The results of the deep borehole investigations are overviewed in Appendix 5.

References

1) Japan Nuclear Cycle Development Institute: "H12: Project to Establish the Scientific and Technical Basis for HLW Disposal in Japan", Project Overview Report, JNC TN1410 2000-001 (2000).
2) K. Shimizu, T. Seo and H. Yoshida: "Geological disposal of high-level radioactive waste and geological environment in Japan", J. Min. Mater. Process. Inst. Jpn., 117, pp. 775-784 (2001). (in Japanese with English abstract)
3) Nuclear Safety Commission of Japan: "Environmental Requirements to be Considered at the Selection of the Preliminary Investigation Areas for High-Level Radioactive Waste Disposal", Advisory Board on High-Level Waste Repository Safety, 30th Sep. 2002 (2002). (in Japanese)
4) Nuclear Energy Agency: "Features, Events and Processes (FEPs) for Geologic Disposal of Radioactive Waste – An International Database", OECD/NEA, ISBN 92-64-18514-3 (2000).
5) M. Mazurek, F.J. Pearson, G. Volckaert and H. Bock: "Features, Events and Processes Evaluation Catalogue for Argillaceous Media", OECD/NEA, ISBN 92-64-02148-5 (2003).
6) National Cooperative for the Disposal of Radioactive Waste: "Project Opalinus Clay: FEP Management for Safety Assessment", Demonstration of disposal feasibility for spent fuel, vitrified high-level waste and long-lived intermediate-level waste (Entsorgungsnachweis), Nagra Tech. Rep. NTB 02-23 (2002).
7) Nuclear Waste Management Organization of Japan: "Evaluating Site Suitability for a HLW Repository – Scientific Background and Practical Application of NUMO's Siting Factors", NUMO-TR-04-04 (2004).
8) Atomic Energy Canada Limited: "Environmental Impact Statement on the Concept for Disposal of Canada's Nuclear Fuel Waste", AECL-10711, COG-93-1 (1994).
9) Posiva Oy: "The Final Disposal Facility for Spent Nuclear Fuel – Environmental Impact Assessment Report" (1999).
10) U.S. Department of Energy: "Final Environmental Impact Statement for a Geologic Repository for the Disposal of Spent Nuclear Fuel and High-Level Radioactive Waste at Yucca Mountain, Nye Country, Nevada", Readers Guide and Summary, OCRWM, USDOE, DOE/EIS-0250 (2002).
11) Japan Nuclear Cycle Development Institute: "Horonobe Underground Research Laboratory Project Investigation Report for the 2000 Fiscal Year", JNC TN1400 2001-008 (2001). (in Japanese)
12) S. Yamasaki, N. Nakatsuka, N. Ogata, N. Eki, T. Moriya, R. Takeuchi, T. Kunimaru and N. Shirato: "Horonobe Underground Research Project – The Result on URL Area Selection Performed along with Field Investigations of FY2001/2002", JNC TN1400 2002-017 (2002). (in Japanese with English abstract)
13) Japan Nuclear Cycle Development Institute: "Horonobe Underground Research Laboratory Project Investigation Report for the 2002 Fiscal Year", JNC TN5400 2003-001 (2003). (in Japanese)
14) Japan Nuclear Cycle Development Institute: "Horonobe Underground Research Laboratory Project Investigation Report for the 2003 Fiscal Year", JNC TN5400 2004-001 (2004). (in Japanese)
15) Japan Nuclear Cycle Development Institute: "Horonobe Underground Research Laboratory Project Investigation Report for the 2004 Fiscal Year", JNC TN5400 2005-001 (2005). (in Japanese)
16) H. Matsui, T. Niizato and T. Yamaguchi (Eds.): "Horonobe Underground Research Laboratory Project Investigation Report for the 2005 Fiscal Year", JAEA-Research 2006-073 (2006). (in Japanese with English abstract)

3. Selection process for the URL area and site

Phase I of the Horonobe URL project consisted of selecting a URL area (the main area of 3 km × 3 km square for the surface-based investigations) and a URL site (the site for constructing the underground and surface facilities), which involved establishing fundamental factors relating to the geological environment and safety, surface-based investigations of the geological environment, stepwise narrowing down of target areas (sites) from the whole area of Horonobe Town through candidate URL areas and, finally, to a URL site. This selection process was based on information on the geological environment acquired by the investigations and took social and environmental conditions into consideration.

This chapter describes the selection process for the URL area and the URL site. Section 3.1 describes the technical requirements and social and environmental conditions considered in the selection of a URL site and the selection procedure, while Sections 3.2 and 3.3 summarise the process leading from establishing potential URL areas to selecting candidate URL areas. Section 3.4 describes the selection of the URL area and Section 3.5 the selection of the URL site. Finally, technical findings are summarised in Section 3.6. It should be noted that the requirements and conditions described here are those that apply specifically to the selection of a URL site and will be different from those used for selecting a final disposal site.

3.1 Basic strategies for the selection process of the URL area and site

3.1.1 Requirements for the URL site

As stated in Chapter 1, the underground facilities in the Horonobe URL project (referred to as the URL in this chapter) provide an R&D platform for testing geological disposal techniques in an actual geological environment, with a view to enhancing their reliability and confirming their practicality and applicability. Of importance will be to develop investigation and evaluation techniques and engineering methods that are applicable to the various geological environments found in Japan. The URL is also expected to be used as a location for promoting a wider understanding of geological disposal. Therefore, the criteria used for selecting the URL site are clearly different from those taken into consideration when selecting a final disposal site[1),2)].

Two criteria were defined as being fundamental for the selection of a URL area and a URL site, viz.:

- the presence of a suitable rock formation and groundwater (geological environment criteria);
- a sufficient volume of rock for the safe construction of the URL and the execution of R&D activities (safety factor)[3)].

Specific technical requirements for the criteria and social and environmental conditions, which had to be taken into consideration are described below.

(1) Rock mechanical properties

Based on data of the rock mechanical properties obtained from a deep borehole (D-1) drilled at Horonobe by the Power Reactor and Nuclear Fuel Development Corporation (PNC; now JAEA) before the start of the Horonobe URL project[4)], it was considered possible to safely construct the URL up to a maximum depth of 500 m, taking into account current engineering technologies and rock properties investigated.

(2) Geological structure

It was realised that excavation of a shaft or drift at a location with a steep bedding plane (e.g. near the fold axis) could result in a landslide along the bedding plane, leading in turn to a high risk of tunnel collapse. It was also expected that, at such a location, the horizontal variation of rock type will be significant and it is likely that the rock formations that overlie or underlie the target formation will be encountered during deep underground excavation of a drift. Thus, as a preference in terms of geological structure, it was considered that an area or site with a small dip should be selected to ensure safe construction of the URL and to improve the chance of encountering the particular target formation.

(3) Geology

Neogene sedimentary formations, which are widely distributed throughout Japan, were selected for investigation in the Horonobe URL project. As described in Chapter 1, Japanese legislation (i.e. the Act) states that HLW should be disposed in deep geological formations at depths greater than 300 m below the ground surface to isolate the waste from the human environment over the long-term. In addition, the required formation thickness was defined assuming that the shaft would reach a maximum depth of 500 m. Hence, an area had to be selected where the target Neogene sedimentary formation distributes in a depth range of 350–500 m and two or more formations outcropping in the drifts should be avoided.

(4) Groundwater chemistry

Groundwater chemistry was not considered when selecting the URL site. However groundwater had to be present to allow investigation of hydrochemical conditions and groundwater flow. Based on the D-1 borehole investigation results[4], it was assumed that saline groundwater with high mineralisation is present in the sedimentary formations in the Horonobe Town area. It was thus necessary to develop disposal techniques and safety evaluation methods for such a geological environment.

(5) Social and environmental conditions

Since there are a variety of organisations, individuals and regulations, it was considered important to perform preliminary surveys of the potential URL areas before starting field activities. Social conditions include, for example, designation as a special area such as a national park, or environmental protection areas such as a wildlife sanctuary, land use (designation as a forest reserve, river source or farming area), land ownership (housing, farmland, forestry areas, hot springs and mining rights) and historic relics or ruins. Environmental conditions include impacts associated with the URL construction on flora and fauna or peripheral environments (river water, groundwater, soil etc.). In particular, more attention will be required regarding development in the habitats of rare animal and plant species.

3.1.2 Stepwise selection process for the URL site

The selection process of the URL site in the Horonobe Town area proceeded stepwise as shown in Subsection 3.1.1, by defining technical requirements and relevant social and environmental conditions, selecting two or more areas or sites that meet these requirements and conditions through investigations based on existing information and field exploration and, finally, comparing these areas or sites in terms of technical criteria and a comprehensive evaluation taking social and environmental conditions into account.

In order to make efficient use of time and resources, surveys based on existing literature references and open information and hearings at the sites were conducted as far as possible before starting the field investigations in order to identify areas that seemed likely to meet the requirements for the URL area. Field investigations were conducted to acquire detailed information on the geological environment, by increasing the level of detail from aerial reconnaissance surveys through ground exploration to borehole investigations[3].

3.2 Selection of potential URL areas

3.2.1 Requirements for potential URL areas

One of the technical requirements for the selection of potential URL areas was that a target formation exists where the URL could be constructed and maintained safely; the formation would occur at a depth of around 350 m with a thickness of about 150 m. Although groundwater chemistry was not a factor for selecting the URL area as described in Subsection 3.1.1, as there was a need to investigate saline groundwater, preference was given to areas where saline groundwater was expected.

3.2.2 Review of existing information

Information on geology and geological structure, topography, meteorology etc. in the Horonobe area was compiled for the purpose of selecting potential URL areas within Horonobe Town. Existing information includes literature data and geological maps, as well as the results of oil exploration (as the sedimentary formation in and around the Horonobe area is oil and gas bearing), gravity and seismic explorations and the D-1 borehole investigations[4)]. The information is summarised below. The geological map and geological profile prepared based on the acquired information are shown in Figures 3.2.2-1 and 3.2.2-2 respectively.

The geology of the Horonobe area can be characterised as follows: Horonobe Town is located at the eastern end of the Tenpoku Sedimentary Basin and has a distribution of Cretaceous basement rock overlain by the Palaeogene Haboro and Magaribuchi Formations, the Middle Miocene Soya Coal-bearing, Onishibetsu and Masuporo Formations, the Middle Miocene – Pliocene Wakkanai and Koetoi Formations (the Koetoi Formation subdivided into upper and main facies but presently the upper facies corresponding the lower section of the Yuchi Formation), the Pliocene – Early Pleistocene Yuchi and Sarabetsu Formations, Middle Pleistocene and Holocene sediments and terrace sediments deposited after the Middle Pleistocene and Holocene[5)]. Of these formations, the Haboro and Magaribuchi Formations have not been observed at the surface, but were encountered in the existing MITI (the Ministry of International Trade and Industry; now the Ministry of Economy, Trade and Industry) Tenpoku borehole[6)]. The Wakkanai, Koetoi Yuchi and Sarabetsu Formations are a series of sediments consisting of abyssal → shallow marine → half-terrestrial → terrestrial deposits that are overlain unconformably[5)]. Each formation consists mainly of shale, diatomaceous mudstone, fine-grained sandstone, conglomerate, sandstone and siltstone. The geological structure in the Horonobe area is divided into three parts by the Horonobe Fault and the Omagari Fault, which have a strike of NNW-SSE[7)]: the eastern part with the Horonobe Fault, the part between the Horonobe Fault and the Omagari Fault and the western part with the Omagari Fault. Each part can be characterised as follows: a distribution of Cretaceous – Neogene formations with numerous folds and faults in the eastern part, the Wakkanai and Koetoi Formations with en echelon folds with a strike parallel to the fault in the middle part and the Yuchi and Sarabetsu Formations with moderately sloping folding structures in the western part[8)]. Structures active in the Quaternary, such as faults, flexures and tilts, are also found in the eastern and western parts[9)].

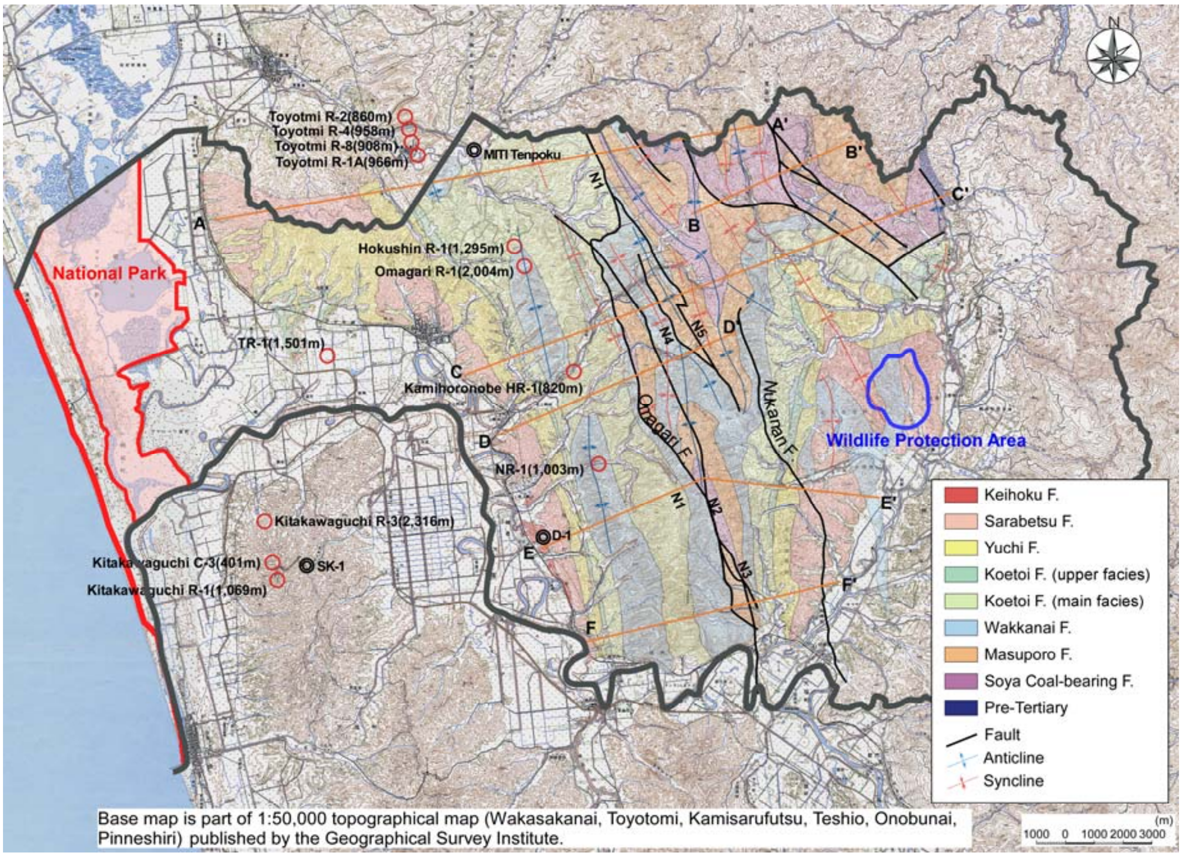

Figure 3.2.2-1 Geological map with the locations of existing boreholes for regional exploration in the Horonobe area before the start of the Horonobe URL project

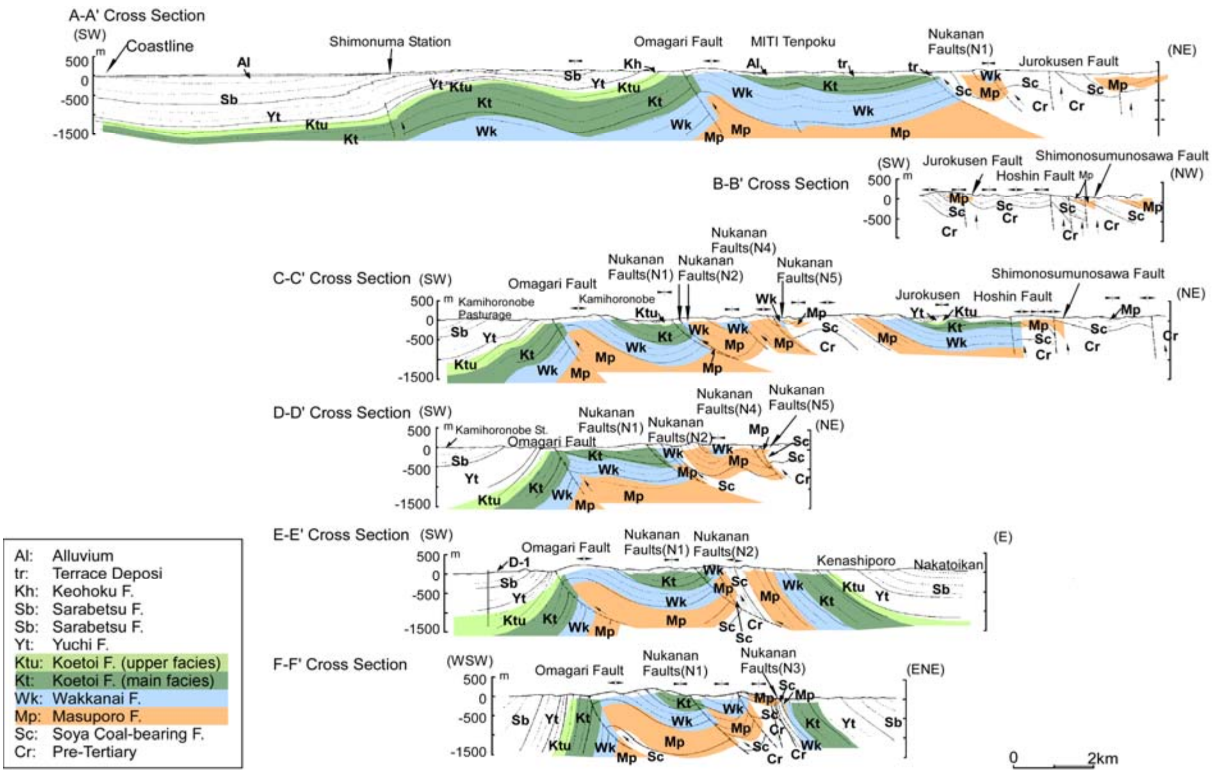

Figure 3.2.2-2 Schematic geological profiles thorough the sedimentary formations at Horonobe

Cross-sections along the A-A' to F-F' lines shown in Figure 3.2.2-1

Exploration and development of coal, oil and natural gas deposits has been carried out in the Tenpoku region, including the Horonobe Town. The eastern part of the Nukanan Fault (Figure 3.2.2-1) was exploited as the Tenpoku Coal Field and coal mines were also developed at some locations in Horonobe Town. The west side of the Nukanan Fault contains the Tenpoku Oil Field, where a geological survey was carried out around 1910. Mining and exploratory excavation of oil and natural gas deposits trapped in anticlines was also carried out, mainly in the Masuporo Formation, but no oil field was developed. Natural gas, however, has been produced for about 36 years in the Toyotomi Gas Field, neighbouring the northern part of Horonobe Town; the cumulative production is estimated to be about 200 million m^3 [10)].

The climate in this area can be classified into two types, viz. an oceanic climate and an inland climate, since the area is located in the northernmost part of Hokkaido and faces both the Japan Sea and the Okhotsk Sea. The part facing the Japan Sea receives the effects of the monsoons prevailing in winter, but the atmospheric temperature is higher compared with the part facing the Okhotsk Sea; the maximum temperature is observed in August and the lowest temperature in January. The average annual rainfall for northern Hokkaido is 1,195 mm, almost the same as the average for the whole Hokkaido area, and the rainfall inland is higher with 1,400 mm or more[11)]. The trend is the same for weather observations conducted at several points in Horonobe Town[12)]. Existing data on rivers obtained by measuring discharge once a year indicated a specific discharge of 0.2–0.69 $m^3\ s^{-1}$ per 100 km^2 for most of the rivers investigated. The influence of seasonal variation of rainfall was not taken into account owing to lack of information. With regard to groundwater chemistry, the concentrations of Na^+ and K^+ are high, which indicates a potential effect of windborne salt or spring water[11)]. The investigation of groundwater chemistry described in this report was conducted for groundwater sampled at a relatively shallow depth (approximately 100 m) and information on deep groundwater chemistry is not included.

Information on the hydraulic properties, deep groundwater chemistry and rock mechanical properties is included in the report on the D-1 borehole investigations[4)]. Methane (CH_4) gas was found in saline groundwater from the Koetoi Formation. The head distribution is hydrostatic in general.

3.2.3 Selection of four potential URL areas

The selection of potential URL areas was based mainly on geological structure and distribution. Based on existing information from gravity explorations, seismic surveys and available borehole data[13)], a geological map (Figure 3.2.2-1) and geological profile (Figure 3.2.2-2) were produced for the whole area of Horonobe Town and three areas (A, B and C) were selected as the areas where Neogene sedimentary formations of interest for the Horonobe URL project (i.e. the upper part of the Masuporo Formation, the Wakkanai Formation and the main part of the Koetoi Formation) were assumed to be distributed horizontally with a thickness of about 150 m at a depth of about 350 m. Area B is larger than areas A and C and the sedimentary formations are continuous from north to south for greater than 10 km. In order to investigate its heterogeneous geological properties, area B was divided into two sub-areas, B1 and B2 (Figure 3.2.3-1).

The groundwater flow system was ascertained preliminarily by simulation covering the whole area of Horonobe Town, using existing information on topography, geology and hydrogeology[14)]. In the groundwater flow simulation, the change in groundwater level around the site for construction of the URL was estimated assuming the groundwater flow field (flow direction and flow velocity) prevailing in the Horonobe area.

After the above technical review, the aims and schedule for the investigations in each area were decided based on existing information on groundwater chemistry, land use classification and infrastructure. A summary of the characteristics of each area based on existing information, as well as potential problems and recommended investigation items to confirm the suitability of the area are given below. In selecting a URL area from a number of potential or candidate investigation areas, it is important, with a view to optimising costs and time, to define technical requirements in such a way as to restrict the items to be addressed in the field investigations.

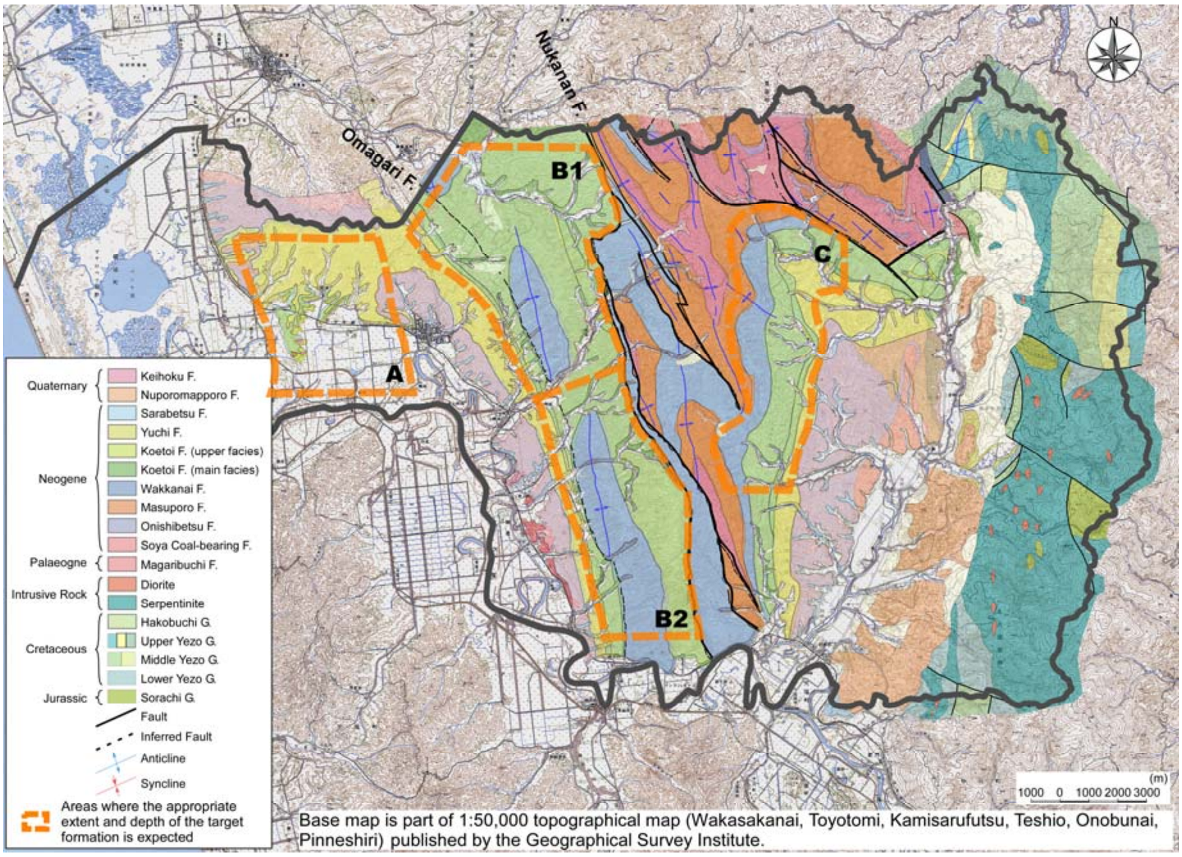

Figure 3.2.3-1 Four potential areas selected for URL construction in Horonobe Town

(1) Background of area A

1) Geological structure and distribution

In this area, the depth of the Neogene sedimentary formations is located at around 150 m at the top of the anticline in the south and at about 250 m in the north. The moderate dip of 30° or less generally indicates a horizontal distribution of the Neogene sedimentary formations over several kilometres. The lithofacies of the target horizon indicate that the main part of the Koetoi Formation consists mainly of massive argillaceous rocks. These suggested that the Neogene sedimentary formations have a stable geological structure with sufficient extent and thickness. The area was thus judged as meeting the requirements in terms of geological structure and distribution.

2) Safety of URL construction

Based on existing information, the sedimentary formations are expected to have moderate dip and a stable geological structure and hence it was assumed safe to construct and maintain the URL.

3) Social and environmental conditions

A study of land use, landowners and mining rights holders, as well as environmental monitoring, was found to be essential for areas A, B1, B2 and C. Based on existing information, a large portion of this area is privately owned land. The northern part of this area is hilly and infrastructure such as roads has not been developed, whereas the middle to southern part is flat and infrastructure including roads is well developed. Although it was recognised that other regulations would need to be considered, construction of the URL would thus be possible in principle.

4) Potential investigations

Since saline groundwater with a temperature of 34–38°C had previously been found in borehole investigations in the past for oil and natural gas exploration, it was assumed that saline groundwater was distributed throughout this area. It was considered possible to investigate the saline – freshwater interface (boundary between fossil seawater and freshwater) and hydrogeological investigations of the differences in density between saline groundwater and freshwater would be possible.

5) Recommended investigations to further confirm area suitability

It was recognised that, in principle, some or all of the following should be checked in order to confirm the suitability of area A as a URL area:

- The area is located in the anticline part of a fold structure and investigations conducted to date for oil and natural gas exploration suggest the possibility that the sedimentary formation contains a lot of gas. It is therefore important to confirm the amount of dissolved gas in the groundwater in this area.
- If the depth of the URL is near an unconformable interface with the Quaternary system, rock conditions may have deteriorated owing to alteration or weathering. Depending on the depth of the actual top surface and distribution of the Neogene sedimentary formations, construction of the URL may not be possible. Hence, rock mechanical properties (strength and competence) and the depth of the actual top surface and distribution of the Neogene sedimentary formations need to be investigated.
- Since this area is located on the west side of the Omagari Fault, where geological classification and stratigraphy are not well established, investigations to determine the age, sequence and distribution of the sedimentary formations would be required.

(2) Background of area B1

1) Geological structure and distribution

In this area, the Neogene sedimentary formations are distributed from the ground surface to a depth of 500 m or more and are expected to continue horizontally in an E-W direction for 8 km or more across the Omagari Fault. The horizons to be investigated are the Wakkanai Formation and the main part of the Koetoi Formation, consisting primarily of massive argillaceous rocks. In addition, the sedimentary formations in this area show moderate folding with a long wavelength and a stable geological structure with no subdivision by discontinuities such as faults.

2) Safety of URL construction

Since the sedimentary formations may have a steep dip of 60° or more on the west side of the Omagari Fault, measures against rock fall may be required for construction and maintenance of the URL. On the other hand, on the east side of the Omagari Fault, the sedimentary formations have a moderate dip of about 30° and the Neogene sedimentary formations are distributed from the ground surface to 500 m or deeper. Thus, it was considered that the URL could be safely constructed and maintained.

3) Social and environmental conditions

Privately owned land is widely distributed in this area. In addition, with the exception of a national forest covering the eastern part of this area, flat and moderately sloping land are common and infrastructure such as roads is also well developed. Although details of area-specific legal restrictions are unknown, it was considered that construction of the URL would not present a problem.

4) Potential investigations

The Omagari Fault is considered to be active and could be a target for investigation in this area because it runs in an NW-SE direction in the western part and may be encountered directly in the URL, depending on where it is constructed. Since saline groundwater with a temperature of 30°C had been found at a depth of around 600 m in boreholes drilled in the past for oil and natural gas exploration, it might be possible to conduct investigations on the profile of the fossil seawater and the saline – freshwater interface.

5) Recommended investigations to further confirm area suitability

It was recognised that in principle some or all of the following should be checked in order to confirm the suitability of area B1 as a URL area:

- The potential presence of oil and natural gas would need to be taken into account in the investigations because this area is located in an anticline and is in the vicinity of the Toyotomi Gas Field. The results of oil and natural gas exploration indicated that a gas reservoir is located at depths blow 650 m and a gas production rate of 3,600 m^3 d^{-1} has been measured in a section of 955–971 m depth. In these exploratory boreholes, 350–550 m^3 d^{-1} of gas blowout was recorded from the Wakkanai Formation and the main part of the Koetoi Formation, which are located in the upper part of the gas-bearing formation. It is thus important to investigate the amount of dissolved gas in groundwater.
- It will be necessary to acquire information about the location of the Omagari Fault and the rock mechanical properties of the surrounding rocks as it may not be possible to construct and maintain the URL safely, depending on the location and scale of the Omagari Fault and accompanying faults.
- The sedimentary formations may dip steeply in the vicinity of the Omagari Fault and the Masuporo Formation, in the lower sequence of the Wakkanai Formation, may also be a potential target horizon. Since the Masuporo Formation is considered to contain oil and natural gas and it is assumed that its geological structure is more complicated than the Wakkanai and Koetoi Formations, the extent of the Masuporo Formation and its suitability as a target for investigation would need to be evaluated.

(3) Background of area B2

1) Geological structure and distribution

In this area, the Neogene sedimentary formations are found from the ground surface to a depth of 500 m or more and are expected to continue horizontally in an E-W direction for at least 4 km across the Omagari Fault. The target horizons are the Wakkanai Formation and the main part of the Koetoi Formation, consisting mainly of massive mudstone.

2) Safety of URL construction

Since the sedimentary formations have a moderate dip of about 30° on the east side of the Omagari Fault, which indicates a more stable geology than on the west side of the Omagari Fault, and the Neogene sedimentary formations occur from the ground surface to a depth of 500 m or more, the URL could be constructed and maintained safely.

3) Social and environmental conditions

Areas outside those restricted by regulations, such as natural parks and wildlife sanctuaries, would come into question for construction of the URL. However, most of the east side of the Omagari Fault is hilly and covered in a national forest and minimum infrastructure such as roads has not been developed. Thus, it has to be taken into account that the URL construction would have to be done from the west side of the Omagari Fault, where privately owned flat and moderately sloping land are widely distributed and infrastructure such as roads is relatively well developed.

4) Potential investigations

The Omagari Fault is considered to be an active fault. This fault is located in an NNW-SSE direction in the western part of this area. The fault may therefore be encountered directly in the URL. Investigation of the hydraulic characteristics of fossil seawater and the saline – freshwater interface may also be possible since fossil seawater was observed in borehole D-1 drilled on the west side of the Omagari Fault[4)].

5) Recommended investigations to further confirm area suitability

It was recognised that in principle some or all of the following should be checked in order to confirm the suitability of area B2 as a URL area:

- The dip of sedimentary formations may be steep near the Omagari Fault. Therefore, the Masuporo Formation in the lower sequence of the Wakkanai Formation may be a target horizon for investigation. Since the Masuporo Formation is considered to contain oil and natural gas and is assumed to have a more complex geological structure than the Wakkanai and Koetoi Formations, the extent of the Masuporo Formation and its suitability as a target horizon would need to be evaluated.
- It would be necessary to acquire information about the location of the Omagari Fault and the mechanical properties of the surrounding rocks as it may not be possible to construct and maintain the URL safely, depending on the location and scale of the Omagari Fault and associated faults.
- The potential presence of oil and natural gas would need to be taken into account in the investigations because an anticline is located in the area; the Masuporo Formation contains oil and natural gas and may be one of the horizons to be investigated and very small-scale oil and natural gas indications have been found at the ground surface. The information about the amount of oil and natural gas in this area is currently insufficient.
- The stratigraphy, rock classification and age are not sufficiently clear to the west side of the Omagari Fault and hence would need to be studied further.
- It would be necessary to evaluate the feasibility of, and check the restrictions on, construction of the URL in the national forest on the east side of the Omagari Fault.

(4) Background of area C

1) Geological structure and distribution

In this area, the Neogene sedimentary formations are distributed from the ground surface to a depth of 500 m or more and are expected to continue horizontally in an E-W direction for several kilometres across the Omagari Fault. The main target horizons are the Wakkanai Formation and the main part of the Koetoi Formation, consisting primarily of massive mudstone. The dips of the formations are steep, with 40°–60° in the western and southern parts of this area. In the middle to eastern part, the dip is 30° or less, suggesting a stable geological structure and appropriate distribution of the Neogene sedimentary formations. However, the Masuporo and Yuchi Formations may be encountered in this area.

2) Safety of URL construction

The dips of the sedimentary formations are expected to be steep in the western and southern parts of this area – hence there are large horizontal changes in lithology. Measures against rock fall may be required during construction and operation of the URL in the western to southern parts of this area. On the other hand, in the middle to eastern parts, the sedimentary formations have a moderate dip and the Neogene sedimentary formations are distributed from the ground surface to a depth of 500 m or more. The URL could thus be constructed and maintained safely. However, for the Yuchi Formation, which consists mainly of sandstone, precautions would be required for the safe construction and maintenance of the URL.

3) Social and environmental conditions

Since this area is adjacent to a wildlife sanctuary, care will be necessary in planning the investigation programme because the URL construction may affect the sanctuary, even though the area is actually outside restricted areas such as natural parks and wildlife sanctuaries. In addition, the URL construction may not be straightforward because, except for a small, moderately sloping region along the prefectural road in the northern part of this area, hilly country prevails, without infrastructure such as roads.

4) Recommended investigations to further confirm area suitability

It was recognised that in principle some or all of the following should be checked in order to confirm the suitability of area C as a URL area:

- This area is located in the Tenpoku Coal Field and relatively few investigations have been conducted on oil and natural gas. This means that the geology and the geological structure are not as clear compared with other area. Hence, investigations to determine the age, stratigraphy, geological structure and extent of the rock formations of interest would be required.
- The URL in this area may encounter the Masuporo and Yuchi Formations. Since the Masuporo Formation is considered to contain oil and natural gas and it is assumed that the geological structure is more complex than that of the Wakkanai and Koetoi Formations, the extent of the Masuporo Formation and its suitability as a target rock formation would need to be checked. For the Yuchi Formation, which consists mainly of soft, fine grained sandstone, rock mechanical strength and suitability as a target for investigation would need to be evaluated.
- Since most of this area is covered with the Teshio Experimental Forest of Hokkaido University, it would be necessary to evaluate the feasibility of, and check the restrictions on, the URL construction.

3.3 Selection of the candidate URL area

3.3.1 Requirements for the candidate URL area

The requirement that construction of the URL should not affect hot springs around Horonobe Town was added to the requirements and conditions described in Subsection 3.2.1. The information on the distribution of hot springs around the town was acquired after the start of the field surveys.

3.3.2 Aerial reconnaissance surveys

Aerial geophysical surveys were conducted for the potential URL areas, with the primary aim of checking the geological structure estimated on the basis of existing information.

(1) Methods and approach for the surveys

Aerial geophysical surveys are considered to be particularly effective in the initial stages of regional investigation programmes as they can provide information on large-scale regional geological structures by combining techniques such as electromagnetic, magnetic and radiometric surveys. The electromagnetic method is suitable for obtaining information on differences in rock types, the magnetic method can be used to identify large-scale or deep geological structures and the radiometric method to identify large-scale near-surface discontinuities.

Aerial geophysical surveys were planned for all four areas where the Neogene sedimentary formations were assumed to occur to a depth of around 500 m with sufficient extent and thickness, except for area C where permission was refused from the land owners. Line spacing was 250 m for the main survey lines and 2 km for the cross survey lines; flying height was 60–120 m (Figure 3.3.2-1).

(2) Results of the surveys

The data from the aerial electromagnetic surveys indicated a high specific resistivity of 30–500 Ω m in the area of the Yuchi and Sarabetsu Formations, which consist mainly of sandstone and conglomerate. In the area where the Masuporo, Wakkanai and Koetoi Formations are found, a low specific resistivity of 1–10 Ω m at a depth of tens of metres or more was observed, while a high specific resistivity of 50–200 Ω m in the range from the ground surface to tens of metres in depth was observed (Figure 3.3.2-2).

The results obtained using the electromagnetic method and aerial magnetic surveys were generally consistent, except for abnormal NNW-SSE magnetics observed at the boundary between the Yuchi Formation and the Sarabetsu Formation. In addition, a magnetic anomaly with low continuity was also observed in the area where the Masuporo Formation is found to the east of the Nukanan Fault. These magnetic anomalies were considered to correspond to the occurrence of sandy formations, which is consistent with the trend of the regional magnetic map prepared using existing geological information[15] (Figure 3.3.2-3).

The results of a radiometric survey showed a trend with natural radioactivity being high in the bottomland along the Teshio River and in streams in hilly areas whereas low in the area where the Neogene sedimentary formations are distributed. There was no trend showing high radioactivity at locations where large-scale discontinuities such as the Omagari Fault are assumed to occur.

From the above results, characteristics such as lithology and chemical composition would appear to be fairly homogeneous in the area where sedimentary formations occur (presenting a low resistivity contrast) and it was assumed that homogeneous sedimentary formations occur at a depth of around 500 m where the URL would be constructed. On the other hand, some features that show a low specific resistivity were found in the area where the Omagari Fault is assumed to be present, but the results of aerial geophysical surveys were not sufficiently clear to allow identification of the exact location and configuration of the Omagari Fault. However, the results of such aerial surveys indicated that the distribution of geology and geological structures is consistent with that estimated during the selection of potential URL areas in general and is also in agreement with the results obtained using borehole D-1[4]. Therefore, the conclusions regarding the selection of potential URL areas (areas A, B1 and B2) can be considered to be appropriate.

In addition to the above technical findings, the importance of providing advance information on planned activities was acknowledged because stock farming prospers in Horonobe Town and the impact of noise from the helicopters used for the aerial surveys was an issue of concern.

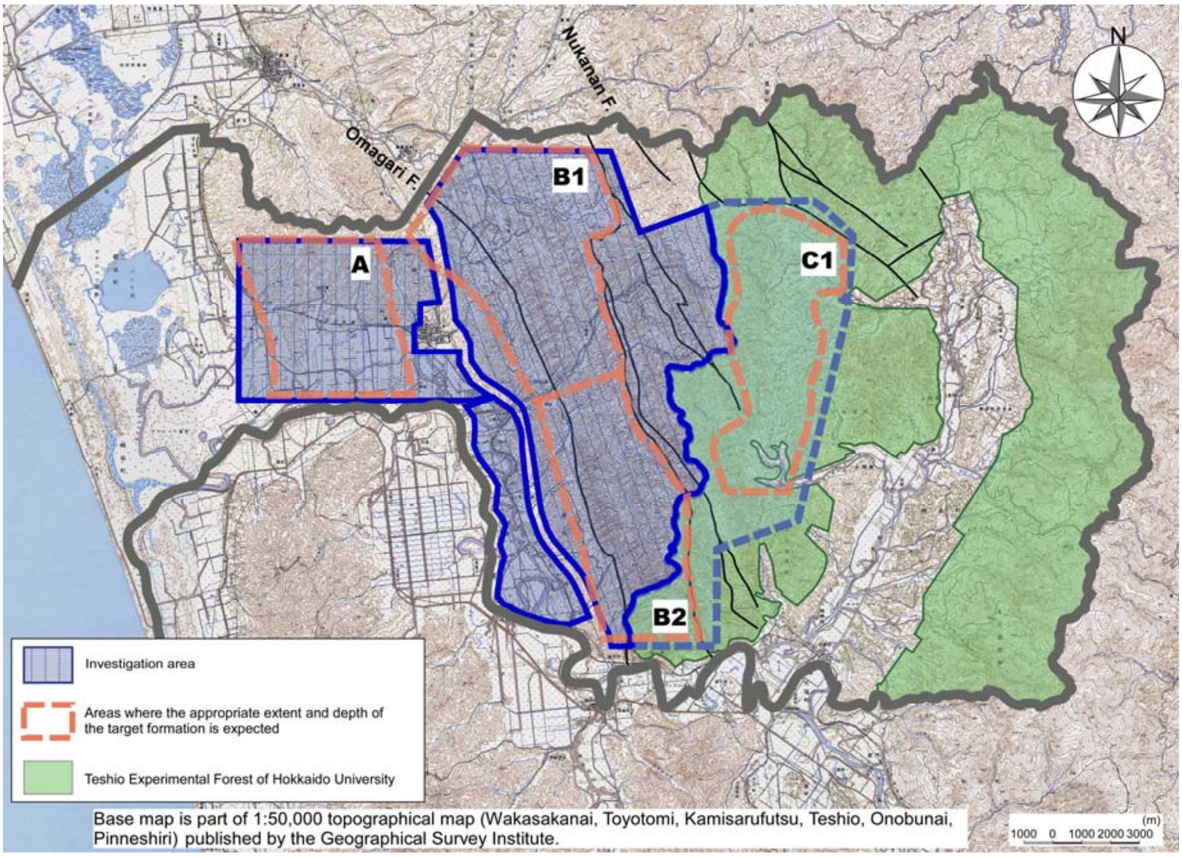

Figure 3.3.2-1 Areas for aerial reconnaissance surveys in Horonobe Town

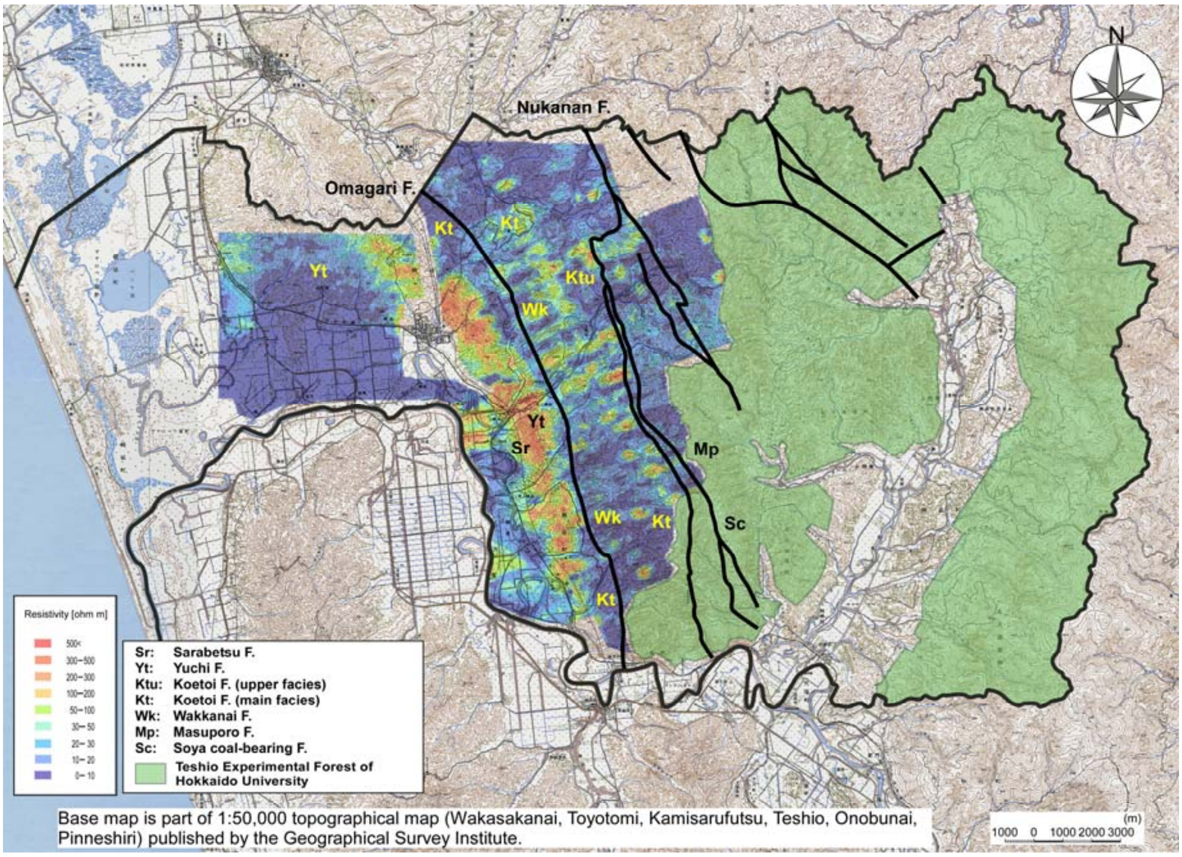

Figure 3.3.2-2 Image of resistivity distribution observed by airborne electromagnetic survey

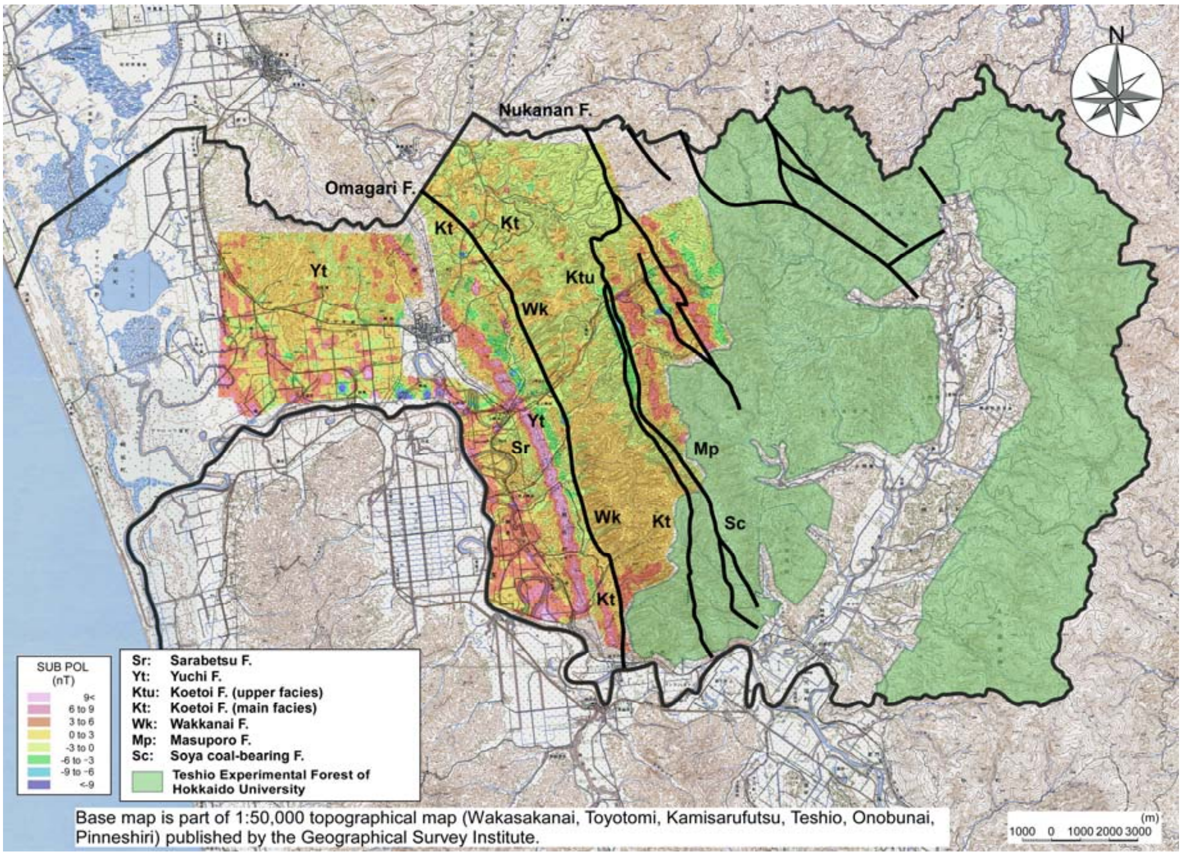

Figure 3.3.2-3 Image of resistivity distribution observed by airborne magnetic survey

3.3.3 Investigations from the surface

The stratigraphy of the Neogene sedimentary formations in the Horonobe area has not yet been established because they consist of massive mudstone with little change in lithofacies. The Omagari Fault, which cuts through the centre of Horonobe Town, is assumed to be a thrust fault dipping to the east with a vertical displacement of several hundreds to more than a thousand metres; it is also assumed to have been active in the Quaternary[16]. Since fault outcrops have not been observed in the Horonobe Town, sufficient data have not yet been obtained on the location and dip of the Omagari Fault and the presence of fracture zones or fault activity.

Surface-based investigations were conducted with the aim of enhancing confidence in the results of aerial geophysical surveys, checking existing geological information and obtaining mineralogical data. The investigations included ground geophysical surveys (electromagnetic), surface geological investigations and mineralogical examinations of rock samples (microscopic examination, mode analysis, X-ray diffraction, whole rock analysis, microfossil analysis, RockEval analysis, palaeomagnetism analysis and geochronometry)[17].

(1) Ground geophysical surveys

Existing data from seismic surveys[13] carried out to date suggest that these have not provided sufficient data on the geological structure for this area. Magnetotelluric (MT) and audiomagnetotelluric (AMT) electromagnetic surveys that had not previously been used here, as well as a 2D resistivity analysis of the data, were therefore attempted in order to investigate geological structure (Figure 3.3.3-1). The results showed an NNW-SSE trend for horizontal distribution of the resistivity, which is consistent with the geological structure of this area. The resistivity obtained in the shallower subsurface environment showed a clear contrast, reflecting the differing rock types with different resistivities between the west and east sides of the Omagari Fault; the Yuchi Formation consists mainly of sandstone on the west side of the Omagari Fault and the Koetoi Formation consists mainly of mudstone on the east side of the Omagari Fault. On the other hand, the results obtained for a depth of around 500 m showed an ambiguous contrast (Figure 3.3.3-2). This is because the Wakkanai and Koetoi Formations both consist mainly of mudstone and are distributed on the west and east sides of the Omagari Fault. These data indicate that mudstones with a low resistivity contrast and similar physical properties are found at a depth of 500 m in this potential URL area.

The geological structure assumed from the aerial and ground geophysical surveys is thus consistent with that assumed based on existing information, indicating that the rock formations of interest are distributed homogeneously around a depth of 350 m. It was concluded that the potential URL areas (areas A, B1 and B2) investigated here meet the technical requirements in terms of geological structure and distribution (Figure 3.3.3-3).

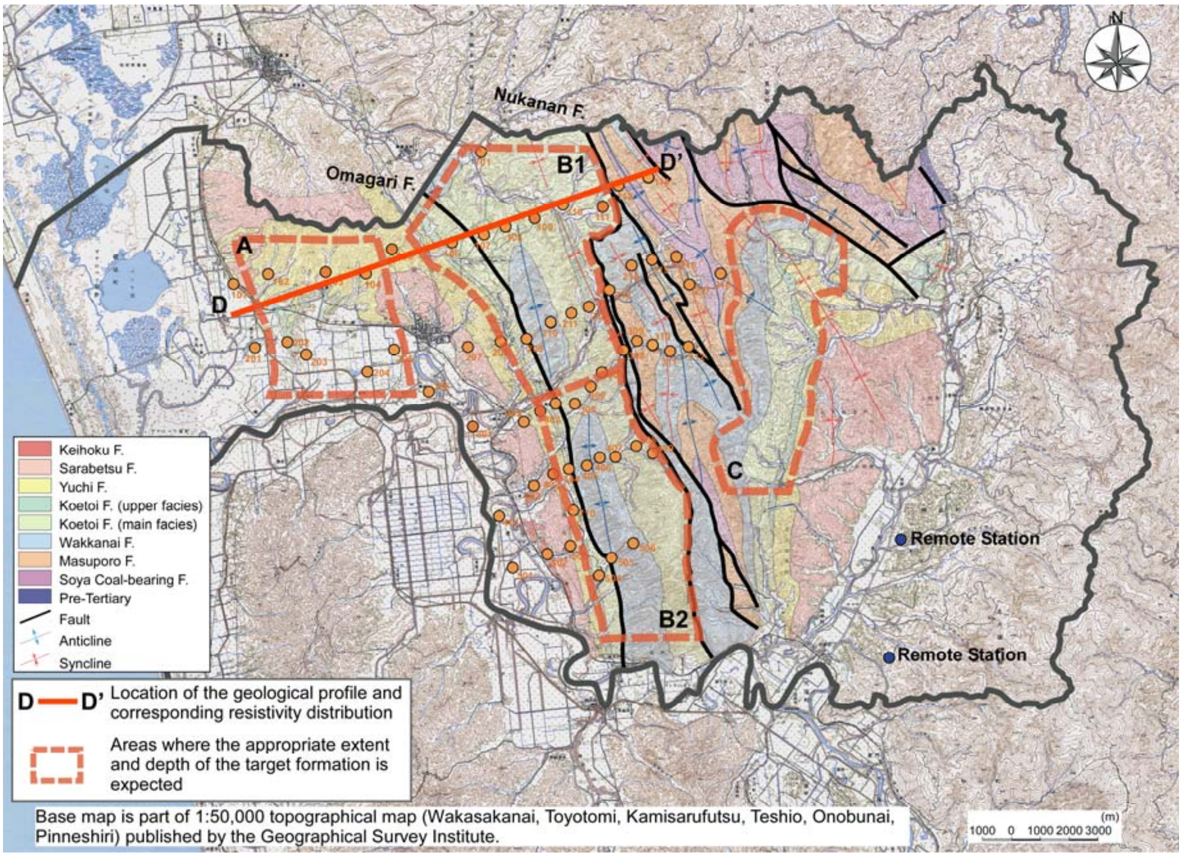

Figure 3.3.3-1 Station points for ground geophysical survey by MT and AMT methods

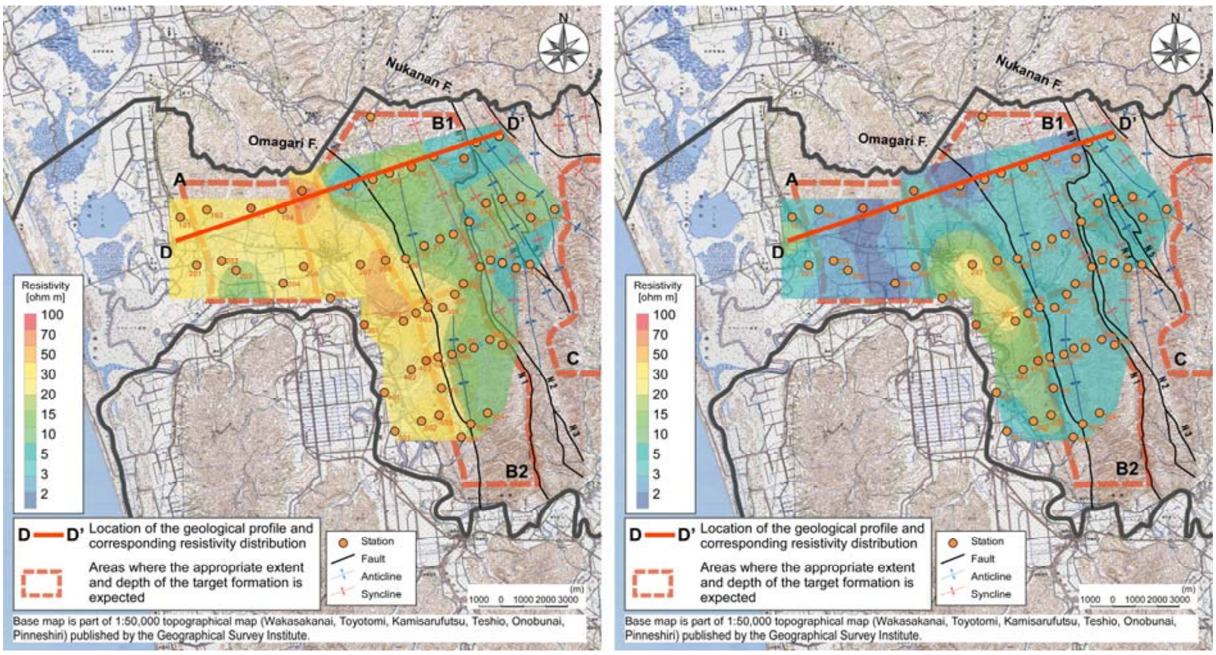

Figure 3.3.3-2 Images of resistivity distribution at 0 m (left) and -500 m (right) elevation

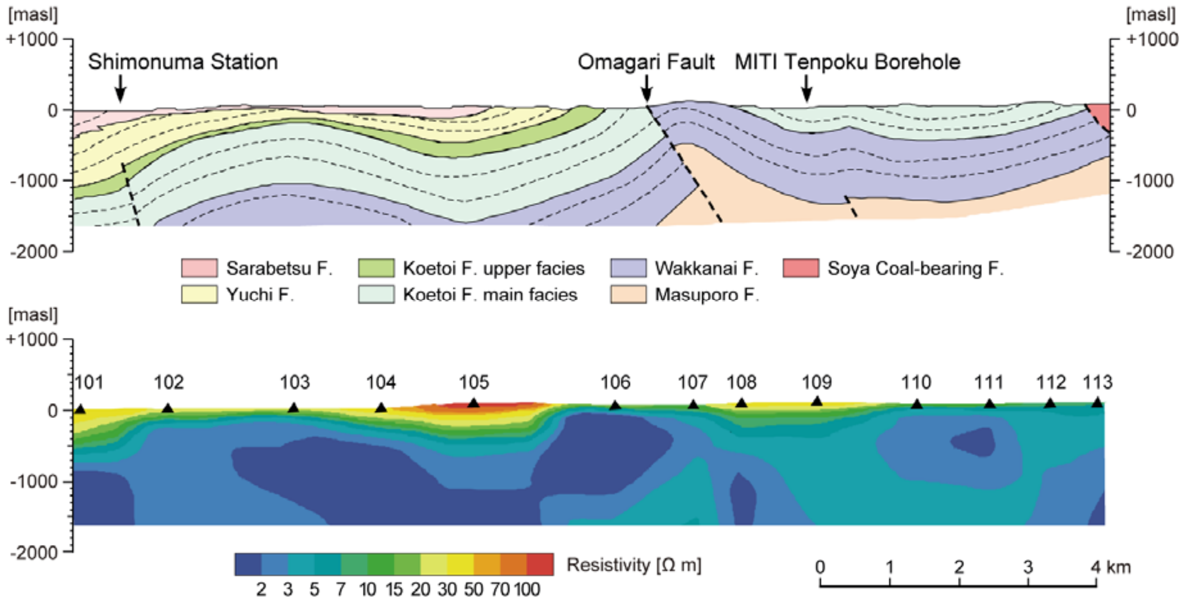

Figure 3.3.3-3 Comparison of schematic geological and corresponding resistivity profiles

(2) Surface geological investigations

Surface geological investigations were performed to confirm the stratigraphical distribution of the sedimentary formations and the geological structure assumed based on existing information (Figure 3.3.3-4). A good correlation was found between the results obtained and the conclusion drawn by Yanagida[16)], because bioturbation features several centimetres in diameter remain in the diatomaceous mudstone in the main part of the Koetoi Formation and hard mudstone similar to that found in the Wakkanai Formation is observed in the lower section of the main part of the Koetoi Formation on the east side of the Omagari Fault. It was also found, for most of the area where surface geological investigations were conducted, that the main part of Koetoi Formation occurs on the west side of the Omagari Fault, while the Wakkanai Formation is distributed mainly on the east side of the Omagari Fault. In addition, some data that were obtained indicate a dip with a higher angle than that described in the existing literature although data of the angle and shape for Omagari Fault could not be obtained. New data and information on the geological properties were generally consistent with the existing geological information.

It was concluded from the results presented above that existing information was generally reliable, but some open aspects regarding stratigraphy and the distribution of geology were identified, including the fact that the lithofacies boundary between the Wakkanai Formation and the Koetoi Formation was not clear with some parts of each formation being misinterpreted as the other formation.

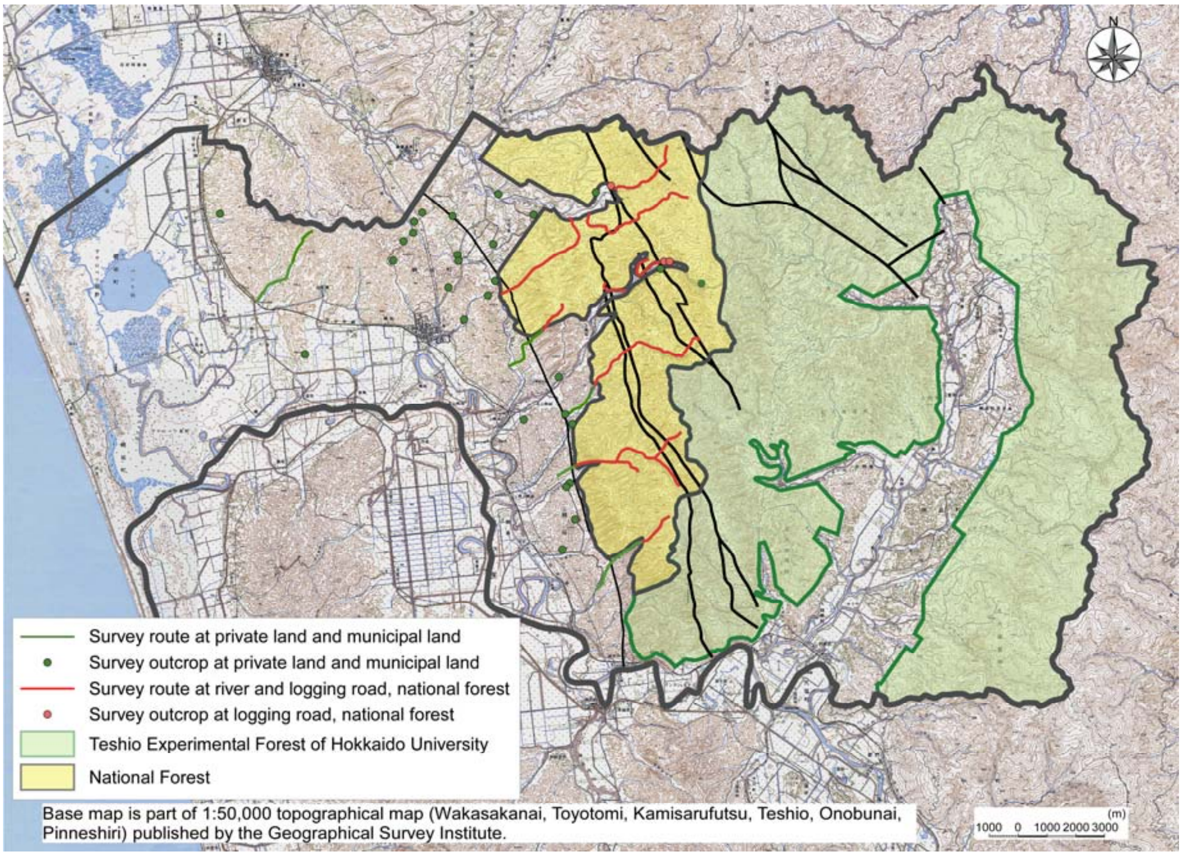

Figure 3.3.3-4 Surface geological investigations in Horonobe Town

3.3.4 Borehole investigations

The first borehole investigations in the area of interest were conducted with the main objective of checking whether the area meets the technical requirements, as well as obtaining direct data on the characteristics of the geological environment. A further objective was to establish borehole investigation techniques, including suitability of drill bits, composition of drilling fluids and casing programmes; this was because, despite recent technological advances, borehole drilling is often associated with problems due to unexpected geological conditions.

(1) Selection of the borehole investigation site

Based on the results of aerial and surface-based investigations and the situation with regard to land use, two areas (areas B1 and B2) that met the technical requirements and social conditions were selected from the potential URL areas and locations for borehole investigations were selected in these two areas.

Area A was eliminated from borehole investigations because a large-scale geological feature known as the Sarabetsu Anticline was identified and it is reported that about 10,000 m^3 d^{-1} or more of gas was released during the borehole drilling for oil and natural gas exploration in the past, leading to terminating of these investigations[10),18)]. This suggests that safe borehole investigations or construction of the URL would be less feasible here compared to other areas. Although it might have been possible to make the elimination when it was first found, based on existing information, that the sedimentary formation in the area contains gas, i.e. before conducting the aerial and surface-based investigations, elimination as a candidate URL area was postponed at this point because the possibility of dissolved gas being present in the groundwater was considered to be common to all the potential areas and no criteria had been set in this respect.

Area C was also eliminated because aerial and surface-based investigations could not be conducted because permission was refused from the land owners. Even if these investigations could have been carried out, construction of the URL would have been difficult owing to these restrictions on land use. However, areas A and C may still be investigated as candidate URL areas if areas B1 and B2 are found not to be suitable.

For the areas B1 and B2, locations where the rock formations of interest are located at a depth of around 350 m with a thickness of around 150 m were identified based on the aerial and surface-based investigations and several of these locations were selected as borehole investigation sites. The locations of the boreholes were on the west side of the Omagari Fault in area B1 and on the east side of the Omagari Fault in area B2. The reasons behind selecting the borehole investigation sites were to understand the geological properties, their heterogeneities and the influence of the Omagari Fault. When selecting the borehole investigation sites, it was important to consider data that would be useful when selecting a URL area and a URL site, as well as the need to check the technical reliability of geological conceptualisation based on existing information. The locations of boreholes HDB-1 and HDB-2 were finally selected for areas B1 and B2 respectively considering the land use and the ease of formalities (Figure 3.3.4-1; see also Appendix 4). Although the location of borehole HDB-2 is near the boundary between areas B1 and B2, comparison of data obtained in the two boreholes will provide information on the heterogeneity of the geological environment, since the sedimentary formations in areas B1 and B2 are continuous and the two boreholes are located at a distance from one other.

(2) Overview of the investigations

The borehole investigations were conducted with the main aim of confirming that the rock formations of interest are located at a depth of around 350 m with a thickness of 150 m, as well as obtaining data on rock mechanical properties for designing the URL, data required for developing hydrogeological models and analysing groundwater flow and confirming the presence of saline groundwater. The data will be used for identifying suitable techniques for evaluating the geological environment, reviewing geological environment models and improving the reliability of groundwater flow analyses by comparing them with existing information collected and compiled on the geological environment before starting the field investigations. Generally rock mechanical data should be obtained in the vicinity of the URL for designing the underground facility. However, since the Wakkanai Formation is rather homogeneous, it was considered possible that sufficient information could be obtained from the initial borehole investigations.

A drilling depth of 500 m would be sufficient from the viewpoint of obtaining data on rock mechanics and information to be used as input for construction of drifts at depths between 350 m and 500 m in the URL. However, for the groundwater flow analysis covering an area up to 5,000 m in depth, it will be necessary to build confidence in the results of the analysis based on existing information using data on the hydraulic regime (including hydraulic conductivity and pore pressure) from much deeper than 500 m. It was finally decided to drill the boreholes to a depth of 720 m with a view to obtaining the data on hydraulic properties required for analysing the impact associated with the construction activities[19),20)].

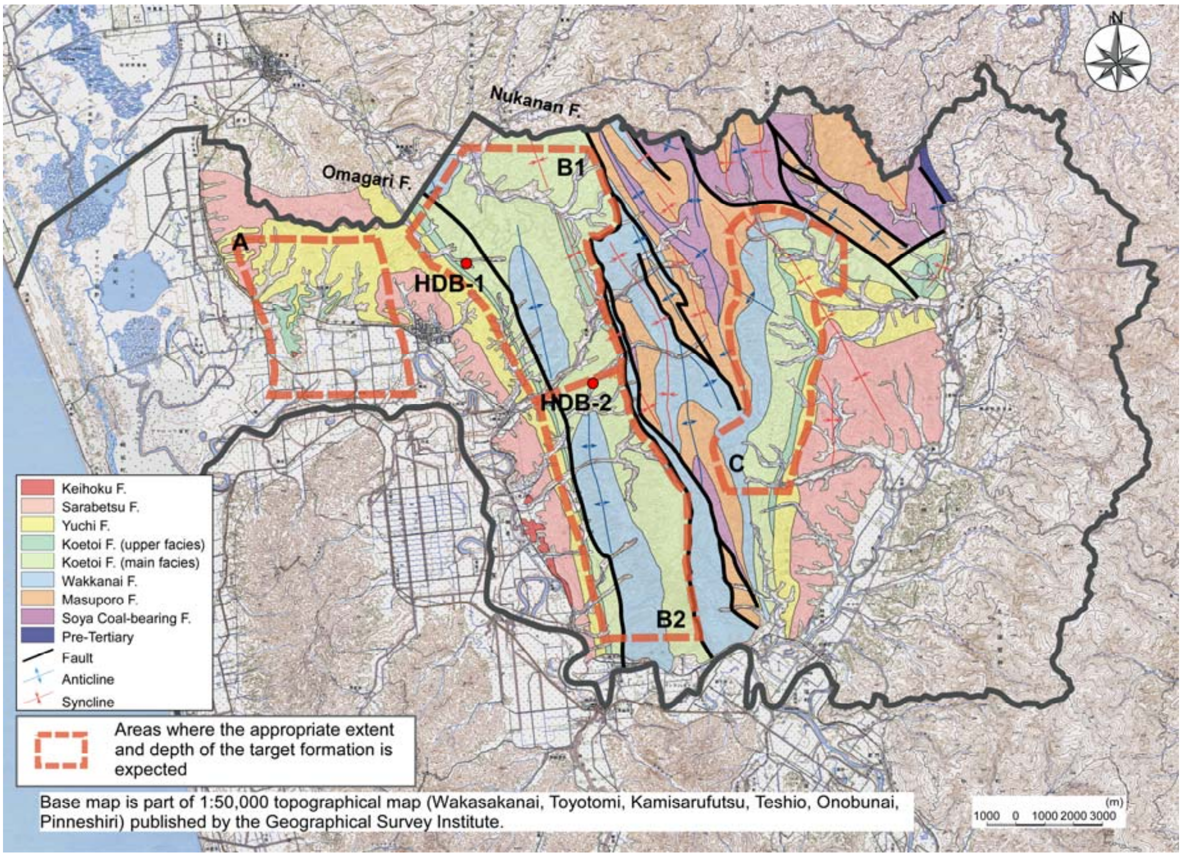

Figure 3.3.4-1 Borehole investigations at HDB-1 and HDB-2

(3) Results of the investigations

The discussions surrounding the selection of a URL area are summarised here. Details of the investigations will be presented in Chapter 4. Data obtained in boreholes HDB-1 and HDB-2 indicated that the target rock formations (the Wakkanai Formation and the main part of the Koetoi Formation) can be found from near surface to a depth of 720 m. The boundary between the Wakkanai Formation and the main part of the Koetoi Formation was observed at a depth of 321.0 m (now revised to 325.0 m) in borehole HDB-1 and at 56.7 m (now revised to 41.4 m) in borehole HDB-2. The section from the boundary to the bottom of the boreholes was made up of the Wakkanai Formation (see Appendix 5). Core samples were subjected to an unconfined compression test, which indicated a mechanical strength of 10–35 MPa at a depth of 500 m. Stress measurements in the boreholes indicated maximum principal stresses of 12.37 MPa for borehole HDB-1 (585.0 m depth) and 13.94 MPa for borehole HDB-2 (535.5 m depth). The ratio of maximum principal stress to minimum principal stress in the horizontal plane was less than 1.5 for both boreholes, suggesting that there is no significant anisotropy. These data support the assumption that the URL could be safely constructed and maintained in both areas[21)].

With regard to the hydraulic properties of the sedimentary formations, the hydraulic conductivities were in the order of 10^{-10} m s^{-1} in borehole HDB-1 (interval of 370.0–395.0 m depth) and 10^{-9} m s^{-1} in borehole HDB-2 (interval of 344.9–404.9 m depth). In general, sedimentary rocks are treated as porous media and compared to fractured media, the hydraulic conductivity is relatively homogenous. Since low hydraulic conductivities were measured in both boreholes HDB-1 and HDB-2, the hydraulic conductivity for the whole area was thus assumed to be low. Although contamination with the drilling fluid employed was not completely eliminated, the salinity of the groundwater sampled during hydraulic tests was found to be lower than that of current seawater by a factor of 2–3 (Figure 3.3.4-2). The same result was obtained from analysis of the porewater squeezed from the cores.

With regard to dissolved gases in the groundwater, gas blowout was observed during hydraulic packer tests in borehole HDB-2. The source of the gas was considered to be dissolved gas in the groundwater in the test interval, because the hydraulic pressure in the test interval decreased as a result of the gas blowout. No significant gas blowout was observed, by contrast, during the hydraulic tests in borehole HDB-1. Data from gas analyses of mud used as a drilling fluid and gases sampled during hydraulic tests and gas blowout from cores indicated that the gas is composed mainly of CH_4, although some contamination with air is observed (Figure 3.3.4-3).

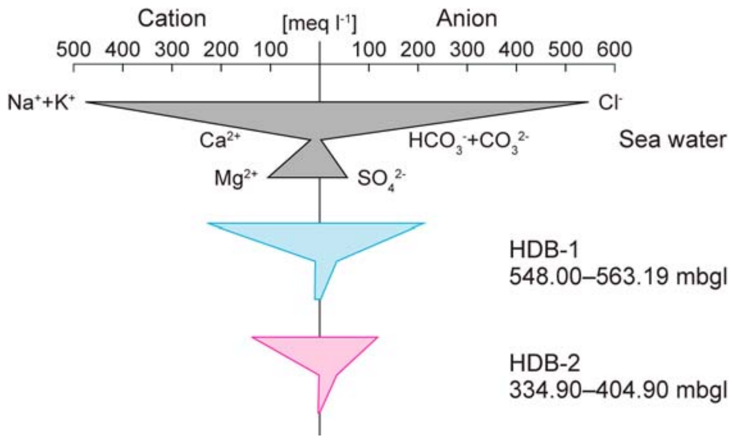

Figure 3.3.4-2 Hexadiagram of groundwater sampled from the Wakkanai Formation

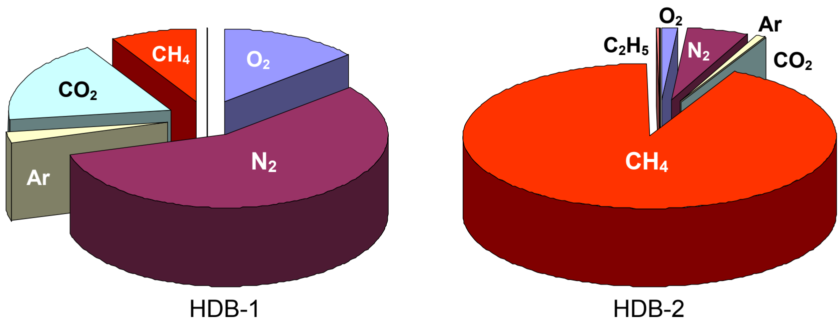

Figure 3.3.4-3 Composition of dissolved gas in groundwater at boreholes HDB-1 and HDB-2

3.3.5 Environmental assessment

As a baseline reference for selecting a candidate URL area (Figure 3.3.5-1), a regional environmental assessment was conducted for rare animal and plant species and water supplies (whether or not well water is used) in the potential URL areas (areas A, B1, B2 and C, except for the Teshio Experimental Forest of Hokkaido University).

Investigations of flora and fauna identified 36 species as being key species, including endangered species. The number of key species identified was more or less the same in areas A, B1 and B2. The habitat for these species was also clarified for each area[3]. Details of these investigations will be discussed in Section 6.2.

The water supply in Horonobe Town consists of groundwater for public, private and industrial use in coastal areas (in the Shimonuma, Hamasato and Azahoronobe districts and central Horonobe; see Appendix 2) and surface water for mountain areas (in the Hokushin, Kamihoronobe, Kaishin, Yukou, Toikanbetsu, Nakatoikan and Kamitoikan districts). Well water is not used in the Yukou, Toikanbetsu, Nakatoikan and Kamitoikan districts.

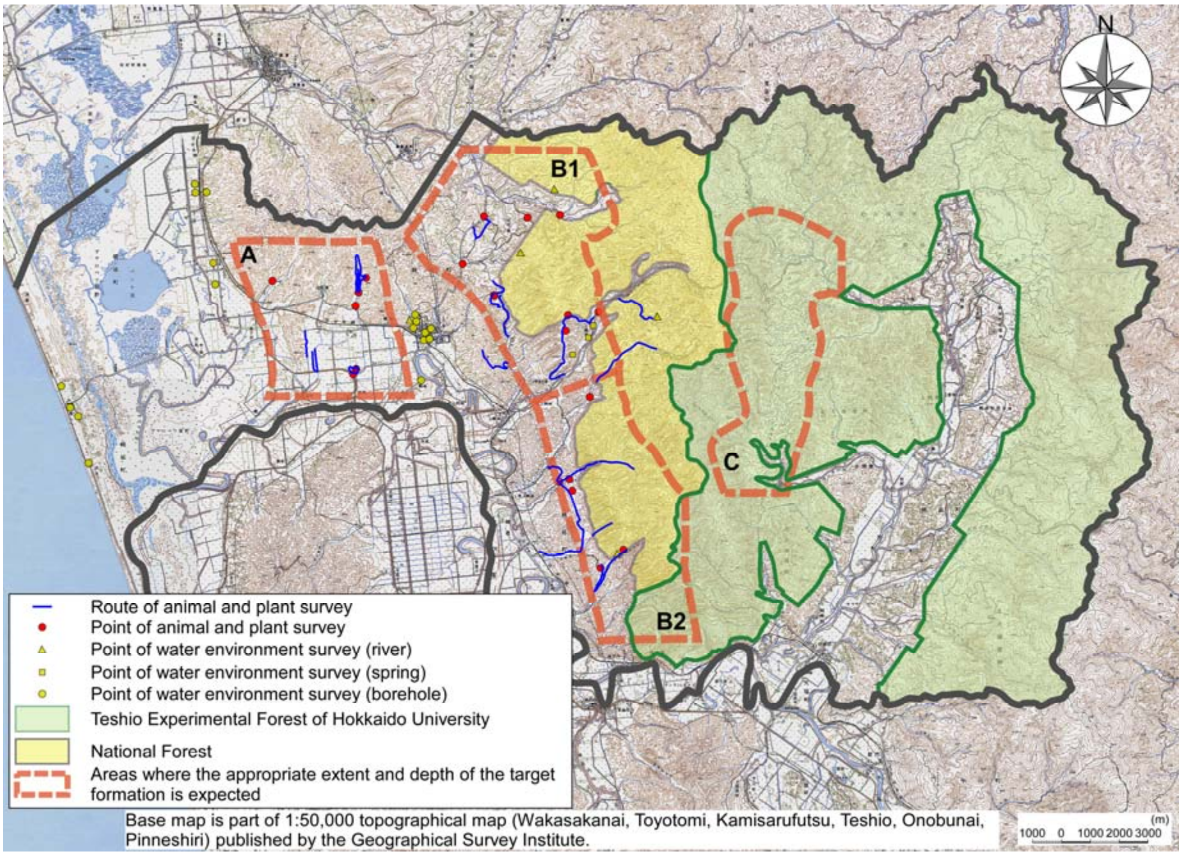

Figure 3.3.5-1 Environmental assessment in Horonobe Town

3.3.6 Evaluation of the investigation results and selection of the candidate URL area

Data collected by compiling existing information, aerial and ground geophysical surveys, surface geological investigations, deep borehole investigations and environmental assessment in areas B1 and B2 were evaluated in the light of technical requirements.

- Data obtained by aerial and ground geophysical surveys, surface geological investigations and borehole investigations indicated that there is a boundary between the Wakkanai Formation and the main part of the Koetoi Formation at a depth of 321.0 m (now revised to 325.0 m) in borehole HDB-1 and at 56.7 m (now revised to 41.4 m) in borehole HDB-2; the Neogene sedimentary formations are located at a depth of 350 m with a thickness of more than 150 m.
- The stability of the shaft and drift was analysed using the rock mechanical properties of the Neogene formations, based on data obtained in a range of laboratory tests using cores and borehole hydraulic fracturing tests (unconfined compressive strength of 15 MPa at a depth of around 500 m in borehole HDB-1 and tensile strength was set at 1/10 of the unconfined compressive strength). The results of the analysis indicated that the URL could be constructed and maintained safely using conventional tunnel support. Many fractures were observed in deeper sections of borehole HDB-2 and a discontinuum analysis was conducted to evaluate the scale and location of potential rock falls. The results indicated that these could be prevented by increasing the strength of the tunnel support. Temporary values for fracture properties were used in the discontinuum analysis and more accurate values will be used in the detailed design[22)].
- Variation of the initial stress condition in the Horonobe area will be confirmed. The directions of the drifts, strength of support measures and configuration of drift cross-sections will be finalised based on site-specific information after the URL site has been selected.
- The amount of gas blowout expected during construction of the URL was estimated based on data on hydraulic conductivity and gas volume obtained from borehole investigations, since it was assumed that deep subsurface gas would not be present as a gaseous phase and would be dissolved in groundwater. Safety during construction of the URL would be assured by using ventilation systems which could handle the estimated volume of gas blowout and using construction methods with explosion-proof specifications.
- The analysis of groundwater and porewater from boreholes HDB-1 and HDB-2 indicated that there is saline groundwater at deeper part of 300 m or more in both areas.

These results suggest that both areas B1 and B2 meet the technical requirements for a URL area and would be appropriate as candidate URL areas. However, the fact that there is less dissolved gas in the groundwater in area B1 indicates that this area would be more suitable for safe construction of the URL.

Social conditions were reviewed for areas B1 and B2; this included looking at land use planning and development of water supply and sewage systems, as well as roads capable of accommodating large vehicles. As a result, most of area B1 consists of moderately sloping terrain, except for the national forest in the east part of the Hokushin district. Major roads have been developed and sites for constructing the URL or boreholes drilling could be easily found. The north side of the major roads of Toikan – Horonobe line in area B2 is mountainous, with both national and private forests. Transport networks other than prefectural roads have not been developed in this area; this would mean selecting a URL site on farm land or private land or in forest along the prefectural roads and could hinder the progress of investigations.

Area B1 was ultimately selected as the candidate URL area, because it would be more advantageous in the URL construction and investigations as there is greater development of the required infrastructure.

3.4 Selection of the URL area from the candidate URL area

3.4.1 Requirements and preferences

The process of selecting a URL area started after area B1 had been selected as the candidate URL area. A range of surface-based investigations will be conducted in the URL area. Technical criteria for the URL area include occurrence of the sedimentary formations of interest at a depth of around 350 m with a thickness of about 150 m, safe construction and maintenance of the URL and the presence of saline groundwater. An additional criterion at this stage was that the URL construction should not have an adverse effect on the hydrology at the site, because area B1 is close to the Toyotomi Hot Springs in the north. Since the reliability of the regional groundwater flow analysis at this stage is not high, confidence in the analysis will be enhanced by iteratively improving the relevant dataset and the hydrogeological model during construction of the URL.

The Omagari Fault, a large-scale discontinuity in the centre of area B1, was not taken into account in the selection of the URL site, because the effect of such a feature on a geological disposal system is one of the topics for a later R&D programme.

3.4.2 Selection of the URL area

The results of a series of investigations indicated that the Neogene sedimentary formations (the Wakkanai and Koetoi Formations) are located with an N-S strike and saline groundwater is present on both sides of the Omagari Fault which runs through the centre of area B1. With regard to infrastructure, there is one prefectural road that connects central Horonobe with Wakkanai City and several local roads crossing the prefectural road in the northern part of the area. These conditions are considered favourable for securing material transport routes and constructing an access road to the URL site and borehole investigation sites. On the other hand, it would be difficult to secure land for investigations and for constructing the URL in the southern part of the area, where there is no road infrastructure and national forests extend over large areas (Figure 3.4.2-1)

Based on the above considerations, the northern part of area B1 (the Hokushin district) where infrastructure is well developed was selected as the URL area (Figure 1.2.2-1; see also Appendix 2). The Yuchi Formation is found in the south-western part of the URL area. This is not a target rock formation for constructing the URL but the influence of this overlying formation on the Wakkanai and Koetoi Formations will be investigated.

3.5 Selection of the URL site from the URL area

3.5.1 Requirements and preferences

When selecting the URL site from a URL area where technical requirements and preferences and social conditions were met, as described in Section 3.4, additional social conditions and the opinion of local government had to be taken into consideration and respected appropriately.

3.5.2 Borehole investigations

Borehole investigations were conducted in the URL area for the purpose of obtaining data for selecting the URL site, designing the URL and development of geological environment models. The locations of boreholes HDB-3 to HDB-5 were selected such that data would be obtained on the characteristics of the geological environment on both the west and east sides of the Omagari Fault and the continuity of the sedimentary formations along the strike would be determined, considering that the strike of the formations at the URL site is NNW-SSE, which is parallel to the Omagari Fault (see Appendices 2 and 4).

The results of the borehole investigations suggested that the Wakkanai and Koetoi Formations meet the technical requirements and preferences. They also indicated that the depth of the boundary between the Wakkanai Formation and the Koetoi Formation is shallower in boreholes HDB-4 and HDB-5 located on the east side of the Omagari Fault than in boreholes HDB-1 and HDB-3 located on the west side. Sections with many fractures and higher permeability were found in boreholes HDB-4 and HDB-5 on the east side of the Omagari Fault compared to boreholes HDB-1 and HDB-3 on the west side.

3.5.3 Evaluation of the investigation results and selection of the URL site

The URL site was selected on the west side of the Omagari Fault, given that fewer fractures were encountered and no features indicating higher permeability (e.g. loss of circulation during drilling) were identified. The site near boreholes HDB-1 and HDB-3 was selected, taking advantage of the fact that the data from borehole investigations obtained to date could be used in the design of the URL and the technical reliability of the investigation results could be checked using information obtained in subsequent investigations. Finally, the site shown in Figure 1.2.2-1 (see also Appendix 2) was selected within the URL area, considering the social and environmental conditions; existing transport routes are available, the topography is flat and regulatory procedures would be simple because of wilderness areas and privately owned land.

3.6 Summary

This chapter described the process of selecting a URL site from the whole area of Horonobe Town, including strategy, technical requirements and social and environmental conditions. This was a real case of selecting areas and a site for performing characterisation of the deep geological environment and represents the only case in the URL programme in Japan.

When pursuing a stepwise site selection process, defining the importance of technical requirements and social and environmental conditions at an early stage will facilitate the planning of the programme. The approach in which several areas (sites) are selected in each step and, finally, a comprehensive evaluation is carried out taking social conditions into account to identify a site, ensures transparency and objectivity and enhances public acceptance. In the case where a clear difference cannot be drawn based on technical requirements and preferences, an assessment based on social and environmental conditions will become important. The criteria for the selection of the URL site in the Horonobe URL project should be distinguished clearly from those for the actual disposal programme, but there may be many aspects of the social and environmental conditions that will be common to both.

References

1) Nuclear Safety Commission of Japan: "Environmental Requirements to be Considered at the Selection of the Preliminary Investigation Areas for High-Level Radioactive Waste Disposal", Advisory Board on High-Level Waste Repository Safety, 30th Sep. 2002 (2002). (in Japanese)
2) Nuclear Waste Management Organization of Japan: "Evaluating Site Suitability for a HLW Repository – Scientific Background and Practical Application of NUMO's Siting Factors", NUMO-TR-04-04 (2004).
3) S. Yamasaki, N. Nakatsuka, N. Ogata, N. Eki, T. Moriya, R. Takeuchi, T. Kunimaru and N. Shirato: "Horonobe Underground Research Project – The Result on URL Area Selection Performed along with Field Investigations of FY2001/2002", JNC TN1400 2002-017 (2002). (in Japanese with English abstract)
4) Power Reactor and Nuclear Fuel Development Corporation: "Site Investigation of Storage Technology Research Center – Deep Layer Boring", PNC TJ 1027 98-012 (1987). (in Japanese with English abstract)
5) T. Oka and Y. Igarashi: "Latest Cenozoic formations in the northern part of Teshio Plain, Hokkaido – Sedimentary facies and pollen stratigraphy", In: M. Kawamura, T. Oka and T. Kondo (Eds.) Commem. Vol. Prof. M. Kato, pp. 341-365 (1997). (in Japanese with English abstract)
6) Japan National Oil Corporation: "Report on the MITI Tenpoku Drilling" (1995). (in Japanese)
7) T. Oka: "Distribution and tectonic evolution of Late Cenozoic basins in Hokkaido", Monogr. Assoc. Geol. Collab. Jpn., No. 31, pp. 295-320 (1986). (in Japanese with English abstract)
8) M. Akiyama and K. Hoyanagi: "Neogene, Tenpoku Area", Regional geology of Japan part 1: Hokkaido, Kyoritsu Shuppan, pp. 105-106 (1990). (in Japanese)
9) T. Nakata and T. Imaizumi (Eds.): "Digital Active Fault Map of Japan", Univ. Tokyo Press (2002). (in Japanese)
10) E. Hirooka: "Petroleum geological study on Tenpoku district in Hokkaido, Japan", J. Jpn. Assoc. Petrol. Technol., 27, pp. 113-134 (1962). (in Japanese with English abstract)
11) T. Hirota, H. Sagayama, E. Yokoyama, T. Suga and H. Matsunami: "Hydrogeological Map of Hokkaido: No.1 WAKKANAI", Explanatory Notes, Geol. Surv. Hokkaido (1983). (in Japanese with English abstract)
12) R. Imamura, N. Wakamatsu and S. Odagawa: "Planning of Subsurface Hydrology Observation System in Horonobe Underground Research Project", JNC TJ1410 2001-001 (2001). (in Japanese with English abstract)
13) T. Kanekiyo: "Collection and Arrangement of the Geological Data in the Northern Part of Hokkaido", JNC TJ1440 99-005 (1999). (in Japanese with English abstract)
14) H. Imai, R. Yamashita, K. Amemiya and I. Shiozaki: "Study on Regional Groundwater Flow Analysis Method in Sedimentary Rock Mass", JNC TJ1410 2001-002 (2001). (in Japanese with English abstract)
15) M. Makino, Y. Okubo and T. Nakatsuka: "Magnetic Map of the Japanese Islands", Explanatory Notes, 1:2,000,000 map series No. 23, Geol. Surv. Jpn. (1992). (in Japanese with English abstract)
16) M. Yanagida: "Study on Geology of Northern Area in Hokkaido", JNC TJ1400 98-001 (1998). (in Japanese with English abstract)
17) Japan Nuclear Cycle Development Institute: "Annual Report of Research and Development on HLW Geological Disposal in 2001", JNC TN1400 2002-003 (2002). (in Japanese)
18) Hokkaido Mining Promotion Committee: "Petroleum and Natural Gas Resources in Hokkaido,

Exploration and Development (1977–1988)”, Resour. Energ. Div., Dept. Comm., Ind. Tourism Labour, Hokkaido Pref. Govt. (1990). (in Japanese)

19) T. Yamamoto, M. Shimo, Y. Fujiwara, H. Hattori, T. Tadokoro, H. Iwama, M. Nago and S. Kumamoto: “HDB-1 Borehole Investigations in Horonobe Underground Research Center”, JNC TJ1400 2002-010 (2002). (in Japanese with English abstract)

20) T. Yamamoto, M. Shimo, Y. Fujiwara, H. Hattori, T. Tadokoro, H. Iwama, M. Nago and S. Kumamoto: “HDB-2 Borehole Investigations in Horonobe Underground Research Center”, JNC TJ1400 2002-011 (2002). (in Japanese with English abstract)

21) S. Niunoya and H. Matsui: “The Investigation on Rock Mechanics in HDB-1 and HDB-2 Boreholes in Order to Select the URL Area”, JNC TN5400 2005-012 (2005). (in Japanese with English abstract)

22) S. Kubota, M. Noda, M. Toida and K. Iwasa: “Feasibility Study on Construction Horonobe URL”, JNC TJ1400 2002-003 (2003). (in Japanese with English abstract)

4. Characterisation of the geological environment from the surface

Important issues to be addressed during Phase I of the Horonobe URL project are enhancing understanding of the deep geological environment and establishing the technical basis for systematic techniques for characterising the geological environment throughout stepwise surface-based investigations. With this in mind, investigations were conducted for two areas at different scales, viz. 'the whole Horonobe Town area' and 'in and around the URL area', which involved surveys of existing information, aerial reconnaissance surveys, ground exploration and borehole investigations. The key properties of the geological environment and processes involved, which would be of great relevance for geological disposal, were generally understood. Systematic characterisation techniques from the surface were then developed through integration and interpretation of the investigation results, associated modelling of the geological environment and, importantly, enhancement of confidence in the results and models.

Sections 4.1–4.5 describe the results of the investigations of geology and geological structures, hydrogeology, hydrochemistry, rock mechanics and long-term stability of the geological environment respectively. Based on experience accumulated and the investigation results, Section 4.6 provides the basic methodology for systematically characterising the geological environment and discusses assessments of key issues relating to the safety of the geological disposal system. Section 4.7 focusses on a range of techniques applied to characterise the geological environment. Finally, Section 4.8 gives a summary of the achievements of stepwise characterisation of the geological environment from the surface.

4.1 Geological investigations

4.1.1 Aims

The investigations of geology and geological structures were carried out to acquire the information necessary for hydrogeological, hydrochemical and rock mechanical characterisation and to establish relevant investigation techniques. The areas covered included topography, geological heterogeneity, thickness of the overburden (unconsolidated deposits) and features that are important such as solute transport pathways.

4.1.2 Surface-based investigations covering the whole Horonobe Town area

(1) Investigation aims and methods

The main aims of the investigations during this stage were to clarify the topography, geological heterogeneity, thickness of the overburden and features important for solute transport for the whole area of Horonobe Town. The information obtained represents an important basis for understanding the area of interest and will provide input for hydrogeological and hydrochemical modelling. The investigations conducted in this stage include:

- survey of existing information;
- aerial and ground reconnaissance surveys;
- borehole investigations.

Information on topography, stratigraphy and geological age, unconsolidated surface (terrace) sediments and discontinuities such as faults was compiled from open literature, including the results of oil and natural gas exploration in the Tenpoku region[1]. Reconnaissance surveys[2], airborne geophysical surveys[3),4] and MT electromagnetic surveys[4),5] were conducted in order to acquire the information needed to clarify the geological heterogeneity of rock formations and features potentially important as solute transport pathways.

For the MT electromagnetic survey, all traverse lines were aligned at right angles to the strike of fault and fold structures to provide a better understanding of these structures. During deep borehole investigations (boreholes HDB-1 and HDB-2), specifically core logging and mineralogical investigations were carried out with the aim of understanding the geological heterogeneity of the rocks.

(2) Investigation results and interpretation

1) Topography

The Soya Hill, located in the northern region of Hokkaido, is divided into west, central and east parts by the Omagari and Horonobe Faults, the two major structural features that run north to south[6),7)]. The URL area selected for this investigation phase is located near the boundary between the west and central parts (Figure 4.1.2-1). The west part is dominated by the Teshio Plain consisting of the Sarobetsu Lowland and the Ubushi Lowland, with hills at 80–190 m elevation, stretching in an N-S direction. The central part is located between the Omagari Fault and the Horonobe Fault and has hilly terrain with altitudes of 100–300 m elevation[8),9)]. The E-W extent gradually narrows towards the south.

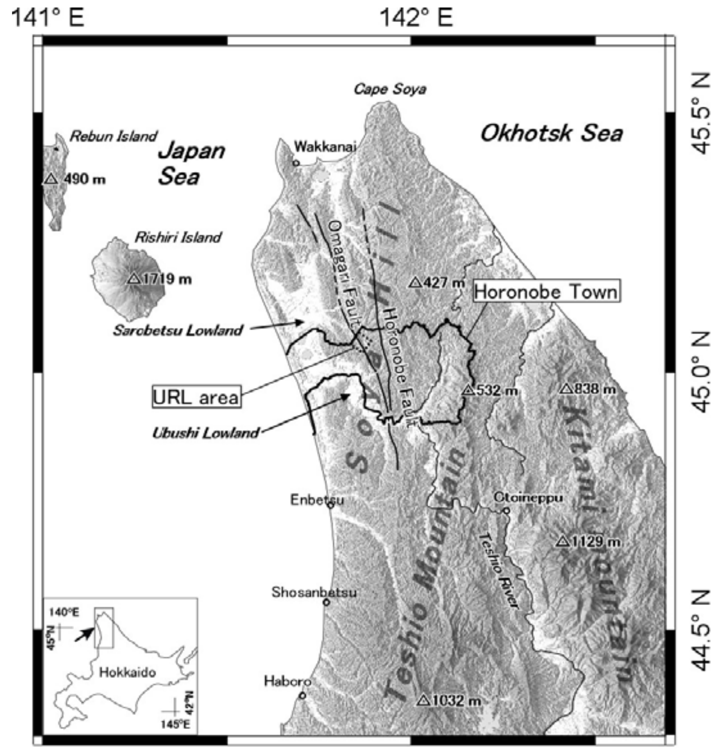

Figure 4.1.2-1 Outline map in and around Horonobe Town

Modified from Niizato and Yasue[9)]

2) Geological heterogeneity

Existing literature indicates that Horonobe Town is located at the eastern edge of the Tenpoku sedimentary drainage basin, where the Palaeogene Haboro and Magaribuchi Formations, the Soya Coal-bearing, Onishibetsu and Masuporo Formations (Early–Middle Miocene), the Wakkanai and Koetoi Formations (Late–Middle Miocene to Pliocene), the Yuchi and Sarabetsu Formations (Pliocene to Early Pleistocene), terrace sediments later than the Middle Pleistocene and Holocene sediments are distributed on Cretaceous bedrock[10)]. Of these formations, the Haboro and Magaribuchi Formations were not identified from the ground surface but were observed in deep borehole investigations[11]. The Wakkanai, Koetoi, Yuchi and Sarabetsu Formations consist of a series of sediments made up of abyssal → shallow marine → semi-terrestrial to terrestrial deposits that unconformably overlie the Masuporo Formation[10],[12],[13]. The Wakkanai and Koetoi Formations consist of siliceous rocks, while the Yuchi and Sarabetsu Formations consist of coarse-grained clastic material. The stratigraphy is based primarily on the classification of lithofacies. It should be pointed out that the boundaries of the formations do not necessarily coincide with the boundaries of geological eras[12]; there are heteropic facies between the Koetoi Formation and the Yuchi Formation and between the Yuchi Formation and Sarabetsu Formation[10],[13]. In the following paragraphs, a general description for the formations distributed in and around the URL area is given; the Masuporo, Yuchi and Sarabetsu Formations are discussed first, followed by the Wakkanai and Koetoi Formations, the latter being the main formations to be characterised.

The Masuporo Formation consists of alternating layers of conglomerates, sandstones and mudstones, often intercalated with slumping beds. The thickness of the formation varies between around 900 m and 1,000 m.

There are diverging opinions on the definition of the Wakkanai and Koetoi Formations. Focussing on lithology, Nagao[6] and Mitani et al.[14] classified the formation consisting primarily of so-called “hard shale” (siliceous shale or siliceous mudstone – both are mudstones consisting of silica minerals with low crystallinity, i.e. opal CT) as the Wakkanai Formation and the formation above this, consisting primarily of diatomaceous mudstones (mudstones consisting of non-crystallised amorphous silica minerals, i.e. opal A), as the Koetoi Formation. On the other hand, Fukusawa[13] focussed on the sedimentary structure and reclassified the formation consisting of siliceous or diatomaceous shale with clear bedding as the Wakkanai Formation and the formation above this, consisting of siliceous mudstones or diatomaceous mudstones with no clear bedding, as the Koetoi Formation. The latter also demonstrated by lithological examination that the diatomaceous shale had been hardened to form siliceous shale in the Wakkanai Formation and the diatomaceous mudstone to siliceous mudstone in the Koetoi Formation through progressive burial diagenesis of siliceous minerals. Although there are differing views on the definition of the Wakkanai and Koetoi Formations, the definition of Nagao[6] and Mitani et al.[14] was adopted for the Horonobe URL project, because only geological maps based on the definition of Nagao and Mitani et al. are widely available. These studies were a basis for regional groundwater flow analysis (e.g. hydrogeological model shown in Figure 4.2.2-2) that was needed at the initial stage of the investigation (see Subsection 4.2.2). In short, the Wakkanai Formation consists primarily of siliceous mudstones with no clear bedding or siliceous shale with clear bedding; the upper part of the formation is a transition zone to diatomaceous mudstones. The thickness of the formation varies between around 600 m and 1,000 m and the lower boundary age is estimated to be 13 Ma based on the radiometric age of volcaniclastic rocks[13] formed at the base of the siliceous shale. The Koetoi Formation consists primarily of diatomaceous mudstone that appears massive on first inspection and gradually changes in an upward direction to sandy mudstone. The thickness of the formation varies between around 400 m and 700 m.

The Yuchi Formation consists of soft fine-grained sandstone. The thickness of the formation varies between around 400 m and 800 m. It should be noted that what JNC previously defined as the upper part of the Koetoi Formation (see Subsection 3.2.2) is treated as part of Yuchi Formation here

The Sarabetsu Formation consists of alternating layers of conglomerate, sandstone and siltstone, intercalated with a lignite seam. The maximum thickness of the formation is about 700 m and the age is presumed from shell and pollen fossils to be about 1.3–0.7 Ma[10].

The results of the reconnaissance surveys and the borehole investigations showed that the distribution of each formation is generally consistent with the information in the literature[1),2)]. Data obtained from the airborne geophysical surveys also support the information in the literature[3),4)]. For example, the apparent resistivity structure obtained from airborne electromagnetic surveys generally corresponded well with the distribution of the formations; resistivity was high where the Yuchi and Sarabetsu Formations, with coarse-grained rocks such as sandstone and conglomerate, are found, while it is low in the area where the Wakkanai and Koetoi Formations, with fine-grained rocks such as mudstones and shale, are distributed. For the airborne electromagnetic surveys, the area with a high electromagnetic anomaly matched closely with the distribution of the Sarabetsu Formation, which is assumed to contain a serpentinite gravel with high magnetic susceptibility. Although influenced by topography, the γ-ray intensity obtained from the radioactivity survey also corresponded well with the distribution of the formations; it was high in the areas where the Sarabetsu and Yuchi Formations occur and low in the area where the Wakkanai and Koetoi Formations are found. Also, the results of the MT electromagnetic surveys were similar to those from the airborne electromagnetic surveys[3),4)].

3) Thickness of the overburden (unconsolidated deposits)

Existing literature indicates that terrace sediments are widely distributed near the surface in the form of unconsolidated deposits with a maximum thickness of several metres near the URL area, about 25 m in the east part of Horonobe Town and a maximum of about 15 m in the Sarobetsu and Ubushi Lowlands in the west part of Horonobe Town[1)]. They also indicate that the Pleistocene Keihoku Formation, with lithofacies similar to the terrace sediments, is distributed with a maximum thickness of about 50 m in the west part of Horonobe Town[1)].

4) Features potentially important as solute transport pathways

In the central part of Horonobe Town, the features known as the Horonobe Fault (N1–N5 faults) and the Omagari Fault, which are large enough to be shown on the geological map, run parallel in an NNW-SSE direction. These faults may be important as solute transport pathways. Information on these features based on the available literature is discussed below.

The Horonobe Fault consists of several individual faults (N1–N5 faults) with a strike of NNW-SSE and right-echeloning with a step width of about 1 km. Although fault traces can be identified as a lineament in the topography, no change in the topography in the Late Pleistocene is observed.

The Omagari Fault extends more than 25 km[6)] in length and connects to the Tono Fault in the south[15),16)]. The location of the fault at the surface is assumed to be primarily at the boundary between the Wakkanai Formation in the east and the Koetoi Formation in the west[14)]. On the east side of the fault, a fold structure with an axis in the direction N20–15°W is aligned en echelon[15),17)]. The fault was interpreted as being a normal fault tilted to the west since the fault plane inclines westward at the ground surface and the east side of the fault uplifts[6),18)]. However, on the basis of a later geophysical survey, the fault was interpreted as being a reverse fault with uplift on the east side[11),14),19),20)]. Oka[21)] also interprets this fault as a reverse fault. Fukusawa[16)] reports that, from the distribution of the thickness of the Wakkanai Formation, there was a 30 km lateral movement to the left along the fault after the sedimentation of the Wakkanai Formation. Regarding recent activity history, a report by the Research Group for Active Faults of Japan[22)] suggests tilting movements in the area where the fault crosses the Teshio River, while Ikeda et al.[23)] identify no topography showing active faults or flexures in areas other than the above.

Despite the reconnaissance surveys, airborne geophysical surveys and the MT electromagnetic surveys, no new information was obtained on the location and formation of the Horonobe and Omagari Faults.

At this stage of the investigations, no particular examination of fractures was undertaken because these were not considered important as solute transport pathways. However, existing literature indicates that there are a number of fractures in the Wakkanai and Koetoi Formations in and around the URL area. According to Mitani et al.[14)], these can be classified into three types depending on their nature: an E-W system (shear fractures), an N-S system (tensile fractures) and an NE-SW/NW-SE system (combination of shear and tensile). These systems are discussed in the context of the axes and limbs of the anticline, with the E-W type being distributed in the anticlinal axis and limb, the N-S type in the anticlinal axis and the NE-SW/NW-SE type in the anticlinal axis and limb. Other than the above anticlinal structures, fractures parallel to the bedding plane with fault rock were also observed.

4.1.3 Surface-based investigations in and around the URL area

(1) Investigation aims and methods

The main aim of the investigations at this stage was to acquire more detailed information on the geological heterogeneity of the rock formations, the thickness of the overburden (unconsolidated deposits) and features that are important as solute transport pathways in the vicinity of the URL area, building on the geological information acquired in the previous stage. Methods of surface-based investigations and borehole investigations, conducted in this stage, are described below.

1) Surface-based investigations

The investigations carried out include:

- reconnaissance surveys to clarify geological heterogeneity[24)–27)];
- topographical surveys to examine terrace facies and reconnaissance surveys to determine the thickness of the overburden[28)];
- topographical surveys (lineament investigations)[8),29),30)], reconnaissance surveys[31),32)], AMT electromagnetic surveys[31),33)], ground-penetrating radar surveys[34)], reflection seismic surveys[9),31),35)], re-analysis of data from previous reflection seismic surveys[36)] and gravity surveys[37),38)] to clarify structures potentially important as solute transport pathways.

Of these investigations, the reconnaissance surveys included outcrop sketches of the Omagari Fault[31)] and a sketch of the fractures at the stripped horizontal outcrop[32)]. The latter was based on the findings of the hydrological analyses in this stage, indicating that fractures in the rocks have a significant influence on groundwater flow[39)]. For the AMT electromagnetic and seismic reflection surveys, all traverse lines were aligned at right angles to the strike of the Omagari Fault to obtain a clearer understanding of the structure. In order to check the reliability of the measurements with the AMT electromagnetic and reflection seismic surveys in the previous stage, a high density electrical survey[40)] and a high density reflection seismic survey[38)] were conducted with the traverse lines aligned in the same way as in the original surveys. The applicability of these surveys is described in Subsection 4.7.2.

2) Borehole investigations

Deep borehole investigations (boreholes HDB-3 to HDB-11) were conducted to clarify the geological heterogeneity of the rock formations and shallow borehole investigations[25),41)] were used to determine the thickness of the overburden (unconsolidated deposits). The deep borehole investigations, as well as gas investigations[42),43)] in the shallow boreholes, were also aimed at clarifying features that could be important as solute transport pathways. The gas investigations involved measurement of the concentrations of CH_4 and CO_2 immediately above the groundwater surface in the boreholes (maximum depth of 30 m). The boreholes for the measurements were aligned so as to cross the strikes of the faults at right angles to better determine the influence of the Omagari Fault.

(2) Investigation results and interpretation

1) Geological heterogeneity of rock formations

The investigation results for geological distribution in this stage are generally consistent with those from the previous stage. By taking all the results up to this point, a geological map and geological profile were obtained as shown in Figures 4.1.3-1 and 4.1.3-2 respectively.

Various findings were obtained on lithology and physical properties and geological age of each formation by accumulating substantial amounts of data from the investigations conducted up to this stage. The detailed findings are discussed in the following.

Based on microscopic and electron microscope examinations, elemental mapping and powder X-ray diffraction analysis, typical minerals constituting the Wakkanai and Koetoi Formations were identified to be silica minerals (opal CT/opal A), small amounts of quartz, feldspar, clay minerals (kaolinite, smectite, illite and chlorite), pyrite and carbonate minerals (siderite, magnesite). The Wakkanai Formation consists primarily of opal CT, while the Koetoi Formation does not contain opal CT[44)]. Pyrite and carbonate minerals were found only in the formations deeper than about 10 m and deeper than several tens of metres respectively. In the shallow subsurface, they were almost completely dissolved due to oxidation and dissolution[45)]. The depth profile of silica mineral content is considered to be constant in both formations[44)], since there were no substantial changes in SiO_2 or Al_2O_3 in the whole rock chemical composition.

With regard to the chemical composition of the rocks, eluviation of elements such as Na was observed in rocks in the shallow subsurface that were in contact with meteoric water permeating through the shallow formations from the ground surface[44)].

The following findings have been made concerning the physical properties of the various formations[25),26)].

- Masuporo Formation: specific density of the rock with natural moisture content approximately 18 kN m^{-3}, porosity approximately 45% and the rigidity (Ld value) approximately 250–400.
- Wakkanai Formation: specific density of the rock with natural moisture content approximately 17 kN m^{-3}, porosity approximately 40% and rigidity (Ld value) above 400.
- Koetoi Formation: specific density of the rock with natural moisture content approximately 15 kN m^{-3}, porosity approximately 58% and rigidity (Ld value) approximately 300–400.
- Yuchi Formation: specific density of the rock with natural moisture content approximately 18 kN m^{-3}, porosity approximately 45% and rigidity (Ld value) approximately 250–350.
- Sarabetsu Formation: rigidity (Ld value) approximately 200–450.

The porosity was measured according to Japanese Industrial Standards (JIS) A1109 (specific density and water absorption test method for fine aggregate) and the rigidity was measured using the Equotip portable hardness tester manufactured by Proceq SA of Switzerland.

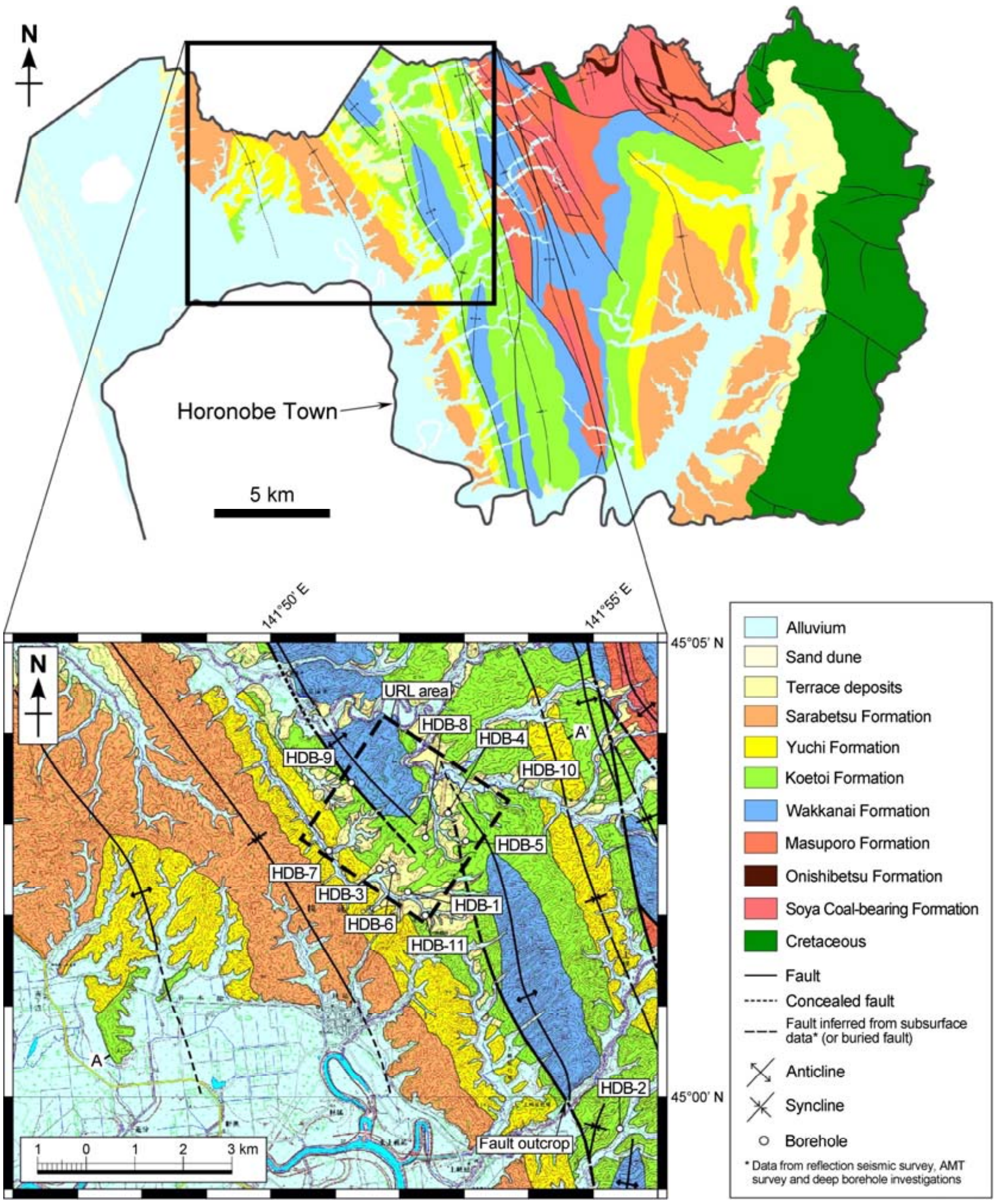

Figure 4.1.3-1 Geological map in and around the URL area

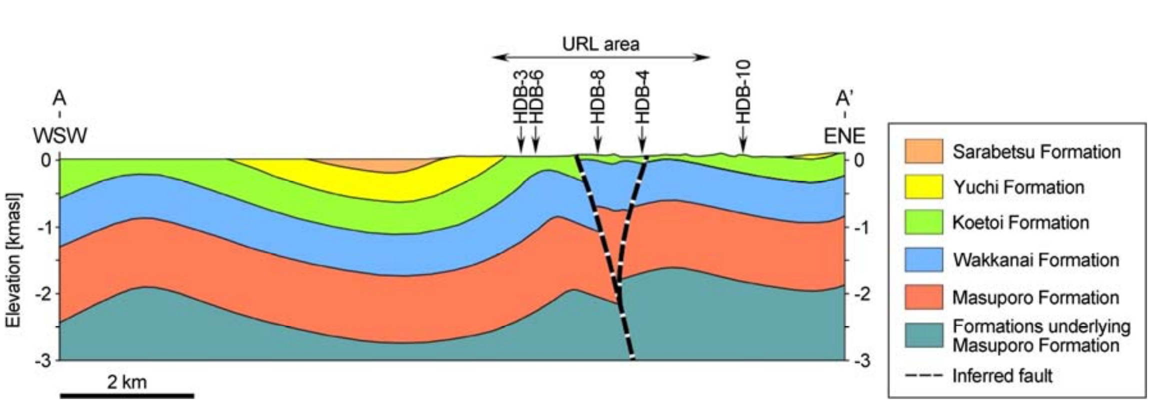

Figure 4.1.3-2 Geological cross-section along the A-A′ line shown in Figure 4.1.3-1

Based on Niizato and Yasue[9)] and Ishii et al.[31)]

Regarding the ages of the formations, intercalation of tuff was observed near the boundary between the Wakkanai Formation and the Koetoi Formation in borehole HDB-2 close to the anticlinal axis and in borehole HDB-10 far from the anticlinal axis. The fission track (FT) dating of the tuff layer was 3.9 ± 0.3 Ma in borehole HDB-2 and 2.9 ± 0.1 Ma in borehole HDB-10[46]. This means that the age at the boundary of the two formations near the URL area may differ depending on the location relative to the anticlinal axis (the formation interface does not form a synchronous surface). The age was estimated to be in the range of approximately 2.9–3.9 Ma. To determine the age of the boundary between the Koetoi and Yuchi Formations, diatom analysis and FT dating measurements of the tuff layer were carried out in the upper Koetoi Formation at a location about 5 km west of the URL area. The results verified the existence of the *Neodenticula Koizumii* Zone (2.6/2.7–2.0 Ma), the production of *N. Seminae* indicating an age later than approximately 2.4 Ma and a FT age of 2.3 ± 0.1 Ma[27]. The age of each formation in the URL area estimated taking all the above findings into consideration is summarised in Figure 4.1.3-3.

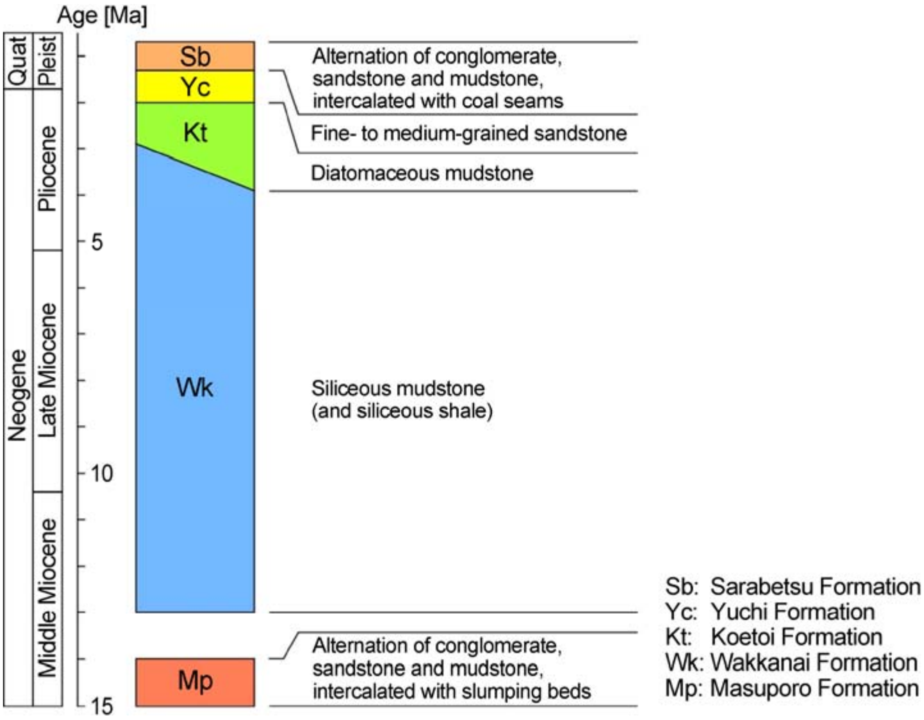

Figure 4.1.3-3 Schematic columnar section in and around the URL area

2) Thickness of the overburden (unconsolidated deposits)

The topographical surveys (terrace surface interpretation) and reconnaissance surveys in the URL area indicated that the terrace surfaces were distributed along small valleys and dissected terrace surfaces at a location higher than the terrace surfaces (at about 70–80 m elevation)[47] as shown in Figure 4.1.3-4. The terrace sediments were considered to be low-lying sediments that formed a buried valley owing to periglacial processes such as solifluction (soil creep) in the last glacial period, based on the fact that the terrace surface consisted primarily of breccia gravel mudstone, the ^{14}C dating of plant remains in the peat layer above the terrace indicated about 14,000 BP and the initial motion analysis of refracted waves in the reflection seismic surveys[35] indicates a deep buried valley structure in the middle of the terrace surface[28]. The low-lying terrace sediments were found to be about 20 m thick at the thickest part, i.e. the middle of the terrace, based on results from the shallow borehole and deep borehole investigations[28]. The dissected terrace surface consists of horizontal alternating layers of mud, silt and sand, which contain diatoms that lived in river and/or bay/shore areas. The terrace was thus considered to be a high-lying terrace formed near shores strongly influenced by rivers[28)]. The thickness of the high-lying terrace sediments is estimated to be several metres from the results of the reconnaissance surveys. Based on the above findings, it was considered that terrace sediments cover the base rock with a thickness of over 20 m in and around the area around the URL.

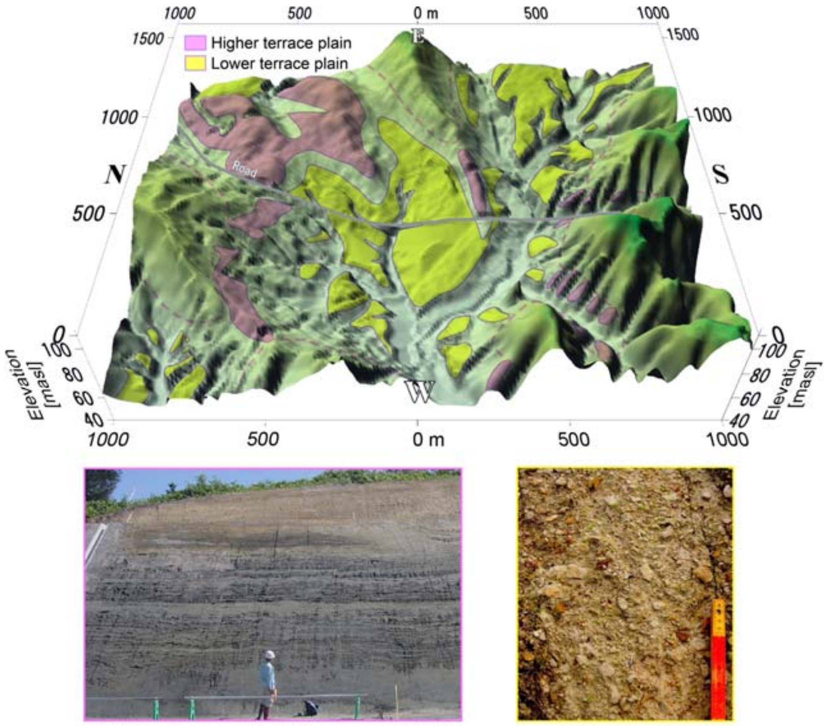

Higher terrace deposits composed of mudstone, siltstone and sandstone

Lower terrace deposits composed of rubble

Figure 4.1.3-4 Terrace deposits in the URL area

3) Features important as solute transport pathways

Here findings on the Omagari Fault are discussed, followed by those on minor faults (outcrop and sample-sized faults) and finally on joints.

Reconnaissance surveys were conducted in the Hokushin district where the URL area is located to clarify the location and the nature of the Omagari Fault. Most of the Hokushin district is covered by terrace sediments and it was difficult to identify outcrops of the bedrock. The Omagari Fault was observed in outcrop 5 km south of the URL area. At this location, a fault plane about 10–20 cm wide containing fault breccia was observed, forming the boundary between the Wakkanai Formation and the Koetoi Formation, as well as a cluster of minor faults containing fault breccia about 1–10 cm wide or fault gouges 0.5–3.0 cm wide, which were dominant in the range of about 120 m from the above fault plane. This indicates that the Omagari Fault consists of a 10–20 cm wide fault nucleus and a damaged zone about 120 m wide[31)] (Figure 4.1.3-5). From the topographical surveys (lineament surveys) performed near the fault outcrop, small lineaments were traced on the extension of the strike direction of the fault (NNW-SSE direction) that would indicate the existence of the fault[8)]. Some information on the location of the fault had already been obtained from the geophysical surveys. From a re-examination of existing reflection seismic data, the reflector that would correspond to the limbs of the anticline on the west and east side of the Omagari Fault in the deep underground of the outcrop could be observed[36]. In addition, a structure concordant with the strike direction of the fault that could be related to the fault was observed by the ground-penetrating radar surveys near the fault outcrop[34].

Reflection seismic surveys were conducted near the URL area, but most of the reflected events in the profiles were not clear enough to predict the location and geometry of the Omagari Fault (Figure 4.7.5-7). However, from the results of the AMT electromagnetic surveys, the 3D distribution of the Omagari Fault with high confidence was predicted as shown in Figure 4.1.3-6[31]. This prediction involved interpreting the results of the above fault outcrop surveys, the borehole investigations up to borehole HDB-8 (core logging, borehole wall observation, resistivity logging and chemical analysis of waters) and the reflection seismic surveys. The findings used in the interpretation include:

- According to the observations at the fault outcrop, the Omagari Fault may form a fault zone approximately 120 m wide that consists primarily of a damaged zone. This sort of structure would tend to be a permeable zone.
- While the location of the fault could not be predicted by the reflection seismic surveys conducted in the previous stage, the depth information on formation boundaries from boreholes HDB-6 and HDB-8 drilled in this investigation stage allowed the location to be predicted.
- The match between the position of the Omagari Fault predicted from the seismic reflection surveys and that of the high resistivity zone from the AMT electromagnetic surveys was good; the shape of the high resistivity zone presents a flower structure.
- The relationship between the resistivity of the formation and the salinity of the formation water would suggest that the high resistivity zone could be an area where meteoric fresh water infiltrates into the deep subsurface.
- There is a section dominated by minor faults in the rocks deeper than 380 m in borehole HDB-4. This section corresponds to the high resistivity zone.
- Based on the results presented above, the high resistivity zone is considered to correspond to the zone where meteoric fresh water infiltrates preferentially along the Omagari Fault. Based on the continuity of the high resistivity zone, the fault distribution is suggested to be as shown in Figure 4.1.3-6.
- Based on the striation direction in the fault plane of the Omagari Fault, the analysis of minor faults and information from the existing literature, the displacement sense of the Omagari Fault consists of both a vertical component and a left-lateral component of uplift on the east side. The fault distribution shown in Figure 4.1.3-6 can be interpreted as part of the flower structure formed by faults with such a displacement sense.

The distribution of the Omagari Fault as predicted above was consistent with the position where changes in the gravity anomaly that may be an influence of the fault were observed in the gravity survey[43].

The results for gas measurements in the shallow boreholes indicated that the concentration of CO_2 was less than a few hundred ppm in the area away from the predicted location of the fault, while it was more than a few thousand ppm near the predicted location[43]. The reason for this is considered to be that CH_4 produced deep subsurface moves up to the surface along the Omagari Fault and is oxidised to produce a high concentration of CO_2 in the oxidising environment in the proximity of the ground surface. This suggests that the Omagari Fault may be important as a solute transport pathway and needs to be examined in detail using the results of isotope measurements.

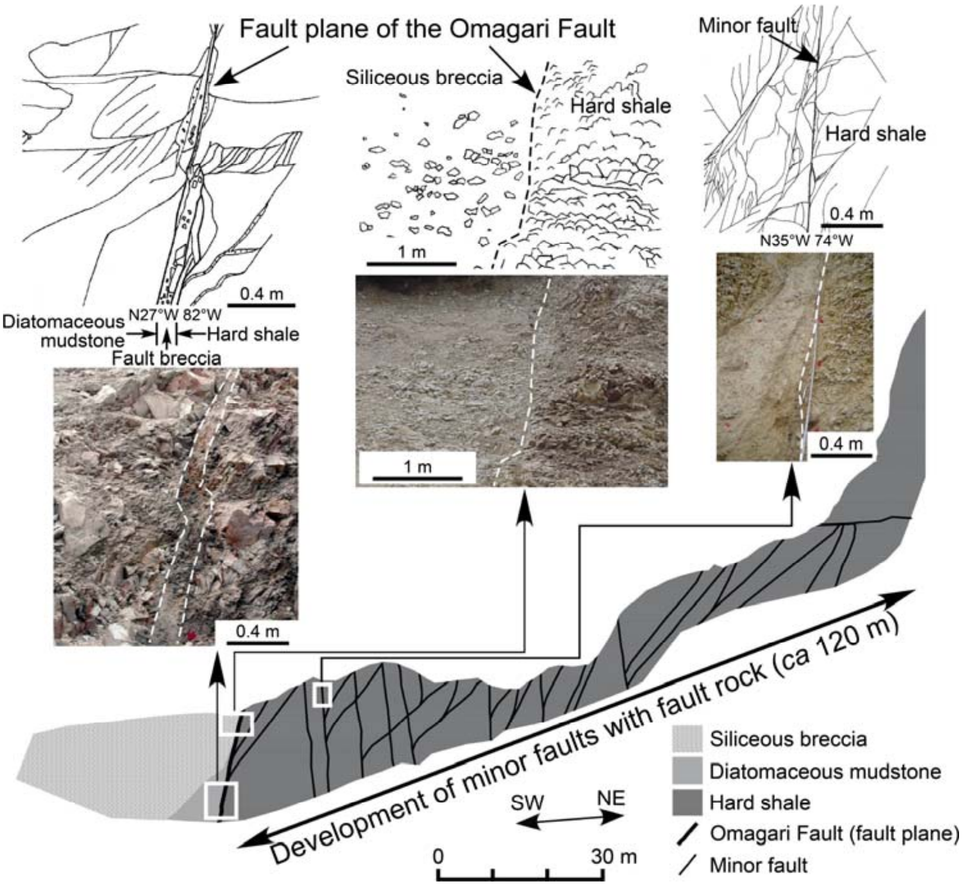

Figure 4.1.3-5 Outcrop photos and sketches of the Omagari Fault

Based on Ishii et al.[31)]

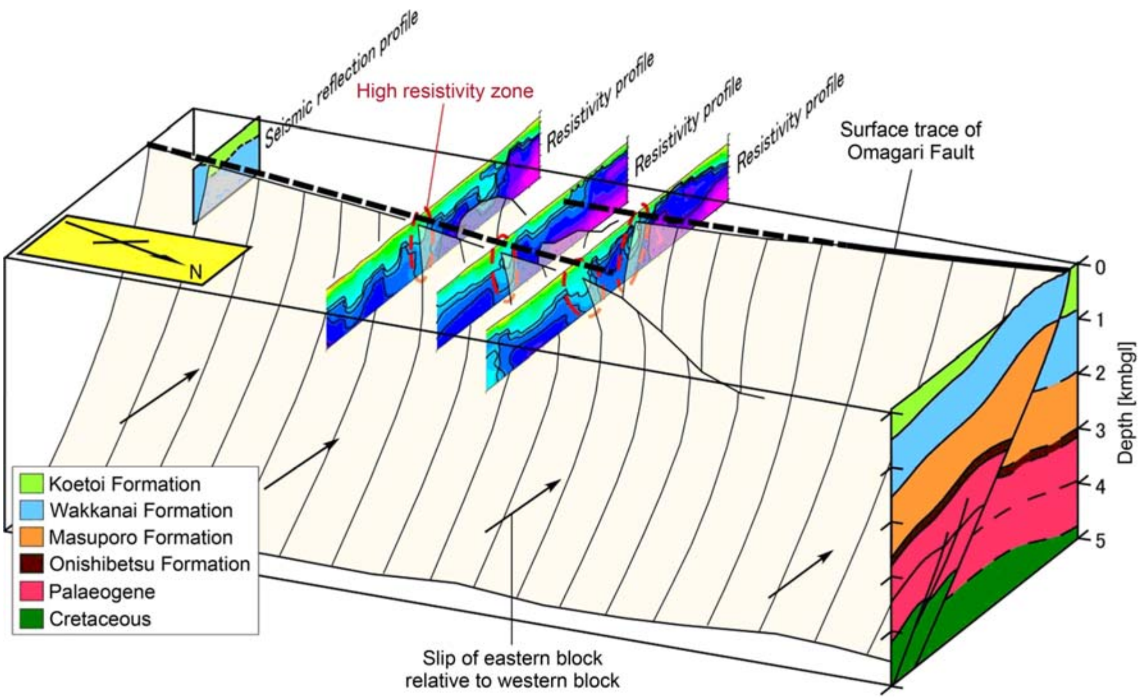

Figure 4.1.3-6 Schematic diagram of the Omagari Fault in and around the URL area

Based on Ishii et al.[31)]

In the boreholes HDB-4 and HDB-5, there were numerous fractures and circulation loss sections during drilling, suggesting that these fractures may be important as solute transport pathways. More detailed investigations will therefore be required in the latter half of this stage.

Examining the results of the deep borehole investigations (core logging, borehole wall image analysis), most of the fractures observed in the boreholes were judged to be shear fractures, based on the intercalation of fault rocks and the presence of striations and slickensides on the surface of the fractures. The fractures can be divided into either minor faults at a high angle to the bedding plane or those parallel to the bedding plane. In addition, since the former minor faults tend to gather densely, the clustered zone was defined as a fracture or fault zone[48)]. The sections where drilling fluid was lost during drilling and also where the hydraulic conductivity was high during in situ hydraulic tests corresponded to a fault zone.

The hydrological analysis taking the above fracture zone into account indicates that the fracture zone has a large influence on groundwater flow[39)]. Further examination of the distribution and nature of fractures in the rocks was thus conducted, including drawing sketches of fractures at artificially generated stripped horizontal outcrop surfaces. The results of the investigations were as follows[32)]:

- The minor faults can be divided into those that are strike-slip with a high angle to the bedding plane and those parallel to the bedding plane with a dip-slip, based on the relationship between the fault direction and the bedding plane and fold axes and the displacement sense (Figure 4.1.3-7).
- The formation age of the minor faults at a high angle to the bedding plane was estimated to be mostly younger than the age of the folding and very different from the age when the Omagari Fault was formed and the youngest among faults observed in the rocks, based on the intersection relationships of the faults, the stress field at the fault movement (estimated by the analysis of minor faults), the relationship between the minor faults parallel to the bedding plane and fold activity and existing information on the Omagari Fault.
- The minor faults at a high angle to the bedding plane were possibly formed by the compressive stress originating from the residual stress that had accumulated at the time when the fold was formed and are assumed to be distributed widely along the fold structure, based on the relationship between the stress field at the time of faulting estimated by the minor fault analysis and the direction of the fold axis, formation processes of faults and existing literature information. The minor faults that are parallel to the bedding plane are considered to have been formed by bedding slips associated with flexural-slip folding and are assumed to be distributed widely along the fold structures, in particular in the limb area, based on the relationship between the fault direction and bedding plane and that of the displacement sense and the direction of the fold axis.
- Minor faults at a high angle to the bedding plane tend to be gathered densely and connect with each other en echelon (Figure 4.1.3-8), forming a fault zone with a length of the order of 10–100 m.
- Based on the development of the oxidised zone along the fault near the surface, the occurrence of intercalated fault rocks, distribution density and formation processes and the relationship between the fault direction and stress field, it can be concluded that the minor faults at a high angle to the bedding plane (or fault zones) are likely to be major groundwater pathways, while minor faults parallel to the bedding plane are not.

The trends in the direction and distribution density of lineaments that were interpreted or recognised by the topographical (lineament) investigations in and around the URL area were consistent with those of the minor faults at a high angle to the bedding plane. However, minor faults (in fault zones) or joints that can be actually traced at the surface as lineaments were not identified[30)].

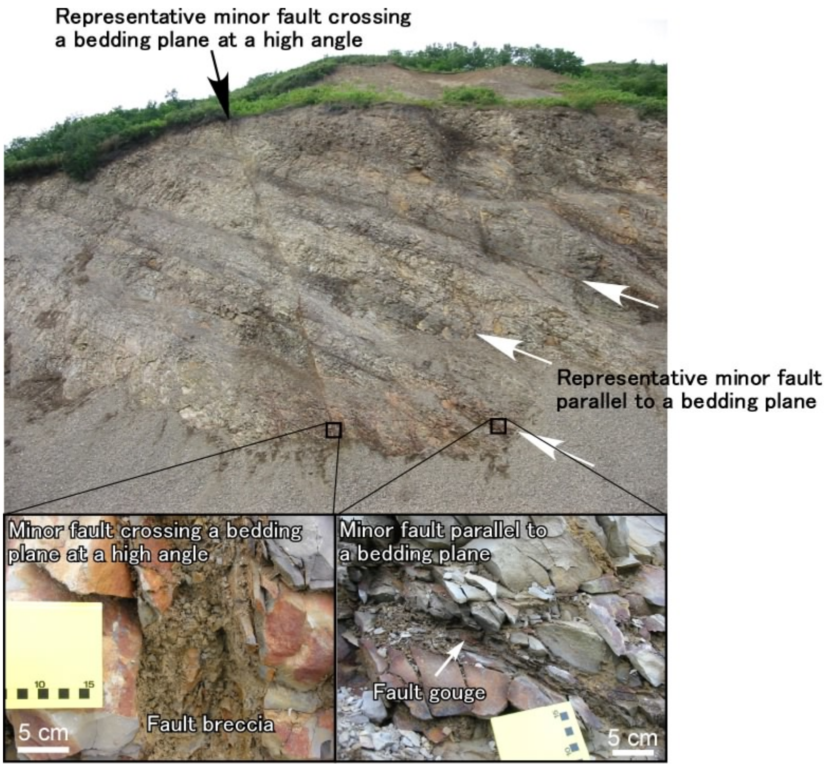

Figure 4.1.3-7 Photographs of representative minor faults

Based on Ishii and Fukushima[32)]

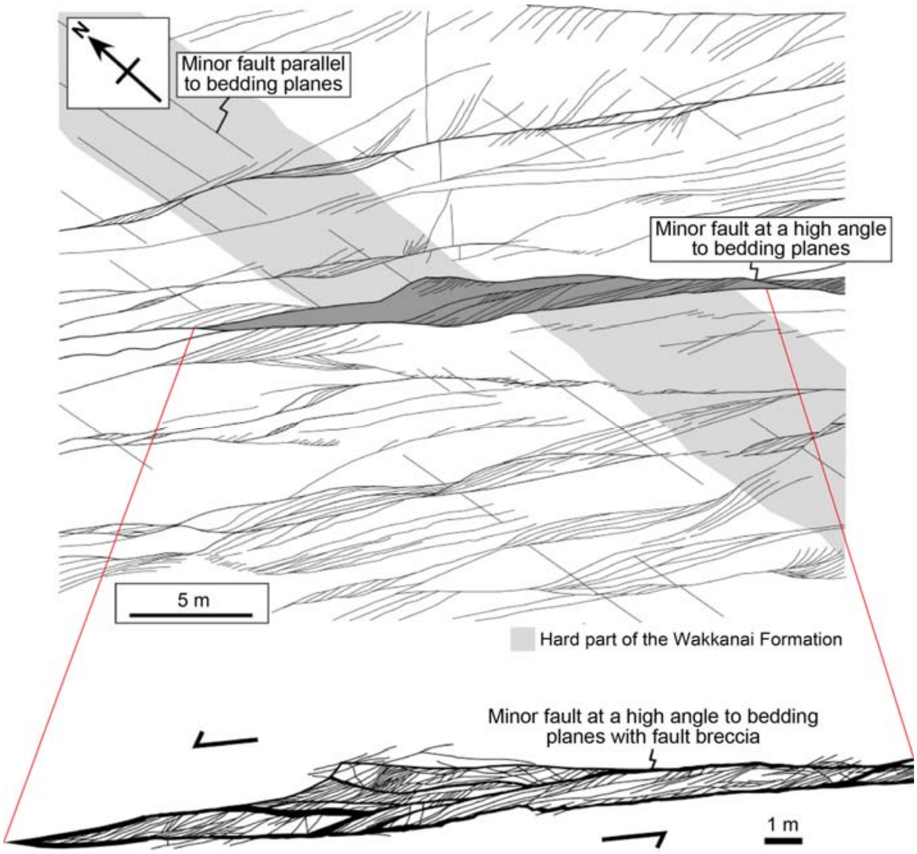

Figure 4.1.3-8 Sketch of minor fault at a high angle to bedding planes

Based on Ishii and Fukushima[32)]

Mitani et al.[14] pointed out that joints are observed in the anticlinal axis. It was found in analyses of the gravity surveys conducted in this stage that the gravity anomaly identified during the surveys could be well explained by assuming a decrease in the density of the formation at the anticlinal top on the west side of the estimated position of the Omagari Fault[37]. This might be due to the development of fractures at the anticlinal top. If this assumption were correct, the decrease in the density of the formation at the anticlinal top would be consistent with the trend of distribution of the joints, as was indicated by Mitani et al.[14]

4.1.4 Geological modelling

The conceptual model of the geological structure in and around the URL area is shown in Figure 4.1.4-1. Distributed in the area are the Wakkanai Formation consisting of siliceous mudstones (or siliceous shale), the Koetoi Formation consisting of diatomaceous mudstones and the Yuchi Formation consisting of sandstones. Discontinuities present in the rocks include the large-scale Omagari Fault and minor faults at a high angle to the bedding plane where dip-slip prevails and almost parallel to the bedding plane where strike-slip prevails, associated with the fold structure (minor faults that are almost parallel to the bedding plane tend to develop in the limb rather than axis of the fold). Minor faults at a high angle to the bedding plane tend to form fault zones by distributing densely together en echelon; these features, in particular the fault zones, are likely to function as preferential pathways for groundwater. On the other hand, minor faults parallel to the bedding plane are not likely to function as groundwater flow paths. The development of joints has not been fully examined and joints are therefore not shown in Figure 4.1.4-1.

Of the above structures, the Omagari Fault and the fault zones can be identified as the structures deserving attention in terms of their effect on groundwater flow and solute transport because they are highly likely to function as preferential water flow paths. They must be represented appropriately in the geological and hydrogeological models. The distribution of the Omagari Fault zone can be predicted deterministically by reconnaissance surveys and geophysical surveys. However, predicting the distribution of the fault zones would be impossible in practice using a deterministic approach and has to be based on stochastic methods, since there are no fault zones whose continuity has been confirmed in the area between the boreholes and at lineaments. This means that fault zones cannot be expressed in the geological structure model that was constructed deterministically (Figure 4.1.4-2), but may be taken into account in a model that combines deterministic and stochastic approaches.

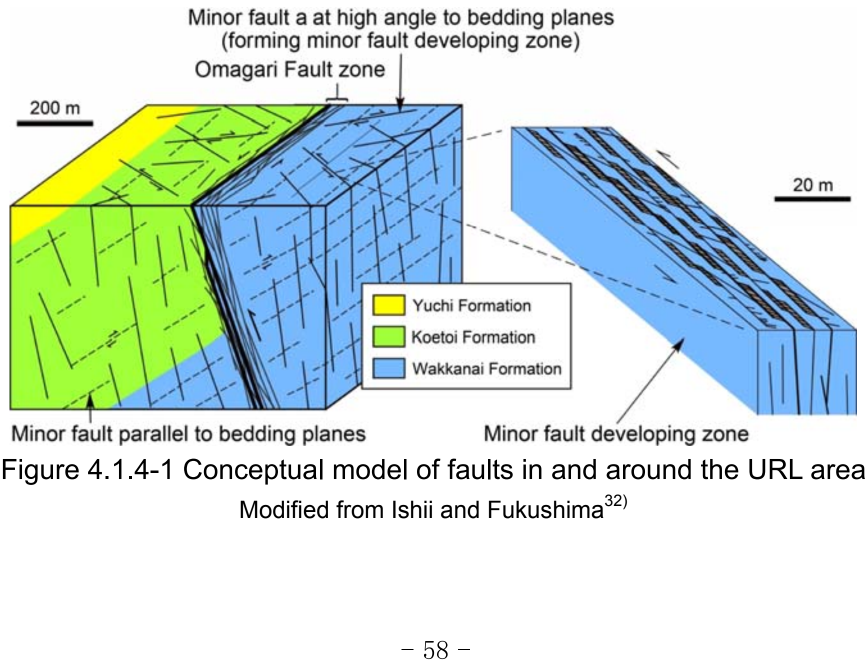

Figure 4.1.4-1 Conceptual model of faults in and around the URL area
Modified from Ishii and Fukushima[32]

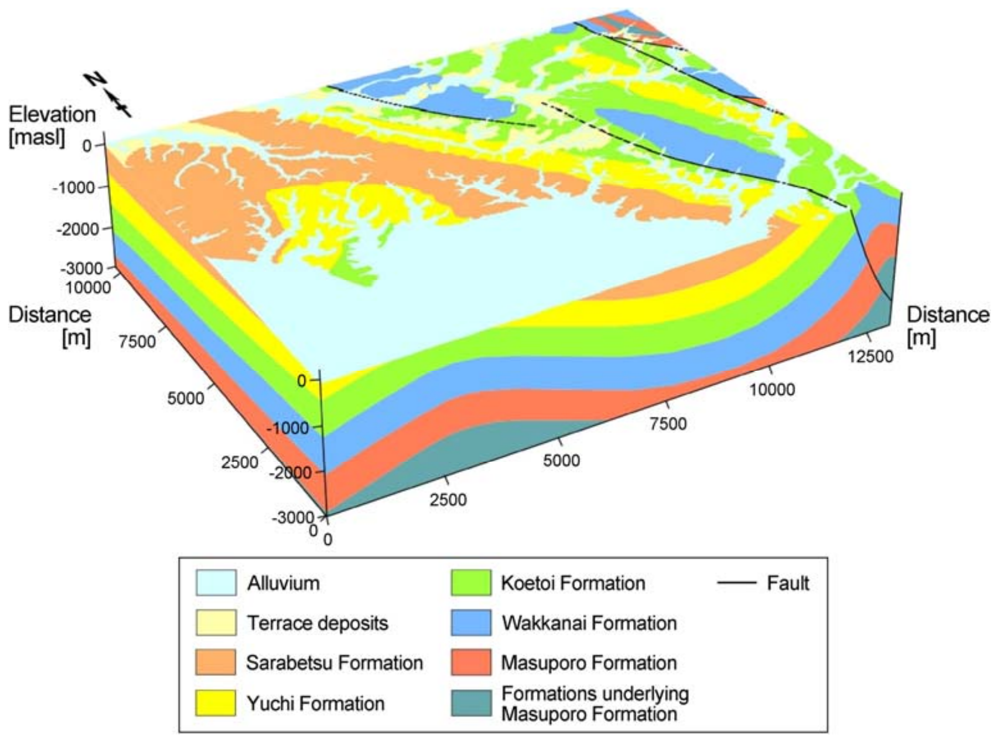

Figure 4.1.4-2 3D model of geological structure in and around the URL area

Modelled area corresponding to the detailed geological map shown in Figure 4.1.3-1

The discussion below presents some simplifications, primarily from a geological point of view, in generating fault zones realisations using a stochastic method.

- Fault zones can be represented as a flat (disk) object with a certain direction, length (radius), width and transmissivity (Baecher et al.[49] have developed a well known model using a disk medium). This means that modelling the whole cluster of fractures, rather than modelling each individual fracture within a fault zone, would be more efficient, given the scale of the section length (1–10 m) of the actual hydraulic test in a borehole and given the need to consider the matrix of fault zones as water flow paths. The fault zones can be considered as geological structures consisting of fractures and the matrix between the fractures.
- The orientation of the fault zones (strike and dip angle) can be represented as the average of the directions of all the fractures in each zone. Since actual fractures are concentrated in an en echelon alignment, the direction of the densely fractured zone will be slightly diagonal across the average direction of the fractures. For simplification of the modelling, the direction of the fault zone will be represented with the average direction of the fractures in the model.
- The strike of fault zones at a high angle to the bedding plane crosses obliquely (to parallel) to the perpendicular direction of the fold axis (average 40°)[32].
- The dip angle of each fault zone is in the range of 45–90° (vertical predominant). Minor faults at a high angle to the bedding plane form a sub-vertical angle at surface outcrop and are strike-slip predominant[32]. Many of such faults are considered to be less influenced by tilting movements as they were likely to be formed after the folding. However, vertical minor faults at a high angle to the bedding plane may not be represented well in the data on dip angles obtained in boreholes as the boreholes are drilled vertically. Therefore this data is not taken into account at this stage.

- The length (radius) of a fault zone is assumed to be 10 times the width actually measured in boreholes and surface outcrops[32].
- Fault zones are assumed to be uniformly distributed in the rock. The 3D density distribution is obtained by inversion modelling from the 1D distribution density obtained from boreholes using a virtual water injection test method proposed by Shimo et al.[50]

For the distribution of fault zones that are difficult to represent deterministically, a more realistic prediction would be possible by generating such zones stochastically considering the above limitations. The limitations on stochastic modelling of such zones should be determined based on the obtained data and their geological interpretation. Information on origin, structural characteristics and formation processes of minor fault developing zones could be used for this purpose. A number of fault zone models using the stochastic method have been developed[39],[51] One example is the application of an equivalent heterogeneous continuum model[52], where information on the spatial distribution of fractures is reflected in the spatial distribution of hydraulic characteristics in the continuum model.

4.2 Hydrogeological investigations

4.2.1 Aims

The aims of the hydrogeological investigations and modelling during the surface-based investigation phase are to clarify groundwater flow characteristics in and around the URL area, to predict the evolution of the hydrogeological environment associated with the construction of the underground facilities and to propose efficient and systematic methods for facilitating investigations during Phase II and/or Phase III such as development of methodologies for understanding the groundwater flow field. According to Darcy's law, the absolute value for groundwater flow velocity (Darcy flux) can be expressed as the product of hydraulic conductivity and gradient. It is thus necessary to acquire data on hydraulic conductivity and gradient and their distributions for the Wakkanai and Koetoi Formations. To understand groundwater flow, the hydraulic conductivities of these formations, recharge rate and hydraulic head distribution were also investigated.

An effective way of clarifying the groundwater flow system in and around the URL area and predicting the evolution of the system associated with the construction of the underground facilities would be to integrate and interpret investigation results, developing a hydrogeological model for analysing groundwater flow[53)]. The development of models and groundwater flow analyses reduces uncertainties as field investigations progress and also makes it possible to propose targeted investigations for subsequent phases.

4.2.2 Surface-based investigations covering the whole Horonobe Town area

(1) Investigation aims and methods

Based on the principle of conservation of physical quantities, groundwater flow can be described primarily by a constitutive law such as Darcy's law, physical properties such as hydraulic conductivity and boundary conditions. When analysing groundwater flow in an area of interest, it is not always possible to establish appropriate boundary conditions for the area. This means that a wider analysis domain may need to be selected and physical properties estimated for this area.

Firstly, information on groundwater flow has to be compiled from the literature. This survey of existing information, which includes compilation of available borehole data and literature information on groundwater use, need to precede shallow subsurface hydrological investigations and borehole investigations. In particular, existing information from boreholes will be used not only as a guideline for how to perform subsequent investigations, but could also be relevant because borehole drilling and pumping of water could disturb the natural groundwater flow system. Information on the rock formations outside the area to be characterised is based essentially on surveys of existing information. In addition, information from oil and natural gas exploration carried out by MITI would be particularly useful for the hydrogeological investigations since it is related to groundwater flow. Such exploration was conducted both onshore and offshore throughout the country, with Niigata and Akita Prefectures at the centre. Boreholes up to 5,000 m depth were drilled to acquire information on deep geological structures and reservoirs. In the URL area, the MITI Tenpoku borehole (5,050 m depth) was drilled at a location about 3 km north of the URL site[11)].

In the Horonobe area, other borehole investigations have been conducted for the development of underground resources. The Kitakawaguchi SK-1 borehole (4,505 m depth) in Teshio Town, for example, was drilled to a sufficient depth to provide valuable information on deep geological formations that were relatively unknown. In borehole D-1, hydraulic tests were carried out in the Sarabetsu Formation on the rock layers of interest[54),55)]. In boreholes HDB-1 and HDB-2 drilled at the time of selecting the URL area, hydraulic tests were carried out for both fractured zones and matrix parts (i.e. background fractured rocks) in order to determine the average hydraulic conductivities of the Wakkanai and Koetoi Formations[56),57)]. Groundwater is used for water supply and for hot springs. At the Toyotomi Hot Spring located 3 km northwest of the URL area, around 180 l min^{-1} of water have been pumped out from a depth of around 900–1,300 m.

In general, pumping out groundwater could affect natural groundwater flow because of a change in the water pressure (hydraulic head) at depth. It is also important for hydrological investigations because of the change in the hydrological balance. In cases where boreholes are not backfilled, they could also act as a water conducting feature. Even for boreholes with casing, the casing may corrode, leading to the formation of a water conduit. These issues need to be investigated as the important factors to affect groundwater flow.

(2) Integration of existing information

Of the existing boreholes, those located close to the URL area that provide relevant information on hydrogeological structures include those at the Toyotomi Hot Spring in Toyotomi Town (north of Horonobe Town), the Tenpoku borehole drilled to the north of the URL area and boreholes HDB-1 and HDB-2 drilled at the time of selecting the URL area. The origin of the hot water at the Toyotomi Hot Spring is assumed to be a fracture-type reservoir[58)]. The formation producing the hot spring is assumed to be the Makubetsu Formation, the upper part of the Masuporo Formation[14)]. Given the occasional occurrence of lost circulation in the Wakkanai Formation and the upper Masuporo Formation during the drilling of the Tenpoku borehole, fractured zones may exist in these formations. According to hydraulic tests carried out in boreholes HDB-1 and HDB-2, the hydraulic conductivity of the Wakkanai and Koetoi Formations is as low as 10^{-11}–10^{-9} m s^{-1}.

Re-analysis of the hydraulic tests conducted in borehole D-1[11),54)] resulted in a hydraulic conductivity in the order of 10^{-7} m s^{-1} for the Yuchi Formation and 10^{-6} m s^{-1} for the Sarabetsu Formation and the Quaternary sediments[59)]. A large aquifer is present in the Sarabetsu Formation and provides a supply of clean water to Horonobe Town.

The observed water pressure head was higher than the hydrostatic pressure by about 150 m in borehole HDB-2. The possibility of abnormally high pressure in the Masuporo Formation was also indicated by the results of a density log from the Kitakawaguchi SK-1 borehole, about 800 m east of the anticline axis of the Kitakawaguchi Anticline[20),60)]. On the other hand, no abnormally high pressure was observed, although the water pressure was pressurised at about +10 m, in borehole HDB-1 located in the URL area. Abnormally high pressure is unlikely in the Wakkanai and Koetoi Formations near borehole HDB-1, but whether such high pressure exists in the URL area has not been confirmed yet.

The presence of gas in the groundwater in the area has been confirmed, as has the presence of high salinity groundwater[61)].

Based on existing borehole investigations, the presence of fractured zones cannot be ruled out, but it can be concluded that the hydraulic conductivity and its variation are low in the Wakkanai and Koetoi Formations.

(3) Modelling of hydrogeological structures and groundwater flow analyses

1) Analytical conditions

The aim of the investigation stage covering the whole Horonobe Town area was to acquire data for describing the general characteristics of groundwater flow (distribution of hydraulic conductivities and hydraulic gradients in the sedimentary formations) in and around the URL area and to propose efficient and systematic investigation methodologies for subsequent stages. Specifically, the geological and hydrogeological structures are predicted based on existing information and sensitivity analyses are carried out by changing the hydraulic conductivity within a possible range for each formation. Formations that may affect the distribution of hydraulic head and flow velocities of the groundwater around the URL are also predicted.

Sensitivity analyses of groundwater flow were carried out for an area of 50 km × 50 km square, including the whole area of Horonobe Town, to estimate the groundwater flow system in the URL area. The analytical region was defined widely enough to avoid affecting the analytical results for groundwater flow directions in the URL area. Taking this into consideration, the eastern boundary was defined as the Teshio Highlands, which are located at the east end of the Teshio River drainage basin, and the western boundary was defined at about 10 km off the coastline. As there was no clear drainage basin boundary to the north and south, the boundaries were defined at locations far from the URL area. The depth for modelling was defined as 5,000 m below the ground surface. Because hydraulic conductivity generally decreases with depth and no large-scale aquifer had been observed in the Tenpoku borehole, the impermeable boundary was conservatively assumed to be at a depth of 5,000 m below the ground surface. The analytical area is shown in Figure 4.2.2-1 and the analytical mesh and boundary conditions are shown in Figure 4.2.2-2.

As described in paragraph (2), the existence of fractured zones cannot be ruled out based on existing borehole investigations, but it can be concluded that the hydraulic conductivity and its variability in the Wakkanai and Koetoi Formations is low, even if fractures are present, their distribution and hydraulic conductivity are unknown. Therefore, at this stage of the investigation, a numerical finite element analyses applying a continuum model was conducted assuming the rock formations to be porous media. The formations subjected to the analyses were, according to hydrogeological classification, the Cretaceous basement, the Masuporo Formation, the Wakkanai Formation, the Koetoi Formation, the Yuchi Formation, the Sarabetsu Formation, the Quaternary sediments, the Omagari Fault, the Horonobe Fault (N1 fault) and shallow subsurface/terrace sediments.

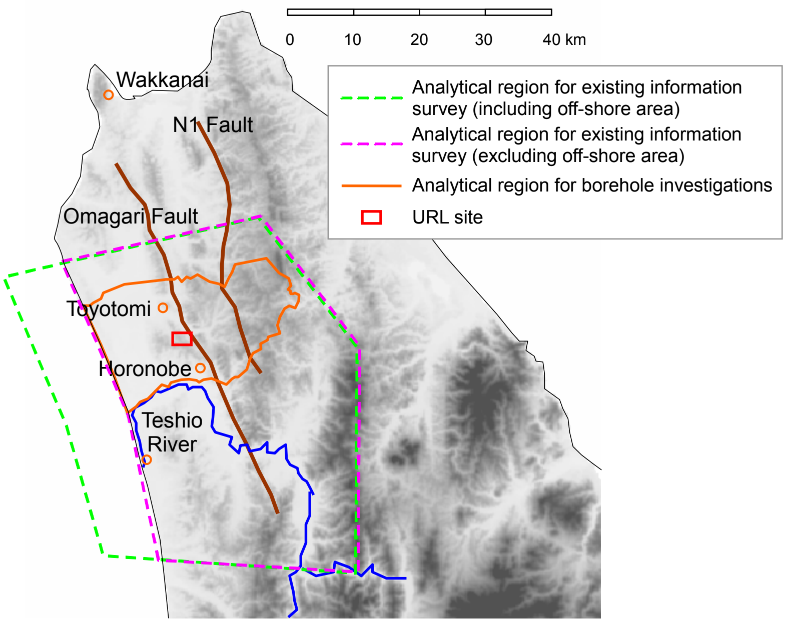

Figure 4.2.2-1 Regions for groundwater flow analysis

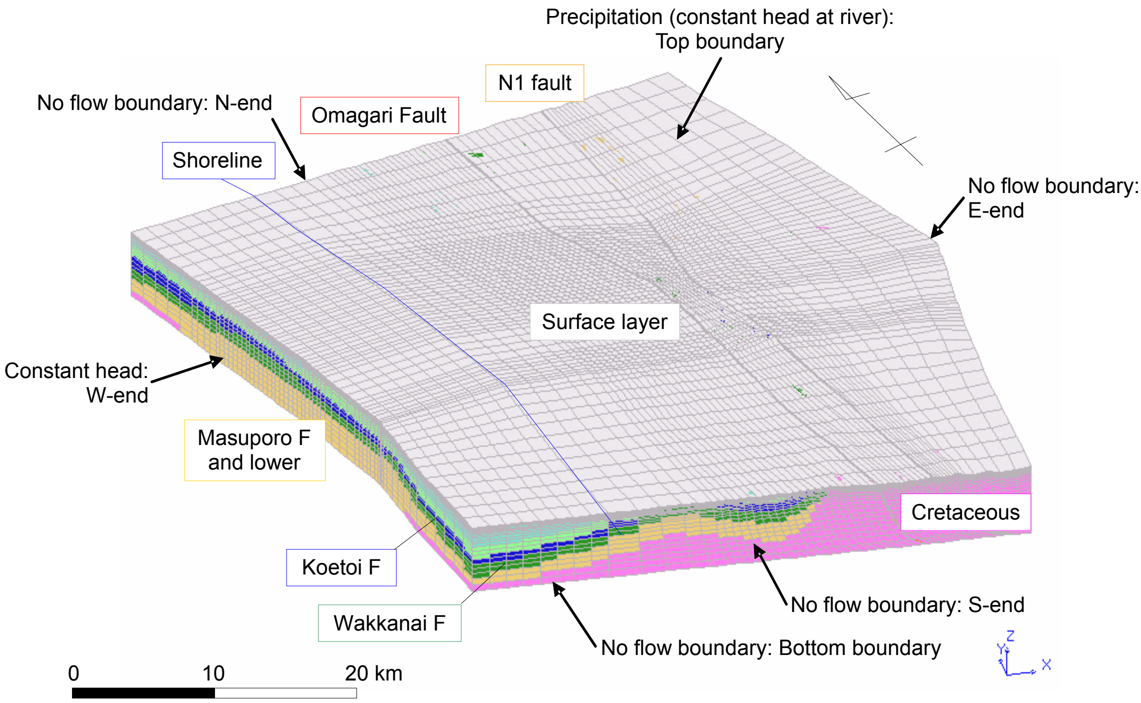

Figure 4.2.2-2 Finite element mesh and boundary conditions

In the investigation stage covering the whole area of Horonobe Town, both the quality and the number of hydraulic tests were limited and sensitivity analyses were therefore carried out using hydraulic conductivities obtained from literatures or by estimation as the reference case and considering the range of variability of hydraulic conductivity. A sensitivity analysis was also conducted for recharge rate[62),63)].

For the reference case, a set of hydraulic conductivities for each formation is shown in Table 4.2.2-1. The hydraulic conductivities in the Wakkanai and Koetoi Formations were derived from the results of hydraulic tests in boreholes HDB-1 and HDB-2, while those for the Yuchi and Sarabetsu Formations and Quaternary sediments were derived from a re-examination[59)] of the results of hydraulic tests in borehole D-1. The hydraulic conductivity of the shallow subsurface/terrace sediments was assumed to be slightly higher than that of the lower formations and slightly larger than that of the upper formation, i.e. the Wakkanai Formation, since the Masuporo Formation consists of gravels and sandstones. For the Omagari Fault, a sandwich structure was assumed, i.e. impermeable in a direction at right angles to the fault plane and highly permeable in the parallel direction, and estimated hydraulic conductivities were used. Cases for the sensitivity analyses are listed in Table 4.2.2-2.

The upper surface boundary was defined as the seepage face in which the water level was fixed when the groundwater level reached the ground surface level at a given rainfall intensity. Rainfall intensity can be obtained by subtracting the amount of evapotranspiration from the amount of precipitation. Imai et al.[64)] define the hydrological recharge rate (precipitation minus evapotranspiration and river runoff) as the rainfall intensity. The recharge rate was estimated based on the average river runoff measured at the Maruyama and Ponpira observatories in the Teshio River drainage basin (1,480 mm y^{-1}), the indicative value of 400 mm y^{-1} for evapotranspiration in Hokkaido determined by the Research Institute of the Ministry of Construction (now Ministry of Land, Infrastructure, Transport and Tourism) and an assumed runoff rate (runoff/rainfall volume) of about 0.7–0.9 based on data for Japanese rivers[65)]. As a result, the recharge rate was calculated as 0–234 mm y^{-1}. In the reference case, it was set conservatively high at 1 mm d^{-1} [64]. The lower boundary was set at -5,000 m elevation as an impermeable boundary. With regard to the lateral boundaries, those on the marine side were defined as fixed water level at the water surface and impermeable at other locations; the lateral boundaries for the other sides were defined as impermeable because they are set along ridges and valleys.

Table 4.2.2-1 Hydraulic conductivity settings for the reference case

Geological structure	Hydraulic conductivity [m s^{-1}]	Basis for setting
Cretaceous	1.0×10^{-11}	Lower than overlying formations, assumed
Masuporo Formation	5.0×10^{-10}	Relatively high hydraulic conductivity because of sandstone and conglomerate, assumed
Wakkanai Formation	1.0×10^{-10}	Based on HDB-1/2 hydraulic test results[56),57)], lower than Koetoi Formation
Koetoi Formation	1.0×10^{-9}	Based on HDB-1/2 hydraulic test results[56),57)]
Yuchi Formation	1.0×10^{-7}	D-1 hydraulic test results[59)]
Sarabetsu Formation, Quaternary	1.0×10^{-6}	D-1 hydraulic test results[59)]
Damaged zone of Omagari Fault	1.0×10^{-8}	Assumption
Core of Omagari Fault	1.0×10^{-10}	Assumption
Damaged zone of N1 fault	1.0×10^{-8}	Assumption
Core of N1 fault	1.0×10^{-10}	Assumption
Surface, sediments	2.0×10^{-6}	Higher than underlying formations, assumed

Table 4.2.2-2 Hydraulic conductivity settings for sensitivity analyses

Cases	Parameters	Values for reference case (AH13)	Values for varying cases
M1	Hydraulic conductivity of Masuporo Formation	5.0×10^{-10} [m s^{-1}]	3.15×10^{-9} [m s^{-1}]
M2			7.92×10^{-11} [m s^{-1}]
W1	Hydraulic conductivity of Wakkanai Formation	1.0×10^{-10} [m s^{-1}]	1.0×10^{-9} [m s^{-1}]
W2			1.0×10^{-11} [m s^{-1}]
K1	Hydraulic conductivity of Koetoi Formation	1.0×10^{-9} [m s^{-1}]	1.0×10^{-8} [m s^{-1}]
K2			1.0×10^{-10} [m s^{-1}]
Y1	Hydraulic conductivity of Yuchi Formation	1.0×10^{-7} [m s^{-1}]	3.16×10^{-6} [m s^{-1}]
Y2			3.16×10^{-9} [m s^{-1}]
Q1	Hydraulic conductivity of Quaternary	1.0×10^{-6} [m s^{-1}]	3.16×10^{-5} [m s^{-1}]
Q2			3.16×10^{-8} [m s^{-1}]
S1	Hydraulic conductivity of surface layer	2.0×10^{-6} [m s^{-1}]	6.32×10^{-5} [m s^{-1}]
S2			6.32×10^{-8} [m s^{-1}]
FOC1	Hydraulic conductivity of core of Omagari Fault	1.0×10^{-10} [m s^{-1}]	1.0×10^{-8} [m s^{-1}]
FOC2			1.0×10^{-12} [m s^{-1}]
FOS1	Hydraulic conductivity of damaged zone of Omagari Fault	1.0×10^{-8} [m s^{-1}]	1.0×10^{-6} [m s^{-1}]
FOS2			1.0×10^{-10} [m s^{-1}]
AR1	Precipitation intensity	1.0 [mm d^{-1}]	1.5 [mm d^{-1}]
AR2			0.5 [mm d^{-1}]

2) Analytical results

The distribution of the hydraulic head obtained from the reference case analysis and the streamlines from the URL area for all cases of the sensitivity analyses are shown in Figure 4.2.2-3. Generally, the main flow direction of the groundwater would be from east to west since the hydraulic head on the east side is higher than that on the west side. The distribution of hydraulic head is relatively complicated owing to the influence of the undulating topography in and around the URL area and the groundwater flow direction varies depending on depth and location. Based on the streamlines, it was confirmed that shallow groundwater flow is governed by local flow systems such as the Shimizu River basin and the Penkeebekorobetsu River basin, while deep groundwater flow is governed by the Teshio River basin, which constitutes a regional flow system.

The sensitivity analysis was conducted using the hydraulic head at -400 m elevation at the URL site, the hydraulic gradient, the groundwater travel time from -400 m elevation to the surface and the travel distance of the groundwater as parameters[62)]. Figure 4.2.2-4 shows the sensitivity gradient ratio for the hydraulic head and the groundwater travel time. Here, the sensitivity gradient means the change in the characteristic values (e.g. hydraulic head) at the focal point when a parameter is changed by one unit (one order of magnitude for the hydraulic conductivity or 1 mm d^{-1} for the recharge rate) and the sensitivity gradient ratio is defined as the value of the sensitivity gradient divided by the characteristic value for the reference case, which is expressed as a percentage. The sensitivity of the hydraulic conductivity to the hydraulic head in relatively shallow formations such as the shallow subsurface/terrace deposits and the Yuchi Formation was found to be large. This can be explained by the fact that the distribution of the hydraulic head is primarily governed by fluctuations in the groundwater level and propagation of the effect of fluctuations in groundwater level to deeper geological formations will be affected by the permeability in the shallower zones. With regard to the groundwater travel time, it is clear that the sensitivity of the hydraulic conductivities of the Wakkanai and Koetoi Formations is large, because most of the streamlines pass through these formations. The sensitivity of hydraulic conductivity of the Omagari Fault is low, but this does not mean that investigations of the fault are not important, since the range of variability of hydraulic conductivity can be expected to be large for large-scale geological structures.

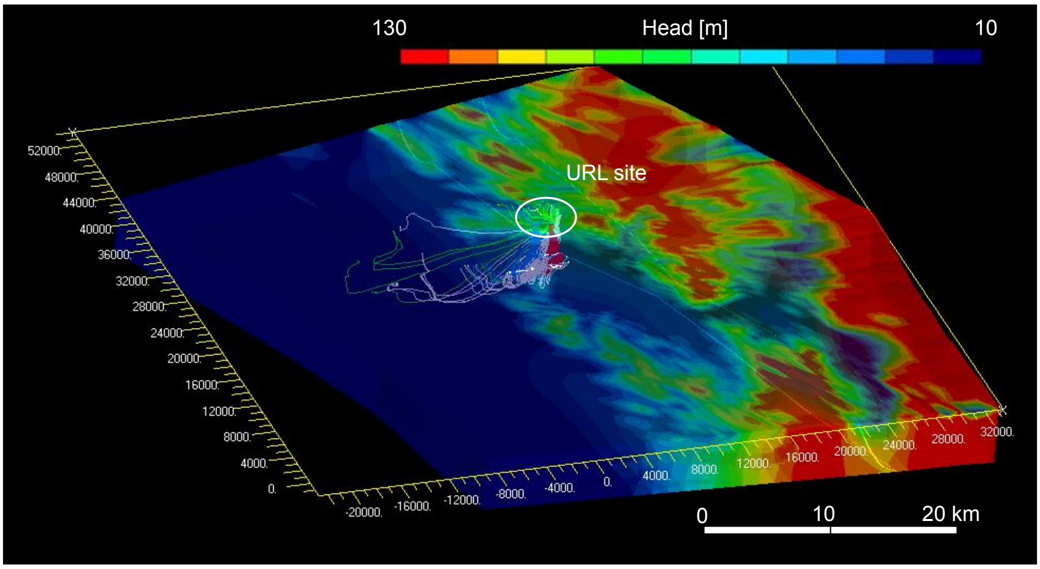

Figure 4.2.2-3 Distribution of hydraulic head for the reference case and simulated streamlines from the URL site

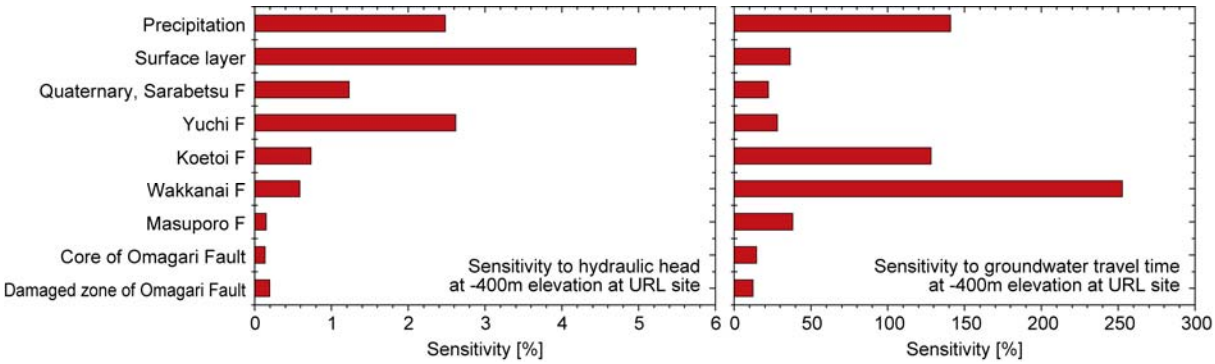

Figure 4.2.2-4 Sensitivity of precipitation and hydraulic conductivity for each geological structure to hydraulic head (left) and groundwater travel time (right) at -400 m elevation at the URL site

The conceptual groundwater flow systems in and around the URL area developed based on the results of groundwater flow analyses are shown in Figure 4.2.2-5. These results indicate that the groundwater flow systems in the area including the URL are governed by the undulating topography and are divided into a local and regional flow system, depending on depth. The boundary between the two systems is located at a depth of about 400 m below the ground surface and groundwater flow near the URL (drifts located at a depth of about 500 m) is highly likely to be governed primarily by the regional flow system.

The investigations in this stage suggest that data acquisition and detailed analyses focussing on the hydraulic conductivity and recharge rate in the formations identified as being important by the sensitivity analyses are important for investigations in subsequent phases, in terms of reducing uncertainties regarding direction and velocity of groundwater flow.

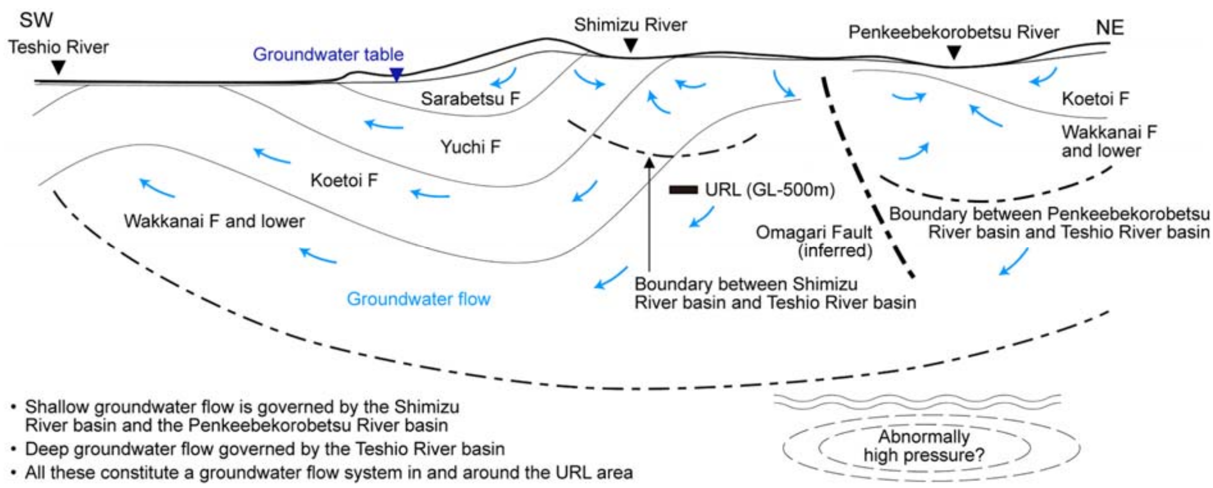

Figure 4.2.2-5 Conceptualisation of groundwater flow in and around the URL area

4.2.3 Surface-based investigations in and around the URL area
(1) Shallow subsurface hydrological investigations
1) Investigation aims and methods

The aims of the hydrological investigations are to acquire data on the distribution of the groundwater levels that affect the distribution of the hydraulic gradient and the groundwater flow systems and to predict the groundwater recharge rate from the surface to deeper sedimentary formations. In particular, with regard to the groundwater recharge rate, a comprehensive evaluation is required using two different methods:

- hydrological balance method: indirect method based on the hydrological balance;
- hydraulic engineering method: recharge rate measurement method using data on the groundwater level and the moisture content in the soil.

In the hydrological balance method, the groundwater recharge rate is obtained by subtracting the river runoff and the total amount of evapotranspiration from the total precipitation in the drainage basin concerned (Figure 4.2.3-1); in the hydraulic engineering method, the vertical seepage volume is obtained based on a geotechnical method from the in situ vertical potential gradient and hydraulic conductivities. Other methods include using a lysimeter and measuring vertical seepage directly using a thermal microflowmeter or a tracer. The direct methods such as the hydrological engineering method can obtain a local groundwater recharge rate at the observation point. Evaluation of the groundwater recharge rate for each drainage basin should be based on prediction by the hydrological balance method. For this purpose, accurate sequential measurements of volumes of precipitation, evapotranspiration, runoff and other hydrological parameters will be required.

A list of the items covered by the hydrological investigations conducted in this stage is given in Table 4.2.3-1[66)–70)]. A map indicating the location of the investigations in drainage basins that are currently targeted for observation is shown in Figures 4.2.3-2 and 4.2.3-3 (see also Appendix 2).

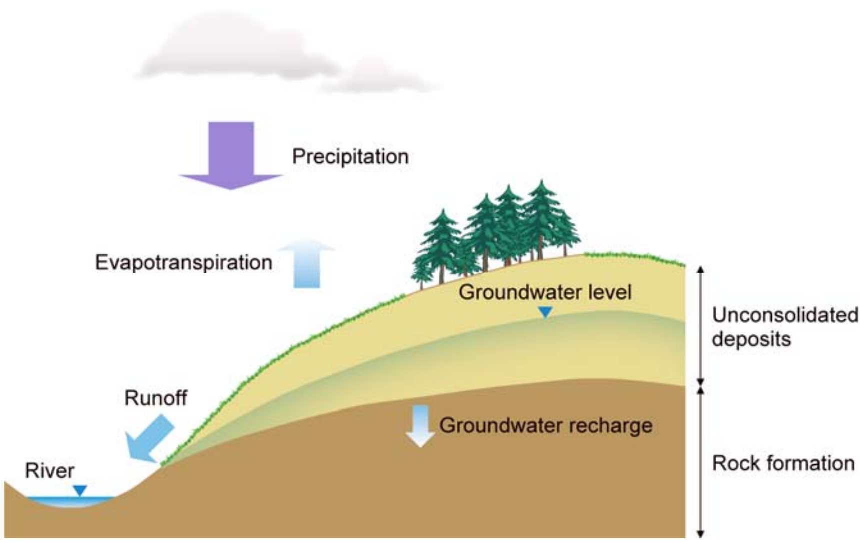

Figure 4.2.3-1 Hydrological balance method for estimating groundwater recharge rate

Table 4.2.3-1 Observation items for shallow subsurface hydrological investigations

<table>
<tr><th>Aims</th><th colspan="2">Methods/specifications</th><th>Items</th><th>Location</th><th>References</th></tr>
<tr><td colspan="6">Hydraulic engineering method</td></tr>
<tr><td rowspan="2">Hydraulic conductivity</td><td colspan="2">In situ hydraulic test</td><td>Hydraulic conductivity</td><td>HGW-1</td><td rowspan="2">Ikeda et al.[67]</td></tr>
<tr><td colspan="2">Laboratory hydraulic test</td><td>Hydraulic conductivity</td><td>(8 samples)</td></tr>
<tr><td>Groundwater level</td><td colspan="2">Pressure gauge/
manual operation</td><td>Groundwater level</td><td>HGW-1</td><td>Ikeda et al.[67]
Seno et al.[69]
Tomura et al.[70]</td></tr>
<tr><td rowspan="2">Groundwater recharge rate</td><td rowspan="2">Soil moisture sensor</td><td>ADR sensor</td><td>Volumetric moisture content</td><td>HGW-1</td><td>Ikeda et al.[67]
Tomura et al.[70]</td></tr>
<tr><td>Laboratory test</td><td>Hydraulic conductivity</td><td>(12 samples)</td><td>Ikeda et al.[67]</td></tr>
<tr><td colspan="6">Hydrological balance method</td></tr>
<tr><td rowspan="5">Precipitation</td><td colspan="2">Rain gauge/
tipping-bucket with heater</td><td>Precipitation; all the year round</td><td>Hokushin</td><td>Nakabayashi et al.[66]
Seno et al.[68]</td></tr>
<tr><td colspan="2">Overflow-type rain and snow gauge</td><td>Precipitation; all the year round</td><td>Hokushin</td><td></td></tr>
<tr><td colspan="2">Tipping-bucket rain gauge</td><td>Precipitation without snow season</td><td>Horonobe
Toikanbetsu
Kamitoikan</td><td></td></tr>
<tr><td colspan="2">Snow depth meter/
laser type</td><td>Snow depth</td><td>Horonobe
Toikanbetsu
Kamitoikan</td><td></td></tr>
<tr><td colspan="2">Snowfall gravimeter/
metal wafer type</td><td>Snowfall weight</td><td>Hokushin</td><td></td></tr>
<tr><td rowspan="9">Evapotranspiration</td><td colspan="2">Thermometer/electrical,
Hygrometer/electrical</td><td>Temperature, relative humidity</td><td>Hokushin</td><td>Nakabayashi et al.[66]
Seno et al.[68]</td></tr>
<tr><td colspan="2">Atmospheric pressure meter/
electrical</td><td>Atmospheric pressure</td><td>Hokushin</td><td></td></tr>
<tr><td colspan="2">Snow surface thermometer/
radiation</td><td>Temperature of snow surface</td><td>Hokushin</td><td></td></tr>
<tr><td colspan="2">Wind vane and anemometer/
pinwheel type</td><td>Wind direction and velocity</td><td>Horonobe
Toikanbetsu
Kamitoikan</td><td></td></tr>
<tr><td colspan="2">Anemometer/three cup</td><td>Ground wind speed</td><td>Hokushin</td><td></td></tr>
<tr><td colspan="2">Sunshine recorder</td><td>Duration of bright sunshine</td><td>Horonobe
Toikanbetsu
Kamitoikan</td><td></td></tr>
<tr><td colspan="2">Actinometer</td><td>Global solar radiation</td><td>Hokushin</td><td></td></tr>
<tr><td colspan="2">Net pyrradiometer</td><td>Amount of net radiation</td><td>Hokushin</td><td></td></tr>
<tr><td colspan="2">Earth thermometer</td><td>Earth temperature</td><td>Hokushin</td><td></td></tr>
<tr><td rowspan="2">River flux</td><td colspan="2">Pressure gauge</td><td>Water level</td><td>P-3, P-4, P-5</td><td>Nakabayashi et al.[66]
Seno et al.[68]</td></tr>
<tr><td colspan="2">Current meter</td><td>River flux</td><td>P-3, P-4, P-5</td><td></td></tr>
</table>

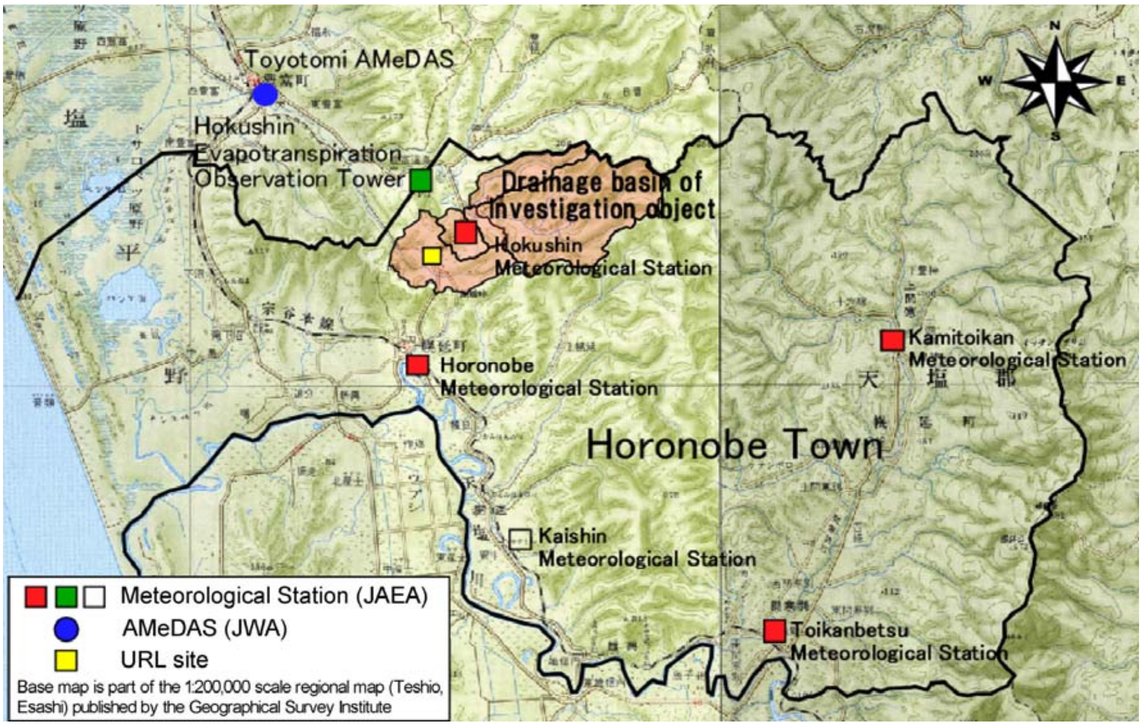

Figure 4.2.3-2 Drainage basin for shallow subsurface hydrological investigations

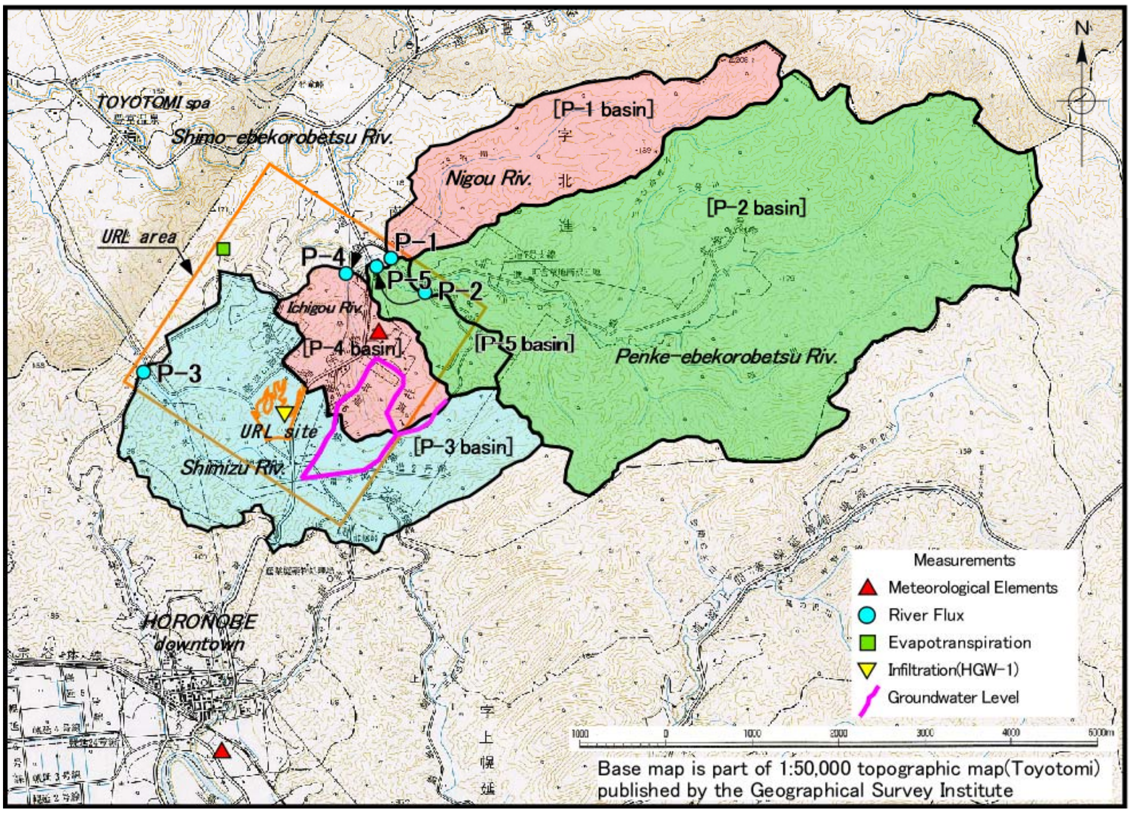

Figure 4.2.3-3 Observation points and basins in and around the URL area

2) Selection of investigation sites

Information on the groundwater recharge rate over the whole analytical region or the groundwater flow systems in the shallow subsurface zone is required to establish upper boundary conditions for the groundwater flow analysis. However, detailed investigation covering the whole analytical region is difficult to achieve and, for this investigation, a sample drainage basin was therefore set up to represent the hydrological characteristics of the analytical region.

Factors that may affect the characteristics of the hydrological balance include geology (lithology), topography (undulation, water systems), overburden (land use, vegetation) and climate (precipitation, temperature, humidity, wind velocity etc.). For the analysis of a wide region, such as studies on regional groundwater flow, the accuracy of the analyses will depend on how well the data used in the analysis represent those in the region. Therefore, for setting up the sample drainage basin, the characteristics of the geology, topography and overburden of the whole Horonobe Town area were interpreted based on the existing hydrology-related literature, aerial photographs and satellite images. A representative drainage basin was then selected with wide ranging conditions and where the regional balance and hydrological characteristics such as the density of water system and other factors were taken into account. In each sample drainage basin, characteristics such as geology, topography and overburden were later converted to numerical data or categorised into patterns. For selection of the actual observation points across the typical drainage basin discussed earlier, factors such as transport access (assuming observations during the snowy season) were compared and a drainage basin where the Neogene sediments to be characterised can be found and with public roads along the river was chosen[66)].

In July 2002, the Hokushin district was selected as the URL site. With this decision, three drainage basins which enclose the URL area were selected for characterisation: the no.2 river drainage basin (P-1 drainage basin) of the Shimoebekorobetsu River basin, the Penkeebekorobetsu River basin (P-2 drainage basin) and the Shimizu River basin (P-3 drainage basin). From November 2004, the observation points were changed to the P-3, P-4 (no.1 river basin of the Shimoebekorobetsu River basin) and P-5 drainage basins (Penkeebekorobetsu River basin) which enclose the URL area, with a view to further improving the data on evapotranspiration and precipitation around the URL area (Figure 4.2.3-2).

The meteorological observations required for measuring precipitation and estimating evapotranspiration are currently being conducted at four meteorological stations in the town (the Hokushin, Toikanbetsu and Kamitoikan districts and central Horonobe) and at the Hokushin evapotranspiration observation tower (Figure 4.2.3-2). Since precipitation and evapotranspiration will vary even in a 3 km × 3 km square area (the Hokushin district), the URL area with two or more meteorological stations should be established to acquire better data.

3) Calculation of groundwater recharge rate

Figure 4.2.3-4 shows the results of river runoff and meteorological observations at the P-1, P-2 and P-3 drainage basins for one year from August 2003 to July 2004. Based on these results, the groundwater recharge rate for each drainage basin in the URL area was calculated by the hydrological balance method[68),70)].

i) Precipitation

The results of precipitation measurements at the Hokushin meteorological station in the period from August 2003 to July 2004 are shown in Figure 4.2.3-5. Since the water equivalent of the snow cover will be underestimated using a conventional hyetometer owing to the low snow catch ratio and the observation point is located in a pasture area with strong winds where the catch ratio of the hyetometer is considered to be particularly low, the precipitation was measured using a hyetometer during the non-snowy season and converted from the snow cover weight during the snowy season. As a result, the total precipitation for one year from August 2003 to July 2004 was approximately 1,620 mm and that from December 2004 to November 2005 was approximately 1,375 mm.

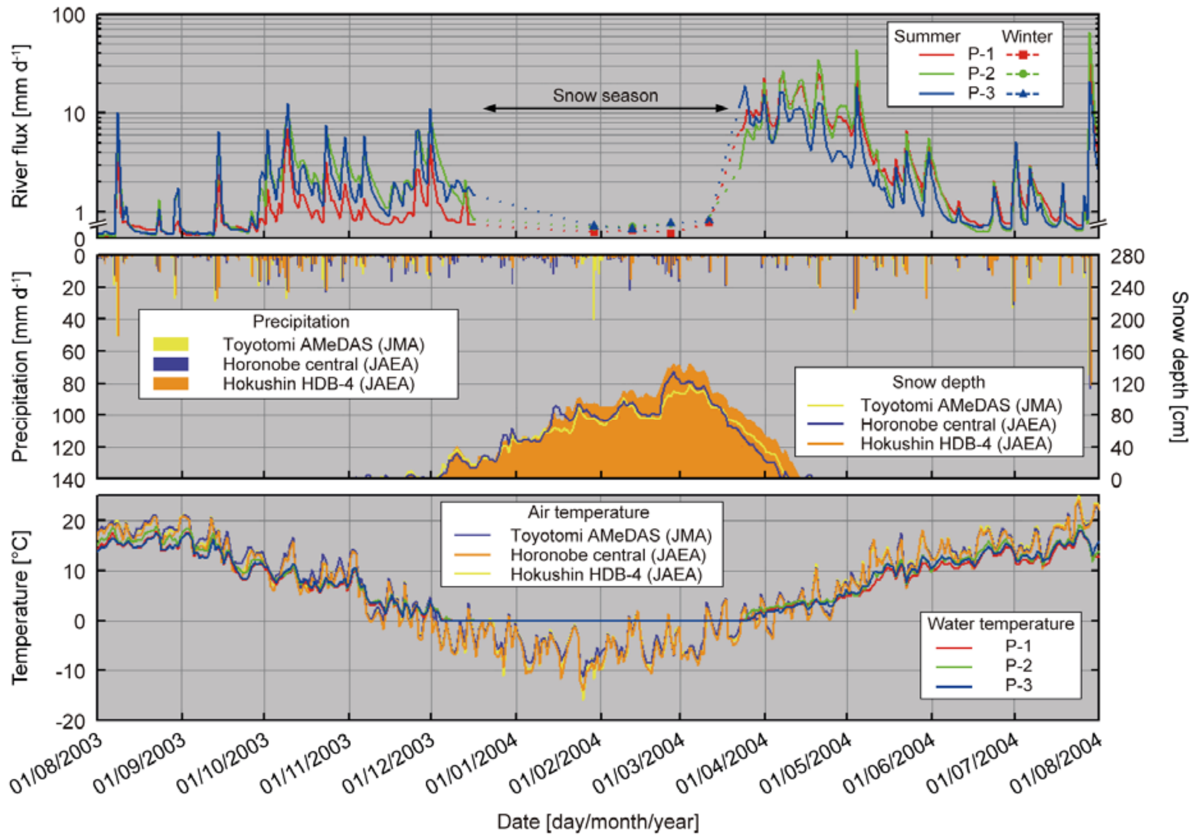

Figure 4.2.3-4 River flux and meteorological observations from August 2003 to July 2004
Observations made by the Japan Metrological Agency (JMA) and JAEA

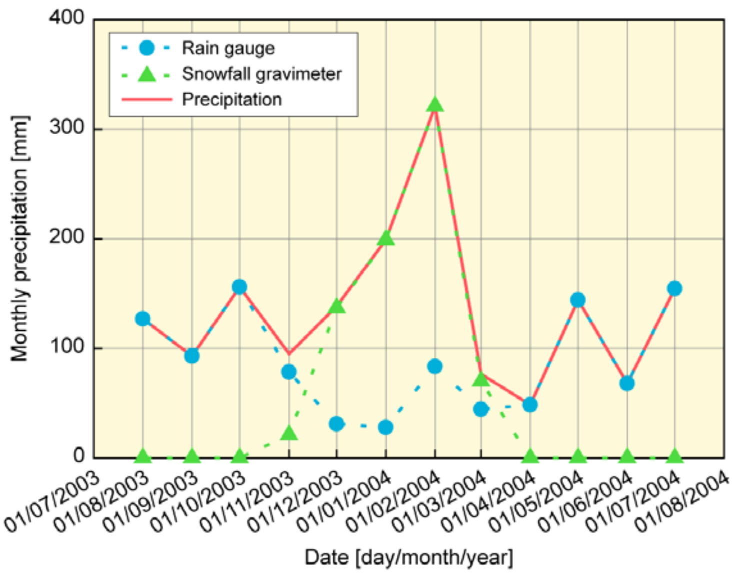

Figure 4.2.3-5 Precipitation measurements from August 2003 to July 2004

ii) Evapotranspiration

The evapotranspiration volumes in the P-1 to P-3 drainage basins from August 2003 to July 2004 were obtained by the Penman method during the non-snowy season and by the bulk method during the snowy season, using the observation results from the Hokushin meteorological station for the pasture area. As a result, the evapotranspiration volume during the year of interest was calculated as being approximately 420 mm. The evaporation volume in the P-3 to P-5 drainage basins in woodland from December 2004 to November 2005 (the period after the change of the observation points) was calculated by the Bowen ratio – energy balance method using the measurements at the Hokushin evapotranspiration observation tower. The volumes in the pasture area were calculated using the Penman method during the non-snowy season and by the bulk method during the snowy season. As a result, the total volume during the year of interest was approximately 260 mm.

iii) Height of river runoff

The height of river runoff, obtained from the river runoff divided by the drainage basin area, is a characteristic value for river runoff that can be directly compared with precipitation. The height of runoff in the P-1, P-2 and P-3 drainage basins in the period from August 2003 to July 2004 was approximately 970 mm, 1,220 mm and 860 mm respectively. The weighted average of the height of runoff considering the drainage basin area (P-1: 4.3 km^2, P-2: 19.7 km^2, P-3: 7.6 km^2, total: 31.7 km^2) was approximately 1,100 mm. The height of runoff for the P-3, P-4 and P-5 drainage basins in the period from December 2004 to November 2005 was approximately 810 mm, 800 mm and 1,070 mm respectively. The weighted average of the height of runoff considering the drainage basin area (P-3: 7.6 km^2, P-4: 2.3 km^2, P-5: 20.8 km^2, total: 30.7 km^2) was approximately 990 mm.

iv) Groundwater recharge rate

The annual groundwater recharge rate for each drainage basin was calculated by adding the monthly volumes of precipitation, river runoff and evapotranspiration for each basin around the URL area. The results are shown in Table 4.2.3-2. The groundwater recharge rate in the period from August 2003 to July 2004 for the P-1, P-2 and P-3 drainage basins were approximately 230 mm, -20 mm and 340 mm respectively, suggesting that P-1 and P-3 are recharge areas and P-2 is a discharge area. The total recharge rate across all the drainage basins was approximately 100 mm.

The groundwater recharge rates in the period from December 2004 to November 2005 for the P-3, P-4 and P-5 drainage basins were approximately 280 mm, 100 mm and 70 mm respectively, suggesting that P-3, P-4 and P-5 are all recharge areas. The total rate across all the drainage basins was approximately 120 mm.

The evapotranspiration volume was approximately 17–26% and river runoff was approximately 53–78% of the annual precipitation, as shown in Table 4.2.3-2. The groundwater recharge rates were in the range -1.1–21% of the annual precipitation and varied depending on the drainage basin. It is not confirmed at this stage whether they are caused by differences in the characteristics of the drainage basins, such as vegetation and geology, and this is an important issue to be addressed in the future.

Table 4.2.3-2 Groundwater recharge rate for each drainage basin

Measurement period		Aug 2003 ~ Jul 2004	Dec 2004 ~ Nov 2005
Annual total precipitation		1621 mm	1375 mm
P-1 (4.405 km^2)	Annual total evapotranspiration Evapotranspiration/precipitation ratio	419 mm 25.8%	–
	Annual total river runoff River runoff/precipitation ratio	965 mm 59.5%	–
	Annual total groundwater recharge rate Groundwater recharge rate/precipitation ratio	237 mm 14.6%	–
P-2 (19.747 km^2)	Annual total evapotranspiration Evapotranspiration/precipitation ratio	419 mm 25.8%	–
	Annual total river runoff River runoff/precipitation ratio	1220 mm 75.2%	–
	Annual total groundwater recharge rate Groundwater recharge rate/precipitation ratio	-17 mm -1.1%	–
P-3 (7.647 km^2)	Annual total evapotranspiration Evapotranspiration/precipitation ratio	419 mm 25.8%	281 mm 20.4%
	Annual total river runoff River runoff/precipitation ratio	860 mm 53.1%	811 mm 59.0%
	Annual total groundwater recharge rate Groundwater recharge rate/precipitation ratio	342 mm 21.1%	283 mm 20.6%
P-4 (2.315 km^2)	Annual total evapotranspiration Evapotranspiration/precipitation ratio	–	377 mm 27.4%
	Annual total river runoff River runoff/precipitation ratio	–	901 mm 65.5%
	Annual total groundwater recharge rate Groundwater recharge rate/precipitation ratio	–	97 mm 7.0%
P-5 (20.798 km^2)	Annual total evapotranspiration Evapotranspiration/precipitation ratio	–	241 mm 17.5%
	Annual total river runoff River runoff/precipitation ratio	–	1070 mm 77.8%
	Annual total groundwater recharge rate Groundwater recharge rate/precipitation ratio	–	64 mm 4.7%
Total	Annual total evapotranspiration Evapotranspiration/precipitation ratio	419 mm 25.8%	261.5 mm 19.0%
	Annual total river runoff River runoff/precipitation ratio	1098 mm 67.7%	993 mm 72.2%
	Annual total groundwater recharge rate Groundwater recharge rate/precipitation ratio	104 mm 6.4%	120.5 mm 8.8%

4) Estimation of shallow subsurface hydrological conditions

The result of about two years of manual measurements of the groundwater levels from December 2003[69] indicates that the levels in all the boreholes drop during the snowy season in winter and rise with the progress of snow melt in early spring. In addition to this annual fluctuation, a short-term fluctuation was also observed, which is assumed to be the influence of rainfall. The range of groundwater level fluctuations, with a maximum of approximately 5 m, varied depending on the location. Figure 4.2.3-6 shows a 2D cross-section of the ground surface along the Hokushin no.6 road and the groundwater level on 2nd December 2004, when the level was relatively low before snow fall, and on 2nd May 2005, when the groundwater level was high after the snow had melted. It is clear from the figure that the local groundwater divide is found near H15-1-1, although the topographical watershed is located near H15-1-4 where the groundwater level is low. When the groundwater divide and the topographical watershed are different, some correction for the drainage basin area, for example, would be required in the hydrological balance calculation.

With regard to the shallow subsurface hydrogeological structure, highly permeable zones were found to exist at depths of 12–13 m and 18–19 m; these were assumed, from the hydraulic tests in boreholes conducted in borehole HGW-1, to be either in the terrace sediments or near the boundary between the terrace sediments and intact rock. In addition, continuous monitoring of the groundwater levels confirmed the hydrological continuity of these highly permeable zones.

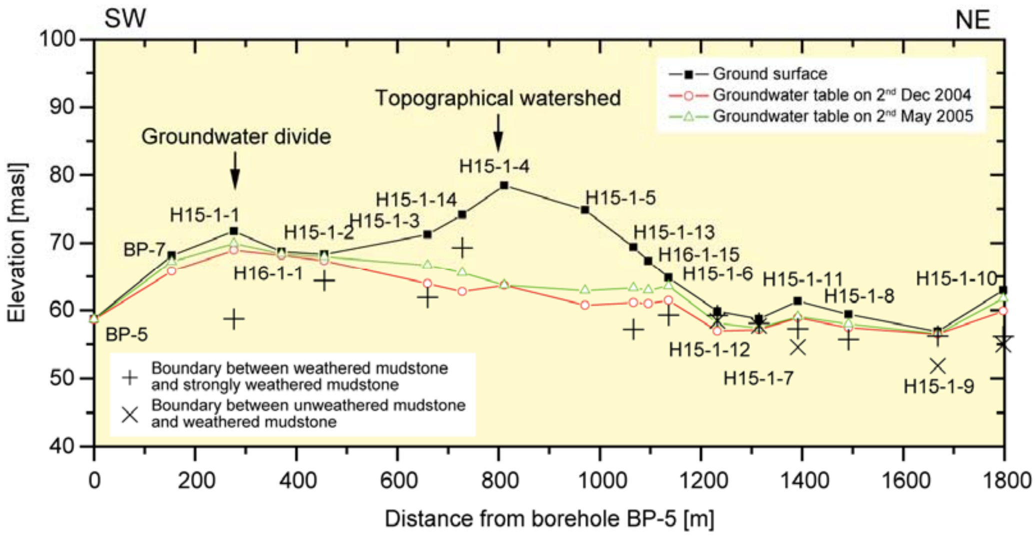

Figure 4.2.3-6 Comparison of groundwater divide and topographical watershed
Data from shallow boreholes drilled along the Hokushin no.6 road

(2) Borehole investigations

1) Investigation aims and items

The borehole investigations include flowmeter logging, flowing fluid electrical conductivity logging, hydraulic packer tests, laboratory tests on cores and long-term monitoring. Fluid logging such as flowmeter and flowing fluid electrical conductivity logging is used to evaluate potential water conducting features and solute transport pathways and their heterogeneity. Data obtained from the hydraulic tests will be used to improve the understanding of the distribution of hydraulic head, hydraulic gradients and hydraulic parameters and to present a conceptual image of groundwater flow. The laboratory tests on cores will be used primarily to determine the hydraulic parameters of the rock matrix without distinct fractures. The aim of the long-term monitoring is to acquire data on the distribution of hydraulic head and hydraulic gradients and their evolution as affected by construction of the URL.

The hydraulic test may be one of the most important investigations as it provides the hydraulic conductivity and hydraulic head. However, it is difficult to conduct hydraulic tests at varying depths with very short intervals because of limited time and funding. Therefore, it is important to acquire data efficiently using fluid logging techniques such as flowmeter logging that provide data in sequence along the borehole and by combining hydraulic test.

In this stage of the investigations, fluid logging was conducted immediately after drilling the boreholes and the sections for the hydraulic tests were selected based on the results of the fluid logging and the results of core inspections. When selecting the test intervals, the objectives of the tests, including obtaining data on the hydraulic characteristics at single points such as representative points (to determine the average hydraulic conductivity in each formation) and water conducting features, and sampling groundwater were taken into consideration. A short test interval was set up to acquire data on the hydraulic characteristics of single points such as water conducting features and a long test interval (approximately 10–150 m) was set up to acquire data on the average hydraulic conductivity in each formation. It may be desirable for the hydraulic conductivity at locations other than the hydraulic test intervals to be calculated by flowmeter logging, but the logging results were used only for the selection of the test intervals for the hydraulic tests. The reason for this is because the flowmeter logging conducted here was strongly affected by collapse of the borehole walls and by drilling mud and almost all boreholes were under artesian condition and it was difficult to calculate the overall transmissivity of the boreholes based on the recovery of the groundwater level after the fluid logging. On the other hand, the results of the flowing fluid electrical conductivity logging conducted in borehole HDB-11 could be used for identifying water conducting features and calculating the transmissivity of them[71)].

Hydraulic tests in the laboratory using core specimen were conducted with the aim of obtaining data on the hydraulic conductivities of rock matrices and complementing the single-hole hydraulic tests in boreholes. Also, in borehole HDB-10, a measurement of the flow direction and velocity of the groundwater in the deep sedimentary formations was conducted using an instrument for measuring very low velocities of 10^{-10}–10^{-5} m s^{-1}. The investigations conducted in each borehole are listed in Table 4.2.3-3[42),56),57),72)–80)].

2) Investigation methods

The subsurface environment of the Horonobe area includes sedimentary rock formations and borehole walls therefore tend to collapse relatively easily. Groundwater is saline and contains dissolved gases. Investigations were pursued in parallel with technology development for application under these conditions. The approach of reducing uncertainties with the progress of the investigations therefore included not only the accumulation of data but also improvement of investigation techniques and their reliability.

The collapse of borehole walls leads to enlargement of the borehole diameter, which makes evaluation of the logging and the hydraulic test results difficult. In addition, the positioning of packers for the hydraulic tests and monitoring of water pressure and chemistry would be restricted and, in the worst case, the investigations might become impossible. For these reasons, drilling mud is used in most stages to decrease the collapse of the borehole wall. However, the drilling mud adheres to the borehole walls and cannot be completely washed off, even though it is replaced by fresh water in the test intervals when logging and the hydraulic test are being conducted. The residual drilling mud may cause disturbance of the data from flowmeter and temperature logging.

When drilling mud was used, the hydraulic tests were conducted based on pumping and drawdown because injection or pressurisation would cause clogging. However, interpretation of the test results may be difficult owing to bubbling of dissolved gases and, in the worst case, the tests will be impossible owing to gas discharge.

Table 4.2.3-3 Hydrogeological investigations in each borehole

Borehole	Flow meter logging (FM) FEC logging (FEC) intervals [mbgl]	Number of in situ hydraulic tests	Number of laboratory hydraulic tests	Long-term monitoring; Number of pressure sensors/ports	Other tests	References
HDB-1	55.0–136.0 (FM) 55.0–206.0 (FM) 191.2–415.2 (FM) 400.0–630.0 (FM)	2	4	MP 4/15		Yamamoto et al.[56)] Yabuuchi et al.[72)]
HDB-2	49.2–403.5 (FM) 399.2–700.0 (FM)	3	4	SPMP 7/7		Yamamoto et al[57)] Yabuuchi et al.[72)]
HDB-3	50.0–307.0 (FM) 250.0–512.0 (FM)	4	13	MP 6/13		Yamamoto et al.[73)] Yabuuchi et al.[72)]
HDB-4	50.0–310.0 (FM) 250.0–512.0 (FM)	4	14 fracture: 9 matrix: 9	MP –/13		Yamamoto et al.[74)] Shimo et al.[75)]
HDB-5	40.0–271.2 (FM/static) 200.0–512.0 (FM)	4	13	–		Yamamoto et al.[76)]
HDB-6	20.0–133.0 (FEC) 50.0–307.0 (FM) 120.0–360.0 (FM) 132.9–360.0 (FEC) 350.0–606.0 (FM)	7	4 fracture: 2 matrix: 4	MP 11/11		Yamamoto et al.[77)] Yabuuchi et al.[72)] Shimo and Kumamoto[78)]
HDB-7	301.2–501.0 (FM)	6	4 matrix: 4	MP 9/9		Yamamoto et al.[79)] Yabuuchi et al.[72)] Shimo and Kumamoto[78)]
HDB-8	20.0–111.2 (FM) 100.0–302.0 (FM) 280.0–463.0 (FM)	7	–	MP 9/9		Yamamoto et al.[80)] Yabuuchi et al.[72)]
HDB-9	25.5–125.0 (FM) 124.2–257.5 (FM) 256.2–520.0 (FM)	8	–	MP 9/11		
HDB-10	24.67–136.0 (FM) 135.08–298.0 (FM) 297.1–500.0 (FM)	9	–	Piezo 11/11	Groundwater velocity and direction measurement	Matsui et al.[42)]
HDB-11	151.95–440.0 (FM) 153.0–453.0 (FEC) 451.6–784.0 (FM) 453.0–803.0 (FEC) 801.0–1005.0 (FM)	12	12	MP 15/19		

In order to resolve the conflict between clogging caused by the increase in pressure and the release of dissolved gas caused by a decrease in pressure, a series of tests were performed by combining two or more test methods based on pumping and drawdown. First, the hydraulic conductivity in the test intervals was determined roughly and the release of dissolved gas associated with a reduction in the pressure was checked by a test which should be minimally influenced by the reduction in pressure (e.g. a pulse test); the differential water pressure was then determined for the subsequent tests to minimise the deterioration in the quality of the test data owing to the release of dissolved gas[81)].

For selection of the intervals for the hydraulic tests, the flowing fluid electrical conductivity was more beneficial for determining inflow points of the groundwater than the flow velocity in the boreholes obtained by flowmeter logging. The flowing fluid electrical conductivity logging was also useful because of the high contrast in electrical conductivity between the saline groundwater (high electrical conductivity) and the borehole water replaced with fresh water (low electrical conductivity).

3) Selection of investigation intervals

During the investigations conducted in boreholes HDB-1 and HDB-2 in 2001, no major loss of circulation or inflow was observed. In addition, no groundwater seepage points were identified in the flowmeter logging. Based on the above results and considering the purpose of obtaining the average hydraulic conductivity to be used in selection of the URL area, the hydraulic test intervals were selected to be in a zone representing the geology of interest and including fractures as well as rock matrix. During the investigations in borehole HDB-4 in 2002, large loss of circulation occurred during drilling (at a depth of 218.45–236.53 m) and this depth was therefore selected as the test interval. A damaged zone of the Omagari Fault was observed at a depth of 380 m or more in borehole HDB-4. At other depths in boreholes HDB-3 to HDB-5 where investigations were conducted in the 2002, the points where changes in the temperature and resistivity of the borehole water were observed during the temperature and flowmeter logging were selected. In the flowmeter logging conducted before 2002, interpretation of the abnormal values was difficult owing to the residues of drilling mud, even after replacement with fresh water. For the investigations in boreholes HDB-6 to HDB-8 in 2003, the test intervals were selected to clarify the variability of hydraulic conductivity and obtain groundwater samples in the zone where abnormal values were detected during flowmeter logging. As the relationship between fractured zones (minor fault zones) and hydraulic conductivity has been established from the results of the hydraulic tests and geological investigations in boreholes HDB-1 to HDB-8, the test intervals were selected to understand the characteristics of the groundwater flow at the points assumed to be fractured zones and points which do not contain such zones in boreholes HDB-9 to HDB-11, where tests were conducted after 2004.

Long-term hydraulic monitoring systems were installed in boreholes HDB-1, HDB-2, HDB-3, HDB-6, HDB-7, HDB-8, HDB-9, HDB-10 and HDB-11 (installed in February 2007). None were installed in boreholes HDB-4 and HDB-5 because of long-term hydrochemical monitoring (HDB-4) and other future investigations (HDB-5).

4) Investigation results

i) Hydraulic conductivity

The hydraulic conductivities obtained from the hydraulic tests were plotted against depths from the ground surface, as shown in Figure 4.2.3-7. The variability of hydraulic conductivity was relatively small in the Yuchi and Koetoi Formations, while hydraulic conductivities in the Wakkanai Formation varied widely in the order of 10^{-12}–10^{-5} m s^{-1}. However, it may not be appropriate to discuss the results statistically because the hydraulic tests did not cover all the drilled sections and the test intervals were selected intentionally as described above. There seems to be an inverse correlation between depth and hydraulic conductivity in every formation but the correlation is fairly low in the Koetoi and Yuchi Formations. In particular, the rate of change of hydraulic conductivity with depth is much greater in the Wakkanai Formation than that in the Koetoi and Yuchi Formations. At the same depth the hydraulic conductivities of the overlying formations are lower, for example, being lower in the Koetoi Formation than in the Wakkanai Formation. All the hydraulic conductivity values obtained in situ are listed in Table 4.2.3-4.

The hydraulic conductivities obtained from the laboratory tests were plotted against porosity (Figure 4.2.3-8) and were found to correlate well with the porosity irrespective of whether they were from the Wakkanai Formation or the Koetoi Formation.

Below are the findings that would be particularly important for clarifying the hydraulic characteristics of the rock formations in the Horonobe area (see Appendix 5):

- Hydraulic conductivity tends to be higher in the shallower zone of the Wakkanai Formation. No obvious differences in lithofacies and development of fractures were observed between the shallower and deeper zones of the Wakkanai Formation.
- The hydraulic conductivities obtained via borehole tests and those from the laboratory hydraulic tests showed approximately the same values in the Yuchi Formation. The values from the in situ tests tend to be much higher in the Wakkanai Formation. The values in the Koetoi Formation lay between the values in the other two formations.
- There was a section/point where the hydraulic conductivity was very high around a depth of 280–290 m in borehole HDB-4, which was confirmed by the flowmeter logging and the temperature logging as being an obvious anomaly. There was also a section where the hydraulic conductivity was very high around a depth of 218–236 m, but no obvious anomaly was observed in the flowmeter logging. The difference in hydraulic head in the two highly permeable zones was as large as several tens of metres, implying no connectivity between them.
- There were highly permeable sections/points around depths of 295–305 m and 392 m in borehole HDB-6, which were confirmed by the flowmeter and flowing fluid electrical conductivity logging to be obvious anomalies.
- There were highly permeable sections/points around depths of 176 m and 206 m in borehole HDB-8. Since the hydraulic heads were the same, these sections/points may be connected.
- There was a highly permeable section/point around a depth of 245 m in borehole HDB-9. This was confirmed by the flowmeter logging.
- Minor faults at a high angle to the bedding plane were dominant at the highly permeable points.
- Hydraulic conductivity suddenly dropped around a depth of 700 m or more in borehole HDB-11. There was no difference in lithofacies and fracture distribution in the zones above or below this depth.

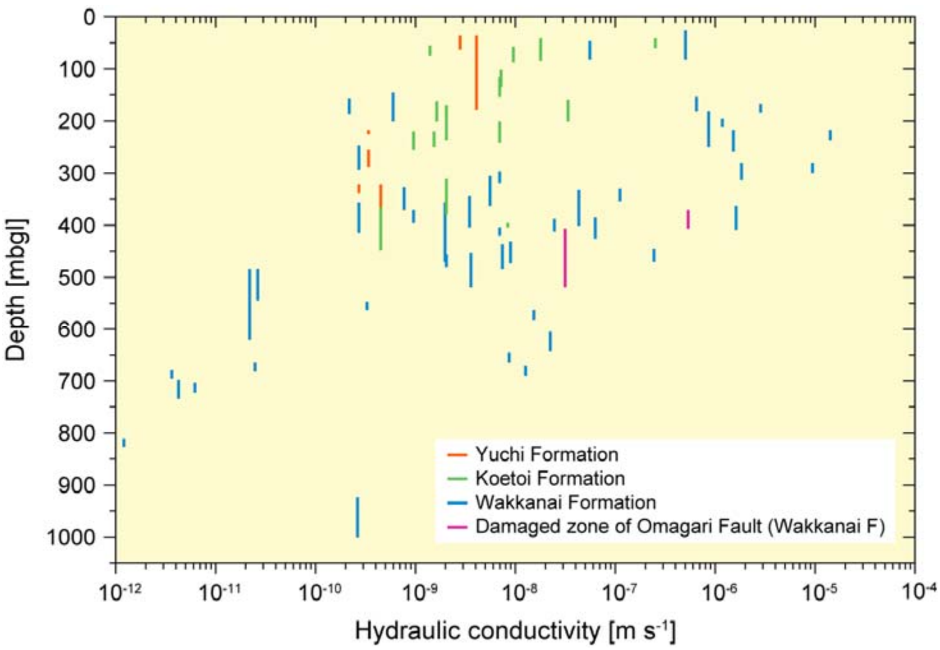

Figure 4.2.3-7 Hydraulic conductivities derived from hydraulic tests in boreholes

Table 4.2.3-4 Hydraulic conductivities and heads obtained via borehole hydraulic tests

Borehole	Interval depth [mbgl]	Interval length [m]	Geology	Transmissivity [$m^2\ s^{-1}$]	Hydraulic conductivity [$m\ s^{-1}$]	Hydraulic head [mbgl]
HDB-1	370.00 – 395.00	25.00	Wakkanai F	2.43×10^{-8}	9.70×10^{-10}	4.00
	548.00 – 563.19	15.19	Wakkanai F	5.00×10^{-9}	3.29×10^{-10}	-0.70
HDB-2	344.90 – 404.90	60.00	Wakkanai F	2.10×10^{-7}	3.50×10^{-9}	-43.00
	666.50 – 682.69	16.19	Wakkanai F	3.97×10^{-10}	2.45×10^{-11}	-147.00
	679.50 – 695.69	16.19	Wakkanai F	5.84×10^{-10}	3.61×10^{-11}	-115.07
HDB-3	160.50 – 200.45	39.95	Koetoi F	1.34×10^{-6}	3.35×10^{-8}	-1.37
	201.95 – 241.90	39.95	Koetoi F	2.81×10^{-7}	7.03×10^{-9}	-3.31
	394.98 – 405.00	10.02	Koetoi F	8.48×10^{-8}	8.46×10^{-9}	-7.28
	454.50 – 520.00	65.50	Wakkanai F	2.36×10^{-7}	3.60×10^{-9}	-8.44
HDB-4	218.45 – 236.53	18.08	Wakkanai F	2.55×10^{-4}	1.41×10^{-5}	3.28
	281.45 – 299.53	18.08	Wakkanai F	1.69×10^{-4}	9.35×10^{-6}	-8.87
	371.90 – 406.43	34.53	Omagari Fault damaged zone	1.85×10^{-5}	5.36×10^{-7}	-11.07
	407.90 – 520.00	112.10	Omagari Fault damaged zone	3.52×10^{-6}	3.14×10^{-8}	-9.85
HDB-5	154.05 – 180.46	26.41	Wakkanai F	1.71×10^{-5}	6.47×10^{-7}	-18.00
	182.05 – 250.46	68.41	Wakkanai F	5.80×10^{-5}	8.48×10^{-7}	-20.04
	331.22 – 402.23	71.01	Wakkanai F	3.12×10^{-6}	4.39×10^{-8}	-11.49
	404.74 – 420.19	15.45	Wakkanai F	1.08×10^{-7}	7.01×10^{-9}	-8.80
HDB-6	41.54 – 84.59	43.05	Koetoi F	7.75×10^{-7}	1.80×10^{-8}	2.14
	218.95 – 250.00	31.05	Koetoi F	4.72×10^{-8}	1.52×10^{-9}	-6.18
	280.95 – 312.00	31.05	Wakkanai F	5.68×10^{-5}	1.83×10^{-6}	-7.58
	363.95 – 409.00	45.05	Wakkanai F	7.39×10^{-5}	1.64×10^{-6}	-7.62
	437.95 – 483.00	45.05	Wakkanai F	3.30×10^{-7}	7.32×10^{-9}	-2.65
	484.95 – 545.00	60.05	Wakkanai F	1.57×10^{-9}	2.61×10^{-11}	-13.37
	484.95 – 620.00	135.05	Wakkanai F	2.93×10^{-9}	2.17×10^{-11}	-10.16
HDB-7	36.36 – 62.91	26.55	Yuchi F	7.33×10^{-8}	2.76×10^{-9}	-0.05
	36.36 – 178.00	141.64	Yuchi F	5.69×10^{-7}	4.02×10^{-9}	0.81
	216.30 – 225.42	9.12	Yuchi F	3.06×10^{-9}	3.35×10^{-10}	-16.18
	256.66 – 287.71	31.05	Yuchi F	1.04×10^{-8}	3.34×10^{-10}	-20.56
	321.21 – 338.86	17.65	Yuchi F	4.85×10^{-9}	2.75×10^{-10}	-18.87
	321.23 – 447.00	125.77	Yuchi F and Koetoi F	5.62×10^{-8}	4.47×10^{-10}	-16.47
HDB-8	57.50 – 89.05	31.55	Koetoi F	3.01×10^{-7}	9.54×10^{-9}	7.38
	168.01 – 184.06	16.05	Wakkanai F	4.59×10^{-5}	2.86×10^{-6}	6.80
	196.01 – 212.06	16.05	Wakkanai F	1.89×10^{-5}	1.18×10^{-6}	6.84
	247.01 – 295.06	48.05	Wakkanai F	1.29×10^{-8}	2.69×10^{-10}	1.90
	303.97 – 362.02	58.05	Wakkanai F	3.29×10^{-7}	5.67×10^{-9}	0.24
	355.97 – 414.02	58.05	Wakkanai F	1.57×10^{-8}	2.71×10^{-10}	-3.99
	355.97 – 470.00	114.03	Wakkanai F	2.27×10^{-7}	1.99×10^{-9}	1.22
HDB-9	25.50 – 82.60	57.10	Wakkanai F	2.86×10^{-5}	5.00×10^{-7}	22.47
	46.37 – 82.60	36.23	Wakkanai F	2.04×10^{-6}	5.64×10^{-8}	26.39
	144.97 – 202.02	57.05	Wakkanai F	3.43×10^{-8}	6.02×10^{-10}	21.53
	157.90 – 187.95	30.05	Wakkanai F	6.55×10^{-9}	2.18×10^{-10}	20.60*
	216.90 – 257.50	40.60	Wakkanai F	6.09×10^{-5}	1.50×10^{-6}	20.31
	326.97 – 370.02	43.05	Wakkanai F	3.28×10^{-8}	7.62×10^{-10}	17.59
	383.97 – 427.02	43.05	Wakkanai F	2.69×10^{-6}	6.25×10^{-8}	16.90*
	430.97 – 474.02	43.05	Wakkanai F	3.84×10^{-7}	8.91×10^{-9}	15.45
HDB-10	41.33 – 59.88	18.55	Koetoi F	4.70×10^{-6}	2.53×10^{-7}	0.62
	101.33 – 136.00	34.67	Koetoi F	2.46×10^{-7}	7.09×10^{-9}	-1.60
	162.84 – 199.89	37.05	Koetoi F	6.11×10^{-8}	1.65×10^{-9}	-3.48*
	219.34 – 256.39	37.05	Koetoi F	3.51×10^{-8}	9.48×10^{-10}	-4.82*
	295.91 – 319.96	24.05	Wakkanai F	1.66×10^{-7}	6.91×10^{-9}	-1.36
	329.91 – 353.96	24.05	Wakkanai F	2.69×10^{-6}	1.12×10^{-7}	-1.32
	387.91 – 411.96	24.05	Wakkanai F	5.99×10^{-7}	2.49×10^{-8}	-1.54
	445.84 – 469.89	24.05	Wakkanai F	5.87×10^{-6}	2.44×10^{-7}	-5.22
	457.34 – 481.39	24.05	Wakkanai F	4.91×10^{-8}	2.04×10^{-9}	-0.62
HDB-11	55.50 – 75.55	20.05	Koetoi F	2.60×10^{-7}	6.96×10^{-9}	0.98
	115.58 – 153.00	37.42	Koetoi F	2.77×10^{-8}	1.38×10^{-9}	0.11
	171.00 – 237.05	66.05	Koetoi F	1.37×10^{-7}	2.07×10^{-9}	-0.14
	311.00 – 380.05	69.05	Koetoi F	1.40×10^{-7}	2.03×10^{-9}	-3.79
	564.00 – 584.05	20.05	Wakkanai F	3.07×10^{-7}	1.53×10^{-8}	-5.51
	606.00 – 644.05	38.05	Wakkanai F	8.60×10^{-7}	2.26×10^{-8}	-5.57
	646.00 – 666.05	20.05	Wakkanai F	1.76×10^{-7}	8.78×10^{-9}	-5.76
	670.00 – 690.05	20.05	Wakkanai F	2.51×10^{-7}	1.25×10^{-8}	-5.08
	697.00 – 735.05	38.05	Wakkanai F	1.61×10^{-10}	4.22×10^{-12}	-11.21*
	704.00 – 724.05	20.05	Wakkanai F	1.25×10^{-10}	6.25×10^{-12}	-14.79
	812.00 – 828.05	16.05	Wakkanai F	1.96×10^{-11}	1.22×10^{-12}	-37.42*
	923.00 – 1000.10	77.10	Wakkanai F	2.01×10^{-8}	2.61×10^{-10}	-41.99

*Unstable when measured

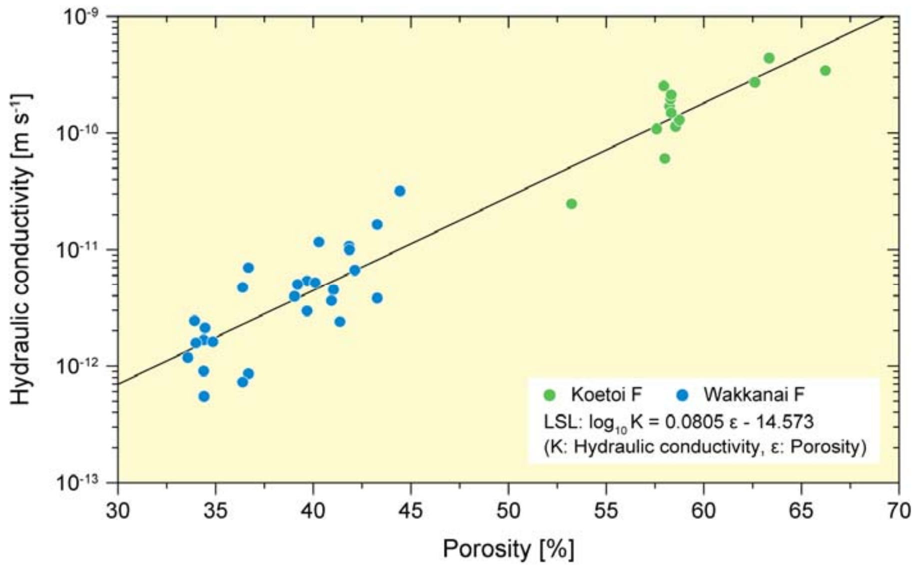

Figure 4.2.3-8 Correlation between hydraulic conductivity and porosity

Data obtained from laboratory measurements on core samples

ii) Hydraulic head/hydraulic gradient

The relationship between the hydraulic heads obtained from the hydraulic tests (Table 4.2.3-4) and the elevation of the borehole mouth is shown in Figure 4.2.3-9. This figure indicates that the distribution of hydraulic head in the formations is correlated with elevation (or topography) and tends to be slightly higher (pressurised) than the elevation of the borehole mouth. One possible explanation could be that the hydraulic head distribution is governed primarily by the topographical gradient and most boreholes were located at a relatively low elevation. The hydraulic head was higher in borehole HDB-2 compared to other boreholes and reached as high as +180 m elevation (+140 m above the ground surface) at around 700 m depth. Also, it was high in the low conductivity zone deeper than approximately 700 m in borehole HDB-11. These facts suggest that the hydraulic head remains high in the deeper zone.

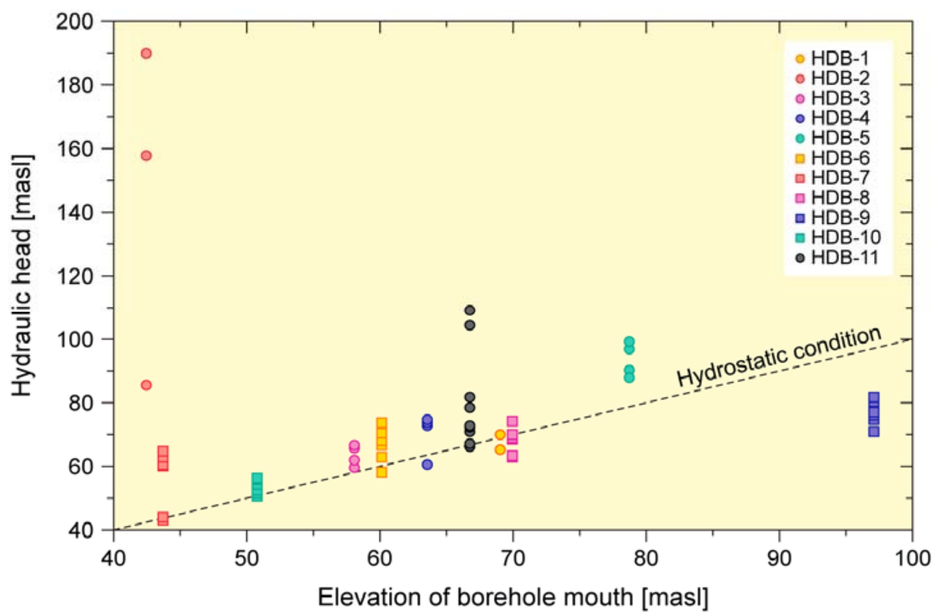

Figure 4.2.3-9 Correlation between hydraulic head and the elevation of borehole mouth

The 3D distribution of hydraulic head obtained by interpolation and extrapolation of measured data is shown in Figure 4.2.3-10. It can be seen from this figure that the general trend of the hydraulic gradient is from east to west and the hydraulic gradients in the direction from boreholes HDB-5 to HDB-4 or HDB-8 were particularly high.

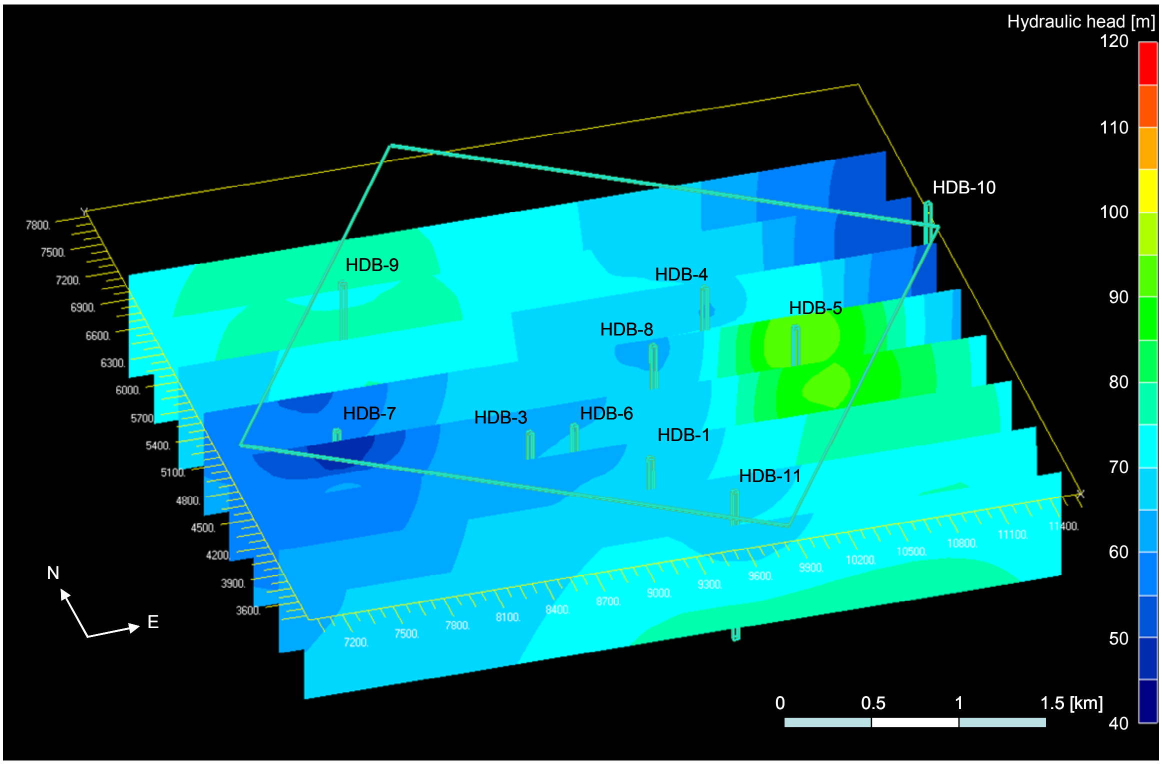

Figure 4.2.3-10 Distribution of hydraulic head estimated by interpolation/extrapolation

iii) Hydrogeological significance of fracture zone

Hydraulic conductivities of fracture zones (or fault zones) were examined using data obtained in boreholes HDB-1 to HDB-8[82]. For the Wakkanai Formation, where hydraulic conductivities show a wide distribution, it was found that the hydraulic properties of the entire formation were significantly affected by the variability of hydraulic conductivity in the test intervals including the fracture zone.

For the Koetoi Formation, no significant difference in the hydraulic conductivity with or without fracture zones was observed. However, a high hydraulic conductivity was seen in the section where fractures prevailed in the shallow zone of borehole HDB-10, indicating that the relationship between fracture zone and hydraulic conductivity also cannot be ignored for the Koetoi Formation.

There were no fracture zones in the Yuchi Formation. Since the variability of hydraulic conductivity was small in the Yuchi Formation and the in situ hydraulic conductivity was not significantly different from that obtained from the laboratory hydraulic tests, the relationship between fracture zone and hydraulic conductivity in the formation is assumed to be insignificant.

iv) Quality of borehole investigations

A composite log would be useful for comparing anomalies in the data and the distribution of hydraulic conductivity and hydraulic head, which were obtained from various logging runs. Detailed comparison of the anomalies obtained from the different logging and test results, water pressures obtained from the hydraulic tests and long-term monitoring and hydraulic conductivities determined from the logging and the hydraulic tests would ensure the quality of the loggings and the tests.

As an example, a composite log of the results from flowmeter logging, flowing fluid electrical conductivity logging, hydraulic tests, laboratory hydraulic tests and long-term monitoring of water pressure in boreholes HDB-6 and HDB-11 is shown together with the fracture density from core observation and the results of temperature logging in Figures 4.2.3-11 and 4.2.3-12 respectively. At depths of around 300 m and 400 m in borehole HDB-6, highly permeable sections were identified, with a hydraulic conductivity of about 10^{-6} m s^{-1}. In addition, at a depth of around 550–700 m in borehole HDB-11, relatively highly permeable sections/points were observed. The flowmeter logging detected a change in the flow velocity around 400 m deep in borehole HDB-6, but anomalies in the flowmeter logging and temperature logging were not obvious at other depths. This suggests that, because of a clear contrast in electrical conductivity between outside the borehole (saline groundwater) and inside the borehole (fresh water), the anomalies in the electrical conductivity profile would be more appropriate for detecting inflow points. The high fracture density sections did not necessarily coincide with the highly permeable sections/points, although, as discussed above, a correlation between minor fault zones and hydraulic conductivity was likely.

The hydraulic conductivities obtained from the laboratory hydraulic tests and single-hole hydraulic tests were very different for all the boreholes except HDB-7 where the relatively homogeneous Yuchi Formation was investigated. The differences in the hydraulic conductivities determined in the laboratory and via borehole tests for the Wakkanai and Koetoi Formations were assumed to be the fact that the laboratory values were for matrix parts while in situ values were for fracture zones. This suggests that the Wakkanai and Koetoi Formations should be regarded as fractured media in terms of hydrogeology.

The hydraulic head values obtained during the hydraulic tests and the long-term monitoring were almost the same for all the boreholes. This suggests that the hydraulic head values obtained by the above testing and logging were appropriate.

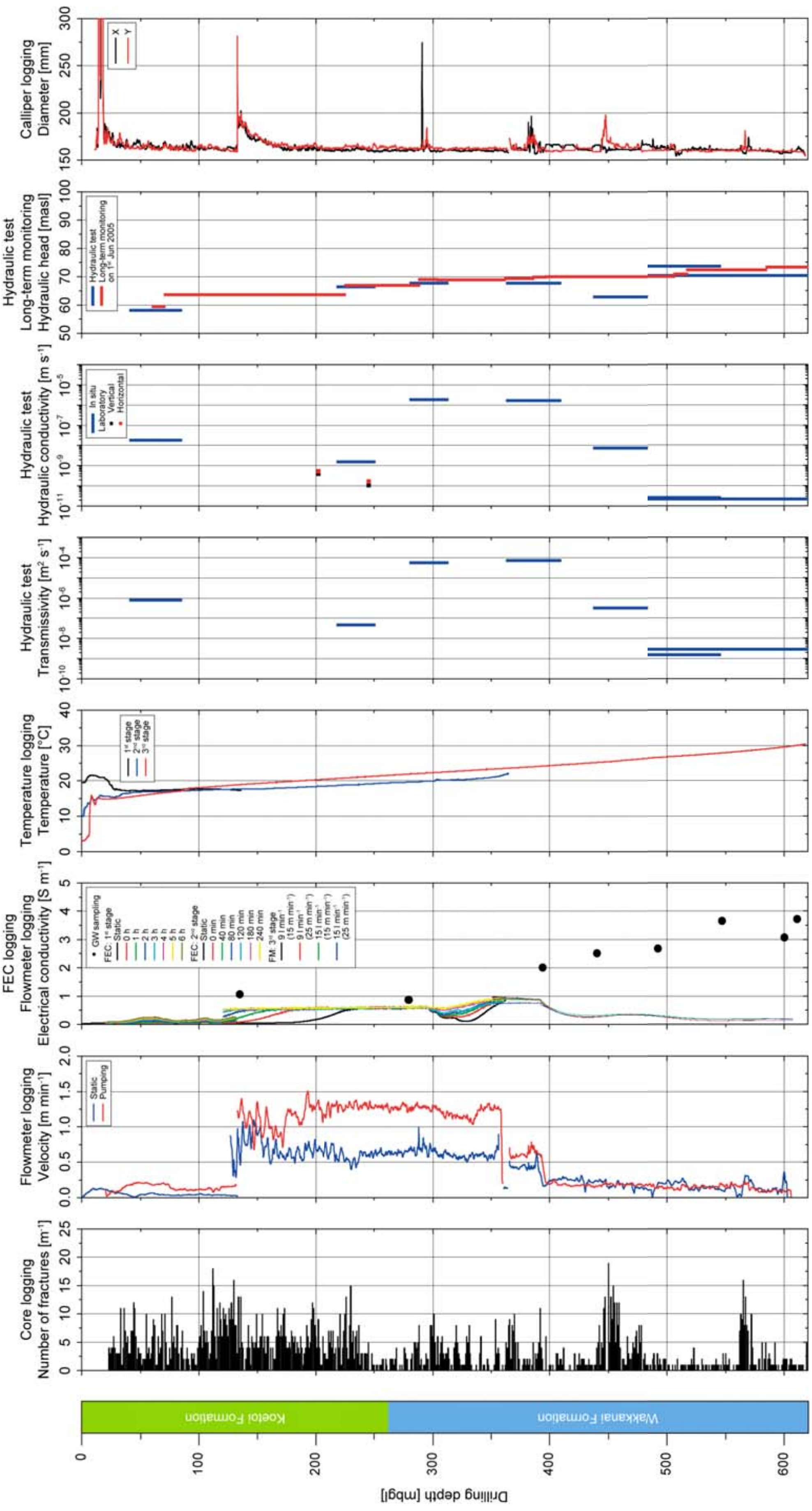

Figure 4.2.3-11 Composite log for borehole HDB-6

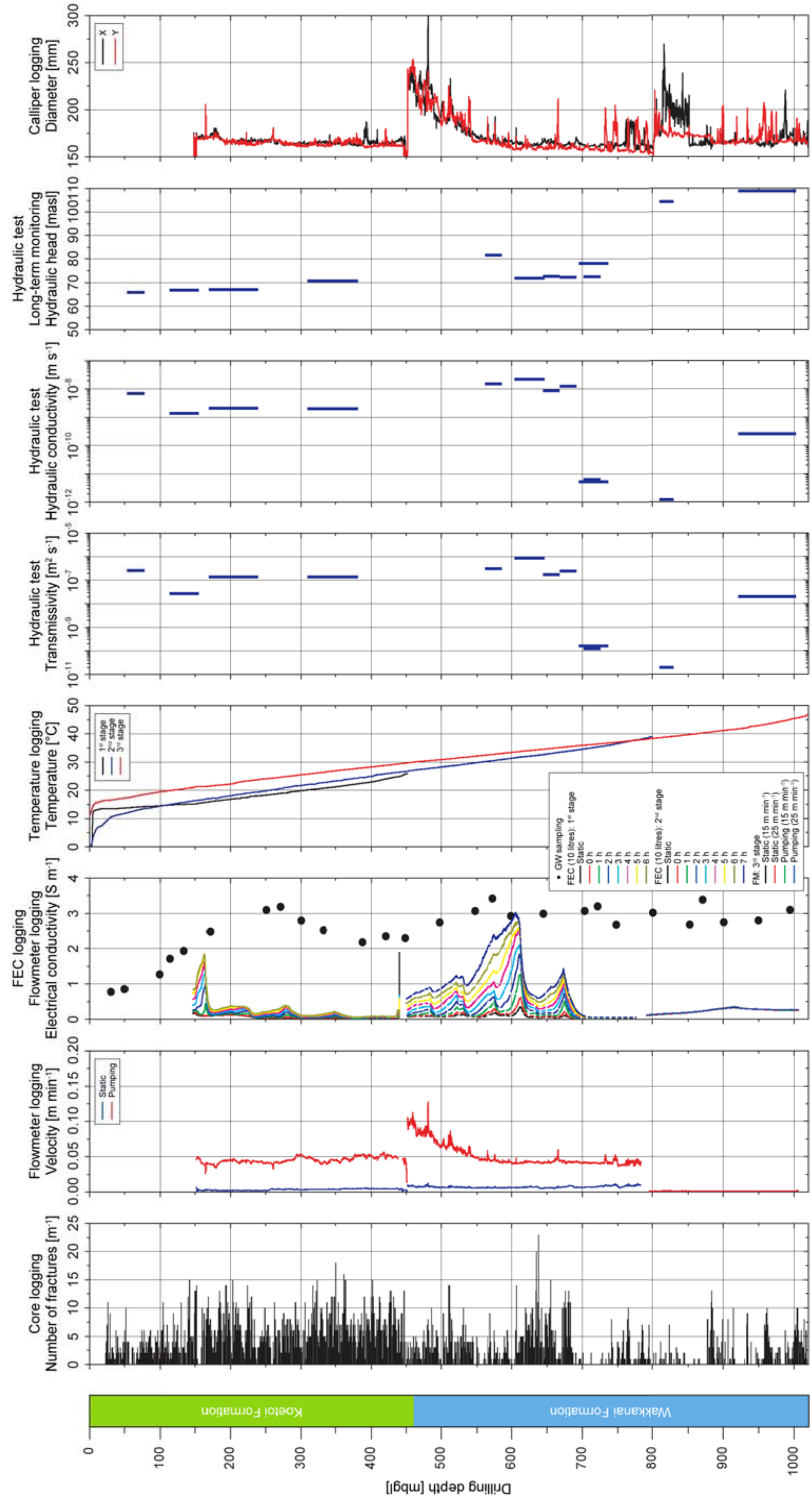

Figure 4.2.3-12 Composite log for borehole HDB-11

4.2.4 Hydrogeological modelling

(1) Approach to modelling hydrogeological structure

The aims of modelling hydrogeological structure and analysing groundwater flow are to enhance the understanding of the characteristics of groundwater flow in and around the URL area by integrating and interpreting the above investigations in order to predict the evolution of the groundwater flow system associated with the construction of the underground facilities and to make proposals for how to conduct investigations efficiently and systematically in Phase II and/or Phase III as development of the methodologies for understanding a groundwater flow field in the geological disposal project. It is of importance to present specific examples of updating of the models and reduction of uncertainties with the progress of the investigations for reviewing the applicability of the safety assessment techniques.

In the Mizunami URL project, a process for reducing model uncertainties has been proposed, involving an iterative approach based on an investigation – modelling – analysis cycle[82)]. In Sweden, an investigation/modelling process is being used for potential repository sites at Forsmark and Simpevarp, in which a database of investigation results are frozen at a certain point in time and models are developed based on the frozen database and subsequently revised[83),84)]. In the Horonobe URL project, modelling and analysis has been updated almost every year based on the most recent data available[53),62),85)–88)]. Table 4.2.4-1 shows the evolution of the major hydrogeological structure models with the progress of the investigations from the time of selecting the URL site to the completion of Phase I. The models shown here represent the final state of modelling and analysis[53),88)] for Phase I, based on the investigations up to and including those in 2005. Modelling and analysis of groundwater flow focussing on the present groundwater flow system is described in this section and an analysis aimed at predicting the evolution of the groundwater flow system associated with the construction of the URL is presented in Subsection 4.6.3.

At the time of selecting the URL area and site and before the model presented in Subsection 4.2.2 was developed, a sensitivity analysis was conducted for an area of 50 km × 50 km square covering the whole area of Horonobe Town and the hydraulic head and the groundwater streamlines were examined for the four potential URL areas[63),64)]. Although the results were not taken into account in the selection of the URL area and URL site, a sensitivity analysis would be beneficial at the selection stage for predicting the outlines of the groundwater flow system in this area.

Other studies now being conducted include development and application of a technique for predicting the distribution of the hydraulic conductivity from the water pressure distribution[89),90)], focussing on abnormally high pressure such as observed in borehole HDB-2, and analyses taking the mechanical influence of water pressure into account. Toida et al.[91)] and Takase et al.[92)] have developed alternative models as part of their studies aimed at ensuring model reliability.

Model development should be pursued together with studies on the long-term stability of the geological environment, because the hydrochemical and hydraulic conditions generated through environmental evolution in the deep sedimentary formations. Against this background, integration and analysis of information on natural phenomena that are presumed to affect the geological environment on the long-term, such as groundwater flow, are currently being conducted[93)]. The process whereby the saline groundwater system confined during sedimentation is mixed with rain water over a long time period is also described analytically in order to review the consistency between actual measurements and the analysis of distribution of the groundwater chemistry[62),94)]. Such an approach, combining groundwater flow and advection – dispersion of the dissolved components, will be critical not only for explanation of the water chemistry distribution, but also for improvement of confidence in the groundwater flow analysis.

Table 4.2.4-1 Progress of hydrogeological modelling and simulation in Phase I

Financial year	Investigations	Characteristics defined (events considered)	Hydrogeological models and groundwater flow analyses (grey cells for models described in this report)	Scale	Issues to be addressed in the next investigations; feedback from groundwater flow analyses
Before 2002	- Existing information - HDB-1/2		Sensitivity analyses for the potential URL areas[63),64)]	Regional scale (ca. 50 km × 50 km square)	Hydraulic conductivities of shallower formations and fault, groundwater table, groundwater age, infiltration rate, depth dependency and anisotropy of hydraulic conductivities and distribution of groundwater salinity
2002		(URL area selected)	Sensitivity analyses for the URL area[62)]	Regional scale	Hydraulic conductivities of the Wakkanai and Koetoi Formations (sensitive on the migration time of groundwater flow), infiltration rate and hydraulic conductivity of shallower formations (sensitive on the hydraulic head)
	- HDB-3/4/5	Variability and depth profiles of hydraulic conductivities			
2003	- HDB-6/7/8 - AMT survey - Runoff (P-1/2/3) - Meteorology - Surface gas	Hydraulic conductivity of fracture zone in the Wakkanai Formation (Location of the Omagari Fault defined)	Sensitivity analyses considering variability and depth profiles of rock hydraulic conductivities; data from HDB-1 to HDB-8[85)]	Local scale (ca. 20 km × 20 km square) Site scale (ca. 3 km × 3 km square)	Consistency with groundwater chemistry (e.g. distribution of groundwater salinity)
2004	- HDB-9/10/11 - Runoff (P-3/4/5) - Evapotranspiration - Groundwater table	Infiltration rates at P-1/2/3 basins	Groundwater flow analysis considering variability and depth profiles of rock hydraulic conductivities, fracture zone hydraulic conductivities in the Wakkanai Formation, infiltration rates and location of the Omagari Fault; data from HDB-1 to HDB-8[87)]	Local scale	
2005	- HDB-11 - Stripping - Hydrology	(Minor fault zone defined)	Groundwater flow analysis considering variability and depth profiles of rock hydraulic conductivities, hydraulic conductivities of minor fault zone in the Wakkanai and Koetoi Formations, infiltration rates and location of the Omagari Fault; data from HDB-1 to HDB-11; prediction of the impact of the construction of the underground facilities on the hydrogeological environment[53)]	Local scale Site scale (ca.4 km × 8 km)	Distribution and hydraulic properties of minor fault zones especially in the Wakkanai Formation (large impact on the amount of groundwater inflow into the underground facilities)
			Sensitivity analyses considering variability and depth profiles of hydraulic conductivities and location of the Omagari Fault; data from HDB-1 to HDB-8 (fracture zone considered implicitly)[62)]	Local scale	
		(Phase I ended; Phase II started)	Optimisation of analysis; data from HDB-1 to HDB-11[88)]	Local scale	Heterogeneity of hydraulic conductivities (impact on distribution of hydraulic head), shallow subsurface hydrology
2006			Groundwater flow analysis for the effect of grouting on the amount of groundwater inflow into the underground facilities and groundwater pressure distribution around the URL	Local scale Site scale	

(2) Outline of groundwater flow analysis

The analysis in the investigation stage covering the whole area of Horonobe Town indicated that the largest groundwater streamline through the URL area was considered to be the one that flows out of the Shimizu River or the upper Penkeebekorobetsu River to the Teshio River in a south or south-west direction from these rivers. The area covering the Shimizu River and the upper stream of the Penkeebekorobetsu River as the upper boundary and the Teshio River as the southern boundary was established as the domain for detailed analysis. The analysis domain is shown in Figure 4.2.4-1.

In the H12 report, it is stated that many rock formations in Japan can be classified as fractured rocks and some Neogene sedimentary formations are classified as rocks with the characteristics of both fractured and porous media[95]. From the borehole investigations, the sedimentary formations were characterised, in terms of hydrogeology, as being fractured or with the characteristics of both fractured and porous media. Although understanding the distribution of the fractures and their hydraulic characteristics will be critical when considering solute transport through the fractured rocks, no generalised method for investigation or modelling has been developed owing to large regional variances. The two types of modelling approach were thus applied for identifying the effects of differences in modelling techniques for the minor fault zones in the Wakkanai Formation on the water pressure distribution and the groundwater streamlines:

- homogeneous continuum model;
- equivalent heterogeneous continuum model.

The homogeneous continuum model, which assumes a stratum with a scale of about 20 km × 20 km square to be homogeneous even if it includes fault zones, can be considered as a generic model without direct consideration of minor fault zones. For the analysis using the homogeneous continuum model, the sensitivity analyses for hydraulic head were conducted using the rainfall intensity and hydraulic conductivities in the Wakkanai and Koetoi Formations and the Omagari Fault as parameters, using average values from the actual measurements discussed in Subsection 4.2.3 or estimates based on the literature as the reference hydraulic conductivity for each geological formation. The results of the sensitivity analysis and the distribution of the water pressure that was actually measured were then compared and the input parameters such as hydraulic conductivity were optimised within a predictable range in order to represent the distribution of the water pressure that was actually measured[88].

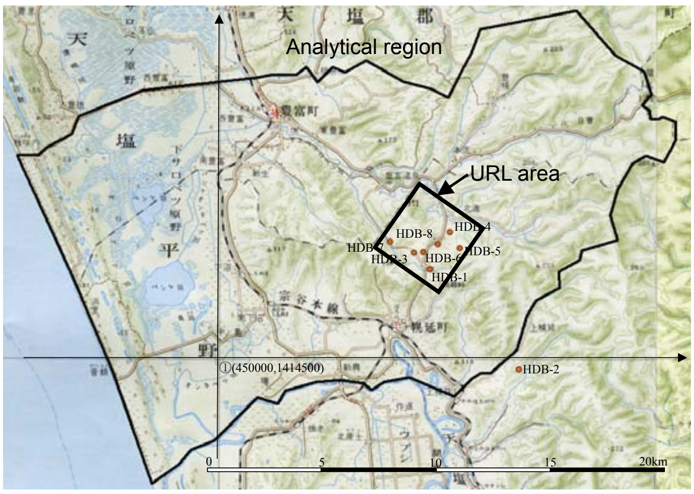

Base map is part of the 1:200,000 scale regional map (Teshio, Esashi) published by the Geographical Survey Institute

Figure 4.2.4-1 Region for groundwater flow analysis

The equivalent heterogeneous continuum model is a method of modelling that reflects information on the spatial distribution of fractures obtained from borehole and outcrop investigations in the spatial distribution of the hydraulic characteristics of the homogeneous continuum model, to represent groundwater flow in heterogeneous and discontinuous rocks[52]. Here, the equivalent heterogeneous continuum model was introduced to model the minor fault zones directly and thereby examine the effect on the groundwater flow of the distribution of highly permeable minor fault zones[53].

(3) Analysis using the homogeneous continuum model

1) Analytical conditions

A finite element code, Dtransu-3D-EL[96], based on the Eulerian – Lagrangian method was used in the analysis of groundwater flow with the homogeneous continuum model, taking the advection – dispersion of salinity into account. However, an advection – dispersion analysis was not conducted here. The formations subjected to the analyses were, according to hydrogeological classification, the Masuporo Formation and lower, the Wakkanai Formation, the Koetoi Formation, the Yuchi Formation, the Sarabetsu Formation, the Omagari Fault, the Horonobe Fault (N1 fault) and the shallow subsurface/terrace sediments. Figure 4.2.4-2 shows the analytical mesh and the boundary conditions.

The hydraulic conductivity in the reference case was estimated based on average values from actual measurements, as discussed in Subsection 4.2.3 (2), and on literature data. The hydraulic conductivities in the Wakkanai, Koetoi and Yuchi Formations were obtained by the least squares approximation line taking into consideration the trend of decreasing hydraulic conductivity with depth as indicated by the interpretation of the results of hydraulic tests in boreholes. The upper limit of the hydraulic conductivities in each hydrogeological classification was set as the maximum value of the in situ hydraulic test results in each formation and the lower limit as the logarithmic mean of the hydraulic conductivities measured by the laboratory hydraulic tests for the rock matrix. The trend of decreasing hydraulic conductivity with depth was also taken into account for the Omagari Fault, although data were as sparse as two points. The gradient of the trend for the Omagari Fault was considered to be equal to, but the overall hydraulic conductivity was set to be one order of magnitude higher than, that of the Wakkanai Formation. For the other formations, there were no measured data and existing investigation results[63] and estimated values were used.

Sensitivity analyses were conducted to determine the influence of rainfall intensity and the hydraulic conductivities of the Wakkanai and Koetoi Formations and the Omagari Fault on the hydraulic head in each borehole. A reference value and twice and half of the reference value were used for rainfall intensity. For the Wakkanai Formation, cases using anisotropic hydraulic conductivity were set, assuming a minor fault zone with a dominant E-W strike in the formation. For the Koetoi Formation, cases where the hydraulic conductivity was either higher or lower by one order of magnitude were set. For the Omagari Fault, there was a case where the hydraulic conductivity was set higher and a case where anisotropic hydraulic conductivity was applied, assuming the existence of a fault core with low hydraulic conductivity.

For the optimisation analysis, an inverse analysis that optimises the input conditions such as the hydraulic conductivity within a predictable range was carried out based on a comparison of the results of the sensitivity analysis and the measured water pressure distribution, to ensure that the measured water pressure distribution would be well represented. An inverse analysis may be better if it is conducted quantitatively using an index such as the deviation between the measured values and the calculated values. However, since issues such as the weighting for the area where data were insufficient remained unresolved, the analysis was conducted on a trial and error basis using qualitative criteria.

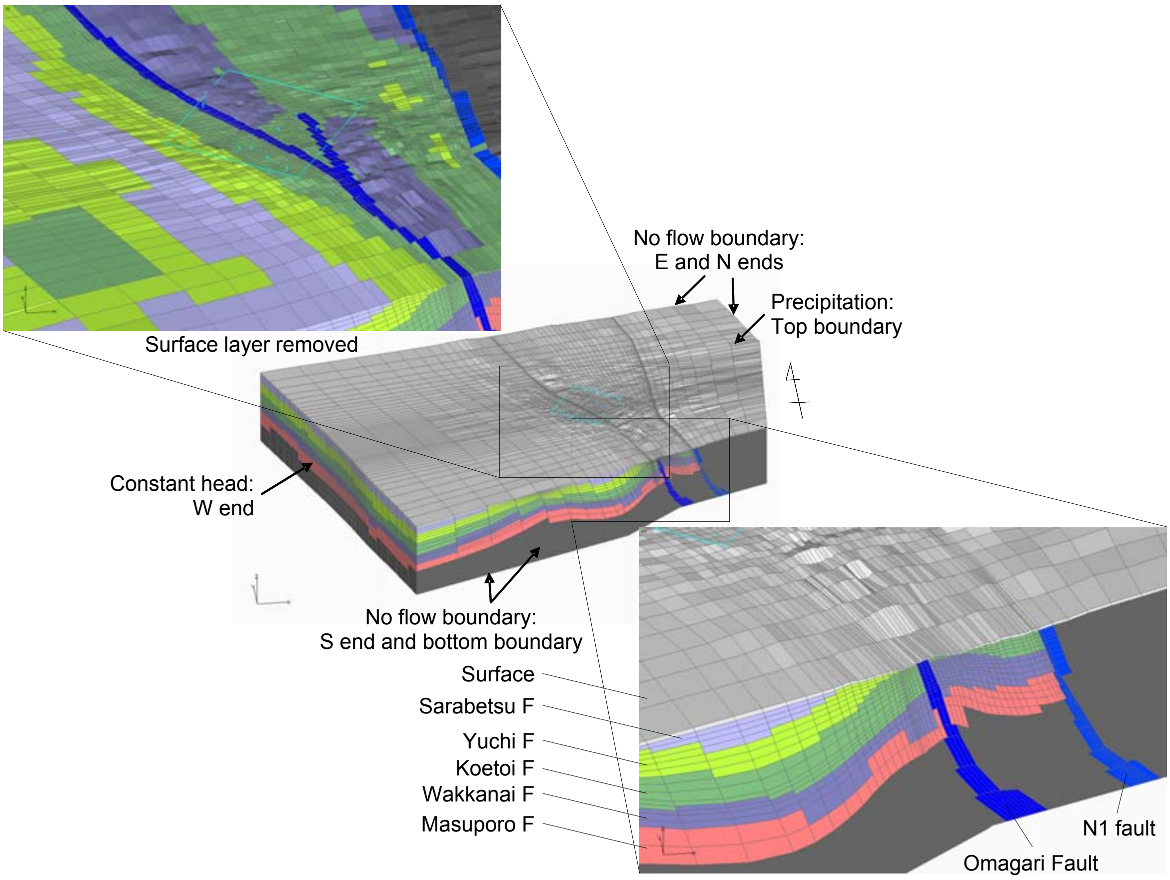

Figure 4.2.4-2 Finite element mesh and boundary conditions

2) Analytical results for groundwater flow

The sensitivity analysis has revealed that rainfall intensity has a strong influence in high elevation areas and that a discontinuity in the distribution of hydraulic head has been lost between the east and west sides of the Omagari Fault in the cases where the hydraulic conductivity of the fault was either high or anisotropic and the hydraulic conductivities in the Wakkanai and Koetoi Formations influences the distribution of the hydraulic head in the drainage basin.

For the optimisation analysis based on the sensitivity analysis, reference hydraulic conductivities and parameters to be optimised were selected by comparing the results of the sensitivity analysis with measured values. As a result, rainfall intensity was changed for the cases which use anisotropic hydraulic conductivity for the Wakkanai Formation and the cases which use the same hydraulic conductivities as those in the reference case for other formations.

Figure 4.2.4-3 shows the result of the optimisation analysis, compared with the measured values. Along with the decrease in rainfall intensity, the hydraulic head in boreholes HDB-5 and HDB-9 were lowered. Owing to the decrease in rainfall intensity, the hydraulic head in borehole HDB-9 approaches the measured value, while that in borehole HDB-5 deviates from the measured value at a depth of around 100 m. The reason why the hydraulic heads of the two boreholes were not represented correctly at the same time could be that the local geological structures (i.e. minor fault zones) controlling the groundwater flow were not correctly reflected in the model and that there was a limitation in applying the hydrogeological classification to the geological structure. For the current model, a rainfall intensity of approximately

0.3–0.7 mm d^{-1} would be an appropriate value. There was almost no influence owing to rainfall intensity in the other boreholes. This is because the elevation of the other boreholes was relatively low and they were influenced by the river water level rather than by the rainfall intensity. None of the high hydraulic heads in the deep zone of borehole HDB-11 could be simulated.

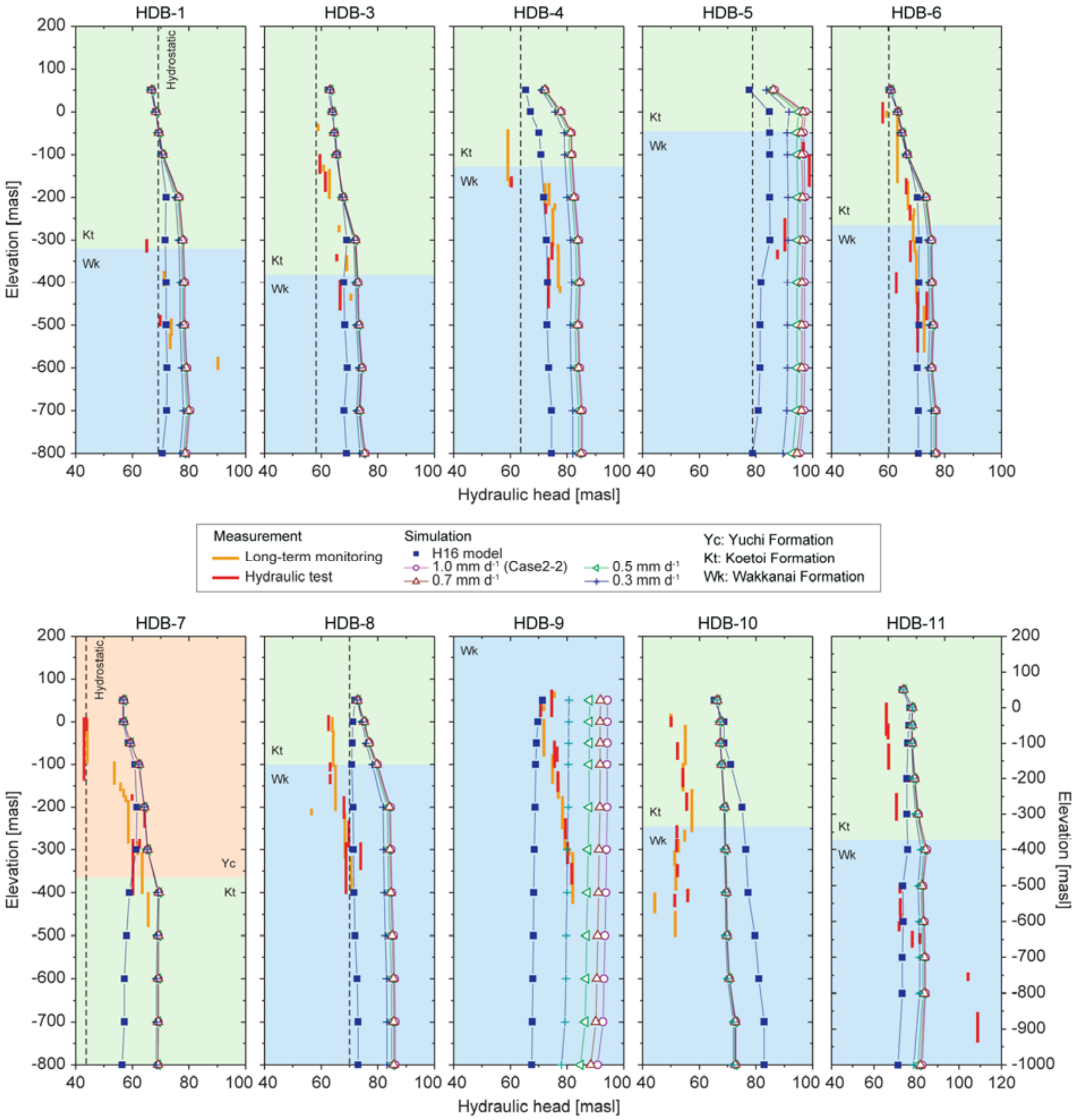

Figure 4.2.4-3 Comparison of hydraulic head between simulation and measurement

Figure 4.2.4-4 shows the distribution of hydraulic head at a vertical cross-section through boreholes HDB-6 and HDB-7 (A-A' cross-section in the figure) in the case of a rainfall intensity of 0.5 mm d^{-1} and the streamline of the groundwater passing through elevations of 0 m, -200 m, -400 m and -600 m in boreholes HDB-4 and HDB-6 to HDB-11. It can be concluded from the hydraulic head distribution that a high hydraulic head is maintained in the mountains on the east side (upper part of the Shimizu River), the direction of the hydraulic gradient is generally from east to west and hydraulic gradients are governed locally by the topographical gradients. These findings were the same as the concept for the groundwater flow system predicted from the analysis results in the investigation stage using existing information and were consistent with the groundwater flow system predicted from the measured values as shown in Figure 4.2.3-10. However, the streamlines indicate that local groundwater flow systems such as the Penkeebekorobetsu River basin and the Shimizu River basin have an influence on deeper zones, compared to the prediction based on conventional models.

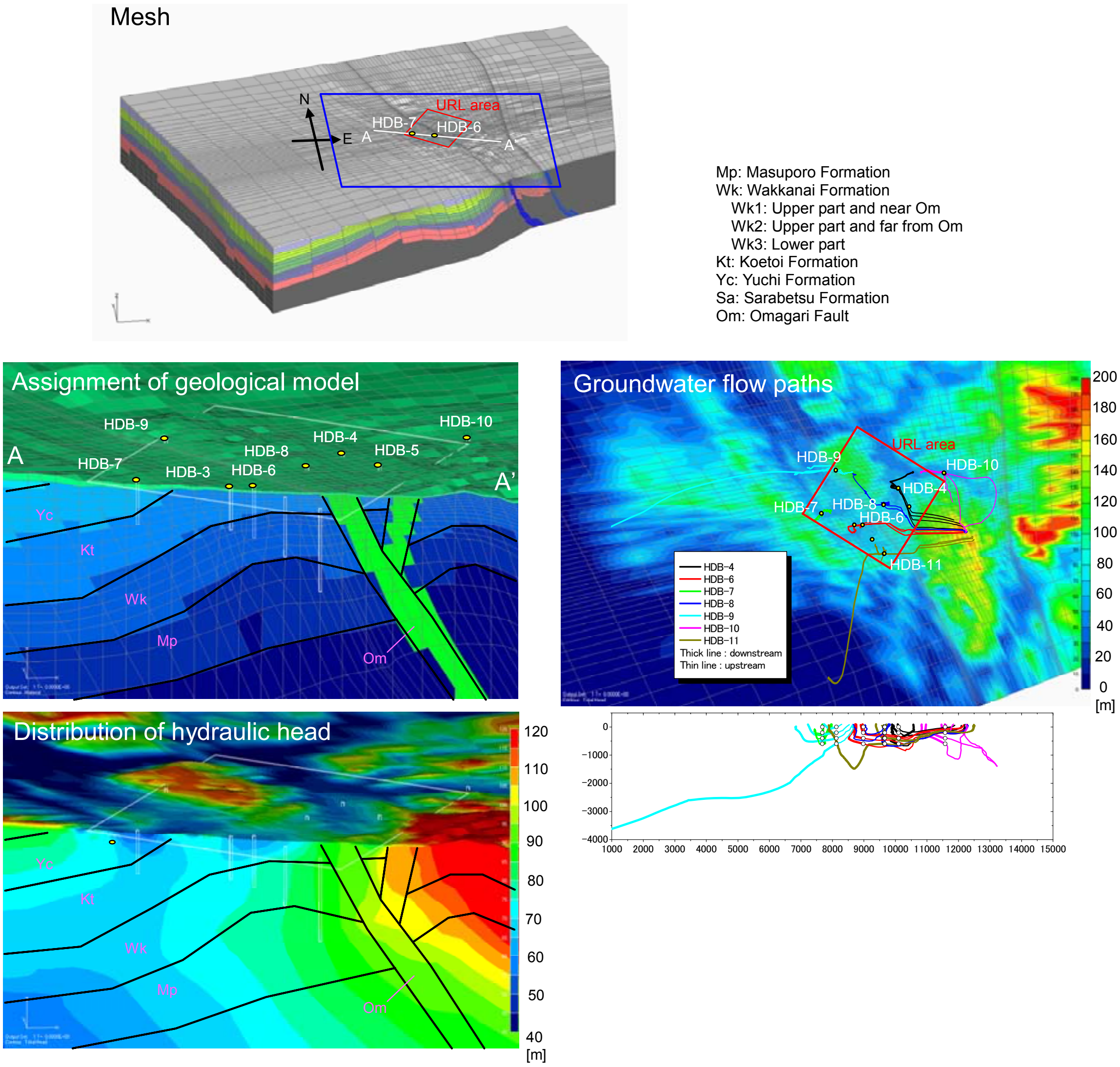

Figure 4.2.4-4 Distribution of hydraulic head and groundwater flow paths through boreholes HDB-4 and HDB-6 to HDB-11, obtained by the optimisation analysis

(4) Analysis using the equivalent heterogeneous continuum model

The equivalent heterogeneous continuum model[52] uses a method in which rocks are substituted with heterogeneous and discontinuous structures such as fractures and has been applied for rocks such as granite, where fractures dominate the groundwater flow[50),97]. This model was applied to the Wakkanai Formation and the Koetoi Formation using the 3D saturation/unsaturation seepage flow analysis code, EQUIV-FLO, based on the finite element method[53].

The formations subjected to the analyses were, according to the hydrogeological classification, the formations below the Masuporo Formation, the Masuporo Formation, the Wakkanai Formation, the Koetoi Formation, the Yuchi Formation, the zone shallower than the Sarabetsu Formation, the Omagari Fault and the Horonobe Fault (N1 fault). A finer mesh was used than that for the homogeneous continuum model.

The selection of the hydraulic conductivities in the formations other than the Wakkanai and Koetoi Formations were the same as those for the analysis using the homogeneous continuum model. For the Wakkanai and Koetoi Formations, minor fault zones assumed to be disks were generated hypothetically based on the 1D density and the strike/dip distribution of the minor fault zones observed in boreholes HDB-1 to HDB-8. The transmissivity and length of the minor fault zones were then estimated by comparing the results of hypothetical hydraulic tests with the actual hydraulic tests. For statistical treatment of the minor fault zones, 10 realisation analyses were conducted by combining the distribution of the minor fault zones generated probabilistically.

The groundwater flow system obtained as a result of the analysis was qualitatively the same as that of the homogeneous continuum model, which suggests that, whether or not the minor fault zones were directly modelled, groundwater flow systems such as recharge and runoff areas could be predicted analytically.

The major benefit of the equivalent heterogeneous continuum model would be that variability in results could be presented by generating minor fault zones probabilistically. The streamlines and the range of the hydraulic head distribution could be predicted to some extent. This should be useful for assessing uncertainties in the case of the actual disposal project. Predicting the amount of groundwater inflow into the underground facilities as described in Subsection 4.6.3 would also be useful for planning the drainage of the facilities.

In the analysis using the equivalent heterogeneous continuum model, a critical achievement would be demonstrating a modelling process in which minor fault zones indicated in the geological structure model were used in the hydrogeological model.

4.3 Hydrochemical investigations

4.3.1 Aims

As described in the previous sections, the Phase I investigations were carried out, which focussed on two main areas: the whole area of Horonobe Town and in and around the URL area. For the hydrochemical investigations, the following four aims were established:

- to clarify 3D distributions of groundwater chemistries;
- to explain the major groundwater evolutions;
- to estimate the origin and residence times of the groundwater;
- to improve the investigation techniques for determining groundwater chemistries.

4.3.2 Surface-based investigations covering the whole Horonobe Town area

(1) Investigation aims and methods

For the whole area of Horonobe Town, surveys of existing information and borehole investigations (HDB-1 and HDB-2) were conducted primarily to acquire data to be used for the selection of candidate URL area and a URL site and for planning investigations in and around the URL area.

(2) Investigations using existing information

A very limited amount of information is available data on the groundwater chemistry in the Horonobe Town area, most of which comes from chemical analyses of well water used for daily water supply[98]. Other information that could be useful includes investigation results from the D-1 borehole investigations.

The maximum depth of wells used for daily water supply is approximately 100 m, which means that water has been sampled mainly from shallower formations (e.g. the Sarabetsu Formation) rather than from the sedimentary rocks of interest (the Wakkanai and Koetoi Formations). Such groundwater has a pH approximately 7 and contains abundant Na^+ and HCO_3^- (concentrations of 13–17 mg l^{-1} and 50–70 mg l^{-1} respectively) and relatively small amounts of other dissolved constituents. On the other hand, the results of the investigations in borehole D-1 indicated the presence of saline groundwater containing the same salinity as that of present sea water deep subsurface (approximately 500–1,000 m depth).

(3) Borehole investigations

Groundwater was sampled in combination with hydraulic packer tests in deep boreholes HDB-1 and HDB-2 (Table 4.3.2-1, see also Appendix 2) drilled in the URL site selection stage. Since the hydraulic conductivities of the sedimentary formation were low over the entire length of the boreholes, the groundwater was sampled from a section with relatively high hydraulic conductivity (approximately 10^{-10}–10^{-9} m s^{-1}).

1) Sampling and analysis of groundwater from boreholes

Groundwater sampling from the boreholes was carried out with the aim of obtaining samples with residual drilling mud of 1% or less, using the concentration of a tracer added to the drilling mud as an indicator[99]. Sodium-naphthionate, a type of fluorescent dye, was selected as the tracer, given its low sorptivity onto rocks and ease of measurement.

Since Na-HCO_3 type groundwater with low mineralisation was assumed to exist in shallower formations, such groundwater from the shallower subsurface was used at the time of borehole drilling. Water chemistry (pH, electrical conductivity, major constituents) and Na-naphthionate were analysed every hour to confirm that no significant change in the water chemistry had occurred during borehole drilling. The concentration of Na-naphthionate added was specified as 10 ± 1 mg l^{-1} in this investigation, considering the desired inclusion level of drilling mud (1% or less) and the lower limit of the in situ quantification of the Na-naphthionate). During pumping tests, the concentration of Na-naphthionate was measured every one to two hours depending on the pumping rate of the water. When measuring the Na-naphthionate concentration, physico-chemical parameters such as pH, redox potential and electrical conductivity were also measured. It would be preferable to pump out groundwater until the concentration of the Na-naphthionate drops below 0.1 mg l^{-1}, however, owing to time and budget constraints for borehole investigations, pumping was stopped and sampled groundwater was analysed for major constituents, various isotopes (H, He, O, C and Cl), dissolved gases and microbes.

Table 4.3.2-1 Groundwater sampling in boreholes

Borehole	Interval depth [mbgl]	Formation*	Tracer [mg l^{-1}]	Total volume extracted / packed-off interval [litre]	pH	EC [mS m^{-1}]	K** [m s^{-1}]	H† [mbgl]
HDB-1	548.00–563.19	Wk	1.4 (14%)	1093 / 305	6.9	2560	3.29×10^{-10}	-0.70
HDB-2	344.90–404.90	Wk	0.9 (9%)	1738 / 1176	7.9	1490	3.50×10^{-9}	-43.00
HDB-3	160.45–200.45	Kt	2.1 (21%)	4140 / 771	6.7	3490	3.35×10^{-8}	-1.37
HDB-4	218.45–236.53	Wk	1.1 (11%)	13102 / 437	7.5	313	1.41×10^{-5}	3.28
	281.45–299.53	Wk	0.4 (4%)	11812 / 437	7.8	430	9.35×10^{-6}	-8.87
	371.90–406.43	Wk	0.6 (6%)	4200 / 753	7.0	1582	5.36×10^{-7}	-11.07
	407.90–520.00	Wk	0.7 (7%)	7800 / 2487	7.0	1681	3.14×10^{-8}	-9.85
HDB-5	154.05–180.46	Wk	0.2 (2%)	1176 / 572	8.5	39.5	6.47×10^{-7}	-18.00
	182.05–250.46	Wk	0.3 (3%)	17524 / 1507	8.3	84.5	8.48×10^{-7}	-20.04
	331.22–402.23	Wk	0.5 (5%)	6240 / 1565	7.0	1301	4.39×10^{-8}	-11.49
HDB-6	280.95–312.00	Wk	0.8 (8%)	17006 / 597	7.3	1199	1.83×10^{-6}	-7.58
	363.95–409.00	Wk	0.6 (6%)	55325 / 872	6.9	1966	1.64×10^{-6}	-7.62
HDB-8	57.50–89.05	Kt	3.7 (37%)	1228 / 639	8.0	209	9.54×10^{-9}	7.38
	168.01–184.06	Wk	1.5 (15%)	39420 / 320	7.6	370	2.86×10^{-6}	6.80
HDB-9	25.50–82.60	Wk	0.3 (3%)	4049 / 3138	6.1	15.8	5.00×10^{-7}	22.47
	216.90–257.50	Wk	1.6 (16%)	19409 / 765	6.9	1239	1.50×10^{-6}	20.31
HDB-10	41.33–59.88	Kt	2.6 (26%)	4813 / 364	8.0	209	2.53×10^{-7}	0.62
	445.84–469.89	Wk	0.8 (8%)	7445 / 465	6.8	2510	2.44×10^{-7}	-5.22
HDB-11	171.00–237.05	Kt	5.5 (55%)	2770 / 1420	7.0	1147	2.07×10^{-9}	-0.14
	606.00–644.05	Wk	0.9 (9%)	17586 / 755	6.2	3796	2.26×10^{-8}	-5.57

*Wk: Wakkanai Formation, Kt: Koetoi Formation; *K: Hydraulic conductivity
†H: Hydraulic head; hydraulic parameters shown in detail in Table 4.2.3-4

2) Squeezing and analysis of porewater chemistries

Porewater was extracted from the core, obtained during borehole drilling, by the squeezing method[100)]. Since the quantity of the squeezed porewater was limited, i.e. a few to a few tens of millilitres, an analysis was conducted for only some of the major constituents and isotopes of H and O. As discussed in Subsection 4.7.3, significantly high SO_4^{2-} concentrations were observed in the porewater from boreholes HDB-1 and HDB-2. This was considered to be due to oxidation of sulphides in the cores, as the squeezing operation occurred a few weeks after the cores were sampled. In order to avoid the chemical disturbance caused by oxidation, soon after the cores were obtained, a photograph was taken and geological observations were made immediately after sampling. The cores were then waxed for storage and transport and porewater was finally squeezed in the laboratory (Figure 4.3.2-1). As well as minimising the time from core sampling to squeezing, the squeezing was conducted for some cores in a glove-box filled with inert gas.

Figure 4.3.2-1 Sealing of core sample in wax for porewater squeezing

3) Chemical and mineralogical analyses of cores

Chemical (major constituents and rare earth elements) and mineral compositions of the rocks were analysed using cores to acquire input data for the hydrochemical analysis discussed later.

The results of investigations in boreholes HDB-1 and HDB-2 indicate that Na-Cl type groundwater with high mineralisation is present in the zone deeper than 300 m from the ground surface in the Wakkanai and Koetoi Formations[56),57)].

Based on the results described above, a concept for hydrochemical characteristics was developed for the groundwater in and around the URL area; Na-HCO_3 type groundwater with low mineralisation is distributed in the shallower subsurface and Na-Cl type groundwater with high mineralisation is found in the deeper formations.

4.3.3 Surface-based investigations in and around the URL area

(1) Investigation aims and method

In this investigation stage, data on hydrochemical characteristics were obtained mainly by investigations in deep boreholes HDB-3 to HDB-11 and data on surface water, such as precipitation and river water, were also obtained. During investigations in boreholes HDB-3, HDB-4 and HDB-5, data on hydrochemical characteristics were obtained with the aim of confirming and improving the applicability of investigation techniques using boreholes (i.e. techniques for groundwater sampling and squeezing porewater) and constructing the conceptual model for the distribution of groundwater chemistries. For the investigations in boreholes HDB-6 to HDB-11, data were collected with a view to improving the conceptualisation of the geological environmental properties established using the results of the investigations in boreholes HDB-3, HDB-4 and HDB-5. Finally, using all the data obtained, a 3D distribution of groundwater chemistries in and around the URL area was predicted and hydrochemical evolution processes were discussed. Through these investigations and analyses, the investigation techniques for hydrochemical characteristics of the groundwater were established for the sedimentary formations.

(2) Shallow subsurface hydrochemical investigations

These investigations cover rain water, river water and groundwater in shallow subsurface (to a depth of tens of metres from the ground surface). Rain and river water were sampled, analysed and monitored in the context of surface hydrology as discussed in Section 4.2. Rain water was collected in sampling bottles each month and the average water chemistry for the month concerned was measured. During the winter period, snow fall over a month was collected, dissolved in an airtight container at room temperature and analysed. River water was collected and analysed once a month. Groundwater in the shallow subsurface was pumped from existing wells in Horonobe Town and analysed[82]. The regular collection and analysis of rain water, river water and groundwater from shallow subsurface allowed clarification of the variation of chemical and isotopic compositions of the waters (Figure 4.3.3-1).

The chemical composition of rain water showed a seasonal change; rain water during the winter (i.e. snow fall) shows higher salinity while that from the other seasons less salinity; this trend has been observed almost every year. The chemistry of river water was the same as the average for Hokkaido[101]. A general trend was observed whereby the salinity was higher during periods when the river surfaces are frozen in winter and lower during the period when snow melts in spring. The above findings were used to establish upper boundary conditions for the hydrochemical model discussed later.

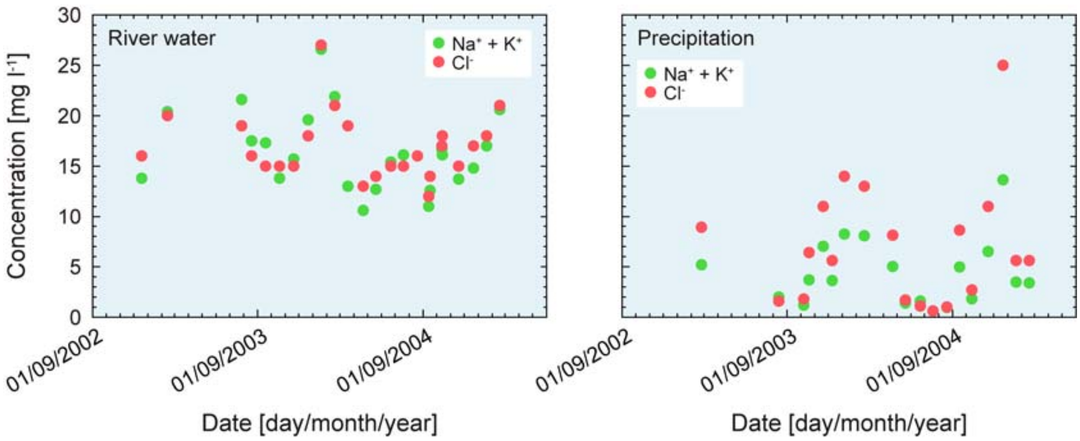

Figure 4.3.3-1 Chemistry of river water and precipitation

(3) Borehole investigations

For the deep borehole investigations, groundwater was sampled in combination with hydraulic packer tests. Groundwater samples were collected from a total of 18 sections from boreholes except HDB-2 (Table 4.3.2-1). Porewater was extracted from cores using the method described above and then analysed.

The hydrochemical study using data from deep borehole investigations was divided into two stages according to the interpretation of the investigation results: a study using data from investigations in boreholes HDB-1, HDB-3, HDB-4 and HDB-5 and those from all the boreholes (HDB-1 to HDB-11).

It was found that, in boreholes HDB-1 and HDB-3, Na-Cl type groundwater with high mineralisation is present from a depth of approximately 200 m, while in boreholes HDB-4 and HDB-5 Na-HCO_3 type groundwater with low mineralisation is present to a depth of 300 m and Na-Cl type with high mineralisation in the formations deeper than 300 m (Figure 4.3.3-2). The variation in groundwater chemistry between boreholes might possibly be attributed to differences in the hydraulic conductivity of the rocks. The measurements of H and O isotopes showed that the Na-HCO_3 type groundwater is abundant in light isotopes (δD of approximately -70‰, $\delta^{18}O$ of approximately -10‰), while the Na-Cl type groundwater is abundant in heavy isotopes (δD of approximately -10‰, $\delta^{18}O$ of approximately +2‰) as shown in Figure 4.3.3-3.

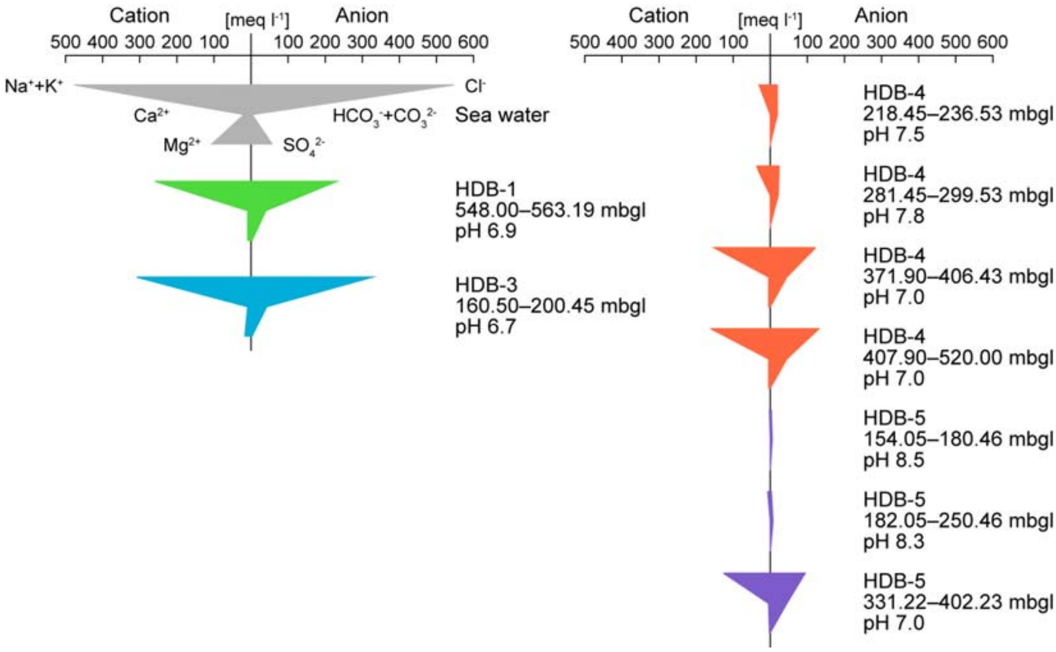

Figure 4.3.3-2 Chemistry of groundwater from boreholes HDB-1 and HDB-3 to HDB-5

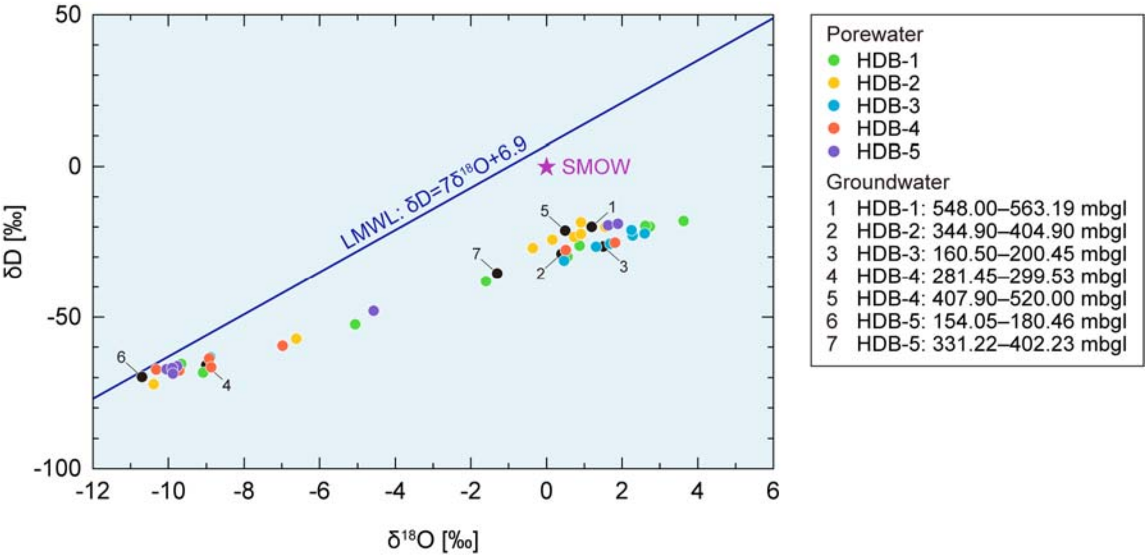

Figure 4.3.3-3 δD vs δ^{18}O for porewater and groundwater from boreholes HDB-1 to HDB-5

Analysis of the stable H and O isotopes in the groundwater samples from boreholes HDB-1, HDB-2 and HDB-3, after correcting the influence of current surface water, showed that δD and δ^{18}O were lower than in the modern meteoric water; differences of δD and δ^{18}O values are approximately 10‰ and 3‰ respectively. This suggests that groundwater recharge occurred during a period being colder than the present and also the depths where precipitation was recharged in the past and present were different, implying that the transition between glacial and interglacial periods, for example, could have been recorded. For depths at which infiltration occurs, a good correlation was found between the amount of influence of infiltration and rock permeability[102)].

Described below are data obtained in boreholes HDB-6 to HDB-11 (Appendix 2) and the findings on the hydrochemical characteristics of the groundwater in the Wakkanai and Koetoi Formations.

1) Major chemistry of groundwater

The groundwater and porewater chemistries are shown in Tables 4.3.3-1 and 4.3.3-2 and Figure 4.3.3-4, indicating that the Na-HCO_3 type groundwater is distributed in the shallower subsurface, while Na-Cl type groundwater is found in deeper formations. The depth where the groundwater changes from the Na-HCO_3 type to Na-Cl type varies for each borehole, which would be attributed to differences in rock permeability.

A significantly high SO_4^{2-} concentration was observed in some porewater samples. This could be due to sulphide in the cores being oxidised and dissolved as sulphate during the core storage and/or the core squeezing process.

The pH measured for the groundwater pumped from the boreholes and squeezed porewater was approximately 7–8. The redox potential measured in situ at 606.00–644.15 m depth in borehole HDB-11 (in the Wakkanai Formation) was approximately -170 mV.

Table 4.3.3-1 Major chemical and isotopic compositions of groundwater pumped from boreholes

Borehole (HDB)		1	2	3	4	4	4	4	5	5	5	6	6	8	8	9	9	10	10	11	11
Sampling depth [mbgl]		548.00 ~ 563.19	334.90 ~ 404.90	160.50 ~ 200.45	218.45 ~ 236.53	281.45 ~ 299.53	371.90 ~ 406.43	407.90 ~ 520.00	154.05 ~ 180.46	182.05 ~ 250.46	331.22 ~ 402.23	280.95 ~ 312.00	363.95 ~ 409.00	57.50 ~ 89.05	168.01 ~ 184.06	25.50 ~ 82.60	216.90 ~ 257.50	41.33 ~ 59.88	445.84 ~ 469.89	171.00 ~ 237.05	606.00 ~ 644.05
Formation*		Wk	Wk	Kt	Wk	Wk	Wk	Wk	Wk	Wk	Wk	Wk	Wk	Kt	Wk	Wk	Wk	Kt	Wk	Kt	Wk
pH		6.9	7.9	6.7	7.5	7.8	7.0	7.0	8.5	8.3	7.0	7.3	6.9	8.0	7.6	6.1	6.9	7.2	6.8	7.0	6.2
EC	[mS m^{-1}]	2560	1490	3490	313	430	1582	1681	39.5	84.5	1301	1199	1966	209	370	15.8	1239	1067	2510	1147	3796
Tracer	[mg l^{-1}]	1.4	0.9	2.1	1.1	0.4	0.6	0.7	0.2	0.3	0.5	0.8	0.6	3.7	1.5	0.3	1.6	2.6	0.8	5.5	0.9
Na^+	[mg l^{-1}]	5140	3120	6900	730	880	3500	3700	86	180	2900	2460	4220	367	787	22	4200	2300	5000	3300	6600
K^+	[mg l^{-1}]	170	51	320	17	21	54	59	4.0	5.4	46	77	110	18	31	1.8	59	110	160	160	140
Ca^{2+}	[mg l^{-1}]	180	24	220	14	23	94	95	0.91	2.2	99	69.0	140	12	12	3.9	84	67	97	40	250
Mg^{2+}	[mg l^{-1}]	120	36	210	5.4	9.9	53	56	0.45	0.96	46	43	110	5.7	7.8	1.1	59	55	140	84	170
Mn^{2+}	[mg l^{-1}]	0.41	0.51	0.01	nm**	0.01	nm	0.03	0.01	0.01	0.03	0.03	0.02	0	0.01	nm	nm	nm	nm	0.02	0.01
Si	[mg l^{-1}]	49	45	27	nm	20	nm	23	20	19	20	24	24	20	20	21	22	26	25	26	27
ΣFe	[mg l^{-1}]	290	nm	0.19	nm	0.05	nm	0.11	0.11	0.13	2.50	0.04	0.04	0.04	0.05	0.02	0.04	0.02	0.03	0.02	0.04
Al^{3+}	[mg l^{-1}]	<0.1	<0.1	nd***	nm	nd	nm	0.02	nd	0.1	0.4	0.02	<0.01	0.06	0.02	0.01	<0.01	0.06	<0.01	<0.01	<0.01
F^-	[mg l^{-1}]	<0.1	<0.1	nd	nm	0.2	nm	0.4	0.4	0.4	0.2	<0.1	0.2	0.1	<0.1	<0.1	0.2	0.3	<0.1	<0.1	0.1
Cl^-	[mg l^{-1}]	7500	4180	11600	630	820	4300	4600	16	67	3250	3050	6300	200	390	14	5100	2400	8100	5100	10000
Br^-	[mg l^{-1}]	<0.1	19	99	nm	29	nm	19	0.1	0.2	10	11	45	<1	1.0	<0.1	33	26	83	42	78
I^-	[mg l^{-1}]	16	12	41	nm	nd	nm	16	nd	nd	13	9	17	<1	<1	<1	15	10	33	16	29
NO_3^-	[mg l^{-1}]	<0.1	<0.1	0.4	nm	nd	nm	0.2	nd	nd	0.6	0.1	0.1	0.5	0.5	<0.1	<0.1	1	0.5	0.3	0.1
NO_2^-	[mg l^{-1}]	0.18	<0.1	nd	nm	0.9	nm	nd	nd	nd	0.1	nm	nm	nm	nm	<0.1	<0.1	<0.1	<0.1	<0.1	<0.1
SO_4^{2-}	[mg l^{-1}]	96.7	2.4	38	4.6	0.3	1.7	7.0	0.5	2.2	6.8	5.9	0.2	23	1.1	10	6.9	1	0.4	11	<0.2
HCO_3^-	[mg l^{-1}]	2155	2120	2463	1123	1184	2600	2610	240	410	2640	41	41	41	41	47	3200	3600	1100	1410	2200
CO_3^{2-}	[mg l^{-1}]	–	–	–	–	60.0	–	–	–	–	–	–	–	–	–	–	–	–	–	–	–
TOC	[mg l^{-1}]	10	44	52	nm	16	nm	42	3	5	30	130	63	25	13	2	9	36	20	19	31
TIC	[mg l^{-1}]	390	400	530	nm	250	nm	570	50	86	580	390	510	170	300	9	630	640	320	260	450
^3H	[TU]	1.4	nm	1.2	nm	<0.4	nm	nm	nm	nm	nm	<0.4	<0.4	1.6	<0.4	2.7	<0.4	<0.4	<0.4	0.8	<0.3
δD	[‰]	-20	-29	-27	nm	-66	nm	-21	-70	-71	-36	-56	-37	-72	-70	-71	-35	-61.4	-42.3	-46.1	-24.2
$\delta^{18}O$	[‰]	1.2	0.4	1.5	nm	-9.0	nm	0.5	-10.7	-10.8	-1.3	-5	-0.6	-10.4	-8.8	-11	0.1	-6.4	-1.9	-3.6	3.5
$^{36}Cl/Cl$	[$\times 10^{-15}$]	3.3	–	0.9	–	7.1	–	1.7	8.0	7.0	5.4	2.2	–	5.6	1.2	172	3.1	0.7	2.1	2.5	2.9

*Wk: Wakkanai Formation, Kt: Koetoi Formation; **nm: not measured; ***nd: not detected

Table 4.3.3-2 Major chemical and isotopic compositions of porewaters

Borehole (HDB)	1	1	1	1	1	1	1	1	1	1	1	1	1	1	1	1	1	1	1	1
Sampling depth [mbgl]	54.00 ~ 56.00	109.30 ~ 111.60	130.00 ~ 131.00	164.03 ~ 165.92	222.70 ~ 224.00	271.23 ~ 273.93	311.10 ~ 312.00	345.00 ~ 346.00	380.00 ~ 381.00	400.05 ~ 401.00	443.00 ~ 444.00	455.00 ~ 456.00	493.00 ~ 494.00	514.00 ~ 515.00	545.00 ~ 546.00	556.05 ~ 556.80	597.35 ~ 598.00	609.70 ~ 610.00	648.20 ~ 650.00	704.15 ~ 705.00
Formation*	Kt	Kt	Kt	Kt	Kt	Kt	Kt	Wk	Wk	Wk	Wk	Wk	Wk	Wk	Wk	Wk	Wk	Wk	Wk	Wk
pH	–	–	–	–	–	–	–	–	–	–	–	–	–	–	–	–	–	–	–	–
EC [mS m^{-1}]	203	378	507	–	–	–	1084	–	1212	1234	1454	–	–	1759	–	1436	–	5923	–	5486
Na^+ [mg l^{-1}]	690	1500	1700	2000	3700	2700	4400	3000	5100	5400	5800	5000	6600	6200	6100	5900	7700	9900	6300	11000
K^+ [mg l^{-1}]	97	130	140	110	190	150	200	120	150	180	190	160	340	120	170	120	330	180	170	190
Ca^{2+} [mg l^{-1}]	220	110	97	59	380	72	150	68	280	290	230	140	316	140	61	180	430	560	210	510
Mg^{2+} [mg l^{-1}]	98	52	36	35	180	54	100	56	150	200	180	110	190	150	84	140	260	890	140	1000
Cl^- [mg l^{-1}]	100	300	600	2000	2000	3400	5000	4100	5300	5300	6900	8100	9700	9500	10000	8700	9700	9400	10400	9700
SO_4^{2-} [mg l^{-1}]	2200	3100	3200	2200	7200	2200	3400	1900	5300	6000	4000	800	3200	1200	900	1700	4800	13100	300	14500
HCO_3^- [mg l^{-1}]	–	–	–	–	–	–	–	–	–	–	–	–	–	–	–	–	–	–	–	–
CO_3^{2-} [mg l^{-1}]	–	–	–	–	–	–	–	–	–	–	–	–	–	–	–	–	–	–	–	–
TOC [mg l^{-1}]	–	–	–	–	–	–	–	–	–	–	–	–	–	–	–	–	–	–	–	–
TIC [mg l^{-1}]	–	–	–	–	–	–	–	–	–	–	–	–	–	–	–	–	–	–	–	–
δD [‰]	-66.0	-68.0	-66.0	–	-52.0	–	-38.0	–	-32.0	-30.0	-27.0	–	–	-20.0	–	-27.0	–	-19.0	–	-19.0
$δ^{18}O$ [‰]	-9.7	-9.1	-8.3	–	-5.0	–	-1.4	–	0.2	0.6	1.4	–	–	2.8	–	0.8	–	2.8	–	3.6

Borehole (HDB)	2	2	2	2	2	2	2	2	2	2	2	2	2	2	2	2	2	2	2	2
Sampling depth [mbgl]	45.00 ~ 45.90	128.00 ~ 130.00	151.00 ~ 157.84	204.00 ~ 205.90	254.00 ~ 255.00	290.00 ~ 290.82	350.00 ~ 351.29	400.90 ~ 401.75	403.15 ~ 401.75	412.59 ~ 413.69	454.00 ~ 464.12	499.00 ~ 499.80	534.75 ~ 543.99	594.00 ~ 594.85	623.00 ~ 624.00	652.69 ~ 654.80	675.00 ~ 676.00	688.00 ~ 689.00	695.00 ~ 696.00	718.50 ~ 719.85
Formation*	Wk	Wk	Wk	Wk	Wk	Wk	Wk	Wk	Wk	Wk	Wk	Wk	Wk	Wk	Wk	Wk	Wk	Wk	Wk	Wk
pH	–	–	–	–	–	–	–	–	–	–	–	–	–	–	–	–	–	–	–	–
EC [mS m^{-1}]	252	753	–	1860	–	2047	–	1809	–	1534	–	1054	–	2099	2066	–	1935	–	2239	–
Na^+ [mg l^{-1}]	500	1700	1600	5500	4300	6300	3300	5500	4000	5200	6100	2400	2600	6000	6600	3100	7300	2800	7400	2700
K^+ [mg l^{-1}]	21	46	80	96	50	120	120	98	130	80	130	27	40	12	22	100	77	30	140	40
Ca^{2+} [mg l^{-1}]	28	85	87	450	280	400	13	440	71	440	–	39	50	500	490	100	44	54	410	63
Mg^{2+} [mg l^{-1}]	24	39	30	250	96	310	47	200	39	170	–	13	17	180	220	27	250	13	260	16
Cl^- [mg l^{-1}]	610	740	1900	3300	4400	3500	4100	3000	5800	3000	8300	2700	3400	3100	2900	3600	2500	3500	2400	3400
SO_4^{2-} [mg l^{-1}]	520	2700	1100	9000	4700	10300	2100	9700	1800	9100	1800	1200	1100	10100	11600	2300	14000	960	15000	990
HCO_3^- [mg l^{-1}]	–	–	–	–	–	–	–	–	–	–	–	–	–	–	–	–	–	–	–	–
CO_3^{2-} [mg l^{-1}]	–	–	–	–	–	–	–	–	–	–	–	–	–	–	–	–	–	–	–	–
TOC [mg l^{-1}]	–	–	–	–	–	–	–	–	–	–	–	–	–	–	–	–	–	–	–	–
TIC [mg l^{-1}]	–	–	–	–	–	–	–	–	–	–	–	–	–	–	–	–	–	–	–	–
δD [‰]	-70.0	-57.0	–	-18.0	–	-20.0	–	-23.0	–	-23.0	–	-25.0	–	-22.0	-22.0	–	-25.0	–	-28.0	–
$δ^{18}O$ [‰]	-10.3	-6.6	–	0.9	–	1.7	–	0.7	–	0.5	–	0.2	–	0.9	0.7	–	0.2	–	-0.5	–

Borehole (HDB)	3	3	3	3	3	3	3	3	3	3	4	4	4	4	4	4	4	4	4	4
Sampling depth [mbgl]	22.12 ~ 23.00	104.09 ~ 106.00	155.20 ~ 155.99	156.20 ~ 156.90	229.30 ~ 229.92	274.30 ~ 274.90	326.00 ~ 327.00	373.00 ~ 373.70	425.20 ~ 426.00	500.10 ~ 501.00	28.93 ~ 30.65	96.73 ~ 97.55	159.40 ~ 160.20	166.78 ~ 168.00	224.00 ~ 224.75	274.25 ~ 275.00	324.00 ~ 325.00	377.00 ~ 377.90	426.00 ~ 426.75	474.00 ~ 474.90
Formation*	Kt	Kt	Kt	Kt	Kt	Kt	Kt	Kt	Kt	Wk	Kt	Kt	Wk	Wk	Wk	Wk	Wk	Wk	Wk	Wk
pH	–	–	–	–	–	–	–	–	–	–	–	–	–	–	–	–	–	–	–	–
EC [mS m^{-1}]	–	–	–	–	–	–	–	–	–	–	–	–	–	–	–	–	–	–	–	–
Na^+ [mg l^{-1}]	850	6000	6500	7600	6200	6600	7100	6800	6500	6600	39	500	1200	1900	770	1200	1700	2800	3500	3300
K^+ [mg l^{-1}]	68	370	360	480	350	340	430	310	220	280	13	38	45	73	31	30	27	39	49	51
Ca^{2+} [mg l^{-1}]	57	150	170	200	75	250	520	280	230	260	7	15	95	300	12	51	51	98	40	18
Mg^{2+} [mg l^{-1}]	36	150	180	190	160	190	290	230	260	220	5	11	56	190	10	34	15	78	66	53
Cl^- [mg l^{-1}]	1100	9900	11000	13000	10000	11000	12000	11000	11000	11000	35	140	160	120	600	530	1600	3300	4400	4700
SO_4^{2-} [mg l^{-1}]	420	880	290	800	500	1100	1800	1700	1100	1300	90	980	2800	5400	810	2000	1500	1900	1600	600
HCO_3^- [mg l^{-1}]	200	50	10	10	50	10	50	10	10	10	0	20	10	10	40	20	10	10	10	10
CO_3^{2-} [mg l^{-1}]	–	–	–	–	–	–	–	–	–	–	–	–	–	–	–	–	–	–	–	–
TOC [mg l^{-1}]	–	–	–	–	–	–	–	–	–	–	–	–	–	–	–	–	–	–	–	–
TIC [mg l^{-1}]	–	–	–	–	–	–	–	–	–	–	–	–	–	–	–	–	–	–	–	–
δD [‰]	-64.0	-32.0	-27.0	-25.0	-26.0	-26.0	-23.0	-23.0	-21.0	-23.0	-67.0	-68.0	-64.0	-66.0	-67.0	-65.0	-60.0	-36.0	-28.0	-25.0
$δ^{18}O$ [‰]	-8.9	0.5	1.3	2.6	1.7	1.9	2.3	2.6	2.2	2.6	-10.3	-9.7	-8.9	-9.6	-8.9	-8.0	-7.0	-1.1	0.5	1.8

Borehole (HDB)	5	5	5	5	5	5	5	5	5	5	6	6	6	6	6	6	6	6	6	7
Sampling depth [mbgl]	27.51 ~ 28.00	60.19 ~ 61.34	124.56 ~ 125.36	174.15 ~ 174.80	225.00 ~ 225.80	278.20 ~ 279.00	324.18 ~ 325.00	373.25 ~ 373.95	426.00 ~ 426.90	473.10 ~ 474.00	78.00 ~ 78.30	135.00 ~ 135.30	279.41 ~ 279.89	394.30 ~ 394.52	440.00 ~ 440.50	492.28 ~ 492.50	547.00 ~ 547.48	600.03 ~ 600.33	610.70 ~ 611.00	41.50 ~ 41.72
Formation*	Kt	Kt	Wk	Wk	Wk	Wk	Wk	Wk	Wk	Wk	Kt	Kt	Wk	Wk	Wk	Wk	Wk	Wk	Wk	Yc
pH	–	–	–	–	–	–	–	–	–	–	8.1	8.2	8.3	8.3	8.5	8.0	8.3	8.3	8.1	8.7
EC [mS m^{-1}]	–	–	–	–	–	–	–	–	–	–	–	–	–	–	–	–	–	–	–	–
Na^+ [mg l^{-1}]	100	92	200	520	630	1600	1800	2400	3900	3400	3400	2500	1800	4100	5244	5200	8205	6400	8591	880
K^+ [mg l^{-1}]	28	15	14	24	19	53	43	36	72	66	160	120	59	74	81	48	135	67	127	42
Ca^{2+} [mg l^{-1}]	220	150	360	27	26	100	27	32	73	19	81	53	43	160	144	120	123	84	329	8.9
Mg^{2+} [mg l^{-1}]	90	56	150	24	13	53	35	64	95	60	57	33	27	120	111	170	216	190	240	7
Cl^- [mg l^{-1}]	77	66	72	68	130	1100	1900	3700	4400	4800	4600	2500	1800	5900	7717	8300	11808	9700	12035	130
SO_4^{2-} [mg l^{-1}]	960	650	1800	1100	1200	2300	1300	190	2600	780	830	800	710	1200	32	610	1546	79	1934	430
HCO_3^- [mg l^{-1}]	30	30	10	50	50	30	20	30	20	20	1600	2100	1500	1200	1039	900	363	1100	667	2100
CO_3^{2-} [mg l^{-1}]	–	–	–	–	–	–	–	–	–	–	500	500	500	500	220	500	120	500	88	500
TOC [mg l^{-1}]	–	–	–	–	–	–	–	–	–	–	100	100	100	100	56	200	–	100	63	100
TIC [mg l^{-1}]	–	–	–	–	–	–	–	–	–	–	400	400	300	300	262	300	–	300	119	500
δD [‰]	-66.0	-67.0	-67.0	-65.0	-69.0	-58.0	-48.0	-31.0	-20.0	-19.0	-36.0	-44.0	-55.0	-36.0	-27.0	-24.0	–	-20.0	–	-63.0
$δ^{18}O$ [‰]	-9.8	-10.0	-9.9	-9.6	-9.9	-6.3	-4.6	-0.4	1.6	1.9	-1.4	-2.4	-6.1	-0.4	1.0	2.2	–	3.4	–	-9.8

*Wk: Wakkanai Formation, Kt: Koetoi Formation, Yc: Yuchi Formation

Table 4.3.3-2 Major chemical and isotopic compositions of porewaters (continued)

Borehole (HDB)		7	7	7	7	7	7	7	8	8	8	8	8	8	8	9	9	9	9	9	9
Sampling depth [mbgl]		131.00 ~ 131.26	320.36 ~ 320.67	343.29 ~ 343.55	398.80 ~ 399.00	442.10 ~ 442.30	496.13 ~ 496.36	506.38 ~ 509.90	63.00 ~ 63.30	101.73 ~ 102.00	283.64 ~ 284.00	344.20 ~ 344.70	400.57 ~ 401.00	449.04 ~ 449.24	465.25 ~ 465.42	36.22 ~ 36.45	54.95 ~ 55.23	78.00 ~ 78.50	151.10 ~ 151.42	198.75 ~ 199.00	222.00 ~ 222.25
Formation*		Yc	Yc	Yc	Kt	Kt	Kt	Kt	Kt	Kt	Wk	Wk	Wk	Wk	Wk	Wk	Wk	Wk	Wk	Wk	Wk
pH		8.5	8.5	8.4	8.3	8.2	8.3	8.1	8.3	8.2	8.5	8.3	8.3	8.6	7.9	7.5	7.8	7.5	8.2	8.1	–
EC	[mS m^{-1}]	–	–	–	–	–	–	–	–	–	–	–	–	–	–	45	220	510	1100	–	–
Na^+	[mg l^{-1}]	2600	9300	10613	9100	10508	9000	10002	660	860	3600	4232	4000	4645	5170	55	290	1100	2300	4134	–
K^+	[mg l^{-1}]	170	420	518	470	474	480	439	40	38	60	72	46	1	68	5.8	18	21	22	51	–
Ca^{2+}	[mg l^{-1}]	25	57	84	120	149	100	163	22	29	52	109	68	128	212	11	36	52	34	87	–
Mg^{2+}	[mg l^{-1}]	33	190	168	170	193	160	175	13	17	87	76	100	82	130	11	29	34	23	46	–
Cl^-	[mg l^{-1}]	1200	15000	16037	14000	15577	14000	14171	330	260	4600	5573	5500	6815	6567	28	180	180	2100	5421	–
SO_4^{2-}	[mg l^{-1}]	3000	140	417	490	20	1200	33	490	1200	770	17	500	10	2125	100	370	1900	360	5	–
HCO_3^-	[mg l^{-1}]	1900	2800	2644	3200	3096	2400	3231	900	1000	1300	1755	900	877	640	47	290	530	1600	2801	–
CO_3^{2-}	[mg l^{-1}]	500	500	366	500	293	500	235	500	500	500	134	500	214	88	0.1	0.9	0.8	11	150	–
TOC	[mg l^{-1}]	100	100	119	100	123	100	120	100	100	100	64	100	77	59	6.3	20	42	64	<24	–
TIC	[mg l^{-1}]	400	600	606	700	661	500	661	200	200	400	363	300	217	116	10	59	110	330	597	–
δD	[‰]	-60.0	-19.0	-20.0	-18.0	-14.0	-17.0	-15.0	-71.0	-70.0	-31.0	–	-18.0	-25.0	–	-65.0	-67.1	-68.8	-56.1	-32.4	-29.9
$\delta^{18}O$	[‰]	-7.5	2.7	2.9	2.8	3.9	2.8	3.8	-10.1	-9.2	0.3	–	2.2	0.4	–	-9.5	-9.8	-9.5	-5.8	-0.3	1.6

Borehole (HDB)		9	9	9	9	10	10	10	10	10	10	10	10	10	10	10	10	10	10	11	11
Sampling depth [mbgl]		251.70 ~ 252.00	347.68 ~ 348.00	456.62 ~ 457.00	516.67 ~ 517.00	32.76 ~ 33.00	43.70 ~ 44.00	59.10 ~ 59.30	148.65 ~ 149.00	195.65 ~ 195.85	249.68 ~ 250.00	301.00 ~ 301.34	355.00 ~ 355.20	397.40 ~ 397.70	447.00 ~ 447.35	466.46 ~ 466.71	484.80 ~ 485.00	505.50 ~ 506.00	548.00 ~ 548.50	30.60 ~ 31.00	49.64 ~ 49.87
Formation*		Wk	Wk	Wk	Wk	Kt	Kt	Kt	Kt	Kt	Kt	Wk	Wk	Wk	Wk	Wk	Wk	Wk	Wk	Kt	Kt
pH		8.5	8.8	8.4	8.1	8.3	8.4	7.7	8.4	8.2	8.2	8.4	–	8.1	8.2	7.8	8.3	8.5	8.3	8.4	8.2
EC	[mS m^{-1}]	2100	2900	2600	2500	800	1100	1100	1300	–	1700	1500	–	–	2600	2200	–	1800	2300	640	820
Na^+	[mg l^{-1}]	4600	6300	5400	5400	1800	2700	2400	2900	3484	3600	3100	–	4301	5100	4300	3529	4000	4600	1400	1600
K^+	[mg l^{-1}]	38	23	38	12	88	116	130	138	193	154	140	–	118	98	58	82	38	50	92	42
Ca^{2+}	[mg l^{-1}]	59	58	62	23	48	63	59	41	66	66	82	–	213	84	160	105	41	93	68	60
Mg^{2+}	[mg l^{-1}]	64	89	58	72	34	50	45	29	38	41	46	–	113	140	110	59.3	86	120	29	28
Cl^-	[mg l^{-1}]	5700	8600	7100	7000	1700	2900	2000	3000	4224	4500	4200	–	7064	7400	6300	5608	5500	6700	1400	1700
SO_4^{2-}	[mg l^{-1}]	120	1400	430	2000	380	320	2800	490	104	170	1300	–	11.9	110	1700	27.9	870	1500	84	220
HCO_3^-	[mg l^{-1}]	2000	1000	1800	1000	1800	2200	380	2200	3606	2000	580	–	1535	980	240	1275	560	320	1500	1400
CO_3^{2-}	[mg l^{-1}]	29	12	22	12	18	27	0.4	26	0	14	19	–	103	6.9	0.7	112	8.2	3.2	18	10
TOC	[mg l^{-1}]	60	20	32	20	53	56	51	59	<24	45	23	–	41	83	39	25.9	27	42	39	52
TIC	[mg l^{-1}]	400	210	360	200	370	450	79	440	723	410	120	–	307	200	50	251	110	64	300	290
δD	[‰]	-27.6	-19.1	-20.4	-23.3	-62.0	-55.3	-60.1	-49.8	-44.5	-47.2	-57.9	-63.4	–	-37.2	-42.6	–	-43.8	-32.5	-63.9	-63.5
$\delta^{18}O$	[‰]	1.0	4.4	2.0	2.8	-7.0	-5.8	-6.2	-4.5	-3.0	-3.8	-5.8	-7.3	–	-2.4	-2.1	–	-2.1	1.1	-7.2	-6.9

Borehole (HDB)		11	11	11	11	11	11	11	11	11	11	11	11	11	11	11	11	11	11	11	11
Sampling depth [mbgl]		99.40 ~ 99.72	114.09 ~ 114.30	134.20 ~ 134.45	171.65 ~ 171.85	251.10 ~ 251.45	271.75 ~ 272.00	300.36 ~ 300.56	332.50 ~ 332.70	388.62 ~ 388.82	421.13 ~ 421.35	448.70 ~ 449.00	498.00 ~ 498.39	547.51 ~ 548.00	572.80 ~ 573.00	599.05 ~ 599.50	644.81 ~ 645.00	703.50 ~ 704.00	722.00 ~ 722.39	748.60 ~ 748.38	800.73 ~ 801.00
Formation*		Kt	Kt	Kt	Kt	Kt	Kt	Kt	Kt	Kt	Kt	Kt	Wk	Wk	Wk	Wk	Wk	Wk	Wk	Wk	Wk
pH		8.8	8.1	8.2	7.9	8.2	7.9	8.1	7.9	7.9	8.2	8.5	8.4	8.4	8.2	7.9	8.4	8.2	8.0	7.8	8.1
EC	[mS m^{-1}]	1300	–	2220	2500	3320	–	2800	2600	2400	–	2660	2800	2900	–	2800	2900	2700	–	2700	2700
Na^+	[mg l^{-1}]	3000	3497	4200	5400	6500	6338	5800	5500	4800	5067	5000	5600	6400	6696	6800	6200	6400	6720	6400	6600
K^+	[mg l^{-1}]	150	180	180	230	270	279	200	170	120	162	140	66	71	124	100	31	54	87	70	34
Ca^{2+}	[mg l^{-1}]	58	80.6	84	150	150	259	190	160	79	143	170	63	42	232	280	49	88	72	200	210
Mg^{2+}	[mg l^{-1}]	63	60.1	71	120	140	154	130	120	110	96.5	130	150	150	158	240	150	150	136	150	130
Cl^-	[mg l^{-1}]	3200	4793	5600	7600	9800	10131	8700	7700	6500	7126	6930	8500	9700	10957	9200	9400	9700	10145	8300	9500
SO_4^{2-}	[mg l^{-1}]	180	86.8	220	730	750	6.64	260	340	210	14.5	1750	590	190	7.76	3300	680	700	7	2400	830
HCO_3^-	[mg l^{-1}]	2100	3160	1900	1600	940	2928	1400	1700	1700	2088	870	550	1000	1163	360	620	430	1707	440	480
CO_3^{2-}	[mg l^{-1}]	67	0	14	6	6.6	0	6	7	7	188	13	7	13	150	1.4	8	3	0	1.4	2
TOC	[mg l^{-1}]	71	169	57	170	42	190	49	33	16	56.4	34	24	40	<24	52	44	65	30	99	100
TIC	[mg l^{-1}]	420	581	390	320	190	492	290	340	340	382	170	110	210	246	72	130	86	301	90	99
δD	[‰]	-53.0	-46.4	-40.4	-35.7	-22.4	-18.7	-30.1	-31.9	-35.6	–	-29.6	-29.0	-26.3	–	-20.1	-23.6	-23.1	–	-20.3	-24.0
$\delta^{18}O$	[‰]	-4.7	-3.5	-1.9	0.2	2.3	3.0	1.1	0.8	-0.2	–	0.2	1.7	2.0	–	2.6	3.3	3.5	–	3.3	3.5

Borehole (HDB)		11	11	11	11	11
Sampling depth [mbgl]		852.80 ~ 853.00	871.00 ~ 871.60	901.30 ~ 901.70	950.00 ~ 950.20	994.00 ~ 994.35
Formation*		Wk	Wk	Wk	Wk	Wk
pH		8.7	8.3	8.6	8.0	8.6
EC	[mS m^{-1}]	2500	–	2600	2700	3000
Na^+	[mg l^{-1}]	5600	6624	5900	6200	6900
K^+	[mg l^{-1}]	20	65.8	20	37	20
Ca^{2+}	[mg l^{-1}]	71	244	58	150	100
Mg^{2+}	[mg l^{-1}]	100	117	120	100	110
Cl^-	[mg l^{-1}]	8300	10838	8500	8700	9800
SO_4^{2-}	[mg l^{-1}]	140	22.9	150	740	550
HCO_3^-	[mg l^{-1}]	790	1270	730	800	590
CO_3^{2-}	[mg l^{-1}]	18	155	13	3.7	11
TOC	[mg l^{-1}]	110	80	110	120	110
TIC	[mg l^{-1}]	160	228	150	160	120
δD	[‰]	-29.0	–	-28.5	-24.9	-27.6
$\delta^{18}O$	[‰]	1.7	–	2.3	2.0	2.9

*Wk: Wakkanai Formation, Kt: Koetoi Formation, Yc: Yuchi Formation

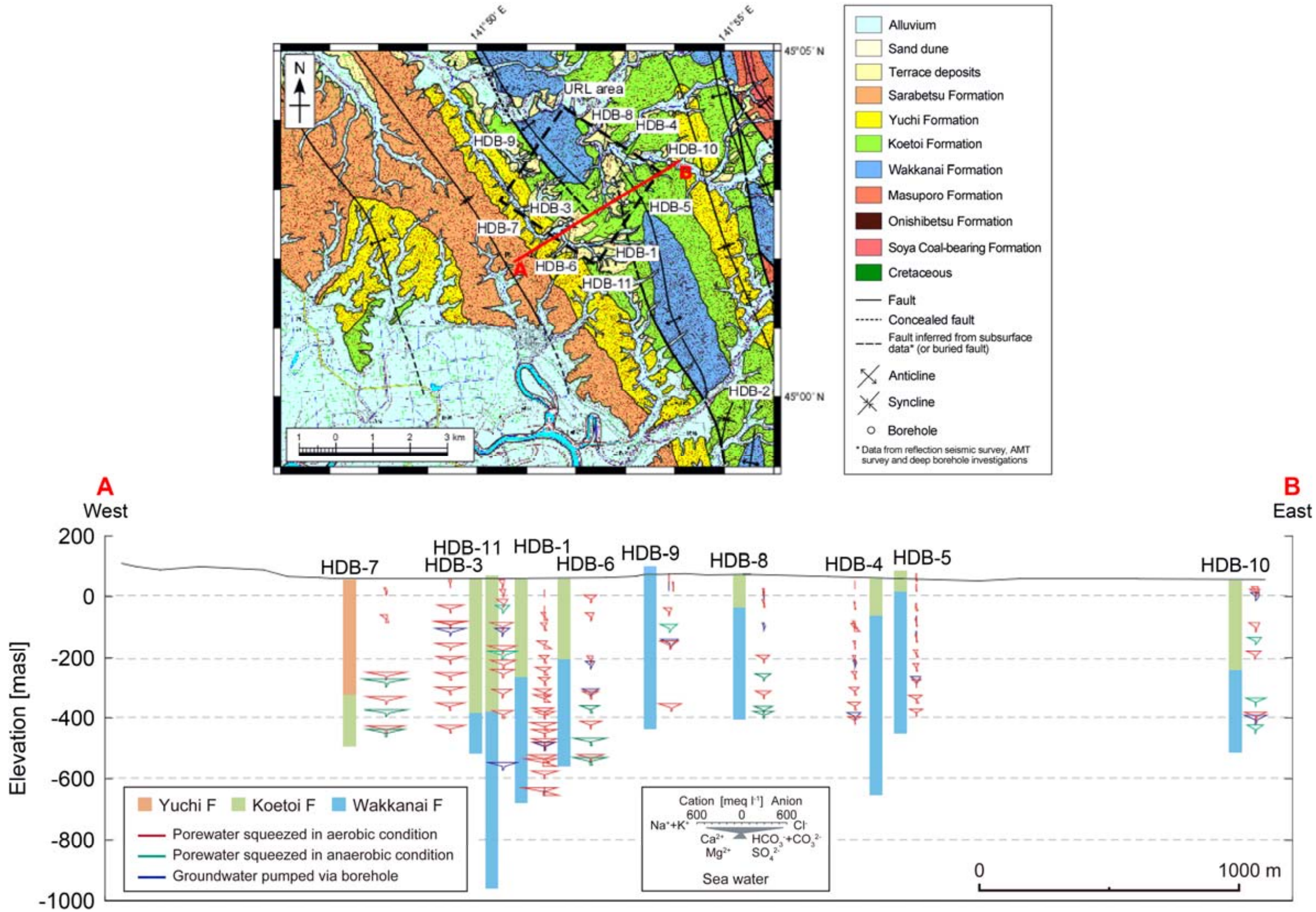

Figure 4.3.3-4 Distribution of groundwater chemistries in and around the URL area

2) Origin of groundwater

The origin of the groundwater was estimated by determining ratios of stable isotopes (δD and $\delta^{18}O$) for the groundwater and the porewater (Figure 4.3.3-5). The groundwater in the shallower subsurface is abundant in both light H and O isotopes (δD of -90 – -60‰, $\delta^{18}O$ of -11 – -10‰), while that in the deeper formations is abundant in heavy isotopes (δD of -30 – -20‰, $\delta^{18}O$ of +2 – +3‰). Mixing of these two types of groundwater could thus be one of the evolution processes for the present groundwater.

It is known for the groundwater in shallower subsurface that the water chemistry was formed by the ion-exchange reaction of Na^+ and H^+ between the liquid phase (recharged with precipitation) and the solid phase (clay minerals in rocks, such as smectite), with evidence that the pH increases with an increasing Na/Cl concentration ratio in the groundwater[44)]. This is consistent with the results from the measurement of the H and O isotopes described above.

The salinity of the deep groundwater is about 1/3–1/2 that of present seawater, with high $\delta^{18}O$ values of +2 – +3‰. The origin of the deep groundwater may be the fossil seawater. However, it cannot simply be explained by mixing with water originating from meteoric water. A groundwater evolution process with this feature would be mixing of fluids released in association with diagenesis[103)].

These results and discussion would suggest that mixing and water-rock reactions are the major processes determining the groundwater chemistry in the Wakkanai and Koetoi Formations.

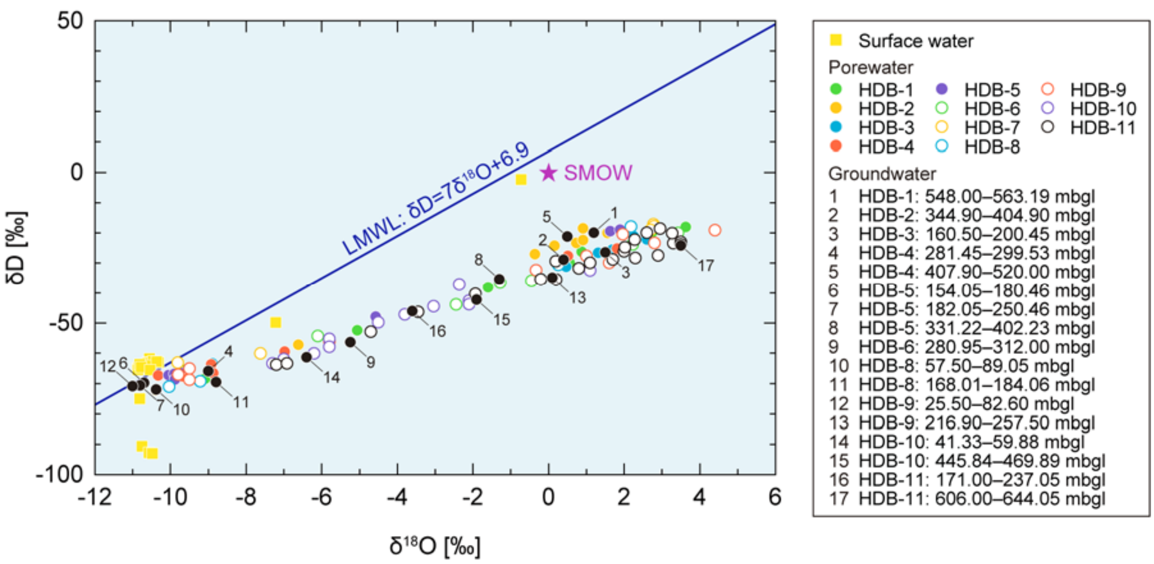

Figure 4.3.3-5 δD vs $\delta^{18}O$ for surface water, porewater and groundwater from all boreholes in and around the URL area

3) Residence time of groundwater

The residence time of groundwater was estimated by measuring radioisotopes (^{3}H, ^{14}C, ^{36}Cl, ^{3}He and ^{4}He). Based on existing information, it was assumed that the origin of the groundwater in the Wakkanai and Koetoi Formations was likely to be fossil seawater and, considering the rock formation age, the residence time of the groundwater in the area would be in the order of one million years. This means that ^{3}H and ^{14}C with relatively short half-lives might not be useful for estimating the residence time. The results of the measurement of ^{3}H and ^{14}C in the groundwater samples showed a ^{3}H concentration of less than the lower the detection limit and ^{14}C with a very low concentration of a few pMC (percent modern carbon) for almost all the samples[104]. These facts indicate that the age of the groundwater in the area is 50,000 years or younger. However, the possibility that the ^{14}C measured here could have originated from oil in the drilling mud or used for lubricating drilling tools cannot be ruled out.

The ^{36}Cl ratios ($^{36}Cl/Cl$) were as low as 1×10^{-14} for groundwater at almost all depths. The $^{36}Cl/Cl$ of the river water in Horonobe Town was $(30–70) \times 10^{-15}$. The residence time, calculated based on assumption that the $^{36}Cl/Cl$ at the time of recharge of the groundwater had the ratio of river water and that ^{36}Cl decayed through radioactive decay, is in the order of one million years. The ratio of ^{36}Cl estimated based on the amount of ^{36}Cl produced in the subsurface, which is based on the neutron flux density estimated from the content of the U and Th in the rocks, is about 10×10^{-15}. Approximately three million years is necessary for $^{36}Cl/Cl$ in the groundwater to reach 10×10^{-15} (radioactive equilibrium). Taking all the above into consideration, the residence time of the groundwater is considered to be in the order of a few million years. However, it is pointed out that the residence time cannot be estimated in the field where mixing of water chemistry is a major groundwater evolution process[105]. Since mixing was considered to be one of the main processes determining the groundwater chemistry in the Wakkanai and Koetoi Formations, the residence time estimated based on the $^{36}Cl/Cl$ ratio should be treated in the light of the limitations of the method.

The He concentration in the groundwater was $10^{-6}–10^{-5}$ cm^{3} STP g_{water}^{-1}, which is two orders of magnitude higher than that dissolved in the groundwater (4.8×10^{-8} cm^{3} STP g_{water}^{-1}) in equilibrium with air. In the case where an excessive amount of He compared to that at equilibrium with air is produced by α-decay of U and Th in the rock, the residence time would be estimated to be a few million years. This confirms the result of the groundwater flow analysis which was conducted separately.

These discussions above suggest that, for estimating the residence time of the groundwater, it is necessary to acquire and compare data on numbers of radioisotopes, variations in water quality and the groundwater evolution processes.

4) Colloids, organics and microbes in groundwater

The types and quantities of colloids, organics and microbes in the groundwater could vary depending on water chemistry (e.g. salinity). Because of the limited time available for the borehole investigations, the contamination of the groundwater samples by the drilling mud was as high as a few to a few tens of %, which was not low enough to acquire high quality information on colloids, organics and microbes. To obtain high quality data on colloids, organics and microbes is one of key research topics for the investigations in Phase II and/or Phase III. Preliminary data collection was conducted to evaluate the applicability of basic techniques, including analysis methods.

The total organic carbon concentration in the groundwater was in the range of a few to a few tens of mg l^{-1} and no clear relationship with the concentration of the principal components was observed. Characterising the properties of organics (mainly humic substances) both in the shallower and deeper groundwaters revealed that the molecular weight distribution of humic substances may be different for the two groundwaters[106].

With regard to microbes in the groundwater, measurements of the total numbers of bacteria and a genetic analysis were conducted for some water samples collected from the boreholes. The total bacteria number was in the range 10^4–10^6 m l^{-1} and trend was not observed that indicates reduction in the bacteria numbers with increasing depth. The ratio between cell division and total number of bacteria (activity index) was a maximum of 5.63% at 280.95–312.00 m depth in borehole HDB-6 (boundary between the Wakkanai Formation and the Koetoi Formation). DNA analysis of the groundwater at the above depth showed that *Gamma-proteobacteria*, particularly those related to the *Pseudomonas* group, were dominant. This could support the high activity index observed[107]. The hydraulic conductivity for this interval was in the order of 10^{-6} m s^{-1}, which was one or two orders of magnitude higher than that for other sections in the borehole HDB-6. These data suggest a potential relationship between the occurrence and activity of the microbes in the groundwater and the permeability of the rocks or groundwater flow.

For organics and microbes in the groundwater, preliminary data collection and confirmation of the applicability of conventional and improved analysis methods for groundwater samples were conducted. In the investigations in Phase II and/or Phase III, it will be necessary to accumulate information on the impact on solute transport by collecting groundwater samples under controlled conditions and acquiring data on colloids, organics and microbes.

5) Chemical and mineral compositions of rocks

The major chemistry in the Wakkanai and Koetoi Formations includes Si (approximately 70 wt%), Al (approximately 10 wt%) and Fe (III) (approximately 2 wt%)[26].

Based on the results of microscopic observations, electron microscopic observations and X-ray diffraction analysis[44], the typical minerals that constitute the Wakkanai and Koetoi Formations were identified as silica minerals (opal CT/opal A) and some quartz, feldspar, clay minerals (kaolinite, smectite, illite, chlorite), pyrite and carbonate minerals (siderite, magnesite). However, there is a large difference in the silica mineral phase between the Wakkanai Formation and the Koetoi Formation; the Wakkanai Formation is constituted mainly of opal CT, which was formed by the burial and diagenesis of diatom remains (opal A), while the Koetoi Formation does not contain opal CT. The depth of the boundary between the two in each borehole is defined by the difference in the silica mineral phases described above.

4.3.4 Hydrochemical modelling

(1) Estimation of distribution of groundwater chemistry

The distribution of groundwater chemistries was estimated from the data obtained in each investigation stage (Figure 4.3.4-1). The inverse distance weighting method included in the Tecplot ver. 10 software was used for the estimation. To the east of the Omagari Fault, groundwater with low mineralisation was found in deeper formations, while in the west, groundwater with high mineralisation was found in the shallower formations. This finding is consistent with the resistivity distribution estimated by the geophysical survey (see Section 4.1). Since the resistivity distribution represents the salinity of the groundwater[108], the estimated result for the distribution of the groundwater is considered to roughly represent the distribution of water chemistry in and around the URL area.

Iterating the data acquisition and modelling and applying two or more investigation methods for the same area would be effective for improving confidence in the investigation and modelling approaches.

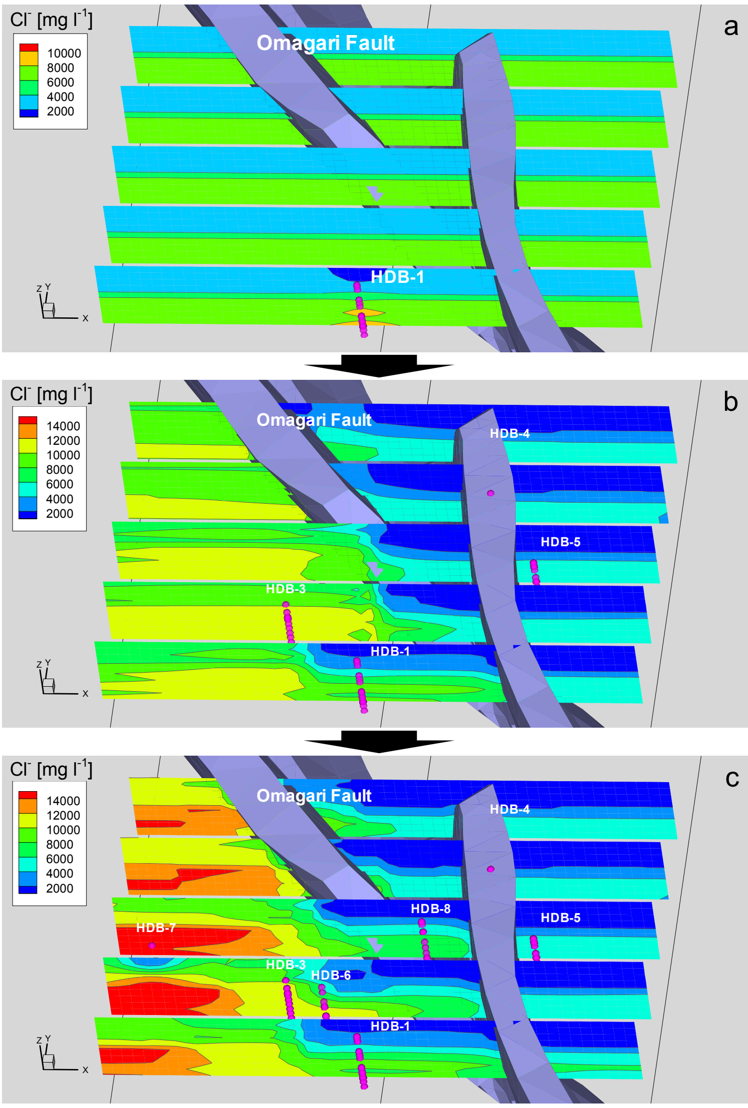

Figure 4.3.4-1 Progress in estimation of 3D distribution of groundwater chemistries

a: Data from borehole HDB-1 only; *b*: Data from boreholes HDB-1and HDB-3 to HDB-5

c: Data from boreholes HDB-1and HDB-3 to HDB-8

(2) Analysis with the M3 method

1) Overview of the M3 method

The groundwater chemistry in the Horonobe area could have been formed from a number of different sources such as river water and fossil seawater. The M3 (multivariate, mixing and mass balance) method[109),110)] is a technique for identifying water chemistry types (reference waters) of different origin and calculating the mixing ratio of the reference waters using the multivariate analysis technique. It also provides an estimate of generated/lost quantities of components owing to chemical reactions such as rock – water interaction, based on the difference between the calculated concentration of components in the complete mixture and the actually measured concentration of the components (mass balance calculation). The following three steps are taken in the M3 method[109),110)]:

- Step 1: Analysis of principal components
  The distribution of water chemistries is expressed visually as a principal component analysis plot and reference waters in the area concerned (end-member of the groundwater chemistry) are identified. Generally, it covers principal components such as Cl^-, SO_4^{2-}, HCO_3^-, Na^+, Ca^{2+} and Mg^{2+}, as well as isotopes such as ^2H, ^3H and ^{18}O. The principal components are calculated by a linear equation multiplying predictor variants (concentrations of components) by some weighting factors. The water chemistry data plotted inside the polygonal shape in the analysis chart can be interpreted based on mixing of reference waters and chemical reactions.

- Step 2: Calculation of mixing ratio
  The mixing ratio of reference waters is calculated for the data of groundwater chemistries. The mixing ratio can be obtained by the distance between the groundwater and the reference water in the principal component analysis. For the 2D analysis (where the secondary components are also included), a mixing ratio can be obtained for up to three reference waters.

- Step 3: Calculation of mass balance
  Once the calculated value using the above mixing ratio matches with the actual measured value, the components can be explained using a complete mixing model. The difference between the calculated and actually measured values can be explained by errors due to uncertainties and/or production/loss caused by chemical reactions.

2) Analytical results

i) Data used for the analyses

The data for groundwater (water pumped from boreholes and porewater squeezed from cores), river water and seawater, those that contain data on the six principal components (Na^+, K^+, Mg^{2+}, Ca^{2+}, Cl^- and SO_4^{2-}) were used in the analyses. As a principal component analysis using the porewater could lead to false conclusions, i.e. the aforementioned SO_4^{2-} concentration might be included in the principal components, the water chemistry data for the groundwater were therefore used for the analyses.

ii) Principal component analysis

The results of principal component analysis are shown in Figure 4.3.4-2 (top). All data were plotted on the straight line connecting two end-members (river water, groundwater from the interval of 160.50–200.45 m depth in borehole HDB-3). It was found that there was no need to use seawater as an end-member.

iii) Calculation of the mixing ratio

The distribution of the mixing ratios calculated based on the results of the principal component analysis is shown in Figure 4.3.4-2 (middle).

iv) Calculation of mass balance

The concentration of principal components estimated based on the mixing ratio calculated assuming mixing of the above two end-members and the measured concentration were compared (Figure 4.3.4-2, bottom). The estimated Na^+ concentration, among the reactive elements, was smaller than the measured one. This indicates that Na was added by rock – water interaction.

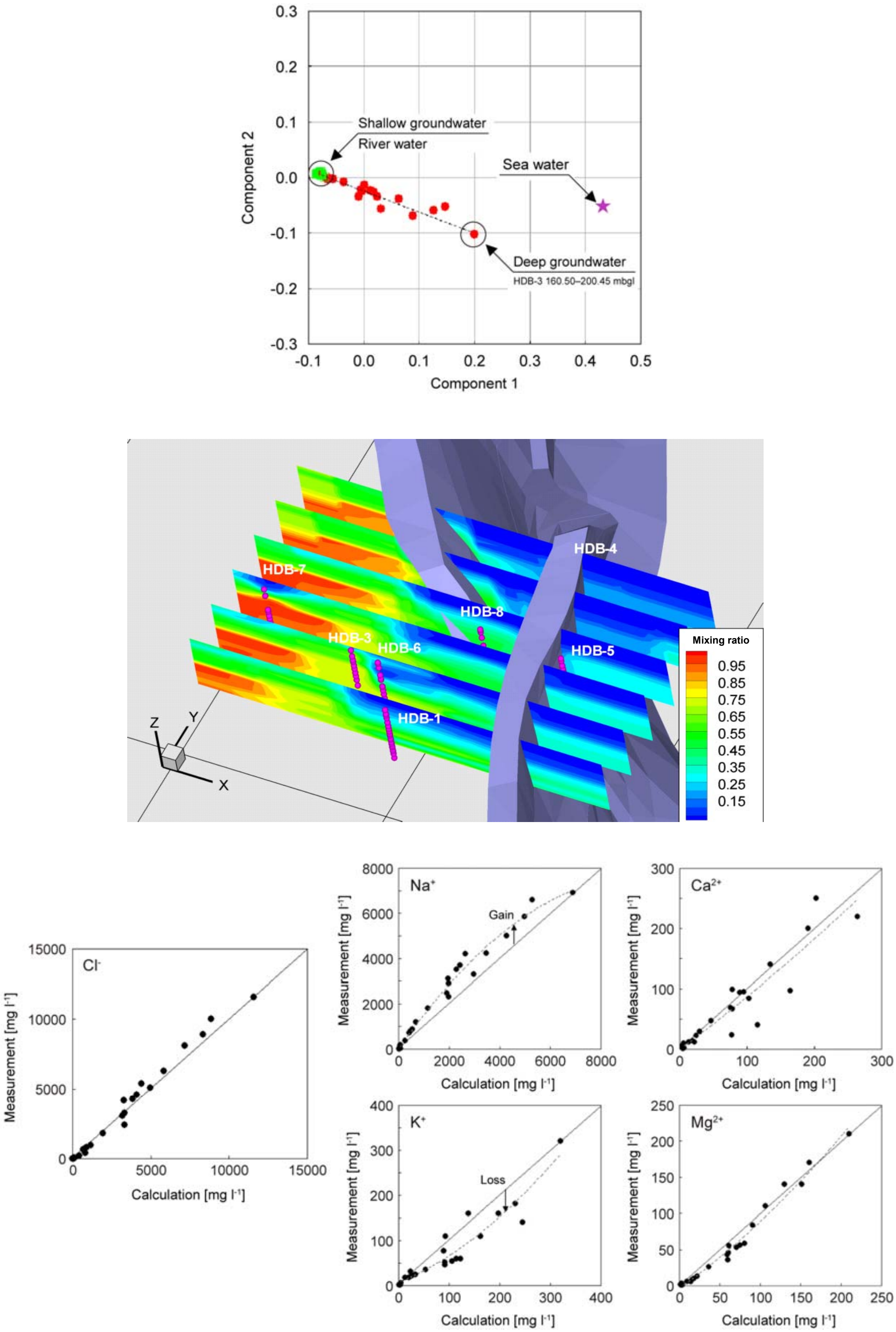

Figure 4.3.4-2 Results of analysis with M3 method

Top: Results of principal component analysis; *Middle*: Distribution of estimated mixing ratios of deep groundwater
Bottom: Comparison of calculated and measured concentrations of principal components; After Shimo et al.[87)]

4.4 Rock mechanical investigations

4.4.1 Aims

The main goals of the rock mechanical investigations in Phase I were to clarify the rock mechanical properties of the geological environment and to establish methodology for evaluating the impact on the tunnel near-field of the underground facilities. More specifically the aims of the investigations were:

- to acquire information on rock mechanical properties from near-surface to deep subsurface for the selection of a URL area and a URL site;
- to acquire the data necessary for designing the underground facilities;
- to estimate the mechanical impact of constructing the underground facilities on the tunnel near-field.

It is thus necessary to enhance confidence in the investigation techniques applied and the modelling and analyses performed in Phase I through investigations during tunnel excavation (Phase II).

4.4.2 Surface-based investigations covering the whole Horonobe Town area

(1) Investigation aims and methods

The geological environment has more or less site-specific characteristics and hence there is no standard investigation technique for acquiring information. The basic approach for investigations aimed at improving understanding in this area is iterative development of a field concept, formulation of an investigation plan based on the developed concept, implementation of the plan and evaluation of the investigation results. Taking the above into account, in this investigation phase a programme was formulated to achieve the aims described in Subsection 4.4.1, based on existing information.

(2) Integration of existing information

The sedimentary rocks to be characterised are the Neogene sedimentary formations, based on the requirements relating to distribution of formations for the URL site as shown in Subsection 3.1.1. A geological structure was predicted in which rocks with almost identical properties are continuously distributed horizontally. The Koetoi Formation has been assumed to consist of mechanically fragile mudstones, based on the results of laboratory tests on cores from the D-1 borehole[54)]. Based on the existing information, the concepts for mechanical properties were initially assumed as below:

- Neogene sedimentary formations form a porous continuum with relatively homogeneous properties and a wide horizontal extent. The rigidity of the rock is classified as ‘soft’ in an engineering sense.
- Because the rocks are soft, fractures formed by diastrophism are not easily opened and they are smaller compared to those in crystalline rock. In addition, information exists on the hardness of these sedimentary rocks, which has been obtained by geophysical logging and is similar to results obtained from laboratory tests[111)]. Therefore, the differences between the properties of the in situ rock mass, including fractures, and those of rock samples are relatively small.
- As mudstones generally consist of clay minerals, there is a concern that rocks may be influenced by increased pressures owing to clay swelling during excavation. Also, deterioration of the rocks around the tunnel caused, for example, by slaking could occur.

The basic principles for planning the investigation programme were formulated as follows, considering the URL site selection process:

a) Data should be obtained so that the features of the geological structure can be compared and the relationships between them defined. Because the rock properties can be considered to be equivalent to the properties of rock cores determined in laboratory tests if the rocks are relatively soft and homogeneous and the influence of fractures on the mechanical properties of the in situ rock mass are relatively small, the mechanical properties of widely extending rock bodies can be evaluated using limited data.

b) The rocks may be deformed both upwards and downwards owing to the influence of folding, thereby having heterogeneous mechanical properties. Data should therefore be obtained with a frequency that allows assessment of properties on the minimum scale required to realise the specified aims.

c) The investigation programme must be formulated taking into account the progress in a stepwise site selection process, as well as individually examining the data requirements in each selection step.

d) Because of the relatively short investigation cycle (execution of investigations → analysis/assessment of the results → planning for subsequent years), i.e. as short as one year, the basic approach to the investigations should be a qualitative assessment cycle: conceptualisation of the rock mechanical properties → planning of the investigation programme based on the concept → implementation of the programme and evaluation of the results → refinement of the initial concept. Quantitative modelling should be made at the stage when the mechanical impact of tunnel excavation will be predicted.

For principle (a), data obtained continuously from near-surface to deep subsurface using a method such as geophysical logging were compared with point data on physical and mechanical properties obtained by laboratory tests and geological structures. The modelling/analysis scale for achieving the aims of this investigation was smaller than that for other types of investigations, such as the hydrogeological investigations. From the viewpoint of evaluating mechanical impact, the diameter of the tunnels to be excavated in the underground facilities should be a measure for determining the scale.

For principle (b), at the start of the investigations, a scale of approximately 50 m in diameter was regarded as the minimum for the investigations and data were to be obtained from more than one location on this scale, given the diameter of the tunnel (5 m) for a repository in soft rock described in the H12 report[112)].

For principle (c), before selection of the URL site in the investigation stage in/around the URL area, data collection and evaluation should be focussed on clarifying 3D mechanical features in the URL area; after selection of the site, the data required for designing the underground facilities should be the focus.

For principle (d), since the testing of the conceptual model has to be completed in a single year, the evaluation was conducted using data primarily from laboratory tests, except triaxial compression tests, and geophysical logging (e.g. density logging) in a borehole, which could be obtained quickly but reflecting the rock mechanical properties of the sedimentary formations of interest.

Evaluation of the rock mechanical behaviour of the tunnel near-field during excavation is necessary from the viewpoint of designing the underground facilities and predicting the impact during tunnel excavation. This requires information on the in situ stress conditions as well as the rock properties. It was decided to conduct minimal measurements to acquire information on changes in stress with depth and the principal stress ratio in this investigation, given that the influence of the rock properties and fractures on the stress field was assumed to be small and the installation of casing would be inevitable for protecting the borehole wall during investigations, since the rocks were soft down to a range of a few hundred metres depth.

The effect of long-term rock behaviour on the EBS will be characterised in R&D on geological disposal technology and relevant data therefore need to be obtained. Since there were no standard methods for evaluating the long-term behaviour, laboratory testing methods (triaxial creep test, uniaxial creep test, uniaxial compression test with changing strain rate) were used to study long-term rock behaviour.

(3) Investigations before selection of the URL area

Rock mechanical investigations were conducted for selection of the URL area using boreholes HDB-1 and HDB-2 (both 720 m depth). Based on the principles described in Subsection 4.4.2, physical and mechanical properties were measured by laboratory tests using standardised domestic and international methods based on the International Society for Rock Mechanics (ISRM) guidelines and JIS, in order to evaluate various properties of the Neogene sedimentary rocks in and around the URL area and to compare the results with data on properties of Neogene sedimentary rocks found in other areas of Japan. Specific test targets include density, specific weight, effective porosity, elastic wave velocity, uniaxial and triaxial compression and Brazilian tests, which were planned so as to evaluate the engineering characteristics (confined compression dependence and anisotropy caused by the sedimentary structure) generally shown by soft sedimentary rocks[113)]. Laboratory tests were also conducted separately to evaluate the swelling and slaking characteristics of the rocks described above using standard methods.

In situ stress is measured, in principle, by in situ measurements which are now considered to be highly reliable. The in situ stress measurement was also attempted on core samples from soft sedimentary rocks for the case where the in situ test cannot be conducted owing to borehole breakout and its applicability was evaluated. The hydraulic fracturing method was used as the in situ measurement method because the boreholes in question are vertical deep boreholes and are always filled with water and the vertical downward direction can be considered as one of principal stress directions as found in the existing measurement cases[114)]. The acoustic emission (AE) method developed in JAEA Tono Geoscience Center was employed as a stress measurement method for core samples.

The depth profiles of the physical and mechanical properties of sedimentary rocks characterised in boreholes HDB-1 and HDB-2 are shown in Figure 4.4.2-1. In borehole HDB-1, the rock physical (i.e. density, effective porosity) and mechanical properties (elasticity modulus, uniaxial compressive strength and tensile splitting strength) tend to increase with depth, while for borehole HDB-2 no such clear trend was recognised. The results of measurements of mechanical properties of the Wakkanai Formation were 1.41–6.35 GPa for the elasticity modulus (E_{50}), 8.9–34.9 MPa for the uniaxial compressive strength and 0.168–0.337 for Poisson's ratio; those for the Koetoi Formation were 0.38–1.03 GPa, 1.44–9.80 MPa and 0.220–0.467 respectively. This means that, in an engineering sense, rocks classified as soft sedimentary rock are found down to approximately 700 m in depth. The tensile splitting strength was approximately 1/10 of the uniaxial compressive strength in both the Wakkanai and Koetoi Formations. Figure 4.4.2-2 shows the comparison between the physical and mechanical properties of Neogene sedimentary rocks (mudstones and tuff) distributed throughout Japan as identified in the H12 report[115)] and those obtained in boreholes HDB-1 and HDB-2. The physical and mechanical properties (except for effective porosity) of the rocks near boreholes HDB-1 and HDB-2 were within the variation range of properties of Neogene mudstones and tuff found throughout Japan and the mode value of the properties was also approximately the same. The effective porosities were within the range of variability, but were relatively higher, with 34.9–51.9% for the Wakkanai Formation and 52.2–65.2% for the Koetoi Formation.

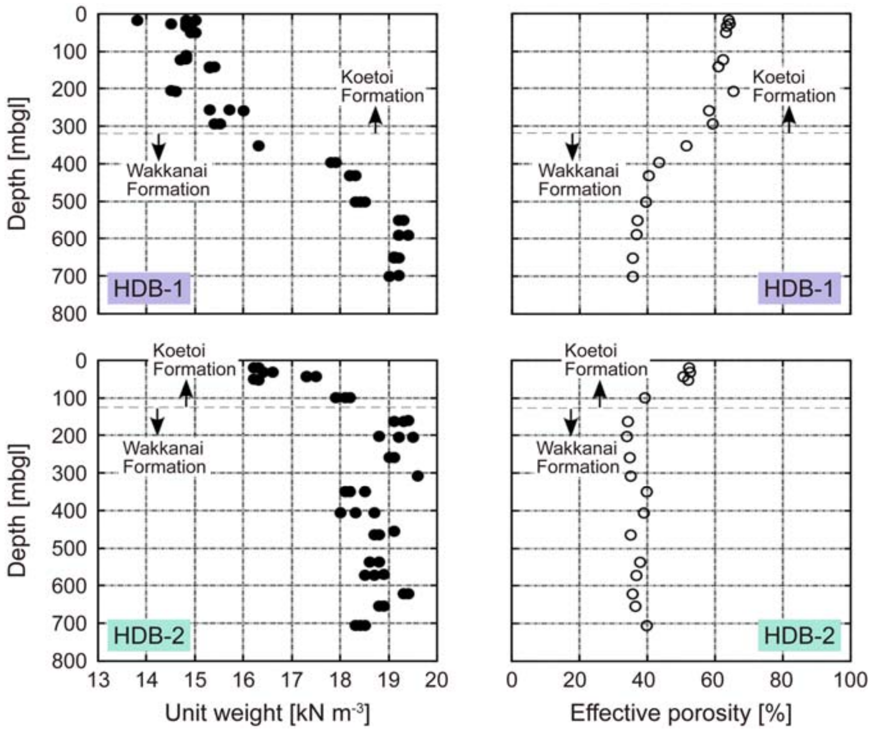

Figure 4.4.2-1 Distribution of rock physical properties characterised in boreholes HDB-1 and HDB-2

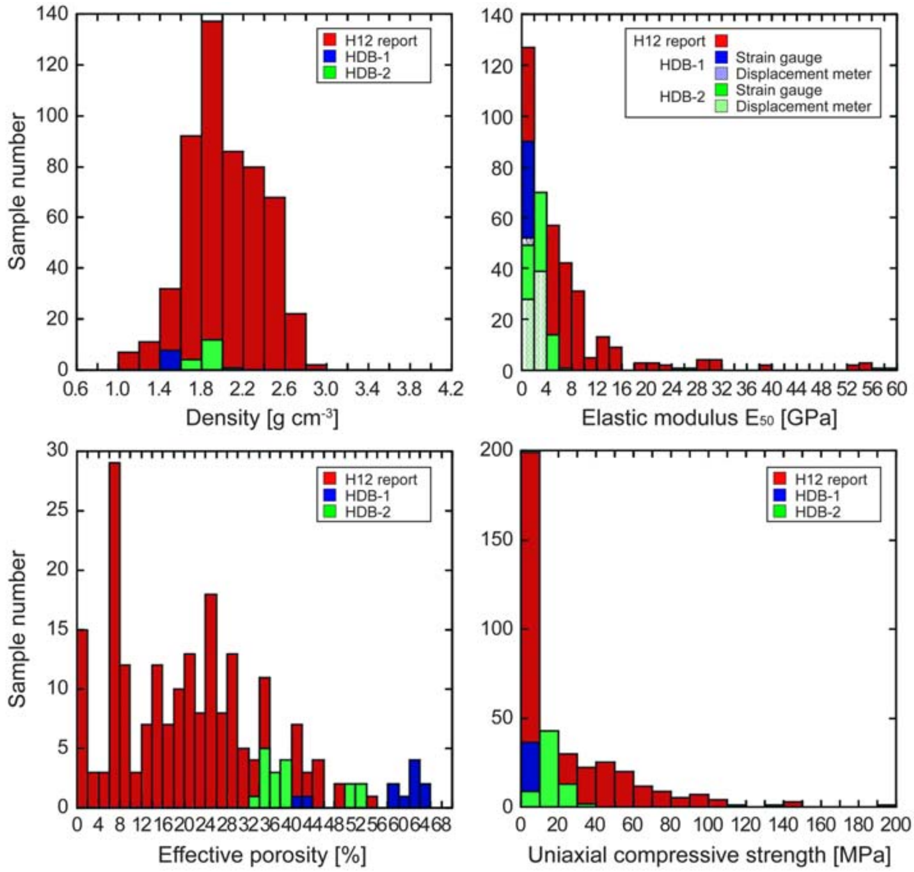

Figure 4.4.2-2 Comparison of rock properties characterised in boreholes HDB-1 and HDB-2 and for Neogene sedimentary rocks in Japan

The comparison between data on elastic velocity measured for the rock mass by geophysical logging and for the rock cores is shown in Figure 4.4.2-3. Although the elastic velocity for the crystalline rock obtained from geophysical logging was smaller than that for the cores[116), data obtained by geophysical logging and by core measurement for the Wakkanai and Koetoi Formations are very consistent. In addition, local changes in the velocities during geophysical logging were smaller, compared to those in the crystalline rocks. This could be due to differences in nature between crystalline rocks and soft sedimentary rocks; the crystalline rocks form larger-scale fractures with rigid faces that are easily opened by displacement whereas soft sedimentary rocks form smaller-scale fractures that are not easily opened.

From these results, the concepts for mechanical properties, which were assumed before the investigations, were confirmed to be appropriate; the rocks would constitute a porous continuum and could be classified as soft rock in an engineering sense and the influence of fractures in the rock mass on the mechanical properties would be small.

Contrary to the assumption before the investigations, rocks down to a depth of 700 m from the ground surface in boreholes HDB-1 and HDB-2 showed little swelling and the slake durability was also high[117)]. This means that both the Wakkanai and Koetoi Formations contain small amounts of smectite, but not so much as to affect the characteristics of these formations. Thus, for the rocks around boreholes HDB-1 and HDB-2, deterioration of rock properties, caused by squeezing during tunnel excavation, and the repetition of drying and wetting cycles over a short period of time would be unlikely.

The results of the in situ stress measurements are shown in Figure 4.4.2-4. Although the initial plan included tests at three depth levels in boreholes HDB-1 and HDB-2, tests were conducted at only two depth levels, since the stress measurement system applied was not suitable for measurement in the drilling mud and the device often became jammed. However, since borehole breakout occurred continuously in the section at approximately 400 m and deeper in borehole HDB-1 and locally in borehole HDB-2, an attempt was made to use the phenomenon in estimating the in situ stress and the direction of the principal stress in the horizontal plane.

Although the number of measurements was small, the direction of the major principal stress in the horizontal plane would be almost constant in an E-W direction at a depth of 300–700 m, given the estimates based on borehole breakout. This direction is consistent with the strain direction of the maximum horizontal compression obtained from the analysis of the seismic ground motion[118)]. The minimum principal stress in the horizontal plane was estimated to be almost equal to the estimated overburden pressure and the major principal stress was estimated to be higher than the minimum principal stress by a factor of about 1.2–1.3. In the rocks around borehole HDB-2, the depth profile of the principal stress was very similar to that in borehole HDB-1, but the principal stress direction in the horizontal plane was not constant. One of the reasons for this could be the fact that borehole HDB-2 is located close to the Omagari Fault identified at the surface and borehole was drilled in an area where changes in stress caused by fault activity might still occur.

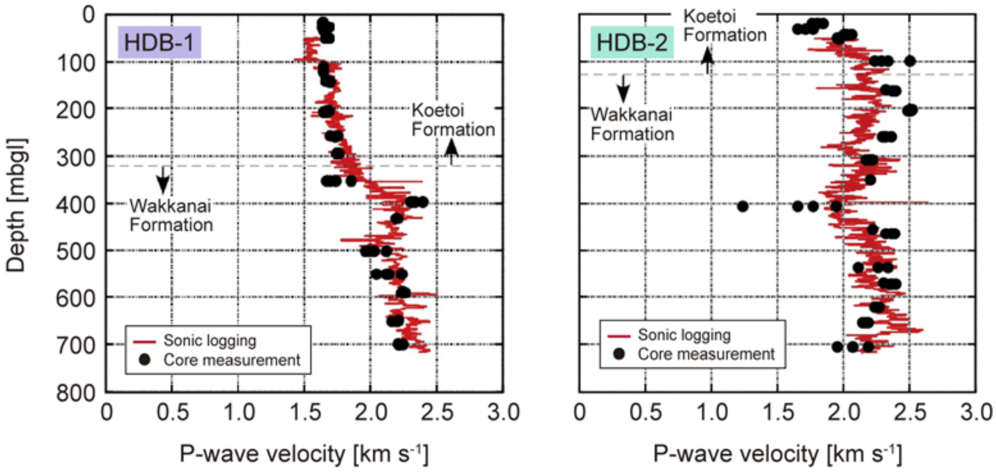

Figure 4.4.2-3 Comparison of P-wave velocities measured on cores and in situ for boreholes HDB-1 and HDB-2

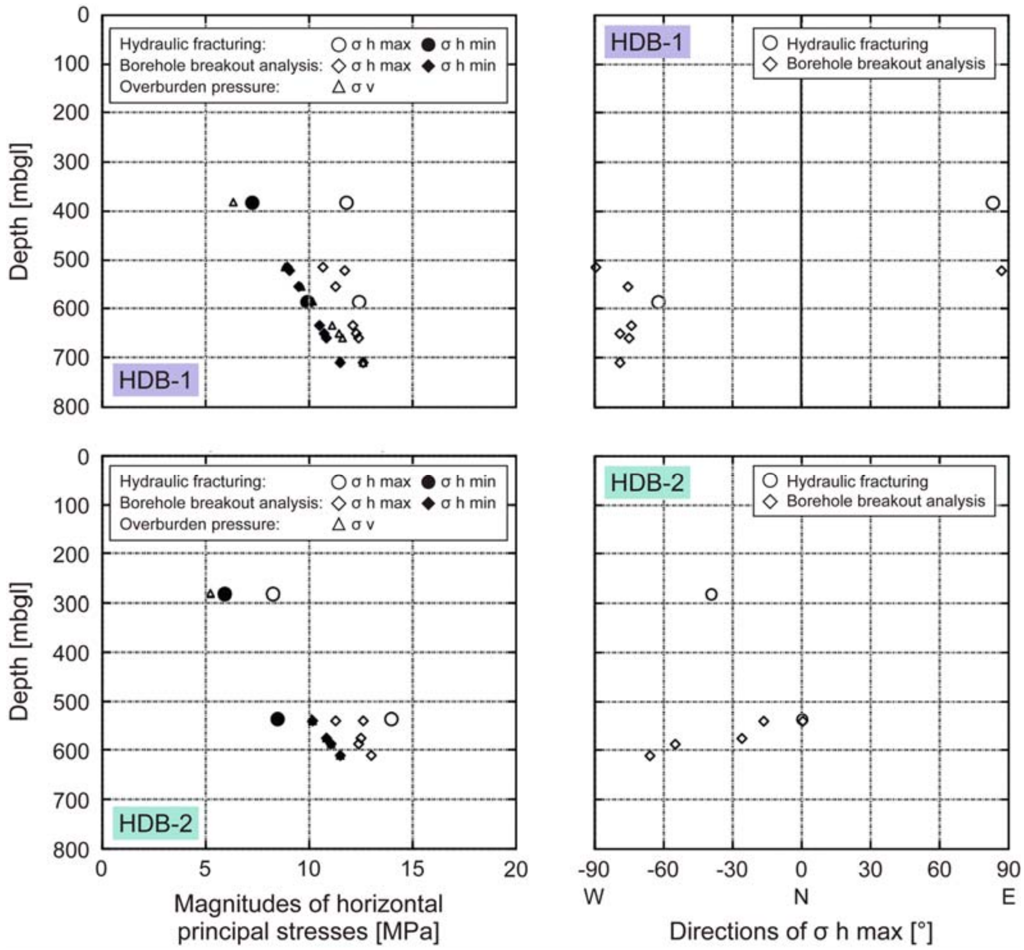

Figure 4.4.2-4 Measured and estimated principal stresses and directions with depth in boreholes HDB-1 and HDB-2

4.4.3 Surface-based investigations in and around the URL area

(1) Investigations prior to selection of the URL site

The results of geophysical logging and laboratory tests during investigations in boreholes HDB-3, HDB-4 and HDB-5 in the URL area are shown in Figure 4.4.3-1, in conjunction with the investigation results from boreholes HDB-1 and HDB-2. Borehole HDB-3 was located on the west side of the inferred location of the Omagari Fault in the URL area and boreholes HDB-4 and HDB-5 on the east side, as shown in Subsection 3.5.2 and Appendix 2, the aim being to acquire information on the geological environment on both sides of the fault. The same investigation methods and items as for boreholes HDB-1 and HDB-2 were used for the investigations in these boreholes so that the data obtained could be directly compared with the results from borehole HDB-1. The applicability of the investigation methods, other than the hydraulic fracturing, to the formations distributed throughout the URL area (the Wakkanai and Koetoi Formations; see Appendix 5) was confirmed by the investigation results in boreholes HDB-1 and HDB-2.

Figure 4.4.3-1 indicates that the rocks around each borehole have features in common with the rocks around borehole HDB-1 drilled before the selection of the URL area in that the investigation results show the same trend of physical properties increasing in strength, P-wave, density etc. with increasing depth. The results of geophysical logging and laboratory tests are almost consistent and physical properties change significantly at certain points. With regard to the distribution of properties, it was found that the rocks in and around the URL area could be classified into three major zones within a range down to 700 m depth. These three zones, classified on the basis of rock quality, correspond, in descending order, to diatomaceous mudstones, the transition zone from diatomaceous mudstones to siliceous mudstones and siliceous mudstones.

Taking the above findings into consideration, the results of geophysical logging and laboratory tests compared with the results from borehole HDB-1 as reference values are shown in Figure 4.4.3-2. It can be seen from this figure that the depth profiles of the physical and mechanical properties of sedimentary rocks in and around the URL area are uniform when fault-slip such as from the Omagari Fault is adjusted. The depth profiles of the rock physical and mechanical properties investigated in the boreholes on the same side of the Omagari Fault (i.e. HDB-1 and HDB-3 on the west side; HDB-4 and HDB-5 on the east side) are almost the same with depth. Comparing with the profiles on either side of the fault, the profiles are almost the same by correcting fault-slip (about 200 m). Hence the 3D distribution of the rock properties can be estimated taking the geological structure into account.

The results of the in situ stress measurements for each borehole are shown in Figure 4.4.3-3. The stress measurement system used was the hydraulic fracturing method that can be used even in drilling mud and is unlikely to become jammed. This method was used for the measurements in boreholes HDB-3, HDB-4 and HDB-5. The depths for the measurements were similar to those for the stress measurements in borehole HDB-1, to allow comparison of the stress conditions between the east and west sides of the fault. When comparing the maximum/minimum principal stress in the horizontal plane measured for each borehole, those in boreholes HDB-1 and HDB-3, located on the west side of the fault, were slightly higher than those for boreholes HDB-4 and HDB-5. The direction of the maximum principal stress was mostly in an E-W direction, whatever the side of the fault. The reason for this could be the influence of the regional stress field, with a maximum principal stress axis in the horizontal plane in an E-W direction.

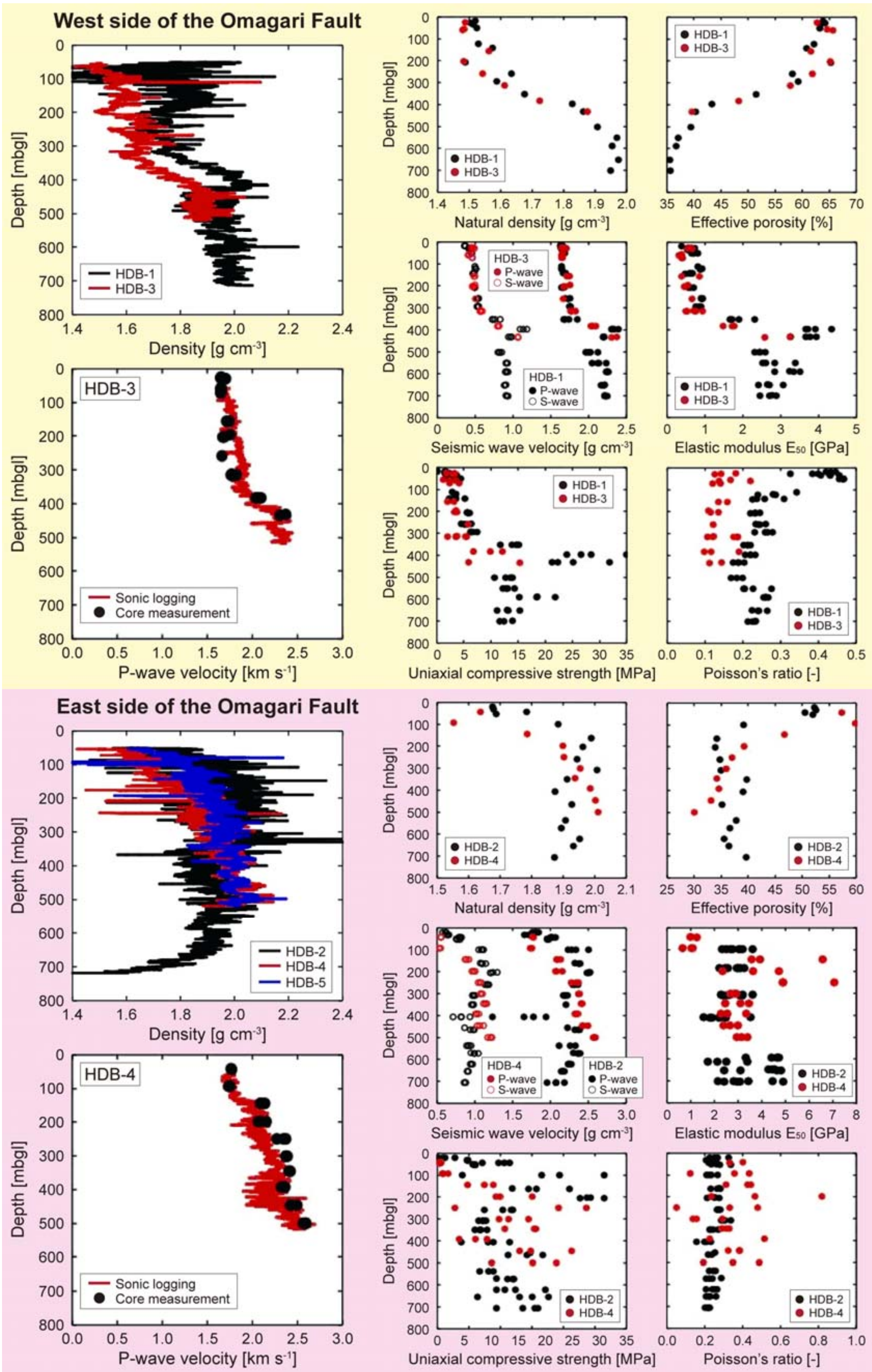

Figure 4.4.3-1 Comparison in physical and mechanical properties of sedimentary rocks between the west and east sides of the Omagari Fault

West side of the fault: HDB-1 and HDB-3; *East side of the fault*: HDB-2, HDB-4 and HDB-5

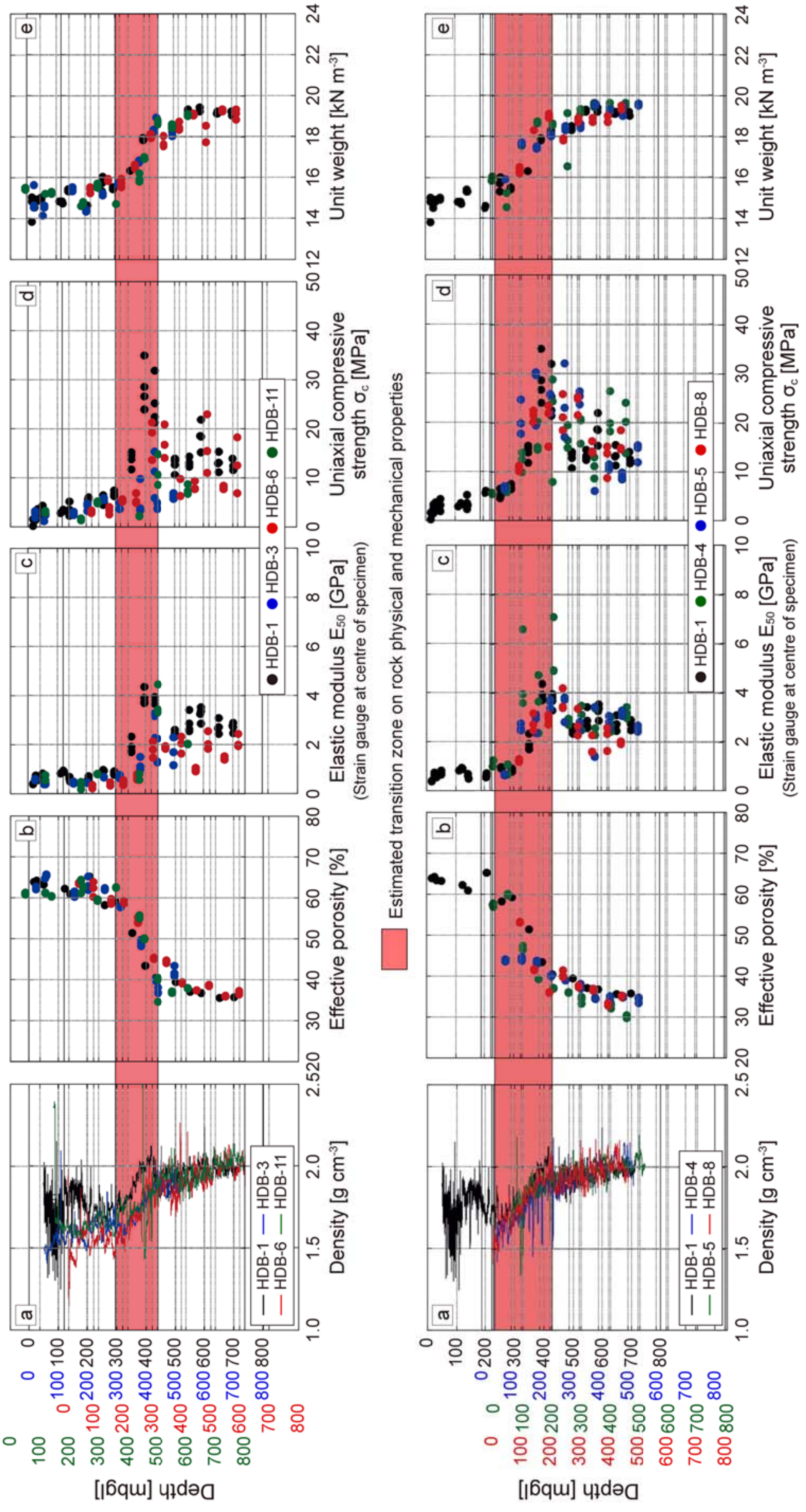

Figure 4.4.3-2 Depth profiles of rock physical and mechanical properties characterised in boreholes HDB-1, HDB-3 to HDB-5, HDB-8 and HDB-11

a: In situ measurement in borehole; *b–e*: Laboratory measurement on core

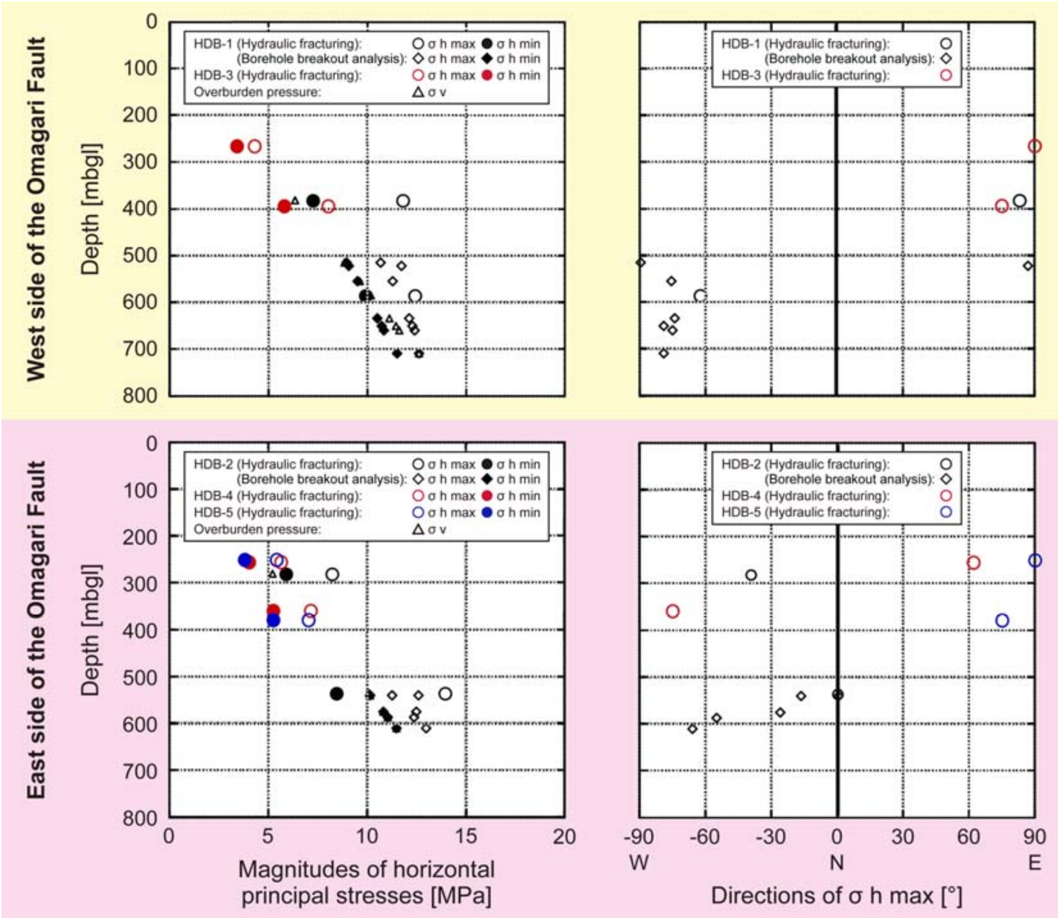

Figure 4.4.3-3 Measured and estimated principal stresses and directions with depth in boreholes HDB-1 to HDB-5

(2) Investigations after selection of the URL site

During the investigations in boreholes HDB-6, HDB-7 and HDB-8 after selection of the URL site, various tests were conducted focussing on borehole HDB-6, which is located nearest to the URL site, to acquire data necessary for designing the underground facilities. More specifically, in situ borehole expansion tests were conducted to clarify the influence of fractures on the mechanical behaviour of the in situ rock mass; this had been identified as one of the subjects to be investigated at the start of the design of the underground facilities. The number of triaxial compression tests and in situ stress measurements was also increased. A borehole expansion test device which can be applied down to a depth of approximately 500 m was not available in Japan and an isobaric loading type testing device made by Solexperts AG, Switzerland was therefore used[119]. Although boreholes HDB-7 and HDB-8 were well away from the URL site and investigations and tests were not necessary from the viewpoint of obtaining data for designing the underground facilities and evaluating excavation damage, laboratory tests were nevertheless conducted in order to acquire supplementary data for clarifying the geological structure because it is hard to distinguish the Wakkanai Formation and the Koetoi Formation by core observation only. The methods and items for the laboratory tests before and after selection of the URL site were the same, allowing the data to be compared.

Various physical properties obtained from the laboratory tests and geophysical logging in borehole HDB-6 is shown also in Figure 4.4.3-2, compared with those for HDB-1 to HDB-5. This figure indicates that the physical properties of the rocks around borehole HDB-6 and their depth profile are almost the same as those obtained from the investigations in boreholes HDB-1 to HDB-5. According to the results of borehole expansion test shown in Figure 4.4.3-4, the rigidity of the in situ rock mass without fractures in the Wakkanai Formation at low stress levels corresponds more or less to the elasticity modulus obtained from the uniaxial compression tests under non-confined compression. With an increase in the stress level, the rigidity becomes close to the dynamic elasticity modulus obtained from the velocity logging, or close to the rigidity that corresponds to the minimum deformation of the rocks under confined compression. The rigidity of the in situ rock mass without fractures in the Wakkanai Formation can thus be estimated from the results of the uniaxial compression tests and geophysical logging. Even in the fractured zone of the Wakkanai Formation, a decrease in rigidity owing to fractures was not observed. From the above results, it can be concluded that the influence of fractures on the rigidity of the in situ rock mass in the Wakkanai Formation is small. In the Koetoi Formation, the dynamic elasticity modulus obtained by velocity logging was larger than that obtained from the borehole expansion and laboratory tests and a difference in rigidity was observed between the in situ rock mass with and without fractures. The larger dynamic modulus of elasticity is owing to larger S-wave velocity obtained from the results of the velocity logging than that in the laboratory tests. The cause is currently unknown. With regard to the Koetoi Formation, the rocks near the location of the borehole expansion test may have been in an almost failed condition owing to the effects of potential fractures generated in association with the formation of the minor fault zones distributed along the fold structure as described in Subsection 4.1.4.

Borehole HDB-8 was drilled near the inferred location of the Omagari Fault and was initially expected to cross the fault. However, core observation indicated no fracture zone corresponding to the Omagari Fault in the borehole and depth profiles of rock properties did not show any gaps or repetitions that may be caused by the fault (Figure 4.4.3-2). The borehole was thus not considered to cross the fault. The depth profiles of the rock physical and mechanical properties measured in borehole the HDB-7, which was drilled primarily in the sandstone of the Yuchi Formation, showed different features from those of rocks in the other boreholes (Figure 4.4.3-5). Specifically, there was almost no change in the physical properties with depth and the density was higher but the mechanical properties were smaller than for the Koetoi Formation. In the zone deeper than 400 m in borehole HDB-7, a transition zone from the Yuchi Formation to the Koetoi Formation was observed.

The results of the measurements of in situ stresses in boreholes HDB-1, HDB-3 and HDB-6, located to the west of the Omagari Fault, are shown in Figure 4.4.3-6. In borehole HDB-6, the in situ stress of the Koetoi Formation that had not been obtained in the previous borehole investigations was measured. The figure indicates that the direction of the maximum principal stress in the horizontal plane of the rocks located on the west side of the Omagari Fault was approximately E-W from the surface down to a depth of approximately 700 m. It also indicates that the minimum principal stress in the horizontal plane was similar to the estimated overburden pressure and the maximum principal stresses were within the range of 1.5 times the minimum principal stress. Although there are few data for the Koetoi Formation, the stress conditions measured in the horizontal plane could be more isotropic than those of the Wakkanai Formation. One of the reasons for this could be the large difference in the rigidity of the rocks of the Wakkanai Formation compared with that of the Koetoi Formation. It was found that, in general, the in situ stress conditions in and around the URL area are not significantly different from those measured for rocks with similar densities in other parts of Japan[120)], as shown in Figure 4.4.3-7.

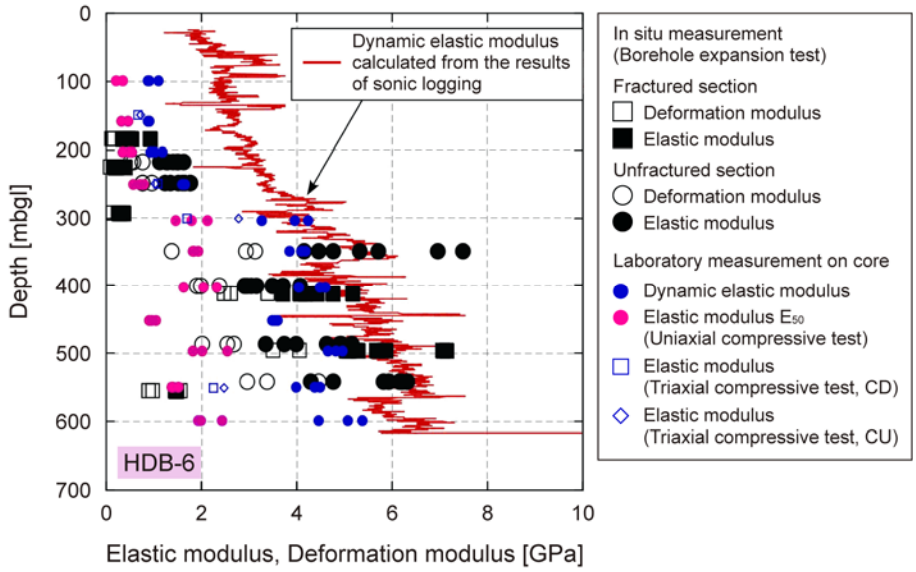

Figure 4.4.3-4 Distribution of elasticity and deformation moduli measured in borehole HDB-6

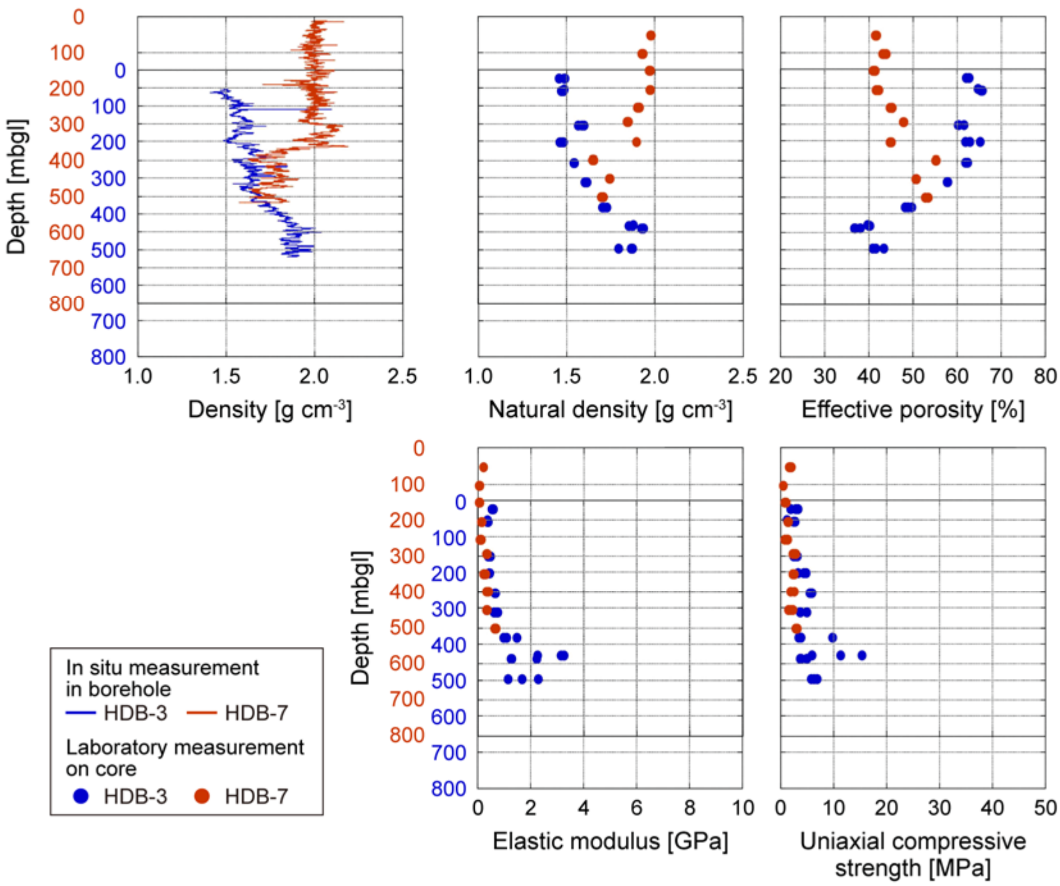

Figure 4.4.3-5 Comparison of rock physical and mechanical properties between boreholes HDB-3 and HDB-7

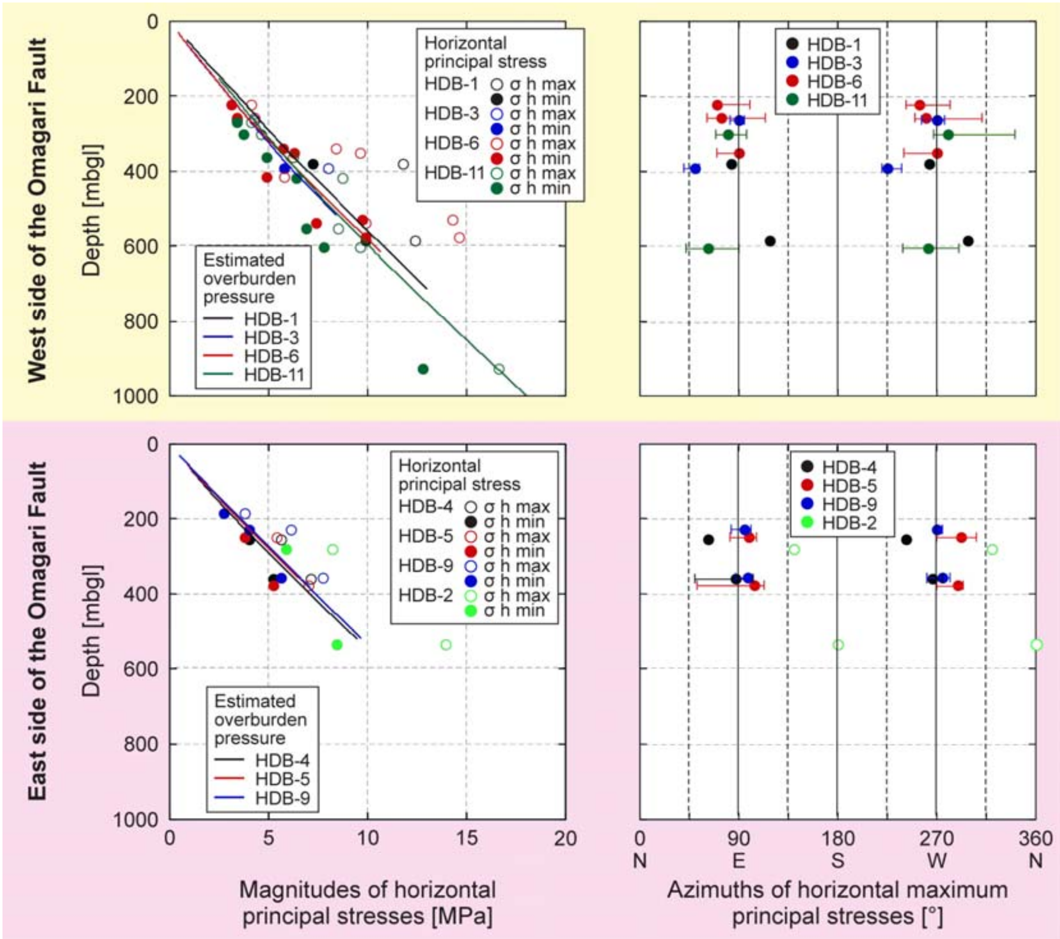

Figure 4.4.3-6 Measured horizontal principal stresses and directions with depth in boreholes HDB-1 to HDB-6, HDB-9 and HDB-11

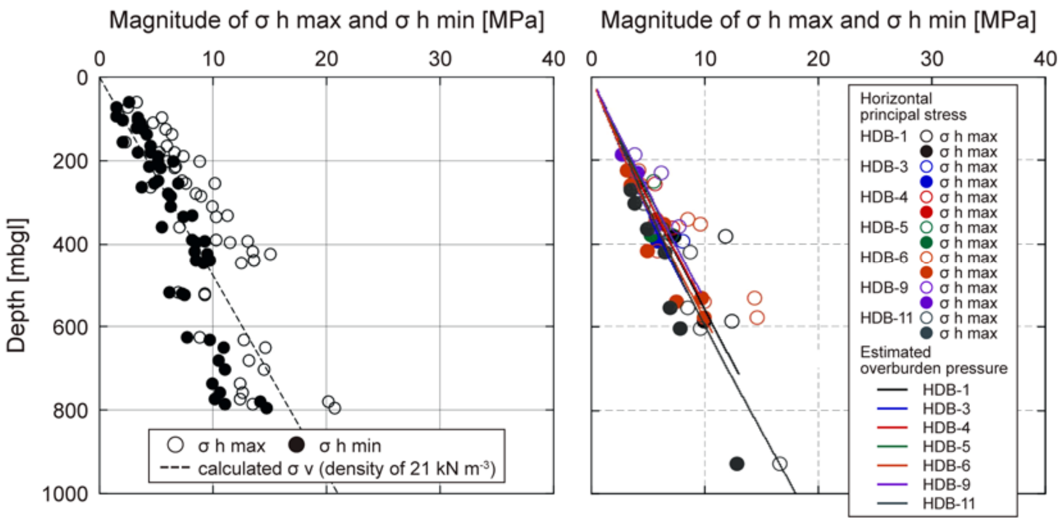

Figure 4.4.3-7 Comparison of magnitudes of principal stresses measured at Horonobe and for similar sedimentary rocks in Japan

Left: Data for sedimentary rocks with similar densities (20–22 kN m^{-3}) from eight different locations in Japan

Right: Data for sedimentary rocks in boreholes at Horonobe, shown also in Figure 4.4.3-6

The last borehole investigation campaign in Phase I was in boreholes HDB-9, HDB-10 and HDB-11. Since these boreholes are located near the boundary of the URL area, laboratory tests to acquire supplementary data for evaluation of the geological structure as well as isotropic compaction tests to acquire data necessary for modelling rock mechanics were conducted, as was the case in boreholes HDB-7 and HDB-8.

The results of the geophysical logging and the laboratory tests in borehole HDB-11 are shown also in Figure 4.4.3-2, in conjunction with those in boreholes HDB-1, HDB-3 and HDB-6; all these boreholes were drilled to the west of the Omagari Fault. Down to a depth of 1,000 m, similar trends were observed. The rocks can be classified into three zones based on their physical properties. In the isotropic compaction tests, the yield phenomenon due to the isotropic pressure was not seen even under a high pressure of 40 MPa (approximately three times the operating in situ stress) in the Wakkanai Formation. The Mohr – Coulomb type yield standard would therefore be applicable for the modelling and analysis of the rocks in the Wakkanai Formation. The rocks in the Koetoi Formation were plasticised at an isotropic pressure of approximately 10 MPa.

A similar comparison was made for the investigation results in boreholes HDB-9 and HDB-10. Some different trends were seen compared to the results for boreholes HDB-1, HDB-3, HDB-6 and HDB-11. Specifically, the distribution of physical properties in borehole HDB-9 was considered to be similar to that for borehole HDB-2, as shown in Figure 4.4.3-8. The reason for this could be that both boreholes HDB-2 and HDB-9 are located relatively near to the inferred surface location of the Omagari Fault and show the direct effects of large-scale deformation (e.g. vertical displacement) generated by fault activity. In addition, changes in rock physical and mechanical properties in the shallower zone (50–250 m in depth) in borehole HDB-10 were similar to those for the transition zone from the Yuchi Formation to the Koetoi Formation around the bottom (350–550 m in depth) of HDB-7 (Figure 4.4.3-8).

The results of the in situ stress measurements in boreholes HDB-11 are shown also in Figure 4.4.3-6, compared with those in boreholes HDB-1, HDB-3 and HDB-6. These in situ stress measurements were also conducted to obtain data from ZONE 2 (see Figure 4.4.4-11 in Section 4.4), where physical properties change sharply and fewer data have been obtained, and the zone deeper than 500 m where there were very little measured data for the sedimentary rocks. The results of the measurements showed that the linear depth-dependent trend was the same as in the results previously obtained, but the relationship between maximum/minimum principal stresses in the horizontal plane and the estimated overburden pressure were different from the previous results in the zone deeper than 500 m. Specifically, the estimated overburden pressures were larger than the maximum/minimum principal stresses, which indicates normal fault-type stress conditions. The direction of the maximum principal stress was consistently in an E-W direction from near-surface to approximately 1,000 m depth, which was the same as the previous results. In borehole HDB-11, borehole breakout was found in the zone deeper than 300 m, as was the case in boreholes HDB-1, HDB-3 and HDB-6, and the estimated direction of the maximum principal stress was E-W. The reason for the changes in the relationship between the estimated overburden pressure and maximum/minimum principal stresses at around 500 m depth is unknown at this point. In situ stress measurements were also conducted in borehole HDB-9 and resulted in the same trends as the previous measurements. Therefore, it is unlikely that the in situ stress field near the Omagari Fault was changed owing to the presence of the fault.

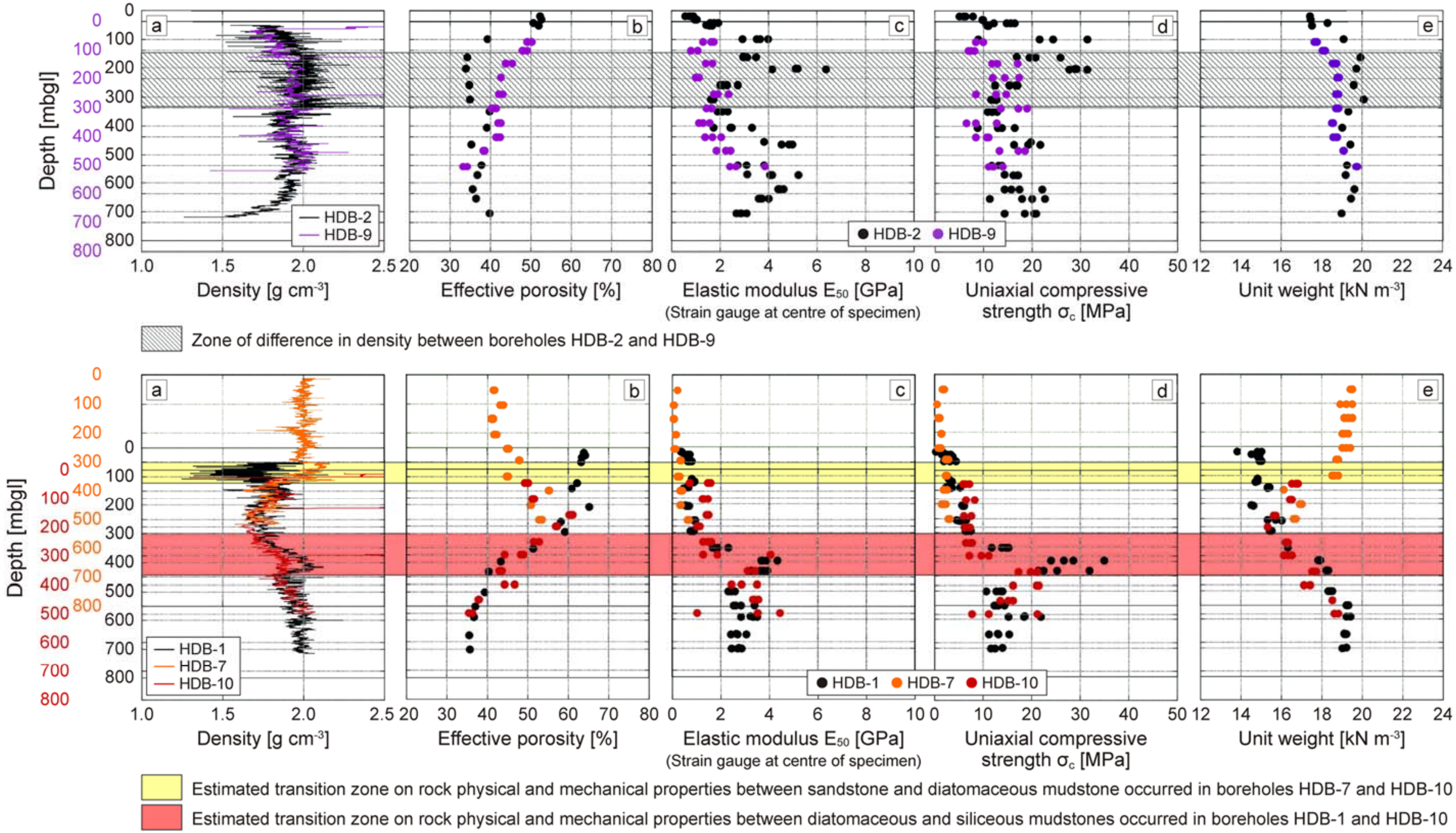

Figure 4.4.3-8 Comparison of depth profiles of rock physical and mechanical properties in boreholes HDB-2 and HDB-9 and boreholes HDB-1, HDB-7 and HDB-10

4.4.4 Rock mechanical modelling

Rock mechanical models and mechanical analyses for geological disposal have to be developed for design, construction, operation and closure of the repository and evaluation of post-closure behaviour of the repository system over the long-term. Specifically, it is necessary to consider the following aspects:

- Design, construction and operation
  Designing tunnel support is one of the most important aspects in the design of a disposal facility. For designing tunnel support, the stability of cavities will have to be evaluated analytically. In this case, the period to be covered in the evaluation will be the operational period of the repository (several decades), which is not so different from the operating period of URL constructed in the fields of resource engineering and civil engineering. Considering only the construction and operation of the repository, evaluating the stability of rocks outside the support infrastructure (e.g. the extent of the plastic zone) will not be so important, as long as the stability of the ultimately designed support can be maintained. However, for the design and safety assessment of plugs, a cavity stability analysis and an evaluation of the extent of the excavation damaged zone (EDZ) and its properties will be required.

- Closure
  Although it depends on the particular closure concept, in the case where a repository is backfilled, leaving the tunnel supports as they are, re-analysis of the cavity stability at this time would not be necessary. However, in the case where the repository is backfilled concurrently with the removal of the tunnel supports, re-analysis of the cavity stability will be required for the conditions that reproduce the backfilling situation. This is not only for ensuring the safety of the operational work but also for analysing the stability of the backfill material immediately after construction, because the EDZ associated with construction and operation may lose stability and change significantly in terms of its extent and characteristics.

  In the case where plugs are to be installed, a design that will achieve the plugs' main objective – sealing off the groundwater flow through the EDZ – and an analysis for evaluating mechanical stability for installing key zones in the existing tunnels would also be required. The period of evaluation in this case would be the lifetime of the engineered barriers or longer.

- Post-closure
  Re-evaluation of the mechanical stability of the cavities would be required only in the case where emplaced waste packages were to be retrieved.

The details of the modelling and mechanical analyses in Phase I were defined in the light of the relevance of the mechanical analysis for an actual repository programme as described above:

a) estimating the extent and characteristics of the EDZ in Phases II and III, based on the URL design;
b) evaluating the long-term stability of the EDZ formed during Phases II and III.

The Horonobe URL project started with investigations covering the whole Horonobe Town area, followed by the selection of a URL site for constructing the URL during the surface-based investigations. Before selecting the URL site and finalising the URL design, major efforts were thus focussed on planning the investigation programme and developing the conceptual models required for evaluating the investigation results; detailed predictive analysis was not conducted until the information required for predicting the impact of constructing the underground facilities was fixed. The above item (a) will thus be discussed in detail in Subsection 4.6.3 and the rock mechanical modelling and analyses are overviewed here.

(1) Before selection of the URL area

The conceptual rock mechanical model for the sedimentary formations around borehole HDB-1 is shown in Figure 4.4.4-1. As stated in Subsection 4.4.3, it was predicted that the Neogene sedimentary rocks to be characterised (i.e. the Wakkanai and Koetoi Formations) have the strength and deformation characteristics of soft rock and there is a zone at intermediate depth between the Wakkanai and Koetoi Formations (approximately 300–500 m) where the physical characteristics change sharply. Such change, however, is not discontinuous as seen in crystalline rocks, but continuous through the Wakkanai and Koetoi Formations. These characteristics were considered as being important for the mechanical modelling and were thus reflected in the conceptual model. However, since information on the dependence of the properties on confined compression, which is a feature of soft sedimentary rock, was insufficient, the data volume should be increased in the next investigation phase.

The study for the modelling and analysis described in the item (b) mentioned above was initiated at this point. Specifically, a triaxial creep test using rock cores was carried out and existing information was collected and reviewed in order to select the method for evaluating the long-term stability of the EDZ. Findings in this study include that the results of the creep tests using rock cores can be reproduced by the conventional classic rheology model (Figure 4.4.4-2), important knowledge for the evaluation of long-term stability has been gained (peak strength will be equal to residual strength on a very long-term basis) and creep destruction will not occur under a creep loading stress less than the residual stress[121]. Based on these findings, a scenario for evaluating the effects of long-term rock behaviour on the engineered barriers in the period from construction to after backfilling was established (Figure 4.4.4-3).

Since the mechanical properties of the rocks making up the Wakkanai and Koetoi Formations are classified as those of soft rock, the deformation that would be caused during tunnel excavation was estimated to be large (a few tens of millimetres), given that the proposed depth of the URL is 500 m. Therefore, the finite difference analysis code FLAC® (Itasca, USA) was used for the numerical analysis; this code allows accurate simulation of deformations from small to large scale and has been applied extensively both domestically and internationally. In the triaxial compression tests, a large excessive porewater pressure was observed in the test specimens even when loading was at a very slow velocity and under drainage conditions, despite the rocks having a very high effective porosity (Figure 4.4.4-4). This could affect the evaluation of the mechanical stability of the tunnel near-field.

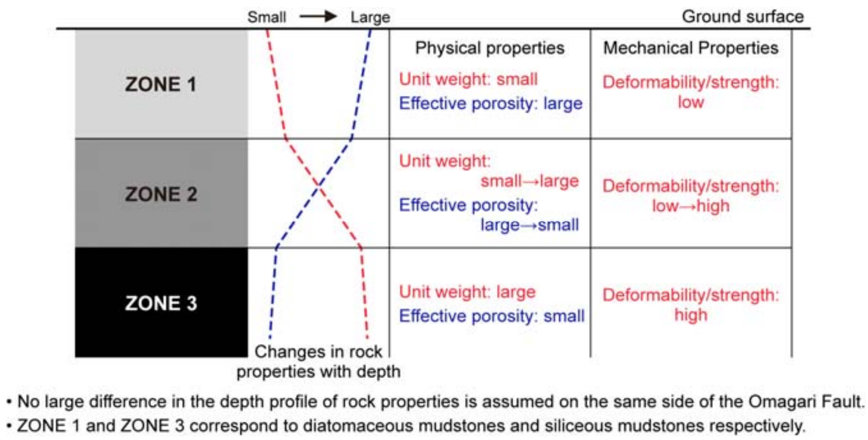

Figure 4.4.4-1 First rock mechanical conceptual model based on the results of investigations in boreholes HDB-1 and HDB-2

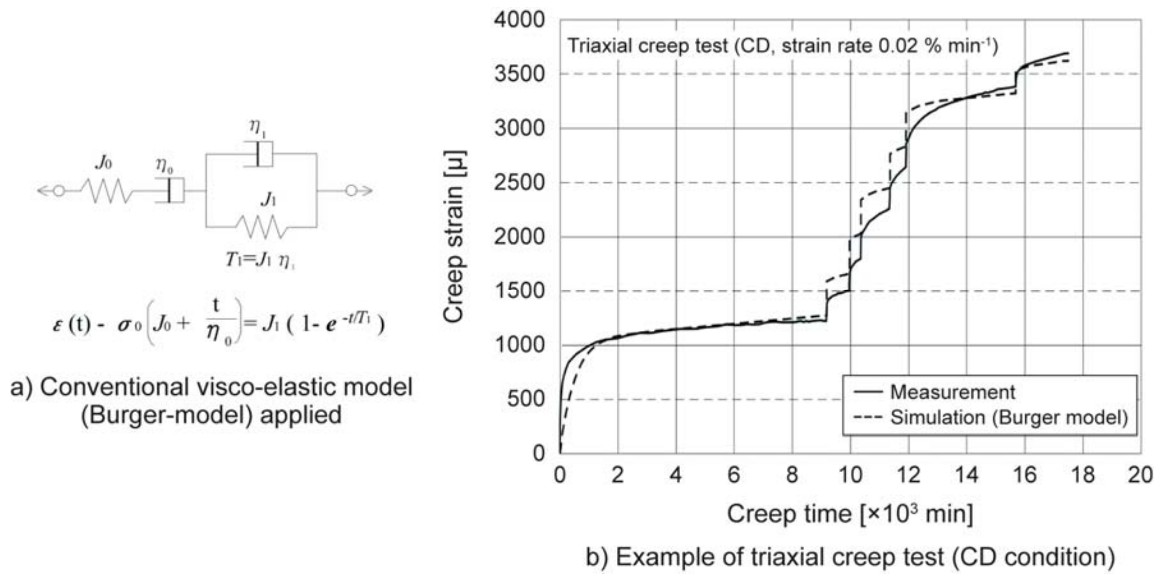

Figure 4.4.4-2 Conventional model applied and fitted curve for the multi-stage creep test

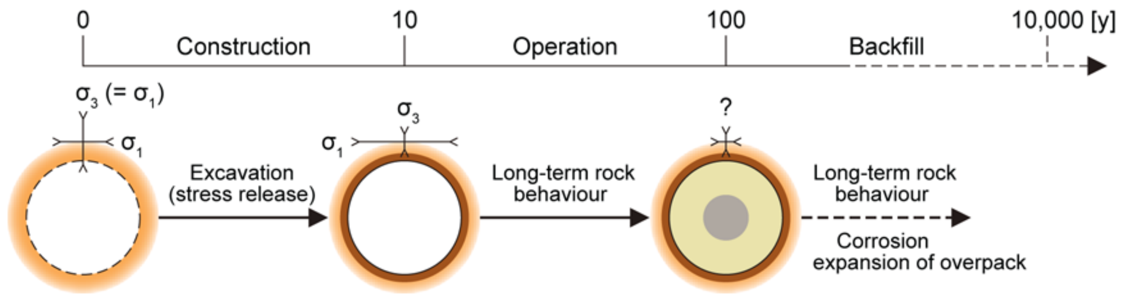

Figure 4.4.4-3 Long-term variation in EBS and surrounding rock mass in the repository

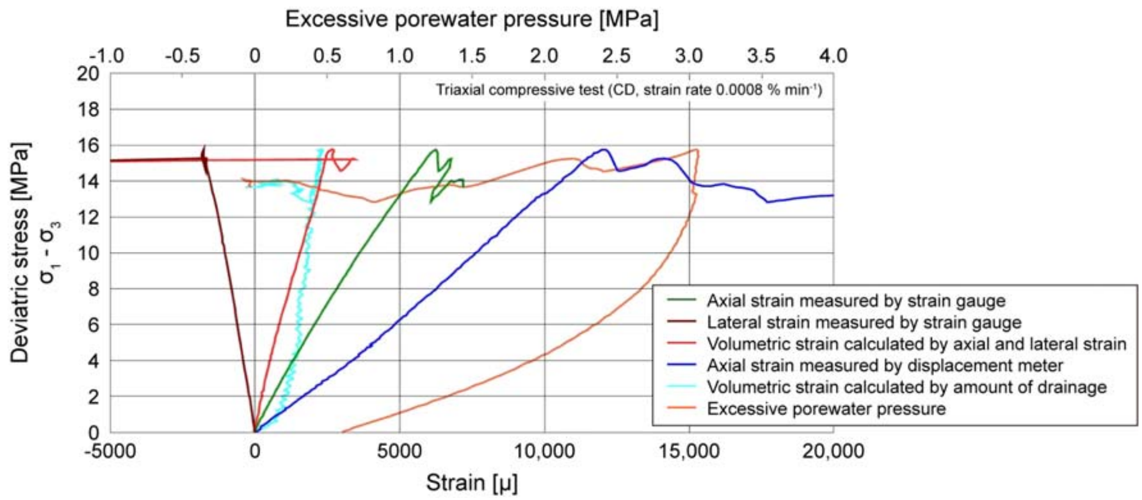

Figure 4.4.4-4 Results of triaxial compression test with drained conditions and very low strain rate

Core specimen from 304.15 to 304.63 m depth in borehole HDB-2

(2) Before selection of the URL site

The results of investigation in boreholes HDB-3, HDB-4 and HDB-5 were available at this point in the project and provided additional information on the distribution of rock properties and in situ stresses in and around the URL area. Specifically, the information obtained from the results of the investigations in these boreholes includes the following: the physical and mechanical properties of rocks on both sides of the Omagari Fault could be explained by simply reflecting the differences in the geological structure and the geology on the west of the fault consisted of three different zones in terms of physical properties. Based on this additional information, the conceptual model was revised as shown in Figure 4.4.4-5.

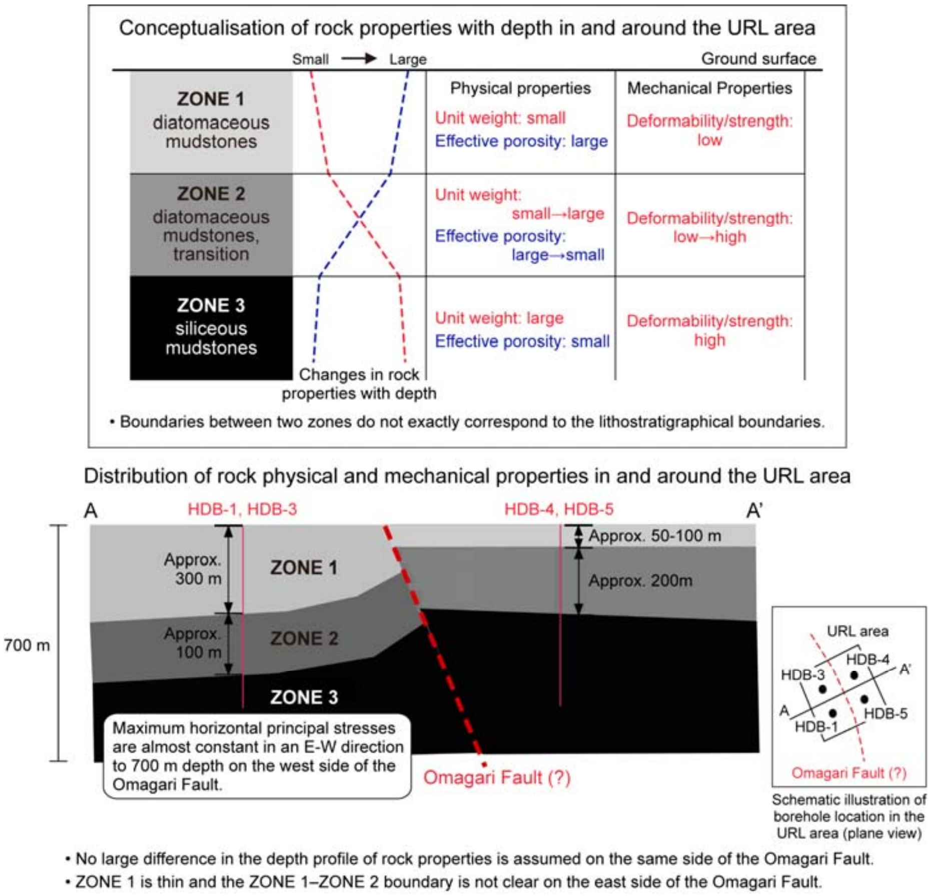

Figure 4.4.4-5 Second rock mechanical conceptual model based the results of investigations in boreholes HDB-1 to HDB-5

The results of the triaxial compression tests in borehole HDB-3 provided information on the dependence of mechanical behaviour of the rocks constituting the Wakkanai and Koetoi Formations on the confined compression. Specifically, the rocks in the Wakkanai Formation showed strain softening behaviour within the range of applied confined compression (approximately twice the estimated overburden pressure), whereas the rocks in the Koetoi Formation changed deformation behaviour within the above stress levels (showing strain softening behaviour under the low confined compression but close to elastic-perfectly plastic behaviour under high confined compression)[122], as shown in Figure 4.4.4-6. In particular, the test samples from the Koetoi Formation under high confined compression did not generate a definite shear surface after destruction (Figure 4.4.4-7). This would be an important finding in evaluating the physical properties of the EDZ. At the stage when these triaxial compression test results were compiled, the Mohr – Coulomb type failure criteria had been considered to be applicable to the rocks in the Wakkanai and Koetoi Formations, but the application resulted in a difference in the apparent cohesion, depending on whether or not there was drainage from the inside of the rocks associated with the deformation (Figure 4.4.4-8). The internal friction angles at the time of peak strength were different depending on the drainage conditions, with approximately 6° (only at the peak time) for siliceous mudstone and approximately 4° for the diatomaceous mudstone, respectively (Figure 4.4.4-8). Laboratory tests were also conducted to acquire parameter values for the coupled hydro-mechanical analysis, in order to investigate the effects of the excessive porewater pressure which was seen during the laboratory tests using cores on the mechanical behaviour of the rocks around the tunnels and on the stability of the tunnel support.

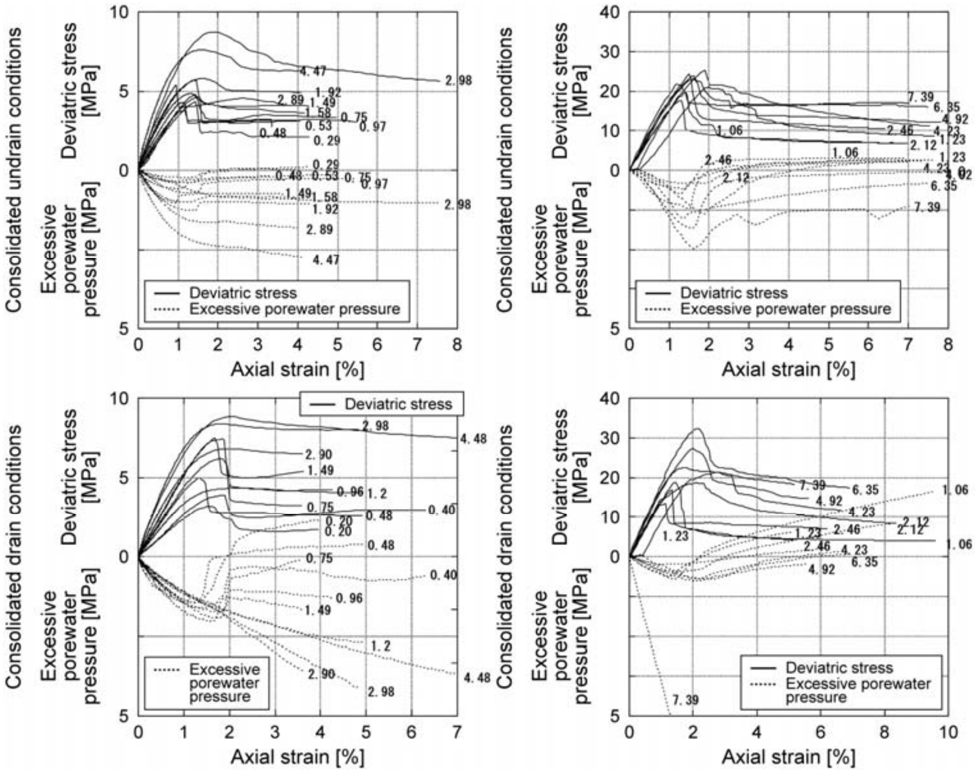

Figure 4.4.4-6 Stress-strain relationship of triaxial compression tests on borehole HDB-3 cores
Left: Diatomaceous mudstone; *Right*: Siliceous mudstone; Axial strain measured by external displacement meter

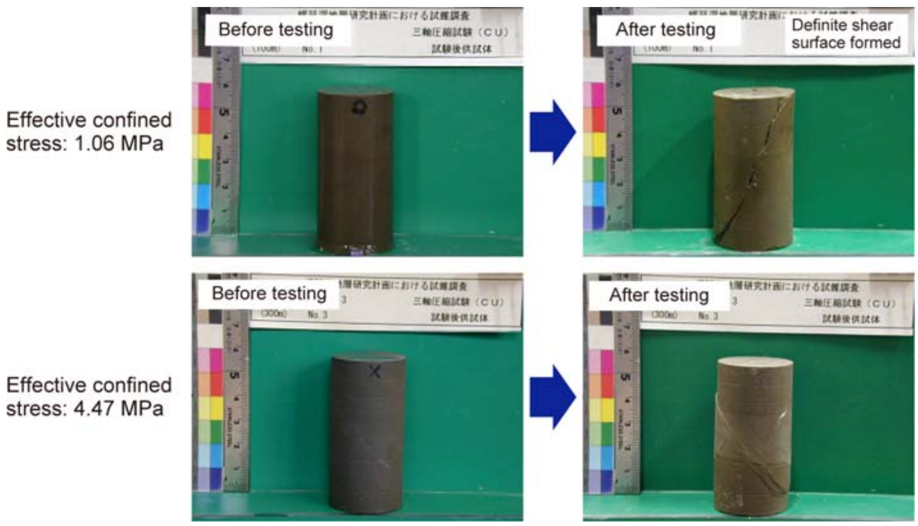

Figure 4.4.4-7 Triaxial compression tests on diatomaceous mudstone specimens

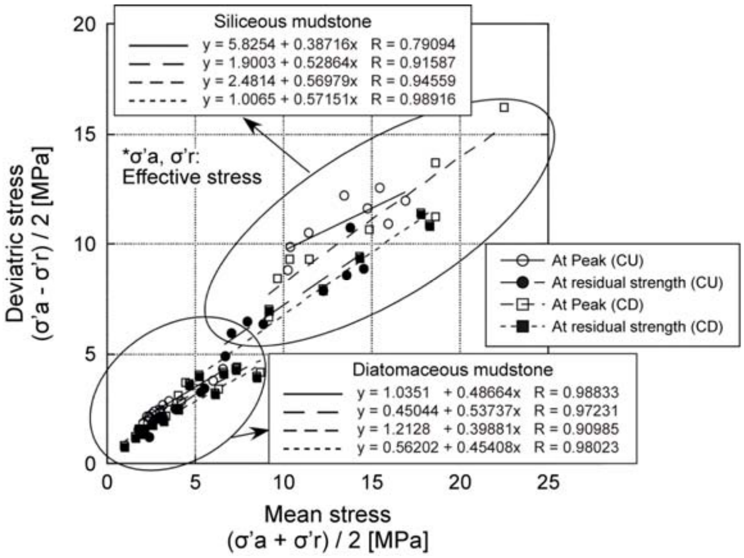

Siliceous mudstone		Cohesion [MPa]	Internal friction angle [°]
CU Tests	At Peak	5.83	21.2
	At Residual strength	1.90	27.9
CD Tests	At Peak	2.48	29.7
	At Residual strength	1.01	29.7

Diatomaceous mudstone		Cohesion [MPa]	Internal friction angle [°]
CU Tests	At Peak	1.04	25.9
	At Residual strength	0.45	28.3
CD Tests	At Peak	1.21	21.7
	At Residual strength	0.56	24.4

Figure 4.4.4-8 Estimation of parameters for the Mohr – Coulomb failure criteria

Based on the above test results, numerical analyses considering the influence of the excessive porewater pressure (during tunnel opening) and strain softening behaviour (after tunnel opening) were conducted for the period extending from the time of tunnel opening to after tunnel closure. Regarding the influence of excessive porewater pressure (Analysis-I), modelling and analysis were carried out considering the technical specifications for tunnel support based on the data from boreholes HDB-3, HDB-4 and HDB-5 and also considering the construction process for the underground facilities (Figure 4.4.4-9). The analysis results of the Analysis-I indicated that the coupled hydro-mechanical processes in the tunnel near-field assumed to occur immediately after excavation would not have a significant influence on the surrounding rock and the stability of the tunnel support (Figure 4.4.4-9).

Parameters for simulation

Ed [GPa]	ν d	G [GPa]	K [GPa]	ø	γ	k [m² Pa⁻¹ s⁻¹]	
2.82	0.287	1.10	2.20	0.35	19.0	5.0×10^{-16}	
Kf [GPa]	Ks [GPa]	α	β	M [GPa]	Ku [GPa]	Eu [GPa]	ν u
2.1	40.0	0.945	0.731	6.02	8.22	3.15	0.436

Model

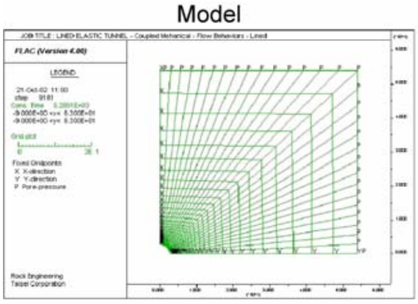

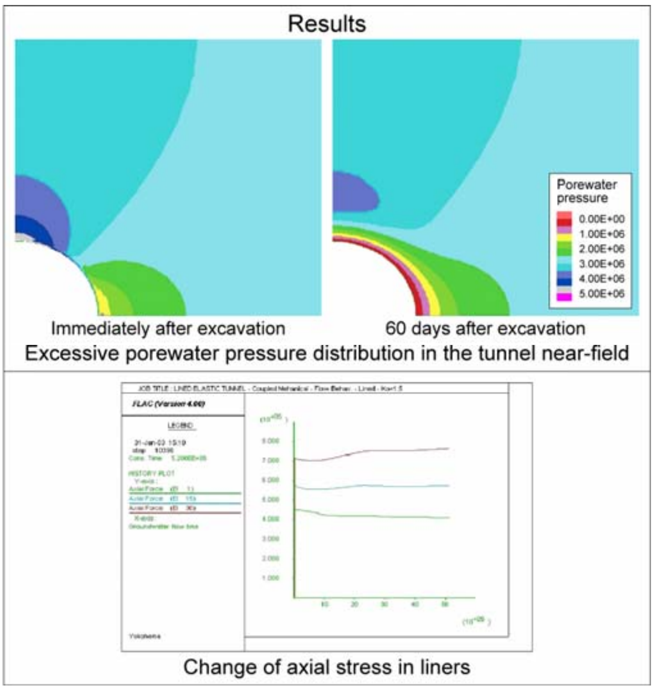

Figure 4.4.4-9 Model and simulation results for hydro-mechanical coupled phenomena
Analysis carried out for siliceous mudstone

For the analysis of the stability of the tunnel near-field during opening (Analysis-II), taking strain softening behaviour into consideration, analyses and assessments of the Analysis-II were conducted focussing on the time-dependent behaviour of rocks for the period from immediately after excavation (Analysis-IIa), when no tunnel support is installed, to the time when the tunnel support is constructed, and on the influence of long-term rock behaviour on the backfill materials (Analysis-IIb) (Table 4.4.4-1). The parameters for the Analysis-IIa were determined by a simulation based on the results of the triaxial creep tests. The result indicates that rocks would not be unstable even without the support. The analysis results of the Analysis-IIb indicated that deformation of the backfill material might occur beyond failure strain especially on shear strain (Figure 4.4.4-10). The methodology used for the Analysis-IIb would be most effective for designing the backfill.

Table 4.4.4-1 Assumptions and scenarios for the numerical simulation of long-term rock behaviour associated with tunnel excavation and its impact on backfill materials

(a) Assumption of parameters for backfills

Backfill materials	Constitutive law	Density [kg m^{-3}]	Young's modulus [kN m^{-2}]	Poisson's ratio [-]	Cohesion [kN m^{-2}]	Friction angle [°]
Crushed diatomaceous mudstone + Bentonite	Elasto-perfect plastic	846	1,975	0.2	9.4	28.8
Crushed siliceous mudstone + Bentonite	Elasto-perfect plastic	1,081	5,153	0.3	17.3	32.6

(b) Assumption of parameters for rock mass

Depth [mbgl]	Constitutive law	Elastic modulus		Strength		Residual strength		Dilation angle
		E_{50} [MPa]	ν_{50}	C [MPa]	ø [°]	Cr [MPa]	ør [°]	ψ [°]
250 (diatomaceous mudstone)	Strain-softening	520	0.050	2.59	14.7	0.492	30.7	4.0
500 (siliceous mudstone)	Strain-softening	1,350	0.272	2.97	32.4	0.451	33.2	4.0

● Support material is assumed to be elastic (38 GPa corresponding to shotcrete with 20 cm thickness).

(c) Simulation cases

Case	Scenario	Depth [mbgl]	σH / σv	Horizontal stress σH [MPa]	Backfill material
1	1	250	1.0	4.76	Crushed diatomaceous mudstone + Bentonite
2	1		1.5	7.13	
3	2		1.0	4.76	
4	2		1.5	7.13	
5	1	500	1.0	9.50	Crushed siliceous mudstone + Bentonite
6	1		1.5	14.25	
7	2		1.0	9.50	
8	2		1.5	14.25	

Simulation steps for Scenario 1
(a) Application of the initial stress (overburden)
(b) Release of 65.5% excavation force during excavation; rock mass being elasto-perfect plastic material
(c) Addition of shotcrete
(d) Release of 100% excavation force during excavation
(e) Addition backfill material
(f) Desition of supports
(g) Changing from peak strength to residual strength

Simulation steps for Scenario 2
(a)–(e) Same as Scenario 1
(f) Changing from peak strength to residual strength
(g) Desition of supports

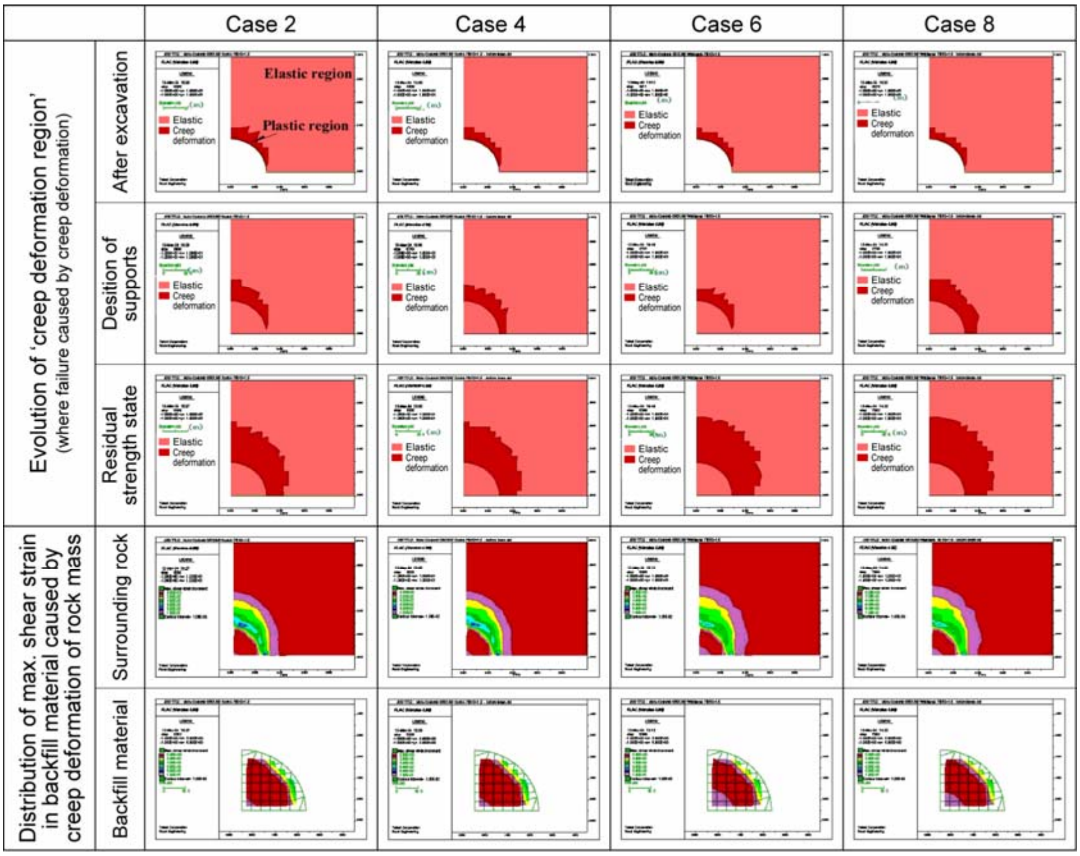

Figure 4.4.4-10 Example of the simulation results of long-term rock behaviour associated with tunnel excavation and its impact on backfill materials

(3) After selection of the URL site

Models were revised as shown in Figure 4.4.4-11 to reflect the results of investigations in borehole HDB-6 conducted after selection of the URL area. Specifically, the characteristics of the confined compression dependence could be taken into account in each zone, based on the results of the triaxial compression tests in boreholes HDB-1 to HDB-6. In addition, the overall characteristics of the in situ stress field in the area to the west of the Omagari Fault became apparent from the results of the in situ stress measurements in borehole HDB-6, which was also reflected in the model. The conceptual model ultimately developed after comparison with the results of investigations from boreholes HDB-1 to HDB-11 is shown in Figure 4.4.4-12. It was concluded that the conceptual model shown in Figure 4.4.4-12 need not be revised, although more detailed information on the 3D geological structure was reflected in the model.

From the viewpoint of evaluating the mechanical influence associated with excavation of cavities on the surrounding rocks, various tests including triaxial compression tests, isotropic compaction tests and laboratory tests for understanding the mechanical properties of shear fractures and their vertical stress dependence were carried out to clarify the mechanical properties of the Wakkanai and Koetoi Formations that will host the underground facilities.

With regard to triaxial tests, large excessive porewater pressure has been observed even at a very slow strain rate and there is some information on strain rate dependence of mechanical properties of soft sedimentary rocks[113]. Considering the above findings, as well as the fact that the deformation rate of the rocks may differ depending on the tunnel excavation method (machine or blasting), the triaxial tests were conducted with different strain rates to confirm the above results. In the strain rate range of 0.1–0.0008%

under the triaxial stress condition, the faster the strain rate was the higher the apparent shear strength was, but such a trend could be explained by a single failure criterion (Figure 4.4.4-13). Thus, the different physical properties of the surrounding rock would not be required in the evaluation of excavation method.

The isotropic consolidation test was conducted with the aim of selecting an appropriate constitutive equation as the model necessary for the numerical analysis, because it was found that the behaviour of the rocks may differ within the range of variation of the stress that is assumed to occur in the surrounding rocks during the tunnel excavation, particularly in the Koetoi Formation. As a result, it was concluded that isotropic compression yield would not occur, at least in the Wakkanai Formation, and the conventional Mohr – Coulomb type failure criteria were therefore applied. Meanwhile, in the Koetoi Formation, isotropic compression yield of the rocks was indicated and it was concluded that a constitutive law such as the Cam-clay model would have to be applied in the future.

Tests on the mechanical properties of fractures and the stress dependence of permeability of the soft sedimentary rocks were conducted focussing on fractures that satisfy both conditions: those with a clear correlation between fractures monitored in situ with borehole televiewer (BHTV) and identified by core logging and shear fractures that could affect the permeability of the rocks based on the investigations in boreholes HDB-1 to HDB-11 (Figure 4.4.4-14). The results of the tests indicated a vertical rigidity and shear rigidity of fractures around one order of magnitude lower than those seen in crystalline rocks. The permeability of the fractures was varied by a factor of 10–100 in the stress range from no pressure to the estimated overburden pressure in both the Wakkanai and Koetoi Formations (Figure 4.4.4-15).

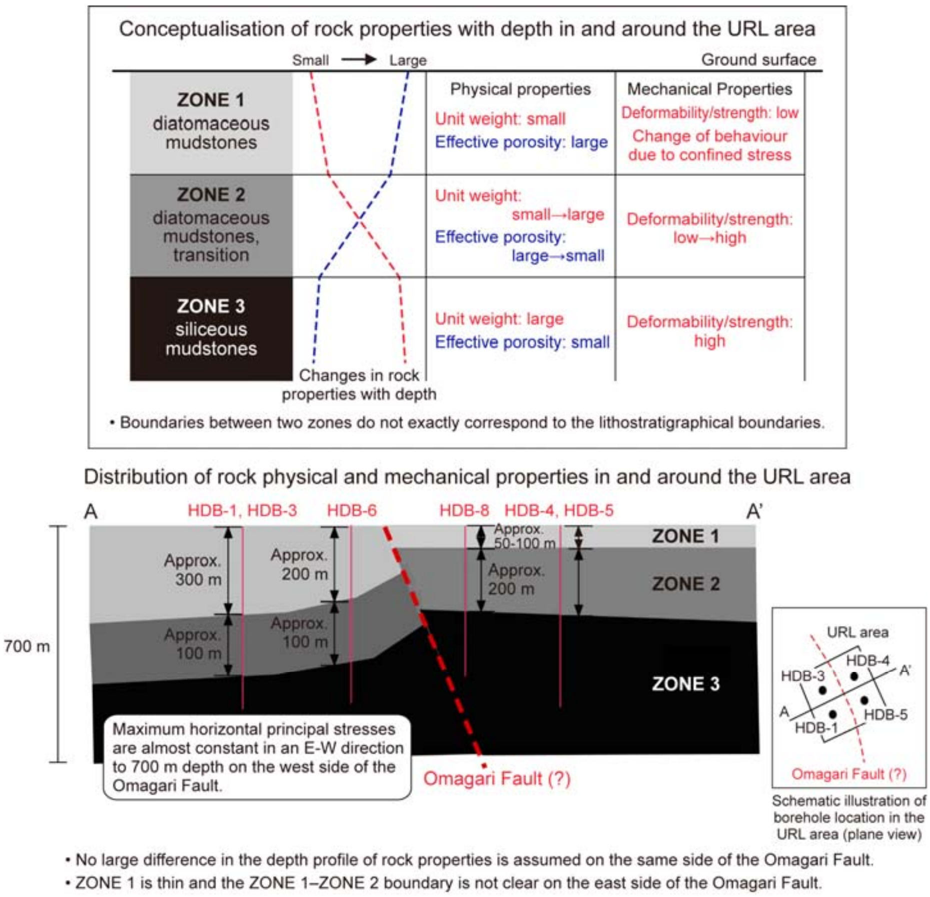

Figure 4.4.4-11 Third rock mechanical conceptual model based the results of investigations in boreholes HDB-1 to HDB-6

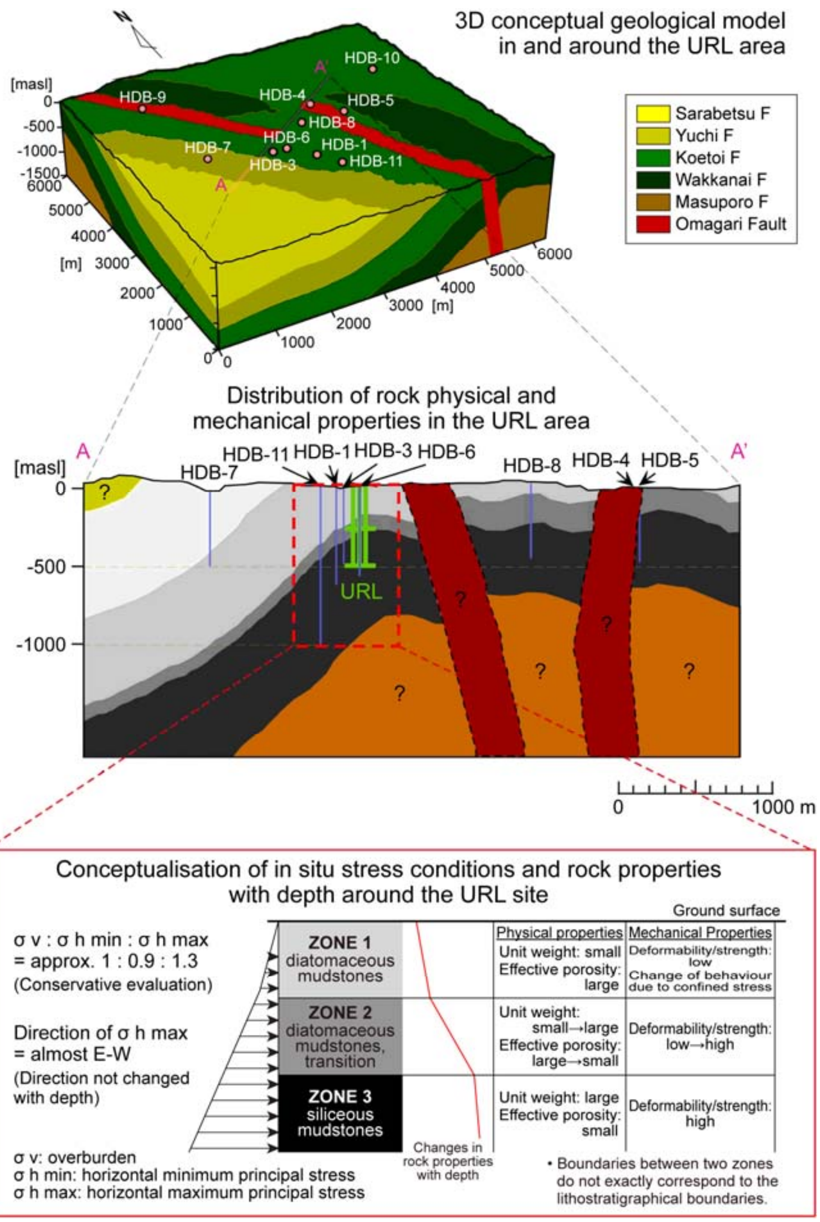

Figure 4.4.4-12 Final conceptual model of rock mechanics

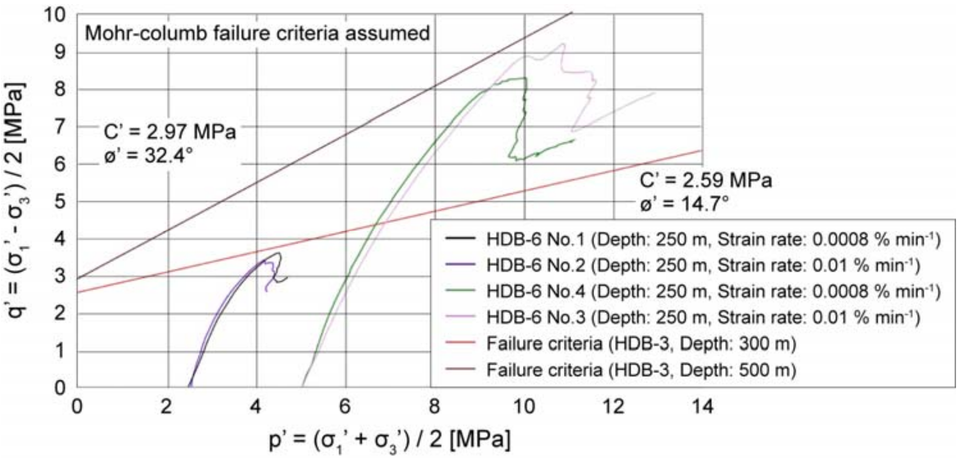

Figure 4.4.4-13 p'-q' plot of stress paths for triaxial compression tests with different strain rates

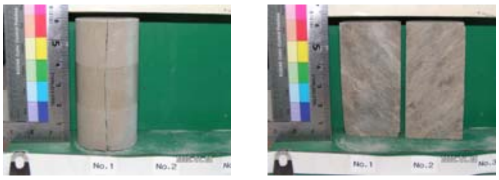

Diatomaceous mudstone
(HDB-11, 238 m depth): K

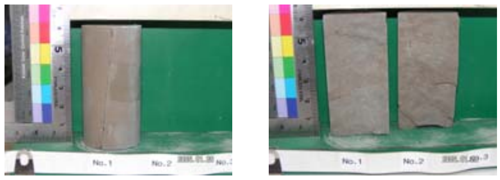

Siliceous mudstone no.1
(HDB-11, 425 m depth): W1

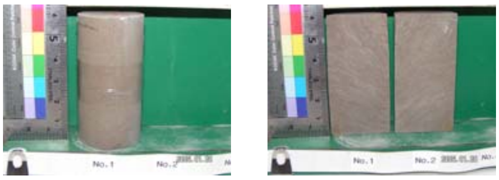

Siliceous mudstone no.2
(HDB-11, 425 m depth): W2

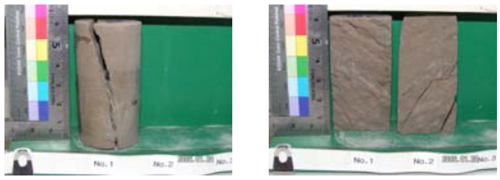

Siliceous mudstone no.3
(HDB-11, 425 m depth): W3

Figure 4.4.4-14 Tested fractures (Type 3) in diatomaceous and siliceous mudstones

K: Koetoi Formation; *W1–W3*: Wakkanai Formation

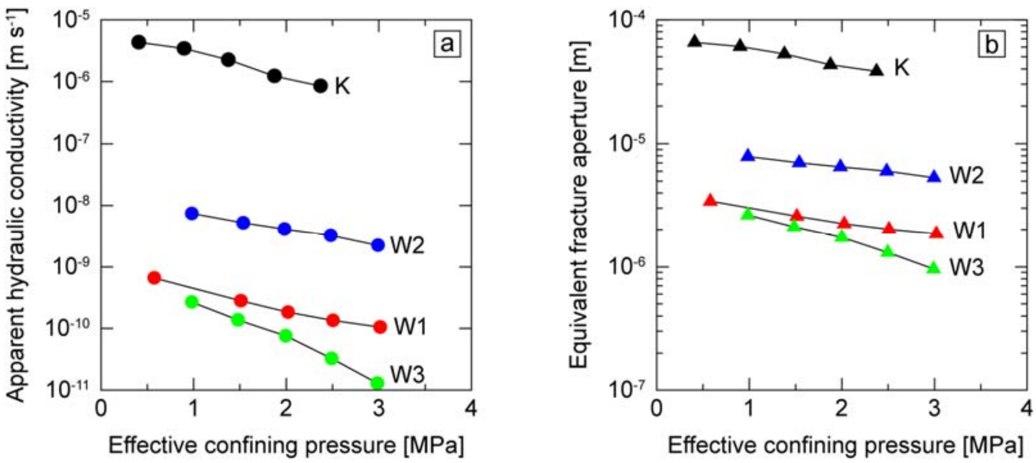

Figure 4.4.4-15 Results of hydraulic tests under different normal stresses for Type 3 fractures

a: Apparent hydraulic conductivity; *b*: Equivalent fracture aperture

Photographs of rock specimens shown in Figure 4.4.4-14

4.5 Study on the long-term stability of the geological environment

4.5.1 Aims

The aim of this study was to establish a series of techniques for modelling and analysing the long-term behaviour of the geological environment in the context of geological disposal (e.g. groundwater flow, groundwater chemistry and solute transport) from the present-day to the future, taking the region of Horonobe Town as a case study. It also aimed to establish methodologies for estimating and evaluating the long-term evolution of the characteristics/properties of the geological environment in specific areas (e.g. coastal region, area where thick sedimentary formations are widely distributed). For the geological disposal project, PIAs will be selected initially based on literature survey. The selection will take place based on factors that would render the geologies to be characterised clearly inappropriate, in order to rule out the possibility of direct damage to the disposal facility or the waste packages and placing excessive limitations on the design of the disposal facility[123)]. Establishing techniques for estimating the long-term behaviour of the geological environment as described here means establishing techniques for investigating and analysing areas with no natural phenomena such as faulting and volcanic activity that could have a significant impact on the geological disposal system, while considering the evolution of the geological environment as affected by phenomena such as uplift, erosion, climate changes and changes in sea-level. In Phase I of the Horonobe URL project, an investigation was conducted with the main aim of determining the temporal and spatial evolution of the natural phenomena in the Horonobe area. This corresponds to the initial stage of the study on the impacts due to natural phenomena[124)] that deals with studies of the long-term stability of the geological environment and the evaluation of such impacts in a consistent manner and the approach using palaeohydrogeological studies[125)].

When evaluating the long-term behaviour of the geological environment, it is of importance to understand not only individual natural phenomena such as faulting, uplift, erosion and changes in climate and sea-level, which have impacts on the geological environment, but also how these phenomena are interrelated and how coupled phenomena affect the geological environment. For example, if local uplift occurs because of a fault movement in addition to the eustatic lowering of the sea-level, the drop in sea-level would be greater than expected lowering of sea-level owing to eustatic sea-level change. Such a drop in sea-level may affect groundwater flow owing to movement of the saline-freshwater boundary and owing to a change in hydraulic gradient, which could possibly affect the hydrochemical environment of the deep subsurface. As explained above, the subsurface geological environment behaves as a system where various phenomena impact on each other, for example interaction among individual natural phenomena, the change in the geological environment brought about by the natural phenomena and the interaction among the individual geological environment conditions. It is reported that, when the above environment is considered, small scale estimates would give only an indirect (limited) understanding of the whole system[126)]. To describe the whole system behaviour, it is necessary to collect the information about every system-component as far as possible. Therefore, in the case where coupled phenomena such as the evolution of the geological environment are being dealt with, it is necessary to link research on natural phenomena such as a sea-level change and faulting with research on hydrogeology and hydrochemistry from the beginning of the investigation[127)]. Taking the above into consideration, this study uses an approach based on palaeohydrogeological studies[125)] that describes the future evolution of the groundwater flow conditions in a certain area on the basis of the temporal and spatial variations of the groundwater flow conditions in association with geological evolution over geological time.

The detailed sequence of the study is as follows (Figure 4.5.1-1):

a) construction of a conceptual model based on the characteristics of the natural phenomena that have occurred in the Horonobe area over geological time;
b) systematic compilation of the impacts of these natural phenomena on the geological environment;
c) acquisition of data on the geological environment required for constructing models of the geological environment ranging from the past to the present and constructing the models;
d) numerical analyses for the groundwater flow conditions and other parameters;
e) checking of the consistency of the analytical results by comparing the results with hydrochemical data;
f) description of the future evolution of the geological environment based on the temporal and spatial variation of the geological environments from the past to the present-day.

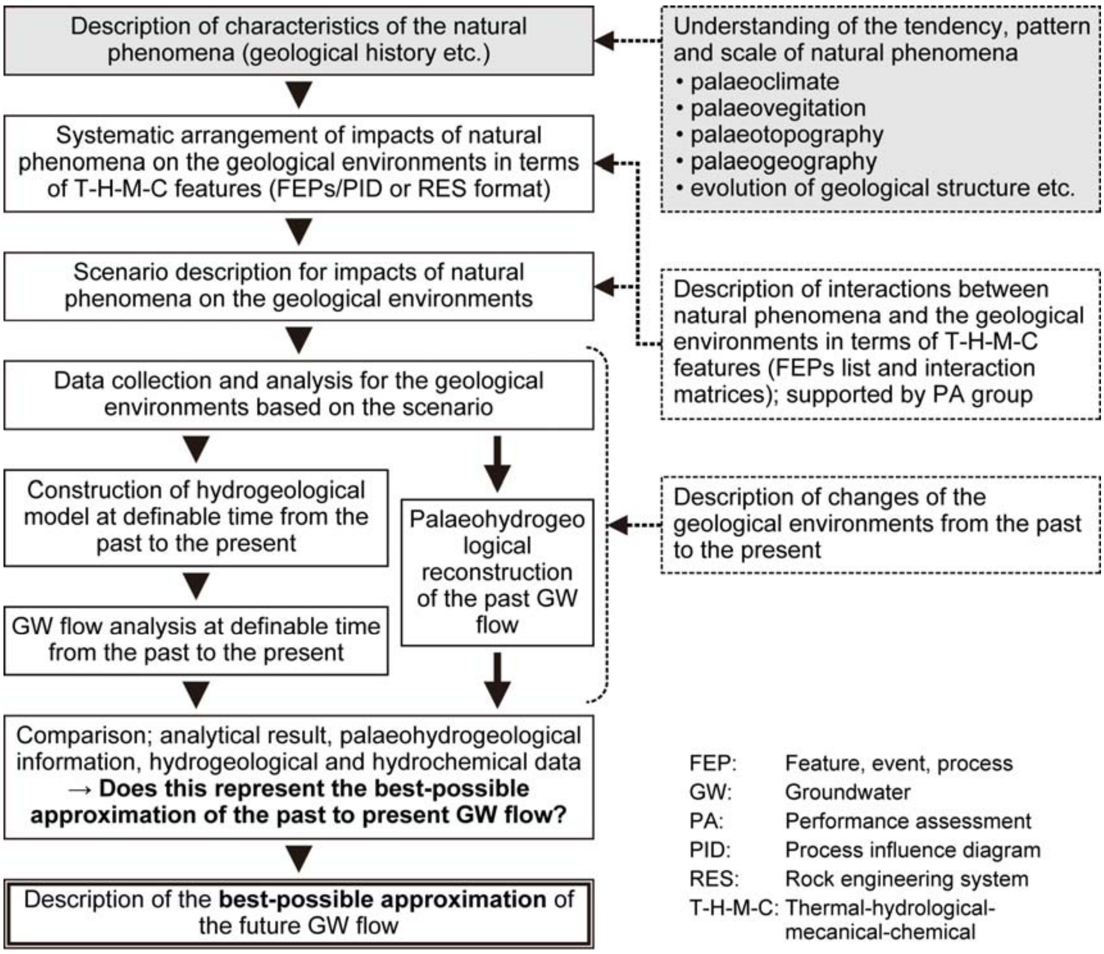

Figure 4.5.1-1 Scope of Phase I (grey square) in the sequence of tasks involved in studying the long-term stability of the geological environments in and around the Horonobe area

With respect to the future evolution of the geological environment, the focus was on understanding the evolution of groundwater flow conditions, considering that, of all the key properties and processes of the geological environment that are important for geological disposal (Figure 2.2.1-1), this is relatively easy to comprehend (see Chapter 2). It is clear that, in addition to groundwater flow conditions, understanding the evolution of the geochemical characteristics of groundwater is also of importance. However, it was decided that this topic would be addressed in Phase II and/or Phase III. When modelling of the geological environments considering with its temporal variation, the processes and mechanisms by which natural phenomena affect the geological environment will be systematically compiled and the evolution of the geological environment originating from these natural phenomena will be documented to provide a basis for establishing methods for estimating the future evolution of the geological environment.

4.5.2 Methodology

The first investigation to be carried out was a survey of the natural phenomena that had occurred in the Horonobe area in the past, based on existing information. Based on this information, the investigation topics and spatial scales to be characterised were then defined and the data flow diagram for each spatial scale and each investigation stage was established. As described below, the spatial scale was divided into five levels and the investigations into three stages (survey of existing information, surface-based investigations and borehole investigations).

The spatial scale to be characterised was determined by considering the features of natural phenomena that had occurred in the Horonobe area in the past, as well as the scale of the occurrence and the range of the impact of individual natural phenomena (Figures 4.5.2-1 and 4.5.2-2). The scale covering the sea surrounding Hokkaido and the whole of Hokkaido was defined as the scale for understanding the regional tectonic setting which provides the geological context for natural phenomena in the Horonobe area. It includes the plate boundaries around Hokkaido and the major mobile belts. As it has been proposed that information on the plate motions should be collected based on surveys of existing information, the spatial scale was set to be fairly large. The spatial scale covering northern Hokkaido was aimed at understanding the outline of the palaeoclimate, together with seismicity and volcanic/hydrothermal activities occurring around the Horonobe area. This scale was set taking into consideration the neotectonic division of the whole of Hokkaido, the extent of the Tenpoku Sedimentary Basin, which includes the Horonobe area, the lowering of the sea-level during glacial periods and the submarine topography to the west of the Horonobe area. The spatial scale for the Horonobe area and the sea area to the west was set orthogonally to the geological structure with an NNW-SSE trend in northern Hokkaido, also considering the spatial extent of the Tenpoku Sedimentary Basin. The geological evolution and the palaeogeography of the Horonobe area were the primary investigation targets in this scale. For the spatial scale for the Horonobe area (land area), existing seismic reflection profiles and results from the borehole investigations were available and the analyses therefore focussed primarily on uplift and subsidence histories that required more detailed data. The spatial scale for the Hokushin district of Horonobe Town (in and around the URL area) was set primarily with the aim of understanding the geomorphological processes. It was also set so as to include the major sedimentary formations found in the Horonobe area, since it is known that the characteristics of the topography in the area differ depending on the lithology.

The data flow diagram indicates how investigations are implemented in order to achieve the overall aims of the investigation including types and combination of investigations, types of data to be acquired, interpretation of the data and integration of information obtained from different fields. This is an example of a systematised investigation methodology consisting of investigations, analyses and evaluations. In this study, the data flow diagram was drafted for each spatial scale to be characterised and for each investigation stage to make clear what investigations were to be conducted at which point (Figure 4.5.2-3a–d). Understanding the geological environment will be improved by iterating the sequence of investigation, analysis and evaluation processes according to the data flow diagram. This data flow diagram is not conclusive; the subjects for investigation and analysis should be reviewed and the links between the subjects revised according to the progress of the investigations. Figure 4.5.2-3a–d shows the data flow diagram at the final point of the Phase I investigations. It will be revised with the progress of the investigations in Phase II and/or Phase III.

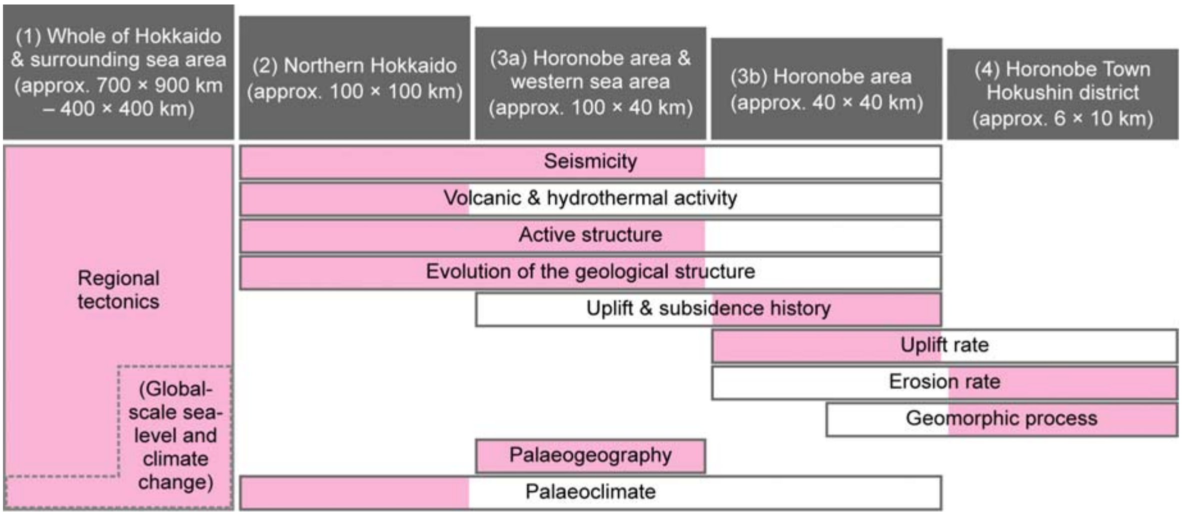

Figure 4.5.2-1 Spatial scales and items for study on the long-term stability of the geological environment in and around the Horonobe area

Pink representing the area covered by studies carried out in Phase I

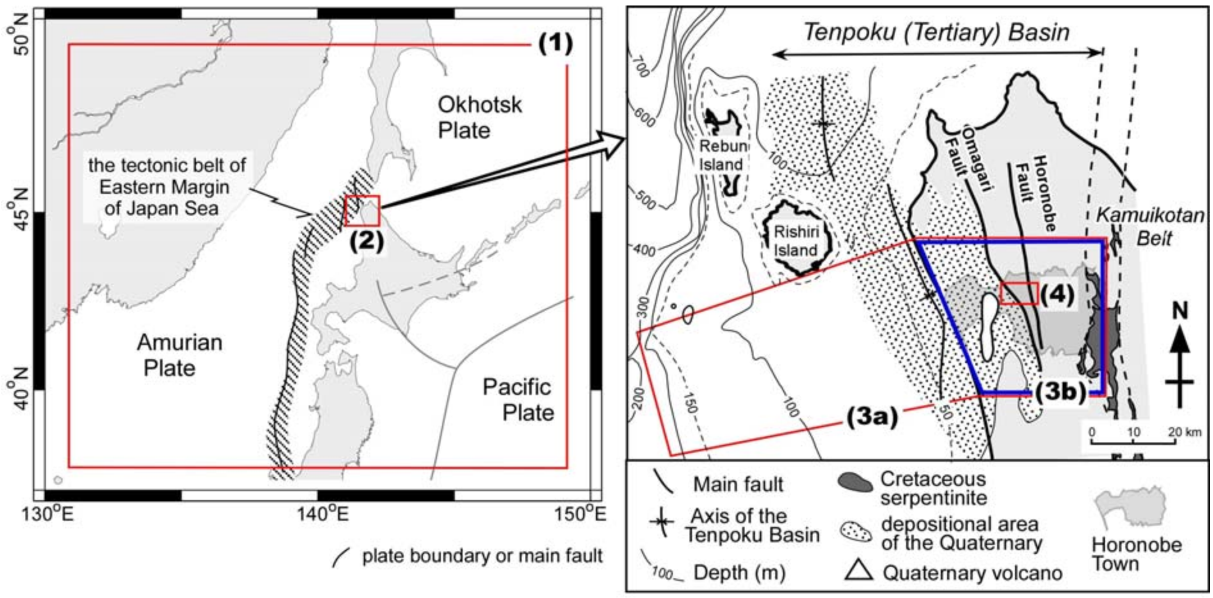

Figure 4.5.2-2 Areas for study on the long-term stability of the geological environment in and around the Horonobe area

Number in parentheses corresponding to Figure 4.5.2-1

Left: Distribution of plates after Taira[128]; *Right*: Tectonic division in northern Hokkaido modified from Oka[21]

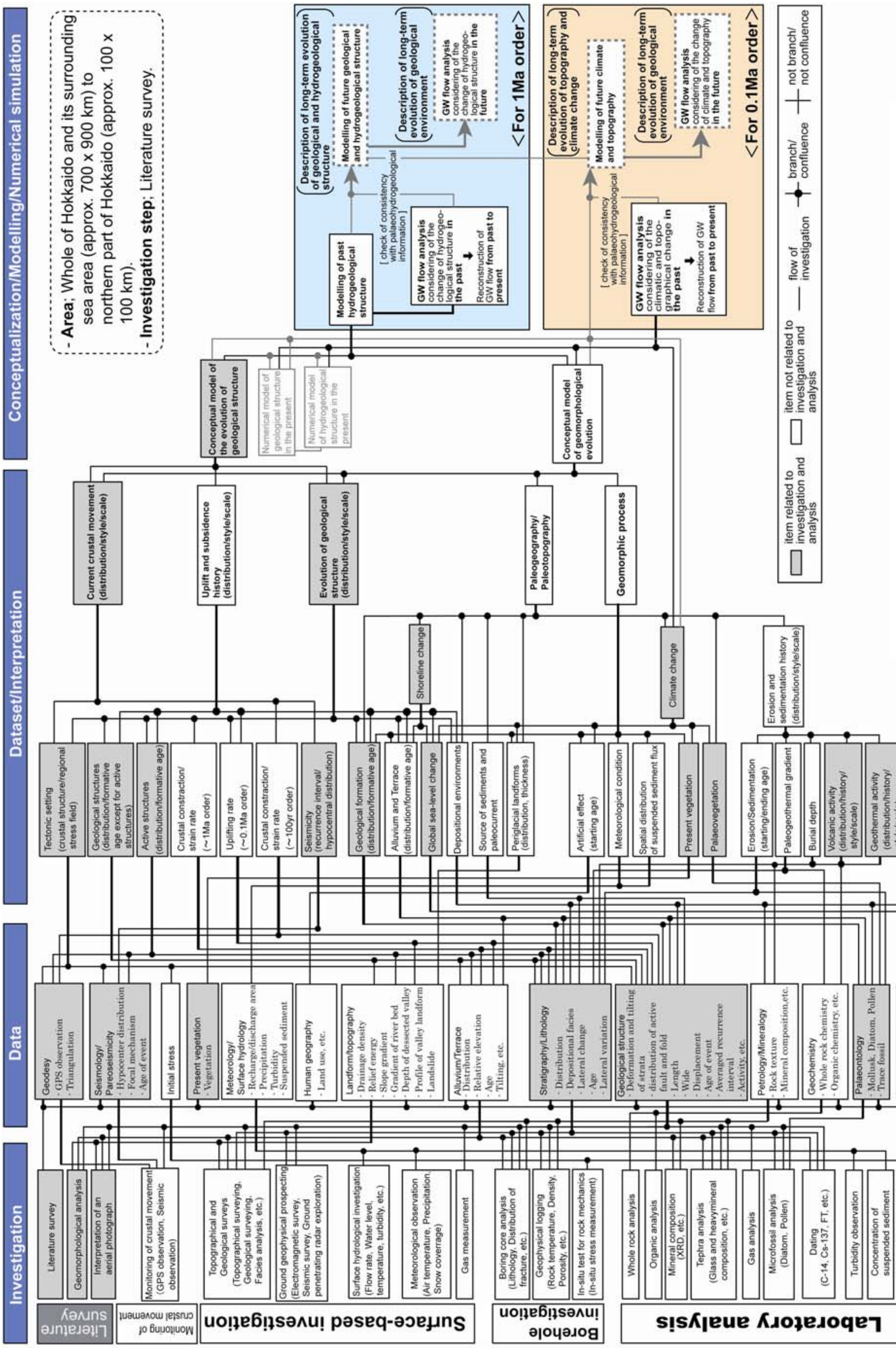

Figure 4.5.2-3a Data flow diagram (palaeohydrogeology)

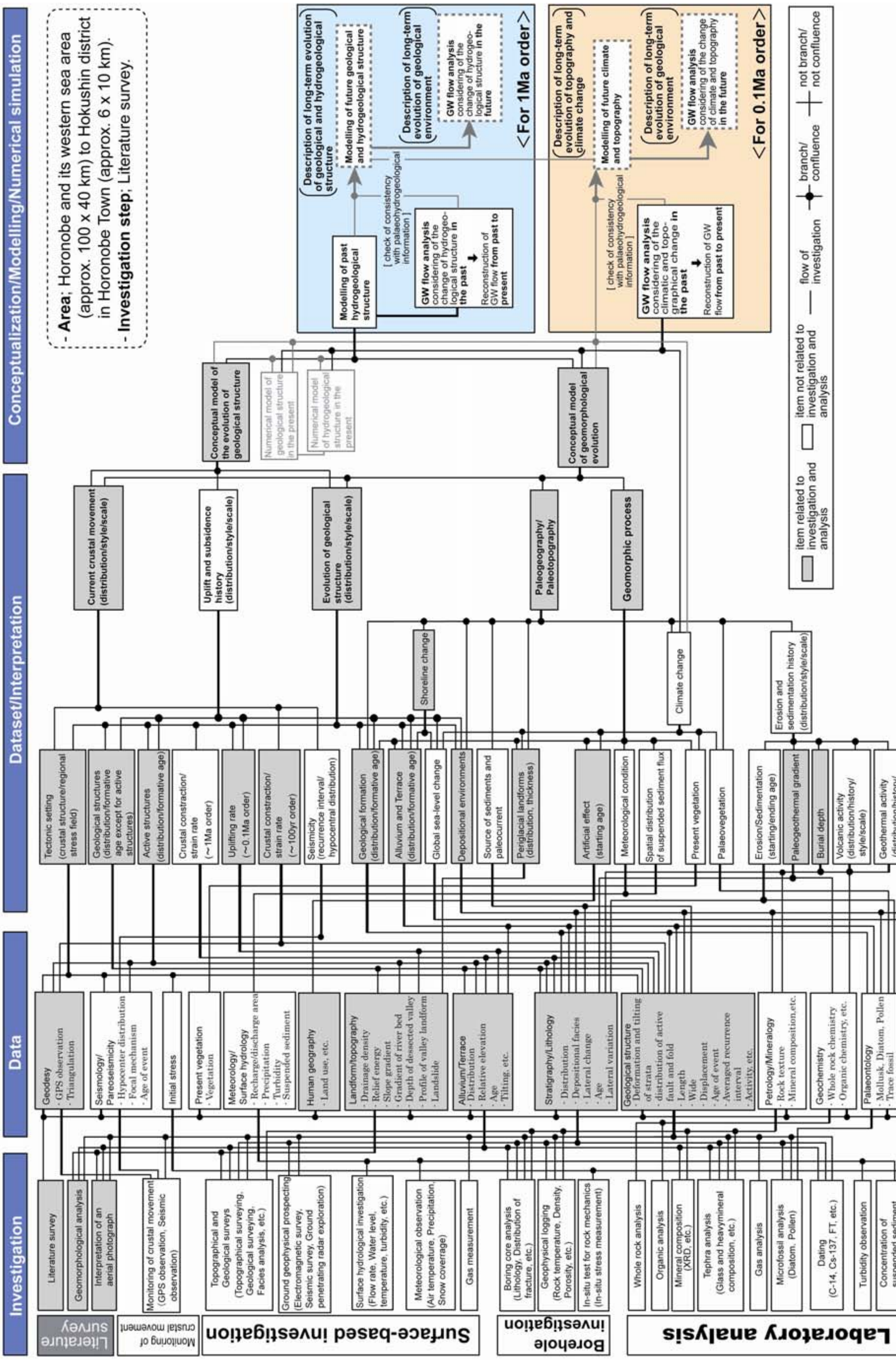

Figure 4.5.2-3b Data flow diagram (palaeohydrogeology)

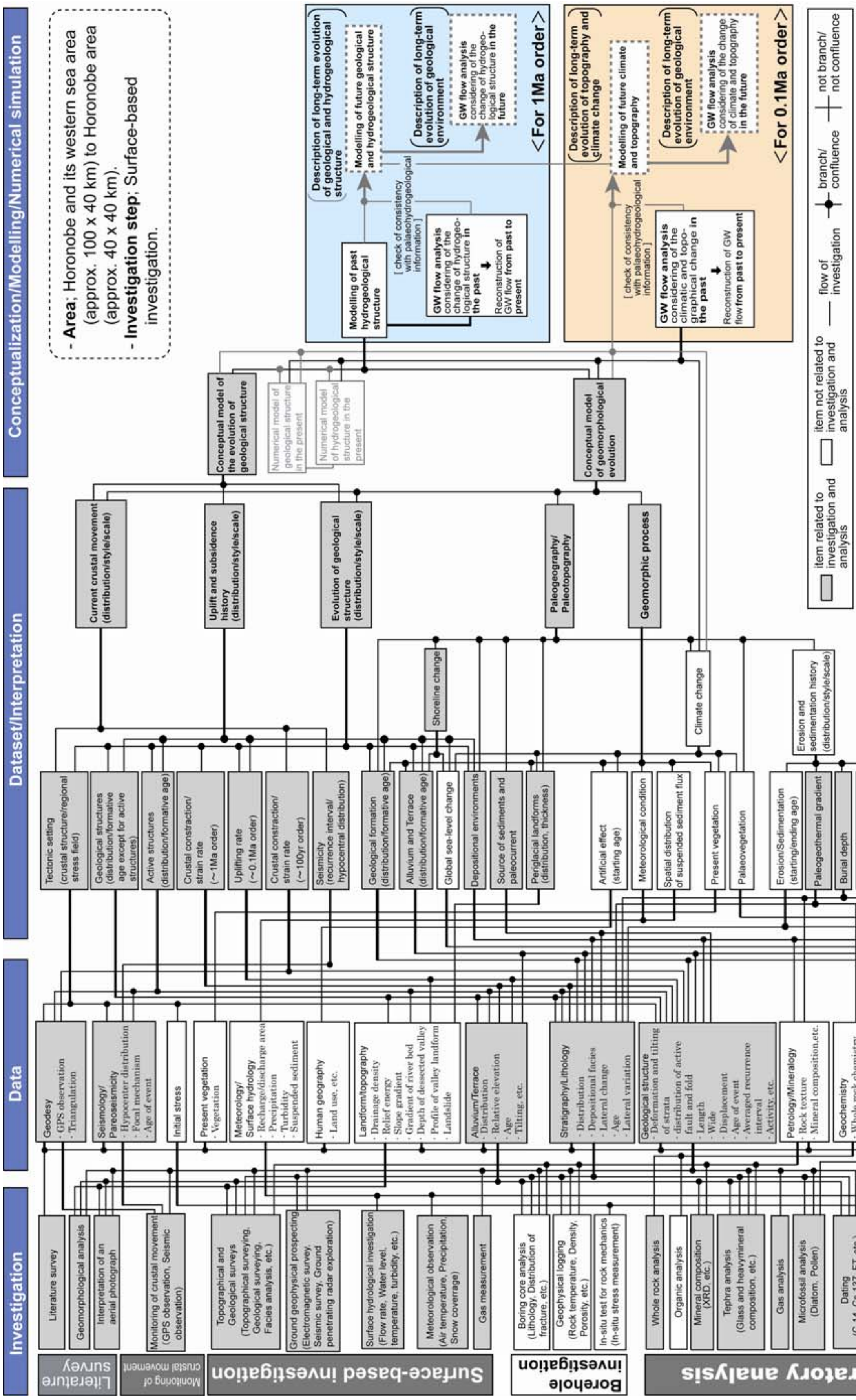

Figure 4.5.2-3c Data flow diagram (palaeohydrogeology)

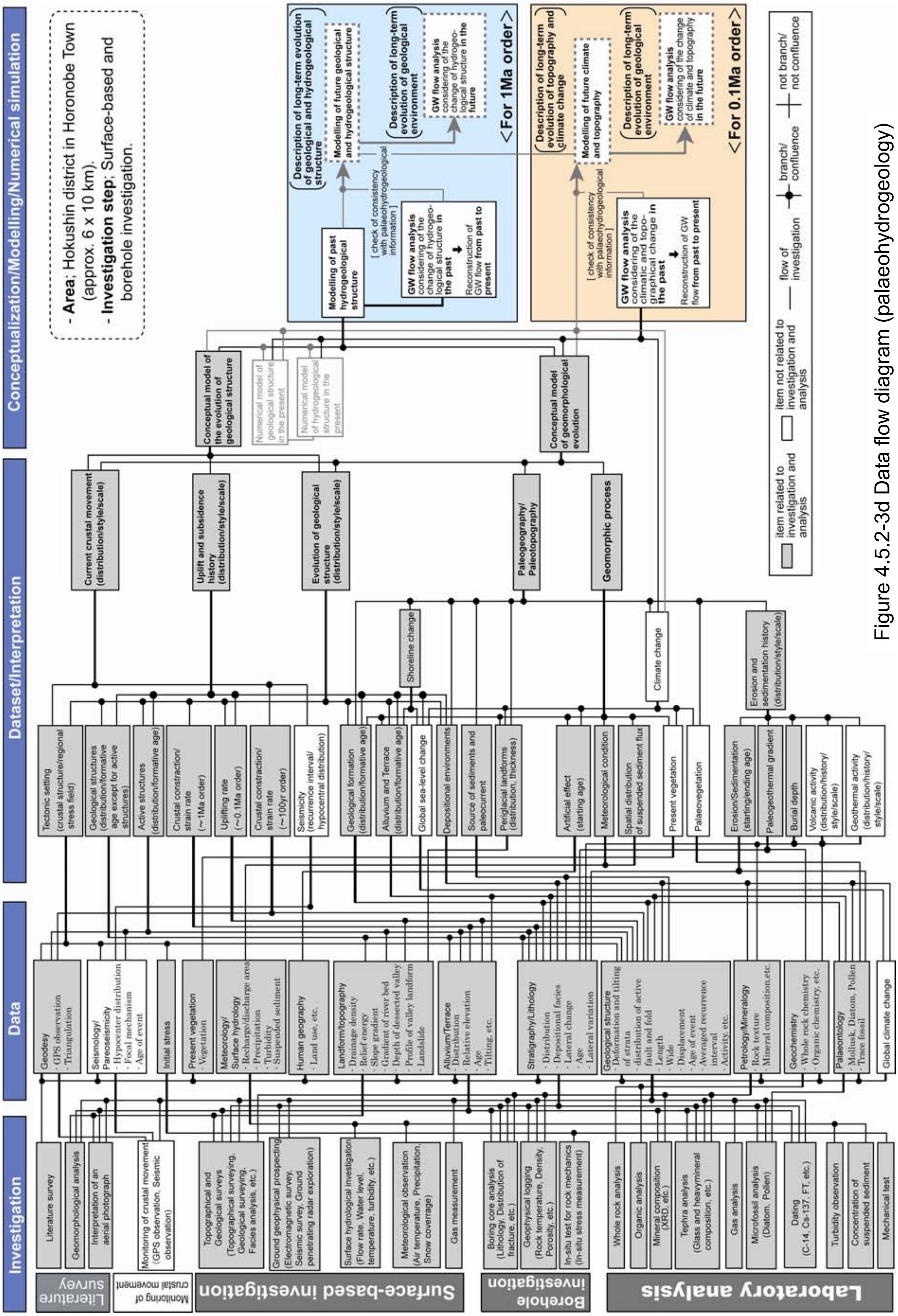

Figure 4.5.2-3d Data flow diagram (palaeohydrogeology)

(1) Investigations and analyses based on existing information

For the area in and around Horonobe, the investigations based on existing information involved an overview of the evolution and scale of earthquake/faulting, volcanic/igneous activity, uplift/subsidence/erosion and changes of climate/sea-level, which are the natural phenomena to be considered for geological disposal. Based on the information above, the natural phenomena and the areas to be characterised could be specified for the more detailed investigations in the stage of surface-based investigations, borehole investigations and the subsequent stages. It was important that the investigations were not limited to the Horonobe area only but include both the Horonobe area and its surroundings and at least the tectonic zone (or geological body) that encompasses the Horonobe area.

Investigations based on existing information were conducted referring to publications and databases[129),130)] of research results covering the whole of Japan and investigation results from in and around the Horonobe area (e.g. academic reports and geological maps published by the Geological Survey of Hokkaido). The estimation of past seismicity and uplift rates were based on analyses of the information compiled as well as on a compilation of existing information. The analysis method is described below.

With regard to past seismicity, the locations and cycles of earthquakes were examined using the method of historical seismology[131)] that studies past earthquakes (historical earthquakes) based on historical literature and records (historical documents). The historical documents surveyed include information of the Ainu handed down by word of mouth and their historical records as well as documents and compilations of the Matsumae and the Tsugaru Clans and “Nikkanki” – a temple diary preserved at the Akkeshi Kokutaiji Temple, one of the three official temples in Ezo (Hokkaido) constructed by the Edo Shogunate government. Other sources include literature by Usami[132)] and the Earthquake Research Committee, Headquarters for Earthquake Research Promotion of the Prime Minister’s Office, Japan[133)]. An interpretation of each earthquake was constructed based on judgments formed on the basis of detailed examinations of the selected historical document and of seismic and geological deliberations. The interpretation of the historical earthquake is generally following the procedures outlined by Ishibashi[134)].

Hokkaido has experienced a unique historical evolution different from that of Honshu. A period commenced from the 12th–13th centuries is called the Ainu cultural period. For examining the seismicity during the Ainu cultural period, historical documents were collected from Ainu oral communications, their historical records and ceremonies[135)] from each village. In areas where these data were collected, it was later evaluated whether the occurrence of earthquakes was documented in such Ainu oral traditions and historical records based on:

- whether it was geologically possible for earthquakes to have occurred;
- whether earthquakes occurred in the historical age after the Ainu cultural period;
- whether natural phenomena resulting from earthquakes in historical ages were mentioned in Ainu oral traditions and historical records[136)].

With regard to the historical documents of the Matsumae and the Tsugaru Clans and “Nikkanki”, the documentation of earthquakes was collected not from the original records and the diary but from the secondary historical sources (compilations made later[137)] that were prepared from the originals by researchers[138),139)]). For the interpretation of historical earthquakes based on historical document, the procedure proposed by Ishibashi[134)] described above was generally followed and the reliability of the occurrence of earthquakes was evaluated by examining whether earthquakes occurred at the same time and date as those recorded in the other historical documents, whether the occurrence of earthquakes was identified at several locations and whether sediments from earthquake-related phenomena such as tsunami deposits and traces of liquefaction remained.

The uplift rate in the Horonobe area over the last several hundred thousand years was calculated based on correlation of the marine terrace surfaces with the marine oxygen isotope stages (MIS) described in existing literature[7),130)], using the age and altitude of the marine terrace surfaces distributed in the western part of the area. The uplift rate was estimated using several methods depending on the baseline of the variations[140)]. Marine terraces developed in shore areas are a good index for calculating the uplift rate. In particular, the distribution of marine terraces formed at the peak of the last interglacial period (MIS 5e), about 125,000 years ago, is widely documented throughout Japan and has been used extensively as an index of uplift rate. Marine terraces formed around 300,000–100,000 years ago (MIS 9–5c) are widely distributed around the Sarobetsu Lowland, located western part of the Horonobe area[130)], and the uplift rate can be estimated using such terraces. For the estimation, aerial photographs were interpreted first and a distribution of the marine terrace surfaces in the Horonobe area was then drawn up (Figure 4.5.2-4). The aerial photographs used were taken by US forces in 1947 (map scale: 1/40,000), the Geographical Survey Institute (GSI) in 1977 (map scale: 1/10,000) and by Horonobe Town in 2000 (map scale: 1/20,000). For the studies of the terrace surfaces and the former shoreline, the altitude, dip, continuity, dissection ratio of the terrace surface and the knick point of the topography were referred to. The results of the studies were expressed as a distribution map of terrace surfaces on a 1/25,000 scale topographical map issued by GSI. The altitude of the former shoreline was determined by dividing the contour interval into ten in the 1/25,000 scale topographical map of the Institute. Following the methodology of Koike and Machida[130)], the uplift (vertical crustal movement) was calculated from the relative altitude of the former shoreline indicated by the marine terrace surfaces subtracting the eustatic change in sea-level.

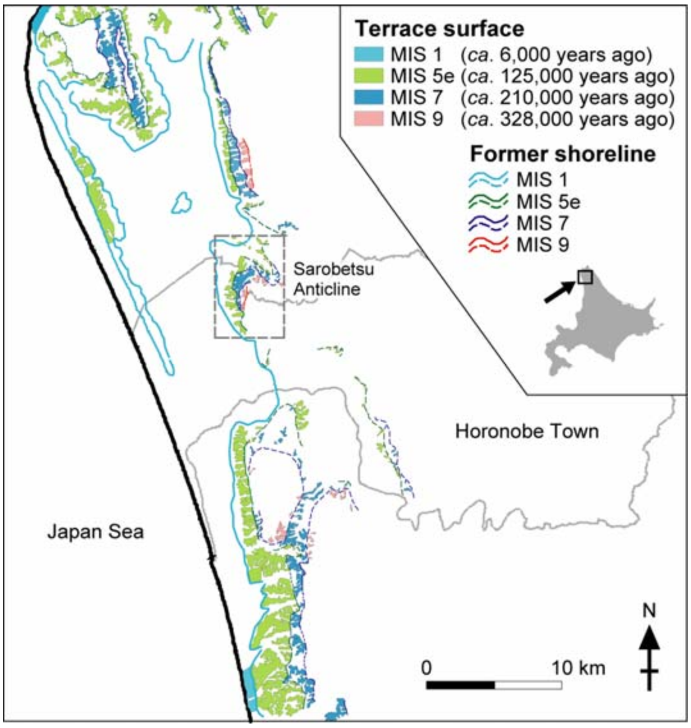

Figure 4.5.2-4 Distribution of marine terraces and former shoreline from MIS 9 to MIS 1

MIS correlation after Koike and Machida[130)]

(2) Surface-based investigations and borehole investigations

i) Seismicity

JMA compiles seismic observation data obtained by various research institutes such as the National University Corporation and determines hypocentres using a nationally uniform seismic velocity structure; the data are published as a database of JMA[129]. The outlines of seismicity in northern Hokkaido can be obtained from this database. However, the seismic velocity structure near the surface on the Japan Sea side of northern Hokkaido is probably significantly different from the uniform velocity structure of Japan, because the total thickness of the Neogene and Quaternary in the area have reached up to 6,000 m. In addition, as the seismic network around the Horonobe area is sparse, the accuracy of hypocentre locations is likely to be low. JAEA, therefore, set up four seismic stations in Horonobe Town (Figure 4.5.2-5) during 2002–2003 to carry out permanent observations and to determine the distribution of hypocentres in and around the Horonobe area by combining the seismic data obtained from the High Sensitivity Seismograph Network Japan (Hi-net)[141].

The analysis was conducted using microseismic clusters observed by the seismic network in northern Hokkaido to relocate the hypocentres, particularly those in the Horonobe area[142]. A hypocentre determination code 'hypomh'[143], which is an attachment of the WIN system commonly used in research institutes in Japan, and a multiplet clustering analysis, which is a highly accurate hypocentre location method, were applied. Multiplets are defined as acoustic emissions and micro-earthquakes that have similarities in waveforms, although the events occurred at different times. The multiplets are thought to be an event that occurs owing to similar mechanisms in the same fault plane or fault system. Multiplet clustering analysis (MC analysis) is an analytical method that combines the detection of arrival time differences by cross-spectral analysis, the relative hypocentre location and the location of relative positions among multiplets (clustering analysis). This method for determining relative hypocentre positions is effective for estimating the strike and dip of each fault and the relative position of the fault and is also able to provide useful information on subsurface structures such as the shape of the fault plane[144].

The distributions of the seismic stations used for the analysis are shown in Figure 4.5.2-5. The analysis covered 4,217 events for which the positions of the hypocentres were determined by Hi-net in the period from 20th December 2002 to 30th September 2005. Of these, 221 events that were measured at more than two of the four seismic stations set up by JAEA were selected as the source data for analysis of waveforms. The seismic velocity structure used was the one determined based on temporary seismic observations in northern Hokkaido[145].

The changes in baseline lengths and groundwater pressures in northern Hokkaido before and after the occurrences of earthquakes were examined to determine the changes in the geological environment associated with the occurrence of earthquakes. Regarding the changes in the base line lengths, these were determined by examining GPS data for the base line length between the HDB-1 GPS station installed by JAEA and the GEONET (GPS Earth Observation Network – the nationwide GPS network) stations installed by GSI (see Subsection 4.7.2). For groundwater pressures, the temporal variation of the groundwater pressures observed in the MP system (see Subsection 4.7.5), which was installed in borehole HDB-1, was analysed. The earthquakes used for examining base line lengths were the 2003 Tokachioki earthquake that occurred on 26th September 2003 with M 8.0[146] and one that occurred on 14th December 2004 with M 6.1[146], with the hypocentre in the southern Rumoi District. The earthquake used for investigating groundwater pressures was the 2003 Tokachioki earthquake.

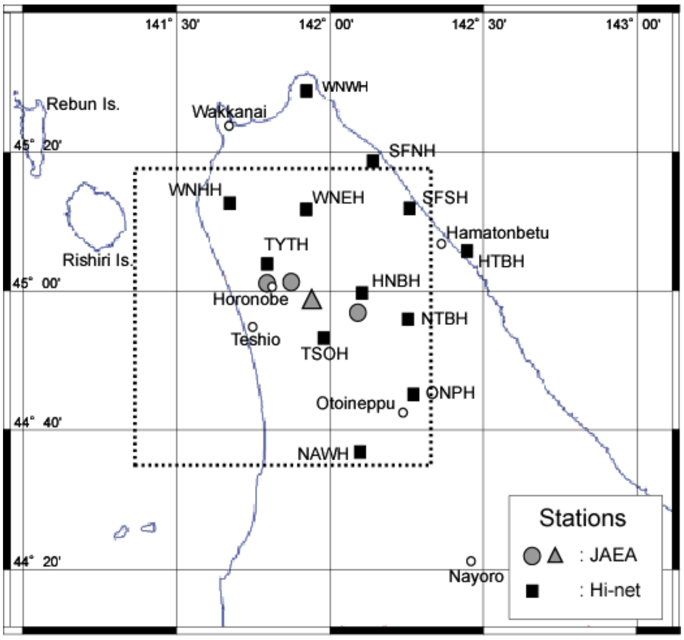

Figure 4.5.2-5 Seismic stations installed in northern Hokkaido
Area surrounded by dashed line corresponding to the area shown in Figure 4.5.3-10
Solid grey triangle for the Kamihoronobe station

ii) Regional tectonics

According to existing information, northern Hokkaido constitutes part of a fold-and-thrust belt in an E-W stress field. The fold structures are thought to have been formed from the east after 2–3 Ma[20),147)]. The rate of crustal movement in northern Hokkaido can be estimated based on the strain rate in the area, which also sets the constraints for restored geological cross-sections by combining uplift, subsidence and erosion rates (see Subsection 4.5.3). The evolution of the geological structure restored in such a way will be essential information for evaluating palaeogroundwater flow conditions (see Subsection 4.2.4). In Phase I, the horizontal strain rates of the crust in northern Hokkaido were estimated by an analysis using GPS observation data and a geological cross-section, in addition to a compilation of existing information from triangulation[148)] and displacement data on active faults[149)]. The geological cross-section from approximately 2.5 Ma to the present (referred to hereafter as the restored geological cross-section) was prepared by referring to existing information and the investigation results for the geology and geological structures in and around the URL area.

For the analysis of the GPS data, data from a total of 17 stations were used: the HDB-1 GPS station[150)], 12 GEONET stations in northern Hokkaido and 4 stations belonging to the International GPS Service (IGS) in East Asia (Figure 4.5.2-6). An observation at the HDB-1 GPS station was started on 1st January 2003. Thus, the analysis covered data during the period from 1st January 2003 to 13th January 2006. The collected data were analysed using a computer code GAMIT, which was developed by the Massachusetts Institute of Technology and the Scripps Institute of Oceanography in the USA. As described before, the Horonobe area is in an E-W stress field. Therefore, the strain rate [y^{-1}] was obtained by using the baseline lengths between the HDB-1 GPS station and GEONET stations (Rishiri, Hamatonbetsu and Esashi stations) for the E-W direction.

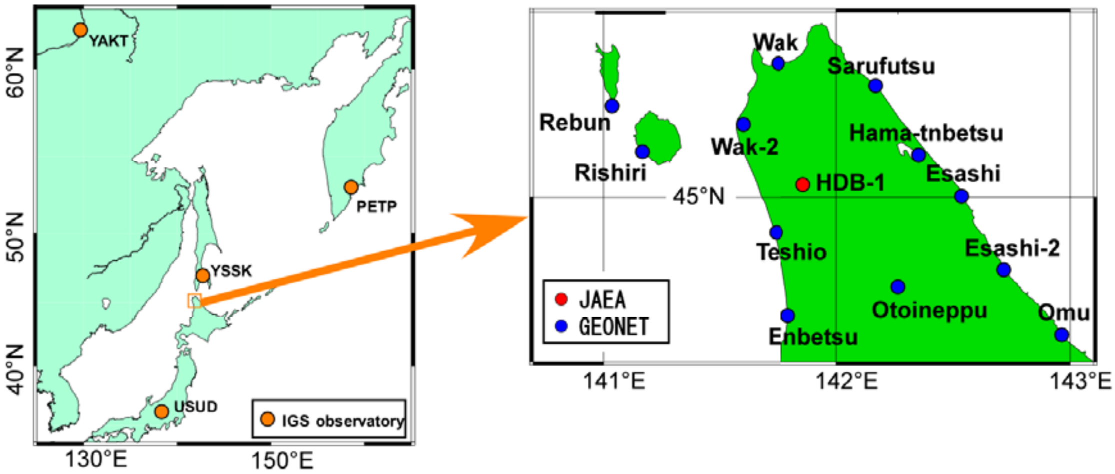

Figure 4.5.2-6 GPS stations in and around the Horonobe area

The analysis was conducted in the following order:

a) determine the change in the baseline lengths during the period of observation;
b) calculate the strain over the observation period (approximately three years) from the ratio between the change in the baseline lengths and the baseline lengths when GPS observations started;
c) convert this ratio into strain rate per year.

The time variation in the baseline lengths was obtained by fitting with a functional form that can express periodical change such as seasonal variance and variance that accumulates over a long period, using the curve-fitting tool in KaleidaGraph version 4.0 of the Synergy Software Co.

In the analysis using the geological cross-section, the horizontal crustal shortening in northern Hokkaido was estimated by applying the procedure of cross-section balancing[151)] to the geological cross-section up to tens of kilometres deep that was derived from the seismic reflection surveys conducted in and around the Horonobe area. The procedure of cross-section balancing draws a cross-section in which the stratification before the deformation, is accurately restored when deformation such as folding and faulting is returned to the condition before deformation, considering that the deformed-state and restored cross-sections maintain constant area[152)]. Here, it is a prerequisite that the cross sectional area of the stratum and the length of a contact in cross section does not changed during the deformation. Shortening was estimated based on the length in the geological cross-section, being the length before the deformation, and the current straight line length, being the length after the deformation, with respect to the basal surface of the formations (the Hakobuchi, Wakkanai and Yuchi Formations) that were assumed to be deposited before the deformation, i.e. development of the anticlinal structure. Ito[147)] interpreted the results of the reflection seismic surveys conducted by the Japan National Oil Corporation in the area from the Sarobetsu Anticline to the Omagari Fault in the western part of the Horonobe area. The fold structure in the Horonobe area was assumed to be formed at the time of deposition of the Yuchi Formation, based on the thinning of the stratum in the anticlinal axis and the thickening of the stratum in the synclinal axis in the seismic profile; it was also assumed that the anticline was developed approximately 2.7–2.6 Ma[147)]. The development of the fold in the Horonobe area was therefore assumed to have started approximately 2.7–2.6 Ma. Based on this assumption, the strain rate was calculated by dividing the strain (extension; the ratio of its change in length to its initial length, where the change in length is the final length minus the initial length) by 2.7–2.6 million years.

The location of the restored geological cross-section was set with the following considerations in mind regarding the results of the shallow subsurface hydrological investigations and the groundwater flow analysis (see information on the recharge area; Subsections 4.2.3 and 4.2.4): it requires to go through the area of the upper Shimizu River and the Teshio River, which is topographically low, and include the area near the shelf break (approximately 140 m deep) in order to take the eustatic sea-level change into account (Figure 4.5.2-7). In addition, the direction of the cross-section is orthogonal to the trend of the geological structure in order to include main components of geological structures such as folds and faults. The present geological cross-section was constructed based on the results of investigations on geology and geological structures in and around the URL area (see Section 4.1) and existing information such as submarine geological structure maps[153], marine seismic profiles[154], interpreted reflection seismic profiles and documentation compiling all of this information[155]. In inland areas, except for in and around the URL area, geological structures refer to existing cross-sections based on the seismic reflection profiles[147] obtained during oil and natural gas exploration in the past and the stratigraphy was taken from geological maps issued by Geological Survey of Japan (GSJ; see Section 4.1 for references). In the sea area, stratigraphy and geological structures refer to existing information, such as submarine geological maps based on the sonic profiles issued by GSJ during the 1970's. Moreover, for the geological structures in sea areas, improvements were made based on the preliminary sonic profiles obtained by GSJ and universities in 1999–2002. If there is contradiction of these data, priority was given to the information obtained in the URL area for both geological structures and stratigraphy. For interpreting the geological structures, the regional structures and tectonics were taken into consideration. In addition, restored geological cross-sections were drafted based on the current geological structure by considering the horizontal crustal strain rate, the rates of uplift/erosion (see Subsection 4.5.3) and the depositional period[6] of the formations in northern Hokkaido.

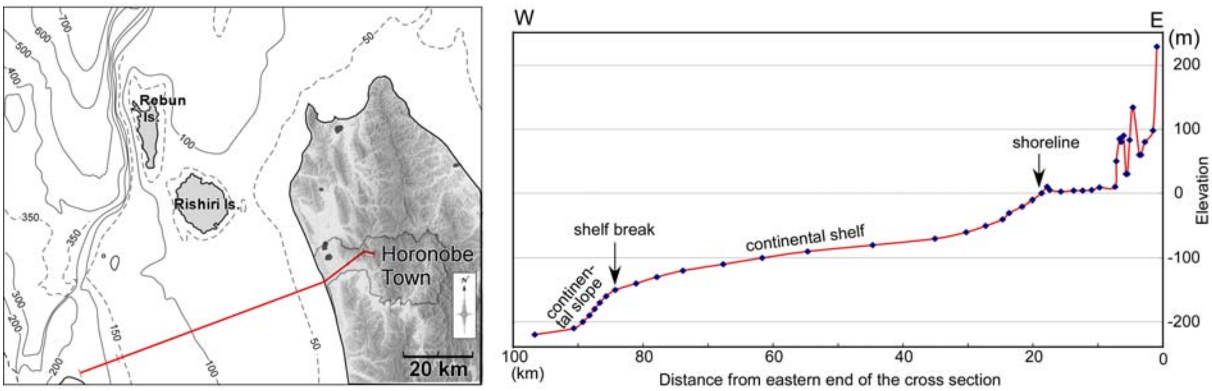

Figure 4.5.2-7 Location of cross-section for restoring geological structure in northern Hokkaido

Left: Sea bed topography after Koaze[7]; *Right*: Geomorphic section along the red line (V:H = 100:1) based on Japan Coast Guard[156]; Red line referring to the restored geological cross-section shown in Figure 4.5.3-15

iii) Estimation of uplift and uplift rate

As described in (1), several different approaches have been attempted to estimate the uplift rate depending on the baseline for calculating the vertical crustal movement[140]. For the analysis based on existing information, the marine terrace surfaces distributed in the western part of the Horonobe area were used as the baseline for calculating of the vertical crustal movement and the uplift rate was calculated according to the MIS correlation as documented in the existing literature[7),130]. However, there is no consensus on the age of marine terrace surfaces in the existing literature. One of the reasons for this is that there are very few widespread tephra beds that can be observed with the naked eye in the strata constituting the terrace surfaces in northern Hokkaido and chronology of the terrace based on tephrochronology would be difficult. A detailed description was therefore prepared of the marine terrace distribution in the Shimonuma district of Horonobe Town, located in the western part of the Horonobe area, and the age of the marine terrace surfaces was estimated by applying the Refractive Index Physical Labor (RIPL) method to the stratum constituting the terrace deposits. The marine terrace surface investigated was correlated with MIS 5e by Koike and Machida[130)].

The RIPL method is used to measure the refractive index of volcanic glass and phenocrysts (e.g. orthopyroxene and amphibole) contained in samples which are collected continuously at 5–10 cm intervals from aeolian deposits and lake/bay deposits. The aim is to identify original tephra material that is invisible to the naked eye and to determine the tephrostratigraphy by statistically analysing the large volumes of data obtained[157)]. This method is possible due to the huge improvement in the accuracy and speed of refractive measurement devices over recent years. Samples were taken at about 5 cm intervals for refractive measurements. Since identification of tephra using refractive index data only can be difficult, the major elements of the volcanic glass were analysed using an energy dispersive electron probe micro-analyser (EPMA). The ^{14}C dating of a charcoal contained in the loess constituting the terrace deposit has also carried out using the accelerator mass spectrometry. The uplift (vertical crustal movement) was then calculated according to the method used by Koike and Machida[130)] by subtracting the eustatic sea-level change from the relative altitude of the former shoreline indicated by the marine terrace surface.

iv) Palaeogeography

Palaeogeographical data, i.e. the evolution of the land – sea distribution and locations/altitudes of mountains in the past are essential for the restoration of historical groundwater flows (see Subsection 4.2.4). For the restoration of the palaeogeography, it is of importance to define the periods of sedimentation of the strata occurring in the area of interest and to estimate the sedimentary environments of the strata based on the sedimentary facies analysis. The information will allow identification of the strata deposited in the same periods and definition of the spatial extent of the sedimentary environments. During Phase I, analysis of fossil diatom, FT dating of volcanic ash, provenance analysis and sedimentary facies and sequence stratigraphical analysis were carried out in order to estimate the depositional age of formations and their palaeoenvironment.

Although the Koetoi and Yuchi Formations have traditionally been examined based on diatom and shell fossils, there were various views on their depositional age and stratigraphy[158),159)]. Existing information is also suggested that the Pliocene – Pleistocene formations in northern Hokkaido facing the Japan Sea have a diachronous relationship[12)]. Therefore, at the western limb of the Sarobetsu Anticline located in the western part of the Horonobe area, identification of fossil diatoms and diatom zones was attempted to the upper Koetoi Formation near the boundary between the Koetoi Formation and the Yuchi Formation and the depositional age of each formation was also examined by FT dating[27)].

Provenance analysis is a method for estimating the source of clastic materials that constitute clastic sedimentary rocks. It is based on the flow direction (palaeocurrent) that supplied the clastic materials and on the lithological and mineralogical examination of the clastic materials. The palaeocurrent is restored using sedimentary structures. The types and volume ratios of the mineral particles and gravels comprising the clastic materials would reflect the strata and rock types in the hinterland and also indicate that the provenance of clastic materials was denudation environment during its sedimentation period. The results of the analysis provide information about sedimentation and denudation environment (approximate land – sea distribution) of the strata and rocks that supplies the clastic materials. The provenance analysis in this case used the composition of the gravels in the Sarabetsu Formation and the content of fossil diatoms in the Koetoi, Yuchi and Sarabetsu Formations (see Subsection 4.7.2).

The Sarabetsu Formation was classified into several sedimentary facies based on information from the lithofacies, sedimentary structures, shape of the basal surface of beds, stacking pattern of sedimentary facies, distribution of the stratum and palaeocurrent direction; the sedimentary environment were reconstructed based on sedimentary facies associations which were integrated from these sedimentary facies (sedimentary facies analysis). From the stacking pattern of sedimentary facies based on the above analysis, the sequence boundaries and sedimentary sequences were identified; the relative sea-level changes at the times of formation of each sedimentary sequence were estimated (sequence stratigraphical analysis). A geological description of continuous outcrops is required for the sedimentary facies and sequence stratigraphical analyses. However the number of continuous outcrops of the Sarabetsu Formation is limited in Horonobe Town. One of these limited continuous outcrops, the location where the lower most part of the Sarabetsu Formation can be continuously observed (Figure 4.5.3-18 for the location of outcrop) was selected for the analyses.

The diagrams of land – sea distribution were prepared for the period after MIS 7 (approximately 210,000 years ago), taking into consideration the formative age and the distribution of the marine terraces in the western part of the Horonobe area (see Subsection 4.5.3), the submarine topography to the west of Horonobe area and the eustatic sea-level changes.

v) Estimation of the amount and rate of erosion

Various methods[160] have been attempted for estimating the rate of erosion. Similarly to the case for the uplift rate, it depends on the length of the period and areas to be covered. The method most used is that based on data on the volume of sediments accumulated in dams. This method is used to calculate the sediment production rate in the drainage basin of a dammed lake, based on the volume of sediment accumulated and the elapsed time since completion of the lake. The advantage of this method is that the average rate of erosion in the drainage basin can be determined quantitatively. However, there is a weakness in that the long-term trend of the erosion rate cannot be determined well, since the observation period for the volume of sediment in the dam can only be as long as about 40 years. Another method involves using geomorphic surfaces such as marine terrace surfaces as an indicator. The rate of downward erosion can be calculated using the depth of the dissected valley on marine terraces. An accurate estimate of the age and original topography of geomorphic surface before dissection is a prerequisite for the application of above method. In any case, applicable methods must be selected considering the characteristics of the investigation area.

The Wakkanai and Koetoi Formations which composed of biogenic fine-grained siliceous rocks are distributed in the Horonobe area. Silica minerals contained in a siliceous sediments were transformed from amorphous silica (opal A) to low-temperature cristobalite (opal CT) and then to low-temperature quartz[161] owing to burial processes and temperature increase. The transformation of the silica minerals, along with zeolite and feldspar with an abundance of Na and Ca, is known as the mineral index of burial diagenesis. The transformation of silica minerals in particular is strongly controlled by changes in temperature owing to the burial of sediments[162]. For this reason, the temperature estimated for the silica minerals in the sediments represents the highest temperature experienced by the sediments during burial diagenesis, provided volcanic activity, hydrothermal activity and hydrothermal alteration associated with these activities did not occur after the sediments had experienced the alterations caused by burial diagenesis.

This means that the palaeogeothermal gradient can be calculated in a borehole if the current depths of occurrence of both opal CT and quartz are obtained in the borehole. Once the palaeogeothermal gradient is known, the depth profiles of opal A, opal CT and quartz at the time of acquiring the palaeogeothermal gradients can be estimated by assuming the temperature of transformation to opal CT or quartz and the ground surface temperature at the period of acquiring the palaeogeothermal gradients. The amount of erosion (amount of denudation) from the time of acquiring the palaeogeothermal gradient to the present is given by subtracting the current depths of opal CT and quartz from the depths of those at the time of acquiring the palaeogeothermal gradient.

There is no large-scale dam in the Horonobe area and marine terraces are limited to coastal area. Although there are flat surfaces that are assumed to be the uplifted marine terrace surfaces in and around the URL area, the age and the original landform of these flat surfaces have not been accurately determined. On the other hand, the Wakkanai and Koetoi Formations, consisting of siliceous sedimentary rocks, are distributed widely in and around the URL area. Based on these findings, the amount of erosion was estimated using the transformation of silica minerals contained in the formations as an indicator.

There are some reports on the transformation temperatures for silica minerals. According to Aoyagi and Kazama[161)], the temperature required for amorphous silica minerals to transform from opal A to opal CT by diagenetic alteration is 45°C and that from opal CT to quartz is 69°C; according to Yoshimura[163)], these temperatures are 50°C and 80°C respectively. However, it should be noted that palaeogeothermal gradients cannot be obtained from the above information only if complicated uplift and subsidence have occurred. In the discussion in Subsection 4.5.3, the amount and the rate of erosion (denudation amounts and rates) were estimated according to the work flow diagram in Figure 4.5.2-8, using the transformation temperatures of silica minerals indicated by Aoyagi and Kazama[161)] and Yoshimura[163)].

vi) Geomorphological processes

All types of physical and chemical changes that alter the topography, i.e. the configurations of the land surface, are called geomorphological processes[164)]. The processes include the formative processes of topography and mechanisms and processes of topographical change. The formative processes and topographical change was estimated to understand the primary processes, such as weathering, erosion, transport and sedimentation. In Phase I, for the Hokushin district of Horonobe Town, where almost all the formations occurring in the Horonobe area are found, the geomorphological processes due to the interactions of the above processes were studied. Firstly, a map of the drainage system, a ‘zebra map’, and a distribution map of relief energy, drainage density and landslide landforms were prepared based on information from morphometry of topographical maps and interpretation of aerial photographs. The ‘zebra map’ was drawn by painting every alternate belt of 25 m in altitude. In addition, field investigations were conducted in order to confirm the landslide landform and landform materials. The current topography were characterised based on the integration of the above information. The geomorphological processes in each of the formation found in the Hokushin district were then examined based on a comparison between the characteristics of the current topography and the geology (see Section 4.1 and Appendix 1 for the geological map). The amount of suspended sediment flux in each basin of the river that encompasses the Hokushin district was calculated based on measurements of the turbidity of the rivers. The characteristics of current geomorphological processes for each drainage basin were studied by comparing the drainage basin characteristics, including vegetation, land use and geology, with the amount of suspended sediment flux. The drainage basin for this study was the same as that for the shallow subsurface hydrological investigations carried out for the Hokushin district in Horonobe Town (see Subsection 4.2.2).

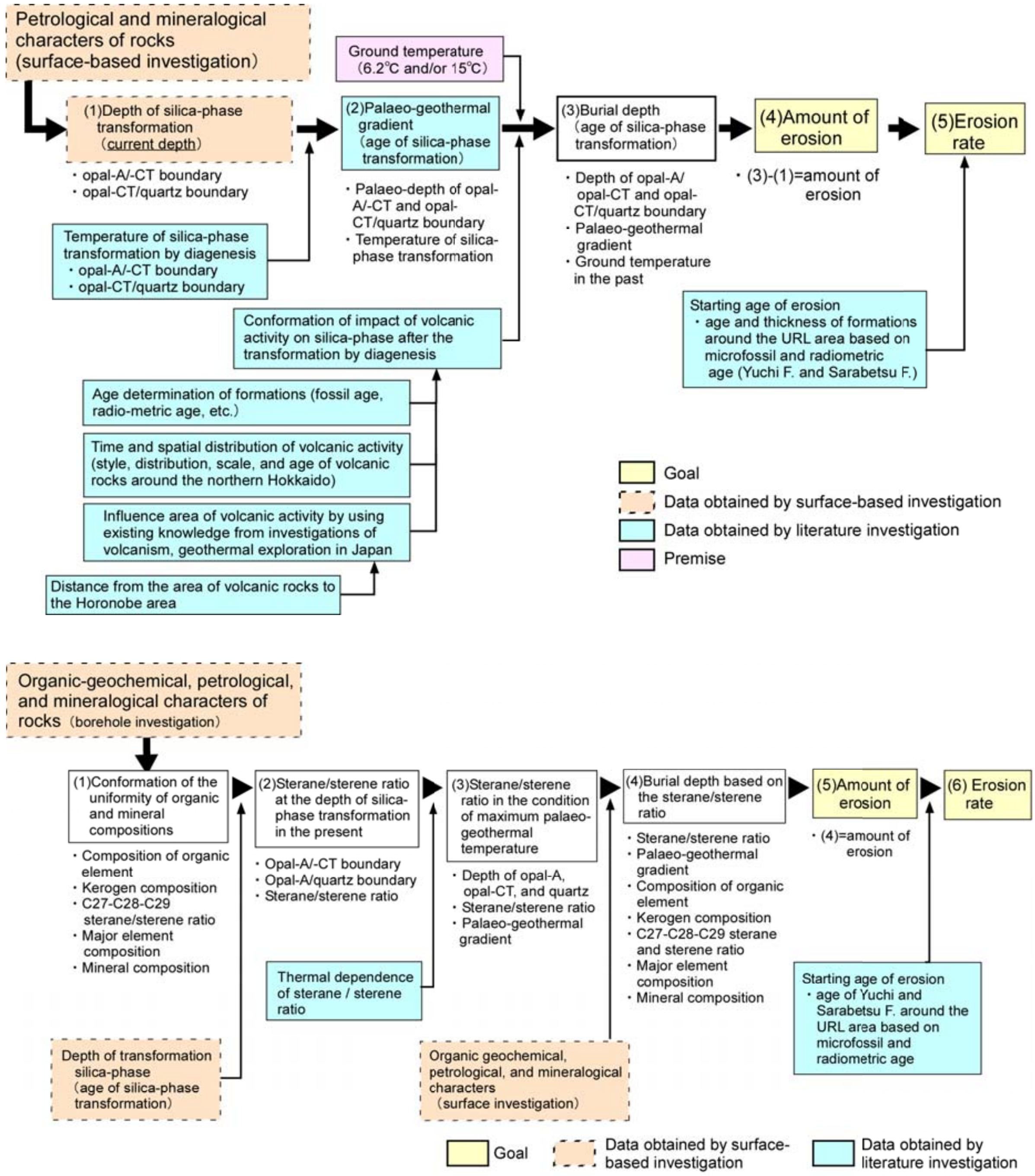

Figure 4.5.2-8 Work flow for estimating erosion rate using the transformation of silica mineral phase (upper) and changes in sterane/sterene ratio (lower)

After Takahashi et al.[165)]

For the preparation of the map of drainage system and distribution map of the relief energy, a topographical map with scale 1/25,000 issued by GSI was used. For the drainage system map, the valley line shown as being concave in the contour line and all rivers shown in the topographical map were traced regardless of the stream order in the drainage system. For the relief and drainage density, the topographical map was overlaid with grids of 500 m square according to Suzuki[166)]. The relief was obtained from the difference between the highest and lowest altitudes (relative altitude) within the grids by visual observation.

The drainage density was obtained by counting the total number of exterior (1st order stream) links and interior (2nd order stream and above) links as the number of valley lines and dividing it by the area of the grid. The landslide landform was read from an aerial photograph on a scale of 1/10,000 taken by GSI in 1977 and the map for assessing the landslide landform was prepared by drawing the above landslide landforms onto a topographical map in the scale of 1/25,000 issued by GSI. According to Yamagishi[167)], all topography consisted of combination of slip scarp and slide block, i.e. the basic elements of the landslide landform, were interpreted as landslide landform. For the large-scale landslide landform, it could be subdivided into smaller blocks and the interior landform, such as the secondary scarps, cracks, mounds and depressions (concave structures) could be seen. Such interior landforms were excluded from the map.

The conventional method of measuring the concentration of suspended sediment in a river is to sample the river water and measure the concentrations at the laboratory. The problem with this method, however, is not being able to acquire continuous data. The concentration of suspended sediment was therefore derived using the turbidity, which can be observed continuously using a special device and correlates with the concentration of suspended sediment. Combining this method with the river flow rate, the volume of suspended sediment was calculated for each drainage basin defined for the shallow subsurface hydrological investigations (see Subsection 4.2.4; Figure 4.2.2-2). This measurement was carried out at the time when Typhoon no.14 passed through in early September 2005, when the river level was significantly raised and lowered over a short period of time and continuous data on turbidity and concentration of suspended sediment could be obtained during the course of the change in the river level. The turbidity (unit in [NTU]) was continuously monitored every 10 minutes for 24 hours with turbidity metres installed together with devices used to measure the river flow rate at points P-3, P-4 and P-5. Turbidity metres with a resolution of 1 NTU and a measurement range of 0–800 NTU are suitable for measuring turbidity even for large outflows of water such as during the time of a typhoon. For the two days when Typhoon no.14 was passing through, river water was sampled at P-3 and P-5 for 24 hours and the sampled water was analysed for turbidity in the laboratory. The continuous data on the concentration of suspended sediment, C [mg l^{-1}], was obtained by determining the correlation formula of turbidity and the concentration of suspended sediment based on these measurements, together with the analytical results for turbidity from the laboratory for 90 samples taken in the Hokushin district of Horonobe Town. The volume of suspended sediment flux, F [g s^{-1}], was calculated using the concentration of suspended sediment, C [mg l^{-1}], and the river flow rate, Q [m^3 s^{-1}], in the formula of F = C Q[168)]. It should be noted that the suspended sediment flux obtained by the above method is the sediment flux transported by suspension out of all the sediment produced by erosion at locations upstream of the points where the turbidity meters were installed in each drainage basin.

4.5.3 Results and synthesis

(1) Study covering the whole of Hokkaido, the surrounding sea area and northern Hokkaido, based on existing information

i) Seismicity

Improved seismic network and temporary seismic observations in Hokkaido since the 1980’s have revealed a number of micro-earthquakes (M < 3) in northern Hokkaido. Such seismicity is dominant in the area facing the Japan Sea and includes the Kamuikotan Belt; the seismicity in the area facing the Okhotsk Sea is very low. A high-seismicity zone with a width of about 50 km running from north to south has been observed and many earthquakes have occurred at depths of 15–30 km in north-western Hokkaido[145),169)], as shown in Figure 4.5.3-1. The seismicity of micro-earthquakes is particularly high along the coastal area of the Japan Sea. Focal mechanisms of such earthquakes are strike-slip faults with reverse dip-slip component and an E-W stress as the maximum principal stress in the zone shallower than 10 km in depth and normal faults at a depth of around 20 km. It is also known that earthquake swarms have sometimes occurred in northern Hokkaido. Within the Horonobe area, earthquake swarms occurred in 1975, 1986 and 1992. The maximum magnitude of the 1992 swarm was M 4.3[170].

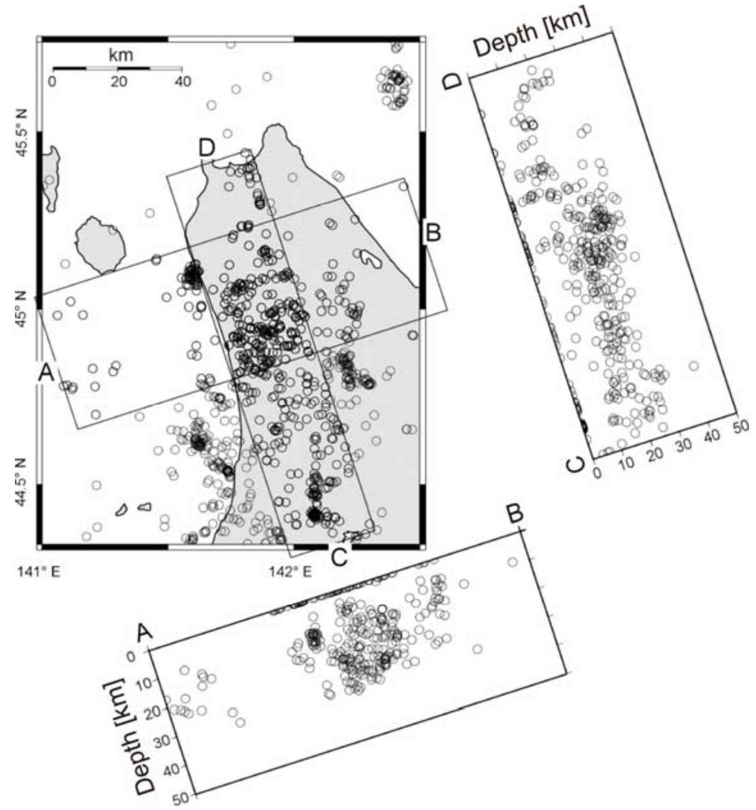

Figure 4.5.3-1 Hypocentre distribution of earthquakes with depths of 50 km or less observed during 2000 to 2002

After JMA[129]

Information on seismicity that occurred before the seismic observations started (historical earthquakes) was collected by examining records of earthquakes in the historical documents. The results indicated that the areas affected by earthquakes or tsunamis possibly caused by earthquakes were found more often along the Pacific Coast of Hokkaido, in particular the coast of Uchiura Bay, and the Iburi – Hidaka and Kushiro coastal areas. For inland areas, the middle Saru River basin, the middle Tokachi River basin, the east of Lake Saroma and around Lake Kussharo also experienced such phenomena (Figure 4.5.3-2). This distribution of the areas, for occurrence of earthquakes, is similar to that of epicentres of destructive earthquakes[132].

The above situation is considered to have existed for the last 800 years, based on comparison with oral traditions relating to earthquakes and tsunamis handing down during the Ainu period and based on the duration of this period[136]. No description by which a specific year or age can be estimated has been found in oral traditions on the Ainu period. The events relating to earthquakes that are mentioned in such traditions are presumed to have occurred during the Ainu cultural period or earlier.

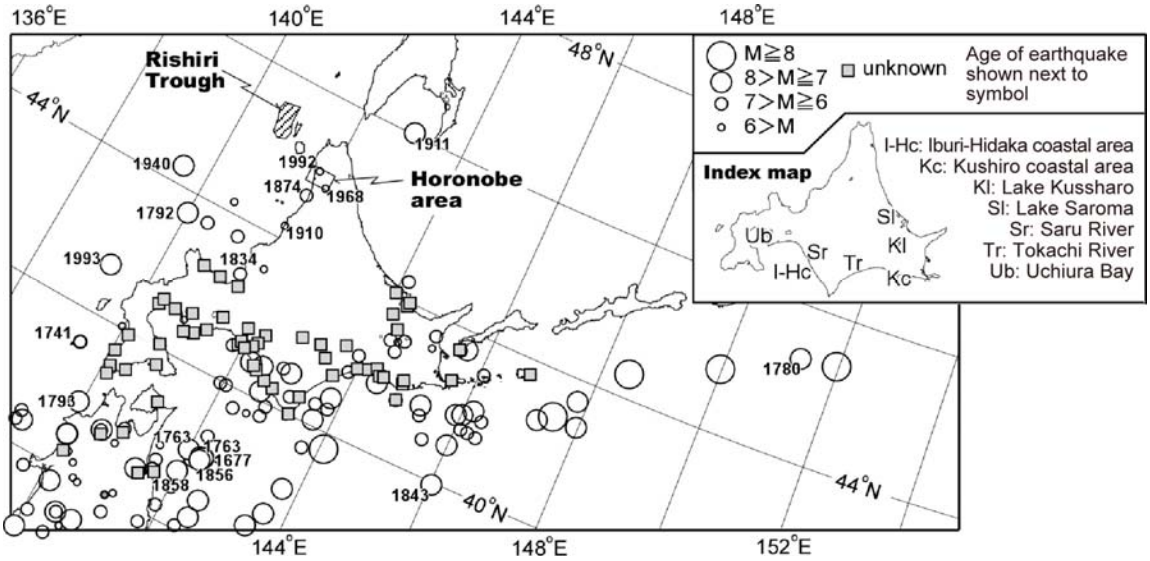

Figure 4.5.3-2 Epicentres of destructive earthquakes and locations associated with the past earthquakes and tsunamis

Circles for epicentres of destructive earthquakes after Usami[132)], Tamura et al.[145)] and Takahashi and Kasahara[171)]
Squares for the past earthquake and tsunami locations after Niizato et al.[136)], Takashimizu[172)] and this study

In historical documents written by people who lived in Honshu Island, 146 earthquakes (i.e. earthquakes that could be felt) that had not been previously known were found to have occurred during the period from 1611 to 1880. All the earthquakes that occurred after 1881 could be confirmed in the records of Usami[132)]. In these records, only earthquakes that occurred in southern Hokkaido were recorded in the early days, starting with one that occurred in the Aizu District (the Keicho – Sanrikuoki earthquake in 1611). Earthquakes that occurred in eastern and central Hokkaido started to appear in the documents since 1780 and 1792, respectively (Figure 4.5.3-3a). After 1816, the earthquake records for the Akkeshi area increased (Fig 4.5.3-3b) and records covering seismicity for the whole of Hokkaido, including inland events (Hidaka District), started to be kept (Figure 4.5.3-3c). With regard to the history of Hokkaido, the Matsumae Clan was established in 1604, the Akkeshi Basho (trading point) opened for the period 1624–1644 and Kunashiri Basho opened in 1754[138),173)]. Incidents including natural disasters around the Akkeshi area after 1816 were recorded in the “Nikkanki” temple diary by the chief priest of the Akkeshi Kokutaiji Temple. In the period from the middle of the Meiji era (around 1890) to the Taisho era (1912–1926), explorers migrated all over Hokkaido and a seismic network was installed by the Meteorological Observatory. The earthquake records collected sporadically by era, followed by an increase in the recorded events, are therefore due to progress made by the Japanese population of Hokkaido. It is however hard to confirm that such records truly illustrate the regionality and cycles of the earthquakes.

It is therefore difficult to investigate the characteristics and cycles of earthquakes by era based on the historical seismology in and around Hokkaido. However, regarding the regionality of the earthquakes, a trend can be seen whereby fewer earthquakes were recorded in northern Hokkaido and more in the coastal areas of the Pacific Ocean from the beginning of the Ainu period up until the present (Figure 4.5.3-3). As described previously, the regionality can be considered to have existed for the last 800 years or so, since the 12^{th}–13^{th} centuries. Ikehara[174)] found two turbidite layers, considered to be landslide deposits from the time of an earthquake, in submarine sediment cores collected from the Rishiri Trough, located to the west of Rebun Island off Hokkaido. Based on the results of age determination for the cores, the recurrence interval of the large earthquakes forming landslide deposits near the Rishiri Trough was estimated to be slightly over 3,000 years. Based on all the above findings, the recurrence interval of major earthquakes (of the size that causes submarine landslides) in northern Hokkaido is estimated to be about 800–3,000 years, a longer period than can be traced from the historical documents.

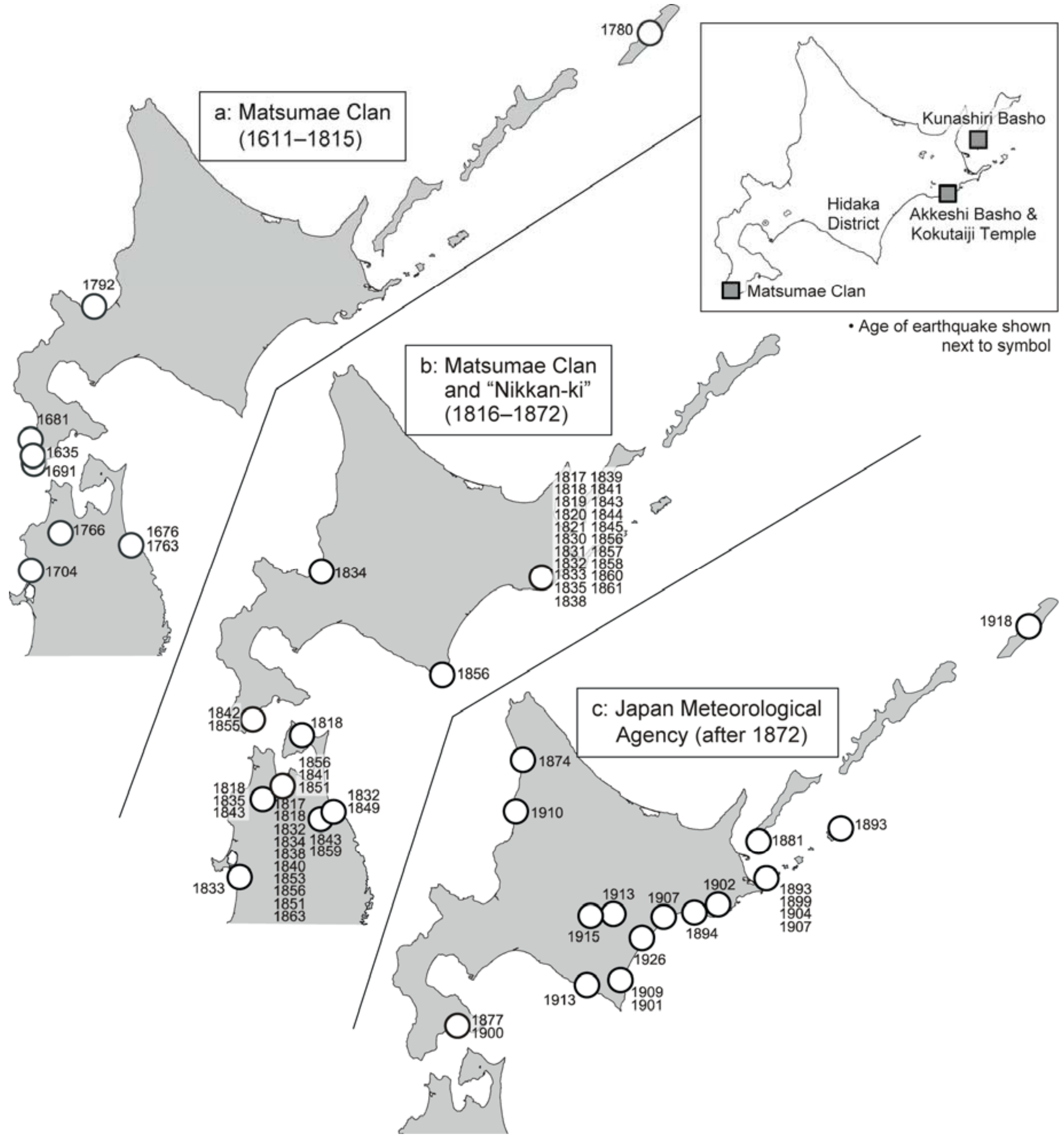

Figure 4.5.3-3 Historical records of earthquakes from the Ainu period to the present
Locations of “Basho” after Kono[175)]

Since the number of historical documents collected to date is limited and all of them are compilations made later, the distribution of the locations where earthquakes that could be recorded and the quake damage that would have been described in the source documents were not well understood. For example, in one of these secondary historical documents, “The New Chronology of Hokkaido History”[138)], original writings are summarised for the purpose of making a chronology and there are cases where the description of seismic ground motion and names of earthquake-affected area have been omitted (personal communication with Prof. M. Kobayashi, Hokusei Gakuen University). The distribution of locations where earthquakes and the quake damages were recorded would be essential information for estimating the magnitudes of the earthquakes and their hypocentres. Therefore, the descriptions in the original historical documents recording earthquake-related events should be checked and historical documents relating to earthquakes that occurred in the areas facing the Japan Sea should be collected.

ii) Active structures (active faults, folds and flexures)

In northern Hokkaido, the Sarobetsu Flexure Zone, the Horonobe Fault Zone and the Toikanbetsu Fault Zone are recognised as an active fault zone from west to east (Figure 4.5.3-4, right). The Sarobetsu Flexure Zone corresponds to the Teshio Fault Zone[23)] and the Sarobetsu Fault Zone[176)] in the existing literatures and the Horonobe Fault Zone is located to the north of the Horonobe Fault. In addition to these active faults, the Omagari Fault and the Horonobe Fault are present as a geological fault from west to east. In this chapter, geological faults are those faults that have no evidence of fault movement during the most resent geological period, especially during the Quaternary. For those active fault zones, the location of fault traces and the displacement and the age for the reference plane of displacement have been obtained based on interpretation of aerial photographs, reflection seismic surveys and borehole investigations[23),177)]. The Horonobe Fault Zone (the “Horonobe Fault Zone”[177)] and “Horonobe Fault”[22)] that were identified as an active fault together constitute the “Horonobe Fault Zone” in the definition here) extends over about 20 km with an NNW-SSE direction in the northern part of the Soya Hill and consists of two fault traces running in parallel a few hundred metres apart. The main fault is in the east side in the Horonobe Fault Zone. This has developed low fault-scarp uplifted eastern side of the fault and displaced the surface of the marine terrace. The southern half of the fault zone is a reverse fault with uplifted western side of the fault and diverging out from south to north. In addition, a graben-like lowland has formed between the reverse and the main faults. The Sarobetsu Flexure Zone, consisting of a number of faults with a length of about 10 km that extend in an NNW-SSE direction, is an active fault zone with total length of about 40 km, located at the margin of the Sarobetsu Lowland. It appears at the ground surface as a flexure, which causes displacement on hill slopes and marine terrace surfaces. The margin of the Sarobetsu Lowland is bounded by the flexure extending from north to south. The Toikanbetsu Fault Zone runs for about 20 km through the hills along the Toikanbetsu River, roughly from south to north. The southern half of the fault zone consists of a fault trace that diverges out from south to north and the northern half consists of a right-stepping fault trace. The fault causes a displacement of the terrace surface uplifting western side of the fault in most cases and results in low fault and flexure scarps[177)]. For the sea area, a submarine active structure map has been prepared based on the analysis of multi-channel seismic-reflection profiles, combining high resolution bathymetric maps and geological data such as the results of borehole investigations[178)]. According to the map, there are two submarine active fault systems in northern Hokkaido (Figure 4.5.3-4, left). The Wakkanai Fault System is a submarine active fault system that runs in the direction northwest to southeast and is considered to be a seaward extension of the land active structures. The Musashi Fault System runs from the Shakotan Peninsula to Musashi Bank and Rebun Island in an N-S direction.

It can be concluded that the distribution of active structures on land is concentrated at the geological boundary (the Toikanbetsu Fault Zone) such as between the Kamuikotan Belt and the Neogene sedimentary rocks and in a depositional area of Quaternary sediments (the Sarobetsu Flexure Zone) such as the Sarabetsu Formation. Those in the sea are unevenly distributed in the Japan Sea area (the Wakkanai and the Musashi Fault Systems).

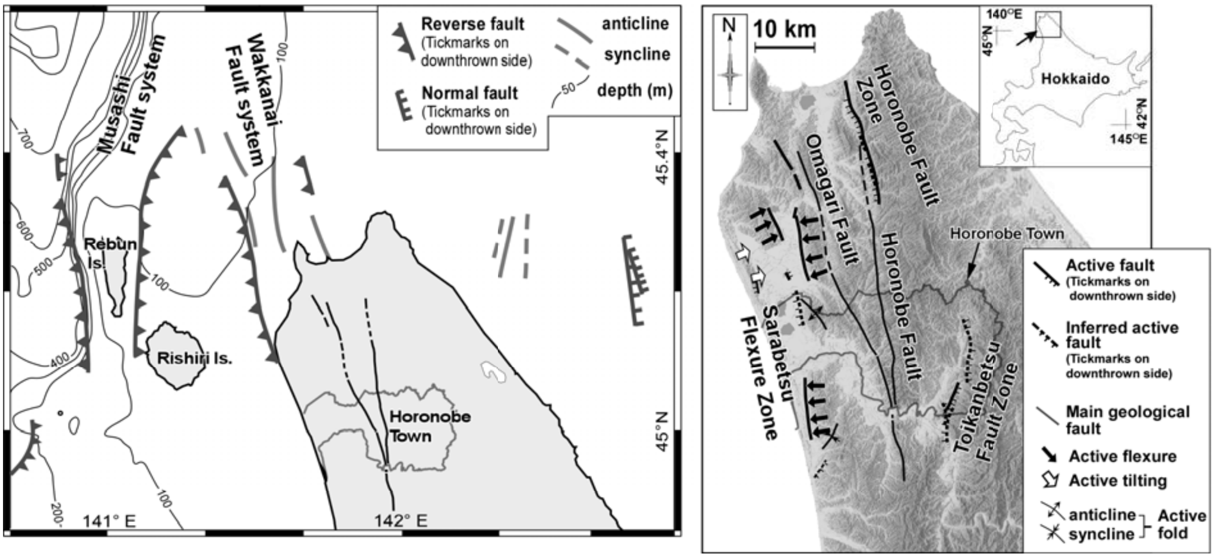

Figure 4.5.3-4 Distribution of active structures in and around the Horonobe area
Shaded relief map after GSI[179)]

iii) Regional tectonics

The basic framework for the neotectonics of Hokkaido and the surrounding sea area is formed by the interaction of the Okhotsk, the Amurian and the Pacific Plates (Figure 4.5.3-5a). There is an E-W compressive stress in the western half of Hokkaido, including the eastern margin of the Japan Sea, oblique subduction of the Pacific Plate and south-westward migration of the Kuril forearc sliver as a result of the oblique subduction of the Pacific Plate along the Kuril Trench.

Hokkaido and the surrounding sea areas can be divided into six tectonic provinces based on differences in the tectonics, the distribution and trend of geology and geological structures and their characteristics[180)] (Figure 4.5.3-5b):

- Province I is bounded by the Okushiri Ridge at the western edge and a series of uplifts connecting the Kabato Mountains and Rebun Island at the eastern edge. It includes the eastern margin of the Japan Sea, south-western Hokkaido and the Ishikari Depression. Its topography, geology and geological structure are mostly in an N-S direction and are seen as being a northward extension of the western part of the principal mountain ridge of the Tohoku District. This tectonic province basically is under the influence of an E-W compressive stress, but the south-western Hokkaido and the Ishikari Depression, which are considered to form the junction of the Northeast Japan arc and the Kuril Arc, are affected by the south-westward migration of the Kuril forearc sliver.
- Province II is directly affected by the subduction of the Pacific Plate and is constituted of a so-called accretionary prism.
- Province III is divided into four sub-provinces based on topographical and geological features:
  - III-1: continental slope of Kushiro – Nemuro offshore;
  - III-2: uplift zone of Kushiro – Nemuro pre-Neogene rocks;
  - III-3: a series of sedimentary basins between the forearc and backarc of the Kuril Arc, in order from the south;
  - III-4: the group of uplift and subsidence zone arranged like an arc and convex to the west, located to the west of the above three sub-provinces. This extends north to south, with mountains

and subsidence basins formed mainly at the end of the Caenozoic age with a convex configuration to the west (the Tokachi Plain, the Hidaka Mountains and the Umaoi Hill). Crustal movement is highly active in this province.

- Province IV is a volcanic arc, with high volcanic/geothermal activity, with volcanic uplift zones and a series of sedimentary basins in a right-handed en echelon arrangement. Provinces II, III and IV are tectonic provinces formed by the subduction of the Pacific Plate in the Kuril island arc – trench system and the south-westward movement of the Kuril forearc sliver related to the subducting plate (particularly in Province III-4). The distribution of the geology and geological structures of the provinces are in an ENE-WSW direction, except for Province III-4.
- Province V is assumed to be an active province and is an oblique collision zone at the plate boundary in the middle to late Miocene. However, crustal movement has been quiet since the Pliocene with very low seismicity as discussed later.
- Province VI covers the range from the Kamuikotan Belt to Teuri and Yagishiri Islands and then to Rebun Island. Crustal movement is active in this province, with subsidence areas and basins formed after the Quaternary, such as the Toikanbetsu Tectonic Basin and the Sarobetsu Lowland. Province VI, like Province I, is characterised by E-W compressive tectonics. Both provinces are considered to form part of the tectonic belt of the eastern margin of the Japan Sea[181),182)]. Horonobe area belongs to Province VI.

As described before, the tectonic belt thought to correspond to the boundary between the Okhotsk Plate and the Amurian Plate[181),182)] occurs at the eastern margin of the Japan Sea, west of the Horonobe area (Figure 4.5.3-5a). It is called “the tectonic belt of eastern margin of Japan Sea”. It is estimated that the tectonic belt formed about 2–3 Ma[128)], from the results of deep sea drilling at Okushiri Ridge and the stratigraphy obtained from reflection seismic profiles conducted in the area of the eastern margin of the Japan Sea. The fold structures developed in the western part of the Horonobe area belong to a part of the geological structures in a fold-and-thrust belt in the above tectonic belt. The folds were formed from east to west by the E-W compressive stress, based on the study of the focal mechanism of micro-earthquakes and the reflection seismic profiles described above[20)]. From the above findings, it is considered that, since the Late Pliocene, the Horonobe area has been in the tectonic setting of the E-W compressive stress field, the same as the current stress field.

In northern Hokkaido, where the Horonobe area is located, an uplift zone of the Mesozoic rocks with an N-S direction, including the Kamuikotan Belt, exists near the central area of northern Hokkaido and Caenozoic sedimentary basins are found on both sides of the uplift zone. The sedimentary basin in the west, where the total thickness of sediments from the Neogene to the present has reached up to 6,000 m, is called the Tenpoku Sedimentary Basin[183)]. This has a width of about 60 km and is divided into three tectonic provinces (east, middle and west) by the Omagari Fault and the Horonobe Fault, which are the main tectonic lines running roughly in an N-S direction (Figure 4.5.3-5c). These tectonic provinces correspond to the Tenpoku Coal Field area, the Wakkanai – east Toyotomi area and the Teshio Plain area[21)] respectively. In the east province, the pre-Upper Miocene formations occur as an en echelon folds and overlie the Cretaceous rocks. In the middle province, the uppermost part of the Middle Miocene formation to the lowermost part of the Pliocene formation are present and are folded in en echelon pattern. In the southern part of the middle province, asymmetric anticlines that are steep to the west and gentle to the east have developed. The western part of the Horonobe area is a latest sedimentary basin with a distribution of mainly the Pliocene – Quaternary formations and fold structures with a larger wavelength compared to the other tectonic provinces. The surface outcrop of the Palaeogene formations cannot be observed in this province, but it has been confirmed by deep boreholes drilled after 1970[61] that the Palaeogene formations are widely concealed subsurface in this area. As shown by the amount of subsidence during the Quaternary and the distribution of active structures and hypocentres, crustal movement can be considered to be most active in the western part of the Horonobe area[9] (Figures 4.5.3-1 and 4.5.3-4).

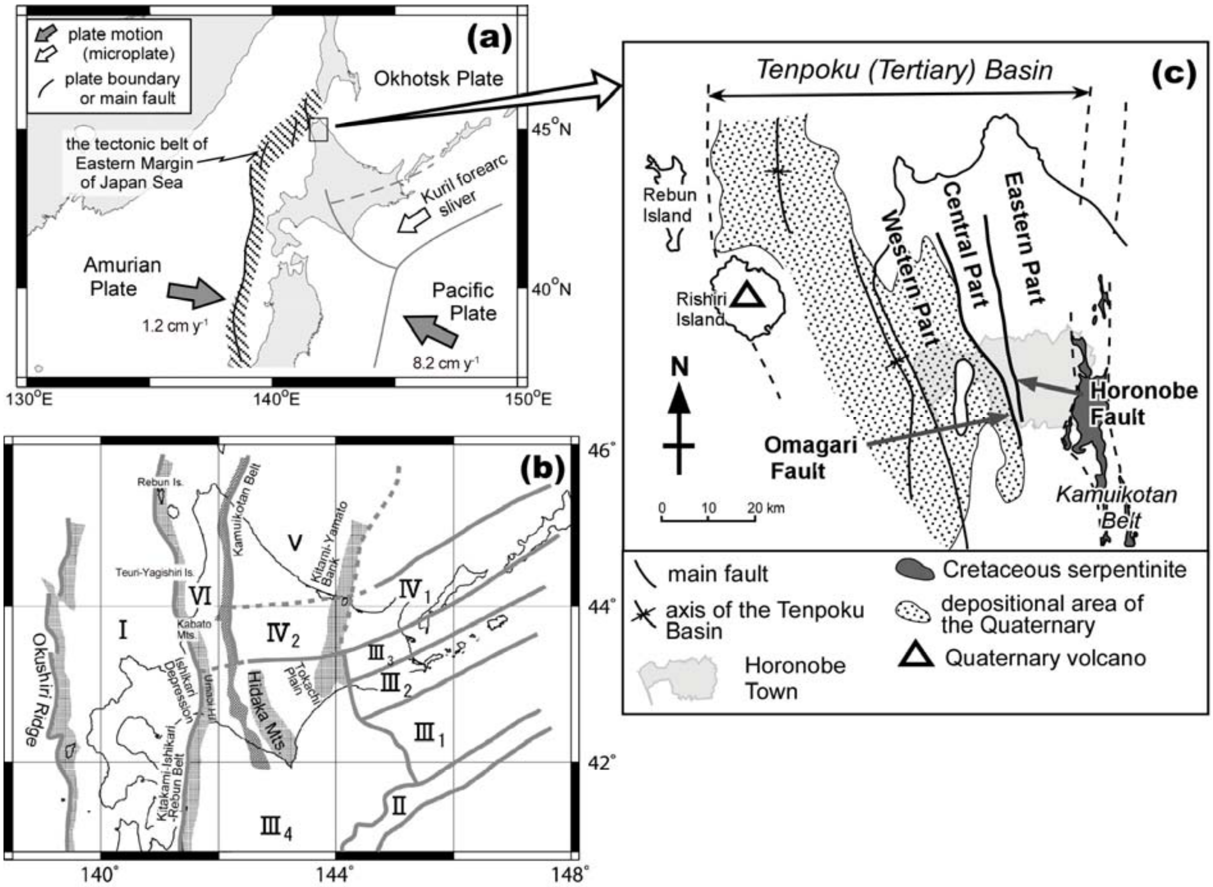

Figure 4.5.3-5 Current tectonic setting and tectonic division in and around Hokkaido
a: Distribution of plates after Taira[128], direction and rate of plate movement after Wei and Seno[184]
b: Tectonic division modified from Oka[180]; *c*: Tectonic province in northern Hokkaido modified from Oka[21]

iv) Volcanic and geothermal activity

The distribution of volcanic rocks in Hokkaido since the Neogene is summarised in Figure 4.5.3-6. Hirose and Nakagawa[185] divided Hokkaido into two provinces: central to eastern Hokkaido, i.e. the east side of the Ishikari depression which is considered to be the junction between the current Northeast Japan arc the Kuril Arc, and central to western Hokkaido, i.e. the west side of the depression. The temporal and spatial variation of volcanic activity in Hokkaido since the Neogene was discussed, based on large volumes of data from K-Ar dating and whole rock chemical compositions, as well as the style of volcanic activity such as volume, rate and mode of eruption and edifice shape in these areas. The correlation between tectonics and volcanic activity in and around Hokkaido was also studied. According to the results, the evolution of volcanic activity in central to eastern Hokkaido since the Miocene would have reflected changes in the tectonic setting of Hokkaido, such as the spreading of the back-arc basin (19–14 Ma; probably the Japan Sea Basin), the significant oblique subduction of the Pacific Plate (9–1.7 Ma) and the jump of the plate boundary.

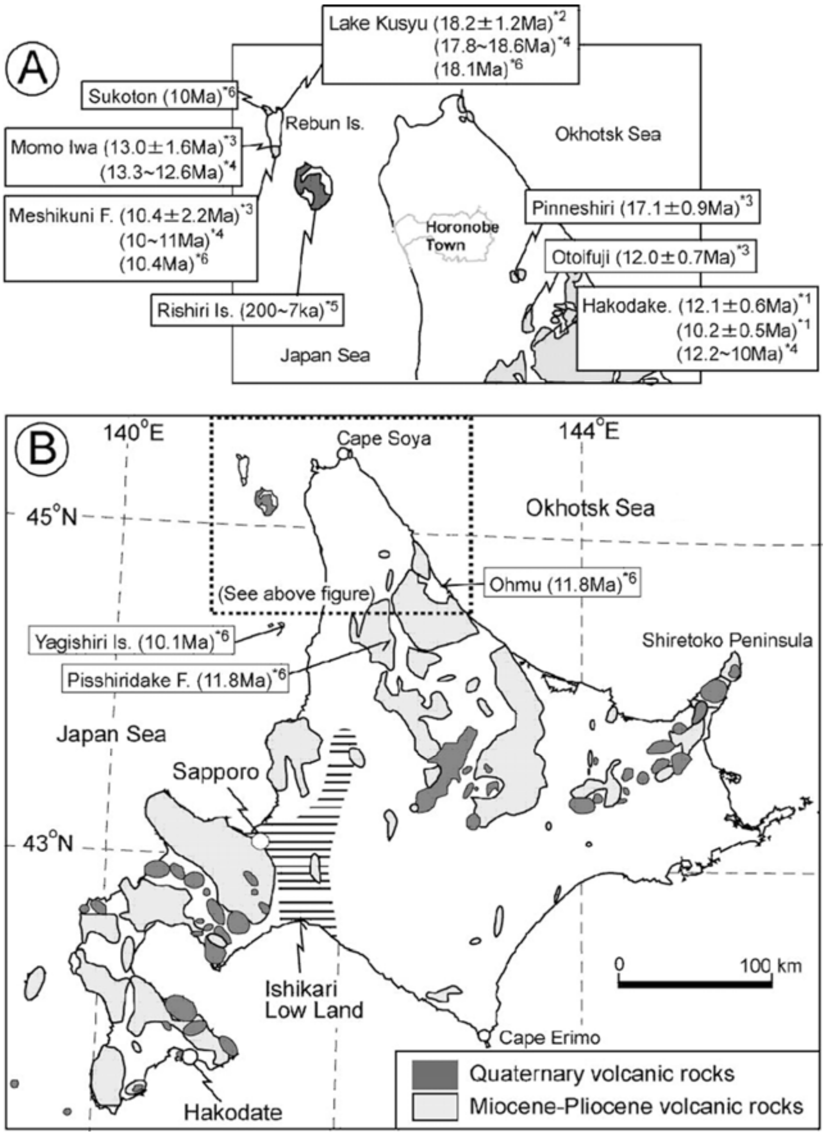

Figure 4.5.3-6 Distribution of Late Caenozoic volcanic rocks in Hokkaido

Simplified from Hirose et al.[186]; K-Ar ages from (*1) Watanabe and Yamaguchi[187], (*2) Goto and Wada[188], (*3) Goto et al.[189], (*4) Hirose and Nakagawa[185], (*5) Ishizuka[190] and (*6) Shuto et al.[191]

For the Rishiri volcano, the Quaternary volcano, which is located northwest of the Horonobe area, the mode of eruption, volume and rate of eruptions and the changes in lithology over time have been closely studied[190], together with a geological investigations of volcanic bodies, K-Ar dating of the major eruptive products and existing tephrochronological studies in northern Hokkaido[192]. According to these studies, the activity of the Rishiri volcano was presumed to have started abruptly around 200,000 years ago, with the most recent eruption a few thousand years ago. Since the temporal variations in both eruption rate and magmatic temperature of the volcano are consistent with a diapir model for a thermal source of magma generation, the eruptive history of the Rishiri volcano can be explained by the ascent and cooling of a single heat source (diaper). Northern Hokkaido, including the Rishiri volcano, is not considered to be a geological setting where the thermal source is constantly ascending, because there is no evidence of other volcanic activity such as fumarole activity in the last few thousand years and there are no Quaternary volcanoes around Rishiri volcano. This is supported by the fact that the geothermal gradient and the terrestrial heat flow in northern Hokkaido are lower than at the volcanic front area (this area extends from the Shiretoko Peninsula to the south side of Sapporo and reaches Hakodate)[193].

The hydrothermal activity and mineralisation in Hokkaido was summarised by Yahata[194]. According to this, there are over 400 hydrothermal metallic deposits formed in the Late Caenozoic and 50 hypothermal alteration zones including sulphur deposits and hydrothermal clay deposits. Those distributed over west Hokkaido, east Hokkaido and the northeast of central Hokkaido (Figure 4.5.3-7). Based on the K-Ar ages of hydrothermally altered mineral, categorisation was made on the modes of occurrence of ore deposit and stratigraphy of the host rocks, the stages of the hydrothermal activity and the mineralisation. Relationships between the characteristics of the hydrothermal activity and mineralisation in each stage and the tectonics around Hokkaido were then discussed. As a result, the hydrothermal activity and the mineralisation of Hokkaido can be categorised as follows: the formation of skarn deposits associated with igneous activity in the continental areas (west Hokkaido, late Early Miocene), the formation of Kuroko deposits, Kuroko-type deposits and bedded manganese deposits developed under the influence of the tectonics of the spreading system in the Japan Sea (north-west of Hokkaido, Middle Miocene) and the beginning of the formation of vein-type deposits (eastern part of central Hokkaido, Middle Miocene), hydrothermal activity and the formation of vein-type deposits on land developed under the influences of the E-W compressive stress field, regional uplift and associated igneous activity (west Hokkaido metallogenetic province and north-east Hokkaido metallogenetic province, Late Miocene) and the formation of magnetic pyrite (FeS) deposits and sulphur deposits in the area along the current volcanic front (Pliocene – Pleistocene). The study suggested that a close relationship between tectonics and hydrothermal activity in Hokkaido[194].

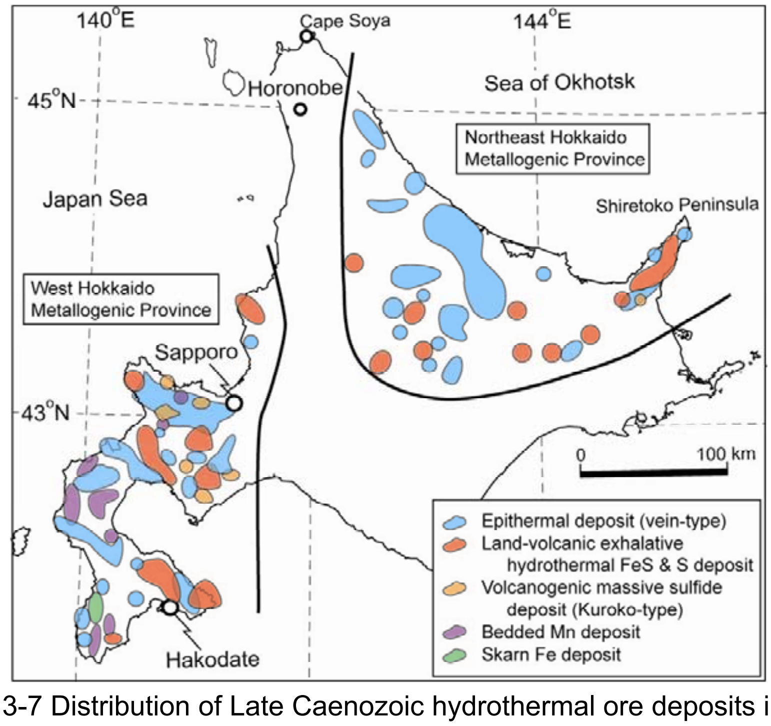

Figure 4.5.3-7 Distribution of Late Caenozoic hydrothermal ore deposits in Hokkaido
Simplified from Yahata[194]

According to existing information, as described above, the evolution of volcanic activity in Hokkaido in the Caenozoic age is closely related to the tectonics in and around Hokkaido. Hydrothermal activity and mineralisation associated with this type of volcanic activity have also evolved. This would indicate that, as long as current tectonics do not change in the future, the area currently showing high volcanic and hydrothermal activity (the Shiretoko Peninsula to the south of Sapporo to Hakodate) would not change significantly in the future. This suggests that the possibility of volcanic and hydrothermal activity would be low in northern Hokkaido in the future. However, the above perspective is based only on surveys of existing information and the possibility cannot be ruled out that the existing information may have ignored such small-scale or low temperature hydrothermal activity and mineralisation without any formation of ore deposits. Although the thermal structure of Japan can be overviewed based on existing data for geothermal gradient and terrestrial heat flow, the current situation is that there are insufficient data to determine more detailed thermal structure, for example when identifying areas where geothermal gradient is changing[195]. In the future, it will be necessary to improve information based on existing information by studying the possible existence of magma and high-temperature fluid in the deep subsurface of northern Hokkaido, using not only geological approaches but also geophysical methods[196] such as seismic wave tomography and the MT method, in conjunction with model calculations and simulations.

v) Palaeoclimate

Global climate changes can be reconstructed from changes in the oxygen isotope ratio of foraminiferal shells in deep-sea sediments[197]. The climate changes in the Quaternary are characterised by repeated cycles of glacial and interglacial periods. The cycles tend towards a colder climate during the Caenozoic era. The cycles during 2.5–1 Ma are different from those in the last 1 Ma and amplitude of the cycles is becoming larger. The principal cycle in the former period was about 40,000 years; in the latter it is about 100,000 years. The change in cycles was not sudden but gradual during the period from 1.2–0.7 Ma[197]. According to the climate change curve based on the change in the oxygen isotope ratio, the change from a temperate climate in the interglacial period to a cold climate in the glacial period progressed gradually during the era when the 100,000 year cycles were dominant, while the change to the temperate climate period was sharp. The current climate is considered to be in a stage slightly after the peak of the temperate climate in the interglacial period. The altitude above sea-level of the Sarobetsu Lowland, which occupies most of the western part of the Horonobe area, is about 2.5–3 m on average and is mostly below about 5 m. The area to the west of the Horonobe area is sea with a depth shallower than 100 m, extending about 30–45 km offshore in horizontal distance. For this reason, changes in the shoreline in the Horonobe area owing to sea-level change and associated spreading or receding of the land area are foreseen for the next 100,000 years and longer. When considering the palaeoclimate of the Horonobe area, important points are that the continental shelf extending to the west of the Horonobe area emerged extensively owing to lowering of the sea-level during the glacial period, the Horonobe area was an inland environment for most of the last glacial stage owing to the connection of the Soya Strait and Sakhalin by a land bridge[198] and the Japan Sea and the western part of the Okhotsk Sea were thought to be frozen during the winter season[7] in a glacial period.

The temporal variation of the palaeoenvironment in northern Hokkaido under the global climate changes described above was estimated from the types and distribution of fossil periglacial landforms formed in the glacial period and by reconstructing the vegetation based on pollen analyses.

In present-day northern Hokkaido, currently in the period slightly after the peak of the temperate climate of the interglacial period, there are woodlands consisting of sub-arctic trees (e.g. Sakhalin fir) and cool-temperate broad-leaf trees (e.g. Japanese oak), randomly mixed as single trees or as grove and forming ‘pan-mixed’ forest (mosaic-like mixed forest with broad-leafed and coniferous trees)[199]. From the results of reconstruction of the vegetation history in Hokkaido, the above forests are considered to have been developed over 5,000–8,000 years ago, at the beginning of the most temperate period of the Holocene[200]. However, the results of pollen analysis of boring cores obtained from Koetoinuma (pond) in Wakkanai City, that are considered to illustrate the evolution of the vegetation from about 8,000 years ago until recent times in northern Hokkaido, show that the appearance of forest consisting of Japanese oak as the principal variety was found in the upper part of the core sample[201]. The present climate of northern Hokkaido is thus concluded to have become developed later compared to other areas of Hokkaido.

The palaeoclimate of northern Hokkaido since the last glacial stage was estimated from the analysis of pollen sampled from the Kenbuchi Basin located south of the Horonobe area[202] (Figure 4.5.3-8). Based on the reconstructed vegetation history for the last 32,000 years or so, taiga consisting of Ezo spruce (*Picea jezoensis*) and Sakhalin spruce (*Picea glehnii*) as the main varieties together with Dahurian larch (*Larix gmelini*), which is comparable with the current vegetation in central Sakhalin, was prevalent 25,000–32,000 years ago. The Steppe with open Siberian dwarf pine (*Pinus pumila*) forest as the main varieties, which can be currently seen in the north of Sakhalin, would have been present 16,000–25,000 years ago, during the Last Glacial Maximum (LGM – the time of maximum spread of the ice sheets, coldest climate period, during the last glacial stage). A significant drop in the numbers of Dahurian larch and Siberian pine was seen 12,000–16,000 years ago during the interstadial period and the coldest climate period corresponding to the LGM returned 10,000–12,000 years ago. After this period, the temperature gradually became warmer and the current forests are presumed to have been developing about 8,000 years ago.

In northern Hokkaido, fossil periglacial landform in the glacial period is found[7]. Since the conditions are different for each periglacial phenomenon, the environment when the phenomenon was formed can be estimated from the combination of fossil periglacial phenomena. Miura and Hirakawa[203] re-examined the fossil periglacial wedges in particular and reconstructed the permafrost environment at the time of occurrence of the periglacial wedges. According to their results, during the last glacial stage the area extending from the Okhotsk Coastal Plain to the Konsen Plain formed the southern limit of the continuous permafrost zone with an average annual air temperature of -7°C between 12,000 and 42,000 years ago. The Tokachi Plain and the north area facing the Japan Sea had discontinuous permafrost conditions with an air temperature range of -7 – -3°C. The annual temperature range was large and winters were very cold. The southern limit of the discontinuous permafrost is more or less consistent with that of the open forests consisting of Dahurian larch and Siberian pine during the LGM (Figure 4.5.3-8).

As outlined above, the palaeoenvironment of northern Hokkaido during the glacial period was quite different from the current environment and is estimated to have been similar to that of present-day northern Sakhalin. Given that climate change is periodical, there is a high chance that the vegetation as reconstructed above will be repeated in the future. However, since vegetation changes depend on altitude, precipitation and distance from the shoreline, the estimation of the palaeoenvironment in the Kenbuchi Basin and Koetoinuma of Wakkanai City would not necessarily be applicable to other areas of northern Hokkaido. On the other hand, once past vegetation has been reconstructed, not only the temperature but also the precipitation in the past can be determined to some extent by comparing the reconstruction with vegetation currently found on earth. Since precipitation and vegetation are important parameters for the estimation of the recharge volume in the future, it is important to reconstruct the vegetation by analysing pollen samples obtained from the Horonobe area and also to reconstruct the palaeoenvironment, including temperature and precipitation.

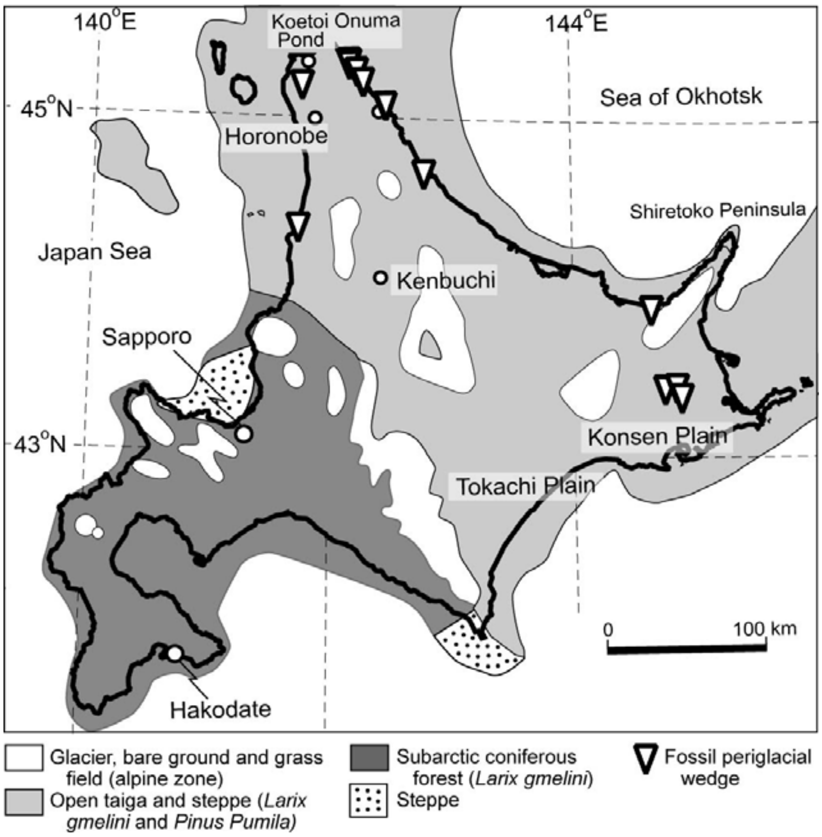

Figure 4.5.3-8 Vegetation during the Last Glacial Maximum in Hokkaido with location of the fossil periglacial wedge

Vegetation after Igarashi[200]; Fossil periglacial wedge after Miura and Hirakawa[203]

(2) Study covering the Horonobe area and the western sea area

1) Investigations based on existing information

i) Uplift rate

The uplift rate calculated based on the marine terraces in the western part of the Horonobe area is shown in Figure 4.5.3-9. The estimations of the uplift rate showed a maximum difference of about a factor of two owing to differences in the MIS correlation of the marine terraces in the existing literature[7),130)]; the uplift rate estimated based on MIS 7 was about 0.29–0.34 m ky^{-1} by Koike and Machida[130)] whereas it was about 0.16–0.26 m ky^{-1} according to Koaze et al.[7)] The uplift rate near the Sarobetsu Anticline (the area surrounded by the dashed line in Figure 4.5.2-4), an active fold, was estimated to be larger than that for the surrounding area, based on the MIS correlation by Koike and Machida[130)]. Taking MIS 5e as an example, it is about 0.60 m ky^{-1} at the anticlinal axis and about 0.48 m ky^{-1} at the fold limb. This indicates local uplift at the anticlinal axis owing to the activity of the Sarobetsu Anticline[9)]. The Sarobetsu Anticline plunges forward more or less north-west. In this case, the altitudes of the marine terraces classified as being of the same MIS stage would show a trend of being lowered towards the north in a direction perpendicular to the fold axis. However, this trend was not observed for the Sarobetsu Anticline. When considering the plunging of the fold axis, the influence of local uplift at the anticlinal axis was even larger.

MIS correlations of marine terraces are important for investigation using marine terraces. Depending on the correlation, the estimations of uplift rates and of the former shoreline vary greatly. For example, Koike and Machida[130] estimated the formative age of the marine terrace surfaces from age of the tephra covering the surface of the marine terrace exposed at Keihoku in Wakkanai City and extended the MIS correlation to the marine terrace in the Horonobe area, based on the geomorphic features of the terrace surface; Koaze et al.[7], on the other hand, extended the MIS correlations for the marine terrace surface of MIS 5e to the Horonobe area based on stratigraphical and geomorphic features such as the tephra stratigraphy constructed in the Tomamae – Haboro area (Figure 4.1.2-1) and the dissection ratio of the marine terrace surfaces. In neither of the above cases is the formative age of the marine terraces obtained by undertaking field surveys in the Horonobe area. The formative age of the marine terrace surfaces in the area should therefore be clarified by field surveys and the MIS correlation in and around the Horonobe area should be improved using the marine terrace surface whose formative age has been clearly defined. Precise age-determination and MIS correlation of marine terrace surfaces by field investigation should be carried out at the base for high resolution estimates of uplift rate and more detail examination of the time and spatial distribution of the uplift rate. When estimating the spatial distribution of uplift and uplift rate, it is important to consider the active structures in the area, as derived from the case of the Sarobetsu Anticline.

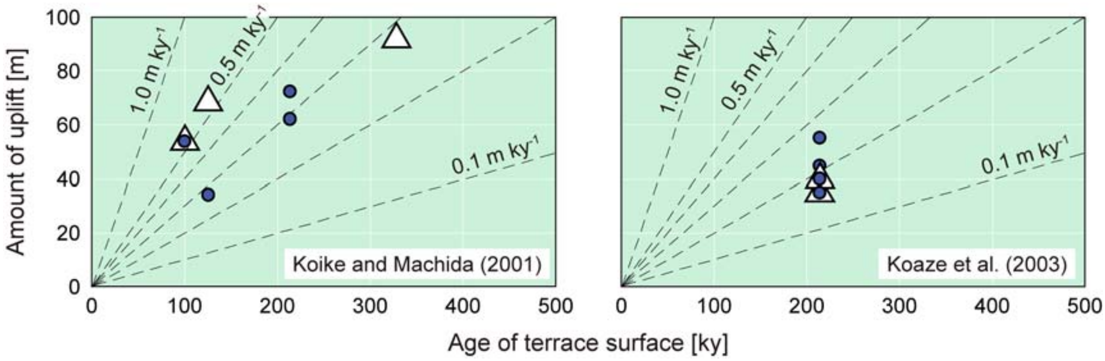

Figure 4.5.3-9 Plot of uplift versus time for a sequence of marine terrace surfaces
Open triangles for marine terrace surfaces at the Sarobetsu Anticline shown in Figure 4.5.2-4

ii) Current topography

It has often been pointed out that the topography and the drainage systems at the Soya Hill and the northern Teshio Mountains (Figure 4.1.2-1), where the Horonobe area is located, are related to the penetration pattern of valleys that reflects geological structures and lithologies[7]. When considering the overall pattern of the drainage system for the northern half of the Soya Hill, the consequent valleys (valleys formed along the fall line of the ground surface) extending E-W from the ridgeline of the hill aligned in an N-S direction and the subsequent valleys (valley with flow paths adapted to the geological structure) in an N-S direction along the strikes of the stratum, form a reticular pattern. At a detailed level, the patterns of the drainage system vary depending on the stratum; parallel or sub-parallel and the geomorphic quantity, for example, the drainage density also varies[7]. Existing information[204] also explains differences in the hills morphology based on differences in the combination of physical properties of the rock, i.e. the physical strength and the hydraulic conductivity (or infiltration capacity), by comparing data on the physical properties of each stratum and on geomorphology.

The above facts illustrate that the geomorphological processes in the Horonobe area developed under rock control. Hence during the surface-based investigations, data on the geomorphology and the physical properties of the rock need to be acquired for each stratum; for simulating the future evolution of the topography in the Horonobe area based on the obtained data, a programme that will use different parameters for each stratum should be applied.

2) Surface-based investigations

i) Seismicity

The distribution of hypocentres calculated using 'hypomh' and multiplet clustering (MC) techniques and focal mechanisms are shown in Figure 4.5.3-10. The spatial variation for hypocentres is large in the analysis utilising 'hypomh' since the error in determining the hypocentres is large. In contrast, in the MC analysis, some concentrations of hypocentres were observed because the accuracy in determining the relative positions of hypocentres and hypocentre clusters is considered to be better than 'hypomh' analysis, i.e. the average value for RMS in each multiplet group is as small as 0.09–0.16 s. In particular, there are concentrations of hypocentres in zones A and B as shown in Figure 4.5.3-10. From the results of the MC analysis, it can be seen that hypocentres become deeper toward the west and the distribution is close to the N-S or NNE-SSW direction. This direction is consistent with the N-S trending geological structures of the near surface in northern Hokkaido.

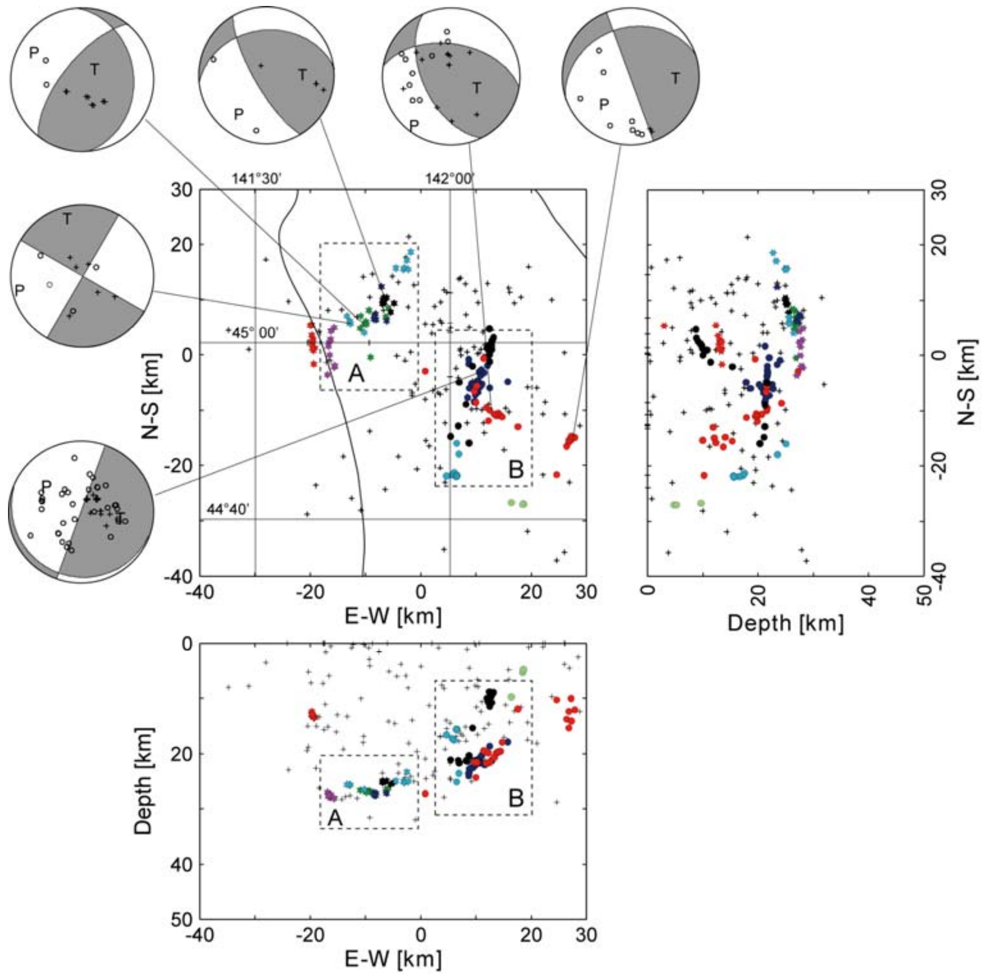

Figure 4.5.3-10 Hypocentre distribution relocated by 'hypomh' (cross) and MC analysis (colour solid circle and hexagon) and focal mechanisms (top-left)

Origins of the coordinates of figures for the Kamihoronobe seismic station shown in Figure 4.5.2-5

Areas denoted A and B in the top-left figure corresponding to those in the lower-left figure

Differences in plot symbol and colour representing different groups of multiplets

Focal mechanisms were also estimated based on data on first motion polarity of the P-wave in this analysis, assuming the hypocentre forces to be a double-couple. FP FIT[205] was used for the analysis. According to these results, reverse type and lateral type faults were in the majority and the area is assumed to be in a horizontal and compressive stress field, although variability in the direction of the P axis was observed.

As described above, the boundary of the North American (Okhotsk) Plate and the Eurasian (Amurian) Plate is assumed to be at the eastern margin of the Japan Sea located to the west of northern Hokkaido[206]. This assumption is based on the distribution of the high-seismicity zone and active structures extending from N-S to NNE-SSW, the direction of the slip vectors of earthquakes, and recent data on crustal movement obtained with GPS. However, this plate boundary is hard to represent as a single line and it may be more realistic to assume multiple boundaries in the wider mobile belt, including the old plate boundary in Hokkaido. Ohtake[207] pointed out that the above plate boundary should not be interpreted as a simple subduction zone but as a collision boundary where various fault activities may occur depending on local conditions. This is based on the fact that the fault plane of the Hokkaido Nanseioki Earthquake (M 7.8) in 1993, which occurred in the above mobile belt, was complex in configuration; dipping east in the northern part and west in the southern part.

The hypocentre of the micro-earthquake cluster in the Horonobe area is thus distributed in an N-S or NNE-SSW direction under a horizontal compressive stress field, but directions for the P axis and the fault planes are assumed to vary widely, reflecting the complex structure at the eastern margin of the Japan Sea.

Since the data used in this analysis were obtained over a short time period of slightly less than three years, the number of events identified as multiplets was very small and the certainty of the results cannot be fully guaranteed. For example, Moriya et al.[208] identified multiplets for 5,000 or more earthquakes and studied the relationship between the distribution of hypocentres and the subsurface structures based on a large number of multiplet data. Together with the accumulation of seismic observation data, determination of hypocentres based on the data obtained and a study of the relationships between seismicity and subsurface structures will be required in the future.

With regard to the influence of earthquakes on groundwater pressure, changes in the pressure before and after the occurrence of the 2003 Tokachioki earthquake were investigated. According to data on groundwater pressure obtained over 10 days before and after the earthquake (Figure 4.5.3-11), the pressure increased four days before the earthquake, decreased during the period from two days before the occurrence and increased again immediately after the earthquake in three monitoring intervals of borehole HDB-1. Altogether, the change was around 1 kPa. The significant change immediately after the occurrence of the earthquake was due to electrical noise caused by a power cut.

There are some case studies on the change in groundwater level immediately after earthquakes in Hokkaido. For the case study[209] targeting major earthquakes of more than M 7.5 that occurred in and around Hokkaido during the period 1993–1994, assuming the volumetric strain on the crust owing to the earthquake and seismic motion to be two factors, theoretical studies were conducted for a model where the change in water level was influenced only by the volumetric strain, a model that was influenced only by seismic motion and a model combining the two factors. The extent of the change in groundwater level immediately after the earthquakes that were reported in various locations in Hokkaido could be explained consistently by the regional crustal strain caused by the fault movement as a whole. The response sensitivity was estimated as 1.6–19.6 mm per 10^{-8} strain. In the study of the 2003 Tokachioki earthquake[210], the distribution of theoretical volumetric strain in Hokkaido was calculated using the source fault model and the correlation between groundwater level and artesian flow volume immediately after the earthquake was investigated. The theoretical volumetric strain near the Horonobe area caused by the 2003 Tokachioki earthquake was about 10^{-7} and the response sensitivity of the water level against strain was estimated as 1.5–17.9 mm per 10^{-8} strain[210]. According to these calculations, a variation in groundwater level of about 1–10 cm might have been observed in the Horonobe area before and after the earthquake in 2003 had measurements been made.

The changes in groundwater pressure seen before and after 26th September 2003 might be due to the earthquake. However, similar changes in groundwater pressure were also observed at times other than when earthquakes occurred (Figure 4.5.3-11, data obtained on 2nd October 2003). The data on groundwater level have to be compared with diurnal changes due to tides and precipitation and data collection and analysis should be continued in the future.

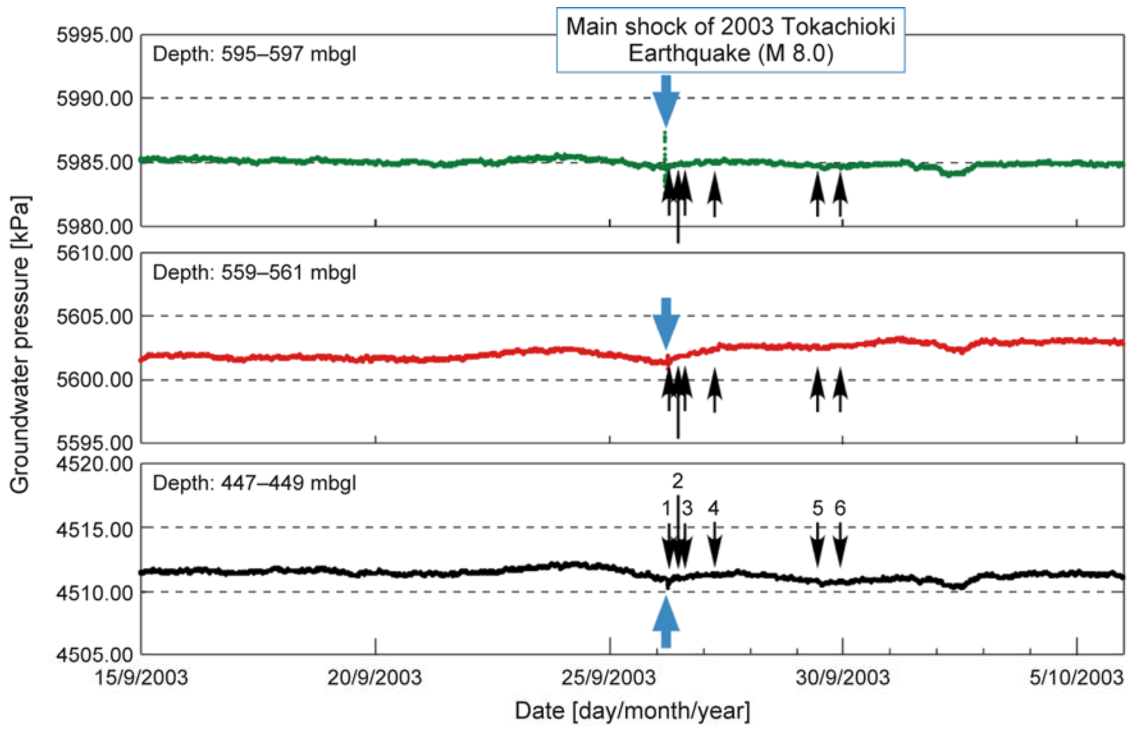

2003 Tokachioki Earthquake		Magnitude	Origin time [hour:minute:second]	[day/month/year]
Main shock		8.0	4:50:11	26/9/2003
Aftershock	1	7.4	6:08:03	26/9/2003
	2	6.1	11:35:14	26/9/2003
	3	6.3	15:26:55	26/9/2003
	4	6.2	5:38:23	27/9/2003
	5	6.5	11:36:55	29/9/2003
	6	6.0	23:22:13	29/9/2003

Figure 4.5.3-11 Variation with time in groundwater pressure observed in borehole HDB-1 before and after 2003 Tokachioki earthquake during 15th September to 6th October 2003

Earthquake data from National Research Institute for Earth Science and Disaster Prevention[141]

ii) Regional tectonics

The amount of horizontal shortening and the horizontal strain rate around the Horonobe area were estimated by a geodetic method using GPS observation data and triangular survey data and by a geological method using active tectonics data and geological cross-sections. The estimate for the strain rate in the area was 10^{-8}–10^{-7} y^{-1} with the geodetic method and 10^{-9}–10^{-8} y^{-1} with the geological method. The values obtained using the two methods were similar; the strain rate from the geological method was smaller than that from the geodetic method by a maximum of a factor of 10 (Figure 4.5.3-12).

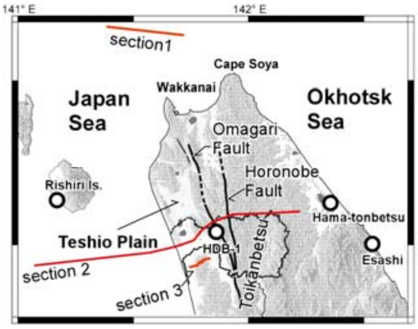

Method	Horizontal strain rate [y^{-1}]		Before 2003 Tokachi earthquake	After 2003 Tokachi earthquake
GPS	10^{-8}–10^{-7}	HDB-1–Rishiri	-1.02×10^{-7}	-6.14×10^{-8}
		HDB-1–Hamatonbetsu	7.94×10^{-8}	-1.55×10^{-7}
		HDB-1–Esashi	1.63×10^{-7}	-1.32×10^{-7}
Triangulation	10^{-8}–10^{-7}	Northern Hokkaido	-1.5×10^{-7}	scale error: 5.0×10^{-6}
Active fault	10^{-9}–10^{-8}	Horonobe area	-7.0×10^{-9} – -1.0×10^{-8}	
Geological cross section	10^{-9}–10^{-8}	Section 1	-7.81 – -8.12×10^{-9}	
		Section 2	-2.29 – -2.43×10^{-8}	
		Section 3	-4.00 – -4.15×10^{-8}	

Figure 4.5.3-12 Estimation of horizontal crustal strain rate using different methods

Shaded relief map after GSI[179)]

It is generally the case that estimates using the geological method based on data on active faults and historical earthquakes tend to be smaller than those obtained by the geodetic method by a factor of around 10. Sagiya et al.[148)] argued that such differences were due to the fact that the strain rates estimated by the geodetic method were influenced by local strains, while those estimated by the geological method reflected the long-term plastic strain in the crust. They also pointed out that the short-term strain contains after-shock motion[148)]. In fact, changes in both the trend and the rate of crustal movement were seen before and after the occurrence of the 2003 Tokachioki earthquake, based on the analytical results for crustal movement using GPS data (Figure 4.5.3-13). In addition, a large number of fault and fold structures forming the fold-and-thrust belt can be seen in the geological cross-sections (Figure 4.5.3-14) and the calculated results for the horizontal crustal strain rate using the geological cross-section reflect the plastic strain of the crust.

The period of after-shock motion (2–3 years or over 10 years[155)]) and the period of geodetic observations (several years to around 100 years) are clearly shorter compared to the recurrence interval of major earthquakes with magnitudes over eight around Hokkaido (500–1,000 years[211)]). This means that the GPS data for about three years and the data from triangular surveys around 100 years in the Horonobe area are highly likely to have been influenced by cyclical movements that occur in longer cycles than the observation period used in the geodetic method.

From the viewpoint of the long-term stability of the geological environment, the trend of the crustal movement and the horizontal crustal strain rate should therefore be obtained using the geological method that covers duration of more than several tens of thousands of years. Active fault data obtained using the geological method and the calculated results for strain rate using the geological cross-section would be most suitable for the construction of the restored geological cross-section discussed below.

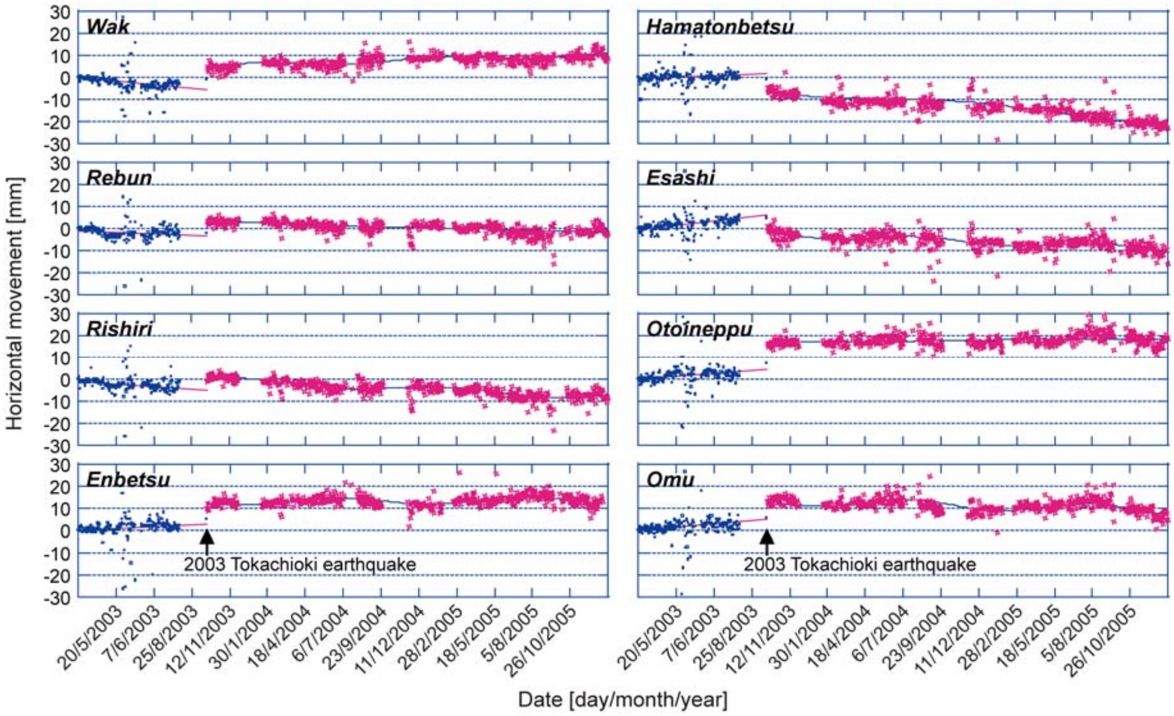

Figure 4.5.3-13 Variation with time in baseline length during 1st January 2003 to 13th January 2006

Location of station shown in Figure 4.5.2-6

Blue square and pink star for baseline lengths before and after 2003 Tokachioki earthquake respectively

Pink straight line and blue sinusoidal curve fitted by the least squares method

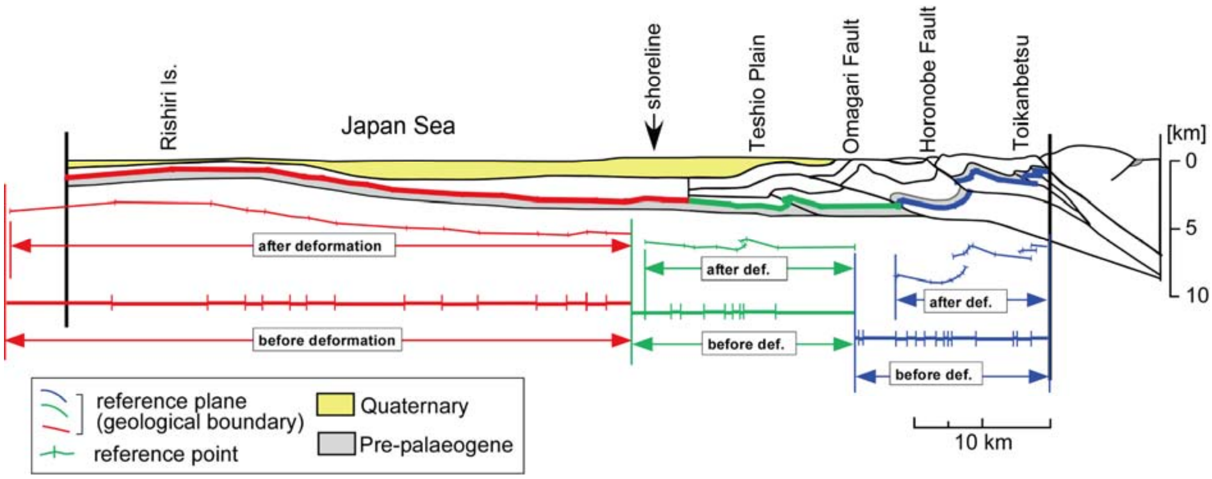

Figure 4.5.3-14 Estimation of horizontal crustal strain rate at Section 2 shown in Figure 4.5.3-12 using the geological cross-section method

Partly modified from Kato and Sato[212)]

The restored geological cross-sections for the last 2.5 million years, prepared by integrating existing information and the results in Section 4.1, is shown in Figure 4.5.3-15. It can be seen from this figure that the Tenpoku Sedimentary Basin located to the east of Rishiri Island has gradually been deepening on a scale of a million years, geological structures of the fold-and-thrust belt has been formed from the east and faults and folds tend to develop on the west side of the cross-sectional area, although these are relatively small in scale. This would indicate that the sedimentary basin has tended to narrow from both the east and west sides, centred on the west of the Horonobe area. In particular, the shortening on the east side is significant. This could be related to the westward migration of the depositional area since the Pliocene in the Horonobe area[27)].

The restored geological cross-sections for the last 2.5 million years were used as input for evaluating the temporal variation of groundwater flow conditions (see Subsection 4.2.4). However, there are factors that have not been taken into account in the cross-section; these include the temporal variation in thickness of formations owing to the consolidation of the stratum by sedimentation and burial diagenesis and to the deformation by E-W compressive stress, In addition, it included balancing the formations before and after deformation and the geometric restriction regarding the formation of fault/fold structures. Moreover, there is a limitation in the sense that the past geological cross-section cannot be restored as accurately as the current cross-section. Therefore, both the current and the past geological cross-sections may have to be treated as conceptual, even though consistency with the investigation results in Phase I (i.e. the geological model in Section 4.1) was taken into account.

The restored geological cross-sections will be revised in the future taking into consideration the temporal variation of the thickness of the formations on balanced cross-sections, based on data obtained with progress of the investigations, in order to make the cross-section more realistic. It should be noted that such cross-sections represents the best-possible approximations of the geological structures that actually existed. For the revision of the cross-sections, it would be of importance to show the premise and data uncertainty and to include the most up-to-date results[213)] of investigations by external research institutes, such as universities.

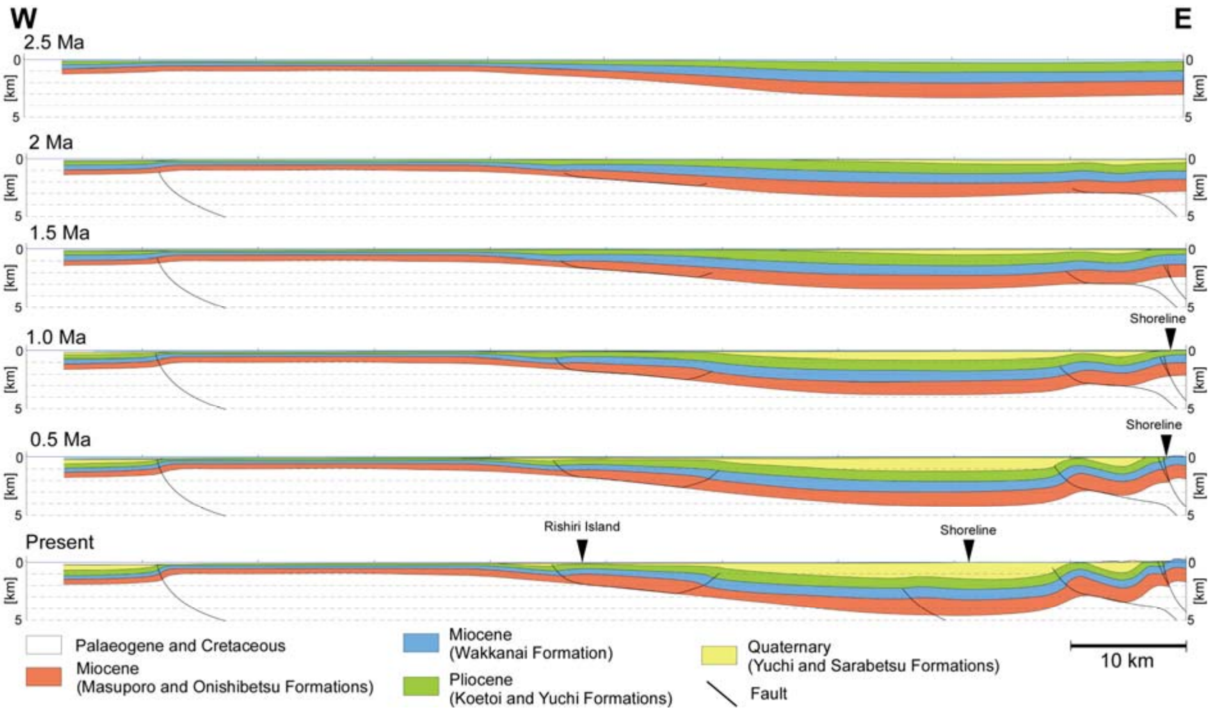

Figure 4.5.3-15 Conceptual reconstruction at the geological cross-section in the Horonobe area

Cross-section along the red line shown in Figure 4.5.2-7

iii) Estimation of uplift and uplift rate

The deposits of the marine terraces in the Shimonuma district of Horonobe Town are about 5 m in thickness and alternating beds of medium- to coarse-grained sandstone and sandy gravelstone. The loess distributed above these is 2 m in thickness and consists of red loess, whitish to pale brown loess, grey tephra and brown loess in ascending order (Figure 4.5.3-16). The terrace deposits contain fragments of volcanic glass, orthopyroxene and amphibole, but it was difficult to identify the key tephra beds because the refractive index of the orthopyroxene and the chemical composition of major elements for the volcanic glass are very variable. On the other hand some tephra was identified in the loess covering the terrace deposits. Two horizons were identified in the red loess, based on the content of heavy minerals such as olivine; three horizons were identified in the whitish to pale brown loess covering the red loess, based on the content of bubble-type volcanic glass and the refractive index of the volcanic glass and the orthopyroxene. Based on these observation and on the results of the EPMA analysis for the volcanic glass contained in the above tephra horizon, the whitish to pale brown loess was inferred to include Kutcharo – Haboro tephra (Kc-Hb; 115–120 ka[214]), Rishiri – Acharu tephra and Shikotu-1 tephra (Spfa-1; 40–45 ka[214]) in ascending order. Since the grey coarse-grained tephra covering the whitish to pale brown loess which is composed mostly of lapilli with about 2 mm in diameter contains a large amount of olivine, it can be correlated to the Rishiri – Hotoku tephra (Rs-Ho; the Latest Pleistocene[192]). The ^{14}C age of charcoal in the brown loess covering the grey tephra was 12,490 ± 60 y BP. Therefore, the whitish to pale brown loess was considered to have been deposited after MIS 5e (about 125,000 years ago).

The red loess, with a thickness of about 1 m, lies below the whitish to pale brown loess. The rate of deposition of aeolian dust in Japan is calculated as 13.5–22.9 mm per 1,000 years for the last glacial stage and 3.6–7.1 mm per 1,000 years for the present (post-glacial period), based on the thickness and the depositional age of loess in the palaeo sand dunes developed along the coastal area of the Japan Sea[215]. Therefore, red loess with thickness of about 1 m is considered to have been deposited over a period of around 100,000 years. Taking into consideration the depositional period for the red loess, the formative age of the marine terrace of interest for the investigations is most likely to be MIS 7 (about 214,000 years ago).

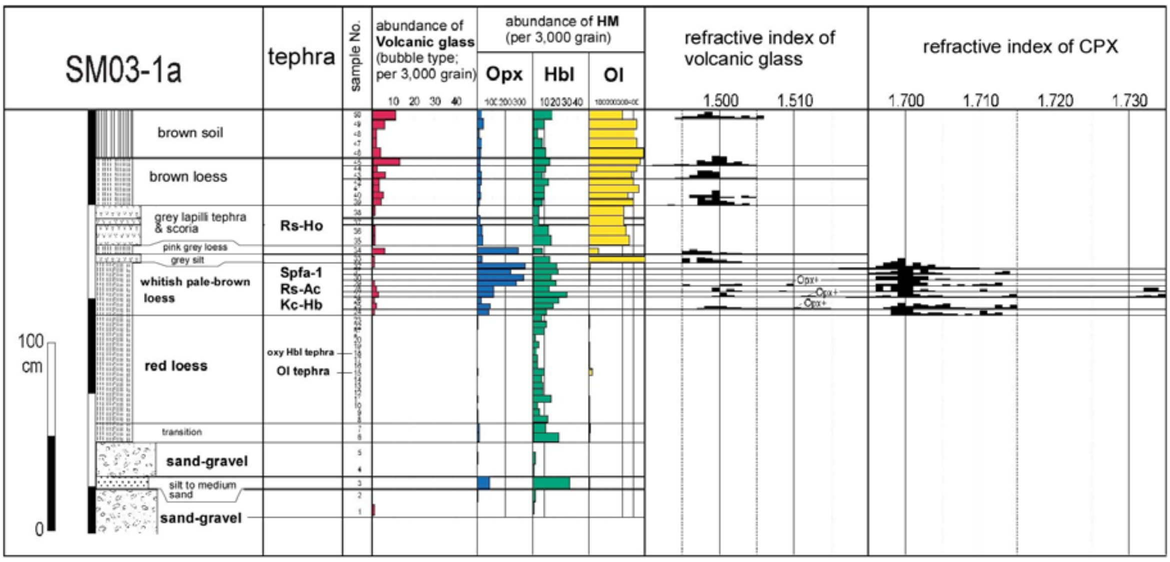

Figure 4.5.3-16 Lithostratigraphical section and histograms showing the refractive indices of constituent minerals and volcanic glass

Location of SM03-1a shown in Figure 4.5.3-17

Uplift rate (vertical crustal movement) was calculated by re-correlating the MIS stages of the marine terraces distributed around the Sarobetsu Anticline in the western part of the Horonobe area; taking into consideration the formation age of the above marine terrace, the current altitude and the eustatic changes in sea-level, the resulting uplift rate is about 0.3 m ky^{-1} (Figure 4.5.3-17).

The formation ages of the marine terraces in the Horonobe area could not be determined in the Phase I investigations except for the Shimonuma district, but could be determined by a combination of geomorphological methods, RIPL methods and dating techniques. The distribution of the marine terraces, their formation age based on the MIS correlation and uplift rates calculated using these methods will represent basic input for the construction of a restored geological cross-section as discussed previously; the restoration of the palaeogeography will be discussed in the next section.

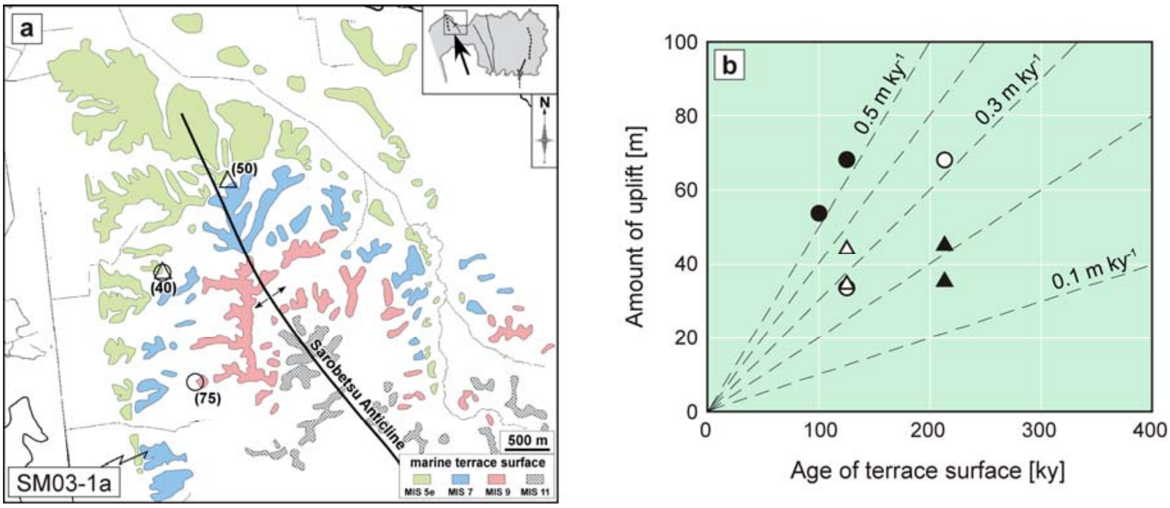

Figure 4.5.3-17 Uplift rate for marine terrace surfaces around the Sarobetsu Anticline

a: Geomorphic map (see Figure 4.5.2-4 for location); *b*: Plot of uplift versus time

Solid circles for estimation by Koike and Machida[130]; Solid triangles for estimation by Koaze et al.[7]

Open circles and triangles from the results of this study

iv) Palaeogeography

The assemblages of fossil diatoms sampled from the upper Koetoi Formation at the western limb of the Sarobetsu Anticline in the western part of the Horonobe area could be clearly correlated with the *Neodenticula koizumii* Zone (Late Pliocene diatom zone)[27]. The assemblage contains fossil diatoms of *N. seminae*, whose first appearance age is about 2.4 Ma. FT age of zircons included in volcanic ash from the upper Koetoi Formation is 2.3 ± 0.1 Ma[27]. This indicates a clear distribution of a late Pliocene diatom zone in the upper Koetoi Formation and the FT age of the volcanic ash is consistent with this zone[27]. These results show the depositional age of the upper Koetoi Formation in the western part of the Horonobe area was confirmed to be about 2.3 Ma. Comparing the depositional age with that of the Koetoi and Yuchi Formations in the eastern part of the Horonobe area[159], there is at least one million years difference in the depositional age between locations in the east and the west with a separation of slightly more than 10 km; the western area is obviously younger than the eastern area (Figure 4.5.3-18). The same trend was also observed near the boundary between the Yuchi Formation and the overlying Sarabetsu Formation; the age of the boundary in the eastern part of the Horonobe area (the Toikanbetsu district) is about 2.4 Ma and that in the western part of the area is about 1.3 Ma[216]. These results could be explained by the fact that the area of maximum deposition (depocentre) in the area migrated towards the west after the Pliocene. This westwards migration of the depocentre is assumed to be largely related to tectonic movements such as faulting and folding, considering that the eastern edge of the depositional area in both the eastern and western areas of Horonobe is bounded by faults and folds. The longitudinal axis of each depositional area zone is coincident with general trend of the geological structures in the Horonobe area, i.e. in the direction of NNW-SSE, and the strain of the stratum is smaller towards the west.

Based on the results of investigations on the gravel compositions of the Sarabetsu Formation in the western part of the Horonobe area, a conglomerate layer containing the Tertiary was found in the formation. The present location of the Soya Hill, where Tertiary sedimentary rocks are widely distributed, was considered to have been at a reasonably high altitude during the depositional period of the Sarabetsu Formation.

From the analytical results of fossil diatoms, it was found that Miocene fossil diatoms of the Masuporo Formation significantly occurs as derived fossil in the Yuchi Formation and that *Neodenticula Kamtschatica*[217)] abundant in the Koetoi Formation is present in significant amounts as a resedimented fossil in the Sarabetsu Formation (Figure 4.7.2-5). The presence of resedimented diatoms is considered to demonstrate a denudative environment during the time of deposition. The area around the western edge of the Soya Hill was thus considered to have been a denudative environment in the latter half of the Late Pliocene considering the abundance of extinct species in the Miocene occurring as resedimented fossils in the Yuchi Formation, the depositional ages of the Yuchi and the Sarabetsu Formations, the distribution of the Masuporo and Koetoi Formations and the frequency of occurrence of resedimented fossil diatoms. Both eastern and western parts of the Soya Hill were considered to have been in the denudative environment since the latter half of the Early Pleistocene when *N. Kamtschatica* was extremely abundant.

As a result of the sedimentary facies analysis of the lowermost part of the Sarabetsu Formation exposed in the eastern part of central Horonobe Town, the sedimentary environments of the Formation were assumed to have been lagoons (seashore lakes), tidal inlets, shorefaces and the beach-shorefaces (Figure 4.5.3-19). In other words, the lower most part of Sarobetsu Formation at the point of the investigation was thus a depositional coastal region with a predominance of ocean waves and storms, i.e. the palaeoenvironment of the area from the inner bay to the barrier. From the results of sequence stratigraphy analysis based on the above, three depositional sequences could be identified with three cycles of change in relative sea-level. With this evidence, the sedimentary environment of at least the lower most part of Sarabetsu Formation at the investigation location was thought to have consistently been a coastal area. Given the result of FT dating of the lower Sarabetsu Formation[48)], the eastern part of central Horonobe Town was considered to have consistently been a coastal area in the earlier half of the Early Pleistocene.

The Teshio River rises from the Mount Teshiodake in the mid Kitami Mountains, flowing north along the eastern foot of Teshio Mountains, crossing the Teshio Mountains near Otoineppu and then the Soya Hill near Horonobe before flowing into the Japan Sea (Figure 4.1.2-1). This demonstrates that the flow channel of the Teshio River was defined before the uplifting of the Teshio Mountains and the Soya Hill.

Summarising the discussions above, the palaeogeography of the Horonobe area over the last three million years can be reconstructed (Figure 4.5.3-20). It can be seen that the land area of Horonobe expanded westwards, with development of structures associated with a fold-and-thrust belt. Based on the formation ages and distribution of the marine terraces in the Horonobe area, the detailed palaeogeography for the last approximately 210,000 years was also reconstructed (Figure 4.5.3-21). Clearly the land area has gradually expanded westwards, along with extensive changes in the shoreline owing to eustatic sea-level changes.

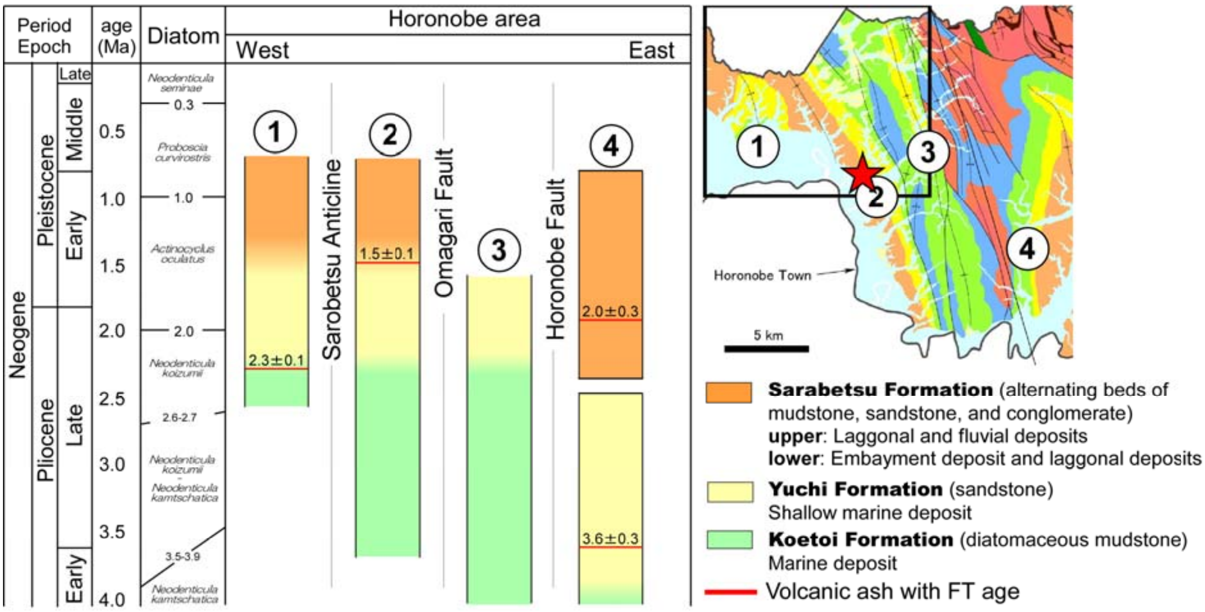

Figure 4.5.3-18 Stratigraphical section and diatom zones for each location in the Horonobe area

Partly modified from Yasue et al.[27]; FT ages taken from Ishii and Yasue[46]

Geological map (right) referring to Figure 4.1.3-1; Red star for the outcrop shown in Figure 4.5.3-19

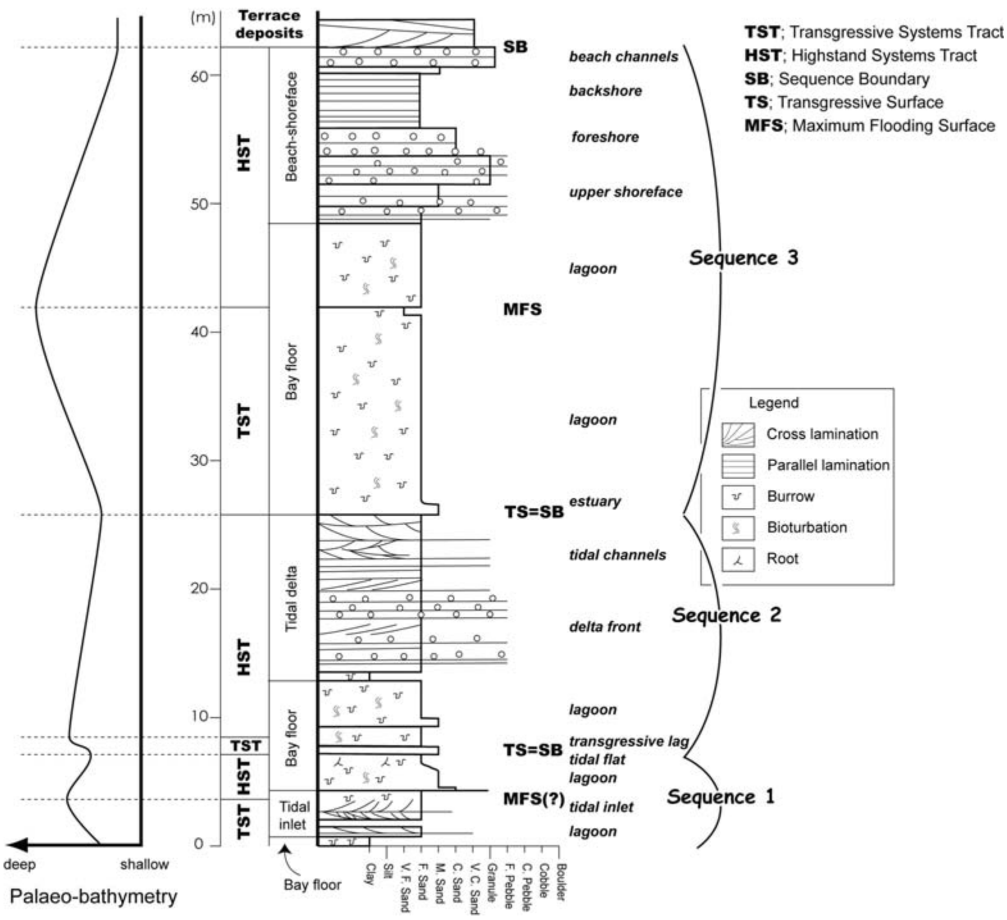

Figure 4.5.3-19 Stratigraphical section in the lower part of the Sarabetsu Formation exposed in the centre of Horonobe Town

Location of the outcrop shown in Figure 4.5.3-18

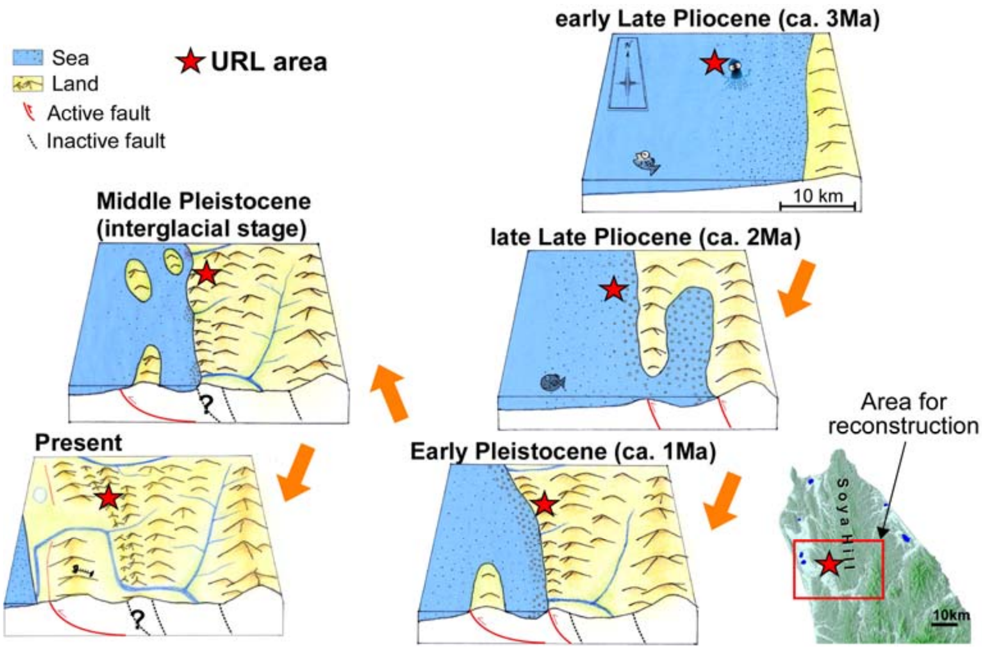

Figure 4.5.3-20 Palaeogeography from the early Late Pliocene (ca. 3 Ma) to the present

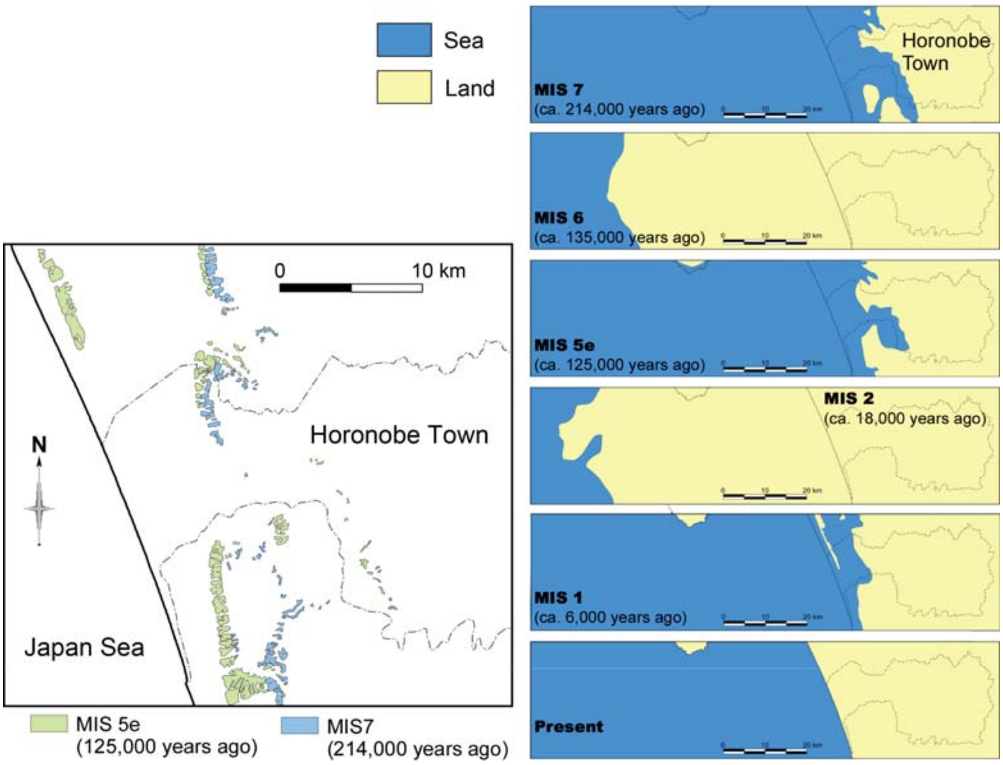

Figure 4.5.3-21 Palaeogeography in and around the Horonobe area from MIS 7 to the present (right), based on the formation ages and distribution and of marine terraces (left)

It is clear that the palaeogeography in the Horonobe area evolved with interaction between tectonics such as faulting and changes in climate and sea-level. In other words, when methods for evaluating an impact of natural phenomena are applied taking the Horonobe area as a case study, it is important to evaluate the influence of interactions among natural phenomena such as faulting, uplift/subsidence and sea-level changes on the deep geological environment, rather than considering these phenomena individually.

(3) Study covering the Hokushin district of Horonobe Town (in and around the URL area) through surface-based and borehole investigations

i) Amount and rate of erosion

The current geothermal gradients of areas occupied by the Tertiary were about 2.0–5.0°C per 100 m in Hokkaido. In particular, gradients of 3.0–4.5°C per 100 m are seen widely over northern Hokkaido[218]. In and around the Horonobe area, palaeogeothermal gradients have been obtained in the north (MITI Tenpoku borehole) and the southeast (Kitakawaguchi SK-1 borehole) of Horonobe Town[11]. From these data, the palaeogeothermal gradient in the Horonobe area was estimated to be 3.5°C per 100 m. For the ground surface temperature of the Horonobe area, the average temperature at the mouth of 13 boreholes, including the MITI Tenpoku borehole[11], and the average ambient air temperature observed at the JMA Teshio Weather Station for 1979–2000 were 15°C and 6.2°C respectively. The amount of erosion (amount of denudation) was estimated, taking these temperatures as the ground surface temperature at the time when the palaeogeothermal gradients were obtained[82].

The ages of the Neogene volcanic rocks in and around the Horonobe area are mostly clarified from radiometric dating; they all show ages older than 10 Ma (Figure 4.5.3-6). No existence of dykes that could be a thermal source and no changes in mineral compositions and degree of thermal maturation associated with hydrothermal activity were reported[11] from the surface geological surveys and borehole investigations in and around the Horonobe area. It could therefore be concluded that the transformation of the silica minerals were attributed to burial diagenesis and were not influenced by igneous and hydrothermal activity after diagenesis.

Given the above conditions, the depth where opal A became opal CT in the past was assumed to be about 860–1,250 m. This is consistent with the burial depth of 800–1,100 m[16] in northern Hokkaido that was obtained from the porosity – depth curve of siliceous rocks. The amount of erosion can be estimated from the differences between these depths and the depth of the current boundary between opal A and opal CT. As a result, the amount of erosion at the locations of the borehole investigation was estimated to be at least 435–820 m (Table 4.5.3-1). The boundary between the Wakkanai Formation and the Koetoi Formation exposed at the ground surface is consistent with the boundary between opal A and opal CT. Thus, the boundary (based on the geological model; see Section 4.1) can be used as the reference surface for estimating the amount of erosion (denudation). A contour map was drawn for the amount of erosion in the Hokushin district of Horonobe Town based on the boundary between opal A and opal CT at the each location of borehole and between the Wakkanai Formation and the Koetoi Formation on the ground surface (Figure 4.5.3-22). In the case where the temperature for opal A to become opal CT is 45°C and the ground surface temperature is taken as 15°C, the amount of erosion is presumed to be in excess of 860 m at the anticlinal axis and about 275 m around borehole HDB-7 at the limb of the anticline. For the areas in and around the Hokushin district, about 860 m and about 1,250 m above the boundary between opal A and opal CT correspond to close the base of the Sarabetsu Formation and in the Sarabetsu Formation, respectively. It can therefore be considered that the Hokushin district has not been a subsidence area since 0.7–1.3 Ma[10], which is the depositional period of the Sarabetsu Formation. The amount of erosion in the Hokushin district discussed so far is the value per one million years over the past. When converting the value into the erosion rate (per 1,000 years), it is estimated as around 0.66–1.79 m ky^{-1} at the anticlinal axis where the uplift is the largest and around 0.21–0.86 m ky^{-1} at the limb of the anticline where it is small (Table 4.5.3-2). According to Koike and Machida[130], the uplift rate in and around the Horonobe area is 0.27–0.55 m ky^{-1}, which is similar to the rate of erosion estimated here.

Table 4.5.3-1 Depth of transition from opal A to opal CT and amount of erosion in each borehole

Borehole	Depth of opal A/ opal CT† boundary [mbgl]	Amount of erosion [m] (Ground temperature: 15°C)		Amount of erosion [m] (Ground temperature: 6.2°C)	
		Opal A/opal CT transformation temperature: 45°C	Opal A/opal CT transformation temperature: 50°C	Opal A/opal CT transformation temperature: 45°C	Opal A/opal CT transformation temperature: 50°C
HDB-1	324.99	535	675	785	925
HDB-2	41.38	820	960	1,070	1,210
HDB-3	426.05	435	575	685	825
HDB-4	100.05	760	900	1,010	1,150
HDB-5	99.95	760	900	1,010	1,150
HDB-6	262.21	600	740	850	990
HDB-7*	nd††	(225)	(350)	(475)	(600)
HDB-8	102.35	760	900	1,010	1,150
HDB-9**	nd	(860)	(1,000)	(1,110)	(1,250)
HDB-10	320.18	540	680	790	930
HDB-11	460.38	400	540	650	790
H15-1-01**	nd	(600)	(725)	(825)	(975)
H15-1-07**	nd	(650)	(800)	(900)	(1,050)

*Amount of erosion based on Figure 4.5.3-22; **Estimation on the basis of relationship between sterane/sterene ratio and palaeogeothermal temperature; †Opal CT detected by XRD; ††nd: not determined (boundary not observed in the borehole)

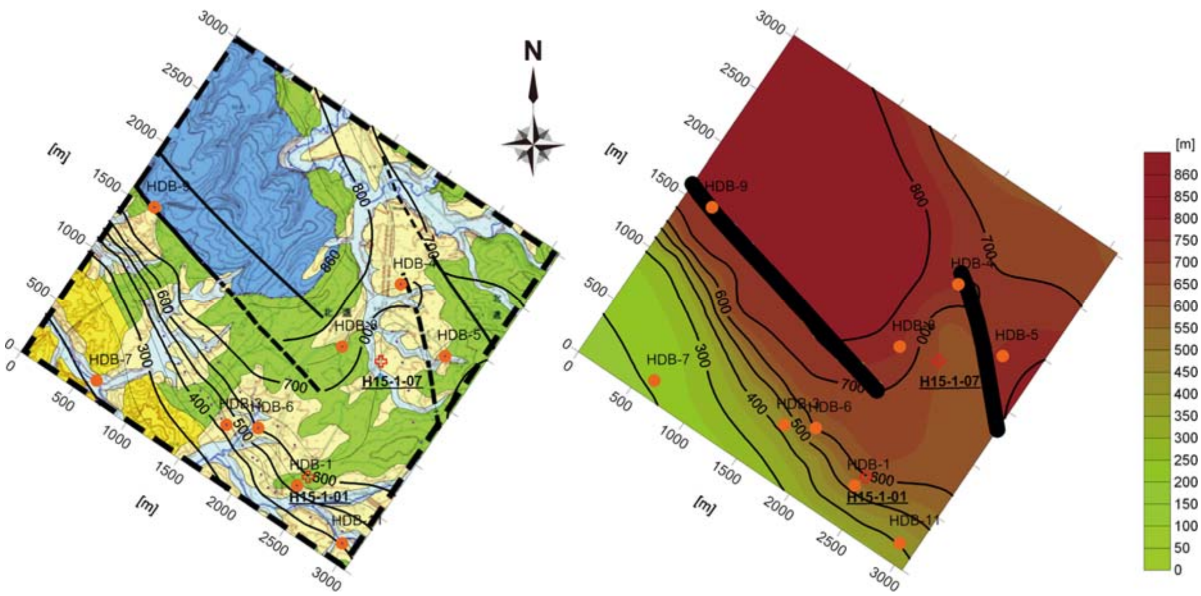

Figure 4.5.3-22 Amount of erosion in the URL area

Contour maps created by build-in-tool (Girding Method) of Golden software “Surfer 8”
Estimation of the amount of erosion based on the depth of opal A/opal CT boundary in boreholes (orange circle) and the geological model by Ishii and Yasue[48)]

Table 4.5.3-2 Erosion rate estimated for each borehole

Borehole	Erosion rate [m ky^{-1}] (Ground temperature: 15°C)		Erosion rate [m ky^{-1}] (Ground temperature: 6.2°C)	
	Opal A/opal CT transformation temperature: 45°C Start of erosion: 1.3 Ma	Opal A/opal CT transformation temperature: 50°C Start of erosion: 1.1 Ma	Opal A/opal CT transformation temperature: 45°C Start of erosion: 0.9 Ma	Opal A/opal CT transformation temperature: 50°C Start of erosion: 0.7 Ma
HDB-1	0.41	0.61	0.87	1.32
HDB-2	0.63	0.87	1.19	1.73
HDB-3	0.33	0.52	0.76	1.18
HDB-4	0.58	0.82	1.12	1.64
HDB-5	0.58	0.82	1.12	1.64
HDB-6	0.46	0.67	0.94	1.41
HDB-7	0.17	0.32	0.53	0.86
HDB-8	0.58	0.82	1.12	1.64
HDB-9	0.66	0.91	1.23	1.79
HDB-10	0.42	0.62	0.88	1.33
HDB-11	0.31	0.49	0.72	1.13

The results of estimation for the amount of erosion depend largely on the reference data such as ground surface temperature, palaeogeothermal gradients and the transformation temperature of silica minerals. Therefore, when estimating the amount of erosion using the mineral compositions of sedimentary rocks, these reference data have to be well understood.

The correlation between palaeogeothermal temperature and the sterane/sterene ratio, a type of cyclic isoprenoids, was investigated by converting depth into palaeogeothermal temperature with the horizon of opal CT as a reference. Isoprenoids are bioorganic matters widely found in animals, plants and micro-organisms. A positive correlation was observed for the palaeogeothermal temperature range of 40–60°C (Figure 4.5.3-23). This demonstrates that the organic ratio in rocks, i.e. the sterane/sterene ratio, is valid as an indicator for the maximum temperature experienced by the rock during diagenetic evolution. If the palaeogeothermal gradient can be estimated, the temperature conditions estimated from the sterane/sterene ratios can be converted into depths. The amount of erosion in the areas of interest could thus be estimated based on the palaeogeothermal gradient and depth profile of sterane/sterene ratio in the present, as is the case for silica minerals.

Siliceous rock (shale, diatomaceous mudstone) formations that have similar characteristics to the Wakkanai and Koetoi Formations are seen in the upper part of the Middle–Upper Miocene in Hokkaido and the petroleum province along eastern margin of the Japan Sea. Examples include the Yakumo Formation in the south-western Hokkaido, the Onagawa Formation in Akita, the Kusanagi Formation in Yamagata and the Nakayama Formation in Sado Island, Niigata[82]. These formations consist primarily of diatoms, with organic compositions similar to those of the Wakkanai Formation. Therefore, the method estimating for palaeogeothermal temperature with the sterane/sterene ratio as an index discussed above could be applied to these formations. It could also be applied to other sedimentary formations if there is not a significant variation of the whole rock chemistry, the mineral and organic compositions in the formation of interest.

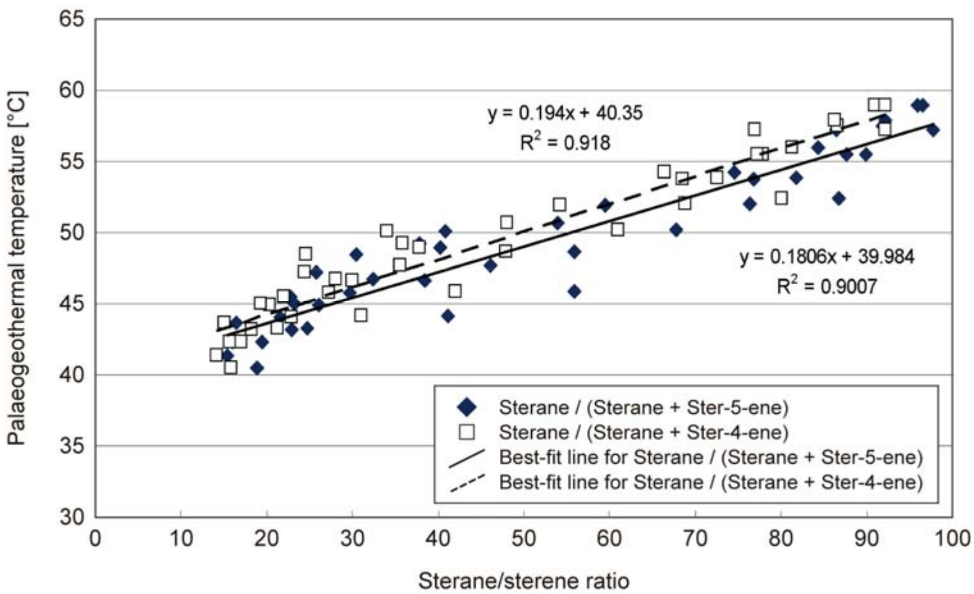

Figure 4.5.3-23 Relationship between palaeogeothermal temperature and sterane/sterene ratio

ii) Geomorphological processes

The spatial distribution geomorphic data in the Hokushin district of Horonobe Town is shown in Figures 4.5.3.24–4.5.3-27. The topographical profiles for each formation and landslide landforms are shown in Figures 4.5.3-28 and 4.5.3-29 respectively. From these figures, it can be seen that the geomorphological processes of the Hokushin district have progressed under the influence of rock control where each process has, to some extent, been influenced by the diverse nature of the landform materials[219)].

In the area where the Wakkanai Formation is found, the drainage pattern is primarily sub-parallel and there are many wide, deep and long straight river valleys (Figures 4.5.3-24, 4.5.3-25 and 4.5.3-28). There are numerous round-top ridges and relatively high-altitude hills with a low drainage density (Figures 4.5.3-26 and 4.5.3-28). High relief energy compared to the Koetoi Formation is found and in many places, the valleys have been filled with alluvial sediments (Figure 4.5.3-27). In this area, fewer terraces considered to have been formed during the last glacial stage are found, compared to the Koetoi Formation. Downward erosion was therefore the primary denudation process in the Wakkanai Formation during both the glacial and post-glacial periods (including the present).

In the area where the Koetoi Formation is distributed, the drainage pattern is sub-parallel in the north-western and south-eastern areas and dendritic in other areas (Figures 4.5.3-24 and 4.5.3-25). The drainage density is greater compared to the Wakkanai Formation and a gentle hill morphology with a low relief energy can be seen, except in the south-eastern area (Figures 4.5.3-26 and 4.5.3-27). The valley-in-valley structure is also seen in the river valleys (Figure 4.5.3-28). It has been formed by incision during the current post-glacial period of bowl-shaped valleys formed during the glacial period and terraces formed in the last glacial stage are found widely in this area (Figures 4.5.3-26 and 4.5.3-27). Since these terraces consist of angular gravel layer composed of breccia to sub-breccia originating from the Koetoi Formation with a muddy matrix and are developed across the valleys, it is inferred that they were formed by periglacial processes; it is concluded that the Koetoi Formation experienced significant sheet erosion due to periglacial processes. In summary, in the current post-glacial period, slopes and their surfaces that became fragile owing to periglacial processes would have collapsed and downward erosion would have been the primary denudation process. It is also concluded that sheet erosion progressed under the sparse vegetation owing to periglacial processes and that lateral erosion associated with bowl-shaped incisions in valleys was the principal denudation process during the glacial period in this area. In the area where the Koetoi Formation occurs, extremely gentle topography was formed owing to periglacial processes.

In the area where the Yuchi Formation is distributed, the drainage pattern is dendritic and drainage density is very high (Figure 4.5.3-24). Different to the Sarabetsu Formation to be discussed later, the Yuchi Formation shows relatively homogeneous lithofacies consisting of sandstone (see Section 4.1). The occurrence of terraces that are considered to have been formed during the last glacial stage is less extensive than in the Koetoi Formation. Given the above, it is inferred that lateral erosion and incision in the valleys were the primary denudation processes during both the inter-glacial and current post-glacial periods. With the development of the dendritic drainage pattern, neighbouring valleys joined together, leading to the development of a topography characterised by wide valleys and a low drainage density.

In the area where the Sarabetsu Formation is distributed, the drainage pattern is dendritic (Figures 4.5.3-24 and 4.5.3-25). The western area of the Hokushin district, where the Sarabetsu Formation is found, has hills with higher altitudes than the Koetoi and Yuchi Formations (Figures 4.5.3-26 and 4.5.3-27). From the geomorphic data, the relief energy is higher compared to the Koetoi and Yuchi Formations and the drainage density is nearly the same as that of the Yuchi Formation (Figures 4.5.3-26 and 4.5.3-27).

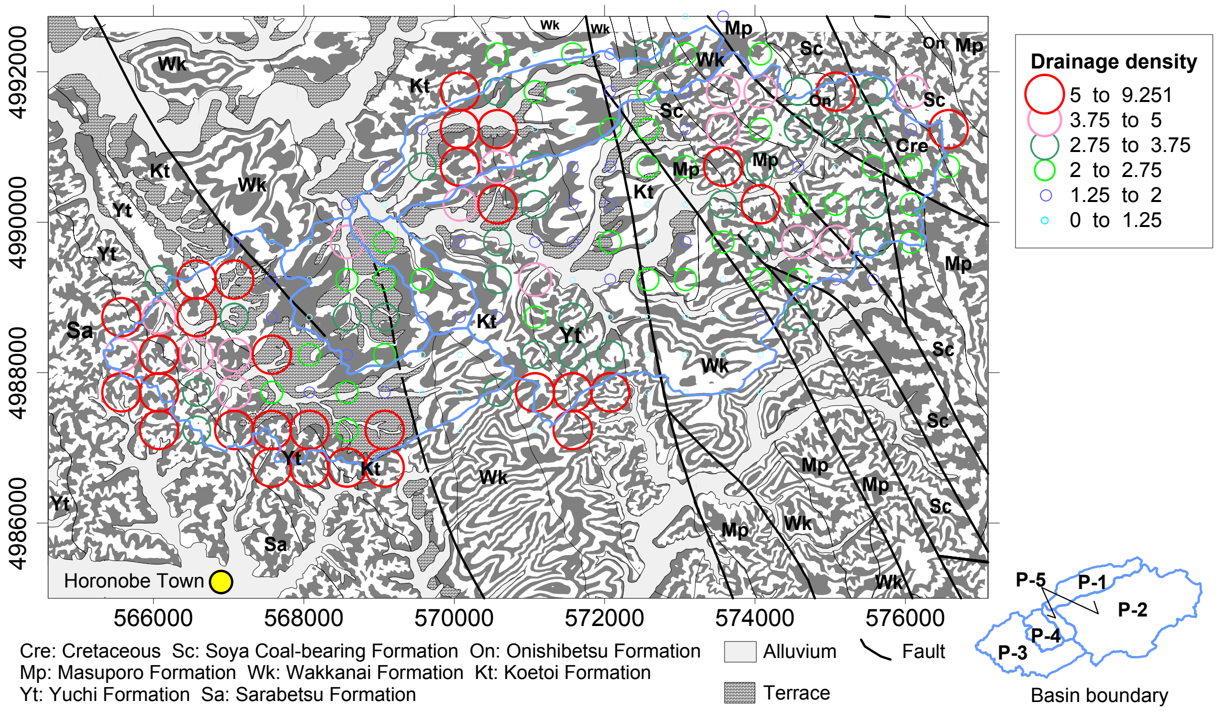

Figure 4.5.3-24 Drainage density [km^{-2}], drainage pattern ('zebra' map) and geology in and around the Hokushin district

UTM (Universal Transverse Mercator system) coordinates used; Every alternate 25 m altitude shaded

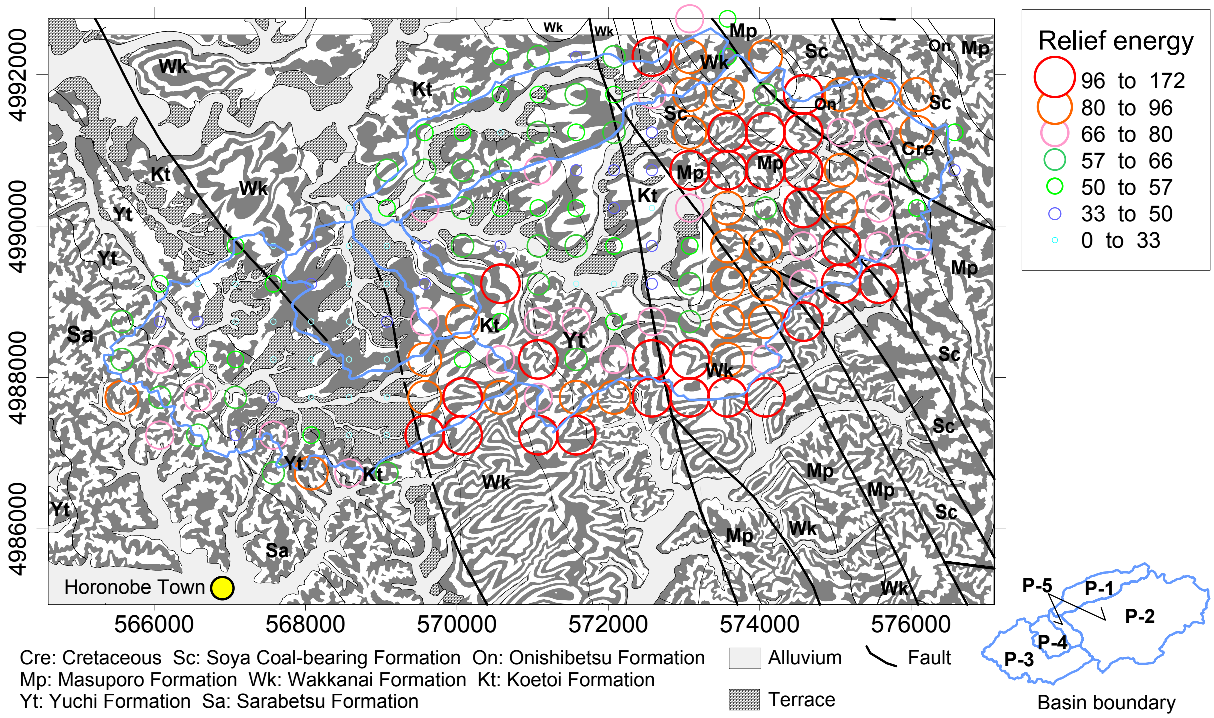

Figure 4.5.3-25 Relief energy [m], drainage pattern ('zebra' map) and geology in and around the Hokushin district

UTM coordinates used; The same 'zebra' map as Figure 4.5.3-24

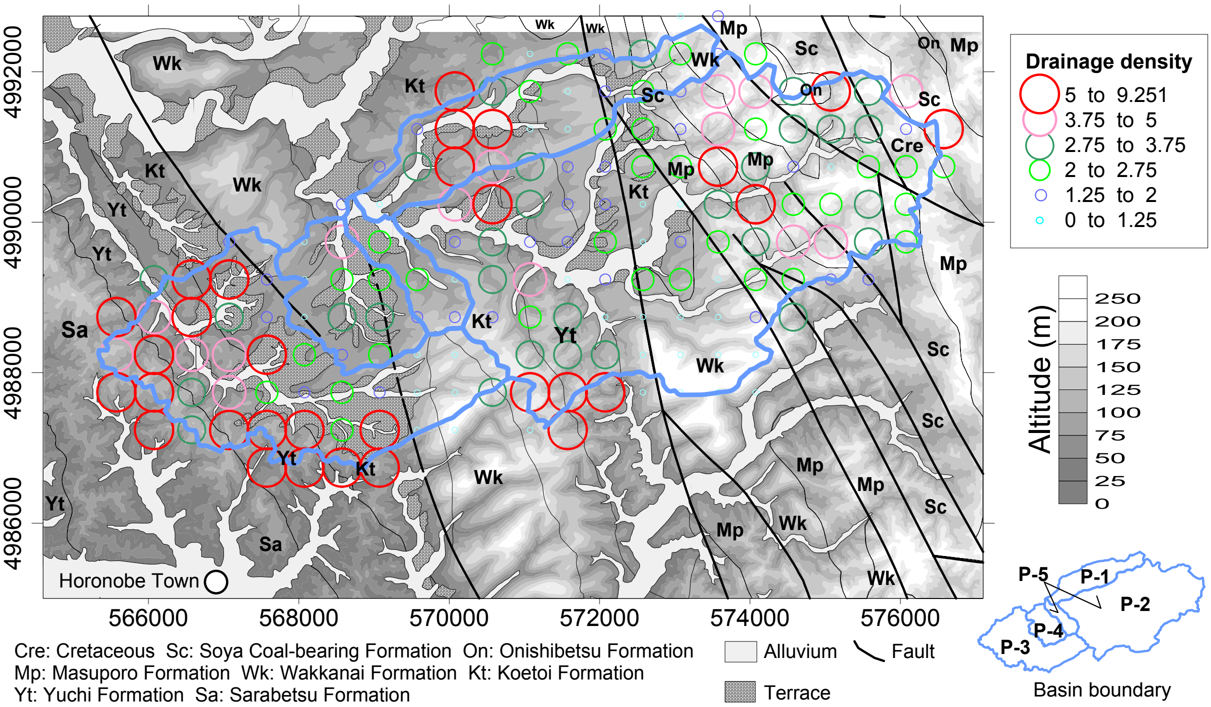

Figure 4.5.3-26 Drainage density [km^{-2}], altitude and geology in and around the Hokushin district

UTM coordinates used

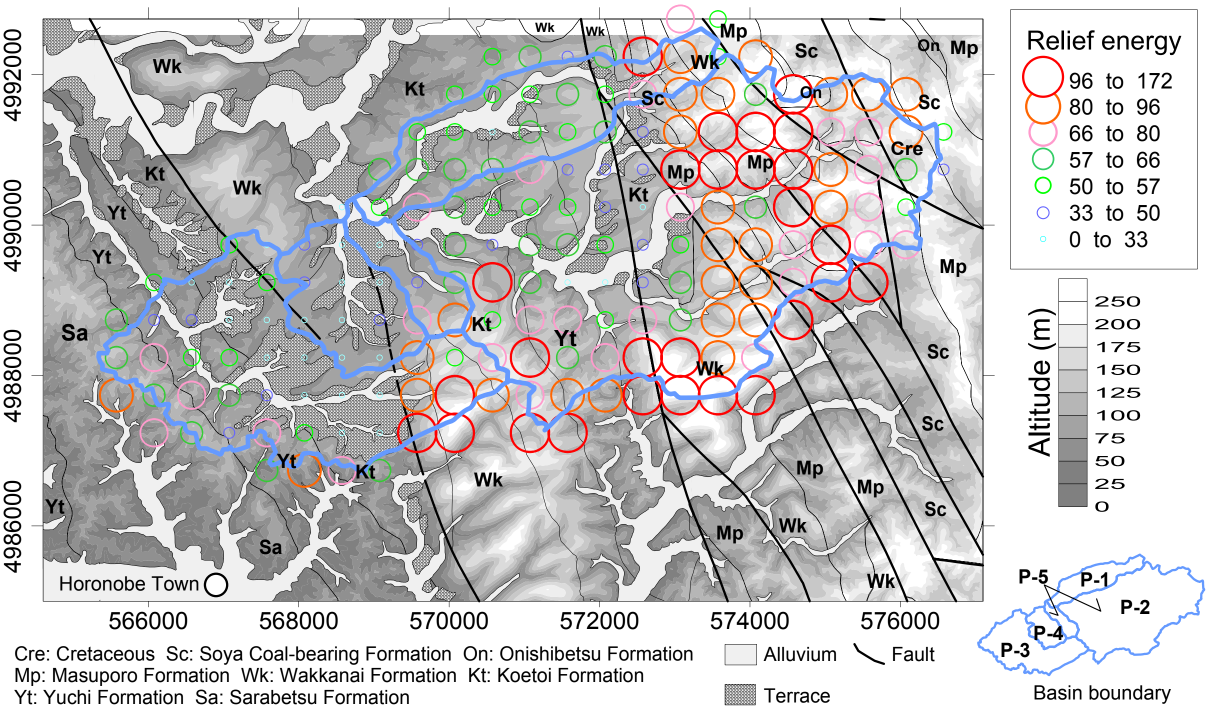

Figure 4.5.3-27 Relief energy [m], altitude and geology in and around the Hokushin district

UTM coordinates used

The Sarabetsu Formation consists of various types of rocks such as conglomerates, sandstones and mudstones (see Section 4.1). Conglomerate layers are dominant along ridges, while mudstones and sandstones are dominant in the valleys. The topographical profiles of the Sarabetsu Formation show the sharp peaked ridge of the conglomerate layer (Figure 4.5.3-28). Thus rock control is considered to be operating within the structure of the Sarabetsu Formation. Based on the above findings, the topography of the area will evolve in the direction to where the relief energy increases, however, once the relief energy exceeds a certain point, the topography would become gentle with low relief energy over a long period of time just like the Yuchi Formation, owing to mass movements and so on.

The formations below the Wakkanai Formation in the eastern part of the Hokushin district form a topographically elevated area and both drainage density and relief energy are high (Figures 4.5.3-26 and 4.5.3-27). The area is characterised by numerous occurrences of landslides (Figure 4.5.3-29). In particular, a landslide landform is concentrated in the Masuporo, Onishibetsu and Soya Coal-bearing Formations. The landslide landform is found for only short distances along faults, except for the formation below the Wakkanai Formation, i.e. a denudation process due to mass movement would be dominate in these formations compared to those above the Wakkanai Formation in the current post-glacial period.

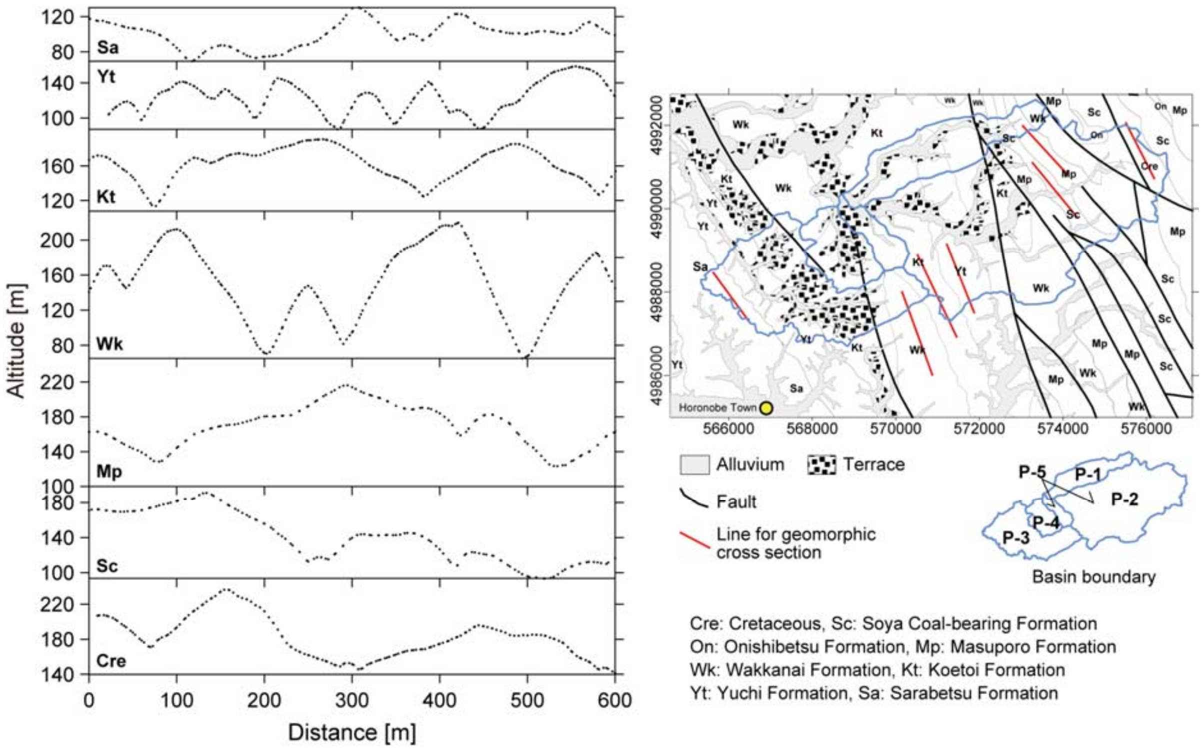

Figure 4.5.3-28 Geomorphic sections for each geological formation in the Hokushin district

UTM coordinates used in the right figure

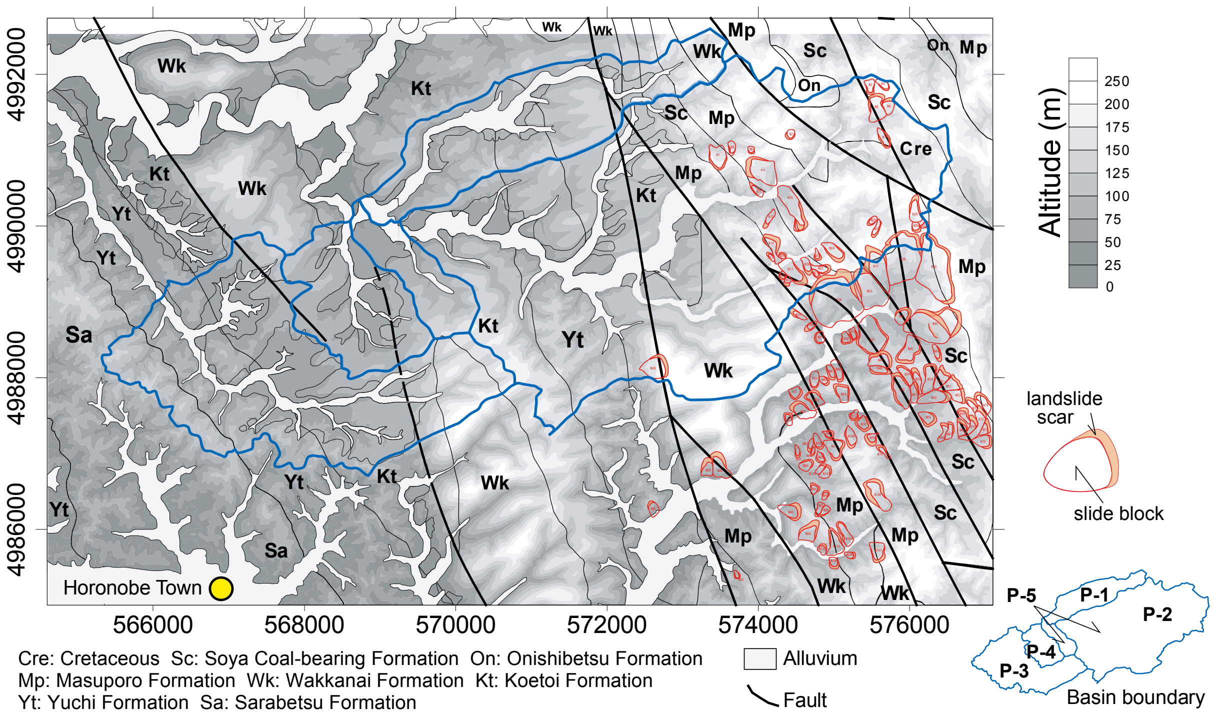

Figure 4.5.3-29 Distribution of landslides and geological map for the Hokushin district

UTM coordinates used

The calculated result for the temporal variation of suspended sediment flux in rivers is shown in Figure 4.5.3-30. In addition, Table 4.5.3-3 shows suspended sediment flux in unit drainage area in the Hokushin district during the Typhoon no.14 (7^{th}–12^{th} September 2005). From this, it is concluded that the differences in the suspended sediment flux at various points in the Hokushin district of Horonobe Town would be a reflection of the geology and vegetation in each basin and that rock control is operating in the erosion process in the area.

Precipitation in the Hokushin district when Typhoon no.14 passed through was 62.5 mm (8 mm maximum per hour) for the two days of 7^{th}–8^{th} September 2005 based on hyetometer data from the Hokushin Meteorological Station installed by JAEA (Figure 4.2.3-2). The river water level rise was associated with an increase in precipitation, with the maximum level being recorded early in the morning of 8^{th} September 2005. The results of the laboratory turbidity analysis of the water samples, taken at the above time, and turbidity data, collected continuously by monitoring devices at P-3 and P-5, are consistent. It was therefore confirmed that turbidity values measured with instrumentation can be used as continuous turbidity data. From the results of the laboratory turbidity analysis of 90 samples taken from rivers in the Hokushin district in the past, it was assessed the relationship between turbidity and concentration of suspended sediment (also termed suspended solids in JIS K 0101 16.1). Both showed a good correlation (correlation factor of 0.996). Based on this, the continuous suspended sediment concentrations were calculated from consecutively observed values for river water turbidity. The flow rate of river water was calculated from continuous observation of the level of river water using the discharge rate curve (H-Q rate curve), which was made on the basis of the shallow subsurface investigations (see Subsection 4.2.3). The peak of the suspended sediment concentration converted from the turbidity was about three hours and six hours ahead of and about half an hour behind the peak of the river flow rate at P-3, P-4 and P-5 respectively. The amounts of cumulative suspended sediment flux from mid-day on 7^{th} September 2005 to mid-day on 12^{th}

September 2005 (the period influenced by precipitation from Typhoon no.14) and the amount per unit area derived by dividing by the area of the basin were obtained. As a result, the amounts of cumulative suspended sediment flux at P-3, P-4 and P-5 were 14.9 t, 0.7 t and 94.0 t respectively. The amounts per unit area were 2.0 km^{-2}, 0.3 km^{-2} and 4.5 km^{-2} respectively, becoming smaller in the order P-5, P-3 and P-4.

Comparing the geology and vegetation in each basin, the sand gravel stratum (the Masuporo, Yuchi and Sarabetsu Formations, terrace deposits and alluvial sediments) that may be a source of suspended sediment occupies almost half of the basin at P-5 and P-3, while it is only about 10% at P-4. 39.7%, 94.9% and 18.7% of areas P-3, P-4 and P-5 are covered by grass, respectively (Table 4.5.3-4). Based on these features of the basins, it is assumed that the larger amount of suspended sediment at P-5 and P-3 compared to P-4 could be due to geological differences and the larger amount at P-5 compared to P-3 could be due to the difference of the percentage of the area covered by grass. The amount of suspended sediment is the amount of sediment provided to rivers by current erosion. Therefore, the differences in the amount of suspended sediment according to area are considered to illustrate the differences in erosion and the evolution rate of the topography of each basin.

As discussed above, there is a strong correlation between with the spatial distribution of the amounts of suspended sediment flux, geomorphic datasets and landslide topography. It is thus certain that current geomorphological processes are progressing under the strong influence of rock control. The amount of suspended sediment flux also relates to the vegetation and the present geomorphological processes are therefore assumed to proceed firstly under rock control and secondly under the influence of the vegetation. When studying future topographical change in the Hokushin district of Horonobe Town, simulation techniques that can take rock control into account will need to be developed and data on geomorphic datasets, required for the simulations must be acquired for each formation.

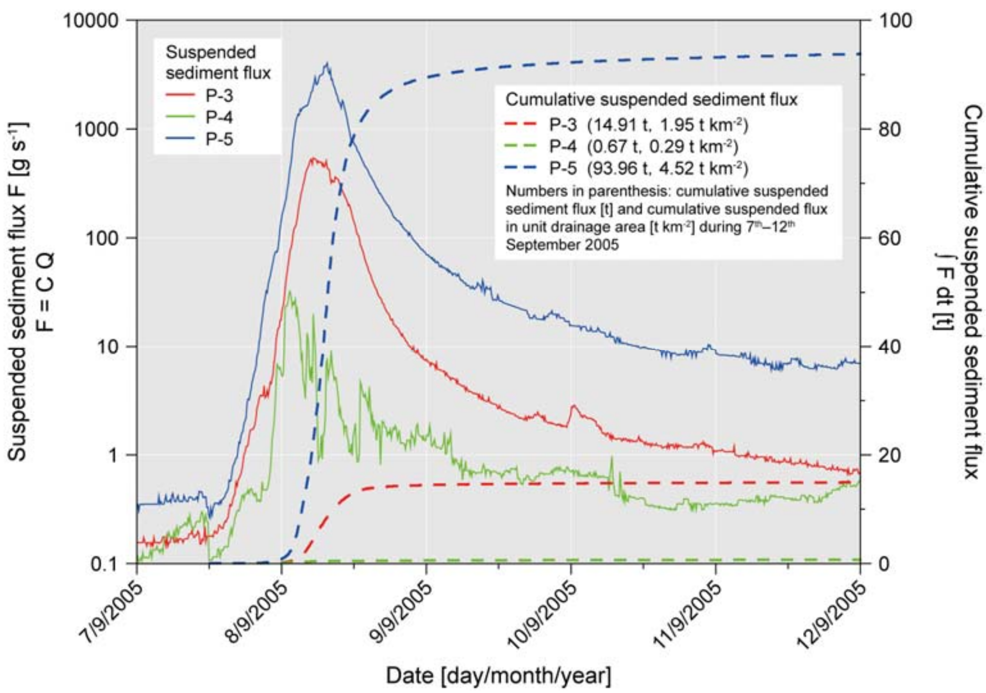

Figure 4.5.3-30 Suspended sediment flux and cumulative suspended sediment flux during Typhoon no.14 from 7th to 12th September 2005 in the P-3, P-4 and P-5 drainage basins

Table 4.5.3-3 Suspended sediment flux in the Hokushin district during Typhoon no.14 from 7th to 12th September 2005

Drainage basin	Drainage area A [km^2]	Cumulative suspended sediment flux ∫ F dt [t]	Cumulative suspended sediment flux in unit drainage area ∫ F dt / A [t km^{-2}]
P-3	7.647	14.91	1.95
P-4	2.315	0.67	0.29
P-5	20.798	93.96	4.52

Table 4.5.3-4 Drainage basin characteristics in the Hokushin district

Drainage basin*	Drainage area [km^2]	River	Characteristics of drainage basin: Geology		Characteristics of drainage basin: Topography	Characteristics of drainage basin: Vegetation [%]
P-3	7.647	Shimizu R.	Lower–middle stream	Western part: Yuchi F. Eastern part: Koetoi F.	High drainage density and low relief energy	Grass field: 39.7 Broadleaf forest: 29.2 Coniferous forest: 19.9
			Upper stream	Mainly Koetoi F. Partly Wakkanai F.		
P-4	2.315	Ichigou R.	Koetoi Formation		Low drainage density and low relief energy	Grass field: 94.9
P-5	20.798	Penke-ebekorobetsu R.	Lower stream	Koetoi Formation	High drainage density and high relief energy	Broadleaf forest: 67.7 Grass field: 18.7 Coniferous forest: 11.1
			Upper stream	Soya Coal-bearing F., Masuporo F. and Wakkanai F		

*Locations of drainage basins shown in Figure 4.2.3-3

4.5.4 Future evolution of the geological environment

(1) Approach to estimating future evolution

Several approaches have been proposed for estimating the future evolution of the geological environment. The principles employed in any approach involve making extrapolations or drawing analogies, or quantitatively estimating the possibility of occurrence of phenomena to obtain the probability, based on the trend of evolution and the extent of influences from the past up to the present. In particular, the extrapolation and analogy approaches would be important for estimating the future evolution of the geological environment over far longer time periods than those covered by experiments. In the extrapolation approach, the future evolution is estimated by extrapolating the historical temporal and spatial evolution trends identified based on analyses of historical evolution into the future. In the analogy approach, phenomena that are similar to the phenomena of interest are studied in order to make generalisations and future evolution of the phenomena of interest is estimated by inferring the future evolution of the generalised phenomena[220]. In any approach, the basis for estimating and evaluating the future evolution is through understanding phenomena in the past.

Information to be used in the future estimation should be obtained during a period similar to, or longer than, that of interest. For example, as described in Subsection 4.5.3, data on crustal movements obtained by geodetic methods such as GPS and triangular surveys cover a period from several to about 100 years and could be influenced by cyclic movements occurring over longer periods than the period of observation. It is possible that the trend and amount of crustal movement obtained using such geodetic methods could be different from those for a period extending over several tens of thousands of years (Figure 4.5.4-1).

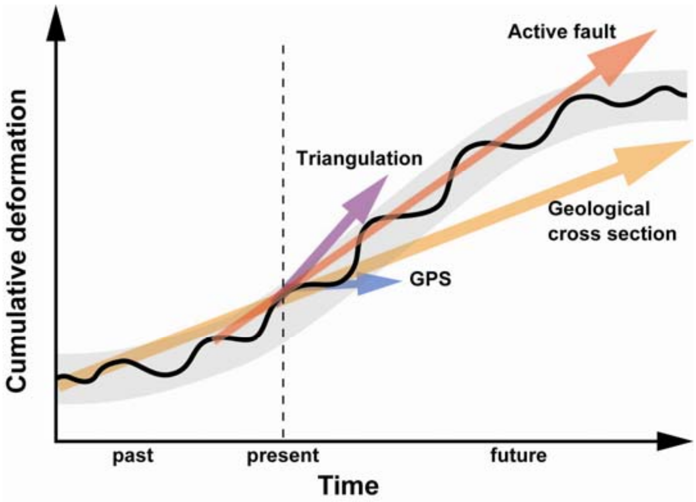

Figure 4.5.4-1 Schematic illustration of variation trend extrapolated from different types of data (GPS and triangulation data, displacement of active faults and crustal strain using a balanced geological cross-section)

Wavy black line showing true deformation path; Broad grey line showing true variation trend

Illustration adapted from Kimura[221)]

(2) Patterns and trends in the occurrence of natural phenomena and changes in the geological environment conditions in the Horonobe area

The natural phenomena to be considered for estimating the future geological environment in the Horonobe area and their interactions and the evolution of the geological environment assumed to occur owing to these phenomena, are summarised in Figure 4.5.4-2a (seismicity/faulting, volcanic/hydrothermal activity, uplift/subsidence and erosion/sedimentation) and Figure 4.5.4.2b (uplift/subsidence, erosion/sedimentation and climatic/sea-level changes). These figures were prepared based on the temporal and spatial variations of the natural phenomena that have occurred in the past in the Horonobe area (see Subsection 4.5.3). In order to illustrate the interactions among natural phenomena, the phenomena were compiled into an interaction matrix[222)]; the characteristics of each natural phenomenon (e.g. pattern of occurrence, style and scale) were allocated as diagonal components and the processes and events that relate to the propagation of influences among phenomena were allocated as off-diagonal components that cross the diagonal components. Based on this matrix, the natural phenomena that should be considered for evaluating the future evolution of the geological environment in the Horonobe area will be uplift, subsidence, erosion and climatic/sea-level changes that progress regionally and slowly. These phenomena would have large influences, in particular, on the hydrology of the bedrock.

Earthquake and activation of fault (including of active structure) · **Earthquake swarm around the Sarobetsu Flexure Zone and the Toikanbetsu (up to M4.2)** · **Interplate earthquake in the Pacific Ocean (ex. 2003 Tokachi-Oki Earthquake)** · **Earthquakes on the eastern-margin of Japan Sea** · **Activation of the Omagari Fault (sinistral reverse oblique movement; lateral,up to 150-200m (topographical evidence); vertical, 200-300m)** · **Formation of significant new fault in the Sarabetsu Flexure Zone** · **Post-seismic crustal movement after the 2003 Tokachi-Oki EarthquakeFault Zone** · change of thermal properties due to temporary heat production along fault · earthquake-induced fluid migraiton in the vertical/subvertical faults · change of porewater pressure in host rock and geosphere due to crustal strain (including of post-seismic crustal movement) · temporary change of porewater pressure and dissipation of overpressure in host rock and geosphere due to crustal strain caused by seismic motion · change of hydrological parameters (hydroulic conductivity etc.) in host rock and geosphere due to formation of fracture and fault rocks · seismic pumping, liquefaction (Hydrological and mechanical effects, also affects to transport property) · change of GW level due to deformation and seismic motion · change of GW flow due to seismic motion · change of mechanical properties of rock due to seismic motion	–	· Topographical change in consequence of the fault movement (Sarabetsu Flexure Zone, Toikanbetsu Fault Zone, and Omagari Fault · Local uplift and subsidence due to activation of the Sarobetsu Flexure Zone,Toikanbetsu and Horonobe Fault Zone (active structures) · Local uplift and subsidence due to activation of the Omagari Fault · Topographical change as a consequence of earthquake-induced landslide
–	**Volcanic and hydrothermal activity** · **Hydrothermal fluid circulation along theOmagari Fault (up to 100^{o}C, based on the preliminary geological survey in the one outcrop)** · **Volcanic and hydrothermal activity will cause heat convection (near the Rishiri and Rebun Island; highly unlikely)** · increase of porewater pressure as a consequence of thermal expansion in host rock and geosphere · change of mechanical and hydrological properties of rock due to heat stress · hydrothermal alternation (change of hyrological and geochemical properties in and around fracture)	· Surface deformation as a consequence of intrusion of magma (highly unlikely in the Horonobe area)
–	–	**Uplift, subsidence/denudation, sedimentation (burial)** · **Regional uplift in consequence of EW compressive stress (uplifting rate is 0.3m/ky in the past 0.3Ma)** · **Change of URL depth (erosion rate is ca.0.21 to 0.66m/ky in the past 1.5Ma)** (uplift, subsidence/denudation , sedimentation wiil cause change of surrounding temperature of URL) · change of hydraulic gradients in magnitude and direction in consequence of topographical change · change of the outcrop area (due to exhumation) of geological formations, this give rise to some change of flow patterns and location of discharge and recharge area · change of porewater pressure due to denudation and sedimentation · change of overburden · change of rock strength due to porewater drainage (sedimentation and burial process) · change of rock strength due to increase of porewater pressure (sedimentation and burial) · change of geochemistry of GW due to porewater drainage · change of geochemical condition due to denudation and/or sedimentation (burial; reduced to oxidized zone or its reverse, to weatherd zone) · possible advective solute transport through the host rock with porewater drainage · change of transport distance

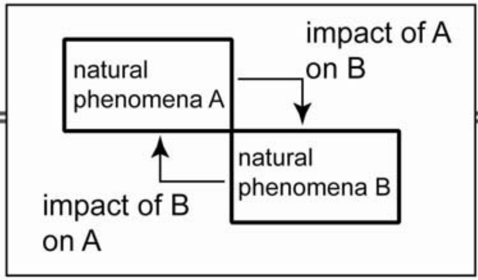

<u>**Bold face**</u>, **natural phenomena;** <u>Regular face</u>, impacts of natural phenomena on geological environments (Thermal, Hydrological, Mechanical, Chemical, transport property)

Figure 4.5.4-2a Natural phenomena, their impact on the geological environment and their interaction as relevant for the future evolution of the geological environment in the Horonobe area

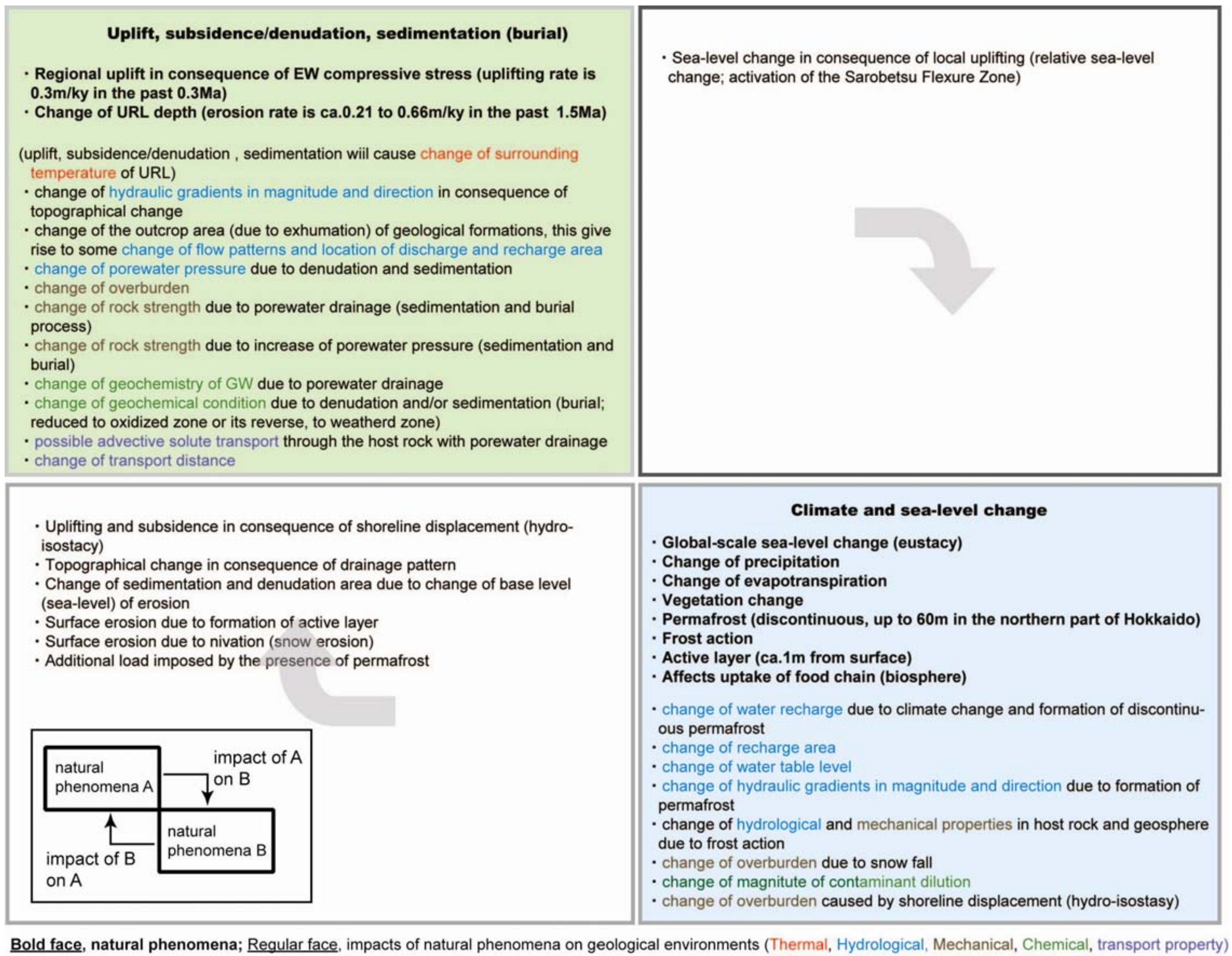

Figure 4.5.4-2b Natural phenomena, their impact on the geological environment and their interaction as relevant for the future evolution of the geological environment in the Horonobe area

As discussed in Subsection 4.5.3, as long as the current tectonic framework does not change, the possibility of occurrence of volcanic/hydrothermal activity is likely to be low in the future. Based on the trend of seismicity for the last approximately 800 years as known from historical documents, the seismicity for the same period in the future can be treated in the same way as volcanic/hydrothermal activity. However, it should be noted that this estimation is based on the trend for the last approximately 800 years. Although sediments reflecting seismic events, such as tsunami deposits and traces of liquefaction, were not found in the coastal area of northern Hokkaido, based on the analysis of submarine sediment cores sampled at the Rishiri Trough to the west of Rishiri Island (Figure 4.5.3-1), the recurrence interval of major earthquakes that would induce landslides of the sea bottom in this Trough is estimated to be about 3,000 years[174]. Evolution of the geological environment in the next several tens of thousands of years should therefore be described considering the influence of seismicity on the geological environment. Based on the temporal and spatial evolutions of natural phenomena revealed in the Phase I investigations, it may be appropriate to adopt the following strategy: the influence of ‘sudden natural phenomena’ occurring over relatively limited geographical ranges would be first obtained from surface-based investigations to understand the current activity and spatial distributions etc. From this, the criteria for selecting faults and hypocentres in order to evaluate their impact would be clarified, followed then by a consequence analysis.

The uplift/subsidence history for the Horonobe area was based on the present depth[9], thickness, deposition period[6] and sedimentary environment of each formation and palaeogeography in the area as discussed in Section 4.1 and this section (Figure 4.5.4-3). Thickness and depositional period of each formation in the Sarobetsu Lowland are taken from the existing information[213),223]. The palaeowater depth during the time of sedimentation of each formation was estimated from the sedimentary facies of each formation[224] on the basis of the relationship between sedimentary facies and water depth[225),226]. Altitudes relative to the current sea-level were obtained from sea levels during the time of sedimentation of each formation using the sea-level change curve[227),228] and palaeowater depth described above (Table 4.5.4-1). This figure represents the overall trend of uplift/subsidence in the Horonobe area, although it is based on some assumptions, including a decrease in the thickness of the formation owing to compaction and isostatic uplift and subsidence. That is, the subsidence trend that has lasted for the last two million years is evolving to an uplift trend in the Sarobetsu Lowland, while uplift will progress until it reaches equilibrium conditions around the URL area and the area near the Sarobetsu Anticline (Figure 4.5.4-3). The different history of uplift/subsidence in each area is correlated with the distribution of the horizontal crustal strain rate reflecting the geological structure of the fold-and-thrust belt in northern Hokkaido; the uplift trend has continued since more than a million years ago in the eastern part of the Horonobe area where the strain rate is high, whereas in the western part of the Horonobe area, where the strain rate is low, evolution from subsidence to uplift is likely to occur. To summarise, considering the future trend of uplift/subsidence in the Horonobe area taking regional tectonics into account, the current uplift trend will continue until it reaches equilibrium conditions in the eastern part of the Horonobe area and the area near the Sarobetsu Anticline, whereas subsidence will evolve to uplift with an increase in the horizontal crustal strain rate in the future and the uplift trend will continue until it reaches equilibrium in the Sarobetsu Lowland.

Regarding climate change, the arrival of a glacial period is expected within several tens of thousands of years, assuming that the approximately 100,000 year cycle that has dominant since about 1.2–0.7 Ma will continue in the future and given that the present time is slightly after the peak of a warm (interglacial) period and about 10,000 years have passed since the start of the post-glacial period[229]. Based on the submarine topography of the Horonobe area, it is highly likely in a glacial period that the continental shelf to the west of the Horonobe area would largely become land owing to the lowering of sea-level, that the

Soya Strait and Sakhalin would be reconnected by a land bridge and that environment in the Horonobe area would change to inland type. Also, based on the results of reconstruction of the vegetation in northern Hokkaido, this area would have a surface environment similar to present-day northern Sakhalin in a future glacial period.

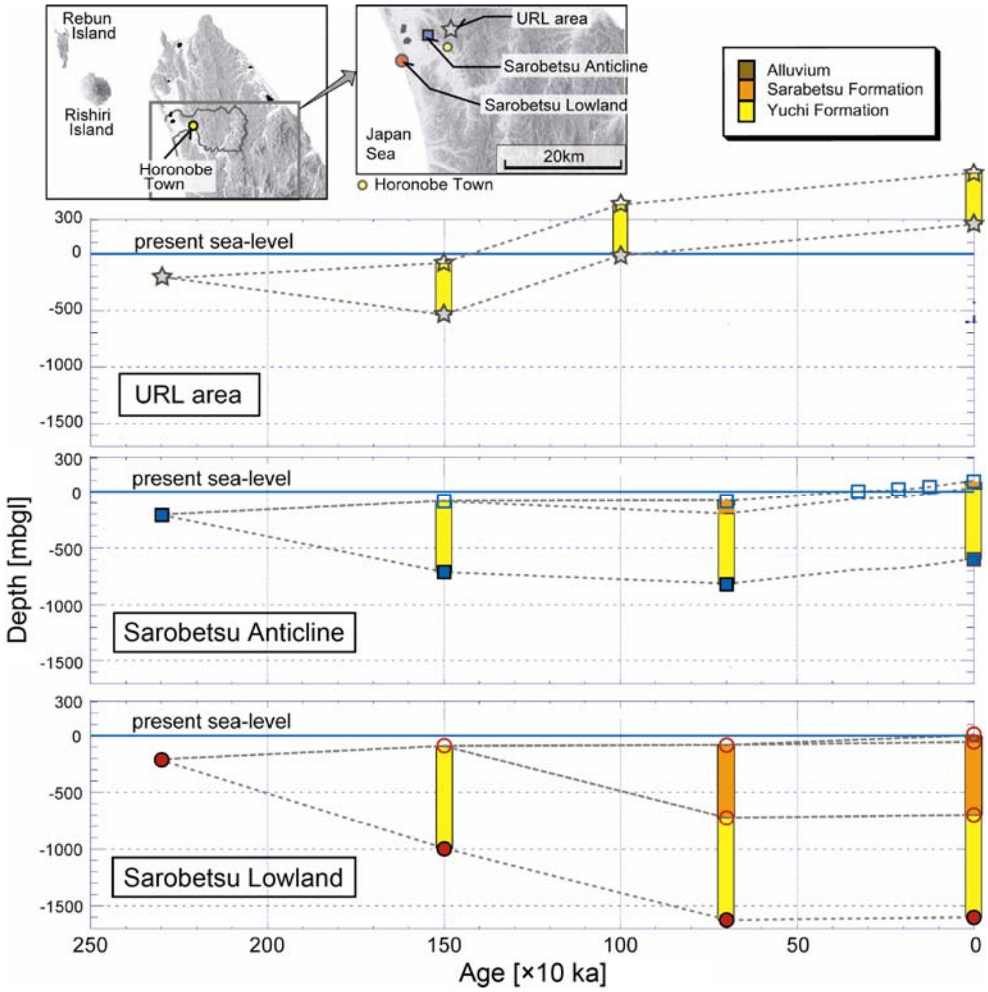

Figure 4.5.4-3 Uplift and subsidence history in the Horonobe area

Shaded relief map after GSI[179)]

Table 4.5.4-1 Description of the Yuchi and Sarabetsu Formations and marine terraces

Formation and terrace	Depositional age (upper and lower ages) [×10 ka]	Terrace altitude [m] Maximum formation thickness [m]	Depositional environment	Water depth [m]	Sea-level [m]
MIS 9	32.8	95	Shoreline	0	+5
MIS 7	21.4	75	Shoreline	0	+5
MIS 5e	12.5	50	Shoreline	0	+5
Sarabetsu Formation	70	625	Lagoon and fluvial	0	-70
	150		Embayment and lagoon	-15	-80
Yuchi Formation	150	900	Shoreface	-15	-80
	230		Outer shelf	-130	-80

Considering the evolution of the geological environment of the Horonobe area for about three million years into the future based on past geological history of the same duration, the development of active structures in the west of the Sarobetsu Lowland, the spreading of the land toward the west and the evolution of the geological structures should be taken into account. These westward movement trends are thought to be part of the contraction of the Tenpoku Sedimentary Basin towards the depocentre. Thus, when covering a period of around one million years into the future, active structures in the eastern part of the Tenpoku Sedimentary Basin have to be included in the study and the uncertainty associated with the estimate will increase.

Summarising the discussions in this section, the surface geological environment and the conceptual cross-section of the geological structure in the Horonobe area covering a period of about 100,000 years into the future were represented as shown in Figure 4.5.4-4. This figure illustrates the situation in the future glacial period. The decrease in the thickness of formations owing to denudation (including erosion), the change in the topography and the development of active faults and folds in the Sarobetsu Lowland to the west of the Horonobe area, as described in Subsection 4.5.3, are included in the figure. The figure is based on the patterns of occurrence of natural phenomena in the Horonobe area in the past and is a conceptual model to be used as a basis for estimating the geological environment of the area in the future. In order to obtain an optimum approximation of temporal and spatial variation of groundwater flow conditions in the future taking the influence of natural phenomena into account based on the conceptual model, quantitative data on natural phenomena and the evolution of the geological environment illustrated in the figure need to be acquired. This would be an issue to be addressed in the investigations of Phase II and/or Phase III.

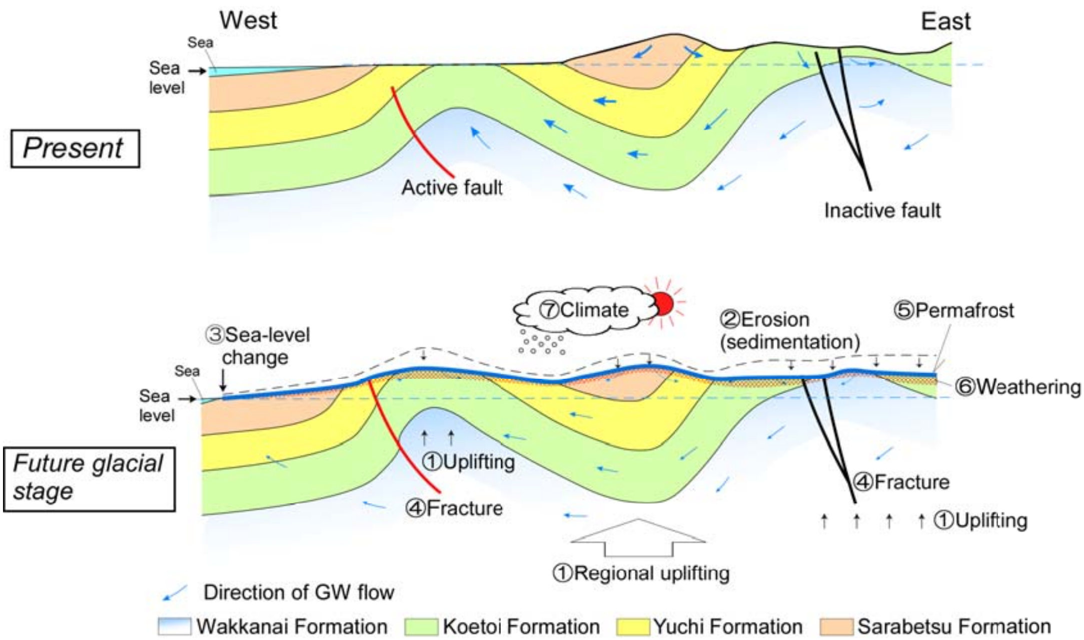

Figure 4.5.4-4 Conceptual model for future geological evolution of the Horonobe area

4.6 Integration of multidisciplinary information

The basic methodology for characterising the properties of the geological environment and processes involved, which are critical for geological disposal, was proposed in the form of a "Geosynthesis Data Flow Diagram"[230] as presented in Subsection 4.6.1. Based on the understanding of the key properties and processes of the geological environment, assessments were attempted of key issues relating to the safety of the geological disposal system[231]. These include solute transport/retardation in the undisturbed geological environment and perturbations induced by construction of the underground facilities. The former was addressed in the context of development of advanced safety assessment methodologies[232] and only the details of the work carried out as part of the geoscientific research and feedback from the solute transport analysis are discussed in Subsection 4.6.2. Regarding the latter issue, prediction of changes in groundwater flow and chemistry and rock mechanical properties in the vicinity of the underground facilities is discussed in Subsection 4.6.3.

4.6.1 Illustration of the geosynthesis data flow diagram

As discussed in Sections 4.1–4.4, during the surface-based investigations most of the key properties and processes of the geological environment in the context of geological disposal (Figure 2.2.1-1) were clarified through investigations using existing information, ground exploration and borehole investigations and modelling of the geological environments (geology, hydrogeology, hydrochemistry and rock mechanics). During the course of the investigations, results such as the combination of investigation techniques in various disciplines and methods for interpretation of investigation results have been achieved by iterating investigations in certain areas on a trial-and-error basis.

Based on this experience and recognising the importance of having a specific roadmap for effectively executing the sequence of activities "investigation → interpretation of results → modelling/analysis → clarification of relevance for geological disposal", the "Geosynthesis Data Flow Diagram"[230] illustrating the linkage between a range of surfaced-based investigations and the key properties and processes of the geological environment was established (see Appendix 6). The case studies referred to in establishing the geosynthesis data flow diagram include the Wellenberg project[233] in Switzerland, where an extensive site characterisation was conducted for selecting an L/ILW repository, and the Mizunami URLproject[234),235], where surface-based investigations on crystalline rocks were conducted. It should be noted that the geosynthesis data flow diagram described here does not anticipate that the conditions of the geological environment will change significantly. The data flow diagram for studies on the long-term evolution of the geological environment and assessment of its impacts on the key properties and processes of the geological environment in the context of geological disposal is discussed in Section 4.5.

The data flow diagram provides a basic roadmap for effectively guiding the characterisation of the geological environment from the surface from the viewpoint of safety assessment and design/construction of the underground facilities. Information contained in the flow diagram includes individual investigation techniques and their combination, the types of information to be acquired, the interpretation of the results and the integration of information obtained from different disciplines for each investigation stage; investigations using existing information, aerial and ground reconnaissance surveys and borehole investigations. The key feature is a systematic framework based on knowledge and experience gained from the surface-based investigations. Effective systematic techniques for characterising, on a step-by-step basis, the geological environment from the surface will be established by testing of the flow diagram based on technical findings accumulated with the progress of the investigations and stepwise optimisation and refinement of the flow diagram.

4.6.2 Solute transport/retardation in the undisturbed geological environment

(1) Approach and details of the evaluation

The outline for the work flow was established by considering the framework for a sequence of evaluation activities in the context of development of advanced safety assessment methodologies for evaluating solute transport/retardation in the deep geological environment in the Horonobe area, using the information obtained from the surface-based investigations (Figure 4.6.2-1). The evaluation was carried out in accordance with the established work flow, with the aims of:

- demonstrating methodologies for evaluation ranging from investigation/analysis of the geological environment to solute transport analysis for sample cases;
- compiling know-how and findings obtained based on a trial-and-error approach to the evaluation.

The tasks conducted primarily by the team responsible for the environmental investigations extend from investigation of the geological environment to analysis of groundwater flow, conducted in accordance with the geosynthesis data flow diagram described in Subsection 4.6.1. In collaboration with the team responsible for the solute transport analysis, a study was carried out to set the parameters for the solute transport analysis and evaluation of the analysis results, bearing in mind the need for feedback to the investigation programme of the geological environment. The information on the geological environment used in the above task was obtained up to the end of March 2005 and may not always be consistent with the description in Sections 4.1–4.3.

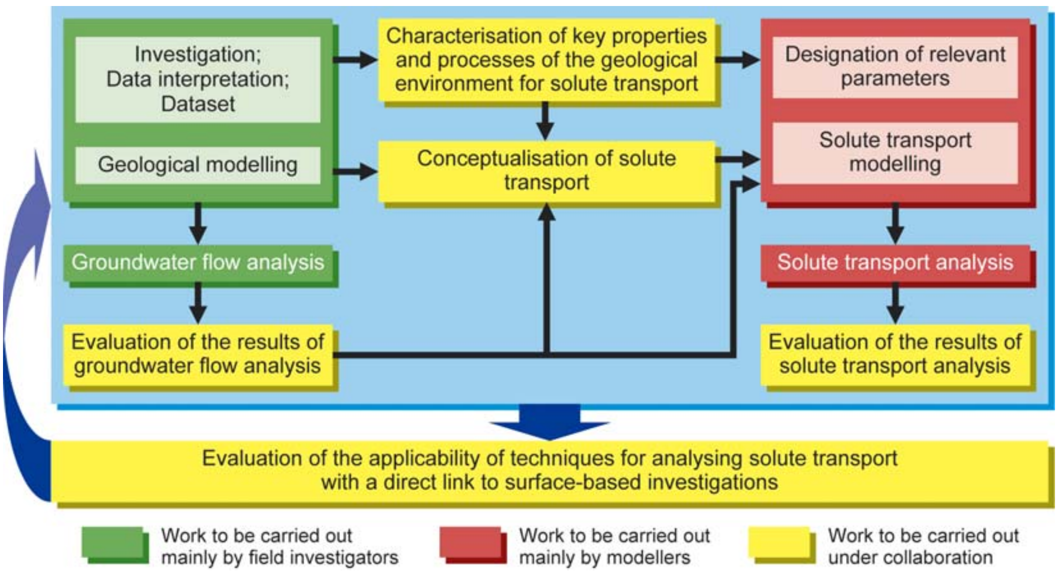

Figure 4.6.2-1 Basic framework for evaluating solute transport, with a direct link to the surface-based investigations

(2) Compilation of geological environment information

Information on the geological environment was compiled for a large area covering the URL area, taking into account that the aims of the solute transport analysis are to clarify the effects of large-scale geological structures (e.g. the Omagari Fault) on groundwater flow and consequently on the performance of the geological disposal system and the EBS and to assess the performance of the EBS and the surrounding geological environment. This corresponds to ‘field investigations’, ‘data’ and ‘interpretation/dataset’ in the geosynthesis data flow diagram.

1) Geology and geological structure

The surface distribution of the Omagari Fault that runs through the URL area has already been clarified. Since it was assumed that fresh groundwater may have infiltrated deeper based on resistivity profiles obtained in the surface-based investigations and the relationship between the resistivity and the porewater Cl^- concentrations, the 3D distribution of the Omagari Fault was estimated based on the distribution of the high resistivity zone (Figure 4.1.3-8). However, detailed information on the Omagari Fault, including geological characteristics and hydraulic properties, has not been obtained. The information, compiled as a geological structure dataset, includes topography, lithostratigraphy, distribution of discontinuity such as faults and fractures and rock properties including density and porosity.

2) Hydraulic properties

It was confirmed by borehole and laboratory hydraulic tests that the hydraulic conductivity of the fracture zone in the Wakkanai Formation is higher by one to four orders of magnitude compared to the background fractured rock. The general trend of hydraulic conductivity with depth (Figure 4.6.2-2), prepared by distinguishing test intervals with or without fractures[62], also indicates that the hydraulic conductivity in an interval with a fractured zone is more likely to affect the overall hydraulic properties of the Wakkanai Formation. On the other hand, a significant difference in hydraulic conductivity for intervals with and without fracture zones is not observed in the Koetoi Formation, although the formation does contain fracture zones. The reason for this is considered to be that the fractures in the Koetoi Formation are less open compared to those in Wakkanai Formation; the rock of the Koetoi Formation is soft and the development of fractures is limited. Data on surface hydrology, such as river runoff, groundwater levels, hydraulic conductivity and hydraulic head, were compiled as the hydraulic property dataset.

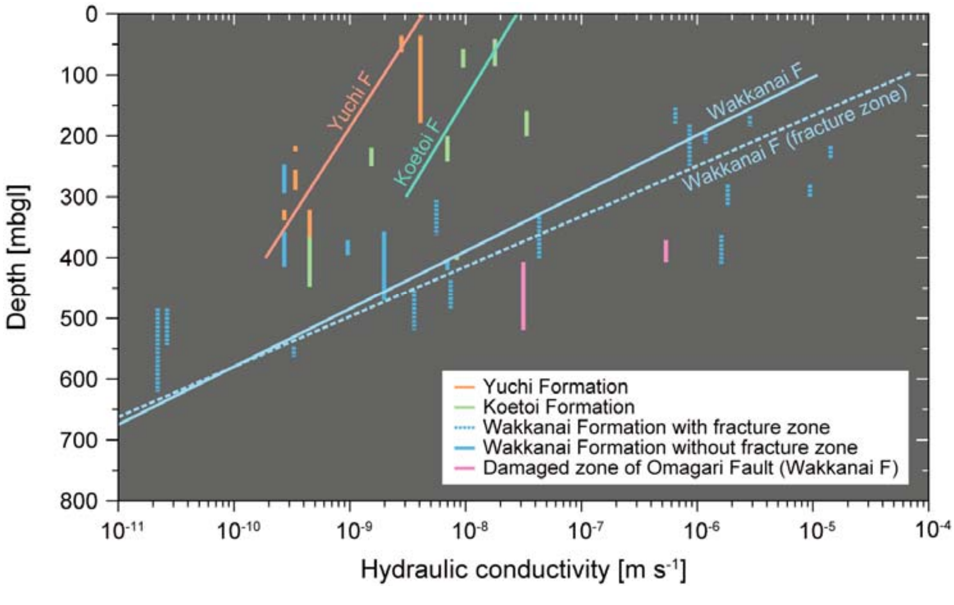

Figure 4.6.2-2 General trend of hydraulic conductivity versus depth for different formations

3) Hydrochemical properties

The occurrence of groundwater with a low concentration of dissolved components (Na-HCO_3 type) in shallower subsurface and a high concentration of dissolved components (Na-Cl type) in deeper subsurface is known based on the results of analyses of groundwater chemistry carried out for samples collected in deep borehole investigations (Figure 4.3.3-2). The Cl^- concentration estimated using the geostatistical method indicates that fresh water has infiltrated relatively deeper in the east of the URL area (Figure 4.6.2-3). The information compiled as a hydrochemical dataset includes chemical compositions of the rocks, mineral compositions and groundwater chemistry.

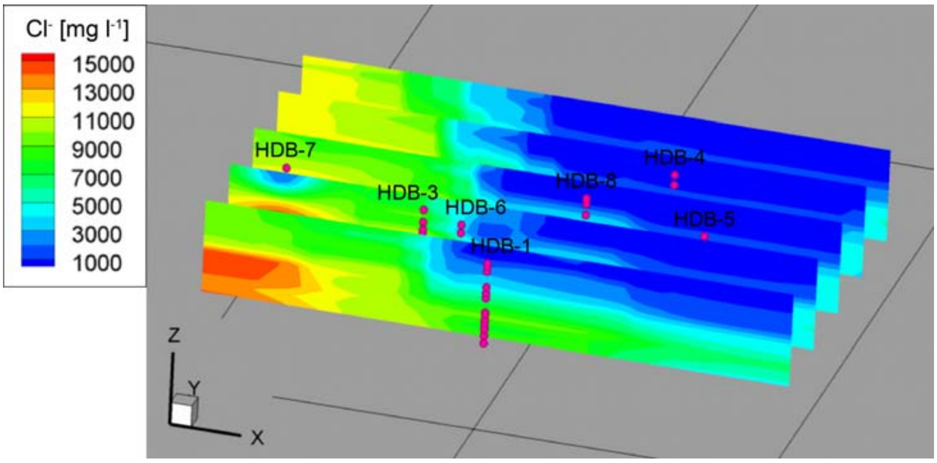

Figure 4.6.2-3 Spatial distribution of Cl concentration in groundwaters around the URL site

(3) Groundwater streamlines

The geological model was constructed[87], as shown in Figure 4.6.2-4, based on the information (datasets) and interpretation of data described above. This model does not incorporate the occurrence of the fractured zones deterministically because of insufficient information on their distribution and hydraulic conductivity However, the Omagari Fault was modelled as having an en echelon structure based on the estimated 3D distribution of the fault. A conceptual model of the hydrogeological structure was also constructed for analysis of groundwater flow based on the geological model and interpretation of the hydraulic properties[62] (Figure 4.6.2-5).

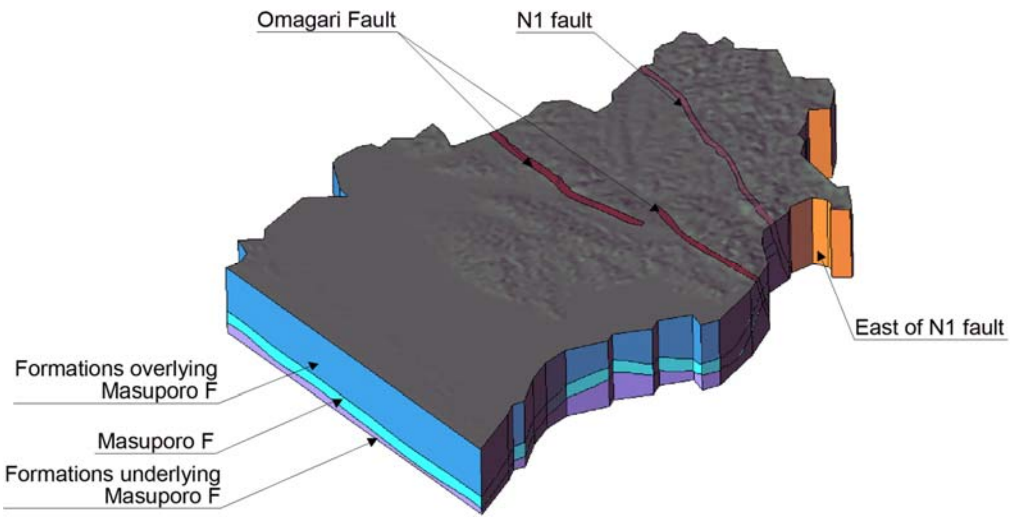

Figure 4.6.2-4 Finite element mesh based on the geological model

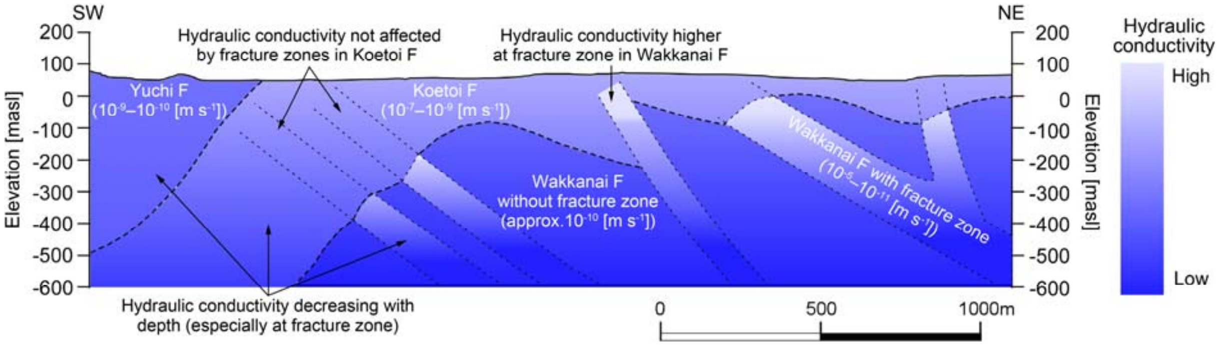

Figure 4.6.2-5 Conceptual hydrogeological model

The analytical region covered an area of about 30 km × 30 km square extending from the eastern edge (the Teshio Mountains) to the western edge (shoreline) of the Teshio River basin, which encompass the whole area of the Horonobe Town. The formations of interest, according to the hydrogeological classification, include the formations underlying the Masuporo Formation, the Masuporo Formation, the Wakkanai Formation, the Koetoi Formation, the Yuchi Formation and the Sarabetsu Formation, as well as surface layers and the Omagari Fault. A set of parameters for analysis was defined, taking into account the uncertainties in measured values and the fact that data on the hydraulic conductivity and upper boundary conditions were not obtained for some formations, as shown in Table 4.6.2-1. The analysis of groundwater flow was then conducted for 18 cases (Cases 001–018; Table 4.6.2-2) using hydraulic conductivity and the upper boundary conditions of each formation as parameters.

Case 001 is the reference case. The parameters for the reference case were determined based on the following, taking the results of the borehole investigations into consideration:

- The hydraulic conductivity of the damaged zone of the Omagari Fault, obtained in borehole HDB-4, is adopted as the hydraulic conductivity of the fault.
- The depth dependence is assumed for the hydraulic conductivity of the Yuchi Formation, since the deviation from the approximation line is smaller and the reliability is better.
- The logarithmic mean is adopted for the hydraulic conductivity of the Koetoi Formation, since the deviation from the approximation line is not as large as in the case of the Yuchi Formation and a significant depth dependence was not observed compared to the Yuchi Formation.
- Bulk hydraulic conductivity is adopted without differentiating between background fractured rock and fractured zones and the depth dependence is assumed for the hydraulic conductivity of the Wakkanai Formation.
- The seepage surface is used as an upper boundary condition, where water level is fixed to atmospheric pressure when the groundwater level has reached the ground surface at a given amount of rainfall.
- A lower impermeable boundary is set at -5,000 m elevation. Sea level forms the upper water level boundary in areas, covered by the sea, and in-land areas, ridges and valleys are set as impermeable boundaries.

In Cases 006–014, the hydraulic conductivities for the Yuchi, Koetoi and Wakkanai Formations were varied within a possible range with reference to measured values. Cases 002–005 and 015–017 are those for the sensitivity analysis focussed on the hydraulic conductivity of the formations without actual measurements. Case 018 was a hypothetical case assuming abnormally high pressure in the deep subsurface.

Comparison with measurements of water pressure obtained by hydraulic tests and long-term monitoring indicates that Case 003 best represents the measured water pressure distribution. This analysis was compared with the recharge rate[68)] obtained from the surface-based investigations and showed relatively good agreement with the measured values. Based on the above results, streamlines to be used in the solute transport analyses were determined, with the starting-point being at the mid-point of three shafts at -390 m elevation (about 450 m depth), as shown in Figure 4.6.2-6. This corresponds to ‘conceptualisation/modelling/simulation’ in the geosynthesis data flow diagram.

Table 4.6.2-1 Parameter settings for analysis

Unit	ID	Hydraulic conductivity [m s^{-1}]	Basis for setting
Surface	Sur1	1.00×10^{-6}	Estimated from general information
	Sur2	1.00×10^{-7}	One order of magnitude lower than Sur1
	Sur3	1.00×10^{-5}	One order of magnitude higher than Sur1
Sarabetsu Formation	S1	1.00×10^{-6}	Derived from re-evaluation of D-1 hydraulic test result
	S2	1.00×10^{-5}	One order of magnitude higher than S1
Yuchi Formation	Y1	$\log_{10} K = -0.0034 z - 8.3665$	General trend of hydraulic conductivity (K) with depth (z)
	Y2	$\log_{10} K = -0.0034 z - 9.3665$	One order of magnitude lower than Y1
	Y3	$\log_{10} K = -0.0034 z - 7.3665$	One order of magnitude higher than Y1
	Y4	7.31×10^{-10}	Logarithmic average
Koetoi Formation	K1	9.07×10^{-9}	Logarithmic average
	K2	9.07×10^{-10}	One order of magnitude lower than K1
	K3	9.07×10^{-8}	One order of magnitude higher than K1
	K4	$\log_{10} K = -0.0032 z - 7.5549$	General trend of hydraulic conductivity (K) with depth (z)
Wakkanai Formation	W1	$\log_{10} K = -0.0105 z - 3.9118$	General trend of hydraulic conductivity (K) with depth (z)
	W2	$\log_{10} K = -0.0105 z - 4.9118$	One order of magnitude lower than W1
	W3	$\log_{10} K = -0.0105 z - 2.9118$	One order of magnitude higher than W1
	W4	1.14×10^{-8}	Logarithmic average
Masuporo Formation	M1	5.00×10^{-10}	Relatively high at depth because of lithofacies
	M2	5.00×10^{-8}	Two orders of magnitude higher than M1
Omagari Fault	D1	1.30×10^{-7}	Logarithmic average obtained in borehole HDB-4
	D2	$\log_{10} K = -0.0121 z - 2.9848$	General trend of hydraulic conductivity (K) with depth (z) for fracture zones in the Wakkanai F
	D3	$K_{parallel} = 1.30 \times 10^{-7}$ $K_{perpendicular} = 1.30 \times 10^{-9}$	Anisotropy assumed
Boundary condition	B1	Sides/bottom: no flow (shoreline: hydrostatic) Top: 1 mm d^{-1} precipitation	Based on existing information
	B2	Top: 3 mm d^{-1} precipitation	Case for examining the influence of precipitation
	B3	Bottom: fixed head 500 m higher than hydrostatic condition	Case for examining the influence of high pressure at depth

Table 4.6.2-2 Analytical cases

Cases	Surface	Sarabetsu F	Yuchi F	Koetoi F	Wakkanai F	Masuporo F	Omagari Fault	Boundary condition
Case 001	Sur1	S1	Y1	K1	W1	M1	D1	B1
Case 002	Sur1	S1	Y1	K1	W1	M1	D1	B2
Case 003	Sur2	S1	Y1	K1	W1	M1	D1	B1
Case 004	Sur3	S1	Y1	K1	W1	M1	D1	B1
Case 005	Sur1	S2	Y1	K1	W1	M1	D1	B1
Case 006	Sur1	S1	Y2	K1	W1	M1	D1	B1
Case 007	Sur1	S1	Y3	K1	W1	M1	D1	B1
Case 008	Sur1	S1	Y4	K1	W1	M1	D1	B1
Case 009	Sur1	S1	Y1	K2	W1	M1	D1	B1
Case 010	Sur1	S1	Y1	K3	W1	M1	D1	B1
Case 011	Sur1	S1	Y1	K4	W1	M1	D1	B1
Case 012	Sur1	S1	Y1	K1	W2	M1	D1	B1
Case 013	Sur1	S1	Y1	K1	W3	M1	D1	B1
Case 014	Sur1	S1	Y1	K1	W4	M1	D1	B1
Case 015	Sur1	S1	Y1	K1	W1	M2	D1	B1
Case 016	Sur1	S1	Y1	K1	W1	M1	D2	B1
Case 017	Sur1	S1	Y1	K1	W1	M1	D3	B1
Case 018	Sur1	S1	Y1	K1	W1	M1	D1	B3

● Parameters deviated from the reference values are given in yellow cells.

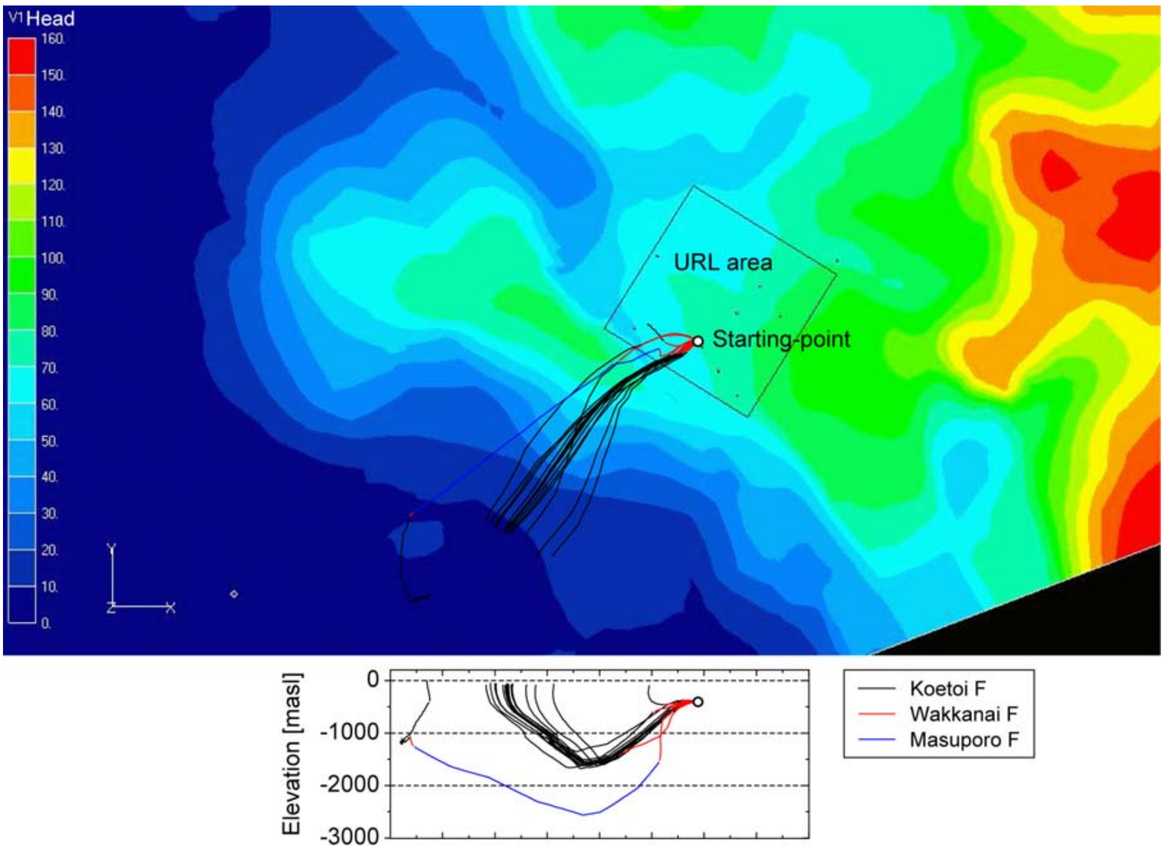

Figure 4.6.2-6 Horizontal distribution of hydraulic head at -400 masl (Case 003) and groundwater flow paths from the starting-point

(4) Compilation of information for solute transport analysis

Information on the geological environment, used directly to describe solute transport in the Wakkanai and Koetoi Formations, was determined as below, based on the information described above and discussions on the streamlines of groundwater:

- hydrogeological structure and hydraulic properties (from the hydraulic dataset and hydrogeological model), involving conceptual hydrogeological model, porosity and hydraulic conductivity;
- solute transport paths (from the results of the groundwater flow analysis), specifically travel time, travel distance and transport paths;
- groundwater chemistry (from the hydrochemical dataset and model);
- mineral compositions (from the geological dataset);
- rock properties (from the geological dataset), particularly porosity and density.

(5) Setting parameters for solute transport analysis

Modelling of solute transport in geological formations was studied for the reference scenario developed in the H12 report[95] and the solute transport for each segment of the trajectory, which was calculated from particle tracking at each time step and/or element, was expressed by applying a 1D porous medium model (Figure 4.6.2-7). For this solute transport model, the following three parameters were examined to describe solute transport in the geological environment, out of the nine parameters required for the solute transport analysis:

- flow vector along the streamline;
- travel distance along the transport path;
- porosity, real density and dry density of the geological formation.

The flow vector along the streamline was obtained from Darcy's velocity divided by the hydraulic effective porosity. Darcy's velocity and travel distance were obtained from the groundwater flow analyses (Figure 4.6.2-8). The analytical results for groundwater flow for the 18 cases previously discussed were used for Darcy's velocity and the travel distance. When the analysis of solute transport was conducted in a way that directly introduced the heterogeneity of the information on the solute transport, Darcy's velocity and the information on travel distance for the segment of trajectory in Cases 003, 010, 013 and 014 were used. On the other hand, when the analysis was conducted in a way that introduced the heterogeneity of the information simplified by a statistical process, Darcy's velocity and the travel distance were based on Case 003 that best represents the distribution of the measured water pressure. The range of uncertainty was established by referring to the variability of other analysis results for groundwater flow.

The hydraulic effective porosity was selected by referring to measurements on rock specimens, taking into account the results of geophysical logging in boreholes, since there were no in situ measurements such as tracer tests. A compound lithological analysis was conducted to obtain the typical porosity of the Wakkanai and Koetoi Formations for the overall interpretation of the results of the geophysical logging, including sonic wave, neutron, natural gamma ray and calliper surveys[77] (Figure 4.6.2-9). The range of uncertainty was set as 1/10, referring to the porosity estimated by applying the existing relationship between the transmissivity and the width of the aperture of water-conducting fractures. The representative values described above and the range of uncertainty were also adopted as the porosity of the stratum. As the real density of the geological formation, that measured for rock cores collected in borehole HDB-6 was adopted. Using this value and established porosities, dry densities were then determined. These values were also adopted to set the diffusion coefficient of the formation.

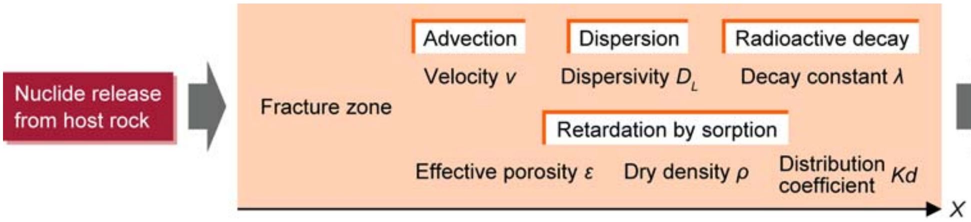

Figure 4.6.2-7 Conceptual solute transport model for porous sedimentary rock

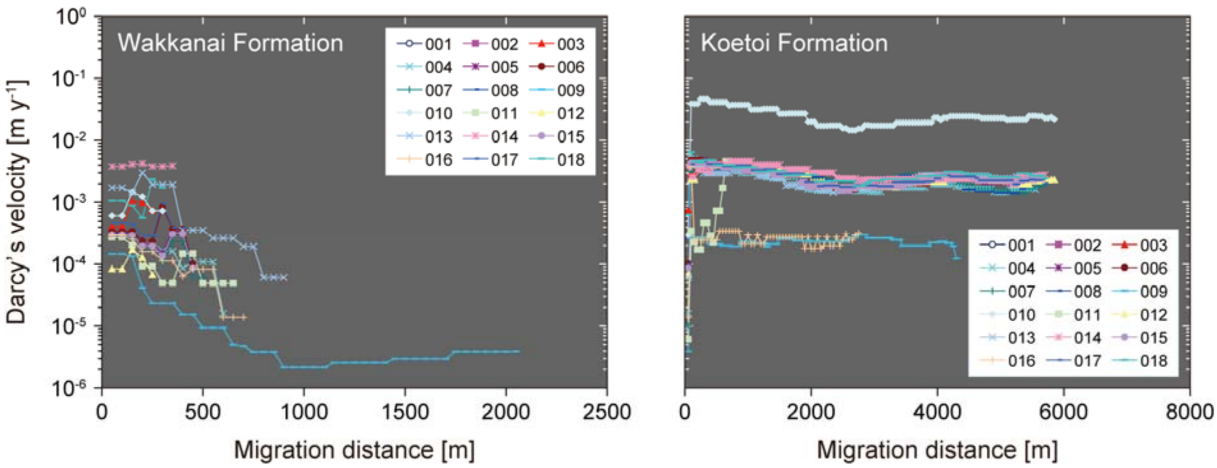

Figure 4.6.2-8 Relationship between Darcy's velocity and migration distance for each analytical case

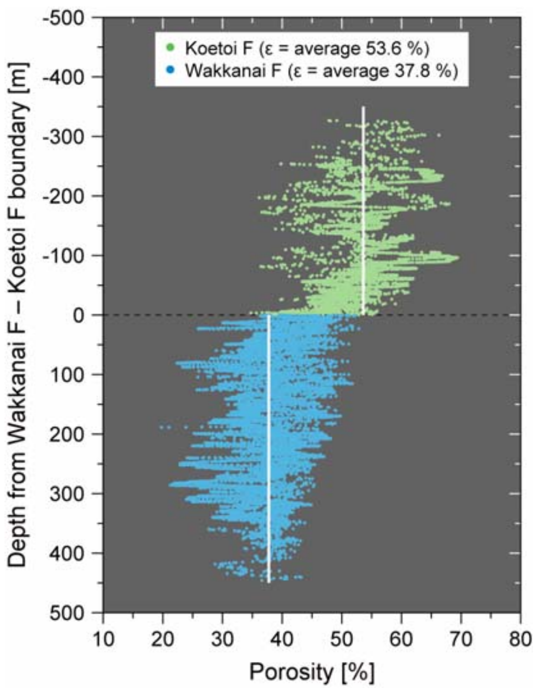

Figure 4.6.2-9 Vertical distribution of porosity estimated by compound log analysis

Information on groundwater composition is of help to establish the distribution coefficient and solubility for the solute transport analysis. Since the groundwater composition around a depth of 450 m was not directly determined in the URL site, the analytical results for the groundwater in borehole HDB-6, closest to the URL, were used for estimation[232] by considering the depth dependency of groundwater chemistry, the results of a thermodynamic analysis of the groundwater and mineralogical information obtained.

For the solute transport analysis, flux in the EDZ, diffusion coefficients and distribution coefficients of rock and buffer materials and solubility in the buffer materials were also determined, in addition to the parameters for describing solute transport in the sedimentary formation. These are described in detail in the Volume “Geological Disposal Research”.

(6) Results of solute transport analyses and feedback to the surface-based investigations

Solute transport analyses were conducted for a total of five cases, considering uncertainties in Darcy’s velocity, streamlines, hydraulic effective porosity and distribution coefficient. As a result, not only could the sensitivity of each parameter be understood, but parameters and models could also be set up and know-how for the analyses compiled.

Looking at the results of the solute transport analyses, a very high retardation effect was indicated both in the Wakkanai and Koetoi Formations. It is however highly likely that the fractured zone in the Wakkanai Formation functions as a streamline, given the distribution of hydraulic conductivity in the formation. In the present study, based on the results of investigations up to the end of March 2005, the concept of a porous medium was adopted because information regarding the characteristics of the fractured zone had not been compiled. Therefore, in addition to understanding the characteristics of the fractured zone in the Wakkanai Formation and defining a strategy for modelling the formation as a fractured medium, an understanding of the characteristics of fractures in the Koetoi Formation that originated from structural movement in the same period as the Wakkanai Formation would also be required. In the case where the involvement of fractures as streamlines is different between the Wakkanai Formation and the Koetoi Formation, this could be used as an example for modelling and analysis of zones with different retardation effects. The method for determining the hydraulic effective porosity, which has a large impact on the results of the solute transport analysis, must be studied in detail.

As knowledge, such as know-how, decision process, obtained following the work flows (field studies, data interpretation, modelling etc.), various uncertainties associated with the solute transport analyses would be reduced. For both existing information and information gained from the investigations of the geological environment, it is necessary to indicate data quality as a range of uncertainties. Review of the methodologies and solute transport analyses based on new geological information and models will be conducted continuously in order to develop advanced safety assessment methodologies.

4.6.3 Perturbations induced by construction of the underground facilities

(1) Geology and geological structure around the underground facilities

For estimating the hydraulic, hydrochemical and rock mechanical perturbations induced by construction of the underground facilities, the geological structure of the area where these perturbations occur (geological environment around the underground facilities) was characterised in terms of distribution of stratigraphy and lithology and water-conducting fractures, based on the geological models as presented in Subsection 4.1.4 (Figure 4.1.4-2).

1) Stratigraphy and lithological distribution

The strata to be encountered around the underground facilities will be, in ascending order, the Wakkanai Formation, the Koetoi Formation and the surface unconsolidated sediments. Since the mineral and chemical compositions, rock mechanical properties and the groundwater flow field are different between the Wakkanai Formation and the Koetoi Formation as discussed in Sections 4.1–4.4 and the highly permeable zone below the terrace sediments is considered to control groundwater flow in the shallower subsurface, it will be of importance to clarify the 3D distribution (boundary depth) of each stratum.

The depth of the boundary between the Wakkanai Formation and the Koetoi Formation was estimated based on information obtained from surveys of outcrops, reflection seismic survey (including high density) and deep borehole investigations (core logging, bedding plane interpretations based on the Electrical Micro Imaging (EMI™) logging results etc.). The thickness of the surface layer was estimated based on information from surveys of topography (terrace surfaces), reflection seismic survey and shallow borehole investigations (description of facies from rock cores and penetration tests). As a result, it was estimated that the terrace sediments occur down to a depth of about 25 m and the depth of the boundary between the Wakkanai Formation and the Koetoi Formation is around 230 m at the locations of the East and Ventilation Shafts; at the location of the West Shaft, these boundaries are estimated to be around 30 m and 280 m respectively (Figure 4.6.3-1).

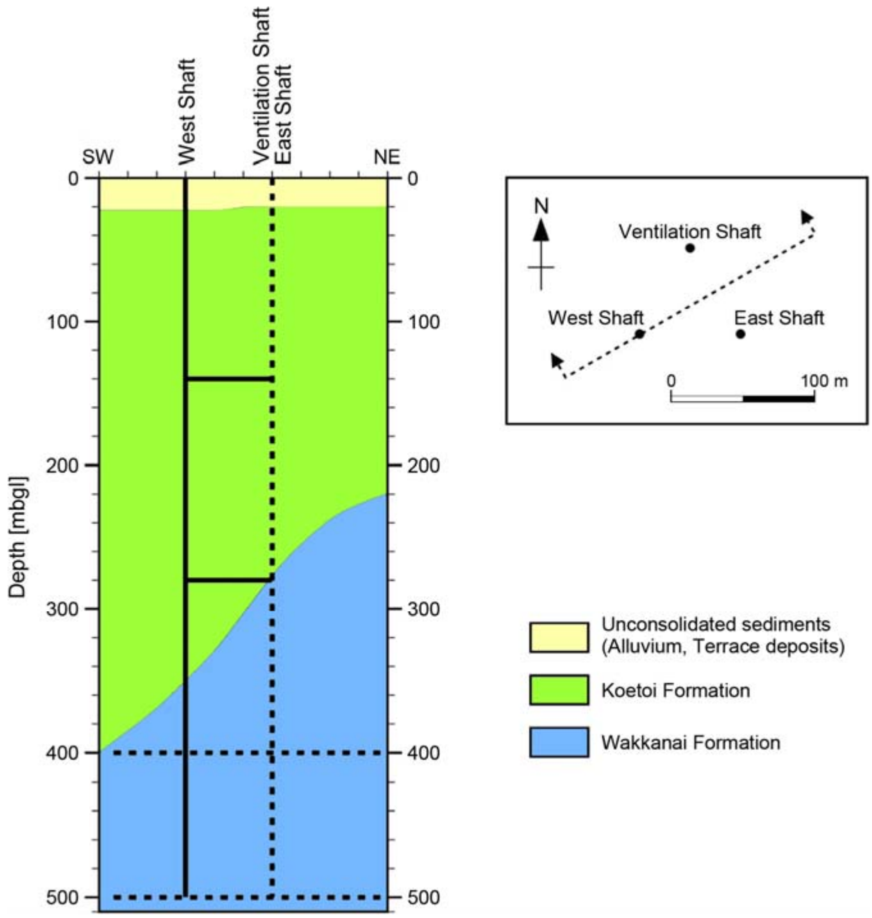

Figure 4.6.3-1 Geological model around the underground facilities

2) Distribution of water-conducting features

The scale and 3D distribution of water-conducting features (WCFs) are of importance for estimating groundwater flow around the underground facilities, particularly the inflow rate generated by construction of the underground facilities. The existence of faults dipping at a high angle to the bedding plane indicating a strike-slip trend, faults horizontal to the bedding plane indicating a dip-slip trend and joints at the anticlinal axis in the Wakkanai Formation was determined by the geological investigations (see Section 4.1). These minor faults may be encountered in the underground facilities but their distribution could not been well characterised from the results of investigations in boreholes HDB-3 and HDB-6, drilled around the underground facilities, or from surveys of outcrops.

(2) Change in groundwater flow associated with construction of the underground facilities

The construction of the underground facilities would induce hydraulic perturbation (e.g. pore pressure decrease around the facilities, hydraulic gradient directed towards the facilities). The change in the regional groundwater flow and inflow rate into the underground facilities was estimated assuming the geological structure discussed above. The analysis for inflow rate was carried out using the equivalent heterogeneous continuum model[53)] discussed in Section 4.2, assuming that groundwater inflow into the underground facilities would be influenced mainly by the distribution of minor fault zones.

1) Analytical method and conditions

A smaller analytical region was established within the domain discussed in Subsection 4.2.4, modelling three shafts and a horizontal drift (Figure 4.6.3-2). The total head obtained in the analysis in Subsection 4.2.4 was used for the lateral boundary condition. The same hydraulic conductivity was used as in the analysis in Subsection 4.2.4. The specific storage was established by fixing the hydraulic diffusivity, i.e. the ratio of hydraulic conductivity and specific storage, at the point where the hydraulic conductivity was 10^{-7} m s^{-1} or higher, taking the compaction rate of the rock and the water filling the pores in the rock into account; this was because the specific storage obtained by hydraulic tests showed abnormal values at points with a hydraulic conductivity of 10^{-7} m s^{-1} or higher. The excavation timeplan assumed in the analysis is shown in Figure 4.6.3-3. An analysis of ten realisations (the same as in Subsection 4.2.4) was conducted.

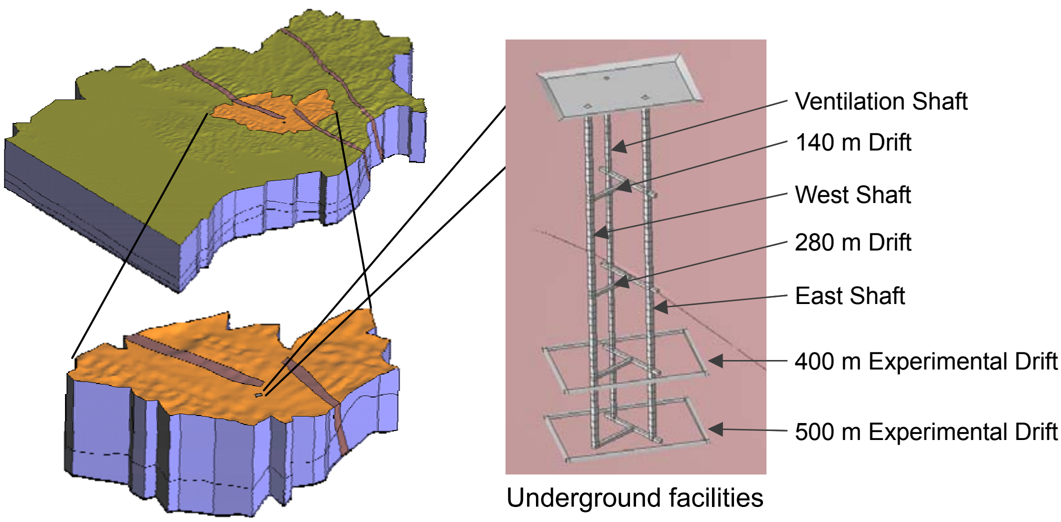

Figure 4.6.3-2 Nested model employed for inflow analysis

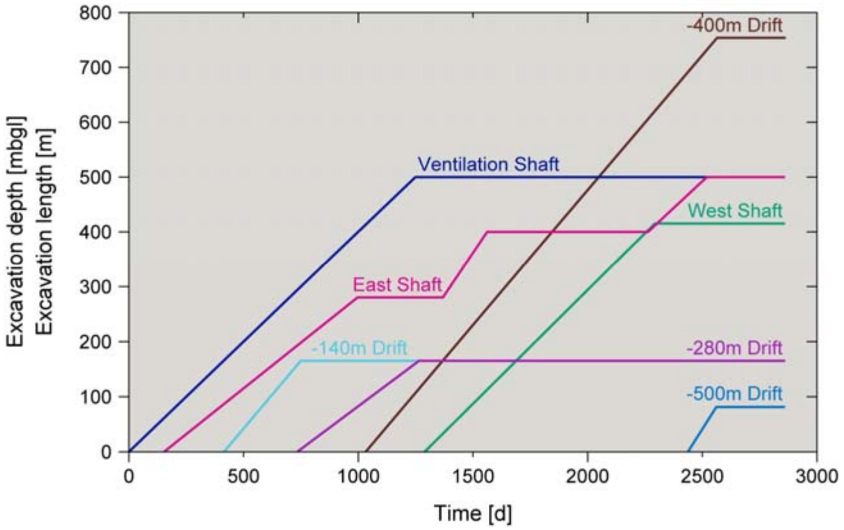

Figure 4.6.3-3 Excavation timeplan assumed in the simulation

2) Analytical results

The results for realisation#1 are shown in Figure 4.6.3-4 as a typical example of the estimation of the inflow rate into the underground facilities. The total inflow rate increased sharply around 600 days after the start of excavation ($\boxed{A}$ and $\boxed{B}$ in the figure) and reached almost the maximum value when completing the excavation of 140 m Drift. In terms of individual shafts and drifts, the inflow rate was large at three locations – the Ventilation Shaft, the 280 m Drift and the 400 m Drift; almost no inflow rate was observed at the East Shaft, the West Shaft and other drifts. This is because the minor fault zones with particularly high permeability in the Wakkanai Formation intersect the above three locations where large inflow rate was observed. The reason for the inflow rate at the 400 m Drift increased while it decreased at the Ventilation Shaft and the 280 m Drift ($\boxed{C}$ in the figure) may be because the 400 m Drift encountered the highly permeable minor fault zones that the Ventilation Shaft and the 280 m Drift had already penetrated.

For all ten realisations where the random value of fault zone formation was changed, the average value and the range of variation of the inflow rate are shown in Figure 4.6.3-5. The plot in the figure indicates the average values for the ten realisations and the bars indicate maximum and minimum values. From this figure, the range of variation due to differences in the distribution of the minor fault zones was as large as 2,000 m^3 d^{-1}. The volume of water inflow started to increase when the Ventilation Shaft, which was excavated ahead of others, reached the Wakkanai Formation (about 600 days after the start) and nearly 80% of the total volume of inflow rate emerged after about 1,250 days, when the shaft excavation was completed. No increase in inflow rate volume was seen at the time when the excavation of the West Shaft began (later than the others). This is thought to be due to the drainage effect, whereby the water pressure around the shaft decreased owing to the inflow rate in the Ventilation Shaft, the East Shaft and the other drifts excavated ahead of the West Shaft.

The distribution of the total head along the vertical cross-section running through the East and West Shafts after construction of the underground facilities is shown in Figure 4.6.3-6 (the result for realisation#1 as an example). For a more comprehensive illustration of the effect of excavating the underground facilities, a contour is shown with the difference from the initial condition before starting the construction. The decrease in total head caused by the construction was distributed as if it were separated by the minor fault zones around the underground facilities, i.e. total head decreased in the area surrounded by the minor fault zones and the impact behind them was small, suggesting the formation of so-called compartments.

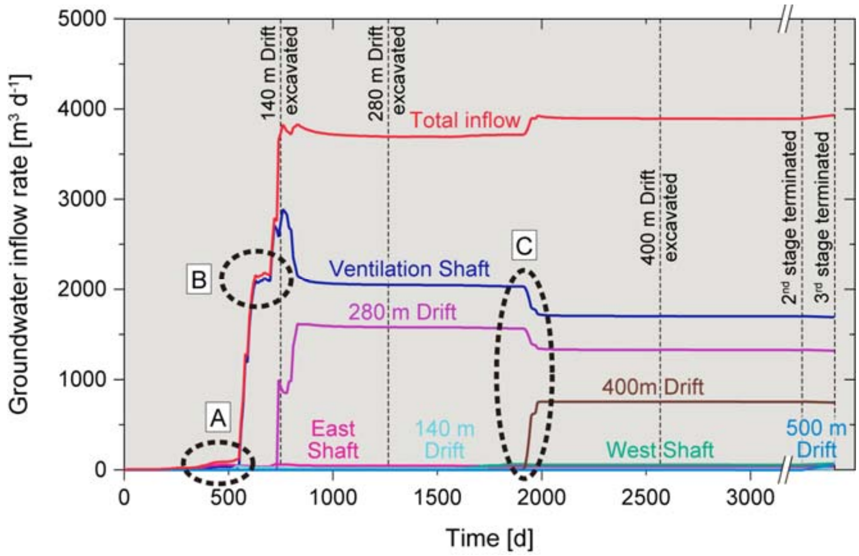

Figure 4.6.3-4 Estimation of groundwater flow into the underground facilities (realisation#1)

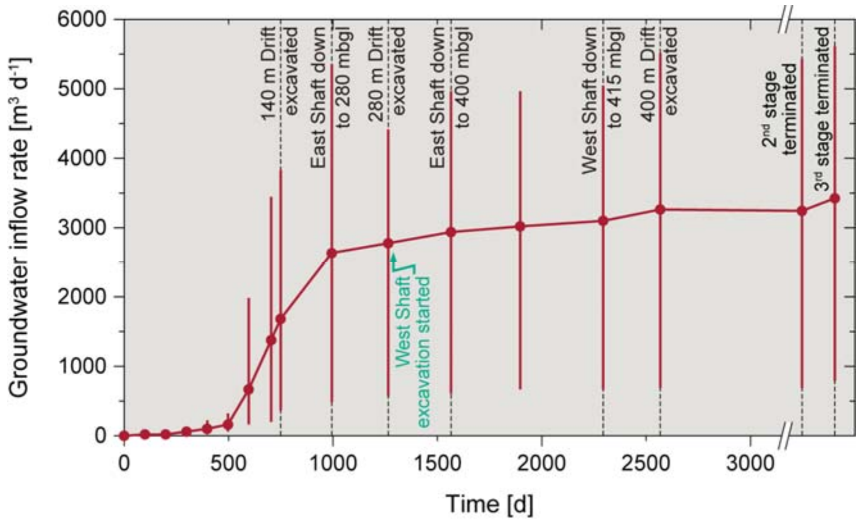

Figure 4.6.3-5 Groundwater flow into the underground facilities (all realisations)

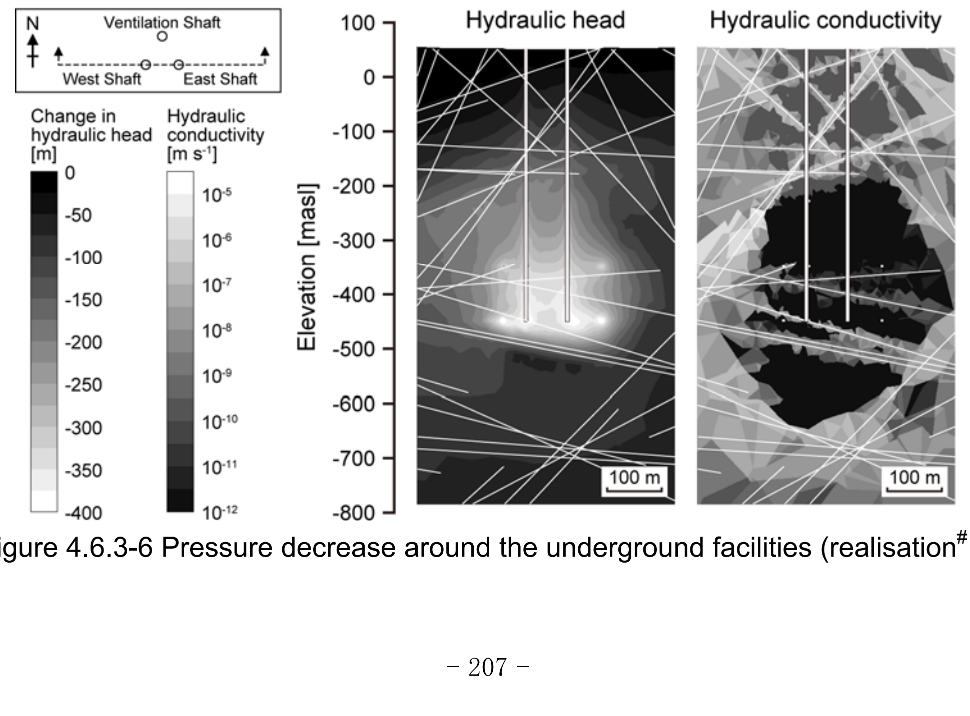

Figure 4.6.3-6 Pressure decrease around the underground facilities (realisation#1)

(3) Change in groundwater chemistry associated with construction of the underground facilities

The construction of the underground facilities would cause a groundwater flow that draws surface water and eventually causes a change in groundwater chemistry by mixing between the meteoric water, shallow subsurface water and deep groundwater. In addition, a flow path created through excavation would supply atmospheric O_2 to the surrounding rock via shafts and drift. For dissolved gases in the groundwater (e.g. CO_2 and CH_4), degassing would be expected owing to the lowered pressure around the shafts. These phenomena constitute hydrochemical perturbations that occur associated with the excavation of shafts etc. and should be interpreted as chemical reactions in the gas phase (i.e. O_2, CO_2 and CH_4), the liquid phase (groundwater) and the solid phase (i.e. concrete lining and rock).

1) Analytical method

The change in groundwater chemistry around the underground facilities induced by construction was analysed on two scales: about 4 km × 8 km around the URL site and approximately 3 km radius around the underground facilities. The computer code TOUGHREACT EOS2[236] was used in this analysis, which was developed based on the non-isothermal/multi-component/multi-phase groundwater analysis code TOUGH2V2.0[237], to which geochemical calculations and a solute transport analysis function were added. The processes that the code can address include transfer of multi-component/multi-phase fluid and heat, migration of chemical species in gas and liquid phases by advection/diffusion, formation of water-soluble complexes, acid-base reactions, redox reactions, dissolution of gas or degassing, dissolution/formation of minerals, cation exchange reactions and surface sorption[238),239].

For the analysis addressing the effects of degassing and the change in water chemistry owing to lowering of the water pressure on a regional scale, the analysis domain was set as the area with about 4 km × 8 km, centring on the URL site (Figure 4.6.3-7). The analysis mesh used to estimate the changes in groundwater chemistry was more elaborate near the underground facilities, where the changes in groundwater flow field and chemistry were expected to be larger (Figure 4.6.3-8).

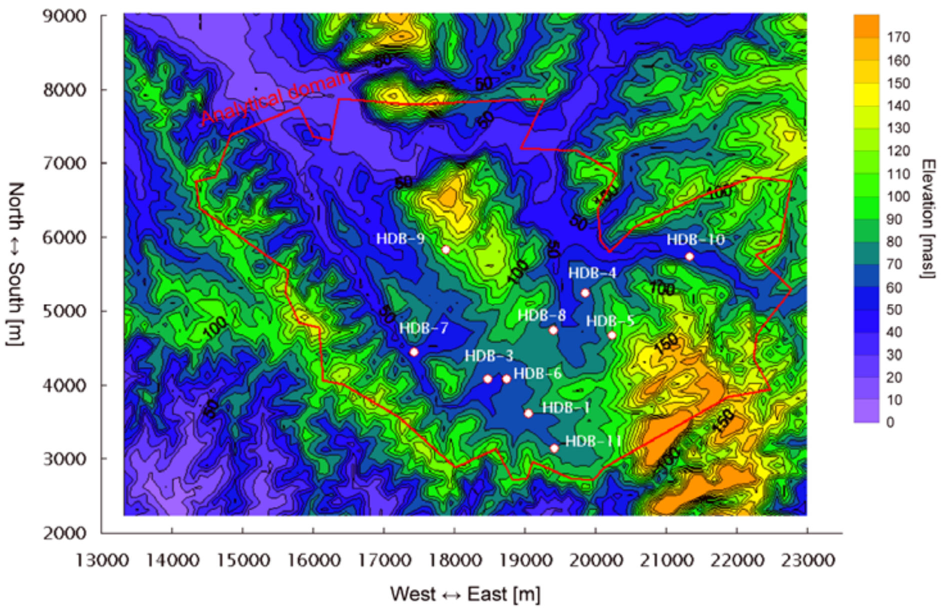

Figure 4.6.3-7 Domain for analysis on a regional scale

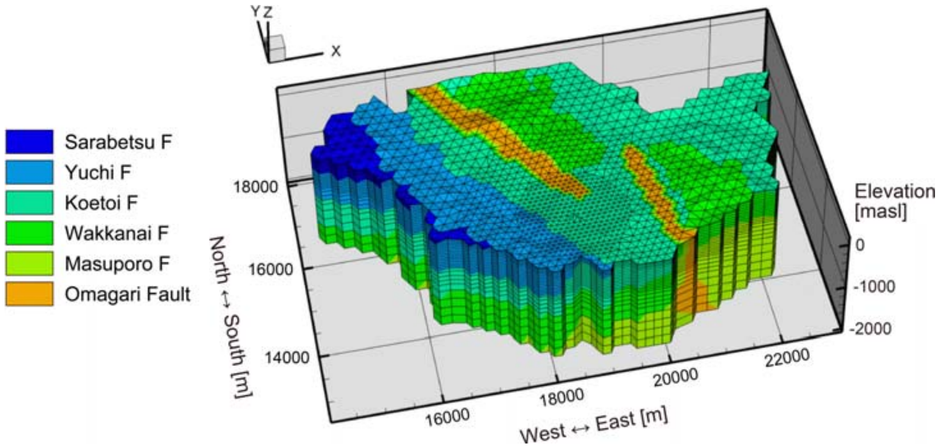

Figure 4.6.3-8 Hydrogeological model for the regional-scale analysis

For the scoping analysis of changes in groundwater chemistry around the shafts owing to degassing of CO_2 from the groundwater, a coupled analysis of a two-phase flow (CO_2 and water) was carried out to examine chemical reactions around the shaft (e.g. pH, calcite precipitation etc.), as shown in Figure 4.6.3-9. A homogeneous 1D axially symmetric model with a 3 km radius and 1 m thickness was applied for analysing the rock – water – (gaseous phase) reaction around the shafts (Figure 4.6.3-10).

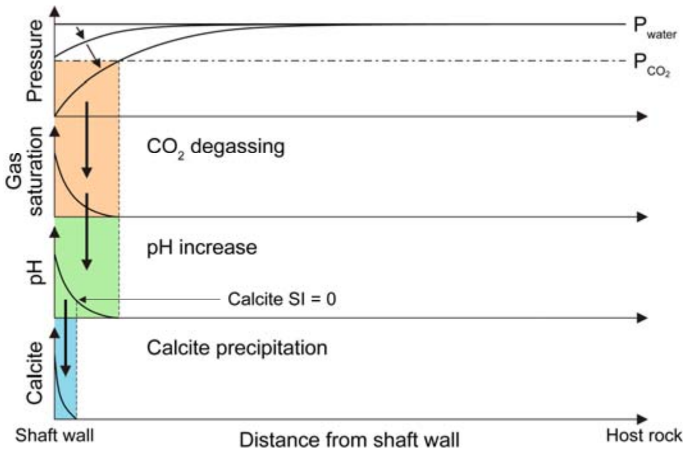

Figure 4.6.3-9 Potential phenomena around the shaft

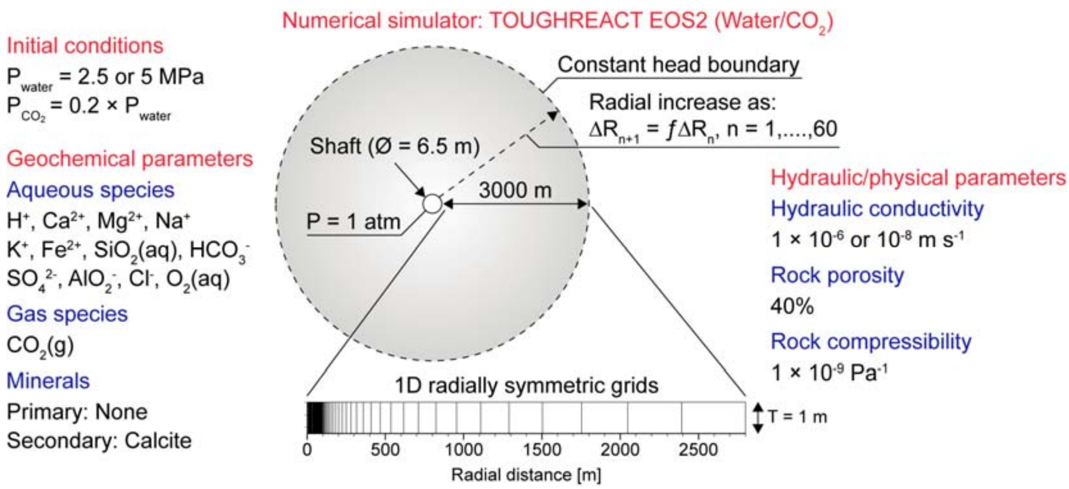

Figure 4.6.3-10 1D model for analysing the rock-water-(gaseous phase) reaction

2) Analytical conditions

For the regional scale analysis, the surface boundary was defined as the rainfall recharge condition and the side and bottom boundaries were defined as being impermeable. In order to establish the rainfall recharge as the surface boundary condition, the groundwater flow analysis was conducted for a rainfall recharge of 3–600 mm y^{-1} and the result was compared with the measurements. Since the hydraulic head of the groundwater changed little compared with the two order of magnitude change in the rainfall recharge, the estimated rainfall recharge around the URL site, 300 mm y^{-1}, was used as the boundary condition. The condition for the shaft walls after excavation had been assumed to be atmospheric pressure, but was actually set considering the flow rate from the grid where the shafts are allocated[239)]. The depth of three shafts was set as 500 m and the excavation process was not taken into account.

For the analysis addressing the rock – water – (gaseous phase) reaction around the shafts, the partial pressure of CO_2 was fixed as 20% of the total pressure and the temperature as 25°C. The pressure at the boundary was fixed. The groundwater chemistry obtained from borehole HDB-6 was used as the initial condition. The groundwater chemistry was calculated assuming that the partial pressure of CO_2 was increased to a certain point. Calcite was selected as the secondary mineral formed as a result of degassing. The calcite tends to be affected by the partial pressure of CO_2 and is easily formed or dissolved over a short period of time. Before setting the partial pressure of CO_2, a hydrochemical calculation was carried out using the Geochemical Workbench for the pH, mineral compositions and sedimentation. The partial pressure of CO_2 was calculated from the HCO_3^- concentration and pH obtained from the investigations in boreholes HDB-1 to HDB-8. As a result, the partial pressure of CO_2 was higher than that in the atmospheric air and was likely to increase to a maximum of 0.02 MPa with increasing depth. Since the groundwater samples were collected at the surface, the partial pressure of CO_2 in situ would be even higher. For the analysis, therefore, the gas phase molar ratio at depths of about 250 m and 500 m was defined as 20% and the partial pressure of CO_2 as 0.5 MPa and 1 MPa at the respective depths. In addition, different water/gas relative permeability curves ($\boxed{a}$ and $\boxed{b}$ in Figure 4.6.3-11) were applied for understanding the effect of gas retention in the groundwater. The analysis was then conducted for five cases (Cases 1–5; Figure 4.6.3-11) using the fixed values of rock porosity and compressibility of 40% and 1×10^{-9} Pa^{-1} respectively.

Parameter	Unit	Case 1	Case 2	Case 3	Case 4	Case 5
Hydraulic conductivity	[m s^{-1}]	1×10^{-6}	1×10^{-8}	1×10^{-6}	1×10^{-8}	1×10^{-8}
Relative permeability curve	-	a	a	a	a	b
Hydraulic pressure	[MPa]	2.5	2.5	5	5	5
Initial P_{CO_2}	[MPa]	0.5	0.5	1	1	1

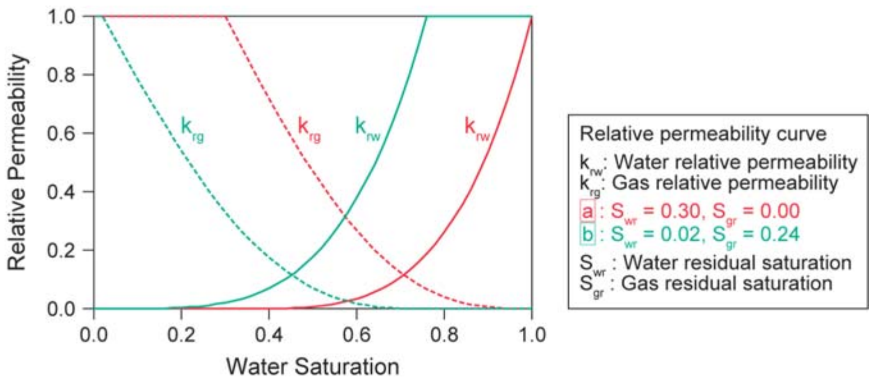

Figure 4.6.3-11 Parameter settings for each analytical case

3) Analytical results

The evolution of the Cl^- concentration is shown as an example of the regional scale analyses in Figure 4.6.3-12. In fractured rock, groundwater would flow preferentially through channels (i.e. interconnected pores) in the fractures. This figure shows the result of an analysis case where the fracture porosity needed for solute transport to occur is extremely small (1%). Groundwater flows towards the shafts, which causes the saline groundwater to be diluted by the fresh water from the ground surface, and a groundwater flow field moving from deep subsurface towards the shafts is formed. From this analysis, the changes in water chemistry depend largely on the rock porosity and on the accuracy of the hydrogeological structure model.

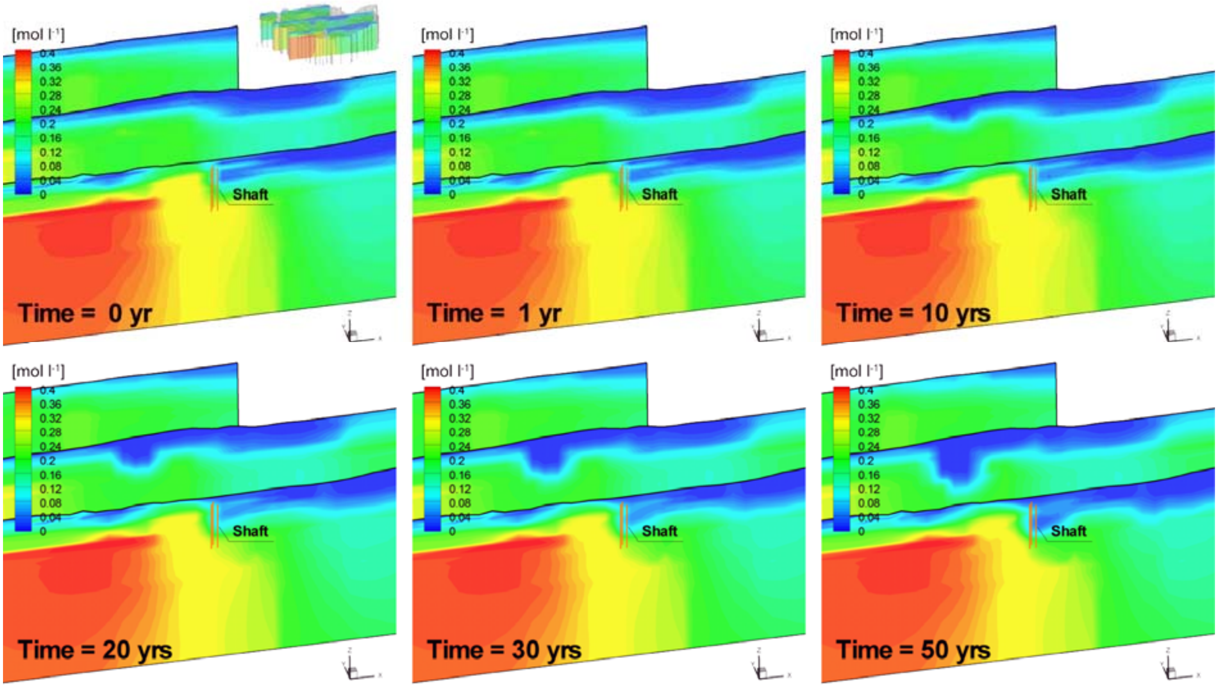

Figure 4.6.3-12 Estimated Cl^- concentration in groundwater during/after shaft excavation

The results of analysis Case 5 are shown in Figure 4.6.3-13 as an example of the analysis addressing the rock – water – (gaseous phase) reaction around the shafts. It indicates that degassing occurs and the partial pressure of CO_2 decreases when the pressure of the groundwater around the shafts becomes lower than the partial pressure of CO_2 (1 MPa) in the groundwater. The decrease in water pressure stops after around five years. The pH decreases in the range where degassing occurs. When the pH is 5.7 or lower, calcite will precipitate.

It has been shown from the results described above that the analysis code TOUGHREACT is applicable for chemical changes (decrease in partial pressure of CO_2 and change in chemical composition), mineralogical changes (such as calcite formation/dissolution) and hydraulic changes (change in hydraulic conductivity with the formation/dissolution of secondary minerals). Together with advances in analytical methods, the accuracy of this approach will be further improved based on observation of changes in water chemistry around the underground facilities associated with the construction of the facilities.

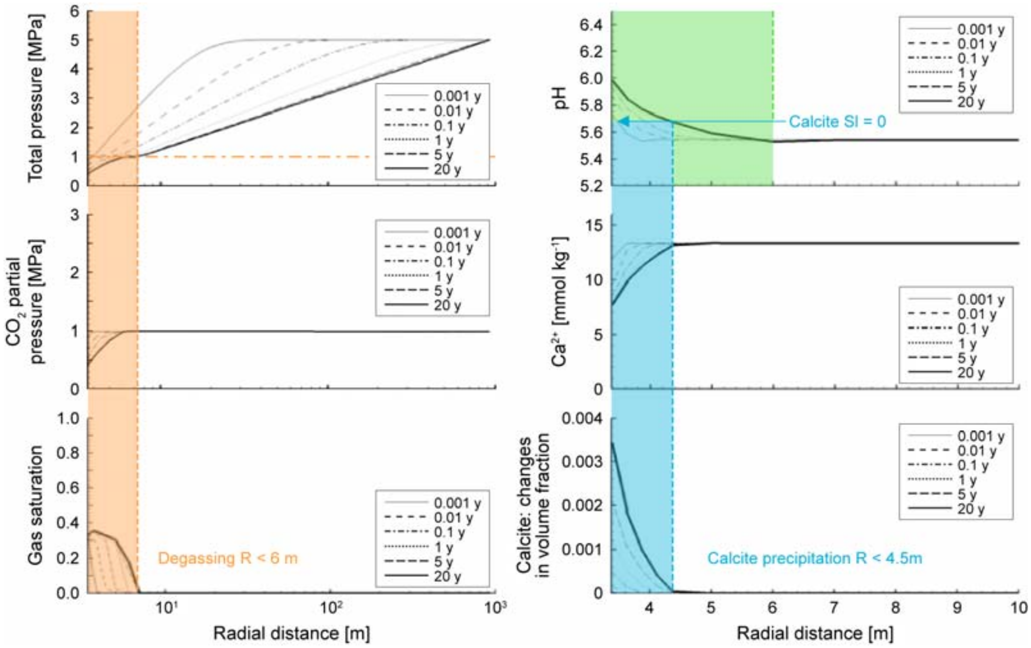

Figure 4.6.3-13 Estimated rock-water-(gaseous phase) reaction around the shaft

(4) Change in rock mechanical properties associated with construction of the underground facilities

A scoping analysis was conducted with the aim of predicting the extent and properties of the EDZ formed in the surrounding rock associated with construction of the underground facilities. The geological structure around the underground facilities shown in Figure 4.6.3-1 and the findings from the investigations discussed in Section 4.4 were taken into consideration.

1) Analytical method and conditions

For modelling the rock, a constitutive law that can express strain softening behaviour was applied for the Wakkanai and Koetoi Formations (Figure 4.6.3-14), based on the findings and conceptual model as discussed in Section 4.4. The rock at the URL site was classified into three zones in terms of its properties in the vertical direction and the properties for the analysis required for the constitutive law were then assigned to each of three zones. Parameters of rock mass properties were determined by fitting the stress-strain curve of the triaxial compression test through trial-and-error in order estimate in situ rock stress conditions. For ZONE 2, where variation of the properties within the zone was large, the analysis was conducted by assigning values separately at the central point of the zone and at the upper boundary (the Koetoi Formation) so that the extent of the EDZ would be large. Mohr – Coulomb type destruction was applied as the standard and the finite difference analysis code FLAC® was used.

The 2D model crossing orthogonally to the shafts and the horizontal drift was used as the basis for the analysis. The cross-sections were selected in the horizontal drifts at depths of 140, 280, 400 and 500 m, where investigations will be focussed in Phase II and data obtained for checking the reliability of the results of the scoping analysis. Since the effects of the strain softening behaviour that will occur with the progress of excavation on the development of the plastic field in the 2D cross-section were unclear, a 3D analysis was also conducted concurrently to visualise the effects (Figure 4.6.3-15). In the 3D analysis, the ultimate specifications and construction processes for the support measures incorporated into the design of the underground facilities was illustrated as close to reality as possible using the model (Figure 4.6.3-16).

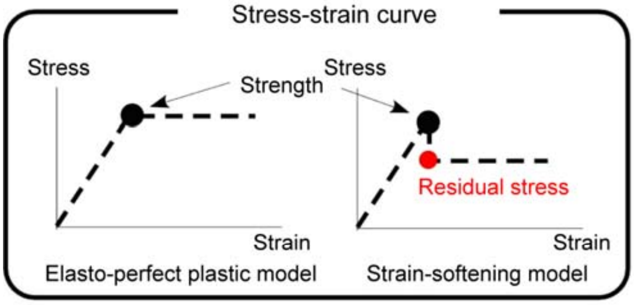

- Strain-softening model was adopted to simulate the exact stress-strain curve.
- Target sections were selected to check the evolution of the EDZ during excavation. The depth was decided based on the results of previous studies.

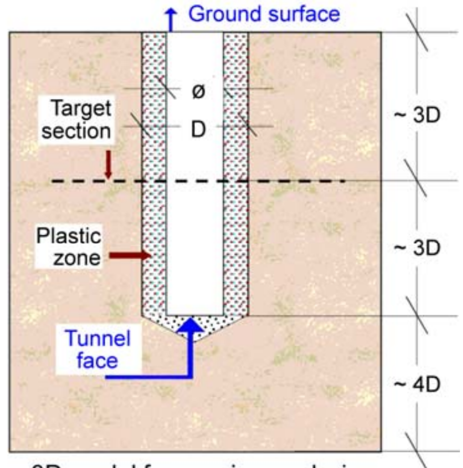

3D model for scoping analysis

Figure 4.6.3-14 Basic concepts for 3D numerical simulation for prediction of the EDZ

Depth [mbgl]	ZONE*	At peak		Residual		Dilation angle ψ** [°]	Unit weight [kN m^{-3}]	Vertical stress [MPa]	Horizontal principal stress†		Elastic modulus E [GPa]	Poisson ratio v [GPa]
		Cohesion C [MPa]	Internal friction angle ø [°]	Cohesion Cr [MPa]	Internal friction angle ør [°]				Maximum σH [MPa]	Minimum σh [MPa]		
140	1	1.50	17.0	0.81	16.4	4.0	15.50	2.13	2.77	1.92	0.30	0.15
220		2.00	12.0	1.08	11.6	4.0	15.70	3.39	4.40	3.05	0.40	0.13
280		2.44	17.5	1.32	16.9	4.0	16.30	4.48	5.82	4.03	0.50	0.08
355	2	1.70 4.10	15.0 25.0	0.80 1.30	17.0 25.0	3.0	15.80 17.10	6.02	7.82	5.42	0.50 0.96	0.10 0.22
400	3	3.56	27.5	0.68	31.2	3.0	18.50	7.26	9.44	6.53	1.25	0.26
450		4.00	27.5	0.76	31.2	3.0	18.70	8.25	10.73	7.43	1.30	0.26

*ZONE defined according to the rock mechanical conceptual model presented in Section 4.4

**ψ: Necessary for strain-softening model

†In situ stress conditions assumed based on the estimated overburden pressure

ZONE 1: σ_H = 4.40 MPa, σ_h = 3.05 MPa; ZONE 2: σ_H = 7.82 MPa, σ_h = 5.42 MPa; ZONE 3: σ_H = 9.44 MPa, σ_h = 6.53 MPa

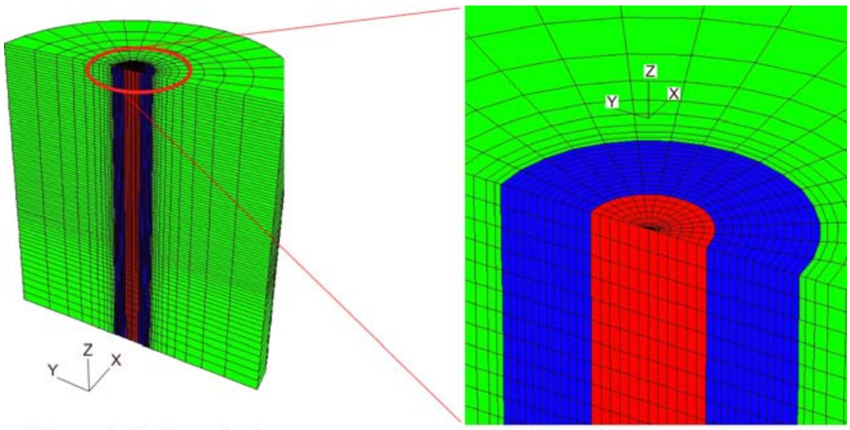

3D mesh (half section)

Red: Shaft, *Blue*: Tunnel near-field

Figure 4.6.3-15 Parameter settings (upper) and 3D mesh (lower) for numerical simulation

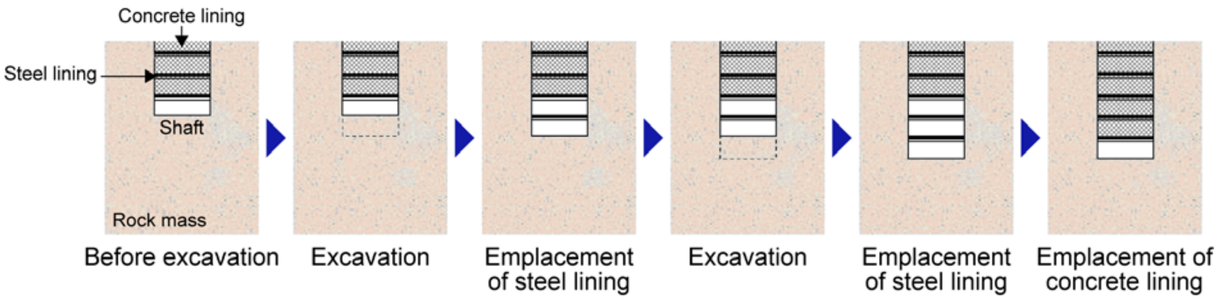

Depth of target section [mbgl]	Scale of 3D modelling [mbgl]	Specifications of supports						
220	190–200	Steel lining (NH-125) H-125 × 125 @ 1.0 m						
		γ [kgf m^{-3}]	E [N m^{-2}]	ν [-]	A [m^2]	Iy [m^4]	Iz [m^4]	J [m^4]
		7.85×10^3	2.10×10^{11}	0.3	30.00×10^{-4}	293×10^{-8}	839×10^{-8}	1.0×10^{-10}
		Concrete lining f'ck = 24 N mm^{-1}						
		γ [kgf m^{-3}]	E [N m^{-2}]	ν [-]	t [m]			
		2.3×10^3	2.5×10^{10}	0.2	0.4			
355	325–425	Steel lining (NH-150) H-150 × 150 @ 1.0 m						
		γ [kgf m^{-3}]	E [N m^{-2}]	ν [-]	A [m^2]	Iy [m^4]	Iz [m^4]	J [m^4]
		7.85×10^3	2.10×10^{11}	0.3	39.65×10^{-4}	563×10^{-8}	1620×10^{-8}	1.0×10^{-10}
		Concrete lining f'ck = 40 N mm^{-1}						
		γ [kgf m^{-3}]	E [N m^{-2}]	ν [-]	t [m]			
		2.3×10^3	2.5×10^{10}	0.2	0.4			
400	370–470	Steel lining (NH-150) H-150 × 150 @ 1.0 m						
		γ [kgf m^{-3}]	E [N m^{-2}]	ν [-]	A [m^2]	Iy [m^4]	Iz [m^4]	J [m^4]
		7.85×10^3	2.10×10^{11}	0.3	39.65×10^{-4}	563×10^{-8}	1620×10^{-8}	1.0×10^{-10}
		Concrete lining f'ck = 40 N mm^{-1}						
		γ [kgf m^{-3}]	E [N m^{-2}]	ν [-]	t [m]			
		2.3×10^3	2.5×10^{10}	0.2	0.4			
450	420–520	Steel lining (NH-150) H-150 × 150 @ 1.0 m						
		γ [kgf m^{-3}]	E [N m^{-2}]	ν [-]	A [m^2]	Iy [m^4]	Iz [m^4]	J [m^4]
		7.85×10^3	2.10×10^{11}	0.3	39.65×10^{-4}	563×10^{-8}	1620×10^{-8}	1.0×10^{-10}
		Concrete lining f'ck = 40 N mm^{-1}						
		γ [kgf m^{-3}]	E [N m^{-2}]	ν [-]	t [m]			
		2.3×10^3	2.5×10^{10}	0.2	0.4			

Figure 4.6.3-16 Model for the excavation process (upper) and the properties of supports (lower)

2) Analytical results

The development of a plastic zone in the rocks around the shafts obtained by the 3D analysis is shown in Figure 4.6.3-17. The result indicates that the plastic zone may extend as wide as a few metres from the tunnel wall, in the case using the properties at the upper boundary of ZONE 2, i.e. the same values as those for the Koetoi Formation. This was inconsistent with the result of the 2D elasto-plastic analysis conducted for designing the underground facilities. This was because the initial stress used for the boundary condition at this cross-section was the value at the centre depth of ZONE 2, which would have been too large. The distribution of stress acting on the tunnel support determined for the working design of the underground facilities was different from the result of the 2D plastic analysis, but, as shown in Figure 4.6.3-18, the stability of the stress distribution was not lost in the 3D analysis.

The extent of the plastic zone obtained by the 3D analysis was compared with that from the 2D analyses, both for the same cross-section as shown in Figure 4.6.3-19. It can be concluded that the extent of the plastic zones derived from both analyses was consistent, with only minor discrepancies. The displacement was larger in the case where strain softening behaviour occurred for the 3D analysis compared to the case for the 2D analysis. Considering the above results, when estimating the extent of EDZ, the sizes of the plastic zone obtained by evaluating the stress and the size of the zone where shear strain exceeds critical shear strain (the Wakkanai Formation: 1.0%, the Koetoi Formation: 0.5%) determined from the laboratory tests were compared and the larger values were taken as the estimated values for the EDZ range.

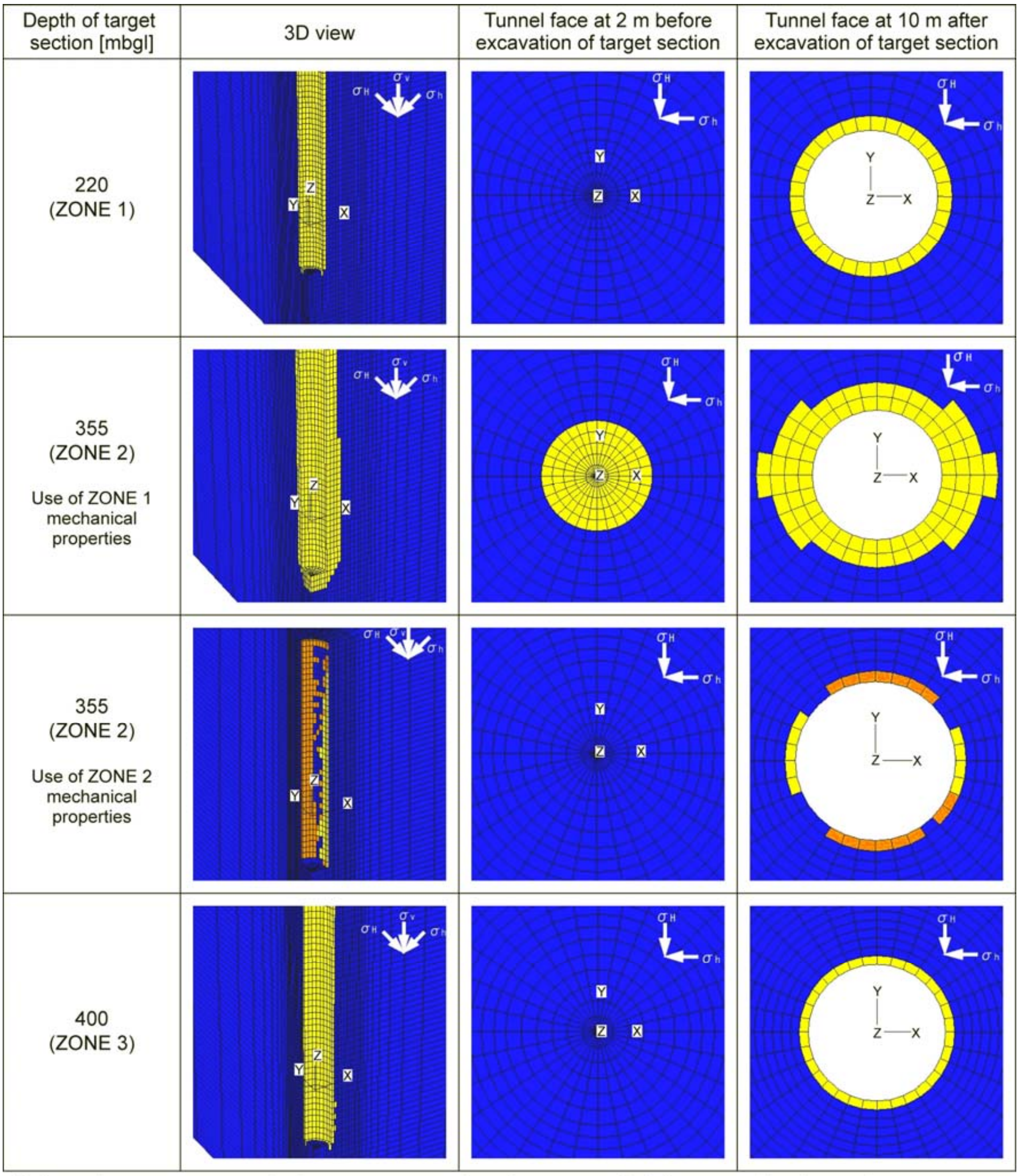

• Yellow colour represents a plastic zone; orange colour shows a tensile failure area (plastic zone).

Figure 4.6.3-17 Calculated extent of plastic zones caused by excavation in the surrounding rock

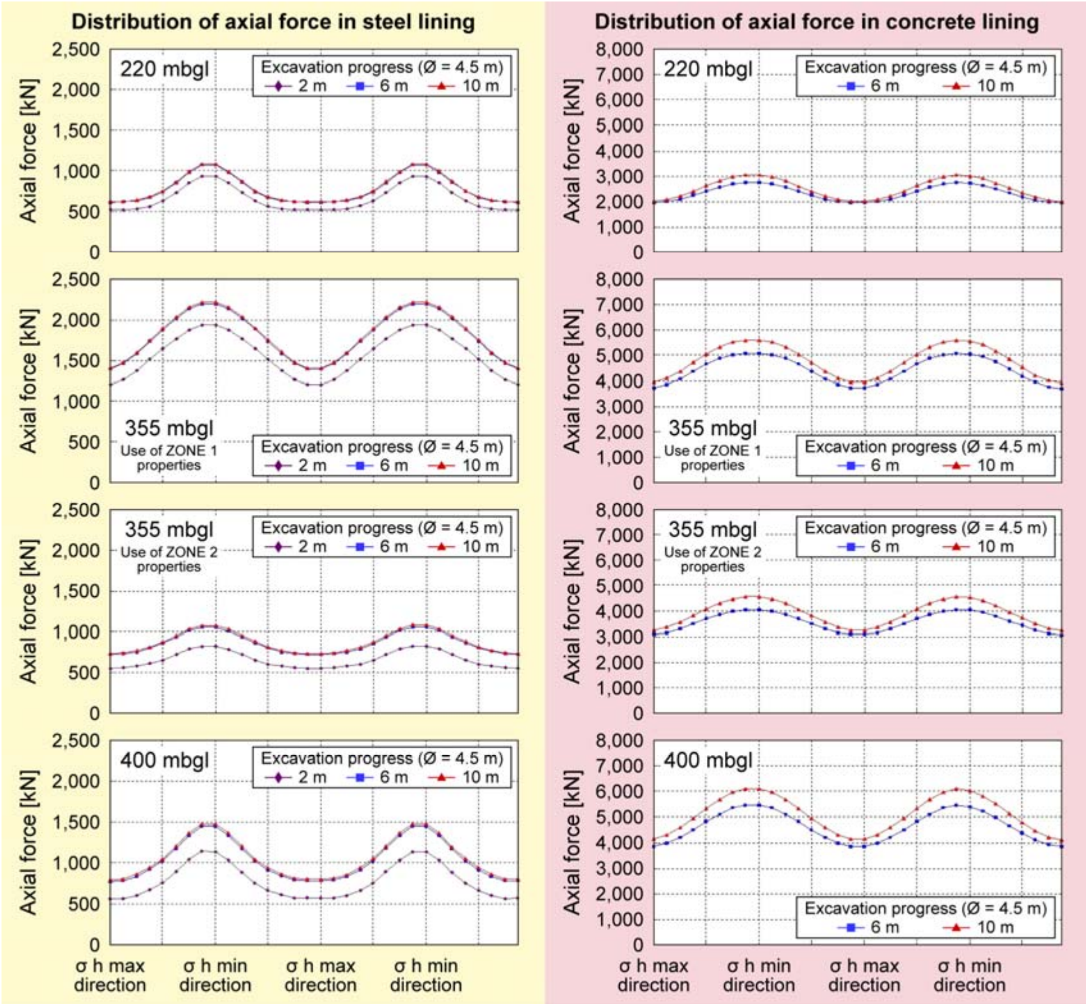

Figure 4.6.3-18 Calculated stresses in the supports of a shaft

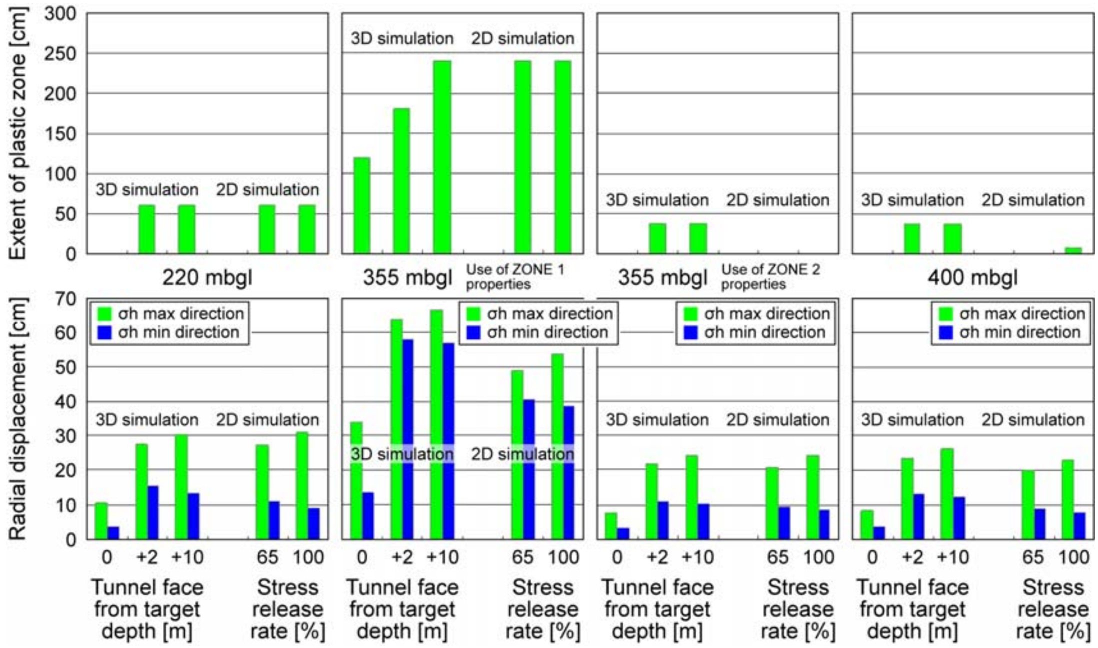

Figure 4.6.3-19 Comparison of the extent of plastic zones (upper) and radial displacements (lower) calculated by 3D and 2D numerical simulation

The conceptual model of the EDZ assumed based on the investigation and test results and the size of the plastic zone estimated analytically, together with the mechanical and hydraulic properties of the plastic zone are shown in Figure 4.6.3-20. The mechanical properties of the EDZ depend on the stress – strain curve in the model; the mechanical properties in the EDZ are under the residual strength and those outside the EDZ are under elastic conditions. The hydraulic properties depend largely on the local shear destruction due to the strain softening and were treated in such a way as to take this dependence into account. Specifically, the range of variation of hydraulic conductivity was determined by considering the depth dependence of hydraulic conductivity and the vertical stress dependence of the hydraulic conductivity of fractures discussed in Section 4.4 and comparing these with the analytically determined stress conditions. As a result, the hydraulic conductivity can vary by about one order of magnitude within the EDZ.

Estimation of the extent and properties of the EDZ (areas A and C)

Depth [mbgl]	ZONE	σv* before excavation [MPa]	σθ* after excavation [MPa]	σθ / σv	Extent of EDZ** [cm]	Area	Degree of property change†				Remarks
							Effective porosity [%]	P-wave velocity [km s^{-1}]	Elastic modulus [GPa]	Hydraulic conductivity [m s^{-1}]	
220	1	4.40	7.0	1.59	60	C	55→45	1.8→2.1	3.0→5.0	10^{-8}→10^{-9}	
280	1	5.82	6.5	1.12	71 Strain-softening	C	55→45	1.9→2.0	4.0→4.4	10^{-9}→10^{-9}	Changes estimated based on σθ on shaft wall
			10.1	1.74		A	55→39	1.9→2.2	4.0→5.8	10^{-9}→10^{-10}	Changes estimated based on $σθ_{max}$ at boundary of yield zone
355	2 Boundary of ZONE1 and ZONE 2	7.82 Middle of ZONE 2	6.3	0.81	240 Strain-softening	C	45→50	2.1→1.9	5.0→4.0	10^{-9}→10^{-9}	Changes estimated based on σθ on shaft wall
			12.1	1.55		A	45→36	2.1→2.3	5.0→6.5	10^{-9}→10^{-10}	Changes estimated based on $σθ_{max}$ at boundary of yield zone
	2 Middle of ZONE 2		13.4	1.71	No area over yield stress or yield shear strain						
400	3	9.44	17.5	1.85	21	A	36→32	2.3→2.2	5.5→5.3	10^{-9}→$5×10^{-10}$	
450	3	10.73	18.5	1.72	37	C	38→34	2.2→2.2	5.2→5.3	10^{-9}→$5×10^{-10}$	

*σv and σθ for the calculated stress at a shaft wall

**Maximum extent over yield stress or yield shear strain

†Evaluated based on a correlation between the distribution of properties and depth

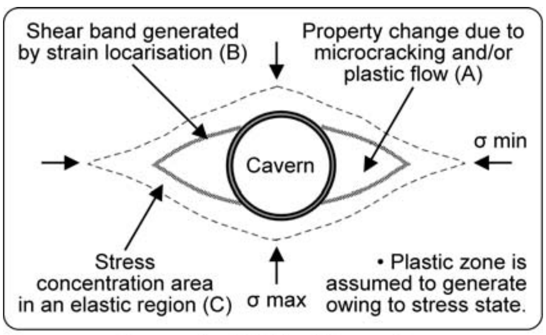

Concept of EDZ at Horonobe

Estimation of the extent and properties of the EDZ (area B)

Depth [mbgl]	ZONE	σθ* after excavation [MPa]	Pore pressure [MPa]	σθ' [MPa]	Max shear strain at boundary of yield zone [%]	Degree of property change
						Internal friction angle [°]
280	1	10.1	4.42	5.68	2.3 Residual stress condition	40.0→38.1
450	3	18.5	7.06	11.44	2.0 Residual stress condition	27.5→26.6

Figure 4.6.3-20 Estimated extent of the EDZ and its mechanical and hydraulic properties

The reliability of the estimations discussed above will be checked through investigations in Phase II. Since the possibility of a large plastic zone was indicated near the boundary between ZONE 1 and ZONE 2 in this analysis, a 3D model including ZONEs 1–3 will be constructed and an analysis/evaluation conducted. As shown in Figure 4.6.3-21, it was found that the zone that will undergo significant destruction due to borehole breakout phenomena would be around half the diameter or the full diameter of the borehole, based on the borehole shape of the horizontal cross-section reconstructed using the results of BHTV logging conducted at a depth of 800 m or more in borehole HDB-11. In a shaft with a shape identical to that of the borehole, significant destruction zones near the shaft wall could occur at a depth shallower than that of the borehole breakout, considering the atmospheric environment inside the shaft and the scale effect of the rock properties. This finding would be important for evaluation of excavation damage and planning of in situ experiments related to the engineered barriers in Phase II and subsequent phases. The analysis to restore destruction phenomena using developed modelling techniques and examination of phenomena on the scale of the shafts and tunnels will be conducted.

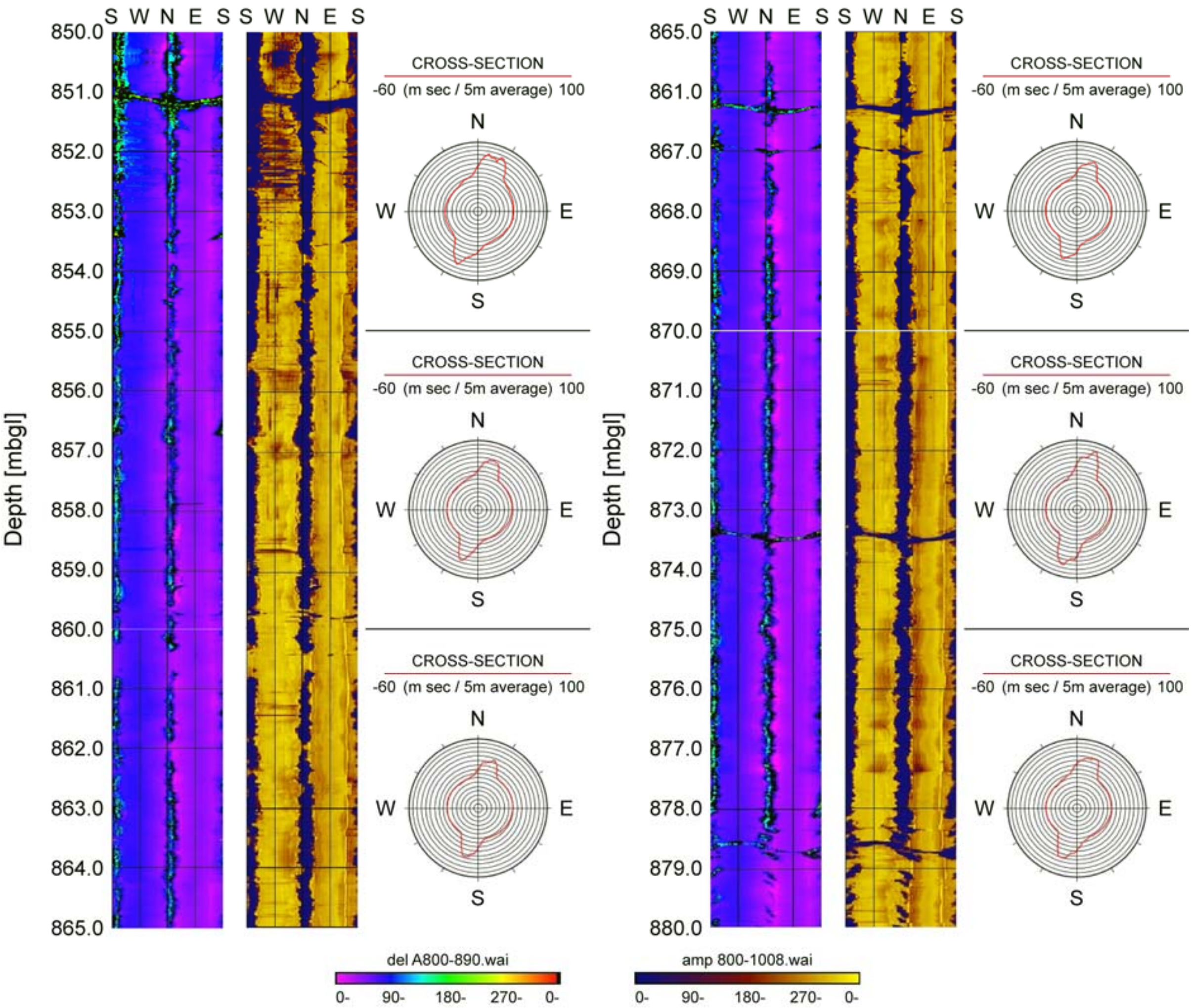

Figure 4.6.3-21 Borehole breakout and reconstructed borehole shapes in borehole HDB-11

4.7 Development of techniques for characterising the geological environment

The techniques used in the Phase I investigations, described in Chapters 3 and 4 (see also Appendix 3), include conventional ones, those modified to achieve specific investigation goals, newly developed techniques and those with improved reliability through combination of several techniques. The results of applying these investigation techniques at Horonobe will provide useful input for planning and implementing investigations of sedimentary formations in areas other than Horonobe in the future. In addition, practical experience (e.g. a wealth of know-how, a number of mistakes) gained through the Phase I investigations will help to come up with ideas and plans to further improve the investigation techniques.

For each of the investigation fields including geological, hydrological/hydrogeological, hydrochemical and rock mechanical investigations, this section summarises the key techniques for acquiring relevant data and for assuring the data quality and the key findings relating to these techniques for sedimentary formations. It also discusses borehole investigation and environmental monitoring techniques that play an important role in the surface-based investigations.

4.7.1 Borehole investigation techniques

A deep borehole programme is the only investigation in Phase I that was able to directly sample rocks and groundwater at depth and observe a variety of properties of the deep geological environment. Because data acquired through borehole investigations will be used in the subsequent modelling and analyses of the geological environment and the final safety assessment and the design of the underground facilities, quality control (QC) of the investigations will be of importance. Since the cost of the borehole investigations increases with drilling depth and the quantity and quality of the investigation, the investigations must be conducted in such a way as to acquire as much information as possible from single borehole. To this end, borehole investigation techniques were optimised in a stepwise manner, which involved the improvement of drilling techniques as a main component.

(1) Planning of the borehole investigations

The borehole investigations require drawing a detailed overall investigation programme and specifying the details of each testing in advance. For this purpose, it is necessary to predict a geological profile showing stratigraphical boundaries and faults and the distribution of hydraulic, hydrochemical and mechanical properties at the drilling site based on all available information before planning the borehole investigations. Based on these predictions, key issues to be addressed in the investigation programme are required to be specified, which will enable the goals of the investigations to be clearly defined. The layout of borehole as well as the investigation targets and methodologies should then be optimised, taking into consideration the time and budget expected for, and restrictions on, the investigations. Although the borehole investigations are suitable and effective for characterising and evaluating the geological environment, drilling itself disturbs the geological environment and consideration should also be given to restricting the impact on the environment to a minimum.

Of great importance is to plan flexibly so that, if an unexpected event such as lost circulation, seepage flow and borehole collapse occurred during drilling, activity can be halted to take appropriate measures and to conduct feasible investigations, providing feedback to the investigation programme. Preparation of measures and backup solutions to major potential problems mentioned above is thus of great importance to gain the promising results of the borehole investigations. It is also required at this stage to prepare QC manuals and systems for the investigations. The investigation targets, methodologies and QC criteria should be revised in an appropriate manner with the progress of the investigations.

Figure 4.7.1-1 shows the investigation programme to be conducted in borehole HDB-11 as an example, which involves drilling steps, casing programme, drilling and reaming diameters, drilling fluid, investigation items and intervals etc. along with the geological and hydrogeological predictions that were made based on the information available before starting the borehole investigations. During the investigations, this plan was optimised in an appropriate manner based on the results of drilling and investigations.

(2) Borehole drilling techniques

1) Selection of drilling fluid

When drilling (soft) sedimentary rocks, much effort should be devoted to maintaining borehole stability for long time periods because the rocks are mechanically unstable and usually have swelling properties. A careful review is therefore required for the selection of suitable drilling mud. Here consideration should be given not only to greater effect on physically protecting the borehole wall but also to less impact on the subsequent investigations in the borehole (e.g. hydraulic tests, groundwater sampling), efficient removal of cuttings from the borehole, safe on-site handling, transparency of product information and fast and easy domestic procurement.

Prior to the first borehole investigations, the applicability of silicate mud for drilling was evaluated as it has the capability of restricting the swelling effects of clay minerals. A laboratory test was first conducted to determine the adhesion of silicate mud on borehole walls and the infiltration of mud into the rock. The results of the test showed that a combination of silicate mud and KCl (rather than silicate mud alone) was more effective because of the higher resistance to swelling and less adhesion to rock surfaces. An application test was then conducted at an off-site field; a borehole was drilled using the silicate mud and KCl mixture to determine the effectiveness of a method for removing mud and the effect on hydraulic conductivity. Although silicate mud could be removed from the borehole wall by NaOH solution, a significant effect of silicate mud was obvious on hydraulic conductivity in highly permeable zones whereas the effect could not be identified in impermeable zones. In any cases, a second exchange by artificial formation water was needed.

Practically it would be difficult to manage the use of strongly alkaline solutions on-site and to take measures such as the use of alkali-resistant drilling tools in the borehole. More seriously, a significant impact of such solutions would be expected on groundwater chemistry[240)]. Since the target sedimentary rocks (the Wakkanai and Koetoi Formations) was found to have low swelling properties owing to a low content of swelling clay minerals, it was decided not to employ silicate mud for drilling boreholes.

For boreholes HDB-1 to HDB-5, in order to minimise the drilling-induced disturbances, drilling with fresh water was conducted from near surface down to the depth range of 54–405 m. As a result, the borehole wall remained mechanically unstable and eventually the borehole enlarged considerably (up to 2.5 times larger than the drilled diameter), thereby not allowing hydraulic tests and groundwater sampling to be carried out in such sections. It was therefore decided to use bentonite mud for further drilling so as to stabilise the borehole wall and lift cuttings efficiently out of the borehole. Based on the practical experience on-site, less dense bentonite mud of 5–6 wt% without any additives was found to be suitable for these purposes. Figure 4.7.1-2 shows the comparison of the borehole diameters of the sections drilled with fresh water and with bentonite mud for boreholes HDB-3 and HDB-4. For boreholes HDB-6 to HDB-11, drilling and long-term stabilisation with bentonite mud were successfully achieved.

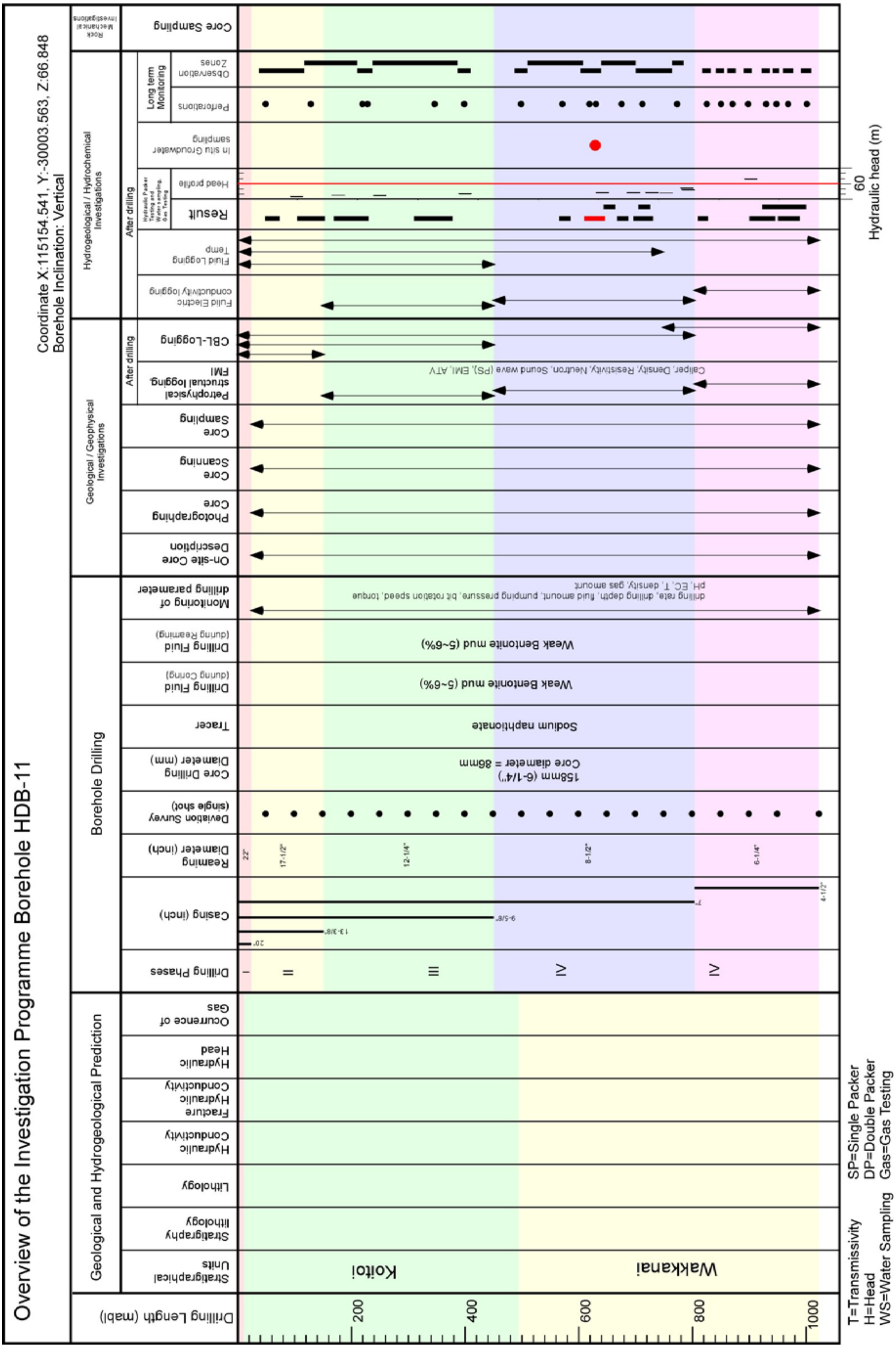

Figure 4.7.1-1 Overview of the HDB-11 borehole investigation programme

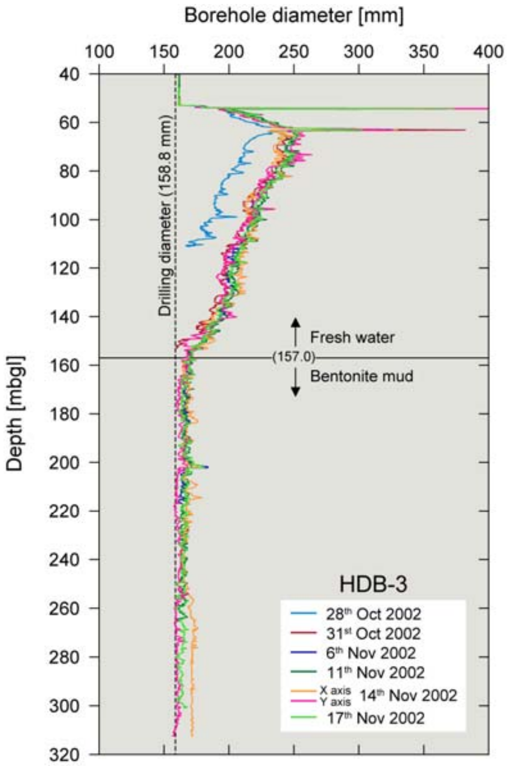

Figure 4.7.1-2 Comparison of borehole diameters between the sections drilled with fresh water and with bentonite mud

2) Protection against explosions of flammable gas

When drilling boreholes in areas where flammable dissolved gas is present in the groundwater, explosion protection measures are required to protect against possible blowouts. The borehole investigations carried out in the past for oil and natural gas exploration indicate possible oil and natural gas occurrences in the Horonobe Town area, meaning that gas blowout could occur during drilling, as described in Chapter 3. For this reason, a blowout preventer (BOP; Figure 4.7.1-3) was installed at the borehole mouth[240]. The Mine Safety Regulations (For Petroleum Mine – 1996 Edition)[241] were applied to determine the stress resistance of various types of valves and BOPs and to manage safety at the drilling site.

Figure 4.7.1-3 Blowout preventer (BOP) mounted at borehole mouth

3) Selection of drilling tools

Basically, the method of all core drilling was applied to the borehole during investigations for acquiring multidisciplinary data on the geological environment. However, the drill rods used in conventional geothermal and resource development are unsatisfactory in terms of pressure resistance and strength to allow installation of the above-mentioned BOP. The drill rods used in oil exploration could not be used for full wireline coring since they are basically designed for partial sampling of cores (i.e. spot coring). A drill rod that can be used with the BOP to allow safe full coring using the wireline technique was therefore manufactured for use in oil or gas bearing sedimentary formations.

4) Drilling and casing installation

Investigations carried out in the borehole include geophysical logging, fluid logging, hydraulic testing, groundwater sampling, rock mechanical testing and long-term monitoring (see Subsection 2.2.2). When conducting these investigations in sedimentary rock, if a casing programme is not formulated, there is a possibility of problems occurring such as borehole collapse or enlargement. Sometimes the borehole itself may become unusable because tools may become jammed owing to borehole collapse. A multi-phase drilling process was therefore adopted in order to achieve a self-supporting borehole and to ensure successful implementation of the investigations. More specifically, the entire drilling process was divided into several steps and the borehole was cased at each step. The layout of the casing pipe was determined based on information on the geological environment at the drilling location taking into consideration key features, such as lithostratigraphical boundaries, fault distribution, location of inflow points, and the plan for the long-term monitoring of groundwater level, pressure and water chemistry after the borehole investigations. The casing programme thus consisted of four stages and casing was installed along the entire length of the borehole.

The rotary wireline drilling method, which is capable of bearing heavy loads in terms of lifting/lowering drilling tools, was used to prevent drilling tools from becoming jammed by collapse of the borehole walls by swelling. In addition, the diameter of fully cored boreholes was determined as 158.8 mm (6 1/4”), which is the basic standard for various drilling tools used in oil exploration and geophysical and fluid logging tools can easily be adapted to these dimensions. The wireline drilling tools used in geothermal development and hot spring surveys could not be used with this borehole size and all tools, including diamond bits and core barrels, had to be newly manufactured.

After completing the drilling and the borehole investigations, the first, second and third stages of the borehole were enlarged using tricone bits with diameters of 444.5 mm (17 1/2”), 311.2 mm (12 1/4”) and 215.9 mm (8 1/2”) respectively. Casing pipes with diameters of 339.7 mm (13 3/8”), 244.5 mm (9 5/8”), 177.8 mm (7”) and 114.3 mm (4 1/2”) were then fixed by using either a single-stage cementing or an inner-string cementing technique. After installation of the casing pipes, jet perforation was conducted at the intervals/depths that were selected based on the investigation results (e.g. distributions of fracture zones, hydraulic conductivity, groundwater chemistry etc.) for long-term hydraulic and hydrochemical monitoring. As an example of borehole completion, the final layout of borehole HDB-6 is shown in Figure 4.7.1-4. However, one of the problems involved in using this method is that water collected from the intervals became contaminated through contact with the cement and the casing pipe (carbon steel).

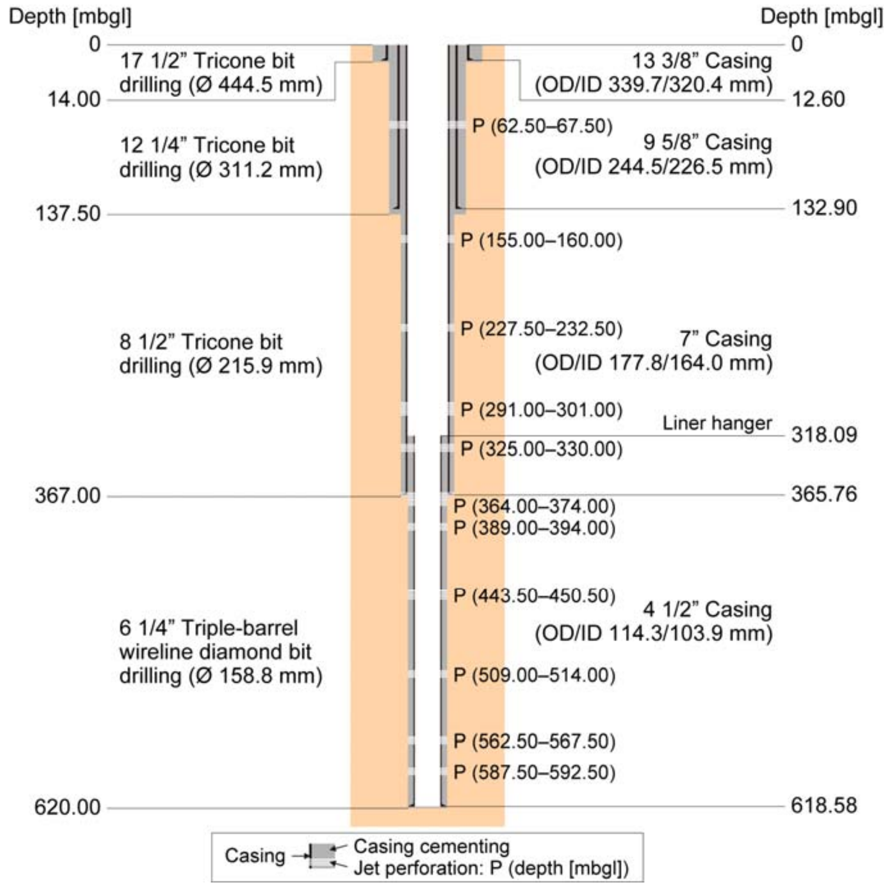

Figure 4.7.1-4 Final layout of borehole HDB-6

5) Drilling parameter monitoring

Monitoring of drilling parameters, such as volume of blowout gas, supply/return and pH of drilling fluid and rotation speed and torque of the drilling rod, is of importance not only for ensuring safety during operations but also for acquiring, although not directly, geological, hydrogeological, hydrochemical and rock mechanical information in real time. As an example, the results of continuous drilling parameter monitoring in borehole HDB-6 are presented in Figure 4.7.1-5. Such monitoring allows identification of any indications of gas blowout, the status of inflow and lost circulation, relative changes in lithology and rock strength etc.

In borehole drilling in Phase I, concern particularly focussed on the concentrations of CH_4 and other gases and supply/return of drilling fluid. The gas concentration was taken into account in controlling the environment at the drilling site and in the safety management of gas blowout. Data on the supply/return of drilling fluid indicated the occurrence of inflow and lost circulation and hence changes in hydraulic conductivity could be estimated. Such a change was indicative of the presence of a water-conducting fracture or a highly permeable zone. For example, when significant lost circulation occurred, drilling was halted to conduct hydraulic testing and groundwater sampling at the interval of lost circulation. Suspending drilling immediately after encountering such feature provides an opportunity to eliminate the effects of drilling fluid and less contaminated groundwater samples can be obtained in a short period of time.

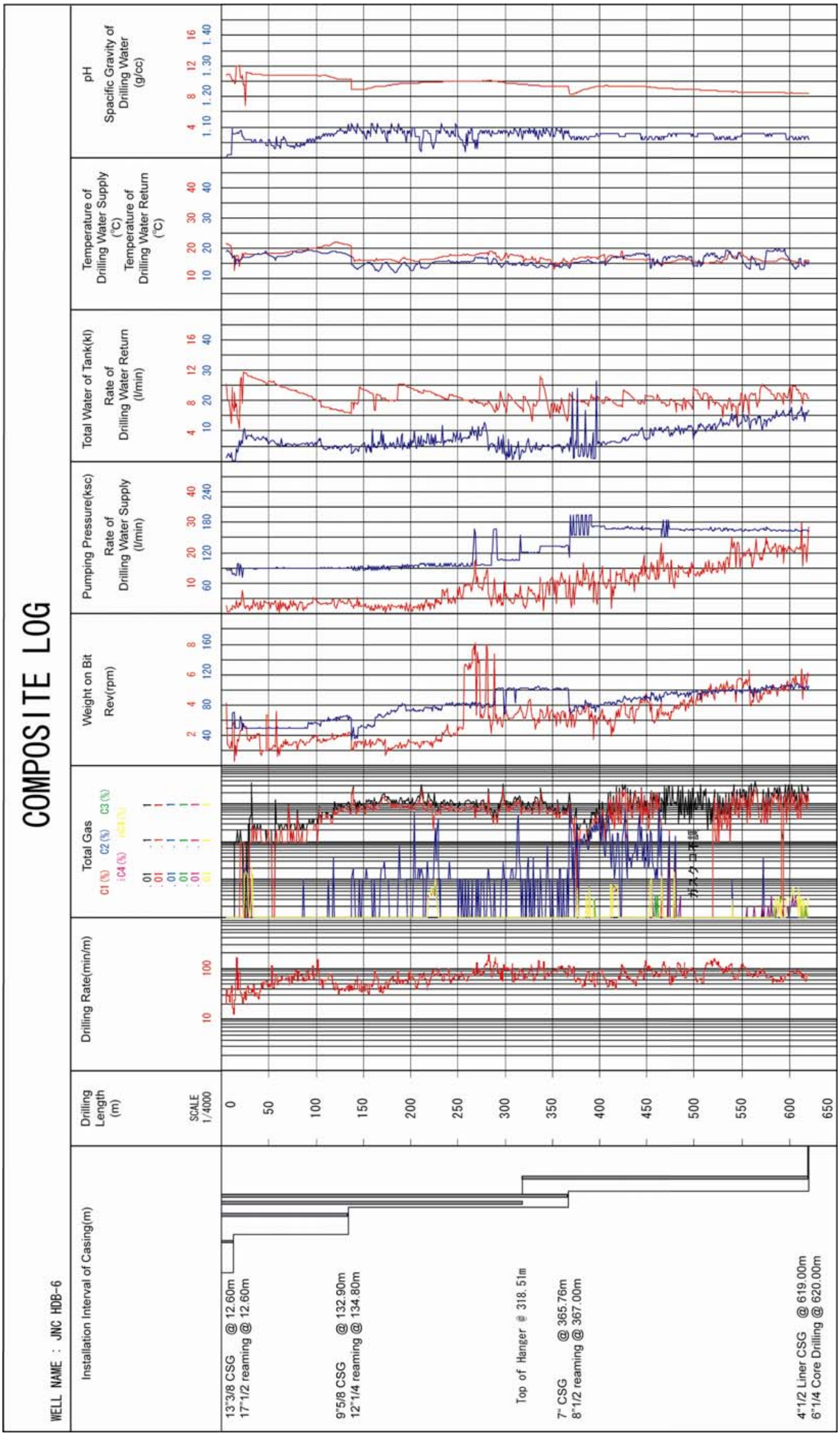

Figure 4.7.1-5 Results of drilling parameter monitoring in borehole HDB-6

4.7.2 Geological investigation techniques

When planning and conducting the geological investigations, concern should be focussed on the following points:

- The costs of borehole investigations and tunnel excavation account for a large proportion of the total cost of the geological investigations. Reducing the financial burden depends on what detail of characterisation can be achieved using geophysical surveys.
- Geophysical surveys are cost-effective, providing data covering wide areas, and non-destructive to the geological environment, in contrast to borehole investigations providing only point but detailed information. Both techniques will play a major role in preliminary and detailed investigations.
- When conducting the geological investigations, it is necessary to formulate area-specific investigation methods and specifications[4)].

The first half of this section focusses on techniques relevant for geological investigations, including aerial electromagnetic surveys, aerial magnetic surveys and aerial radiometric surveys and resistivity surveys and reflection seismic surveys as typical surface-based methods. The relevance of these surveys is discussed from the viewpoint of area-specific characteristics. The latter half of this section highlights investigation techniques for long-term geological stability.

(1) Aerial reconnaissance survey techniques

Aerial geophysical surveys are effective in the initial stages of regional investigation programmes for providing a general understanding of the geological structure over a large area. Electromagnetic surveys are suitable for characterising rock types, magnetic surveys can identify geological structures at greater depth or on a larger scale and radiometric surveys can be used to investigate large-scale near-surface discontinuities.

In this project, a helicopter was used for the aerial electromagnetic, magnetic and radiometric surveys, which required taking measures to protect grazing cattle on the stock farms in the area against helicopter noise[3)]. An electromagnetic sensor was basically kept at a height of 30–60 m above ground and was flown at a speed of 50–80 km h^{-1}. When flying directly above farms located within the survey range, the flight took a 200 m detour to prevent disturbing the cattle. When a detour could not be made, the flying height was increased to 120 m or more. Measures were also taken to accustom the cattle to the noise of the helicopter.

Although the measurement heights mentioned above did not have much impact on the analysis of aerial magnetic and radiometric surveys, they did affect the analyses of aerial electromagnetic surveys to some extent[3)]. Although the standard height from the ground for a magnetic sensor is 45 m, i.e. 15 m higher than for the electromagnetic sensor, all data could be used for the analyses because the data obtained by aerial magnetic survey are measurements of the potential field and, even though the size of the magnetic anomaly that could be detected may vary depending on the measurement height, this variation was small enough to be ignored compared to the order of variation of magnetism indicated by the geological structures. A height correction also had to be also in the aerial radiometric surveys because the gamma radiation from the surface is attenuated by the airspace. However, since it is already known that the intensity of radiation is attenuated exponentially as height above ground increases, data obtained at a height of 180 m above ground can be corrected to allow them to be treated equivalently to the data obtained at the reference height. All the data obtained could therefore be used for the analysis. However, some of the apparent resistivity calculated from data obtained by aerial electromagnetic survey had to be excluded from the analysis because the calculations were based on data obtained at a height beyond the acceptable limit. More specifically, an evaluation was made of the apparent resistivity obtained at 56 kHz, which is most prone to being affected by height. As a result, no significant difference in apparent resistivity was observed between data obtained at a height of up to 90 m and at a height of up to 100 m, while data obtained at a height of up to 110 m showed a significant difference. Measurement data obtained at a sensor height of 100 m or below were used for the analysis.

When conducting aerial geophysical surveys in an area where livestock farms are located, it should be borne in mind that not all data may be used for the analysis because of restrictions based on measurement height (Table 4.7.2-1).

(2) Surface-based investigation techniques

1) Effectiveness of resistivity surveys

In formations consisting of marine sedimentary rock exposed at the ground surface, such as the Wakkanai and Koetoi Formations, mixing of fossil saline water incorporated when the formation was deposited at the sea bottom and freshwater infiltrating from the surface occurs in the shallow parts of the formation. The differences in salinity of the formation water cause a contrast in the resistivity in such a formation; a freshwater infiltration zone can easily be identified from the distribution of resistivity. In particular, in a formation with no significant variation in lithofacies, the distribution of the freshwater infiltration zone is highly likely to be controlled by geological structures (e.g. fault zones) and their hydraulic properties. Consequently, when determining the location of fault zones in such a formation, measuring the resistivity in shallower zones by resistivity survey (e.g. MT electromagnetic survey) would be effective. A series of investigations based on an AMT electromagnetic survey[33] conducted at the Omagari Fault in the URL area (Figure 4.1.3-6) is one case that demonstrates the effectiveness of this approach[31].

The interpretation of the resistivity structure may, however, vary depending on depth, even for the same investigation data. For example, Takakura et al.[242] have highlighted two different approaches for interpreting subsurface resistivity structures in an oil-bearing sedimentary basin similar to the Horonobe area (Higashikubiki area in Niigata Prefecture): reduction of the salinity of the formation water owing to the infiltration of meteoric water for the shallower zone (approximately 1 km or less in depth) and a high content of clay minerals with a high ion-exchange capacity for the deeper part (approximately 1–3 km in depth). In addition, the AMT electromagnetic survey[33] conducted to a depth of 1 km or less in the area indicated a high resistivity zone at a depth of 300–1,000 m. The zone was interpreted to correspond to the zone along the Omagari Fault into which meteoric water has infiltrated[31]. However, high-density electrical surveys conducted at a depth of 300 m or less along the same survey line as the ATM survey indicated that the area assumed to be the Omagari Fault was a zone with a fairly low resistivity (Figure 4.7.2-1). This was interpreted as indicating a high water content in the area along the Omagari Fault[40]. As can be seen from the above, it should be kept in mind that the interpretation of resistivity structures varies depending on depth, even for the same investigation data (Table 4.7.2-1). The target depth for investigation should be set deeper at first and then gradually reduced for conducting effective stepwise resistivity surveys because the resolution of the analyses improves as depth decreases.

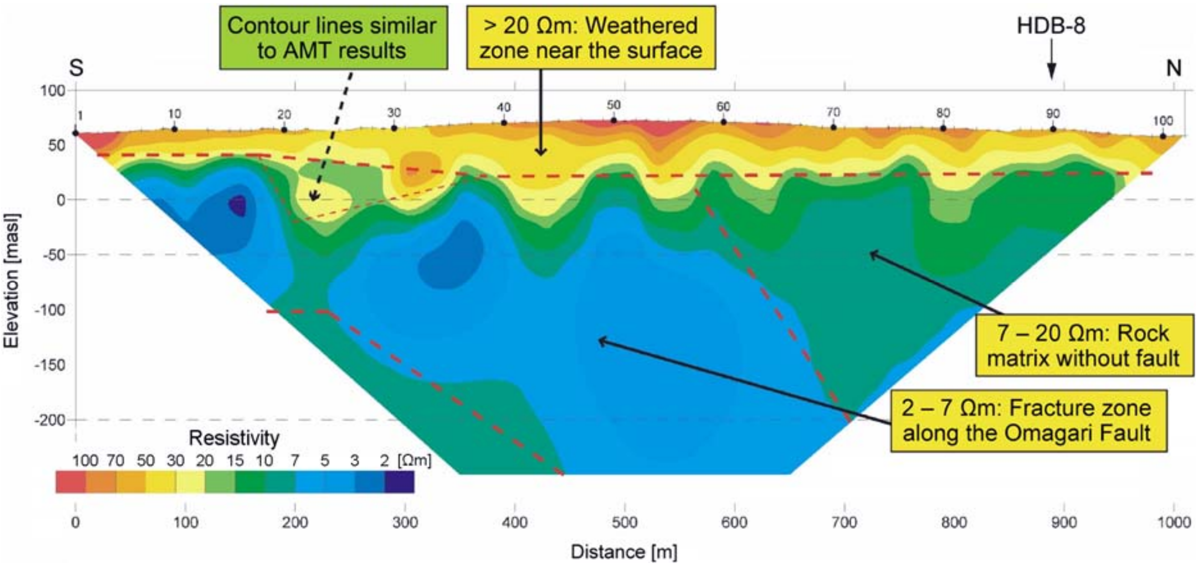

Figure 4.7.2-1 Interpretation of resistivity profiles by high resolution electrical survey

Table 4.7.2-1 Applicability of various geological and geophysical investigations

Availability of data from airborne survey		
Method	Stock farm area	Non-stock farm area
Airborne electromagnetic survey	–	+
Aeromagnetic survey	+	+
Airborne radioactive survey	+	+
Distribution and hydraulic properties of fault in massive marine deposits		
Method	Shallow subsurface (< 1 kmbgl)	Deep subsurface (> 1 kmbgl)
Resistivity investigation	++	–
Resolution of reflector by reflection seismic survey		
Shot/receiver interval	Weakly bedded/laminated rocks	Clearly bedded/laminated rocks
Normal	–	+
Densely	–	++
Recording of seismic data by reflection seismic survey		
Shot condition	Road	Pasture
Vibrator	++	
Impactor	+	+
Image of seismic recreation		
Method	Folding geological structure	Flat geological structure
VSP	–	++
Description of fault		
Method	Strike-slip	Dip-slip
Stripping	++	–
Trench	+	++

++: very good, +: good, –: not good

2) Applicability of reflection seismic surveys

Although reflection seismic surveys were conducted around the URL area[35], the interpretation of the reflecting surfaces proved very difficult[4] because the Wakkanai and Koetoi Formations have homogeneous petrophysical properties and the survey layout was not ideal owing to restrictions on land use. An evaluation was therefore made to determine what difference there would be in the continuity and resolution of the reflector by changing the intervals of shot/receiving points and shot methods for surveys in such formations. The applicability of a multi-offset vertical seismic profile (VSP) survey[38] was also evaluated. Here discussion is also made on how to implement reflection seismic surveys using a stepwise approach.

i) Difference in reflection profile resulting from changing shot/receiving intervals

In order to evaluate the difference in the reflection profile resulting from changing the shot/receiving intervals, measurements based on two different intervals were carried out on the same survey line[38]. The shot/receiving intervals were set at 50 m/25 m for one of the measurements and 20 m/10 m (partially 10 m/5 m) for the other (Table 4.7.2-2). A comparison of the time – migration sections (Figure 4.7.2-2) indicated that the continuity of the reflector observed in both measurements showed no significant difference, although the reflection profile obtained with the higher density measurement showed a slightly higher resolution. These measurements indicate that, when conducting reflection seismic surveys in an area with homogeneous petrophysical properties, the continuity of reflector and the resolution will not always be greatly enhanced even if the shot/receiving interval is set at a higher density.

Table 4.7.2-2 Specifications of reflection seismic surveys

		Reflection seismic survey	High resolution reflection seismic survey
Source	Source	Vibrator, mini-vibrator	Vibrator, impactor
	Shot interval	50 m	20 m or 10 m
	Sweeps	8–60 Hz / 16 sec	10–100 Hz / 16 sec
	Number of stacks	16	5 (vibrator), 20 (impactor)
Receiver	Receiving interval	25 m	10 m or 5 m
	Receiver	SM-7 (geophone, f0 = 10 Hz) 9 / group	SM-7 (geophone, f0 = 10 Hz) 9 / group
Recording system	Recording system	G-DAPS4	G-DAPS4
	Sampling rate	4 msec	2 msec
	Record length	8 sec	5 sec

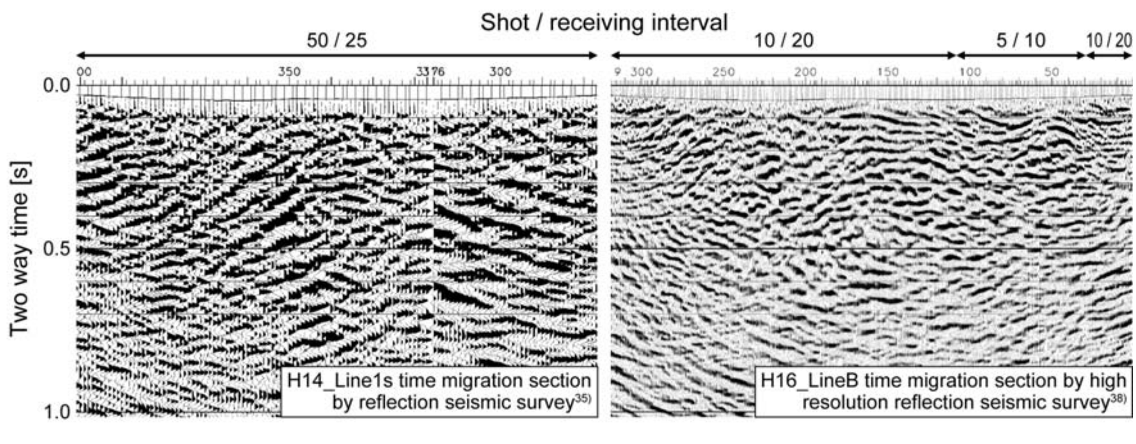

Figure 4.7.2-2 Comparison of time – migration sections at different shot/receiving intervals
Lines shown near the URL site at N-NNE direction with approximately 1.6 km length

ii) Difference in reflection profile resulting from different shot methods

Three measurements were conducted to determine the difference in reflection profile resulting from using different shot methods: vibrator on a gravel road, impactor on the same gravel road and an impactor in pasture land and the same gravel road[38]. A comparison of the stacked profiles (Figure 4.7.2-3) obtained by the vibrator and the impactor indicates that the profile using the former method was superior in terms of the continuity of reflectors at many points. The comparison between the stacked sections obtained by the impactor on the gravel road and the impactor in pasture land indicates that the continuity of reflector and resolution recorded by the two methods are similar. The vibrator method would be preferable to the impactor, but there is no significant difference between the gravel road and pasture land as the shot points.

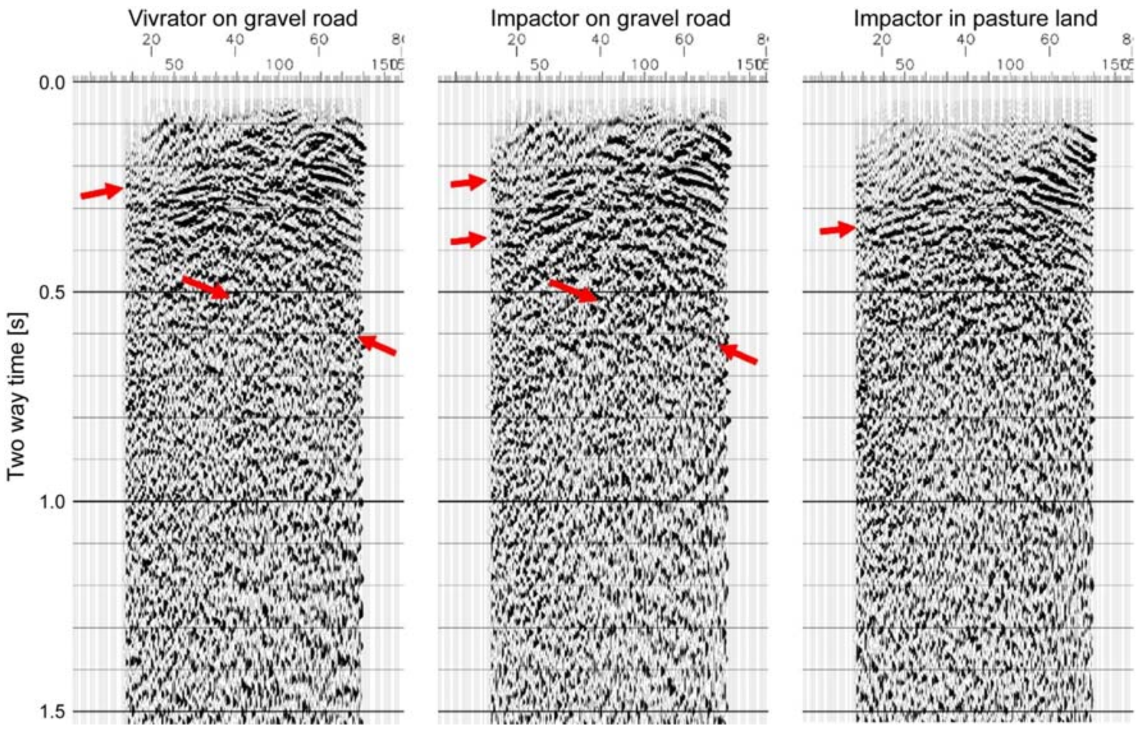

Figure 4.7.2-3 Comparison of stacking record sections by different shot methods

Red arrows showing reflectors to be compared; After Takakura et al.[242]

iii) Applicability of the multi-offset VSP survey

One of the advantages of the VSP survey is that it allows detailed characterisation of geological structures by obtaining high resolution images of reflector. However, this advantage may be less clear if the images obtained depend largely on the assumption of the velocity structures at the time of data processing for analysis. For the multi-offset VSP survey carried out around the URL area, the locations of the reflector obtained by zero-offset processing were more or less consistent with those obtained by the reflection seismic survey[38]. In the common depth point (CDP) mapping carried out by simply assuming a horizontal multi-layered structure, however, the dip direction and angle differed significantly from the result obtained by the reflection seismic survey. This can be attributed to the fact that, in the formation in this area, dip angles and directions vary from place to place. In such a case, consistency between the two methods can be achieved by assuming a velocity structure that takes the dip of the formation into account in the CDP mapping. However, incorporating such an assumption in the velocity structure may decrease the inherent advantage of the VSP survey. Effective implementation of the multi-offset VSP survey would therefore be difficult in an area with a complicated formation dip such as Horonobe area (Table 4.7.2-1).

iv) Procedure for the reflection seismic survey

The above discussion suggests that, in order to perform reflection seismic surveys effectively in a stepwise manner, they should first be carried out according to standard specifications (Table 4.7.2-2); more detailed surveys should then be conducted only when the continuity of reflector and resolution obtained from the first survey are relatively good and the VSP survey should be conducted only when the reflector are more or less horizontal.

3) Applicability of fracture investigations

As described above in Section 4.1, minor faults at a high angle to the bedding plane with a preferential strike slip are found widely in the URL area; these faults are potentially important as transport pathways in the rock. Considering the displacement sense of these minor faults, observations in the horizontal plane would be preferable for characterising basic geological parameters such as displacement and the evolution process of these faults. However, surface outcrops in the Horonobe area are, in many cases, vertical planes exposed by road cutting or similar activities and river bed outcrops are not suitable. In the Horonobe URL project, therefore, a horizontal outcrop was formed artificially by stripping the overburden using heavy equipment (Figure 4.7.2-4). As a result, many important aspects of the above-mentioned minor faults could be characterised[32)]. Generally, the formation of a vertical cross-section (trench survey) is a well-known method for observing active faults with preferential dip-slip, but artificially forming a horizontal outcrop as in the present case is also effective for observing faults with preferential strike-slip (Table 4.7.2-1).

Figure 4.7.2-4 Stripped horizontal outcrop

(3) Investigation of the long-term stability of the geological environment

1) Investigation techniques for the period covering the last one million years

The formation processes of mountains and hills are of importance for determining geomorphological development. A hinterland analysis method using fossil diatoms was developed to investigate these processes[243)] as shown in Figure 4.7.2-5. This method is based on the assumption that the sedimentation/denudation environment (approximate land – sea distribution) in a certain period can be determined based on the assumption that, during the sedimentation period of the horizon bearing resedimented fossil diatom species, the formation in which the species were primarily deposited was in a denudation environment. However, for periods with a large amount of diatoms, resedimented species may not be found owing to its relatively smaller occurrence. Hence, the number of specimens analysed in one sample should be increased so that scarce resedimented species would be identified whilst conducting investigations on palaeocurrent directions, clast component analyses, sedimentary facies analyses and the anisotropy of magnetic susceptibility (AMS) measurements.

Based on the distribution of resedimented fossil diatoms to the Horonobe area, an expansion of the land towards the west was found. The west end of the eastern area of Soya Hill and central Soya Hill were considered to be in a denudation environment from the late Late Pliocene and the late Early Pleistocene, respectively[243].

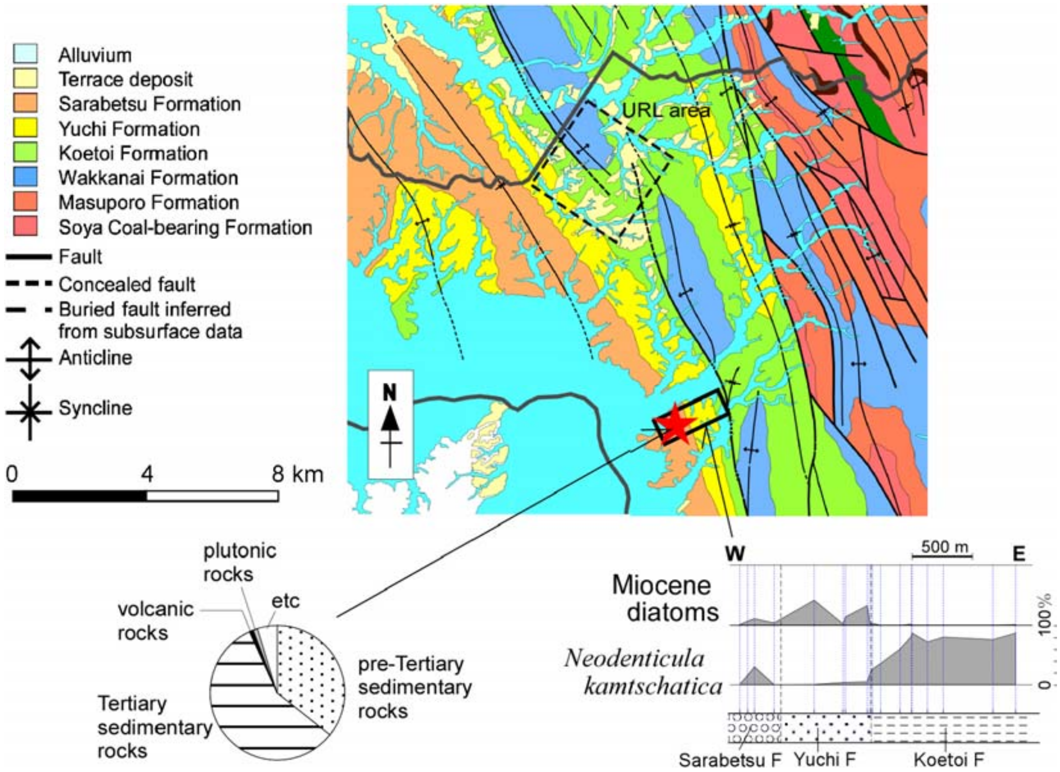

Figure 4.7.2-5 Clast composition of conglomerate in the Sarabetsu Formation and resedimented diatom fossils in the Yuchi and Sarabetsu Formations

2) Investigation techniques for the period covering the last several tens of thousands to several hundred thousand years

The distribution of terrace surfaces and terrace deposits was surveyed based on the aerial photograph interpretation and field investigations and the formation period of the terraces was determined by applying the RIPL method[244] to terrace deposits and loess (aeolian terrestrial sediment formed in the Pleistocene, mainly consisting of silt)[245] (see also Subsection 4.5.2). The terrace deposits examined were approximately 5 m thick with an alternation of medium to coarse sand and gravel layers. The loess distributed on the terrace deposits is around 2 m thick and consists of, from the bottom, red loess, light brown loess, grey tephra and brown tephra.

The results indicate that the grey tephra correlates to the Rishiri – Hotoku tephra. In addition, tephra which is considered to correlate to Kc-Hb and Spfa-1, known as the effective key beds, is also observed in the light brown loess, which implies that this loess was formed after MIS 5e. Based on the formation age of the light brown loess and the fact that the red loess with a thickness of approximately 1 m is found below the light brown loess, and taking the time required for the sedimentation of the red loess into account, it is suggested that the investigated marine terrace surface may have been formed during MIS 7 (214 ka). Provided the terrace was formed during MIS 7, the average uplift rate was estimated to be about 0.3 m ky^{-1}, given that the altitude of the terrace is around 70 m.

It was thus demonstrated that the uplift rate and the land – sea distribution for each period can be determined by applying the RIPL method, in addition to a survey of the distribution of the terrace surfaces based on interpretation of aerial photographs[245)].

3) Investigation techniques for the period covering the last several to several tens of years

Seismic monitoring and GPS surveys are examples of appropriate methods for determining ongoing natural phenomena (particularly crustal movements). The following describes baseline length (distance between survey points) analyses and their results and the results of examining the effects of earthquakes on the baseline length[246)]. It should be noted that the data used in the GPS analyses include those obtained from the HDB-1 survey point in the Horonobe URL project, survey points of the International GPS Service and GEONET (Wakkanai, Wakkanai 2, Sarufutsu, Rebun, Rishiri, Hamatonbetsu, Esashi, Esashi 2, Omu, Otoineppu, Teshio and Enbetsu) of the GSI; the software used was GAMIT, jointly developed by the Massachusetts Institute of Technology and Scripps Institution of Oceanography.

The 2003 Tokachioki earthquake (26th September 2003) and the 2004 Rumoinanbu earthquake (14th December 2004) occurred during the monitoring period. The baseline length, i.e. the distance between survey points, was changed significantly by the occurrence of the 2003 Tokachioki earthquake and post-seismic crustal movements were observed for several months after the incident (Figure 4.7.2-6). In contrast, the baseline length was not changed by the 2004 Rumoinanbu earthquake. The magnitude of the Tokachioki earthquake was 8.0, the seismic intensity in Horonobe Town was 1 and the distance between Horonobe Town and the epicentre was approximately 400 km. The magnitude of the 2004 Rumoinanbu earthquake was 6.1, the seismic intensity in Horonobe Town was 2 and the distance between Horonobe Town and the epicentre was approximately 100 km. The comparison between these two events shows that the earthquake with the greater magnitude had a greater impact on the geological environment around the Horonobe area, even if the hypocentre was far from the town and the seismic intensity was lower. The extent of effects on the geological environment (stress, strain and groundwater level) in the Horonobe area can thus be determined based on the relationship with seismic magnitude and distance from the epicentre by evaluating the results of surveys on the baseline length, while examining the changes in baseline length caused by earthquakes. It should be noted that changes in the baseline length were not caused by any of the earthquakes with a magnitude of 5.0 or greater that occurred off the coast of Tokachi and Nemuro (besides the 2003 Tokachioki earthquake). The geological environment around the Horonobe area is considered to be affected least when a magnitude 8.0 earthquake occurs off the coast of Tokachi.

It could thus be demonstrated that extent of effects on the geological environment (stress and strain) in the Horonobe area can be determined based on the relationship with seismic magnitude and distance from the epicentre by evaluating the relationship between the baseline length and earthquakes[246)].

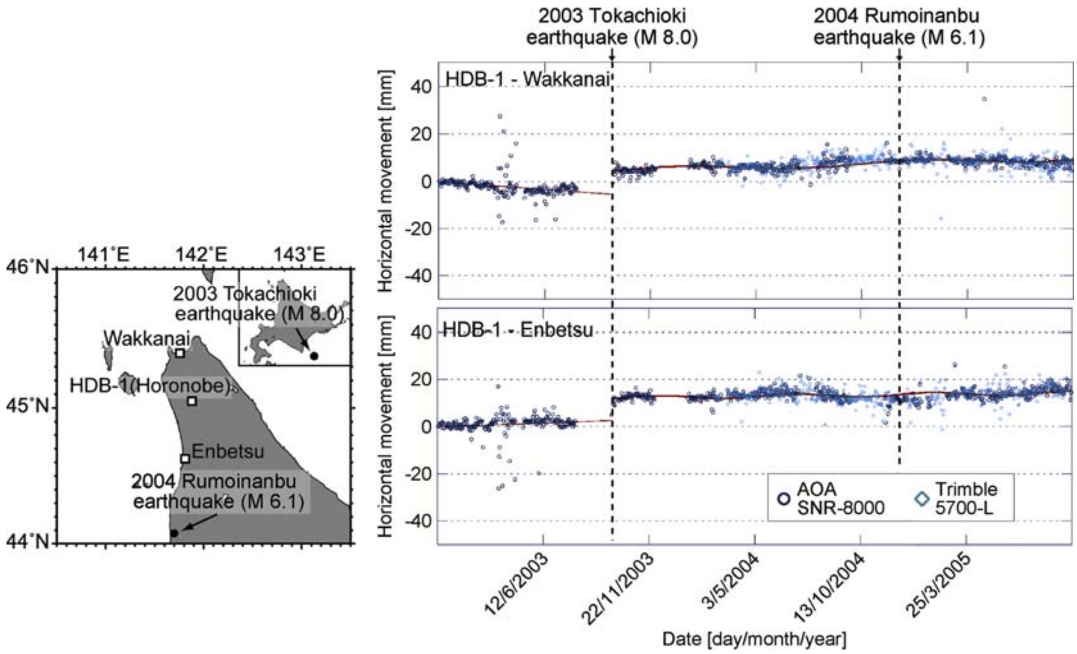

Figure 4.7.2-6 Time variation in baseline lengths from 1st January 2003 to 3rd September 2005
Red lines showing the best-fit curve obtained using the built-in curve-fitting function in KaleidaGraph ver 4.0

4.7.3 Hydrogeological/hydrochemical investigation techniques

(1) Hydrogeological investigations

For the hydrogeological investigations, an input dataset needs to be developed for use in the groundwater flow analyses. Quality-controlled data on hydraulic conductivity, transmissivity and porewater pressure will constitute the primary information in the dataset. Methodologies for measurements and associated analyses of these parameters have already been standardised in the field of civil engineering[247)] etc. However, there are a couple of points that need to be improved with a view to establishing methods for effective and accurate measurement of the parameters in rocks with a wide hydraulic conductivity range in areas where dissolved gases are present.

Since WCFs that control the groundwater flow are suggested to exist in the Wakkanai Formation, as described in Section 4.2 and Subsection 4.6.3, the applicability of a method for identifying WCFs using boreholes and calculating the transmissivity was evaluated.

1) Flowmeter logging and fluid flow electrical conductivity logging

Flowmeter logging and fluid flow electrical conductivity logging are effective for identifying areas with relatively high hydraulic conductivity and the hydrogeological structures that are assumed to control the groundwater flow and permeability. Conceptual diagrams illustrating electromagnetic flowmeter logging and fluid flow electrical conductivity logging are shown in Figure 4.7.3-1. Flowmeter logging was conducted in all boreholes, whereas fluid flow electrical conductivity logging was carried out in boreholes HDB-6 and HDB-11.

For electromagnetic flowmeter logging, the logging probe is moved downwards/upwards at a constant speed and the relative flow velocity of the borehole water is measured using an electromagnetic sensor installed in a flow tube. The longitudinal flow velocity of the borehole water is measured continuously based on the speed of the logging tool, the relative flow velocity and information on the borehole diameter and inflow/outflow points and the flow rate at these points are directly estimated on the basis of the depth profile of the flow velocity. The temperature and electrical conductivity of the borehole water are also measured.

Fluid flow electrical conductivity logging is used to indirectly identify groundwater inflow points using the difference in electrical conductivity between groundwater and borehole water. This method can identify inflow points, when large differences in electrical conductivity exist, and determine the flow velocity in the borehole by analysing the groundwater inflow with a high content of dissolved components (i.e. high electrical conductivity) and the advection – diffusion phenomena of the groundwater in the borehole. First, borehole water is replaced by deionised water with a low electrical conductivity. The logging probe is then moved downwards or upwards at a constant speed while pumping the replaced water at a constant flow rate, thereby continuously measuring the electrical conductivity in the longitudinal direction of the borehole. The measurement is carried out several times at a predetermined time interval to determine the temporal evolution of electrical conductivity.

While the single-hole hydraulic packer test described below can only acquire the hydraulic parameters in the survey area, geophysical logging such as flowmeter logging is capable of continuous acquisition of hydraulic information in the longitudinal direction of the borehole. The hydraulic conductivity in areas other than the hydraulic test intervals and the transmissivity of WCF identified by the flowmeter logging are better calculated based on the results of flowmeter or electrical conductivity logging. However, it is hard to determine hydraulic conductivity precisely because the flowmeter logging in the present project was considerably affected by the collapse of the borehole walls and the drilling mud. Development of methods for evaluating hydraulic conductivity that can eliminate the effects of these factors and logging techniques for use in rocks prone to collapse is a task for the future.

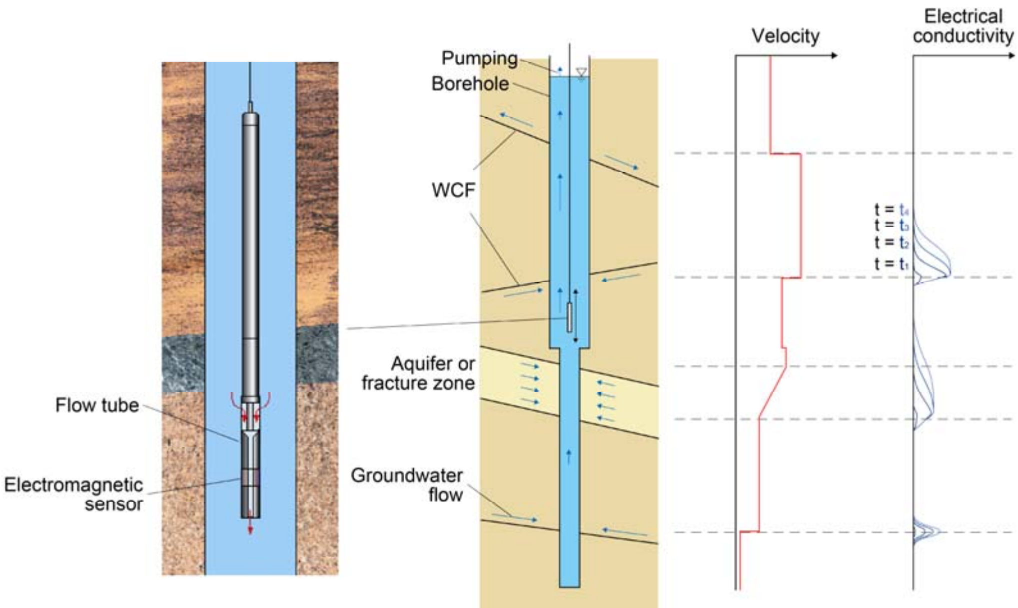

Figure 4.7.3-1 Conceptual illustration of flowmeter logging and electrical conductivity logging

2) Single-hole hydraulic test

In an environment where dissolved gases are present in the groundwater, the release of dissolved gas during testing will affect data quality. When drilling mud is used, a decrease in hydraulic conductivity owing to clogging may also be taken into account. In order to address these issues, test methods were reviewed and the equipment was modified and their effectiveness was finally confirmed[81].

A hydraulic test based on pressurisation or injection may be an effective way of restricting the release of dissolved gases during testing. However, when mud was used for borehole drilling, hydraulic conductivity may decrease owing to the mud penetrating into the rock as a result of the water injection. On the other hand, hydraulic testing based on depressurisation or pumping may reduce the clogging effect, but excessive depressurisation or drawdown may result in the release of dissolved gas in the test interval. Taking this into account, hydraulic tests that have an impact on a small area were carried out first, followed by tests that have an impact over a larger area. During each test, the amount of gas release was checked. The depressurisation or drawdown rate to be used in the subsequent tests was thus set. Figure 4.7.3-2 shows an example of the sequential hydraulic testing procedure.

If the pumping test is performed on groundwater containing dissolved gases, the fluid discharged to the surface would become a mixed gas – fluid phase because of the release of the dissolved gases owing to depressurisation. Therefore, a terrestrially-driven pump that allows the pumping of fluid in a gas – fluid mixed state at a constant rate was used for the hydraulic tests. Since this pump has a sealing capability at the lower part, it can suppress gas release in the closed interval, which allows the tests to be carried out under a single phase state. A gas/fluid separator, a volumetric pumped fluid flowmeter and a gas flowmeter were installed on the ground surface for measuring the pumping rate and flow or released gas in order to calculate the transmissivity and hydraulic conductivity (Figure 4.7.3-3). Also, the durability of the valves of downhole equipment can be improved and orifice diameter increased for carrying out tests with muddy water. Other modifications for this include replacing muddy water in the test interval with freshwater prior to the hydraulic tests or removing mud from the borehole wall[248].

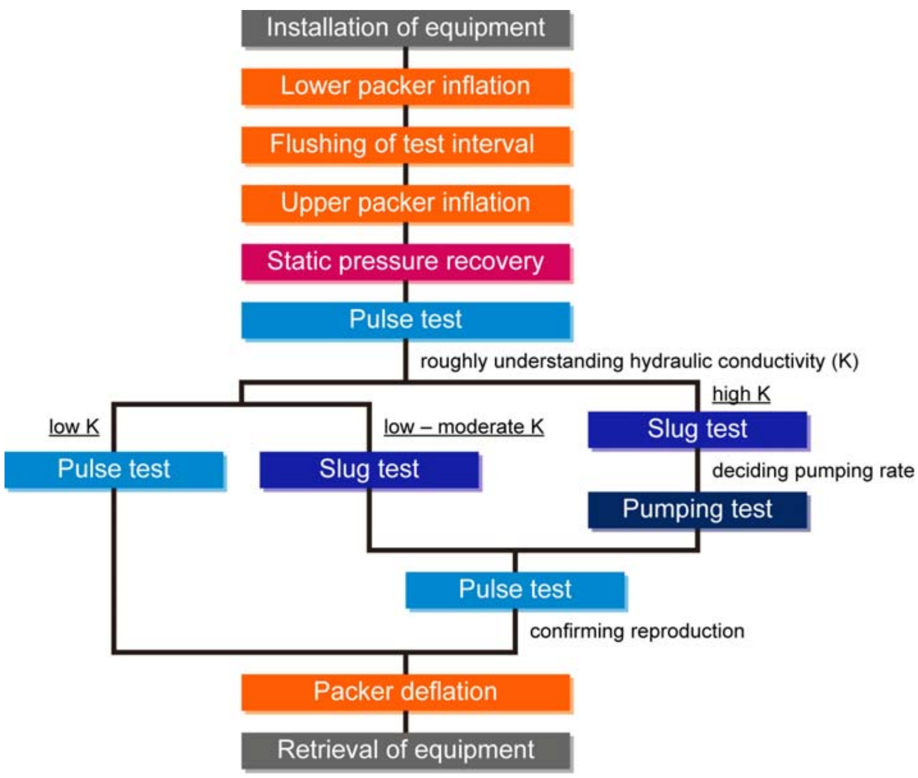

Figure 4.7.3-2 Sequential hydraulic testing procedure

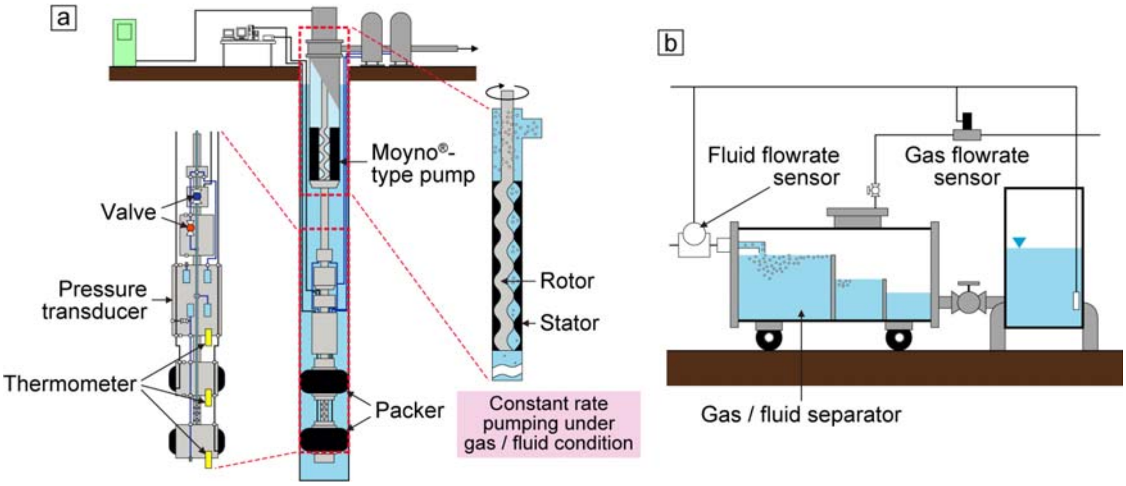

Figure 4.7.3-3 Schematic illustration of hydraulic testing equipment

a: Downhole equipment; *b*: Surface equipment

3) Shallow subsurface hydrological investigation

i) Hydrological balance method

Groundwater recharge rate can be calculated based on the hydrological balance method by subtracting the total amount of river runoff and evapotranspiration from the precipitation in the area of interest. The monitoring conducted in central Japan[249)] can be cited as an example of shallow subsurface hydrological investigations carried out to estimate groundwater recharge rate based on the hydrological balance method. However, a review would be required to determine whether the same methodology can be applied to a region of cold climate such as Horonobe area, because of the occurrence of phenomena peculiar to such areas, such as temporary storage of precipitation on the surface in the form of snow cover during winter and the generation of impermeable areas owing to soil freezing. For example, precipitation during the winter may be supplied to the surface mainly by the thawing of snow cover and determining the snow accumulation/snowmelt rate would thus be as important as (or, in quantitative terms, even more important than) precipitation in summer. The depth and density of snow cover should therefore be investigated in addition to general rainfall measurements. The amount of snowfall may not be indicative of the effective precipitation owing to evaporation from the surface of the snow cover during winter. Thus, the amount of the evaporation has to be determined to establish whether or not it can be ignored.

Two types of rain gauge (a tipping type and an overflow type) were used in the precipitation investigation; snow depth and snow weight meters were installed at the same time. Precipitation in periods with and without snow cover can be calculated by comparing and analysing the data obtained using these gauges. The river water level was continuously monitored using a pressure gauge during the non-freezing period to determine river runoff and the flow rate was determined based on the relationship between water level and flow rate obtained by river flow rate monitoring. However, determining the relationship between water level and flow rate was difficult during times when the ground was frozen because the flow rate decreases. The river flow rate was thus monitored once every week to 10 days to directly determine the flow rate.

The drainage basins in and around the URL area are characterised by the fact that they are located in a cold snowy region with a mixture of fields and forests. The applicability of methods for measuring evapotranspiration to such basins was also evaluated (Table 4.7.3-1). As a result, it was found that the Penman method[250),251)], which is suitable for the water surface or surfaces with a low roughness, and the bulk method[252], which is effective in measuring evapotranspiration from water surfaces or snow cover, were suitable for fields in periods without and with snow cover respectively. The gradient method[251] and the Bowen ratio – energy balance method[253], which calculate evapotranspiration from the crown, would be applicable for broadleaf forests. Although measurements using an evaporimeter provide an indication of evapotranspiration, this method is not used at present because it cannot be used during winter.

Figure 4.7.3-4 shows the monthly total evapotranspiration from 25th November 2004 to 31st December 2005, calculated according to the Penman, gradient, Bowen ratio – energy balance, bulk, Thornthwaite and Harmon methods. In the figure, the measurements of mean monthly evapotranspiration during summer obtained using an evaporimeter in the Kaishin area from 1990–1999 are also shown. The values measured using the evaporimeter indicate evaporation from the water surface. Generally, these values are much higher than those for evapotranspiration over a wider area, but they do serve as a measure of the amount of evaporation and evapotranspiration from vegetation areas. Comparisons were also made with the monthly mean temperature, monthly mean wind speed and monthly total precipitation measured by the meteorological station in the Hokushin area.

As shown in Figure 4.7.3-4, the Harmon and Thornthwaite methods, which are both empirical formulae, show a fairly similar trend, whereas the combination of the bulk method for periods with and without snow cover showed a slightly different trend from the other methods in the periods from July to September 2004 and May to July 2005. The reason for the difference could be that the bulk method is a function of wind speed and depends greatly on its effect and wind speed in the Hokushin area is low during summer and relatively high during spring to early summer. The combination of the bulk method (snow cover period) and the Penman method (period without snow cover) tends to show slightly higher values in periods with high wind speeds, but it generally shows a similar trend to that of the empirical formulae or the measurements using the evaporimeter. The Penman method is thus considered to be effective for estimating evapotranspiration in summer.

Table 4.7.3-1 Applicability of evapotranspiration measurement methods

Evapotranspiration measurement method		Penman	Gradient	Bowen ratio – energy balance	Bulk	Eddy correlation	Thornthwaite	Harmon	Pan evaporation
Check item	a) Effort for acquiring data*	++	+	++	+	–	++	++	++
	b) Measurement item*	+	–	–	+	+	++	++	++
	c) Effect of landform on measurement**	++	++	+	++	–	++	++	+
	d) Measurement in forest†	–	++	++	–	++	–	–	+
	e) Measurement in grass field†	++	++	++	–	++	–	–	+
	f) Measurement on snow cover††	–	–	–	++	–	–	–	–
	g) Measurement during winter††	–	++	++	++	++	++	++	–
	h) Frequent maintenance§	++	++	++	++	–	++	++	++
Evaluation of applicability to	forest (based on a, b, c, d and h)§§	–	++	++	–	+	–	–	+
	grass field (based on a, b, c, e and h)§§	++	+	+	–	+	–	–	+
	snow covered field (based on f and g)§§	–	+	+	++	+	+	+	–

*++: less, +: moderate, –: more, **++: none, +: small, –: large, †++: suitable, +: possible, –: unsuitable, ††++: possible, –: impossible, §++: not necessary, –: necessary, §§+: very good, +: good, –: not good

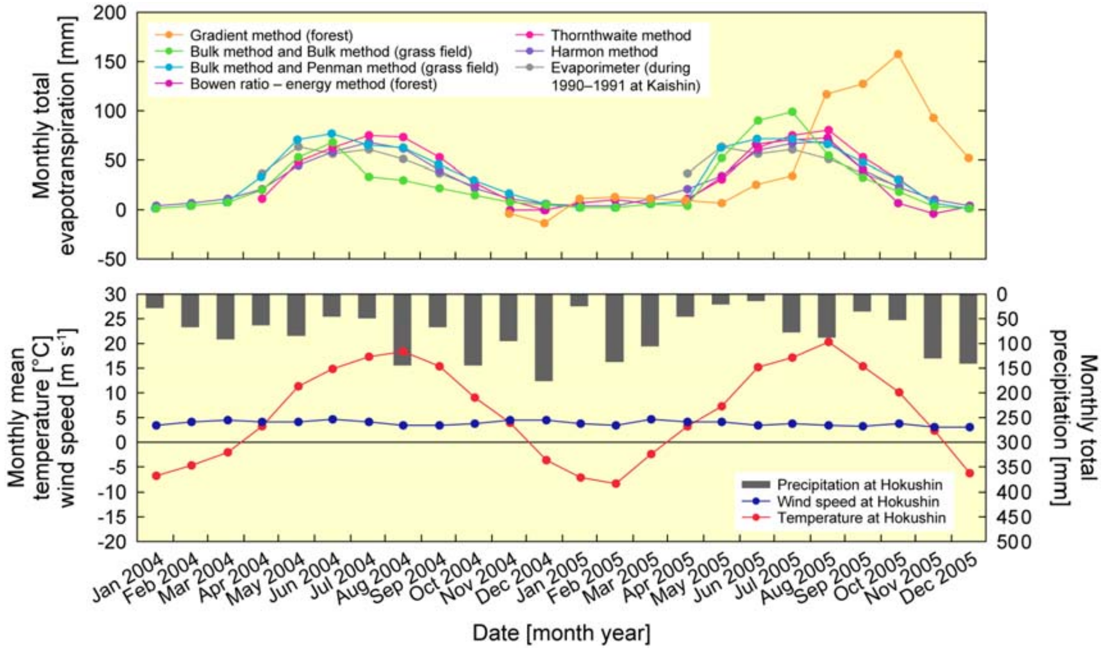

Figure 4.7.3-4 Comparison of evapotranspiration measured by various methods (broadleaf forest)

A comparison was made between the Bowen ratio – energy balance method and the gradient method, which are both intended to estimate evapotranspiration in forest areas. The gradient method showed extremely low values in summer compared to the values obtained using other methods and considerably higher evapotranspiration values during winter when leaves are scarce. These trends are different from those indicated by the evaporimeter measurements. According to Hattori[251)], a stable atmosphere, i.e. a thermally neutral state free from the effect of buoyancy, is important when using the gradient method. Measurement of evapotranspiration in an unstable atmosphere may thus cause some problems with the accuracy of the results. The Bowen ratio – energy balance method is considered to be applicable even in summer because the results agreed well with those of the empirical formulae, provided that a correction is made to compensate for the transpiration that is likely to occur during winter and at dawn.

ii) Hydraulic engineering method

Investigation of groundwater recharge rate using the divergent zero flux plane method was used to confirm the applicability of the hydraulic engineering method. The divergent zero flux plane method is a technique for calculating fluxes in saturated/unsaturated zones based on the difference in pressure heads obtained from the depth distribution of volumetric moisture content and saturated/unsaturated hydraulic conductivities by applying the Darcy’s law to the unsaturated zone. The pressure head in the unsaturated zone can be obtained directly by measuring suction in the soil moisture using a tensiometer. Alternatively, volumetric moisture content can be measured with a soil moisture meter and the pressure head corresponding to the volumetric moisture content is obtained in the laboratory. Field measurements were carried out using a soil moisture meter that is effective for permeable soil, although the influence of hysteresis cannot be ruled out. The soil moisture meter was used because measurement using a tensiometer is difficult since the shallower subsurface at Horonobe area are frozen during winter and because the hydraulic conductivity of the shallower soil was assumed to be relatively high. The measurement points were set at depths of 0.7 m, 1.3 m, 1.8 m and 2.3 m near borehole HGW-1. An amplitude domain reflectometry (ADR) soil moisture meter was used because of its low consumption power and because the accuracy of the device is less affected by salinity. Temperature sensors were also installed.

Figure 4.7.3-5 shows the measurement results for groundwater level, volumetric moisture content and earth temperature. Results of laboratory tests carried out to determine the degree of saturation corresponding to the volumetric moisture content at each depth indicate that all measurement points were more or less saturated. Measurement of groundwater recharge based on the divergent zero flux plane method described above was therefore impossible. This is presumably because the ground at the survey point has a higher content of fine grains than expected and the soil is less permeable. In future investigations, the survey point must be changed to allow the groundwater recharge rate to be estimated using the soil moisture flux. A tensiometer can be used to directly measure suction (negative pressure), although, as described above, using a tensiometer has inherent problems, including frozen piping during winter.

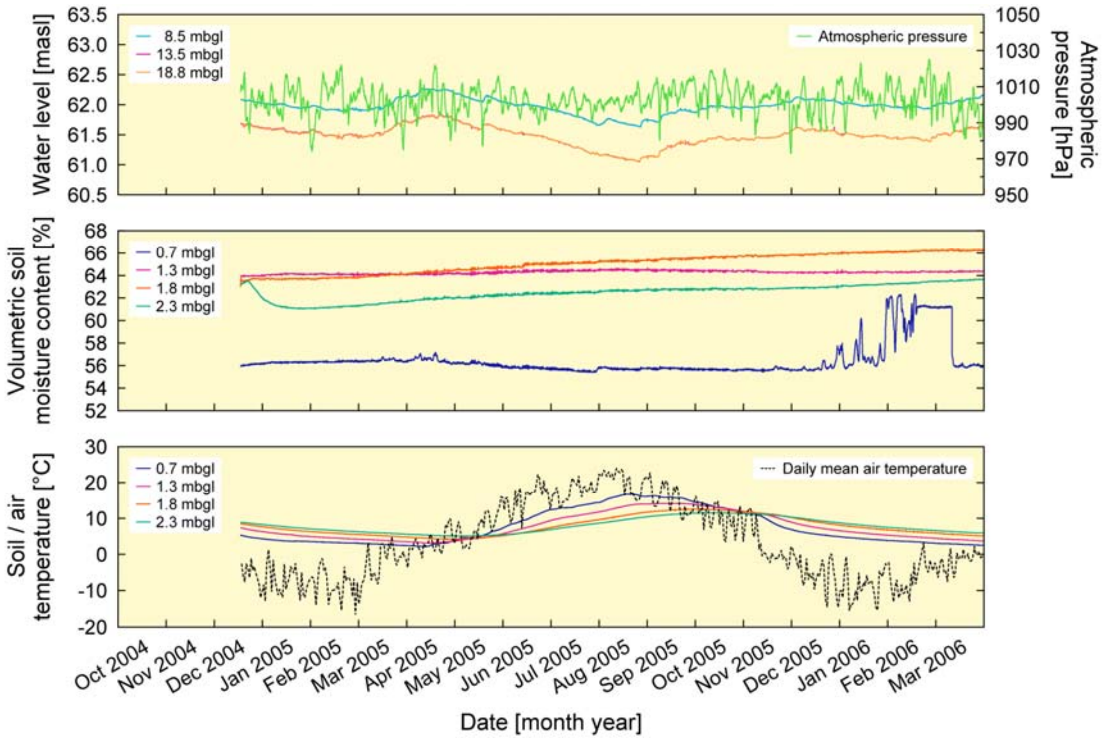

Figure 4.7.3-5 Groundwater level, soil moisture and temperature measurements from October 2004 to March 2006

iii) Other investigations

Other surface-based hydrogeological investigation methods include using river water chemistry and isotopes and groundwater level investigations covering shallower formations by means of electrical exploration; none of which have been used in this project yet.

(2) Hydrochemical investigations

Acquisition of quality-controlled data and hydrochemical analyses based on these data are necessary for characterising the spatial distribution and evolution of groundwater chemistry. During the entire course of the hydrochemical investigations, beginning with data acquisition and ending with analysis, quality assurance/control (QA/QC) of groundwater sampling and analysis is fundamentally of importance. Although QA/QC procedures for chemical and isotope analyses are standardised in the JIS, those for on-site groundwater sampling and sample handling have not yet been established. There are also many issues to be addressed regarding methods for measuring pH and redox potential in situ in boreholes.

1) Groundwater sampling

If the hydraulic conductivity of the host sedimentary formation is low, pumping itself or sufficient time for pumping may not be ensured when groundwater is to be pumped from intervals including fractures (or fracture zones). As a result, it is likely that the volume of data acquired will be insufficient for determining the spatial distribution of groundwater chemistry. In addition, for sedimentary rocks with WCFs, hydrochemical data need to be acquired from both advective groundwater flow through the WCFs and stagnant porewater in the rock matrix. For the characterisation of hydrochemistry in sedimentary rocks, a technique combining two methods – pumping groundwater from boreholes and squeezing porewater from core samples – therefore needs to be developed.

i) Pumping groundwater from boreholes

When groundwater is pumped via a borehole using a submersible pump from the Wakkanai and Koetoi Formations, dissolved gases such as CH_4 and CO_2 are degassed from the groundwater in response to the pressure release. When calculating WCF transmissivity and rock hydraulic conductivity by pumping tests, the amounts of pumped groundwater and the gases separated from the groundwater are required. In general, however, equipment for hydraulic packer test does not have the capability to measure released gas volumes during pumping. The equipment was thus improved to allow use in the investigation (Figure 4.7.3-3).

Degassing of dissolved gases in the groundwater would result in a change in groundwater chemistry. In addition, improving data quality for WCF transmissivity and rock hydraulic conductivity would result in a decrease in data quality for groundwater chemistry. The acquisition of hydraulic data and hydrochemical data at the same time and interval would, however, be very effective for modelling hydrogeological structures and building the technical reliability in the results of groundwater flow analyses. This would also be important in the context of planning an efficacious borehole investigation programme, including reduction of investigation times and costs. Since investigation priorities differ depending on the borehole, groundwater sampling methods have to be selected in an appropriate manner according to the specified aim of the investigation, e.g. measurement of in situ pH over a long period of time or determining the depth profile of salinity over a short period of time. In other words, it is not appropriate to try to achieve perfect results for all investigation targets in a single borehole.

If pumping from a borehole is planned, the chemistry of the drilling water to be used should be selected depending on the groundwater chemistry. In order to confirm that no major changes have occurred in the drilling water chemistry during drilling, analyses (pH, electrical conductivity and major chemistry) should be conducted at a certain time interval. At the same time, analysis of a tracer (Na-naphthionate in this investigation) added to the drilling water should be conducted. During the pumping tests, the concentration of Na-naphthionate should be measured frequently (e.g. every one hour) depending on the pumping rate. At the point when the concentration of Na-naphthionate reaches 0.1 mg l^{-1} or less, the samples for major elements, various isotopes, dissolved gases and microbes are collected. This method has the advantage that several tens to several hundreds of litres of sample can be obtained although degassing occurs.

ii) Extracting porewater by squeezing

Extensive hydrochemical characterisation was conducted on rock matrix porewater. The following points were considered when conducting the hydrochemical analyses[254)]:

- penetration of drilling fluid into the core;
- changes in water – rock interaction owing to drying of the core during storage;
- changes in porewater chemistry during squeezing owing to the fractionation of elements and isotopes;

- changes in porewater chemistry during squeezing owing to oxidation and degassing of porewater and pressure/temperature changes;
- contamination by components of the squeezing tools;
- errors in chemical analysis owing to insufficiency of the squeezed porewater sample.

For this investigation, the procedures and equipment were improved to avoid being affected by the above factors. The results of examination on changes in porewater chemistry during squeezing are described below by way of an example. It should be noted that the examination was carried out under a joint research with the Central Research Institute of Electric Power Industry (CRIEPI).

The system shown in Figure 4.7.3-6 was used to extract porewater. It is a uniaxial compression injection system (available from Seiken Inc., Japan), with a capability comparable to that used by Kiho et al[100]. Porewater with 5–20 ml per sample was squeezed with an axial compression of up to 70 MPa. In order to evaluate the influence on porewater chemistry of the loading pressure owing to squeezing, the chemistry of the squeezed porewater was analysed by stepwise increasing of the loading pressure. As a result, Na and Cl concentrations were found to gradually decrease in the porewater when the loading pressure was increased (Figure 4.7.3-7). The H and O isotope ratios were constant irrespective of loading pressure. The pores observed before squeezing were not observed after the operation. The cause of the changes in the porewater chemistry is assumed to be the fact that absorbed water and interlayer water (low salinity water) in minerals were squeezed out[255].

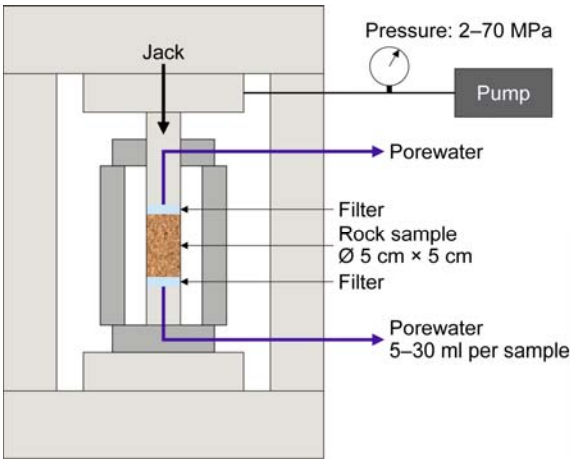

Figure 4.7.3-6 Schematic illustration of equipment for porewater squeezing

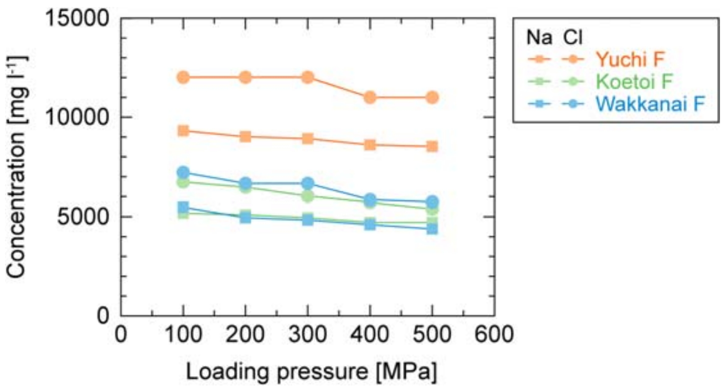

Figure 4.7.3-7 Relationship between loading pressure and porewater chemistry

Based on the results described above, it can be concluded that measurements of the relationship between loading pressure and porewater chemistry would be indispensable as input for QC of data for the porewater chemistry analyses.

iii) Comparison of results of analyses of groundwater pumped from the borehole and porewater

As described above, the possibility cannot be ruled out that groundwater pumped from boreholes and porewater squeezed from cores have different origins and hydrochemical properties. In addition, the chemical composition such as SO_4^{2-} may increase because of oxidation of the core at the time of squeezing. In order to confirm these points, porewater was squeezed from core collected from the interval in the borehole from which groundwater was pumped. The extracted porewater was then analysed and its chemistry compared with that of the groundwater pumped from the borehole. Cores in two different conditions, i.e. ones left for several weeks between sampling and squeezing (borehole HDB-1) and ones that underwent wax solidification immediately after sampling (borehole HDB-11), were prepared and their chemistries compared with each other in order to identify the effects of core oxidation. In addition, for part of the samples, all steps including core shaping and squeezing were conducted in an anaerobic condition. A comparison was then made with the case where the processes were conducted in a normal atmosphere. Figure 4.7.3-8 shows the result of analyses made of the samples obtained in boreholes HDB-1 and HDB-11. Order-of-magnitude differences in concentration were not observed in the comparison of the chemistry of groundwater pumped from the borehole HDB-11 and the porewater.

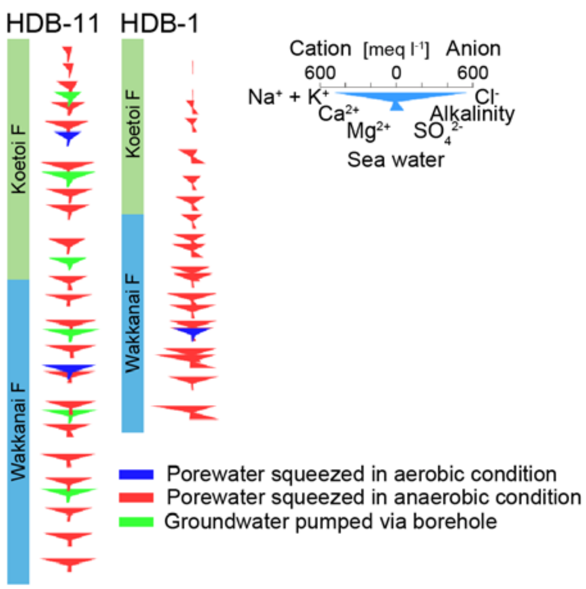

Figure 4.7.3-8 Chemistry of groundwater and porewater in boreholes HDB-1 and HDB-11

The porewater SO_4^{2-} concentration was high for boreholes HDB-1 and HDB-11 but those for the borehole HDB-11 was lower. The difference can be interpreted as follows: the core from borehole HDB-1 was stored in the atmosphere during the period from sampling to porewater extracting and sulphides such as pyrite in the rock were oxidised during this time; eventually SO_4^{2-} was selectively squeezed owing to oxidation occurring during squeezing. This oxidation effect can thus be reduced by squeezing immediately after the core is sampled, as was the case for borehole HDB-11. Figure 4.7.3-9 shows the result of the analysis of principal component in the groundwater and the porewater. In the figure, the factor that controls the second component (PC2) is SO_4^{2-} and the effect appears to be larger in data for borehole HDB-1 compared to the data for borehole HDB-11. If the increase in SO_4^{2-} owing to core oxidation is ignored, the groundwater chemistry in the Wakkanai and Koetoi Formations would be characterised by the SO_4^{2-} concentration. This indicates that even the main component analysis may lead to an erroneous interpretation.

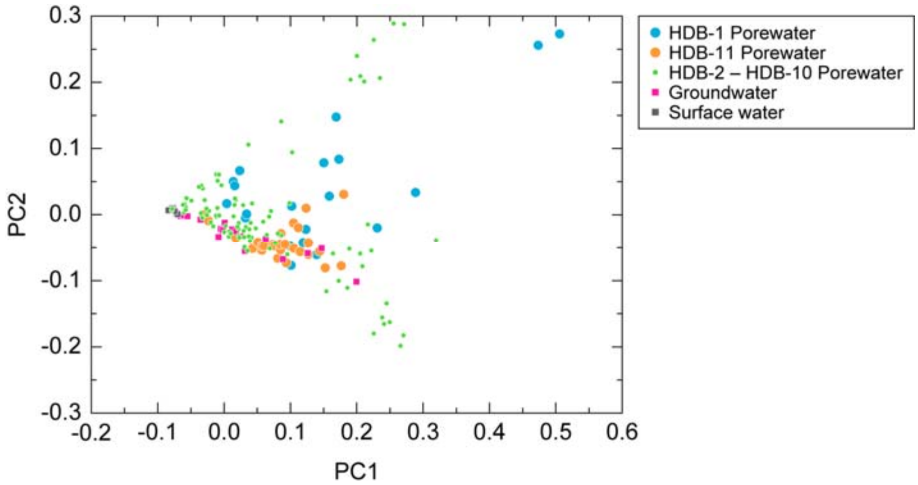

Figure 4.7.3-9 Result of principal component analysis

2) In situ hydrochemical investigations

As described above, pumping groundwater via boreholes involves problems in that groundwater chemistry can be changed owing to degassing and oxidation. To solve these problems, an in situ physico-chemical parameter measurement system and a groundwater sampling technique that maintains in situ pressure were developed[256)].

i) In situ physico-chemical parameter measurement system

This system was developed by combining conventional techniques, based on the assumption that bentonite mud used is left in the borehole. For the measurement equipment which forms the main component of this system, an OCEAN SEVEN 303 Probe developed by Idronaut S.r.l., Italy was selected from the point of view of durability at depths up to about 1,000 m, specified measurement goals and maintainability.

Figure 4.7.3-10 shows the result of the investigation using this equipment. Regarding pH and Eh, results obtained at surface and in situ were different: pH = 6.8 (at surface) and 6.2 (in situ) and Eh = +160 mV (by Au electrode at surface), -60 mV (by Pt electrode at surface) and -166 mV (in situ). These results for other measured items indicate essentially the same values for the surface and in situ measurements. Degassing of CO_2 in the groundwater may be the cause of the higher pH at surface than that measured in situ. Inclusion of small amounts of air may have caused the higher Eh value for the measurements at surface.

ii) In situ pressure confining water sampling equipment

The conventional in situ groundwater sampling technique samples groundwater using the difference in pressure between that in a container and in situ. However this technique reduces the groundwater pressure in the sampling interval when the groundwater is sampled, albeit for only a short period of time. During this time, degassing of dissolved gases may occur owing to the decrease in groundwater pressure, resulting in collection of excess gas in the container. Modifications were required to avoid reducing in situ groundwater pressure when sampling, allowing the amount of dissolved gas in the groundwater to be determined properly. The conventional sampling container designed to prevent reduction in the groundwater pressure could not prevent contact between the content of the container and the groundwater. New sampling containers were therefore manufactured for the deep borehole investigations to acquire data on dissolved gases and microbes in the groundwater.

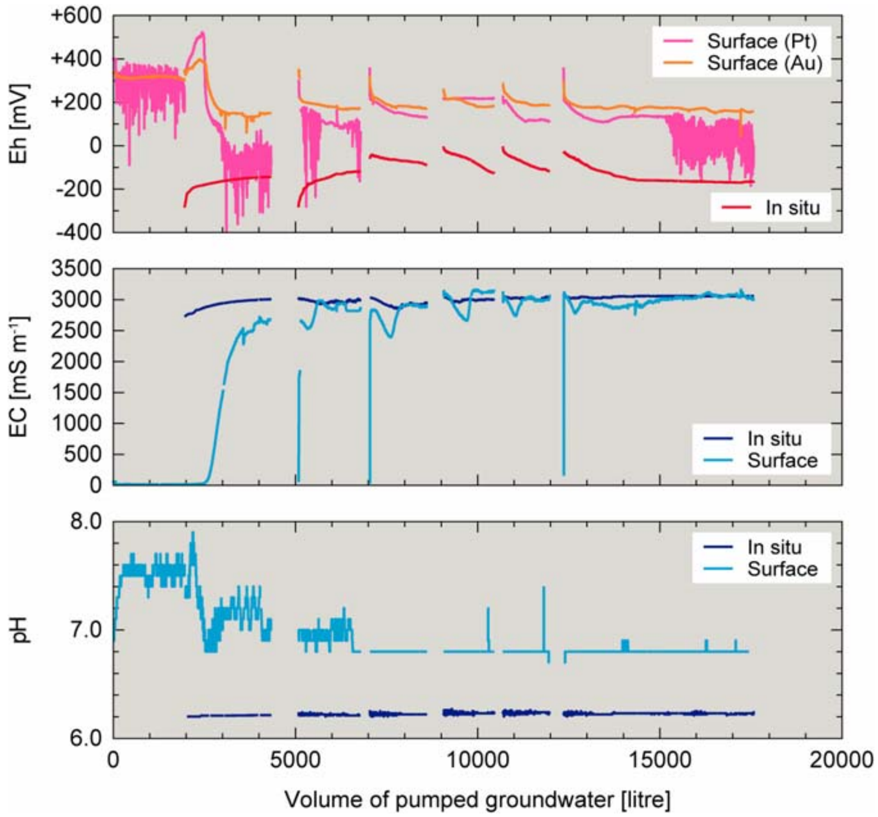

Figure 4.7.3-10 In situ measurement of physico-chemical parameters in borehole HDB-11

4.7.4 Rock mechanical investigation techniques

(1) In situ and laboratory techniques for evaluating rock properties

Conventional testing methods used domestically and internationally were used to evaluate rock mechanical and physical properties for the reasons described in Section 4.4. A certain level of quality is ensured for the acquired data, which has the great advantage of allowing comparison with test results for areas other than Horonobe. However, the following problems associated with using core samples collected during borehole investigations were anticipated owing to the fact that the rocks of interest are from a saline water environment and are soft sedimentary rocks with a high effective porosity and that the vertical depth of the borehole is as much as several hundred metres:

- Mechanical properties may be affected by fine cracks in the cores generated by stress release during borehole drilling.
- Mechanical properties may be affected by using water (for saturation) with a different composition from the original one, since the rocks of interest were stable under saline water conditions.
- The core may dry up in a short period of time as it has an extremely high porosity, even though the slake durability is high. A change in the moisture content may affect mechanical properties.

In addition to these problems, the issues described below were identified during the course of the investigations:

- The specimens could not be standardised to one size as the same test equipment was not always used.
- Measuring the deformation by directly attaching a strain gauge to the specimens was sometimes difficult because the rock was very porous (or siliceous) but with low hydraulic conductivity.

The first problem was solved by carefully sampling the cores to be used in the laboratory tests while allowing for stress release effects during sampling. For the other problems, the following issues were examined in order to ensure the reliability of the laboratory tests:

- Effect of difference in hydrochemistry on mechanical properties
  Examination was conducted using two types of water to saturate specimens for standard uniaxial compression tests; fresh water collected from a well for borehole drilling and groundwater pumped via a borehole. Rock specimens were sampled in the vicinity of the interval where in situ groundwater sampling was carried out. The examination results suggest that the compressive strength may be decreased when a rock specimen in a saline water environment is saturated with non-saline water (Figure 4.7.4-1). It should be noted that the mechanical properties that had been obtained by laboratory tests using specimens saturated with fresh or distilled water may be smaller than those of the rocks in situ[257)].

- Effect of weathering of rocks owing to drying on mechanical properties
  A laboratory test on deterioration of rocks was conducted by simulating the situation where the drying process continues for a long period of time, instead of short-term repetition of drying and wetting. The cores collected from the Wakkanai and Koetoi Formations were firstly cut into test specimens and the specimens were then placed on electronic balances and left in a thermostatic chamber. Measurements of weight change and elastic wave velocity and visual inspections were conducted at specific time intervals. The test results indicate that rock specimens dried up rapidly in the first 100 hours (Figure 4.7.4-2); the elastic wave velocity was reduced and fractures occurred during this time period[117)].

- Effect of difference in size of specimens on mechanical properties
  Specimens with different sizes were sub-samples from the cores collected from the Wakkanai and Koetoi Formations; height was varied while fixing the ratio of diameter to height at 1:2 (2 cm × 4 cm – 5 cm × 10 cm). As a result, no scale effects on mechanical properties were observed within the range covered by these tests.

- Comparison of deformation measured by LDT and strain gauge
  Local deformation transducer (LDT) equipment has been developed and used in the field of soil mechanics as a method for eliminating experimental errors resulting from bedding errors occurring at the top and bottom ends when conducting tests. In the case where a strain gauge cannot be easily bonded to the centre of the specimen, a comparison test was conducted to determine the applicability of LDT to siliceous rock. As shown in Figure 4.7.4-3, strain measured by LDT was equivalent to that measured by a strain gauge. This suggests that LDT could be used in place of a strain gauge when the gauge cannot be bonded to specimens in laboratory tests. In addition, as described in Subsection 4.4.4, the influence of loading rate on the result of a uniaxial compression test, which is considered most likely to be affected, was investigated. The result indicates that loading rates from 0.1 to around 0.002% min^{-1} effectively have no influence (Figure 4.7.4-4).

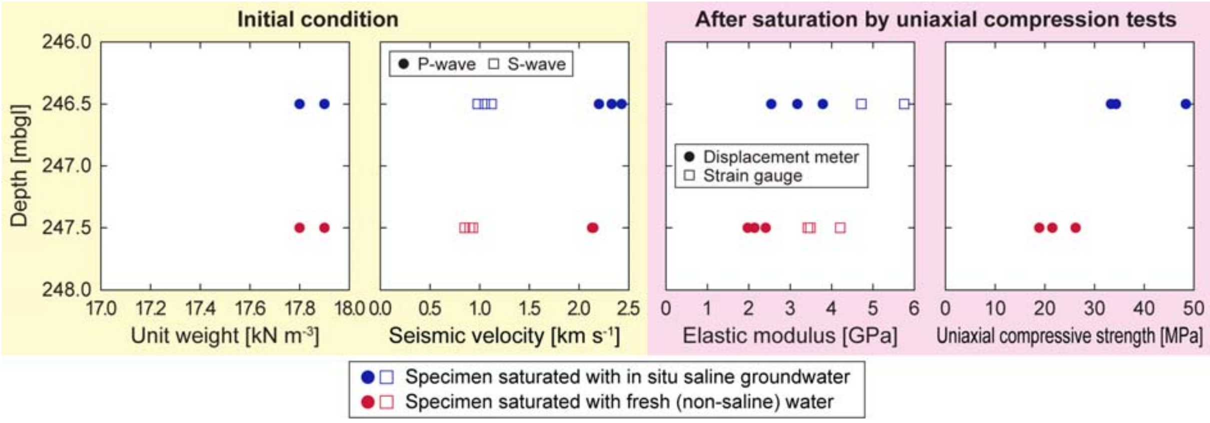

Figure 4.7.4-1 Results of laboratory tests using specimens saturated with different waters

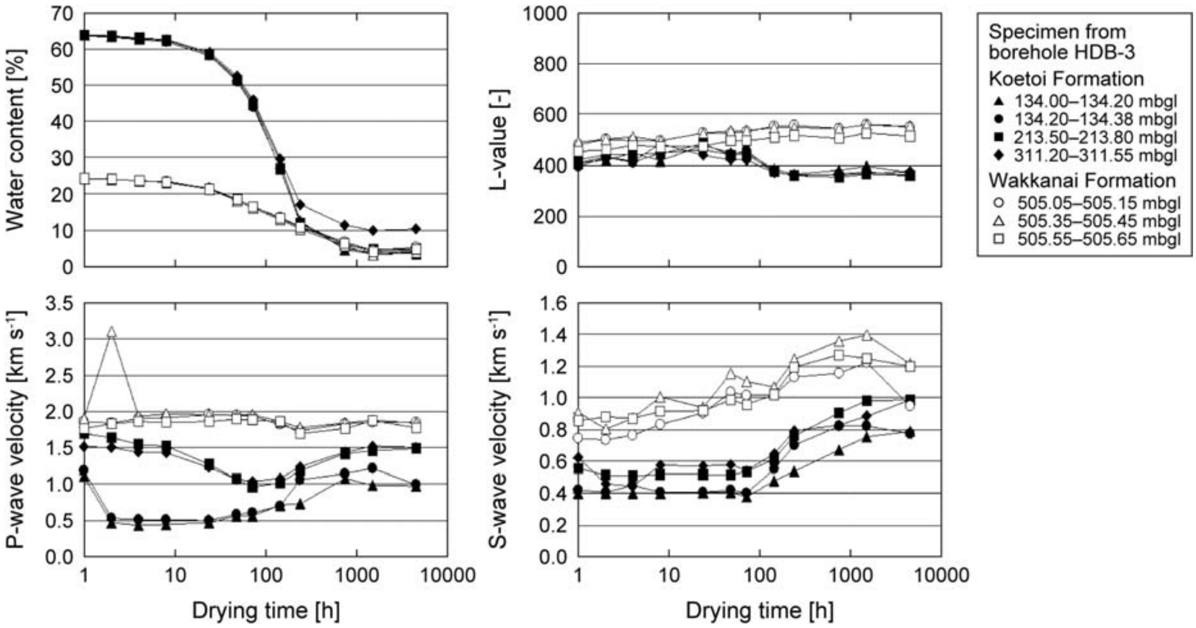

Figure 4.7.4-2 Variation in mechanical properties owing to drying of specimens

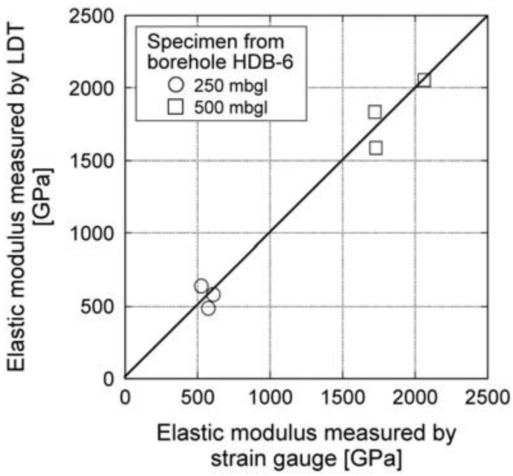

Figure 4.7.4-3 Comparison of elastic modulus measured by LDT and strain gauge

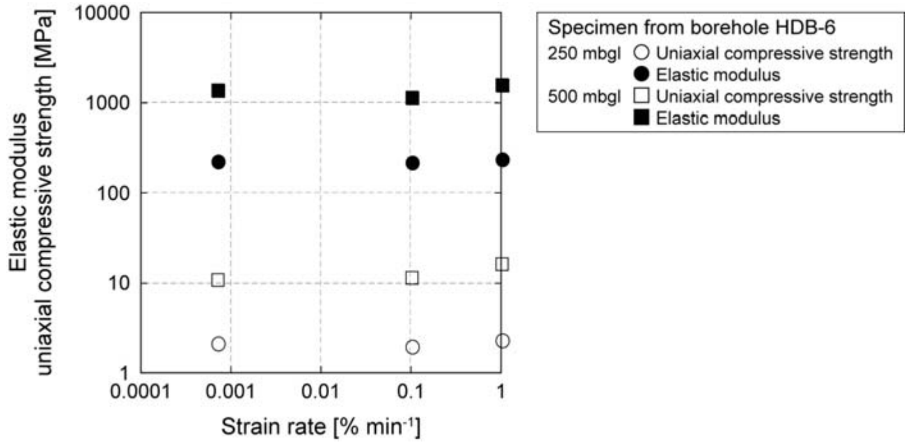

Figure 4.7.4-4 Results of uniaxial compression tests with different strain rates

From the above results, the laboratory test methods used in this investigation generated conservative values in terms of in situ mechanical properties. The data can therefore be compared with each other irrespective of the size of the specimens. However, it was found that a change in moisture content was a major factor causing deterioration of rock properties. Thus, the cores provided for the laboratory test were treated appropriately to prevent moisture content changes soon after drilling. Particular efforts were also made to conduct sampling and testing as soon as practicable. In this respect, a method used in the borehole investigations (plastic wrapping and paraffin coating to retain moisture after core logging) was found to be effective from the viewpoint of long-term storage. The applicability of LDT was confirmed for specimens such as sandstone sampled from the Yuchi Formation to which strain gauges could not be applied.

It is concluded that conventional standardised methods are sufficient for laboratory tests on rock classified as soft sedimentary rock. From the viewpoint of QA of the obtained data, however, the influence on mechanical properties of the geological environment at the investigation site of interest and the petrophysical characteristics specific to each rock type should also be evaluated.

i) Laboratory techniques for characterising long-term rock behaviour

A laboratory test method for characterising the long-term behaviour of rock, which is one of the major mechanics-related issues for geological disposal, has not yet been established either domestically or internationally. Application of pneumatic uniaxial creep test equipment, developed and introduced for macroscopic investigation of the long-term rock behaviour, was made for siliceous rocks in Horonobe in order to acquire data on a range of parameters. The results indicate that the creep behaviour of the siliceous rock was found to be different from that of tuff and sandstone; relatively large creep occurred particularly in the primary creep stage at initial loading (Figure 4.7.4-5). It was also found that the strain rate in the secondary creep stage was not significantly different from that of previous studies and that the confining pressure influenced rigidity at the initial stage of loading, but not creep behaviour in the subsequent stages, compared with the result of a triaxial creep test. The relationship between minimum creep strain rate and failure time can be expressed by a linear relationship[258)], as was previously suggested (Figure 4.7.4-6).

In addition, directionality was also evaluated in terms of the characteristics of long-term behaviour since siliceous rock was known to have a certain degree of mechanical directionality. It was suggested that creep strain may be greater in the vertical direction than in other directions, as is the case for strength, and that the strain level at which creep failure is initiated is close to the strain level obtained by uniaxial compressive strength tests (Figure 4.7.4-7).

A multistage creep test was used as the laboratory test method, recognising the fact that the siliceous rock in Horonobe shows a wide variation in strength in the uniaxial condition. A comparison was made to evaluate the relationship between the multistage creep test and conventional uniaxial creep test methods[259]. However, the multistage creep test method has not yet been fully established to date.

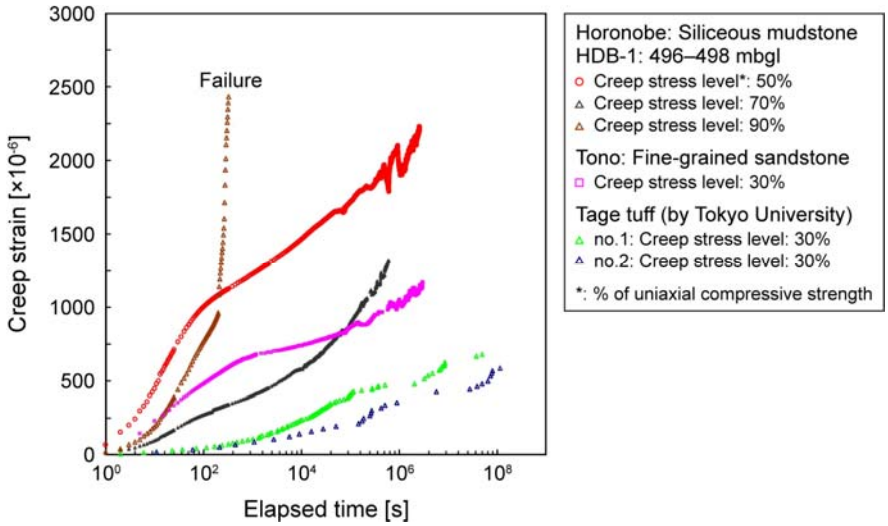

Figure 4.7.4-5 Typical creep strain – time curves for different rocks

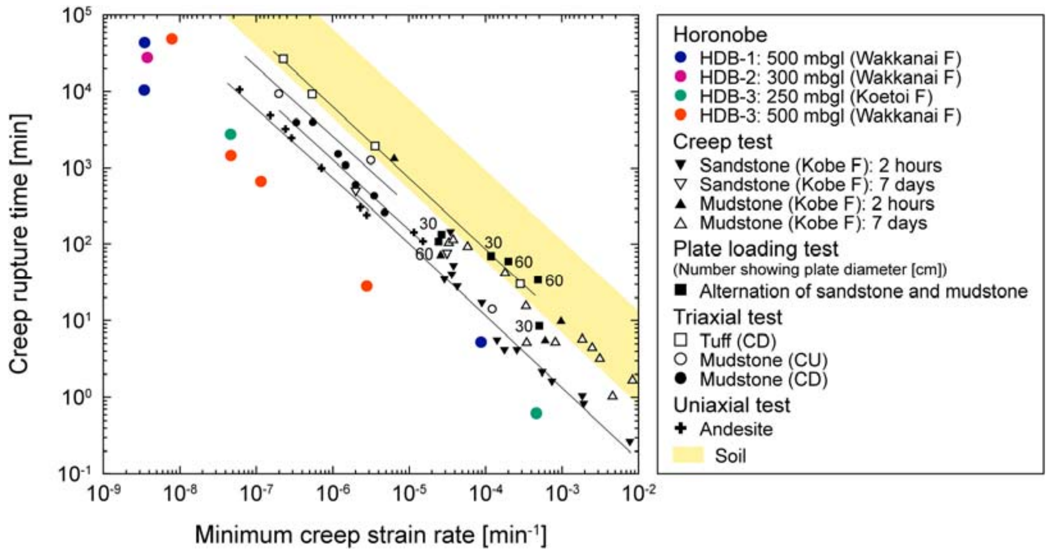

Figure 4.7.4-6 Diagram of minimum strain rate and failure time owing to creep for several types of rock found in Japan

Modified from Yamada et al.[258]

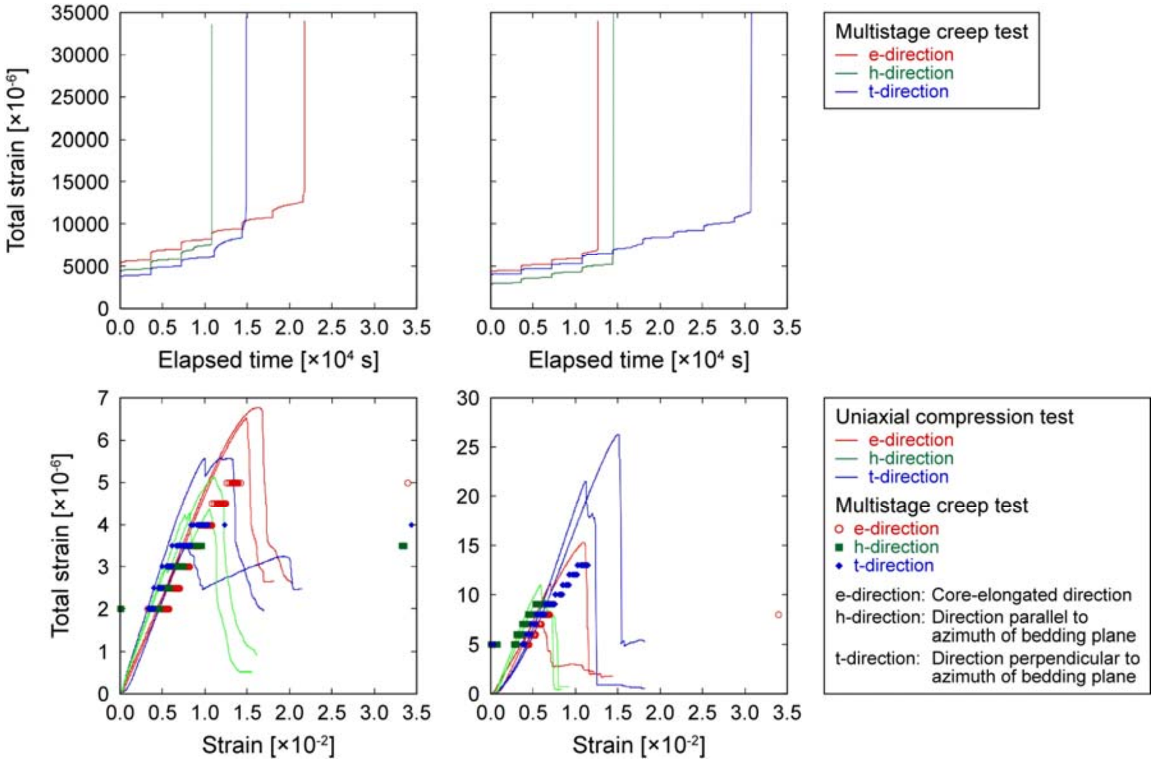

Figure 4.7.4-7 Comparison of stress – strain curves for uniaxial compression tests and multistage creep tests on specimens sampled with different directions in HDB-6

Top: Total strain – time curves by multistage creep tests; *Bottom:* Stress – strain curves by uniaxial compression tests and multistage creep tests; *Left*: Diatomaceous mudstone; *Right*: Siliceous mudstone

ii) Techniques for evaluating in situ rock properties

Data from density and velocity logging were used to evaluate in situ rock mechanical and physical properties. The dynamic elastic modulus and dynamic Poisson's ratio were determined based on P- and S-wave velocities obtained by velocity logging and the results were used to evaluate the in situ rock rigidity. Figure 4.7.4-8 shows some of the measurements. Compared with the results of the laboratory tests, both the P- and S-wave velocities obtained in the Wakkanai Formation agree with the laboratory test results; in the Koetoi Formation, the S-wave velocity was almost twice as high as the core measurement result, although the P-wave velocities agreed well. With respect to the density, the values obtained by velocity logging and laboratory testing showed very good agreement. This could be due to the stress dependence of the elastic wave velocity. Figure 4.7.4-9 shows the results of laboratory tests on stress dependence of the elastic wave velocity[260)]. To conclude, the change in elastic wave velocity caused by the variation in confining pressure was very small and hence the differences mentioned above cannot be fully explained.

Although some questions remain regarding the absolute values for some data obtained from the velocity logging, geophysical logging is considered to be effective for the investigation of rock mechanical and physical properties. This is because comparative evaluations for defining zones that are necessary for developing a conceptual model can be conducted with sufficient accuracy, in both quantitative and qualitative terms, using measured data obtained continuously at high resolution, despite the fact that the targets of the present investigation, the Wakkanai and Koetoi Formations, can barely be distinguished from one other by core logging since they originated from the same diatomaceous rocks and were formed in the same age. Another reason is that suitable positions for the other surveys could be determined using the data from the density logging that provides test results quickly. Unlike the case of crystalline rock, rock mechanical and physical properties determined in situ by the logging agreed well with those obtained by laboratory tests. This would also be advantageous for modelling a 3D field with a small amount of investigation data.

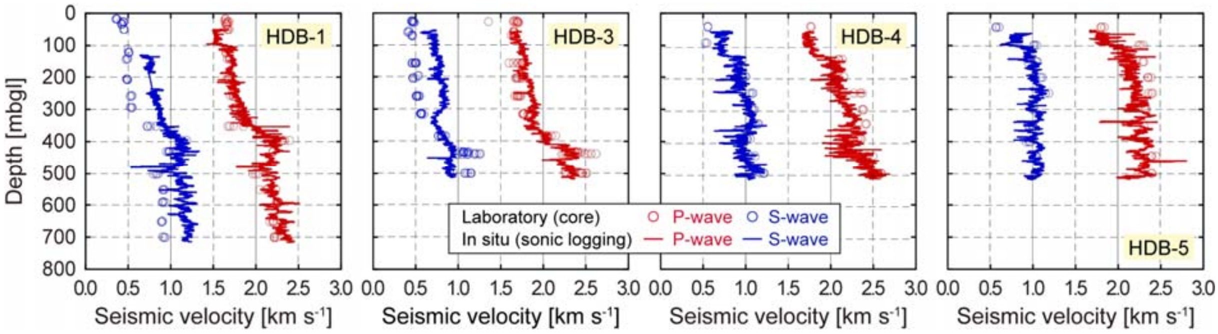

Figure 4.7.4-8 Comparisons of seismic velocities measured in situ and at cores

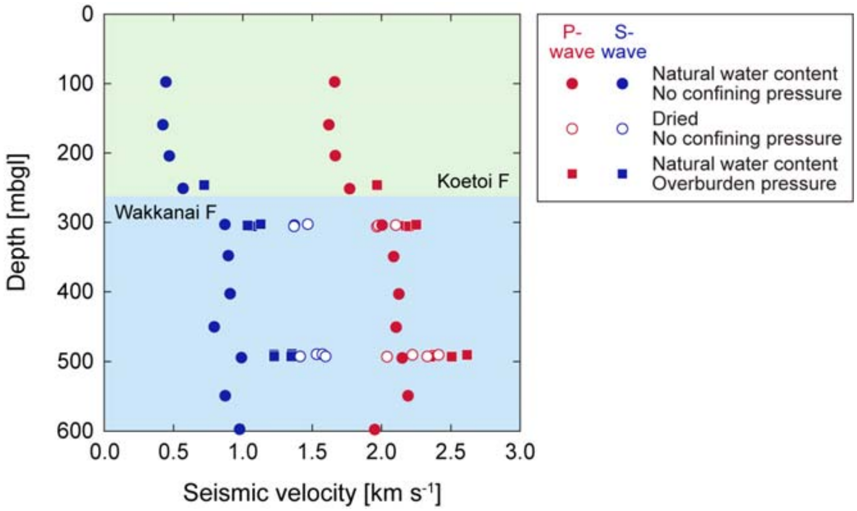

Figure 4.7.4-9 Effect of confined stress on seismic velocities for cores sampled from borehole HDB-6

iii) In situ borehole expansion testing system

The measurement system, developed by Solexperts AG, Switzerland, used in the borehole expansion tests in borehole HDB-6 (Figure 4.7.4-10) proved to be effective because of:

- compact system, allowing use deep subsurface;
- uniform pressure loading type system, allowing application to soft sedimentary rocks;
- capability of determining the directionality of deformation to a certain degree using displacement gauges equipped in three directions.

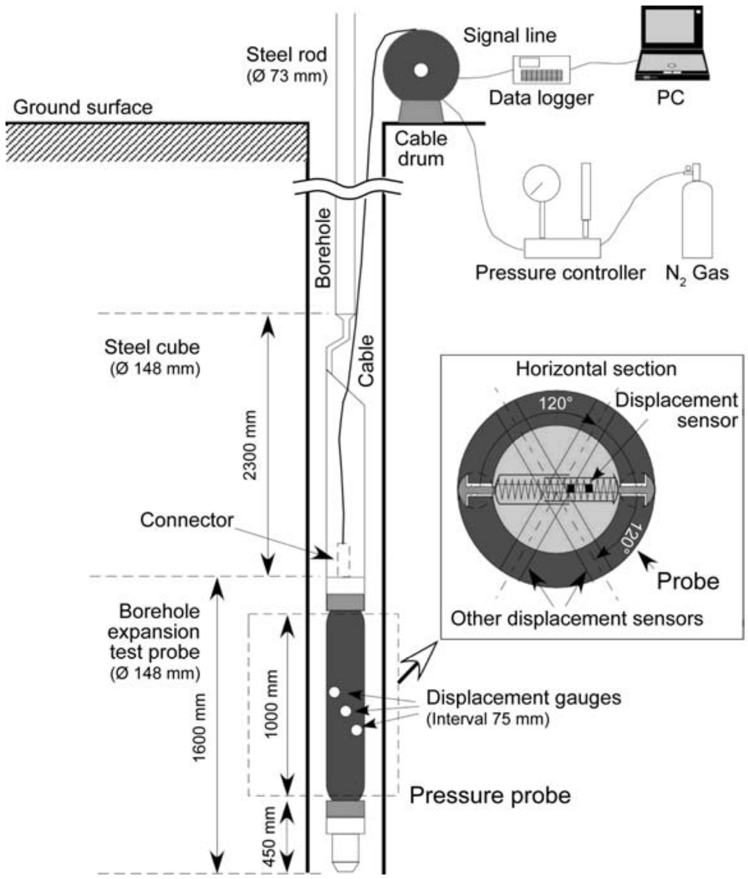

Figure 4.7.4-10 Measurement system for borehole expansion tests in borehole HDB-6

(2) Techniques for evaluating in situ rock stress conditions

The hydraulic fracturing method was applied for characterising the in situ rock stress conditions, considering that the environment was a vertical borehole drilled to great depth where borehole water was always present and one of the directions of principal stress was assumed to be the same as the vertical stress based on the results of previous studies[114)].

For the first investigations in boreholes HDB-1 and HDB-2, a stress measurement system[261)] based on wireline hydraulic fracturing, which had been successfully used in boreholes in the sedimentary formations and granite basement in the Tono area, Gifu Prefecture, was used. The system was developed to allow accurate stress measurement and has the following advantages:

- mechanism called a push valve, allowing injection/drainage of water into/from the packed-off intervals as well as the sections subjected to hydraulic fracturing using one line;
- small clearance between the system and the borehole wall, allowing fracturing using a small amount of water;
- shorter time for measurement than the fracturing system using a rod.

In situ hydraulic fracturing using this system was conducted at two depths, although it was originally planned at three depths. This was because jamming due to the malfunctioning of the push valve and bursting of packers frequently occurred in the borehole during the measurements. These failures were caused mainly by the following factors: when bentonite mud is used for drilling, malfunctioning due to the mechanism of this system tends to occur; since the measurement point was located deep in the soft sedimentary rock, the borehole walls were prone to changes with time; the pulling force for retrieving the tools from the borehole is not sufficient because of the use of a wireline system. Since these problems will be inevitable in future investigations, it was decided to conduct the stress measurement in borehole HDB-3 and subsequent measurements with a rod-type hydraulic fracturing system available from TAM International Inc., USA (Figure 4.7.4-11). As a result, most of the above-mentioned problems affecting the in situ stress measurements were resolved and the measurements could be conducted as planned. However, attention must be paid to the case where dissolved gases turn into bubbles owing to the stress release occurring at the time of borehole drilling, which may affect the measurements using this system.

A phenomenon regarded as borehole breakout was seen as shown in Figure 4.7.4-12 when conducting the investigations in boreholes HDB-1 and HDB-2. The in situ stresses can also be estimated using this phenomenon – omitting the details of the analysis theory, by a comparison between the stress evaluated based on the borehole breakout and that measured by hydraulic fracturing.

As indicated by Figure 4.7.4-13, the maximum principal stress estimated from the borehole breakout agreed well with the result of in situ measurement, although it is slightly lower. Borehole breakout phenomena are repeatedly observed at a depth around 300 m or deeper in boreholes located on the west side of the Omagari Fault, while they are rarely seen on the east side of the fault. Although the Wakkanai Formation is found at a shallower depth on the east side of the Omagari Fault compared to the west side, the mechanical properties in these areas show little difference. The occurrence of the borehole breakout can be interpreted as being due to the difference in in situ stress conditions on the east and west sides of the fault. This interpretation is supported by the fact that the borehole wall is stable, with no deformation in the unprotected borehole sections, at the bottom of, borehole HDB-10 (a depth of 500–550 m) drilled on the east side of the Omagari Fault. These results indicate that borehole breakout phenomena may be useful data for evaluating the direction of the principal stress in the horizontal plane in situ and for qualitative evaluation of the stress field.

When conducting stress measurements based on hydraulic fracturing, it is extremely important to conduct the measurement in a section where no fractures are present in order to ensure the reliability of the results. Although this requirement and the occurrence of borehole breakout are contradictory, stress measurements using hydraulic fracturing in this investigation were intentionally conducted in sections with and without borehole breakout. One reason is that, when damage is limited to the vicinity of the borehole wall, as in the case of borehole breakout, a stress similar to the reopening pressure in the section without fractures would be measured if the artificial fracture generated by hydraulic fracturing reaches deeper than the limited damaged zone from the wall of the borehole, because the analysis of data from stress measurements conducted by hydraulic fracturing uses not the breakdown pressure which develops the primary fracture but a reopening pressure and a shut-in pressure of the developed fractures to calculate the stress. Another reason is that the borehole breakout would provide information on the direction of the principal stress in the horizontal plane.

Since the in situ rock stress conditions may vary depending on the location of interest for the investigation, phenomena associated with stress may also vary. Surface-based borehole investigations therefore need to be flexible to respond to the phenomena occurring at different locations.

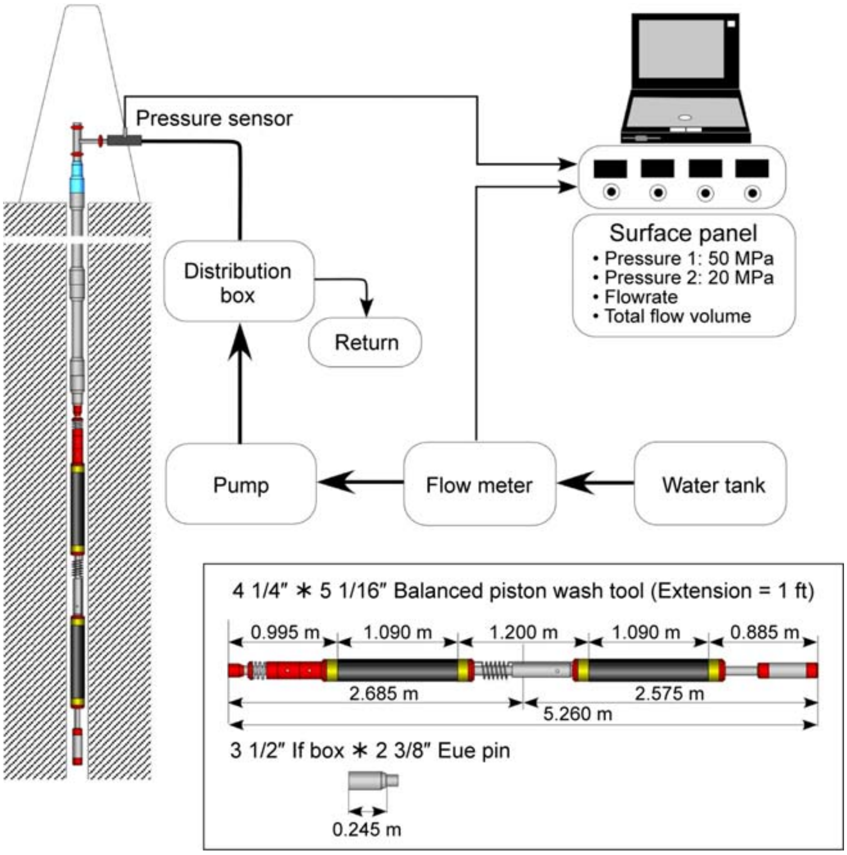

Figure 4.7.4-11 System used for stress measurement with hydraulic fracturing (rod system)

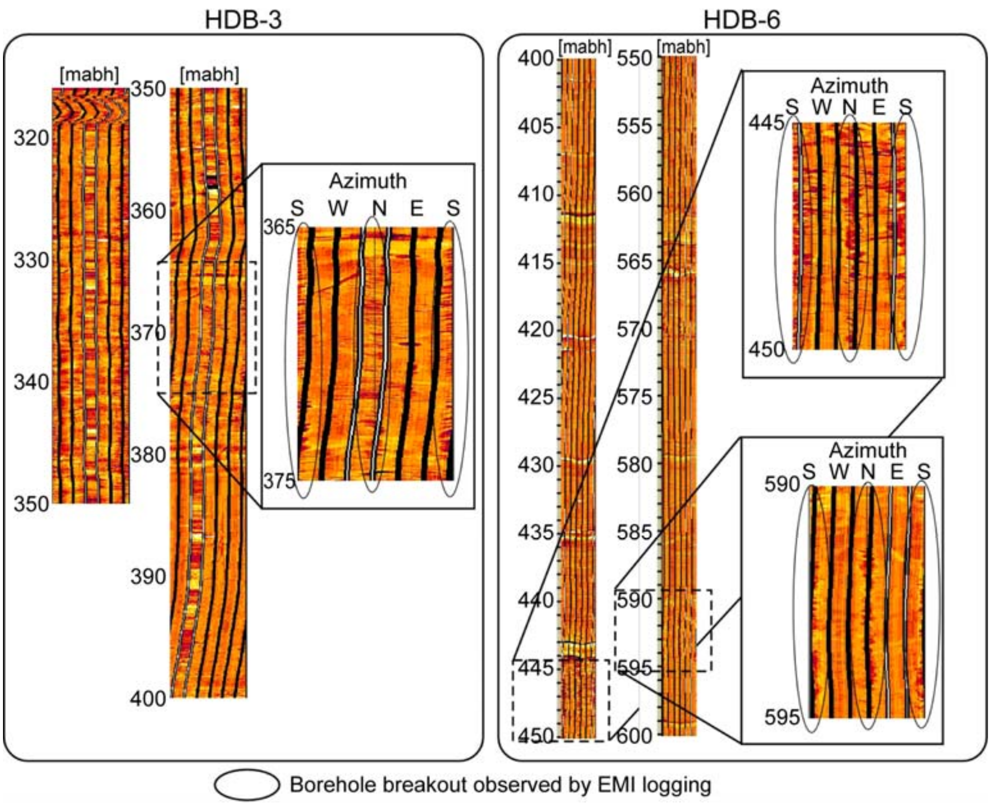

Figure 4.7.4-12 Borehole breakout observed using EMI™ logging in boreholes HDB-3 and HDB-6

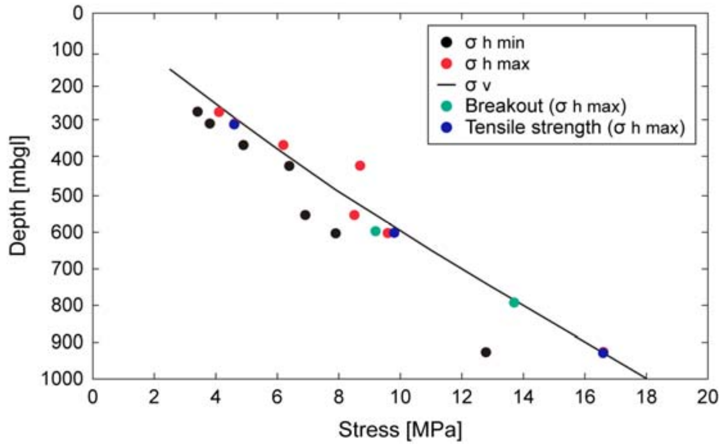

Figure 4.7.4-13 Comparison of the magnitudes of principal stresses measured by hydraulic fracturing and by borehole breakout analysis (HDB-11)

An alternative method for characterising in situ rock stress conditions is that using rock cores. In the case where implementation of in situ measurements had been assumed to be difficult prior to initiating the borehole investigations, as described in Subsection 4.4.2, the applicability of the AE method was evaluated. However, in situ stress measurements based on the AE method were eventually found to be difficult to carry out[262]. One of the reasons could be that the rock-specific effects (e.g. unique characteristics of siliceous rocks characterised) and the effect of degassing of dissolved gases in the groundwater have not yet been understood. Alternatively the anelastic strain recovery (ASR) and differential strain curve analysis (DSCA) methods were also attempted. The ASR method, which estimates stress values and their direction by measuring the minute deformation associated with stress release in the core occurring immediately after borehole drilling, has not been fully tested since it has the disadvantage that the measurement must be started immediately after drilling, the environment (particularly temperature) at the measurement location must be kept constant in order to ensure the accuracy of measurements and the method is not free from the above-mentioned problem of degassing of dissolved gases.

Although the assumption behind its analysis approach – microcracks are generated associated with stress release and closed at the time of reloading – may not strictly coincide with the behaviour of soft sedimentary rock at the time of stress release, the DSCA method was found to be applicable for evaluating the 3D principal rock stresses, at least in the Wakkanai Formation[263] (Figure 4.7.4-14). It was also found that the values provided by the DSCA method were closer to the results of the in situ stress measurements (Table 4.7.4-1). One possible reason could be that the behaviour when the bedding planes in the rock core are opened by stress release is similar to that of microcrack generation.

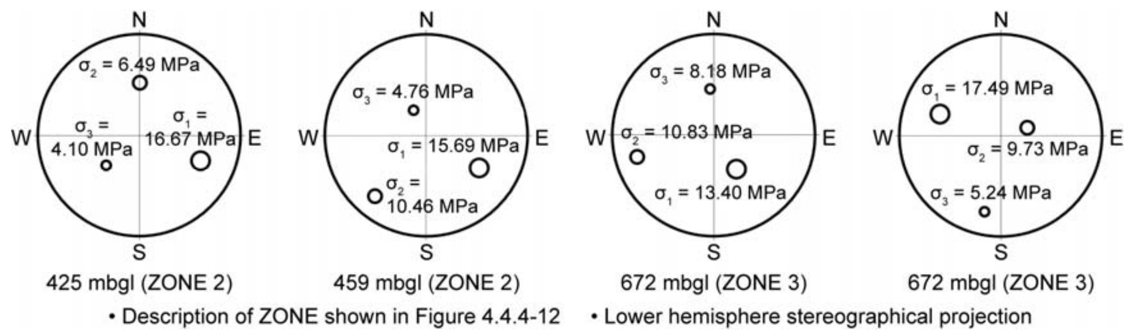

Figure 4.7.4-14 Magnitudes of principal stresses and directions measured by the DSCA method

Table 4.7.4-1 Comparison of the results of hydraulic fracturing and the DSCA method

Method	Depth [mbgl]	Max horizontal principal stress [MPa]	Min horizontal principal stress [MPa]	Direction of max horizontal principal stress
Hydraulic fracturing	302.5	4.5	3.7	N80°E
	602.5	9.7	7.8	N62°E
DSCA	425.0	14.6	5.4	N116°E
	459.0	13.8	10.0	N111°E
	672.0	11.4	10.0	N114°E
	672.0	16.0	5.6	N106°E

4.7.5 Environmental monitoring techniques

Different phenomena that may be induced by construction of large-scale underground facilities can be expected depending on the scale of the facilities, layout, construction method, operating period, distance from the facilities, timing of the observations etc. These phenomena can be classified into two categories: those relating to changes in the state of the environment (e.g. groundwater flow and chemistry) and those related to changes in the field conditions (e.g. hydraulic conductivity and mineralogical compositions) (Figure 4.7.5-1). Work was thus made to establish techniques for monitoring groundwater pressure and chemistry using boreholes and for remotely monitoring various changes in the geological environment. The performance of the systems developed was tested in situ and data were collected.

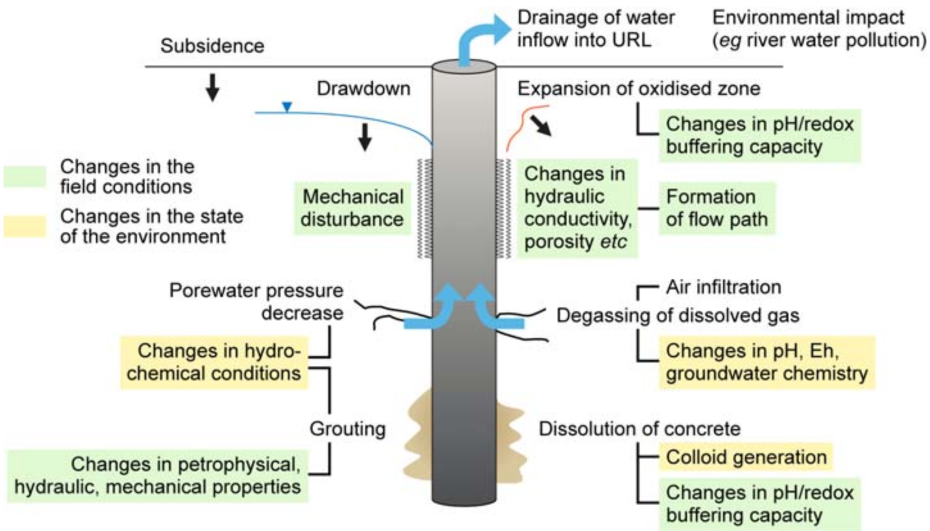

Figure 4.7.5-1 Hydrogeological and hydrochemical changes resulting from shaft excavation

(1) Monitoring using boreholes

The construction of underground facilities may cause changes in the characteristics of the geological environment, such as the hydraulic, hydrochemical and rock mechanical properties in the surrounding areas. The goals of developing monitoring techniques using boreholes include:

- determining the pressure and the groundwater chemistries before and after construction of the underground facilities to identify the impact of construction;
- collecting data not only for hydrogeological and hydrochemical modelling but also for checking the technical reliability in the results of simulation using these models;

- assessing the applicability of conventional long-term monitoring equipment to sedimentary rocks and identifying technical challenges, together with developing new long-term monitoring techniques.

Investigations were conducted of the specifications and application of long-tem monitoring equipment to the rock formations in the Horonobe area, where the climate is cold and the soft sedimentary rocks bear oil and/or gas. Here the selection of the equipment and the results of its field application were described.

1) Completion of boreholes and selection of monitoring locations

In the long-term monitoring of groundwater pressure using boreholes, pressure is measured at packed-off intervals. A steel casing pipe was installed in each borehole to keep the borehole wall from collapsing and then fixed by casing cementing. Following the check of the bonding conditions by cement bond logging (CBL), jet perforation was applied at each monitoring interval in order to allow groundwater pressure measurement in the borehole, as described in Subsection 4.7.1.

The locations subjected to jet perforation and the monitoring intervals were selected based on information on geological structure (stratigraphical boundaries, distributions of fracture zones etc.), hydrogeology (hydraulic conductivity, inflow points etc.), groundwater chemistry as well as the cement – rock bonding conditions.

2) Selection of long-term monitoring equipment

Before starting the long-term hydraulic and hydrochemical monitoring, information on practices followed in other countries in long-term monitoring from the surface to deep subsurface in soft sedimentary rocks was surveyed to determine the applicability of these practices to the rock in this project and to review potential long-term monitoring methods and equipment that could be employed in this project[82)]. For the evaluation and review, consideration was given to the durability of the equipment under conditions characterised by deep oil-bearing soft sedimentary rocks that tend to collapse and deform.

As a result, the Multiple Piezometer (MP) system, produced by Westbay® Instruments Inc., Canada (now joined Schlumberger Water Services), the Stand-Pipe Multi-Packer (SPMP) system, manufactured by Solexperts AG, Switzerland, and the PIEZO system, developed by Dia Consultants Co Ltd., Japan, were selected taking into consideration requirements relating to groundwater pressure measurement, groundwater sampling, applicable depth, borehole diameter, accuracy of groundwater pressure measurement and maintainability.

3) Monitoring of groundwater levels, pressure and chemistry

As shown in Figure 4.7.5-2, conventional monitoring equipment has been used to monitored groundwater pressure and chemistry based on one of the following two methods:

- the direct water pressure measurement method in which water pressure gauges connected in series are installed in a casing pipe so that the position of each gauge matches with the depths of monitoring intervals separated mainly by packers;
- the piezometric head measurement method in which groundwater pressure in a pipe (tube) connected from each of the monitoring intervals is measured separately.

In Horonobe, the MP system using the direct water pressure measurement method and the SPMP and PIEZO systems using the piezometric head measurement method were installed in boreholes and the applicability and durability of each system were evaluated.

The MP system has the advantage that apparatus with a large capacity can be placed in the casing pipe since the pressure measurement gauges are connected in series and inserted in the pipe. On the other hand, the system also has a disadvantage in that groundwater sampling cannot be carried out during hydraulic pressure monitoring. The MP system was installed in boreholes HDB-1, HDB-3, HDB-4, HDB-6 to HDB-9 and HDB-11 (installed in February 2007) and hydraulic monitoring is ongoing in these boreholes except HDB-4.

Both the SPMP and PIEZO systems monitor groundwater pressure using a water pressure gauge installed in an individual pipe connected between the intervals intended for groundwater pressure monitoring and the ground surface. The disadvantage is that groundwater cannot be sampled in a large volume in a short period of time, since the diameter of the pipe connecting the intervals and the ground surface is small (approximately 10–15 mm). By modifying the conventional PIEZO system, a new system for monitoring porewater pressure was developed (Figure 4.7.5-3), which is capable of measuring physico-chemical parameters deep subsurface and acquiring hydraulic conductivity at the same time as conducting groundwater sampling. The SPMP system and the improved PIEZO system are installed in boreholes HDB-2 and HDB-10 respectively and are contributing to the monitoring.

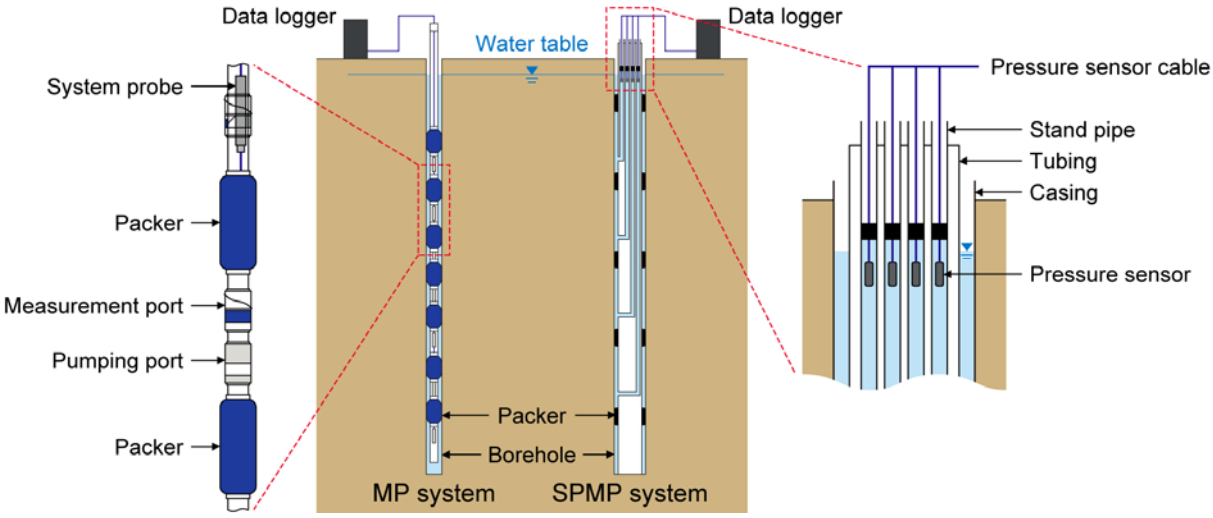

Figure 4.7.5-2 Schematic illustration of the MP and SPMP systems

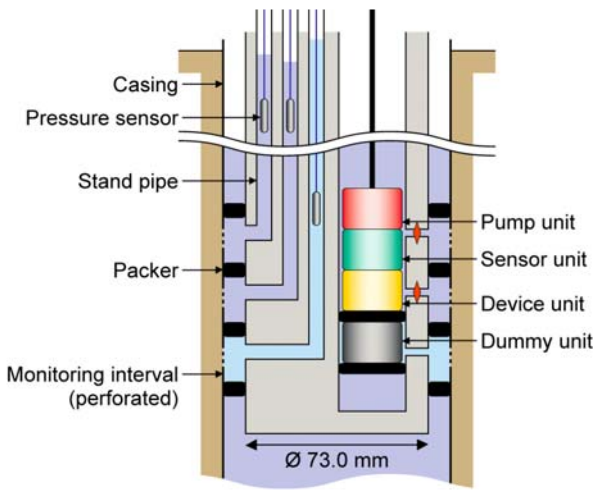

Figure 4.7.5-3 Schematic illustration of the improved PIEZO system

Figure 4.7.5-4 shows some of the hydraulic pressure data measured in borehole HDB-9 as an example. A pressure increase in the thawing season, which is peculiar to snowy regions, as well as an increase due to rainfall were observed in the upper measurement intervals. The values are more or less constant in the remainder of the measurement intervals. Based on the results of monitoring in the boreholes to date, groundwater around the underground facilities is distributed in the range from hydrostatic to slightly artesian conditions.

The results of hydrochemical monitoring in borehole HDB-4[42)] are shown in Figure 4.7.5-5. The data obtained in the borehole investigations indicated that the groundwater chemistry is neutral, viz. pH 7.5, but the pH value increases with the elapse of time. Focussing on the dissolved ions, a decrease in a CO_3^{2-} concentration and an increase in the concentrations of Na^+ and Cl^- are observed. These evolutions are considered to result from the reaction of the groundwater with the cement used when installing the casing pipes. Determining the effects of casing pipes (carbon steel) and cement on groundwater chemistry is an issue to be addressed that is equally important as identifying changes in groundwater chemistry associated with construction of the underground facilities. Groundwater sampling will continue on a regular basis to accumulate monitoring data.

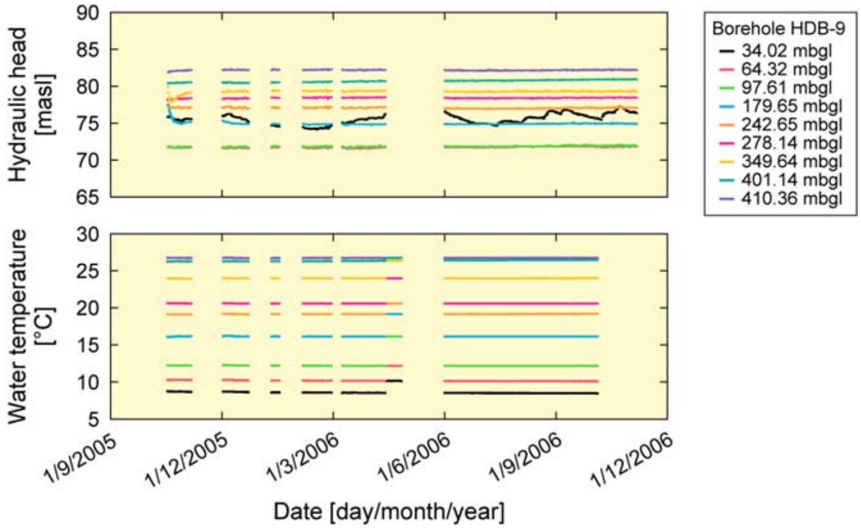

Figure 4.7.5-4 Hydraulic head and temperature monitoring in borehole HDB-9 from October 2005 to November 2006

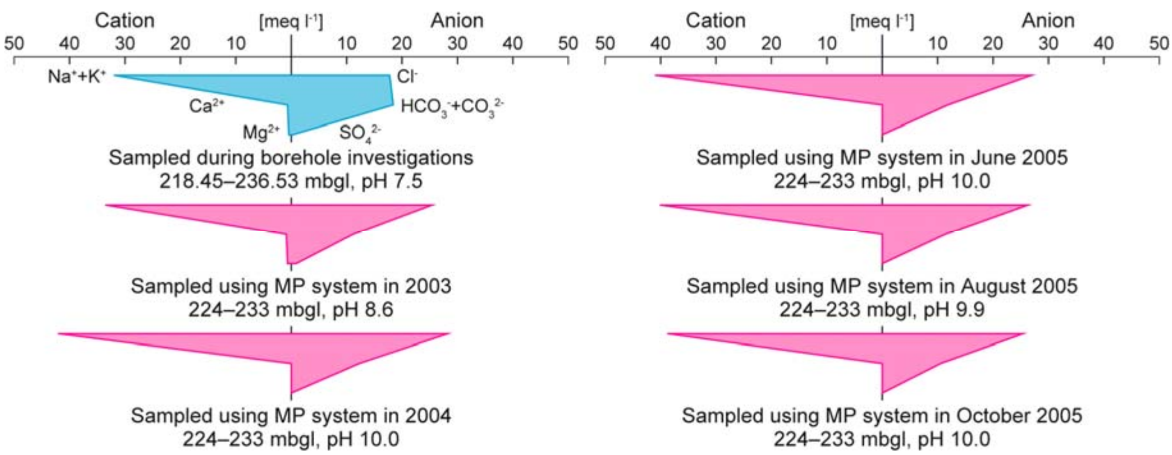

Figure 4.7.5-5 Results of hydrochemical monitoring in borehole HDB-4

4) Future tasks and plans

At present, long-term monitoring data are being sampled at a time interval of 5–15 minutes and are collected periodically, i.e. around once a month given the memory capacity of the data logger and the battery life. In order to monitor the relationship between short-term impact, such as an earthquake, and changes in groundwater pressure, some issues remain to be addressed, such as the expansion of memory capacity, improvement of data writing speed and so forth.

Maintenance of the system is carried out when a malfunction occurs but missing data during maintenance periods which occur more than once a month owing to failure of the logger and malfunctioning of the pressure gauge may be a significant problem. Measures would be required to prevent this problem, such as systematic maintenance plans and preparation of spare components (pressure gauges etc.) in advance, thus establishing a system for smooth restarting of the monitoring equipment as quickly as practicable. Development of the maintenance system would be particularly important for investigations in a remote location such as Horonobe.

In the future, data on pressure and chemistry of groundwater obtained by long-term monitoring systems installed to date will be analysed and methods will be developed for removing natural noise (e.g. earthquakes, atmospheric pressure changes and tidal variations) contained in the data. Improvements will be made to the long-term monitoring systems installed to date in order to assess the application of the systems in the underground facilities and to reduce the system size.

(2) Development of remote monitoring system

Geological disposal is essentially a passive system and, in principle, does not require post-closure management (such as monitoring as part of the institutional control over a repository after closure) to ensure long-term safety[264),265)]. However, post-closure monitoring may be required in some cases owing to social demand[266)]. In order to ensure the long-term repository safety, it is of importance to ensure that, even if hydraulic and hydrochemical conditions, mechanical properties etc. vary owing to perturbations induced by construction and operation of the repository or by natural phenomena, the range of variation would be within the predetermined design-based margin[267)]. For this purpose, R&D on the Accurately Controlled Routinely Operated Signal System (ACROSS) has been pursued to develop a remote monitoring system that allows determination of subsurface structures and assessment of the evolution of rock properties and hydraulic conditions with a resolution higher than that of conventional geophysical surveying techniques.

ACROSS is a method for accurately determining geological structures and their conditions by transmitting continuous seismic and electromagnetic waves to the subsurface while the phases and frequencies are accurately controlled; the data monitored using sensors (e.g. seismometers, magnetometers and electrodes as well as receivers synchronised with the transmission) are then analysed[268)]. Both seismic and electromagnetic waves are used because independent subsurface information (e.g. elastic constants and electrical resistivity) can be obtained, as can responses to the changes in conditions. ACROSS is a Japanese-developed high-resolution non-destructive monitoring technique designed mainly for monitoring of seismogenic zones; it was developed mainly by Nagoya University and JAEA Tono Geoscience Center. In the Horonobe URL project, ACROSS was installed in the Hokushin district with the main aims of developing a system that can identify changes in the geological environment occurring before, during and after construction of the underground facilities and building confidence in the technical reliability of the system. In Phase I of this project, the electromagnetic ACROSS and the seismic ACROSS were installed and experimental monitoring prior to construction of the underground facilities was initiated[269),270)].

1) Selection of transmission and receiving points

ACROSS remotely monitors changes in rock properties and groundwater conditions based on an analysis of minimal changes in the transfer function obtained by monitoring of continuously transmitted seismic and electromagnetic waves. The extent of the signal changes that can be detected after appropriate correction of the frequency characteristics of the transceiver system and measurement of the transmitting signal depends on the signal to noise (S/N) ratio. The transmission and receiving stations, particularly the latter, of the seismic and electromagnetic waves therefore need to be set at locations where ground vibration and electromagnetic waves (referred to hereafter as noise) resulting from factors other than the transmission by ACROSS are sufficiently low. The noise level was therefore investigated in and around the URL area prior to selection of the installation locations of the ACROSS transmission and receiving stations[271)].

In the investigation of noise level for the seismic waves, the levels and characteristics of noise in the monitoring areas were determined by analysing seismograms of seismic reflection surveys conducted in 2002. The locations of the seismic survey lines used for the analysis and the estimated noise levels are shown in Appendix 2 and Figure 4.7.5-6 respectively. Comparing the noise levels in the central Horonobe district and the URL area, the noise level in the URL area is around one order of magnitude lower than that of central Horonobe. Other than intermittent noise caused by vehicles and heavy equipment used for road construction, no major noise sources are assumed to exist on the north side of the survey line. It can be concluded that the noise in the areas remained at a low level except for intermittent noise induced by human activities. It does not indicate the existence of a constant noise source[271)].

The noise characteristics of electromagnetic waves were investigated based on observed data from the MT and AMT electromagnetic surveys conducted in 2001. The noise was characterised by sudden noise lasting for a short period of time with no clustering of any specific frequency. The noise included both natural noise, such as solar activity etc. and human induced noise. Human induced noise was greater at dawn and dusk, more specifically around two to five times greater than that in quiet times. The preferential vibration direction of the noise was to the northeast and the noise was lower around borehole HDB-4.

The seismic ACROSS can be used to determine subsurface conditions by constantly transmitting and receiving seismic waves and analysing the changes in wave groups, such as direct waves reaching the monitoring points and reflected waves from a seismic reflector. The results of the seismic reflection survey conducted in the URL area[272)] indicated an obvious seismic reflector at a depth of approximately 1,000–2,000 m near boreholes HDB-4 and HDB-8 as shown in Figure 4.7.5-7. Monitoring using the reflected wave in addition to the direct wave may thus be possible in this area (Figure 4.7.5-8). The transmission and receiving points were selected as illustrated in Appendix 2, considering that an obvious seismic reflector was found in the area of interest and the noise level is expected to be sufficiently low. Since the surface of the entire area was soft, concrete foundations (ground coupler) with dimensions 10 m × 10 m × 1.3 m, which is larger than used in the previous installations, were constructed at the transmission points. This was intended to transmit the force generated by the system to the ground over a larger area, thus emitting stable seismic waves on soft ground in a non-destructive manner. The seismometer was emplaced to a depth of 2 m or more with a drilling machine to achieve a stable temperature and relatively simple fixing. In order to allow detection of the 3D locations of seismic scatterers in the surrounding area, the seismometers installed at each receiving point were arranged in an L-shaped array made up of 10 units of three-component seismometers, while each of the receiving points was located so as to form a triangle (Appendix 2).

The electromagnetic ACROSS is used to constantly monitor electromagnetic waves transmitted from the transmission points at receiving points and to analyse changes in the monitored electromagnetic waves, thereby determining changes in the conditions of the subsurface environment through which the waves were propagated. It is therefore preferable to arrange the receiving point in line with the transmission point so that the area in which conditions changed can be identified. In order to identify areas with changes, advance knowledge of resistivity structures beneath the receiving point is an important factor in selecting the installation points. Taking the above conditions and the results of noise surveys relating to the electromagnetic waves into consideration, transmission and receiving points were selected as shown in Appendix 2. Two sets of transmission electrodes were installed for the electromagnetic ACROSS for bidirectional transmission in the E-W and NW-SE directions. It should be noted that typical resistivity structures beneath the periphery of each installation station have already been investigated by electromagnetic surveys in and around the URL area[82].

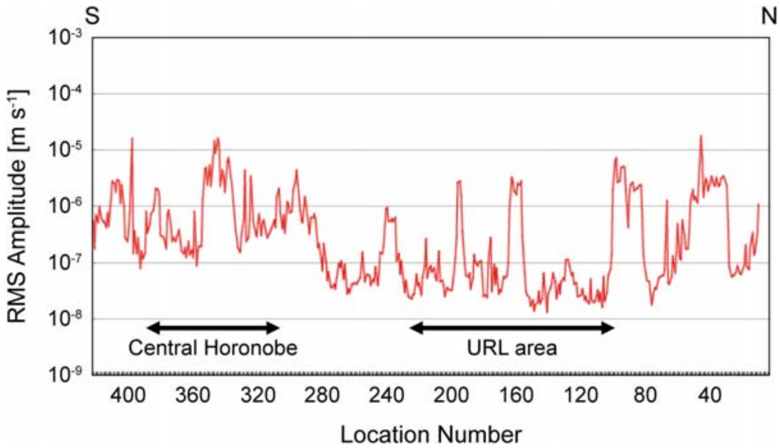

Figure 4.7.5-6 Background noise level around the Horonobe URL

RMS amplitudes of seismograms observed along the seismic survey line shown in Appendix 2

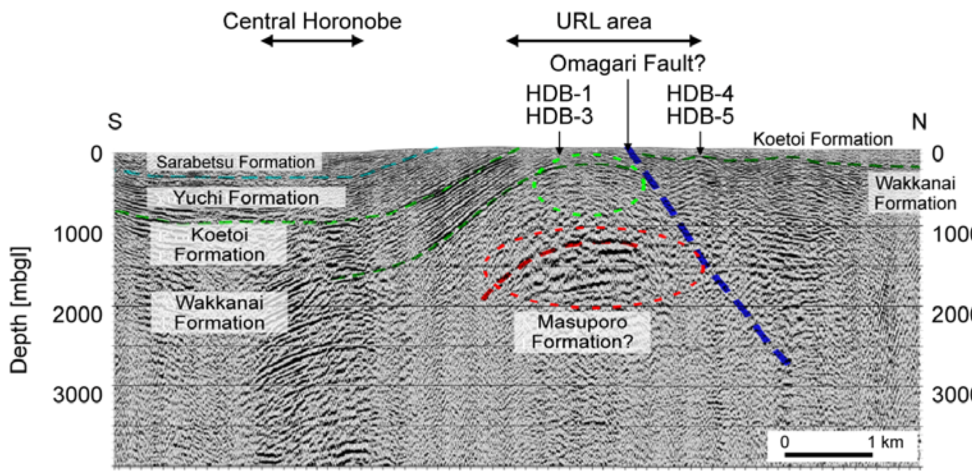

Figure 4.7.5-7 Seismic reflection profile along the seismic survey line shown in Appendix 2

2) Test monitoring

Test monitoring prior to construction of the underground facilities using both seismic and electromagnetic ACROSS was conducted. One of the main purposes of this test was to determine the appropriate signals to be used for monitoring by transmitting design-based signals in advance and conducting an analysis of received signals, while feeding back the results of the analysis to the setting of the transmitting signal frequency etc. Another aim was to make fine adjustments to the installed transmission and receiving equipments.

Test monitoring using the seismic ACROSS started in December 2005 and signals transmitted from the HDB-3 station have been received at the stations HDB-4, HDB-5 and HDB-8. A transmitter that generates power by rotation of the excentric mass[273)] was used for the transmission signals. The rotation direction was reversed once every hour and frequency modulated signals were transmitted, allowing a frequency transfer function corresponding to the linear vibration to be obtained[273)]. In the test monitoring, signals were transmitted by changing the frequency band on a trial-and-error basis in order to find the transmission and receiving signals suitable for monitoring. As an example of receiving signals obtained by such a method, the receiving spectrum of the transmitted signals in the frequency band ranging from 15.43 to 31.41 Hz received at station HDB-5 is shown in Figure 4.7.5-9. This figure shows a frequency spectrum obtained by stacking signals received every 100 seconds over one hour. This spectrum shows that the amplitude in the frequency band of the transmitted signal is higher than those in other frequency bands, which indicates that the transmitted signal was definitely received.

Test monitoring using electromagnetic ACROSS started at the HDB-4 station in December 2004 and at the HDB-8 station in March 2005. In this experimental monitoring, signals were transmitted at different frequencies from two sets of transmitting electrodes in the E-W and NW-SE directions respectively; transmission was conducted by changing the frequency band of the transmitting signal on a trial-and-error basis, as was the case for the seismic waves. Figure 4.7.5-10 shows an example of received signals at the Z receiving point obtained by this test monitoring. The figure shows the sum of frequency spectra of signals received every 100 seconds in one day. Ten transmitting frequencies in the E-W direction were 3.75, 8.75, 16.25, 23.75, 36.25, 58.75, 76.25, 91.25, 111.25 and 136.25 Hz and 11 frequencies in the NW-SE direction were 2.50, 6.25, 13.75, 21.25, 28.75, 38.75, 66.25, 73.75, 88.75, 103.75 and 133.75 Hz. In this figure, frequencies denoted by circles correspond to the transmitting frequencies shown above. The S/N ratios of the received signals in these frequency bands were higher than those in other bands.

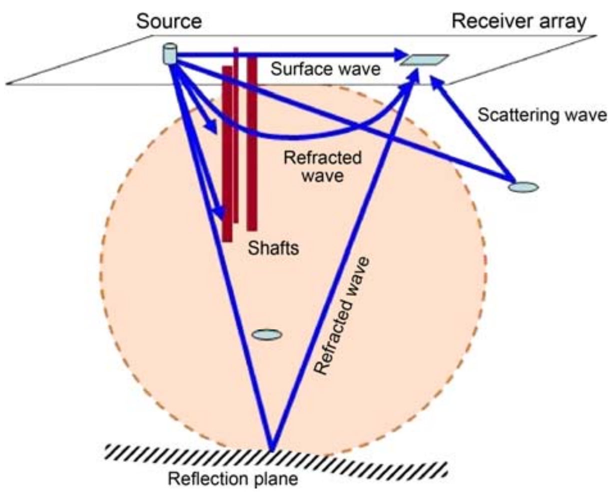

Figure 4.7.5-8 Schematic illustration of a remote monitoring system (ACROSS)

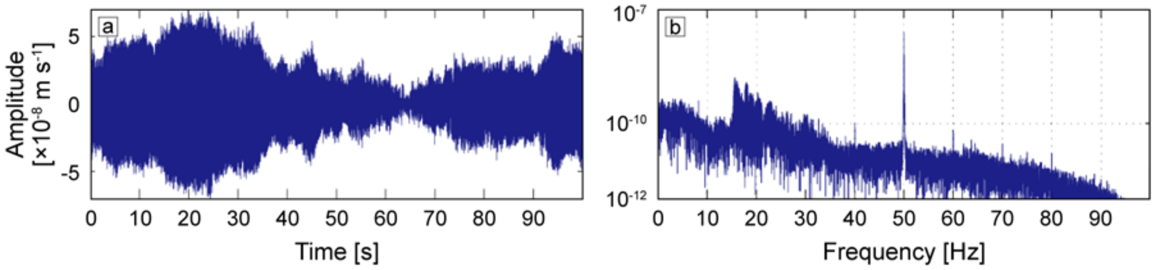

Figure 4.7.5-9 Example of one hour-stacked seismic data observed at station HDB-5

a: Waveform in time domain; *b*: Fourier amplitude spectrum

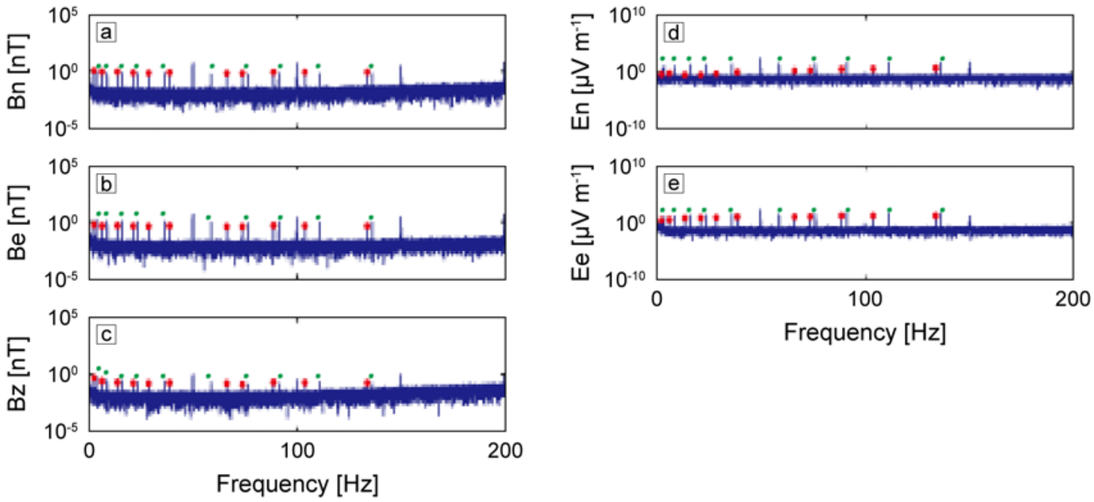

Figure 4.7.5-10 Amplitude spectrum of observed magnetic and electrical fields

a–c: NS, EW and vertical components of the magnetic field respectively

d and e: NS and EW components of the electrical field respectively

Red and green circles representing transmitting frequencies of the NW-SE and E-W dipoles respectively

3) Future plans

The transmission and receiving equipment of ACROSS using seismic and electromagnetic waves as signals was installed and test monitoring was initiated. The monitoring will continue around the URL area in order to develop techniques for monitoring changes in the subsurface geological environment associated with construction of the underground facilities. In parallel with the monitoring, techniques for processing and analysis of observed data will be developed whilst changes of observed data with respect to changes in the geological environment will be evaluated.

4.8 Summary

This section summarises the overall achievements of the surface-based investigations performed to enhance understanding of the deep geological environment and establish the technical basis for systematic techniques for characterising the geological environment, as described in Sections 4.1–4.7. The main results of the investigations of geology, hydrogeology, hydrochemistry, rock mechanics and long-term stability of the geological environment are described, as well as the findings relating to the investigation techniques for the Neogene sedimentary formations at Horonobe, in Subsection 4.8.1. Remaining key issues identified and plans for the Phase II investigations are discussed in Subsection 4.8.2. Finally, Subsection 4.8.3 looks into lessons learnt from the surface-based investigations.

4.8.1 Results of the surface-based investigations

(1) Geological investigations

During the investigations covering the whole area of Horonobe Town, the topography, the geological heterogeneity of the rock formations, the thickness of the overburden and features that could be important as solute transport pathways were overviewed by surveying and interpreting existing information. The results of reconnaissance and aerial geophysical surveys, MT electromagnetic surveys and borehole investigations were largely consistent with the existing information. At the stage of the surface-based investigations in and around the URL area, reflection seismic surveys and borehole investigations were conducted. The results for the distribution of the sedimentary formations were consistent with those obtained in the previous stage. However, a satisfactory interpretation of the location and properties of the Omagari Fault was not achieved. In addition, the results of borehole investigations indicated that fractures might play an important role as solute transport pathways, implying the need for further investigations.

More detailed investigations were therefore carried out, which include topographical studies (interpretation of terrace surfaces and lineament surveys), reconnaissance surveys (description of outcrops of the Omagari Fault and stripped horizontal outcrops in fractures), AMT electromagnetic surveys, ground penetrating radar surveys, re-analysis of existing data from past reflection seismic surveys, gravity surveys, borehole investigations and gas surveys. In terms of the distribution of the sedimentary formations, the results of these investigations were largely consistent with those obtained in the previous stage. A number of new findings were also obtained based on a wealth of data accumulated at this stage. This applied in particular to the mineral composition, alteration, physical properties and geochronology of the Wakkanai and Koetoi Formations, the thickness of the terrace deposits, fractures and the Omagari Fault. Of particular importance in an integrated interpretation of the results were that the 3D distribution of the Omagari Fault was estimated and the hydrogeological significance of the fault zones demonstrated.

(2) Hydrogeological investigations

Data on distributions of hydraulic conductivity and pressure (total head or hydraulic gradient) were accumulated through a series of borehole investigations at the stage of surface-based investigations in and around the URL area. In particular, the spatial variability of hydraulic conductivity correlating significantly with the distribution of minor fault zones was identified. Modelling and groundwater flow analyses taking these results into account enhanced the understanding of the regional and local groundwater flow systems.

Regarding the shallow subsurface hydrological regime, it was found that the groundwater level was not always consistent with the topography and that highly permeable zones lay, either in the terrace sediments or near the boundary between the terrace sediments and intact rock. It was also found that the recharge rate varied depending on the drainage basin.

The hydrogeological model was revised almost every year based on current data as part of the process of reducing uncertainties with the progress of investigations. Prediction of changes in the hydrogeological environment associated with construction of the URL using the latest hydrogeological model, the variation of inflow rate and reduction in the total head were estimated by the groundwater flow analysis. In developing models and performing analyses, it is of importance to show the data and bases behind the assumptions used in the model/analysis in order to examine their reliability and uncertainty. Traceability is also extremely important in that it will constitute the basis for knowledge management in the actual disposal project. Comparing the analyses in the investigation stage covering the whole Horonobe Town area, uncertainties in the surface-based investigations of the geological environment were reduced qualitatively in the sense that the geological model was updated and consistency with the measured values for hydraulic conductivity, water pressure, water chemistry (e.g. salinity) and recharge rate was confirmed.

Lists of specific proposals for investigations from an analytical viewpoint were presented in Table 4.2.4-1 and in Subsection 4.8.2. The investigations have been, and will continue to be, carried out in accordance with a comprehensive strategy (including a strategy for the development of investigation technologies), with discussions involving experts under the restrictions of time and budget. In the analysis carried out to predict the evolution of groundwater flow associated with the construction of the URL, as described in Section 4.6.3, the amount of groundwater inflow into the underground facilities was higher than expected when the URL was designed.

(3) Hydrochemical investigations

Throughout stepwise surface-based investigations with surveys of existing information, shallow subsurface and deep borehole investigations and associated modelling work, hydrochemical characteristics of groundwater which would be of great relevance for geological disposal, in and around the URL area were well understood. Regarding 3D distributions of groundwater chemistries, relatively low salinity groundwater (Na-HCO_3 type) was found in the shallower subsurface whereas relatively high salinity groundwater (Na-Cl type) was found in deeper formations. A clear difference was also seen in groundwater isotopic signatures. Light isotopes were dominant for both H and O in the shallower subsurface groundwater (δD of -90 – -60‰; δ^{18}O of -11 – -10‰), while heavy isotopes dominated in the deep groundwater (δD of -30 – -20‰; δ^{18}O of +2 – +3‰).

Regarding the major groundwater evolutions, current groundwater chemistry would have been formed by mixing two types of groundwater mentioned above. In addition, the shallower subsurface groundwater chemistry would have been formed by rock – water interaction, with ion-exchange of Na^+ and H^+ between the liquid phase (recharged with precipitation) and the solid phase (e.g. smectite) being the main reaction.

(4) Rock mechanical investigations

It was found that the rock formations in and around the URL area was divided into three zones in terms of rock mechanical properties and depth profiles (down to 1,000 m depth). The in situ properties and their distribution in each zone were determined by conducting laboratory tests and in situ experiments (such as borehole loading tests and velocity logging) because fractures in the rock would have only minor effects on in situ mechanical properties. Data for evaluating the initial stress in the zones were obtained by detailed investigation of the initial stress field by borehole investigations on the west side of the Omagari Fault. In particular, an estimate based on the overburden indicated that the vertical stress and the minimum principal stress in the horizontal plane were substantially the same in and around the URL area and that the maximum principal stress was approximately 1.5 times this value. It was also found that the direction of the principal stress was almost constant, viz. in an E-W direction, from near the surface to a depth of approximately 700 m. These results were evaluated and updated step-by-step with the progress of the borehole investigations and served as the base data for selection of the URL area and URL site.

With respect to acquiring the data necessary for designing the underground facilities, the results of the initial stress measurements were used to set the boundary conditions for a cavity stability analysis. In addition, the layout of the experimental drift was determined taking into consideration the direction of the maximum principal stress. Rock mechanical properties were set to conservative values so that the results of borehole loading tests and features such as hairline cracks could be taken into consideration, based on the data obtained from the borehole investigations. Analyses were conducted of processes (e.g. time-dependent deformation, strain softening behaviour and hydro-mechanical coupled phenomena) assumed to occur in the rocks around the shaft and drift when they are actually excavated and compared with the results of stability analyses of tunnel support using the design techniques proposed, for example, in the H12 report.

Of importance in the rock mechanical investigations from the viewpoint of the actual disposal project would be to quantitatively characterise the rock properties and stress conditions in the repository site over several kilometres square and to conduct an analysis of the design of the disposal system based on the properties and conditions characterised. In this respect, for the Neogene sedimentary formations, it may be possible to determine the distribution of mechanical properties in the area of interest if the geological structure covering an area of several kilometres square could be thoroughly understood. Although a significant variation in properties is observed over the range from the surface to several kilometres depth, changes in the initial stress conditions owing to the effects of discontinuities (e.g. stress decoupling) are less likely to occur compared to the case of crystalline rock. In particular, it is believed that no complex changes occur in the direction of the maximum principal stress.

In addition, because phenomena similar to high strain softening are quite likely to be observed in the soft sedimentary rock at the time of fracturing, it will be important to quantitatively evaluate changes due to such localisation of strain, particularly in the prediction and evaluation of the EDZ.

(5) Study on the long-term stability of the geological environment

Based on the results of surveys of existing information, ground exploration and borehole investigations, natural phenomena that should be considered in the evaluation and estimation of the future geological environment in the Horonobe area were successfully identified.

The recurrence interval of past major earthquakes (e.g. those capable of causing landslides) in northern Hokkaido was estimated to be approximately 800–3,000 years, which was too long to trace from historical and ancient documents. At present, although the hypocentre of the micro-earthquakes in the Horonobe area is distributed in an N-S or NNE-SSW direction under a horizontal compressive stress field, the directions of the P-axes and fault planes are believed to show various states that reflect a complex geological structure in the eastern margin of the Japan Sea. In particular, active structures in the land areas are localised at the geological boundary between the Kamuikotan Belt and the Neogene sedimentary rocks (the Toikanbetsu Fault Zone), and at the depositional area of Quaternary sediments (the Sarabetsu Flexure Zone), as well as in the marine area on the side of the Japan Sea (the Wakkanai and Musashi Fault Systems). The geological structures in and around the Horonobe area constitute part of the fold-and-thrust belt in the E-W compressive stress field; the fold structure is assumed to have been formed sequentially from the east to west. The Horonobe area has been in the tectonic setting of an E-W compressive stress field since the Late Pliocene, the same as the current stress field in the area.

With regard to volcanic activity, the possibility of future volcanic and hydrothermal activity is low in northern Hokkaido if the current tectonics in and around Hokkaido do not change in the future.

It is assumed that a change in the position of the shoreline, i.e. the spreading and receding of the land, will take place in the next 100,000 years or longer in the Horonobe area owing to eustatic sea-level change. The land area would reach close to the present locations of Rishiri Island in the future glacial period and marine area to centre of Horonobe Town in the future interglacial period. During a last glacial stage, the surface environment of the Horonobe area can be assumed to be as follows: discontinuous permafrost condition with an average annual air temperature of -7 – -3°C, a large annual range in air temperature and very cold winters. It is also assumed that the area was covered with open forests with mainly Dahurian larch and Siberian dwarf pine and with grasslands. Considering the fact that climate change have occurred periodically during the Quaternary, it is assumed that the present mild global climate and the climate in the glacial period mentioned above will occur alternately.

The reconstruction of the geological structure for the last 2.5 million years indicates that the sedimentary basin probably contracted from both the east and west sides, with the centre of contraction located to the west of the Horonobe area. In particular, the contraction from the east was significant, which means that it could be related to the westward migration of the depositional area since the Pliocene. The land in the Horonobe area would have gradually expanded towards the west, accompanied by periodical and extensive changes in the shoreline location owing to eustatic sea-level changes since over the last three million years.

The current geomorphological processes in the Horonobe area are influenced by rock control, where topographical formation processes are influenced by the properties of the landform materials. Regarding future uplift and subsidence trends, it is considered that the current uplift trend is likely to continue in the eastern part of the Horonobe area and around the Sarabetsu Anticline until equilibrium is reached. The subsidence trend in the Sarabetsu Lowland will change to uplift with an increase in horizontal crustal strain rate in the future and the uplift trend will remain unchanged until it reaches equilibrium.

(6) Development of investigation techniques

A combination of a range of investigation techniques (e.g. airborne and ground geophysical surveys, borehole investigations) applied in Phase I proved to be effective for geological characterisation. A methodology for stepwise surveying with the techniques and integrating the results into model representations actually enhanced the understanding of key geological structures which would be of great relevance for geological disposal.

Techniques for hydraulic testing and flow logging were developed for use in environments such as the sedimentary formations where borehole walls may collapse, as well as environments with saline groundwater and dissolved gases, and their applicability was confirmed. From the shallow subsurface hydrological investigations, the applicability of the methods used for calculating recharge rate in cold weather regions was also reviewed. Techniques for pumping groundwater combined with hydraulic tests and squeezing porewater from cores and analytical methods (e.g. principal component analysis) employed were found to be effective for characterising the groundwater chemistries in the sedimentary formations.

For characterising such rock properties and stress conditions, existing investigation techniques would be sufficient. In addition, a methodology proposed in this project can be used for evaluating the stability of the EDZ which will be required to cover a very long time period when designing special structures (e.g. plugs) rarely used in other conventional underground construction.

From the technical point of view, it would be reasonable to adopt the strain rate obtained by the geological method for discussing the long-term stability of the geological environment as the rate reflected the long-term plastic strain in the crust. In addition, the feasibility of using the sterane/sterene ratio as an index for estimating erosion was suggested; a positive correlation was observed between the palaeogeothermal temperature range of 40–60°C and the sterane/sterene ratio, which are cyclic isoprenoids found in the Wakkanai and Koetoi Formations.

4.8.2 Remaining key issues and plans for Phase II investigations

(1) Geological investigations

The issues to be addressed in Phase II include aspects of discontinuities which have not sufficiently been understood by the Phase I investigations, such as the distribution and continuity of fault zones, development of joints and their modelling. The distribution of fault zones should be determined on a regional scale, not just limited to the tunnel near-field. It is possible that the continuity and geometry of fault zones will be better understood through wall observations in shafts and drifts. As the fault zone characteristics strongly influence groundwater inflow into the underground facilities, a higher priority should be given to characterising the fault zone in the Phase II investigations. It may also be necessary to evaluate the degree of continuity of discontinuities by means of cross-hole tests in the horizontal drifts. In addition, joint development may be better understood by investigating the interior of tunnels because the Ventilation and East Shafts are located near the anticline axis. Since modelling the distribution of such small discontinuities will have to depend on a probabilistic approach, which may involve a great deal of uncertainty, efforts will have to be made to reduce this uncertainty.

(2) Hydrogeological investigations

Some important issues were not sufficiently investigated and still remain as key issues for Phase II and/or Phase III. First, there may be some correlation between hydraulic conductivity and minor fault zones, but variations in hydraulic conductivity of minor fault zones were observed and the flow paths in the minor fault zone are limited to a small part of the zone. Thus, the relationship between hydraulic conductivity and minor fault zones or fractures that constitute these zones would need to be investigated. Second, an extremely high hydraulic pressure that could not be explained by topographical feature alone was observed deep subsurface in borehole HDB-11. A similar phenomenon was also observed in borehole HDB-2. Since such an abnormally high pressure may lead an upward hydraulic gradient, it would be important to study such phenomenon from the viewpoint of reflection to the disposal project. Third, it is assumed that the distribution of groundwater chemistry has been affected by the groundwater flow. In Phase I, an analysis was conducted based on the assumption that the saline water confined during the sedimentation had been washed out by fresh water over a long period of time. However, because this assumption was not thoroughly examined, a further evaluation of consistency with data from geochemical investigation needs to be carried out. In addition, evaluation of consistency with the distribution of groundwater chemistry and abnormally high pressures may involve natural phenomena such as uplift, erosion and changes in climate and sea-level. It will therefore be necessary to develop a comprehensive model considered these factors.

Groundwater flow is an important factor to be considered in the solute transport analysis for the disposal project. However, it will be hard to acquire information on the hydraulic effective porosity required for the analysis from surface-based investigations. Tracer tests for obtaining the parameter will thus be required in the Phase II programme.

With respect to shallow subsurface hydrology, a large variation in data measured by hydrological investigations conducted over the past one or two years indicates a low reliability of the calculated recharge rate. Improving the reliability of the recharge rate should be achieved by continuing observations.

Investigations of the above issues and re-evaluation of data will form part of the Phase II programme. Activities in Phase II should also include formulation of the relationship between hydraulic conductivity and minor fault zones or fractures and characterisation of fracture network structures using tunnel wall observations; borehole hydraulic tests in tunnels, particularly characterisation of hydraulic and solute transport properties of minor fault zones or fractures based on cross-hole hydraulic tests using two or more boreholes or based on tracer tests; acquisition of data on inflow rate into tunnel, hydraulic pressure and groundwater chemistry from long-term monitoring and comparison and confirmation of the data with those predicted in Phase I; updating of geological models and enhancement of data reliability by continuing shallow subsurface hydrological investigations. In addition, uncertainties have to be made clear quantitatively for the actual disposal project and proposing a process for reducing uncertainties, taking the Horonobe case as an example, would be a future issue.

The change in hydraulic conductivity associated with tunnel excavation should also be investigated because the EDZ is likely to become highly permeable in the course of geological disposal. The change in hydraulic conductivity in the tunnel near-field occurs as a result of coupled phenomena with stress release and degassing of dissolved gases in groundwater. Therefore, in the investigations and modelling in Phase II, studies that focus on coupled phenomena, including rock mechanics and hydrochemistry, will be required.

(3) Hydrochemical investigations

Hydrochemical data were acquired mainly through borehole investigations. These investigations are beset with restrictions and difficulties, including some components (such as organic matter, microbes and colloids) not being analysed owing to inevitable contamination of sampled groundwater with drilling fluid, poor quality of analytical values because of the effect of decrease in groundwater pressure (such as degassing) and the limited volume (several tens of millilitres) of extracted porewater, all of which required prioritisation of analysis items. Organic matter, microbes, colloids and dissolved gases are not only important factors for groundwater chemistries but are also indispensable for understanding solute transport processes in the host rock formations. In the Phase II and/or Phase III, it will be crucial to collect data on organic matter, microbes, etc. using boreholes drilled from drifts, with proper management of data quality.

The results from the Phase I investigations revealed that discontinuities such as faults and fractures, which control groundwater flow, are distributed in the sedimentary formations of interest. It is presumed that the groundwater chemistry would be controlled by the distribution and degree of continuity of the discontinuities on a smaller scale. Further investigation should thus be required to confirm this correlation, taking prevailing groundwater flow into account. In addition, it is of particular importance to study the groundwater evolution of the Horonobe area over geological time, up to the present, defining temporal and spatial changes of various characteristics and processes, which include topography, geology and groundwater flow.

(4) Rock mechanical investigations

Although geophysical logging is a relatively effective method for evaluating the properties of rocks such as the siliceous mudstone at Horonobe, where there are almost no changes in lithofacies from the surface to a depth of around 1,000 m, the S-wave velocity for the core sample of diatomaceous mudstone with an extremely high effective porosity is much lower than that obtained from in situ velocity logging. The reason was not fully explained. In addition, although anisotropy in the mechanical properties of rocks was identified quantitatively, anisotropy was not quantified because the factors causing the anisotropy and its characteristics (e.g. relationship with the bedding direction) were not defined. With regard to these remaining issues, methods for evaluating anisotropy are now being reviewed by collecting and analysing existing information from past studies; additional laboratory tests are also being conducted.

Three-dimensional stress conditions were not determined accurately because the hydraulic fracturing method is the only applicable method for measuring the initial stress in a borehole drilled from the surface. The applicability of initial stress measurements using rock cores was not thoroughly evaluated either. Hydro-mechanical coupled behaviour and the time-dependent deformation of the rocks surrounding openings created during tunnel excavation may become the primary mechanisms controlling self-healing of excavation damage over a long time period following the installation of supports, although they are believed to have little influence on the construction of underground facilities. No technique was developed for evaluating the evolution of excavation damage on the rocks surrounding the openings over a long period of time, taking the phenomena mentioned above into account. These issues cannot be adequately addressed in Phase I and should therefore be addressed in Phase II and/or Phase III, along with checking the technical reliability of the rock mechanical investigation techniques developed in Phase I.

The investigations in Phase II can be divided into two categories:

a) validation and updating of models developed in Phase I;
b) investigations that can be conducted only during excavation.

The former category (a) involves investigating both the undisturbed rock and the EDZ, while the latter category (b) involves investigating the mechanisms that generate the EDZ immediately after excavation.

The investigations of the undisturbed rock are aimed at building confidence in the rock mechanical model (distribution of properties and initial stress) developed in Phase I. For this, boreholes, extending over 10 m and covering an area three dimensionally including not only the EDZ but also the entire underground facilities, are drilled from the tunnels to conduct investigations such as density and velocity logging and laboratory tests on rock cores. The target areas for the investigations will be ZONEs 1–3 indicated in the Phase I rock mechanical model. It should be noted that the surveys will be planned mainly as part of borehole investigations from the horizontal drifts, since they are scheduled to be carried out after the excavation of tunnels has been completed.

Building confidence in the predicted results in the category (a) and issues in the category (b) should be addressed before, during and after tunnel excavation because it is necessary to determine the extent, properties and mechanisms of the EDZ formed immediately after excavation. Since the size of the investigation area is limited, and the size of EDZ may vary depending on depth, shaft sinking should be suspended at several depths to allow investigations using boreholes drilled from the interior of the shaft. It should be noted that the time-dependent evolution of the EDZ is one of the items to be investigated for soft sedimentary rocks and, particularly for the area around the shafts, the investigations are planned to be conducted at locations where they can continue even after completion of excavation. Specifically, these investigations will continue in connecting drifts at depths of 140 and 280 m, as well as in two experimental drifts at a depth of 300 m or more. Although the length of the borehole only needs to exceed the range of the EDZ, the boreholes may need to be drilled in several directions in the shaft cross-section since the extent of the EDZ varies depending on the direction of the principal stress. Investigations would include borehole wall observations, borehole loading tests and hydraulic tests, as well as geophysical logging and laboratory tests, allowing changes in in situ rock conditions and properties to be directly determined.

In situ experiments are planned to be conducted mainly in the horizontal drift because these will be required before, during and after excavation in order to understand the generation mechanisms of the EDZ. In situ experiments on the EDZ conducted previously in the Tono Mine may provide input for the design of the in situ experiments.

The models developed in Phase I will be updated on the basis of the results obtained from the Phase II investigations described above. The technical reliability of the initial state obtained from the EDZ-related investigations will be checked by periodical measurement of changes in parameters. The AE technique, which may be difficult to apply in the initial stress measurements, is now being reviewed for use as a method that could be used for non-destructive determination of the extent of the EDZ[274)].

(5) Study on the long-term stability of the geological environment

The investigations and analyses in Phase II will focus on the impacts of natural phenomena on the geological environment based on the results from Phase I. In particular, the past groundwater environment will be reconstructed analytically, taking changes in climate and sea-level, and the evolution of topography and geological structure into account. At the same time, an evaluation will be carried out of whether or not the reconstructed groundwater environment is appropriate in the actual environment using the present rock and groundwater data obtained from the surface and the underground facilities. Concurrently with these analyses, and taking the case of Horonobe as an example, a series of investigation techniques will be developed for modelling and analysing the long-term evolution of the geological environment (including groundwater flow and chemistry and solute transport properties), using an consequence assessment model of faulting and hydrothermal activity being currently under development.

Issues relating to the temporal and spatial changes and style of natural phenomena which remained unsolved by the Phase I investigations will be addressed in the investigations to be initiated in Phase II.

All of the historical documents collected in Phase I to provide information on the past seismicity were compiled long after the occurrence of earthquakes. Hence they did not provide information on the distribution of locations which experience ground-shaking motion, nor about the damage caused by earthquakes, which might be described in the original source texts. The distribution of locations earthquakes that could be felt and the quake damages that were recorded would be essential for estimating magnitude and source of earthquake (i.e. hypocentre), as well as for determining changes in the crustal stress field before and after an earthquake. It will therefore be necessary to check the original historical documents that may have records on earthquakes and to continue collecting historical records on earthquakes that occurred in regions along the Japan Sea. Since the analysis of seismicity in Phase I used seismic monitoring data obtained over a short period of time, i.e. slightly less than three years, the results of the analysis carried out for hypocentre determination are not considered to be particularly reliable due to the lack of data. Further accumulation of seismic observation data and efforts to determine hypocentres based on the data obtained will thus be required to evaluate the correlation between seismicity and the subsurface geological structure.

Restored geological cross-sections prepared in Phase I ignored deformation, i.e. temporal changes in the thickness of formations. The cross sectional areas were not balanced in terms of bed-length and area before and after the deformation, as well as geometrical restrictions related to the development of faults and fold structures. In order to achieve a more practical restoration of the geological cross-section, it should therefore be revised based on new additional data obtained in the course of the next phase of investigations, taking into account the changes thickness of formations. This will enhance the accuracy of the estimating of temporal variation of the groundwater flow conditions taking into account the impact of the natural phenomena, including of the change of geological structure.

For future volcanic and hydrothermal activity, the possibility of the presence of magma and other high temperature fluids at depth in northern Hokkaido should be evaluated using not only geological methods but also geophysical methods such as seismic tomography and the MT method. At the same time, a theoretical evaluation based on simulations should be conducted to improve the reliability of the estimate of the evolution of thermal structures based on existing information. With respect to the temporal and spatial variation of the palaeoclimate associated with the glacial – interglacial cycle in the Horonobe area was reviewed based on the reconstruction of vegetation observed in the Kenbuchi Basin located in the southern part of northern Hokkaido and Lake Koetoi at the northern end of Hokkaido. However, it is well known that vegetation varies considerably depending on altitude, precipitation, and distance from the coast. If the vegetation in the past could be reconstructed, it would be possible to estimate, to a certain degree, not only the palaeotemperature but also the palaeoprecipitation based on the relationship between the present climatic conditions and vegetation. Because the precipitation and vegetation represent key input for estimating the future recharge volume, it will be necessary to reconstruct vegetation using samples collected for pollen analysis in the Horonobe area, and to reconstruct the palaeoenvironment, including temperature and precipitation.

The Phase I investigations revealed only a qualitative trend for topographical changes in the Horonobe area. In future investigations, it will be necessary to develop a simulation model of topographical changes to which the concept of rock control can be applied in order to evaluate the evolution of the geological environment taking topographical changes into account. In this respect, data on geomorphic values required in the simulation should be acquired for each formation. Data uncertainty, reliability of the data, and premises should thus be specified in the analyses related to the impacts of natural phenomena on the geological environments during the Phase II investigations.

(6) Development of investigation techniques

Through the Phase I investigations, techniques for characterising the oil- and gas-bearing sedimentary formations with saline groundwater were developed stepwise and expertise relating to the applicability of these investigation techniques was accumulated as described in Subsection 4.8.1. However, QA/QC for the Phase I investigations proved to be inadequate for some investigation tasks. The reasons identified for this include:

- inappropriate (or lack of) QA/QC methodologies (e.g. strategy, action programme, manual);
- insufficient preliminary evaluation for planning the investigations;
- non-functional organisational system (e.g. information-sharing, decision-making).

In Phase II, an appropriate QA system applicable to all aspects of the investigations should be established, which includes measures to address the issues mentioned above. In addition, since more experience was gained from failure or setback in the course of the Phase I investigations, tacit knowledge and expertise based on such experience should be elicited and integrated as a knowledge database. An important step would also be to pass on key know-how and hard-won experience from researchers who have experienced mistakes to the next generation through the actual work.

4.8.3 Lessons learnt from Phase I investigations

(1) Geological investigations

During the geological investigations from the surface, a lot of successes and setbacks were gained as mentioned in Subsections 4.8.1 and 4.8.2 and the following lessons were learnt from the investigations:

- Some data acquired in the airborne geophysical surveys may be of poor quality because of the limited flying altitude owing to the potential impact on livestock in areas where stock farming is rich and also owing to regulations concerning flying over railways and urban areas.
- When evaluating the location and hydraulic characteristics of a fault zone in a formation composed of marine deposits, an effective investigation method would be to measure the resistivity of shallower rock formations by means of electromagnetic surveys. When interpreting the resistivity structure determined, it would be necessary to consider whether the difference in resistivity is due to differences in the lithofacies or groundwater chemistry. For a stepwise resistivity survey, it would be effective to gradually reduce the depth of the survey.
- When conducting reflection seismic surveys in an area with little variation in physical properties, the continuity of the reflector and the resolution may not be greatly enhanced even if smaller spacing between the shot/receiving points is used. For an effective stepwise reflection seismic survey, a survey according to standard specifications should be conducted first, followed by a more dense survey in the area where relatively good continuity of the reflector and resolution were obtained.
- Multi-offset VSP surveys would be difficult to apply effectively to a sedimentary formation with a complicated dip but effective only when the reflector obtained is considered to be almost horizontal.
- For observation of faults where strike-slip features prevail, it would be effective to artificially form a horizontal outcrop (stripping). For clarifying mountains and hill uplifting processes, the hinterland analysis using fossil diatoms may be applied. Applying the RIPL method to terraces, in particular, would be effective for determining uplift rate and land – sea distribution in each period.
- The correlation between the GPS baseline length (distance between GPS stations) and earthquakes would serve to determine whether earthquakes would have an impact on the geological environment (stress and strain) and, if so, what the level would be based on the relationship between magnitude and epicentre.

(2) Hydrogeological investigations

The discussion below presents lessons learnt from the hydrogeological investigations from the surface, taking into account successes and setbacks described in the preceding subsections:

- For investigations using existing information, full use of the findings of the past surveys (e.g. exploration of natural resources) will be of great importance. Here, the key properties and processes of the geological environment should be focussed on primarily from a hydrogeological point of view.
- The decision as to whether to assume the target rocks as being porous or fractured will be crucial for investigations, modelling and analysis. For example, if the rocks are porous, it would be more cost-effective to conduct hydraulic tests in the laboratory rather than conducting in situ hydraulic packer tests. In contrast, if the rocks are fractured, flow logging would be more important and the length of the test interval for in situ hydraulic tests would have to be carefully determined. When evaluating solute transport properties, investigation methods would be different depending on whether the rocks are considered to be porous or fractured. It will also be required, for groundwater flow and solute transport analyses, to evaluate techniques in accordance with the hydraulic properties of rocks and parameters to be acquired which also vary according to the analytical methodologies. In the

disposal project, it may be necessary, based on existing information or results of investigations in the first borehole, to determine whether rocks are porous or fractured media and to identify important hydrogeological characteristics such as abnormally high pressure. There will then be flexibility to take appropriate measures based on data obtained in subsequent investigations.

- In the shallow subsurface hydrological investigations, it will also be important to characterise the geosphere – biosphere interface. A methodology for determining the water balance on the scale of the drainage basin based on hydrological investigations and defining the distribution of aquifers will be essential as preliminary investigations for the disposal project.
- Borehole investigations would require different methodologies (or a combination of methods) depending on the rock properties and groundwater chemistries of interest. It would therefore be necessary for the disposal project to establish characterisation methods suitable for the site as early as possible so that investigations could be carried out in such a way as to yield results of similar quality in as many boreholes as possible.

(3) Hydrochemical investigations

For investigations of the host sedimentary formations, for instance, in the future disposal project, lessons learnt from the hydrochemical investigations from the surface are described below:

- The individual investigation and analytical techniques applied in the Phase I investigations would be, in general, applicable.
- Since the inadequacy of the Phase I investigations on discontinuities is partly due to insufficient preliminary evaluations and inflexible investigation strategies, investigations for the disposal project should be planned on the assumption that the sedimentary formations may exhibit hydrogeological characteristics inherent to both porous and fractured media.

(4) Rock mechanical investigations

The rock mechanical investigations conducted in the Horonobe project could be considered unusual both domestically and internationally because of the specific geological and rock mechanical conditions. The following findings were obtained in these investigations:

- The rock mechanical investigation of rocks with indistinct lithofacies changes would, for reliable modelling and analysis, require an approach in which successive data are obtained by geophysical logging; for example investigation locations selected based on the obtained data, results of the investigations interpreted and then models developed.
- It is found that rocks assumed to be formed in more or less the same geological age and with significantly high homogeneity in a horizontal direction do not always have a uniform depth profile of properties. This indicates that it is unwise to estimate the 3D distribution of rock properties in an area extending over several kilometres based only on existing geological maps or scant point data. Borehole investigations at several locations would be required to avoid such a situation.
- The effects on the initial stress field of discontinuities of various sizes (faults, fractures etc.) present in the rocks need not be taken into account when determining the layout of a repository to be constructed in sedimentary soft rock. The initial stress may however vary depending on the rigidity of rocks. Therefore, when rocks with different rigidity are present, it will be important to measure the initial stress in each rock in order to enhance the reliability of measured values.

(5) Study on the long-term stability of the geological environment

As a result of the Phase I investigations, some important issues can be highlighted for estimating the future geological environment over a period of ten thousand years. Proposals and lessons learnt for conducting future investigations are described below.

- It will be important to use data obtained by different investigation methods for different time periods concerned. When evaluating the horizontal crustal strain rate over a period of ten thousand years, which will be the case for the disposal project, data obtained using the geological method will form the basis of the evaluation. This illustrates that it is necessary to use an investigation method appropriate for the duration of a period equivalent to, or longer than, that to be evaluated.
- Issues to be considered vary depending on the duration of the time period of interest when estimating future changes of geological environments. An example of the case would be changes in geological structure. Effective investigation results can be achieved by selecting the phenomena to be considered in estimating the future geological environment according to the site-specific characteristics of the natural phenomena.
- It should also be noted that areas which are now coastal may become inland in the glacial period owing to the change in sea-level associated with the glacial-interglacial cycle. In this respect, it is important to collect information on submarine topography in and around the target area in the investigation of coastal regions.
- In addition, when evaluating the effects of natural phenomena on the geological environment, attention should be paid to the fact that the geological environment may be affected as a result of interaction among natural phenomena. In other words, it is important to always be aware of the fact that individual natural phenomena such as faulting, uplift/subsidence or change in sea-level may not affect the geological environment independently but rather the results of interaction among them will have an effect. This means that evaluating the impact of seismicity and faulting alone on the geological environment, for example, may not be appropriate as an evaluation of the impact of natural phenomena on the geological environment in a given location. Natural phenomena up to the present should thus be comprehensively integrated into a geological evolution model before evaluating their impact on the geological environment. This means that consequence assessment models and simulation techniques developed independently to date should be coupled for application when evaluating impacts of natural phenomena on the geological environment and when estimating the future geological environment based on these evaluations. Such a process would be similar to the reconstruction of the geomorphological and geological evolution conducted by researchers in the areas of geomorphology and geology. More specifically it is the integration of individual technologies in which the results of investigations on the current topography and its components, buried landforms, the depositional period and structures of rock formations, micro-fossils found in landform materials etc. are integrated so that historical geomorphology and geological evolution can be reconstructed. Again, the importance of the systematic approach or the palaeohydrogeological method must be emphasised, in which temporal and spatial changes in groundwater flow conditions associated with the geological evolution in a certain location is estimated and the best-possible approximation of a future evolution at that location is described.

(6) Development of investigation techniques

By reviewing the strategies set at the beginning of the Phase I investigations, with the recognition that investigations should be conducted with the key properties and processes of the geological environment and their temporal variations in the context of geological disposal always in mind, the following suggestions are derived in terms of how to conduct investigations:

- A clear strategy for carrying out investigations should be established before starting a programme. Specific goals should be defined first and then a schematic 'workflow' drawn up to specify the procedure leading to the investigation goals; finally a path for achieving the goals should be shown as a 'data flow diagram'. This approach would enable to conduct more efficacious investigations by eliminating excessive efforts and to acquire data on the geological environment, which are crucial for geological disposal, in a comprehensive manner.
- After obtaining the necessary data on the geological environment in a comprehensive manner, more detailed investigation items should be selected. Here, for instance, the sensitivity of the geological environment to the impacts of natural phenomena should be clarified to some extent. Note that geologically significant features are not always important for geological disposal. At the beginning of the investigation, data should thus be collected uniformly for all predetermined investigation items, not for each item in detail. Based on the data collected, items requiring more detailed information should be selected by conducting a sensitivity analysis of system performance.

In addition, with respect to QA/QC for the investigation, lessons learnt from the Phase I investigations are highlighted below:

- To assure the quality of the R&D, 'transparency', 'traceability', 'openness' and 'expert review' are of great importance. As an action programme for realise these requirements, implementation plans should be formulated for each investigation, which define the work timeplan, organisational structures, methods for investigation and analysis, measures against expected problems, procedures involved in each task and for QA/QC and safety assurance etc. They also specify that approval by the person in charge of QA/QC should be gained regarding the content of the programme in question prior to implementation. Particularly when investigations are outsourced to third parties, the goals to be achieved and quality of data required from the investigations should be informed to the parties through clear formulation of the implementation plan.

References

1) H. Funaki, E. Ishii, K. Yasue and K. Takahashi: “Study on Geology and Geological Structure Based on Literature Studies”, JNC TN5400 2004-006 (2005). (in Japanese with English abstract)
2) T. Sawada and S. Okuike: “Geological Survey of Horonobe Area”, JNC TJ1420 2001-037 (2001). (in Japanese with English abstract)
3) T. Igarashi, K. Ikeda, H. Azuma, S. Imamura and M. Oshima: “Air-Borne Geophysical Prospecting Using Helicopter”, JNC TJ1420 2001-035 (2001). (in Japanese with English abstract)
4) N. Eki and S. Yamasaki: “Current status of geoscientific studies being conducted by Japan Nuclear Cycle Development Institute in regard to geological disposal of high-level radioactive waste (part 2) – Horonobe Underground Research Center”, Geophys. Explor., 57, pp. 373-382 (2004). (in Japanese with English abstract)
5) M. Kishimoto, J. Takayama and K. Yokoi: “Geophysical Survey by Electromagnetic Method”, JNC TJ1420 2001-036 (2001). (in Japanese with English abstract)
6) S. Nagao: “Geological Map of Japan: 1:50,000 TOYOTOMI”, Explanatory Text, Geol. Surv. Hokkaido (1960). (in Japanese with English abstract)
7) T. Koaze, M. Nogami, Y. Ono and K. Hirakawa (Eds.): “Geomorphology of Hokkaido”, Regional geomorphology of the Japanese Islands, 2, Univ. Tokyo Press (2003). (in Japanese)
8) K. Yasue and E. Ishii: “Clarification of the accurate distribution of the Omagari–Toyotomi fault in the Horonobe Town, northern Hokkaido”, Active Fault Res., 25, pp. 39-46 (2005). (in Japanese with English abstract)
9) T. Niizato and K. Yasue: “A study on the long-term stability of the geological environments in and around the Horonobe area – Consideration of site specific features in assessing of the long-term stability of the geological environments”, J. Nucl. Fuel Cycle Environ., 11, pp. 125-137 (2005). (in Japanese with English abstract)
10) T. Oka and Y. Igarashi: “Latest Cenozoic formations in the northern part of Teshio Plain, Hokkaido – Sedimentary facies and pollen stratigraphy”, In: M. Kawamura, T. Oka and T. Kondo (Eds.) Commem. Vol. Prof. M. Kato, pp. 341-365 (1997). (in Japanese with English abstract)
11) Japan National Oil Corporation: “Report on the MITI Tenpoku Drilling” (1995). (in Japanese)
12) K. Takahashi, H. Fukusawa, N. Wada, K. Hoyanagi and T. Oka: “Neogene stratigraphy and paleogeography in the area along the Sea of Japan of northern Hokkaido”, Earth Sci. (Chikyu Kagaku), 38, pp. 299-312 (1984). (in Japanese with English abstract)
13) H. Fukusawa: “Late Neogene formations in the Tempoku-Haboro region, Hokkaido, Japan – Stratigraphy reinvestigation of the “Wakkanai” and “Koetoi” Formation”, J. Geol. Soc. Jpn., 91, pp. 833-849 (1985). (in Japanese with English abstract)
14) K. Mitani, F. Hayakawa, K. Takahashi, S. Ishiyama, T. Waki, T. Shigeyama: “Natural Gas Reservoir in the Toyotomi Anticline Area”, Rep. Invest. Miner. Deposits Hokkaido, No. 125, Hokkaido Dev. Agency (1971). (in Japanese)
15) E. Hirooka: “Petroleum geological study on Tenpoku district in Hokkaido, Japan”, J. Jpn. Assoc. Petrol. Technol., 27, pp. 113-134 (1962). (in Japanese with English abstract)
16) H. Fukusawa: “The site of sedimentation of Late Neogene bedded siliceous rocks in northern Hokkaido, Japan”, J. Geol. Soc. Jpn., 93, pp. 37-55 (1987). (in Japanese with English abstract)
17) K. Masaya, M. Fujita, K. Shinbo, F. Akiba, S. Kudo, K. Aoyagi and S. Kobayashi: “Oil and Natural Gas Resource of Japan” Vol. 1: Hokkaido, Jpn. Nat. Gas Assoc. Petrol. Dev. Assoc., pp. 1-92 (1982). (in Japanese)

18) S. Nagao and T. Makino: "Report on the Omagari Oil-Field Investigation in the Teshio District", Rep. Invest. Miner. Deposits Hokkaido, No. 49, Hokkaido Dev. Agency (1959). (in Japanese)
19) H. Yamamoto: "The geologic structure and the sedimentary basin off northern part of the Hokkaido Island", J. Jpn. Assoc. Petrol. Technol., 44, pp. 28-35 (1979). (in Japanese with English abstract)
20) N. Ogura and M. Kamon: "The subsurface structures and hydrocarbon potentials in the Tenpoku and Haboro area, the northern Hokkaido, Japan", J. Jpn. Assoc. Petrol. Technol., 57, pp. 32-44 (1992). (in Japanese with English abstract)
21) T. Oka: "Distribution and tectonic evolution of Late Cenozoic basins in Hokkaido", Monogr. Assoc. Geol. Collab. Jpn., No. 31, pp. 295-320 (1986). (in Japanese with English abstract)
22) Research Group for Active Faults of Japan: "Active Faults in Japan: Sheet Maps and Inventories", Revised Edition, Univ. Tokyo Press (1991). (in Japanese)
23) Y. Ikeda, T. Imaizumi, M. Togo, K. Hirakawa, T. Miyauchi and H. Sato (Eds.): "Atlas of Quaternary Thrust Faults in Japan", Univ. Tokyo Press (2002). (in Japanese)
24) T. Haraguchi, T. Ichihara and H. Ogasawara: "Investigation about Geology and Stratigraphy of the Horonobe Underground Research Laboratory Area and Its Circumference Area", JNC TJ5410 2005-008 (2002). (in Japanese with English abstract)
25) H. Takahata, M. Nagane and N. Matsumoto: "Geological Study of the Neogene Basins in the Horonobe-cho", JNC TJ5420 2004-002 (2004). (in Japanese with English abstract)
26) K. Takahashi: "Data Book of Various Measurements and Analyses on Geological and Drilling Surveys for Horonobe URL Project", JNC TN5400 2005-010 (2005). (in Japanese with English abstract)
27) K. Yasue, F. Akiba, H. Ohira and E. Ishii: "The upper Pliocene diatom zone and fission-track age of the upper Koetoi Formation around the Sarobetsu Anticline, northern Hokkaido", J. Geol. Soc. Jpn., 112, pp. 284-293 (2006). (in Japanese with English abstract)
28) K. Yasue, E. Ishii, N. Eki and T. Fukushima: "Description of terrace deposit in the Hokushin area of Horonobe, north Hokkaido", Abstr. Jpn. Earth Planet. Sci. Joint Meet. 2004, Chiba, Japan, 9-13 May 2004, Q042-P004 (2004).
29) T. Sanga: "A Study of Lineaments in the Horonobe Area", JNC TJ5420 2004-001 (2004). (in Japanese with English abstract)
30) T. Sanga: "A Study of Lineaments and Mapping for the Omagari Fault", JNC TJ5410 2005-006 (2005). (in Japanese with English abstract)
31) E. Ishii, K. Yasue, T. Tanaka, R. Tsukuwi, K. Matsuo, K. Sugiyama and S. Matsuo: "Three-dimensional distribution and hydrogeological properties of the Omagari Fault in the Horonobe area, northern Hokkaido, Japan", J. Geol. Soc. Jpn., 112, pp. 301-314 (2006). (in Japanese with English abstract)
32) E. Ishii and T. Fukushima: "A case study of analysis of faults in Neogene siliceous rocks", J. Jpn. Soc. Eng. Geol., 47, pp. 280-291 (2006). (in Japanese with English abstract)
33) K. Matsuo, T. Negi, K. Yokoi, T. Takahashi and M. Teshima: "The Survey of the Omagari Fault Using Audio Frequency Magnetotelluric Method in Horonobe Research Project for the Subsurface Environment", JNC TJ5410 2004-002 (2004). (in Japanese with English abstract)
34) K. Yasue, T. Niizato and A. Chiba: "Investigation of subsurface geological structure using the Ground Penetrating Radar", Abstr. 113th Annu. Meet. Geol. Soc. Jpn., Kochi, Japan, 16-18 Sep. 2006, p. 273 (2006). (in Japanese)
35) M. Higashinaka, R. Tsukuwi and Y. Ota: "Exploration of the Underground Structure Using Seismic Reflection Method in the Horonobe Underground Research Program", JNC TJ1410 2002-002 (2002).

(in Japanese with English abstract)

36) M. Higashinaka, Y. Sano and T. Ozawa: “Existing Reflection Seismic Data Re-processing”, JNC TJ5410 2005-009 (2005). (in Japanese with English abstract)

37) M. Higashinaka: “Gravity Data Reprocessing”, JNC TJ5410 2004-003 (2004). (in Japanese with English abstract)

38) R. Tsukuwi, T. Nishiki, M. Higashinaka and N. Tsu: “Seismic Reflection, Multi-Offset VSP and Gravity Survey in Horonobe Underground Research Laboratory Project”, JAEA-Data/Code 2006-026 (2007). (in Japanese with English abstract)

39) H. Kurikami, R. Takeuchi, S. Seno, H. Imai, I. Shiozaki, M. Shimo and S. Kumamoto: “Groundwater flow analysis considering fracture zone of Horonobe”, Proc. Fall Meet. 2005 Jpn. Assoc. Groundwater Hydrol., Aomori, Japan, 20-22 Oct. 2005, pp. 100-105 (2005). (in Japanese)

40) K. Matsuo, M. Kishimoto, T. Negi and M. Teshima: “The Survey of the Omagari Fault Using Electric Survey”, JNC TJ5440 2005-001 (2005). (in Japanese with English abstract)

41) T. Watanabe: “Survey Concerning Geology and Geological Structure of Sedimentary Rock at Neogene in Horonobe-cho, Hokkaido, Japan (Part 2)”, JNC TJ5410 2005-005 (2004). (in Japanese with English abstract)

42) H. Matsui, T. Niizato and T. Yamaguchi (Eds.): “Horonobe Underground Research Laboratory Project Investigation Report for the 2005 Fiscal Year”, JAEA-Research 2006-073 (2006). (in Japanese with English abstract)

43) Japan Nuclear Cycle Development Institute: “Horonobe Underground Research Laboratory Project Investigation Report for the 2004 Fiscal Year”, JNC TN5400 2005-001 (2005). (in Japanese)

44) E. Ishii, K. Hama, T. Kunimaru and H. Sato: “Change in groundwater pH by infiltration of meteoric water into shallow part of marine deposits”, J. Geol. Soc. Jpn., 113, pp. 41-52 (2007). (in Japanese with English abstract)

45) E. Ishii, K. Hama, T. Kunimaru and T. Kato: “Water-rock interaction observed in Neogene siliceous rocks in the Horonobe area”, Abstr. 111th Annu. Meet. Geol. Soc. Jpn., Chiba, Japan, 18-20 Sep. 2004, p. 294 (2004). (in Japanese)

46) E. Ishii and K. Yasue: “Stratigraphy and FT Age on Pliocene – Early Pleistocene Tephra in the Horonobe Town, Northern Hokkaido”, JNC TN5400 2005-006 (2005). (in Japanese with English abstract)

47) Japan Nuclear Cycle Development Institute: “Annual Report of Research and Development on HLW Geological Disposal in 2003”, JNC TN1400 2004-007 (2004). (in Japanese)

48) E. Ishii and K. Yasue: “Analysis of Faults and Development of a Geological Model in the Horonobe Underground Research Laboratory Project”, JNC TN5400 2005-008 (2005). (in Japanese with English abstract)

49) G.B. Baecher, N.A. Lanney and H.H. Einstein: “Statistical description of rock properties and sampling”, In: F.D. Wang and G.B. Clark (Eds.) Proc. 18th U.S. Symp. Rock Mech., Golden, USA, 22-24 Jun. 1977, pp. 5C1/1-5C1/8 (1977).

50) M. Shimo, H. Yamamoto, H. Matsui and T. Senba: “Groundwater flow simulation around the Kamaishi in-situ test site using an Equivalent Heterogeneous Continuum Model”, Proc. 28th Symp. Rock Mech., Tokyo, Japan, 30-31 Jan. 1997, pp. 278-282 (1997). (in Japanese with English abstract)

51) H. Takase, T. Noguchi, H. Wakamatsu, A. Martin, K. Yamada, K. Takase and M. Tabara: “Mass Transport Analysis under Uncertainty and Planning of In-Situ Experiments for Horonobe URL Project”, JNC TJ5400 2005-001 (2005). (in Japanese with English abstract)

52) M. Shimo and H. Yamamoto: “Equivalent Heterogeneous Continuum Model Approach for Seepage

Flow Simulation in Fractured Rocks", Taisei Corp. Technol. Res. Ctr. Annu. Rep., No. 29, pp. 257-262 (1996). (in Japanese)

53) S. Kumamoto, M. Shimo, and H. Kurikami: "Predictive analysis of groundwater flow due to the excavation of Horonobe URL", Proc. Symp. 'Groundwater Flow Analysis and Modeling', Jpn. Assoc. Groundwater Hydrol., Tokyo, Japan, 22 Jan. 2007, pp. 43-50 (2007). (in Japanese)

54) Power Reactor and Nuclear Fuel Development Corporation: "Site Investigation of Storage Technology Research Center – Deep Layer Boring", PNC TJ1027 98-012 (1987). (in Japanese with English abstract)

55) Power Reactor and Nuclear Fuel Development Corporation: "Site Investigation of Storage Technology Research Center – Deep Layer Boring", Appended Figures, PNC TJ1027 98-011 (1987). (in Japanese)

56) T. Yamamoto, M. Shimo, Y. Fujiwara, H. Hattori, T. Tadokoro, H. Iwama, M. Nago and S. Kumamoto: "HDB-1 Borehole Investigations in Horonobe Underground Research Center", JNC TJ1400 2002-010 (2002). (in Japanese with English abstract)

57) T. Yamamoto, M. Shimo, Y. Fujiwara, H. Hattori, T. Tadokoro, H. Iwama, M. Nago and S. Kumamoto: "HDB-2 Borehole Investigations in Horonobe Underground Research Center", JNC TJ1400 2002-011 (2002). (in Japanese with English abstract)

58) SK Engineering: "Report on Hot Spring Exploration in Horonobe Town" (1996). (in Japanese)

59) H. Oshima, M. Nishida, T. Maekawa, T. Hirayama, M. Fujihara and M. Arasi: "Study of the Groundwater Flow Analysis in Kaisin Area of Horonobe Town", JNC TJ1400 99-045 (1995). (in Japanese with English abstract)

60) T. Kanekiyo: "Collection and Arrangement of the Geological Data in the Northern Part of Hokkaido", JNC TJ1440 99-005 (1999). (in Japanese with English abstract)

61) Hokkaido Mining Promotion Committee: "Petroleum and Natural Gas Resources in Hokkaido, Exploration and Development (1977–1988)", Resour. Energ. Div., Dept. Comm., Ind. Tourism Labour, Hokkaido Pref. Govt. (1990). (in Japanese)

62) H. Kurikami, R. Takeuchi and S. Seno: "Groundwater Flow Analysis of Horonobe Underground Research Laboratory Project", JNC TN5400 2005-003 (2005). (in Japanese with English abstract)

63) H. Imai, N. Maeda, I. Shiozaki, K. Amemiya and M. Chijimatsu: "Study on Regional Groundwater Flow Analysis Relevant to the Horonobe Underground Research Program", JNC TJ1400 2002-004 (2002). (in Japanese with English abstract)

64) H. Imai, R. Yamashita, K. Amemiya and I. Shiozaki: "Study on Regional Groundwater Flow Analysis Method in Sedimentary Rock Mass", JNC TJ1410 2001-002 (2001). (in Japanese with English abstract)

65) S. Iwai and M. Ishiguro: "Applied Hydrological Statistics", Morikita Publishing (1970).

66) H. Nakabayashi, N. Matsuoka, M. Matsuo and Y. Nakano: "Research for Subsurface Hydrological System in the Planning of Horonobe Underground Research Project", JNC TJ1410 2001-005 (2002). (in Japanese with English abstract)

67) M. Ikeda, T. Sekine and Y. Horiuchi: "Installation of Groundwater Level and Soil Moisture Observation Systems", JNC TJ5410 2004-014 (2005). (in Japanese with English abstract)

68) S. Seno, R. Takeuchi, H. Kurikami and M. Hara: "Estimation of Groundwater Recharge Rate by Water Balance Method in Horonobe Underground Research Laboratory Project – From August, 2003 to July, 2004", JNC TN5400 2005-005 (2005). (in Japanese with English abstract)

69) S. Seno, H. Kurikami, S. Yabuuchi and M. Hara: "Measurement of Groundwater Table in Shallow Boreholes", JAEA-Research 2006-079 (2007). (in Japanese with English abstract)

70) G. Tomura, H. Kurikami, K. Shibano, T. Kunimaru and M. Hara: "Surface Hydrological Investigation of Horonobe Underground Research Laboratory Project", JAEA-Research 2007-063 (2007). (in Japanese with English abstract)
71) C. Doughty, C.F. Tsang, K. Hatanaka, S. Yabuuchi and H. Kurikami: "Application of direct-fitting, mass-integral, and multirate methods to analysis of flowing fluid electric conductivity logs from Horonobe, Japan", Water Resour. Res., 44, W08403, doi: 10.1029/2007WR006441 (2008).
72) S. Yabuuchi, H. Kurikami, S. Seno, M. Hara, T. Kunimaru and R. Takeuchi: "Long-Term Groundwater Pressure Monitoring in Deep Boreholes in the Horonobe Underground Research Laboratory Project", JAEA-Research 2006-056 (2006). (in Japanese with English abstract)
73) T. Yamamoto, M. Shimo, Y. Fujiwara, H. Hattori, M. Nago, T. Tadokoro and M. Kuji: "Borehole Investigations of HDB-3 in the Horonobe Underground Research Program", JNC TJ5420 2004-003 (2003). (in Japanese with English abstract)
74) T. Yamamoto, M. Shimo, Y. Fujiwara, H. Hattori, M. Nago, T. Tadokoro and M. Kuji: "Borehole Investigations of HDB-4 in the Horonobe Underground Research Program", JNC TJ5420 2004-004 (2003). (in Japanese with English abstract)
75) M. Shimo, H. Yamamoto and S. Kumamoto: "Study on Flow and Mass Transport through Fractured Soft Sedimentary Rocks", JNC TJ8400 2003-028 (2003). (in Japanese with English abstract)
76) T. Yamamoto, M. Shimo, Y. Fujiwara, H. Hattori, M. Nago, T. Tadokoro and M. Kuji: "Borehole Investigations of HDB-5 in the Horonobe Underground Research Program", JNC TJ5420 2004-005 (2003). (in Japanese with English abstract)
77) T. Yamamoto, M. Shimo, Y. Fujiwara, H. Hattori, M. Nago, T. Tadokoro and S. Nakagaki: "HDB-6 Borehole Investigations in the Horonobe Underground Research Program", JNC TJ5400 2005-004 (2004). (in Japanese with English abstract)
78) M. Shimo, and S. Kumamoto: "Study on Flow and Mass Transport through Fractured Soft Sedimentary Rocks (II)", JNC TJ8400 2004-011 (2004). (in Japanese with English abstract)
79) T. Yamamoto, M. Shimo, Y. Fujiwara, H. Hattori, M. Nago, T. Tadokoro and S. Nakagaki: "HDB-7 Borehole Investigations in the Horonobe Underground Research Program", JNC TJ5400 2005-005 (2004). (in Japanese with English abstract)
80) T. Yamamoto, M. Shimo, Y. Fujiwara, H. Hattori, M. Nago, T. Tadokoro and S. Nakagaki: "HDB-8 Borehole Investigations in the Horonobe Underground Research Program", JNC TJ5400 2005-006 (2004). (in Japanese with English abstract)
81) R. Takeuchi and Y. Hirata: "A study of ground water investigation under the dissolved gas condition", Proc. 38th Jpn. Natl. Conf. Geotech. Eng., Akita, Japan, 2-4 Jul. 2003, pp. 1259-1260 (2003). (in Japanese)
82) Japan Nuclear Cycle Development Institute: "H17: Development and Management of the Technical Knowledge Base for the Geological Disposal of HLW", Supporting Report 1: Geoscience study, JNC TN1400 2005-014 (2005). (in Japanese)
83) Swedish Nuclear Fuel and Waste Management Company: "Preliminary Site Description Forsmark Area – Version 1.2", SKB Rep. R-05-17 (2005).
84) Swedish Nuclear Fuel and Waste Management Company: "Preliminary Site Description Simpevarp Subarea – Version 1.2", SKB Rep. R-05-08 (2005).
85) H. Imai, K. Fukudome, K. Kayukawa, H. Sasaki, M. Chijimatsu and Y. Moro: "Study on Groundwater Flow Characteristics in Horonobe Underground Research Laboratory Project", JNC TJ5400 2003-009 (2004). (in Japanese with English abstract)
86) H. Imai and I. Shiozaki: "Renewal of the Existing Hydrogeological Model and Groundwater Flow

Simulation", JNC TJ5440 2004-001 (2004). (in Japanese with English abstract)

87) M. Shimo, H. Yamamoto, S. Kumamoto, M. Ono and Y. Fujiwara: "Modeling Study on Geological Environment at Horonobe URL Site", JNC TJ5400 2004-004 (2005). (in Japanese with English abstract)

88) H. Kurikami: "Groundwater Flow Analysis in the Horonobe Underground Research Laboratory Project – Recalculation Based on the Investigation until Fiscal Year 2005", JAEA-Research 2007-036 (2007). (in Japanese with English abstract)

89) H. Inoue, T. Ishiguro, M. Kuji and N. Yoshino: "A Study and Modeling about Groundwater Flow Considering the Properties of Sedimentary Soft Rock", JNC TJ8400 2004-013 (2004). (in Japanese with English abstract)

90) K. Nomoto, M. Matsui, H. Inoue, N. Yoshino, K. Karasaki and K. Ito: "Numerical Simulation in Order to Identify Hydrological Properties of Sedimentary Rock", JNC TJ8400 2005-005 (2005). (in Japanese with English abstract)

91) M. Toida, Y. Suyama, Y. Shiogama, H. Atsumi, Y. Abe and M. Furuichi: "Study on Synthesis of Geological Environment at Horonobe Area: A Technical Review", JNC TJ5400 2003-003 (2003). (in Japanese with English abstract)

92) H. Takase, R. Metcalfe, M. Inagaki, T. Noguchi, Y. Aoyama, K. Takase and M. Tabara: "Study on Synthesis of Geological Environment at Horonobe Area: A Technical Review (Phase 2)", JNC TJ5400 2003-006 (2004). (in Japanese with English abstract)

93) H. Kurikami, K. Yasue, T. Niizato, H. Imai, I. Shiozaki and R. Yamashita: "Analytical study of groundwater flow evolution due to climatic and sea level change", Proc. Symp. 'Groundwater Flow Analysis and Modeling', Jpn. Assoc. Groundwater Hydrol., Tokyo, Japan, 22 Jan. 2007, pp. 59-66 (2007). (in Japanese)

94) H. Yamamoto, T. Kunimaru, H. Kurikami, M. Shimo, and T. Xu: "Long-term simulation of ambient groundwater chemistry at Horonobe Underground Research Laboratory, Japan – Application of coupled hydro-geochemical model", Proc. GeoProc 2006, 2nd Int. Conf. 'Coupled Thermo-Hydro-Mechanical-Chemical Processes in Geosystems and Engineering', 22-25 May 2006, Nanjing, China, pp. 382-387 (2006).

95) Japan Nuclear Cycle Development Institute: "H12: Project to Establish the Scientific and Technical Basis for HLW Disposal in Japan", Supporting Report 3: Safety assessment of the geological disposal system, JNC TN1410 2000-004 (2000).

96) T. Hishiya, M. Nishigaki and N. Hashimoto: "The three dimensional numerical analysis method for density dependent groundwater flow with mass transport", J. Constr. Manag. Eng., No. 638/III-49, pp. 59-69 (1999). (in Japanese with English abstract)

97) M. Shimo, N. Nishijima and K. Fumimura: "Evaluation of uncertainty due to hydrogeological modeling and groud water flow analysis (3) – Taisei Equivalent Heterogeneous Contiuum Model using EQUIV-FLO", Proc. Symp. 'Flow Problems in Fractured Rocks', Tokyo, Japan, 10-11 Sep. 2001, Jpn. Geotech. Soc., pp. 269-278 (2001).

98) T. Hirota, H. Sagayama, E. Yokoyama, T. Suga and H. Matsunami: "Hydrogeological Map of Hokkaido: No. 1 WAKKANAI", Explanatory Notes, Geol. Surv. Hokkaido (1983). (in Japanese with English abstract)

99) K. Hama, T. Kunimaru, and J. Shimada: "Methodology development for the characterization of groundwater geochemistry in the sedimentary rocks – An application to the Neogene sedimentary rocks in the Horonobe, northern part of Hokkaido", Proc. Fall Meet. 2005 Jpn. Assoc. Groundwater Hydrol., Aomori, Japan, 20-22 Oct. 2005, pp. 106-109 (2005). (in Japanese)

100) K. Kiho, T. Oyama, and Y. Mahara: "Production of compaction type pore water extraction apparatus and its application to the deep-seated sedimentary rock", J. Jpn. Soc. Eng. Geol., 40, pp. 260-269 (1999). (in Japanese with English abstract)
101) Groundwater Handbook Editorial Committee (Ed.): "Groundwater Handbook", Constr. Ind. Invest. Cmmte. (1979). (in Japanese)
102) M. Teramoto, J. Shimada, and T. Kunimaru: "Evidences of groundwater regime in impermeable rocks by stable isotopes in porewaters of drilled cores", Jpn. Soc. Eng. Geol., 47, pp. 68-76 (2006).(in Japanese with English abstract)
103) H. Sakai, and Y. Matsuhisa: "Stable Isotope Geochemistry", Univ. Tokyo Press (1996). (in Japanese)
104) T. Kunimaru and R. Metcalfe: "Isotopic study for the estimation of C-14 age of groundwater at the Horonobe, Hokkaido", Proc. 9th Int. Conf. Accel. Mass Spectrom. (AMS-9), Nagoya, Japan, 9-13 Sep. 2002, p. 198 (2002).
105) I. Clark and P. Fritz: "Environmental Isotopes in Hydrogeology", Lewis Publishers (1999).
106) S. Nagao, T. Iwatsuki and K. Hama: "Characterization of groundwater humic substances by high-performance size exclusion chromatography with fluorescence detection", Abstr. Int. Workshop 'Waste Management in Sapporo', Sapporo, Japan, 29-30 Aug. 2005, pp. 3-11 (2005).
107) K. Nagaosa, K. Hama, T. Kunimaru, M. Nakayama, K. Aoki, and K. Kato: "Bacterial community in the groundwater of the Neogene sedimentary rock in Horonobe area, Hokkaido: Phylogenetic analysis with cloning", Abstr. 21st Jpn. Soc. Microb. Ecol. Annu. Meet., Fukuoka, Japan, 30 Oct.–2 Nov. 2005, p. 138 (2005). (in Japanese)
108) Tunnel Research Association, Calamity Science Institute (Eds.): "Underground Visualization and Exploration Techniques", Current status of high-density resistivity survey, Kajima Inst. Publishing (2001). (in Japanese)
109) M. Laaksoharju, C. Skårman and E. Skårman: "Multivariate mixing and mass-balance (M3) calculations, a new tool for decoding hydrogeochemical information", Appl. Geochem., 14, pp. 861-871 (1999).
110) M. Laaksoharju, E.-L. Tullborg, P. Wikberg, B. Wallin and J. Smellie: "Hydrogeochemical conditions and evolution at Äspö HRL, Sweden", Appl. Geochem., 14, pp. 835-859 (1999).
111) K. Ochi, Y. Kim and F. Tatsuoka: "Study into the deformation characteristics of sedimentary soft rock taking into account the strain level-dependency and measurement errors", J. Jpn. Soc. Civil Eng., No. 463/III-22, pp. 133-142 (1993). (in Japanese with English abstract)
112) Japan Nuclear Cycle Development Institute: "H12: Project to Establish the Scientific and Technical Basis for HLW Disposal in Japan", Supporting Report 2: Repository design and engineering technology, JNC TN1410 2000-003 (2000).
113) Japanese Geotechnical Society: "Sedimentary Soft Rocks in Geotechnical Engineering" (1987). (in Japanese)
114) M. Brudy and M.D. Zoback: "Compressive and tensile failure of boreholes arbitrarily-induced to principal stress axis: Application to the KTB borehole Germany", Int. J. Rock Mech. Sci., pp. 1035-1038 (1993).
115) Japan Nuclear Cycle Development Institute: "H12: Project to Establish the Scientific and Technical Basis for HLW Disposal in Japan", Supporting Report 1: The geological environment of Japan, JNC TN1410 2000-002 (2000).
116) H. Matsui, N. Maeda and K. Yoshikawa: "The Results of the Geomechanical Investigations in the MIU-3 Borehole and the Conceptual Geomechanical Model of the Toki Granite in Shobasama Area", JNC TN7420 2001-001 (2001). (in Japanese)

117) H. Matsui, S. Aoyagi and S. Miyanomae: “Examination for the swelling and drying properties of diatomaceous sedimentary rock based on laboratory testing”, Proc. 41st Jpn. Natl. Conf. Geotech. Eng., Kagoshima, Japan, 12-14 Jul. 2006, pp. 495-496 (2006). (in Japanese)
118) T. Moriya: “The crustal stress field being inferred from the earthquake mechanism solution in Hokkaido and its vicinity”, Chikyu Monthly, 21, pp. 557-563 (1999). (in Japanese)
119) S. Niunoya, H. Matsui, T. Yamamoto and K. Sugiyama: “Estimation of deformation properties of sedimentary soft rocks using pressuremeter test in borehole”, Proc. 41st Jpn. Natl. Conf. Geotech. Eng., Kagoshima, Japan, 12-14 Jul. 2006, pp. 559-560 (2005). (in Japanese)
120) A. Cho: “In-situ stress state at the depth of HLW repository”, Proc. 107th SEGJ Conf., Shimizu, Japan, 22-24 Oct. 2002, pp. 118-121 (2002). (in Japanese)
121) T. Yamamoto, T. Aoki, H. Taki and M. Joh: “Investigation on Time-Dependent Behavior of Sedimentary Rock”, JNC TJ5400 2003-001 (2003). (in Japanese)
122) S. Niunoya and H. Matsui: “Geomechanical conceptual model on Neogene diatomaceous rock mass based on laboratory and in-situ measurement”, Proc. 35th Symp. Rock Mech., Tokyo, Japan, 12-13 Jan. 2006, pp. 177-182 (2006). (in Japanese with English abstract)
123) Nuclear Safety Commission of Japan: “Environmental Requirements to be Considered at the Selection of the Preliminary Investigation Areas for High-Level Radioactive Waste Disposal”, Advisory Board on High-Level Waste Repository Safety, 30th September 2002 (2002). (in Japanese)
124) M. Kawamura, T. Ohi, H. Makino, K. Umeda, T. Niizato, T. Ishimaru and T. Seo: “Study on evaluation method for potential impacts of “natural phenomena” on a HLW disposal system”, Proc. 2006 East Asia Forum Radwaste Manag. Conf. (2006 EAFORM Conference), Lung-Tan, Taiwan, 27-28 Nov. 2006, pp. 350-367 (2006).
125) Y. Yusa, K. Ishimaru, K. Ota and K. Umeda: “Geological and geochemical indicators of paleohydrogeology in Tono Uranium Deposits, Japan”, In: Paleohydrogeological Methods and Their Applications, Proc. NEA Workshop, Paris, France, 9-10 Nov. 1992, OECD/NEA, pp. 117-146 (1993).
126) R. Huggett: “Systems Analysis in Geography”, Contemporary problems in geography series, Oxford Univ. Press (1980).
127) E. Sasao, T. Iwatsuki and Y. Amano: “Role of paleohydrogeological studies from the perspective of the natural analogue study of the Tono uranium deposit”, Resour. Geol., 56, pp. 125-132 (2006). (in Japanese with English abstract)
128) A. Taira: “Crustal movement in the eastern margin of the Japan Sea and tectonics of Japanese Islands”, In: M. Ohtake, A. Taira and Y. Ota (Eds.) Active Faults and Seismo-Tectonics of the Eastern Margin of the Japan Sea, Univ. Tokyo Press, pp. 3-15 (2002). (in Japanese)
129) Japan Meteorological Agency: “The Annual Seismological Bulletin of Japan for 2002” (2004).
130) K. Koike and H. Machida: “Atlas of Quaternary Marine Terraces in the Japanese Islands”, Univ. Tokyo Press (2001). (in Japanese)
131) M. Koyama: “A review of historical seismology in Japan: Analyses and proposals for next stage of study of historical documents”, J. Geogr., 108, pp. 346-369 (1999). (in Japanese with English abstract)
132) T. Usami: “Materials for Comprehensive List of Destructive Earthquakes in Japan, [416]-2001”, Latest Edition, Univ. Tokyo Press (2003). (in Japanese)
133) Earthquake Research Committee Headquarters for Earthquake Research Promotion Prime Minister’s Office, Government of Japan: “Seismic Activity in Japan – Regional Perspectives on the Characteristics of Destructive Earthquakes (Excerpt)”, Sci. Technol. Agency (1998).

134) K. Ishibashi: "Problems in the study of old earthquakes", In: Y. Ota and K. Shimazaki (Eds.) Exploring Old Earthquakes, Kokon Shoin, pp. 193-207 (1995). (in Japanese)
135) G. Sarashina: "Folk Tales of the Ainu in Hokkaido" Nire Shobo (1955). (in Japanese)
136) T. Niizato, K. Shigeno and Y. Takashimizu: "Ainu oral traditions and historical records on earthquakes in Hokkaido, Japan", Hist. Earthquakes, No. 21, pp. 121-136 (2006). (in Japanese with English abstract)
137) T. Yata: "Some problems in the recension of the collection of published historical earthquake materials", Chikyu Monthly, 27, pp. 825-829 (2005). (in Japanese)
138) Hokkaido Prefectural Government (Ed.): "The New Chronology of Hokkaido History", Hokkaido Publish Plan. Ctr. (1992). (in Japanese)
139) Aomori Prefectural Government, Department of General Affairs: "Comprehensive List of Earthquakes in Aomori" (1998). (in Japanese)
140) N. Yonekura, S. Kaizuka, M. Nogami and K. Chinzei (Eds.): "Introduction to Japanese Geomorphology", Regional geomorphology of the Japanese Islands, 1, Univ. Tokyo Press (2001). (in Japanese)
141) National Research Institute for Earth Science and Disaster Prevention: "High Sensitivity Seismographic Network Japan", <http://www.hinet.bosai.go.jp> (accessed on 3rd Jun. 2008). (in Japanese)
142) H. Moriya, T. Niizato, I. Kitamura, H. Hotta and H. Ohara: "Analysis of microearthquakes at the Horonobe area, northern of Hokkaido, Japan, by using the Multiplet-Clustering Analysis", Proc. 115th SEGJ Conf., Hakata, Japan, 16-18 Oct 2006, pp. 46-49 (2006). (in Japanese with English abstract)
143) N. Hirata and M. Matsu'ura: "Maximum-likelihood estimation of hypocenter with origin time eliminated using nonlinear inversion technique", Phys. Earth Planet. Inter., 47, pp. 50-61 (1987).
144) H. Moriya, H. Niitsuma and R. Baria: "Multiplet-Clustering Analysis reveals structural details within the seismic cloud at the Soultz geothermal field, France", Bull. Seismol. Soc. Am., 93, pp. 106-1620 (2003).
145) M. Tamura, M. Kasahara and T. Moriya: "Micro-Seismicity and Crustal Structure in the Northern Part of Hokkaido, Inferred from Temporal Observation", J. Seismol. Soc. Jpn., 55, pp. 337-350 (2003). (in Japanese with English abstract)
146) Japan Meteorological Agency: "Destructive Earthquakes in and around the Japanese Islands (from 1996 to 2007)", <http://www.seisvol.kishou.go.jp/eq/higai/higai1996-new.html> (accessed on 3rd Jun. 2008). (in Japanese)
147) T. Ito: "When does the on-going tectonic phase of active tectonics in Hokkaido begin?", Chikyu Monthly, 21, pp. 608-613 (1999). (in Japanese)
148) T. Sagiya: "High strain zone since Meiji Period or later", In: M. Ohtake, A. Taira and Y. Ota (Eds.) Active Faults and Seismo-Tectonics of the Eastern Margin of the Japan Sea, Univ. Tokyo Press, pp. 133-150 (2002). (in Japanese)
149) T. Nohara, Y. Koriya and T. Imaizumi: "An estimation of the crustal strain rate using the active fault GIS data", Active Fault Res., No. 19, pp. 23-32 (2000). (in Japanese with English abstract)
150) R. Tsukuwi: "Data Book on the Results of Long-Term Monitoring in View from Long-Term Stability of the Geological Environment in and around the Horonobe Area – Long-Term Monitoring of Electromagnetic Property and Crustal Movement by Using MT and GPS Equipments", JNC TN5450 2004-001 (2005). (in Japanese with English abstract)
151) Y. Okamura: "Reverse faults and crustal contraction in the offshore area along the eastern margin of

Japan Sea", Chikyu Monthly, 20, pp. 460-465 (1998). (in Japanese)
152) S. Marshak and N. Woodward: "Introduction to cross-section balancing", In: S. Marshak and G. Mitra (Eds.) Basic Methods of Structural Geology, Prentice Hall, pp. 303-332 (1998).
153) Hydrographic Department, Japan Coast Guard: "TEURI TO: Submarine Structural Chart and Report of Survey", Basic map of the sea in coastal waters (1:50,000), No. 6321^{3-S} (1994). (in Japanese)
154) Geological Survey of Japan: "Database of the Marine Seismic Profiles around Japan", CD-ROM Version, Digital geoscience map series M-1 (2001). (in Japanese)
155) M. Ohtake, A. Taira and Y. Ota (Eds.): "Active Faults and Seismo-Tectonics of the Eastern Margin of the Japan Sea", Univ. Tokyo Press (2002). (in Japanese)
156) Japan Coast Guard: "Bathymetric Chart "TEURI TO" (1:200,000)" (1972). (in Japanese)
157) A. Furusawa: "The volcanism found out in the tephric-loess sequences around Yufudake Volcano, central Kyusyu, Japan by RIPL Method", J. Geol. Soc. Jpn., 110, pp. 19-37 (2004). (in Japanese with English abstract)
158) F. Akiba, C. Hiramatsu, I. B. Tsoy, K. Ogasawara and K. Amano: "Diatom biostratigraphy and geologic age of the Maruyama and Kurasi Formations, southern Sakhalin, and their correlation to the Neogene of the Tenpoku area, Hokkaido", J. Geogr., 109, pp. 203-217 (2000). (in Japanese with English abstract)
159) T. Sagayama: "Geologic age of the boundary part between the Embetsu Formation – Koetoi Formation and the Yuchi Formation, northern Hokkaido, Japan: Rubeshube River and Kaminukanan River routes", J. Geol. Soc. Jpn., 109, pp. 310-323 (2003). (in Japanese with English abstract)
160) O. Fujiwara, M. Yanagida, T. Sanga and T. Moriya: "Researches on tectonic uplift and denudation with relation to geological disposal of HLW in Japan", J. Nucl. Fuel Cycle Environ., 11, pp. 113-124 (2005). (in Japanese with English abstract)
161) K. Aoyagi and T. Kazama: "Transformational changes of clay minerals, zeolites and silica minerals during diagenesis", Sedimentology, 27, pp. 179-188 (1980).
162) A. Iijima and R. Tada: "Silica diagenesis of Neogene diatomaceous and volcaniclastic sediments in northern Japan", Sedimentology, 28, pp. 185-200 (1981).
163) T. Yoshimura: "Evaluation of thermal history of sedimentary basin from a mineralogical point of view", J. Jpn. Assoc. Petrol. Technol., 59, pp. 271-278 (1994). (in Japanese with English abstract)
164) E. Yatsu: "Geomorphic processes", In: S. Machida, M. Iguchi, S. Kaizuka, T. Sato, I. Kayane and Y. Ono (Eds.) Encyclopaedia of Geomorphology, Ninomiya Shoten, pp. 393-394 (1981). (in Japanese)
165) K. Takahashi, T. Niizato, K. Yasue and E. Ishii: "Estimation of Erosion Amount by Geochemical Characteristic in the Horonobe Area, Northern Hokkaido", JNC TN5400 2005-011 (2005). (in Japanese with English abstract)
166) T. Suzuki: "Terrace, Hills and Mountains", Introduction to map reading for civil engineers, 3, Kokon Shoin (2000). (in Japanese)
167) H. Yamagishi (Ed.): "Landslides in Hokkaido", Hokkaido Univ. Press (1993). (in Japanese)
168) Y. Kurashige: "Measurements and analysis of the suspended sediment", In: Y. Onda, K. Okuhishi, T. Iida and M. Tsujimura (Eds.) Hydrogeomorphology: The Interaction of Hydrologic and Geologic Process, Kokon Shoin, pp. 132-142 (1996). (in Japanese)
169) Y. Ishikawa: "Identification of high strain zone based on the seismicity in the eastern margin of Japan Sea", In: M. Ohtake, A. Taira and Y. Ota (Eds.) Active Faults and Seismo-Tectonics of the Eastern Margin of the Japan Sea, Univ. Tokyo Press, pp. 151-165 (2002). (in Japanese)
170) H. Shimamura and T. Moriya: "Seismicity in Hokkaido", Hokkaido Univ. Press (1994). (in Japanese)
171) H. Takahashi and M. Kasahara: "Seismic activity in the coastal area of Rumoi Subprefecture and

tectonics in northern Hokkaido, Japan", Geophys. Bull. Hokkaido Univ., 68, pp. 199-218 (2005). (in Japanese with English abstract)
172) Y. Takashimizu: "Ainu oral traditions and historical records on tsunami in Hokkaido Prefecture, Japan", Hist. Earthquakes, No. 20, pp. 183-199 (2005). (in Japanese with English abstract)
173) T. Sasaki, T. Kohara and K. Kojima (Eds.): "The Community Road of Ainu", Yoshikawa Koubunkan (2005). (in Japanese)
174) K. Ikehara: "Large earthquakes recorded as deep-sea turbidites in the Rishiri Trough, Northernmost Hokkaido", The Quat. Res., 39, pp. 569-574 (2000). (in Japanese with English abstract)
175) M. Kono: "History of Ainu/Outline", Hokkaido Publish Plan. Ctr. (1996). (in Japanese)
176) Earthquake Research Committee Headquarters for Earthquake Research Promotion Prime Minister's Office, Government of Japan: "Focused Research and Observation Program in the Future", (2005). (in Japanese)
177) T. Nakata and T. Imaizumi (Eds.): "Digital Active Fault Map of Japan", Univ. Tokyo Press (2002). (in Japanese)
178) H. Tokuyama, E. Honza, M. Kimura, S.-I. Kuramoto, J. Ashi, N. Okamura, H. Arato, Y. Ito, W. Soh, R. Hino, T. Nohara, H. Abe, S.-I. Sakai and K. Mukaiyama: "Tectonic development in the regions around Japan since latest Miocene", J. Soc. Mar. Surv. Technol., 13, pp. 27-53 (2001). (in Japanese with English abstract)
179) Geographical Survey Institute: "Digital Map 50m Grid (Elevation): NIPPON-I" (2001). (in Japanese)
180) T. Oka: "Study on the neotectonics of Hokkaido and its neighboring seas, with notes on the existence of active fault and occurrence of earthquake in Sapporo and its vicinity", In: M. Kawamura, T. Oka and T. Kondo (Eds.) Commem. Vol. Prof. M. Kato, pp. 426-449 (1997). (in Japanese with English abstract)
181) K. Nakamura: "Possible nascent trench along the eastern Japan Sea as the convergent boundary between Eurasian and North American plates", Bull. Earthquake Res. Inst., 58, pp. 711-722 (1983). (in Japanese with English abstract)
182) Y. Kobayashi: "Beginning of plate "Subduction" ", Chikyu Monthly, 3, pp. 510-518 (1983). (in Japanese)
183) H. Yamamoto: "The geologic structure and the sedimentary basin off northern part of the Hokkaido Island", J. Jpn. Assoc. Petrol. Technol., 44, pp. 260-267 (1979). (in Japanese with English abstract)
184) D. Wei and T. Seno: "Determination of the Amurian plate motion", In: M. Flower, S.L. Chung, C.H. Lo and T.Y. Lee (Eds.) Mantle Dynamics and Plate Interaction in East Asia, Geodynamic series, 27, pp. 337-346 (1998).
185) W. Hirose and M. Nakagawa: "Neogene volcanism in central-eastern Hokkaido: Beginning and evolution of arc volcanism inferred from volcanological parameters and geochemistry", J. Geol. Soc. Jpn., 105, pp. 247-265 (1999). (in Japanese with English abstract)
186) W. Hirose, M. Iwasaki and M. Nakagawa: "Transition of Neogene arc volcanism in Central-Western Hokkaido, viewed from K-Ar ages, style of volcanic activity, and bulk rock chemistry", J. Geol. Soc. Jpn., 106, pp. 120-135 (2000). (in Japanese with English abstract)
187) Y. Watanabe and S. Yamaguchi: "K-Ar ages of Miocene volcanic rocks and the tectonics in the Nayoro–Asahikawa region, northern Hokkaido", Earth Sci., 42, pp. 91-99 (1988) (in Japanese with English abstract)
188) Y. Goto and K. Wada: "The middle Miocene alkali dolerite from Rebun Island, northeastern Japan Sea", J. Mineral. Petrol. Econ. Geol., 86, pp. 375-378 (1991).

189) Y. Goto, M. Nakagawa and K. Wada: “Tectonic setting of the Miocene volcanism in northern Hokkaido, Japan: Speculation from their K-Ar ages and major element chemistry”, J. Mineral. Petrol. Econ. Geol., 90, pp. 109-123 (1995). (in Japanese with English abstract)

190) Y. Ishizuka: “Eruptive history of Rishiri Volcano, northern Hokkaido, Japan”, Bull. Volcanol. Soc. Jpn., 44, pp. 23-40 (1999). (in Japanese with English abstract)

191) K. Shuto, Y. Hirahara, H. Ishimoto, A. Aoki, A. Jinbo and Y. Goto: “Sr and Nd isotopic compositions of the magma source beneath north Hokkaido, Japan: Comparison with the back-arc side in the NE Japan arc”, J. Volcanol. Geotherm. Res., 134, pp. 57-75 (2004).

192) H. Miura: “A proposal for the source vent of the Rishiri–Wankonosawa tephra (Rs-Wn), the late Pleistocene marker tephra in northern Hokkaido”, Geogr. Rep. Tokyo Metrop. Univ., 30, pp. 133-145 (1995).

193) A. Tanaka, M. Yamano, Y. Yano and M. Sasada: “Geothermal Gradient and Heat Flow Data in and around Japan”, Digital geoscience map series P-5, Geol. Surv. Jpn., AIST (2004).

194) M. Yahata: “Evolution in space and time of Late Cenozoic hydrothermal activity and ore mineralization in Hokkaido, Japan”, Rep. Geol. Surv. Hokkaido, No. 73, pp. 151-194 (2002). (in Japanese with English abstract)

195) A. Tanaka, Y. Yano, M. Sasada, Y. Okubo, K. Umeda, N. Nakatsuka and F. Akita: “Compilation of thermal gradient data in Japan on the basis of the temperatures in boreholes”, Bull. Geol. Surv. Jpn., 50, pp. 457-487 (1999). (in Japanese with English abstract)

196) K. Asamori and K. Umeda: “Geophysical techniques for detecting magmas and high-temperature fluids; their application to the Onikobe–Narugo volcanic region and the southern Kii Peninsula”, J. Nucl. Fuel Cycle Environ., 11, pp. 147-156 (2005). (in Japanese with English abstract)

197) K. Masuda and A. Abe: “Climate change in the Quaternary”, Chapter 4, In: Iwanami Course on Earth Planetary Science, 11, Iwanami Shoten, pp. 103-156 (1996). (in Japanese)

198) Y. Ono: “The northern landbridge of Japan”, The Quat. Res., 29, pp. 183-192 (1990). (in Japanese with English abstract)

199) Y. Ono and Y. Igarashi: “Forest in Hokkaido”, In: Natural History of Hokkaido, Hokkaido Univ. Press, pp. 81-99 (1991). (in Japanese)

200) Y. Igarashi: “Holocene forest and climate change”, In: Natural History of Hokkaido, Hokkaido Univ. Press, pp. 181-205 (1991). (in Japanese)

201) G. Yamada: “Vegetation history of Hokkaido (1) – north Hokkaido”, In: Y. Yasuda and N. Miyoshi (Eds.) Atlas of Vegetation History in Japanese Islands, Asakura Shoten, pp. 39-50 (1998). (in Japanese)

202) Y. Igarashi, T. Igarashi, H. Daimaru, O. Osamu, T. Miyagi, K. Matsushita and K. Hiramatus: “Vegetation history of Kenbuchi Basin and Furano Basin in Hokkaido, north Japan, since 32,000 yrs BP”, The Quat. Res., 32, pp. 89-105 (1993). (in Japanese with English abstract)

203) H. Miura and K. Hirakawa: “Origin of fossil periglacial wedges in northern and eastern Hokkaido, Japan”, J. Geogr., 104, pp. 189-224 (1995). (in Japanese with English abstract)

204) T. Suzuki, E. Tokunaga, H. Noda and H. Arakawa: “Effects of rock strength and permeability on hill morphology”, Trans. Jpn. Geomorphol. Union, 6, pp. 101-130 (1985).

205) P. Reasenberg and D. H. Oppenheimer: “FPFIT, FPPLOT, and FPPAGE, FORTRAN Computer Programs for Calculating and Displaying Earthquake Fault-Plane Solutions”, USGS Open-File Rep., 85-0739 (1985).

206) Y. Ishikawa: “The tectonic belt in the Japan Sea”, Chikyu Monthly, 20, pp. 490-496 (1998). (in Japanese)

207) M. Ohtake: "Earthquake potential of the eastern margin of the Japan Sea", Chikyu Monthly, 20, pp. 449-453 (1998). (in Japanese)
208) H. Moriya, K. Nakazato, H. Niitsuma and R. Baria: "Detailed fracture system of the Soultz-soultz-sous-Forêts HDR field evaluated using microseismic multiplet analysis", Pure Appl. Geophys., 159, pp. 517-541 (2003).
209) F. Akita and N. Matsumoto: "Coseismic groundwatr level changes in hot spring wells in Hokkaido induced by four earthquakes larger than M 7.5 between 1993 and 1994", J. Seismol. Soc. Jpn., 53, pp. 193-204 (2001). (in Japanese with English abstract)
210) F. Akita: "Hot spring changes induced by the 2003 Tokachi-oki earthquake", Program 42nd Boring Surv. Symp., Sapporo, Japan, 9th Mar. 2004, Geol. Surv. Hokkaido, pp. 79-89 (2004). (in Japanese)
211) F. Nanayama, K. Satake, R. Furukawa, K. Shimokawa, B.F. Atwater, K. Shigeno and S. Yamaki: "Unusually large earthquakes inferred from tsunami deposits along the Kuril trench", Nature, 424, pp. 660-663 (2003).
212) N. Kato and H. Sato: "Active tectonics in the central Hokkaido", Chikyu Monthly, 24, pp. 481-484 (2002). (in Japanese)
213) Advanced Industrial Science and Technology: "Paleoseismology and Activity Study of the Sarobetsu Fault Zone", Report of the additional and complementary survey of the fault zone in the fundamental earthquake survey, No. H17-1 (2005). (in Japanese)
214) H. Machida and F. Arai: "Atlas of Tephra in and around Japan", Revised Edition, Univ. Tokyo Press (2003). (in Japanese)
215) T. Naruse: "Characteristics of an aeolian dust and loess", In: T. Naruse, Aeolian Dust and Loess, Asakura Shoten, pp. 30-46 (2006). (in Japanese)
216) T. Oka and Y. Igarashi: "Plio-Pleistocene in the Toikanbetsu Tectonic Basin, northern Hokkaido: Sedimentary facies and pollen stratigraphy", J. Geol. Soc. Jpn., 99, pp. 365-389 (1993). (in Japanese with English abstract)
217) Y. Yanagisawa and F. Akiba: "Refined Neogene diatom biostratigraphy for the northwest Pacific around Japan, with an introduction of code numbers for selected diatom biohorizons", J. Geol. Soc. Jpn., 104, pp. 395-414 (1998).
218) Y. Yano, A. Tanaka, M. Okubo, Y. Sasada, K. Umeda and N. Nakatsuka: "1:3,000,000 Geothermal Gradient Map of Japan", Cover and Explanation, Geol. Surv. Jpn. (1999). (in Japanese with English abstract)
219) T. Suzuki: "Research on rock control in geomorphological processes – A short history", Trans. Jpn. Geomorphol. Union, 15, pp. 179-201 (1994). (in Japanese with English abstract)
220) K. Tanaka: "Prediction of geological environments – Strategy and present status", Chikyu Monthly, 26, pp. 344-348 (2004). (in Japanese)
221) T. Kimura: "Logics on the long-term prediction of crustal movement", In: T. Kimura, Crustal Movement in Japanese Islands – From A New Perspective, Aichi Shuppan, pp. 1-66 (2002). (in Japanese)
222) Japan Nuclear Cycle Development Institute: "H17: Development and Management of the Technical Knowledge Base for the Geological Disposal of HLW" Supporting Report 3: Safety assessment method, JNC TN1400 2005-016 (2005). (in Japanese)
223) T. Oka, Y. Igarashi and H. Masahiko: "Study of the alluvial deposits (Alluvium) in the Teshio Plain by the analyzing drilling data and pollen analysis", Rep. Geol. Surv. Hokkaido, No. 77, pp. 17-75 (2006). (in Japanese with English abstract)
224) H. Fukusawa, K. Hoyanagi and M. Kiyama: "Stratigraphic and palaeoenvironmental study of the

Neogene formations in northern central Hokkaido, Japan", Mem. Geol. Soc. Jpn., No. 37, pp. 1-10 (1992). (in Japanese with English abstract)
225) R.G. Walker: "Wave- and storm-dominated shallow marine systems", In: R.G. Walker and N.P. James (Eds.) Facies Models; Response to Sea Level Change, Geol. Assoc. Can., pp. 219-238 (1992).
226) E. Seibold, W.H. Berger and N. Niitsuma: "Origin and topography of the ocean margin", In: E. Seibold, W.H. Berger and N. Niitsuma, The Sea Floor – An Introduction to Marine Geology, Springer-Verlag Tokyo, pp. 25-48 (1986). (in Japanese)
227) J. Chappell: "Upper Quaternary sea levels, coral terraces oxygen isotopes and deep-sea temperature", J. Geogr., 103, pp. 828-840 (1994).
228) B.U. Haq, J. Hardenbol and P.R. Vail: "Chronology of fluctuating sea levels science the Triassic", Science, 235, pp. 1156-1167 (1987).
229) N. Yonekura: "Sea level changes of the Quaternary and its prediction", In: Japan Association for Quaternary Research (Eds.) Quaternary Research Looks at the Future of Nature in Japan, Kokon Shoin, pp. 38-59 (1987). (in Japanese)
230) H. Osawa, K. Nakano and K. Ota: "Synthesis of the results from surface-based investigations in the MIU Project", Abstr. 2001 Fall Meet. At. Energ. Soc. Jpn., Sapporo, Japan, 19-21 Sep. 2001, p. 918 (2001). (in Japanese)
231) M. Mazurek, F.J. Pearson, G. Volckaert and H. Bock: "Features, Events and Processes Evaluation Catalogue for Argillaceous Media", OECD/NEA, ISBN 92-64-02148-5 (2003).
232) H. Makino, A. Sawada, K. Maekawa, M. Shibata, H. Sasamoto, H. Yoshikawa, K. Wakasugi, S. Koo, K. Hama, H. Kurikami, T. Kunimaru, E. Ishii, R. Takeuchi, K. Nakano, H. Saegusa, S. Takeuchi, T. Iwatsuki, K. Ota and T. Seo: "A Structure for the Series of Research Activities Ranging from Site Investigation and Evaluation to Mass Transport Analysis – A Study Using Geological Information from the Phase I Programmes (Surface-Based Investigations) at Two Generic Underground Research Laboratories", JNC TN1400 2005-021 (2005). (in Japanese with English abstract)
233) National Cooperative for the Disposal of Radioactive Waste: "Geosynthese Wellenberg 1996, Ergebnisse der Untersuchungsphasen I und II", Nagra Tech. Rep. NTB 96-01 (1997). (in German with English abstract)
234) K. Nakano, K. Ota, S. Takeuchi, H. Saegusa and H. Osawa: "Geoscientific studies in the Mizunami Underground Research Laboratory – Project overview", Abstr. 2005 Jpn. Earth Planet. Sci. Joint Meet., Chiba, Japan, 22-26 May 2005, G018-010 (2005).
235) K. Ota, T. Sato, S. Takeuchi, T. Iwatsuki, K. Amano, H. Saegusa, T. Matsuoka and H. Onoe: "Technical Expertise Gained from the Surface-Based Investigations at the Tono Area", JNC 7400 2005-023 (2005). (in Japanese with English abstract)
236) T. Xu and K. Pruess: "Modeling multiphase fluid flow and reactive geochemical transport in variably saturated fractured rocks: 1. Methodology", Am. J. Sci., 301, pp. 16-33 (2001).
237) K. Pruess, C. Oldenburg and G. Moridis: "TOUGH2 User's Guide", Ver. 2.0, Earth Sci. Div., Lawrence Berkeley Natl. Lab., LBNL-43134 (1999).
238) T. Xu and K. Pruess: "Modeling multiphase fluid flow and reactive geochemical transport in variably saturated fractured rocks: 2. Applications to supergene copper enrichment and hydrothermal flows", Am. J. Sci., 301, pp. 34-59 (2001).
239) H. Yamamoto: "Numerical Simulation of Chemically Reactive Transport in Groundwater – A Simulator TOUGHREACT and Its Application to the CO_2 Sequestration in Deep Underground", Rep. Taisei Technol. Ctr., No. 38 (2005). (in Japanese with English abstract)
240) H. Matsui, M. Sasaki: "Experiences on Deep Borehole Drilling in Neogene Sedimentary Formations

during Surface-Based Investigation Phase", JAEA-Technology 2006-052 (2006). (in Japanese with English abstract)
241) Environmental Protection and Industrial Location Bureau, Ministry of International Trade and Industry (Eds.): "Mine Safety Regulations", For Petroleum Mine – 1996 Edition, Hakua Shobo (1996). (in Japanese)
242) S. Takakura, K. Nakagami, Y. Mitsuhata and R. Murayama: "Petroleum geological interpretation of resistivity structure based in the Higashi-Kubiki area, Niigata, Japan", J. Jpn. Assoc. Petrol. Technol., 62, pp. 59-68 (1997). (in Japanese with English abstract)
243) K. Yasue, F. Akiba and E. Ishii: "Detailed hinterland analysis using reworked fossil diatoms in the Horonobe area, northern Hokkaido, Japan", Abstr. 2005 Jpn. Earth Planet. Sci. Joint Meet., Chiba, Japan, 22-26 May 2005, G016-003 (2005).
244) K. Umeda and A. Furusawa: "Identification of tephras using RIPL method and its application in volcanology", Chikyu Monthly, 26, pp. 395-400 (2004). (in Japanese)
245) K. Yasue, E. Ishii and A. Furusawa: "Period of formation of the marine terraces around the Sarobetsu anticline, northern Hokkaido", Abstr. 112th Annu. Meet. Geol. Soc. Jpn., Kyoto, Japan, 18-20 Sep. 2005, p. 326 (2005). (in Japanese)
246) K. Yasue, T. Niizato and R. Tsukuwi: "GPS observations and the base line analysis in northern Hokkaido", Program Abstr. Seismol. Soc. Jpn. Fall Meet., Sapporo, Japan, 19-21 Oct. 2005, p. 169 (2005). (in Japanese)
247) Japanese Geotechnical Society: "Japanese Standards for Geotechnical and Geoenvironmental Investigation Methods: Standards and Explanations" (2004). (in Japanese)
248) T. Kunimaru, R. Takeuchi and S. Seno: "Geochemical properties of groundwater in Horonobe Underground Research Laboratory Project, northern Hokkaido, Japan", Proc. Fall Meet. 2003 Jpn. Assoc. Groundwater Hydrol., Gifu, Japan, 23-25 Oct. 2003, pp. 36-39 (2003). (in Japanese)
249) T. Yamanoi, M. Sunami, H. Wakamatsu, H. Okazaki and T. Takatoh: "Near-Surface Hydrogeological Investigation in the Tono Area (Part 3)", JNC TJ7440 2001-005 (1996). (in Japanese with English abstract)
250) H.L. Penman: "Natural evaporation from open water, bare soil and grass", In: Mathematical and Physical Sciences, Proc. Royal Soc. London, Series A, 193, pp. 120-145 (1948).
251) S. Hattori: "Explanation on derivation process of equations to estimate evapotranspiration and problems on the application to forest stand", Bull. For. For. Prod. Res. Inst., 332, pp. 139-165 (1985). (in Japanese)
252) H. Nakabayashi, Y. Kodama, Y. Takeuchi, T. Ozeki and N. Ishikawa: "Characteristics of heat balance during the snowmelt season in Ny-Alesund, Spitsbergen Island", Mem. Natl. Inst. Polar Res. Spec. Issue, No. 51, pp. 255-266 (1996).
253) Y. Tsukamoto: "Forest Hydrology", First Edition, Buneido Publishing (1992). (in Japanese)
254) F.J. Pearson, D. Arcos, A. Bath, J.-Y. Boisson, A.M. Fernandez, H.-E. Gabler, E. Gaucher, A. Gautschi, L. Griffault, P. Hernan and H.N. Waber: "Mont Terri Project – Geochemistry of Water in the Opalinus Clay Formation at the Mont Terri Rock Laboratory", Rept. FOWG, Geol. Ser. No. 5 (2003).
255) T. Oyama, K. Nakata, T. Higashihara, T. Hasegawa, Y. Mahara and T. Kitsukawa: "Investigation of squeezed water chemistry from sedimentary rocks depending on the squeezing pressure", Proc. Fall Meet. 2005 Jpn. Assoc. Groundwater Hydrol., Aomori, Japan, 20-22 Oct. 2005, pp. 194-199 (2005). (in Japanese)
256) T. Kunimaru, H. Hirata and K. Ogawa: "The results of physic-chemical parameter monitoring and

groundwater chemistries sampled by pressure remained sampling system in-situ", Proc. Fall Meet. Jpn. 2005 Assoc. Groundwater Hydrol., Aomori, Japan, 20-22 Oct. 2005, pp. 118-121 (2005). (in Japanese)

257) S. Niunoya and H. Matsui: "Strength and deformation properties of Neogene diatomaceous rocks distributing in the salty underground water environment", Proc. 41st Jpn. Natl. Conf. Geotech. Eng., Kagoshima, Japan, 12-14 Jul. 2006, pp. 497-498 (2006). (in Japanese)

258) K. Yamada, S. Matsumura and Y. Nishigaki: "Prediction of long term strength of soft rock", Proc. 8th Japan Symp. Rock Mech., Tokyo, Japan, 29-30 Nov. 1990, pp. 339-344 (1990). (in Japanese with English abstract)

259) K. Hashiba, H. Matsui, T. Sato and Y. Seno: "Effect of stress history on creep behavior of rock", Proc. 35th Symp. Rock Mech., Tokyo, Japan, 12-13 Jan. 2006, pp. 313-318 (2006). (in Japanese with English abstract)

260) T. Ogawa and H. Matsui: "Properties of elastic wave velocities of Horonobe soft-sedimentary rock under confining pressure", Proc. 59th JSCE Annu. Conf., Toyota, Japan, 8-10 Sep. 2004, pp. 865-866 (2004). (in Japanese)

261) H. Kato and Y. Mizuta: "Development of wire-line hydraulic fracturing tool and its application to in-situ stress measurements", J. Min. Mater. Process. Inst. Jpn., 116, pp. 61-63 (2000). (in Japanese)

262) T. Yamamoto, H. Matsui: "Study on the measurement of initial stress on Neogene siliceous rock by acoustic emission method", Proc. 60th JSCE Annu. Conf., Tokyo, Japan, 7-9 Sep. 2005, pp. 675-676 (2005). (in Japanese)

263) M. Yamaguchi, Y. Fujii, K. Fukuda and H. Matsui: "Initial stress measurement of Horonobe siliceous rocks by DSCA method", Proc. MMIJ Fall Meet. 2006, Fukuoka, Japan, 11-13 Sep. 2006, pp. 55-56 (2006). (in Japanese)

264) Nuclear Energy Agency: "Disposal of Radioactive Waste: An Overview of the Principles Involved", OECD/NEA (1982).

265) International Atomic Energy Agency: "The Principles of Radioactive Waste Management", IAEA Safety Series No. 111-F, ISBN 92-0-103595-0 (1995).

266) International Atomic Energy Agency: "Monitoring of Geological Repositories for High Level Radioactive Waste", IAEA-TECDOC-1208, ISSN 1011–4289 (2001).

267) Atomic Energy Commission of Japan: "Guidelines on Research and Development Relating to Geological Disposal of High-level Radioactive Waste in Japan", Advisory Committee on Nuclear Fuel Backend Policy (1997). (in Japanese)

268) M. Kumazawa, T. Kunitomo, Y. Yokoyama, T. Nakajima and K. Tsuruga: "ACROSS: Theoretical and technical developments and prospect to future applications", JNC Tech. Rev., No. 9, pp. 115-129 (2000). (in Japanese with English abstract)

269) H. Ohara, R. Tsukui, T. Kunitomo, T. Nakajima, T. Niizato, K. Aoki, N. Shigeta and M. Kumazawa: "Horonobe Underground Research Laboratory Project – Outline of development of ACROSS", Abstr. 2005 Jpn. Earth Planet. Sci. Joint Meet., Chiba, Japan, 22-26 May 2005, S080-P001 (2005).

270) H. Ohara, R. Tsukui, T. Kunitomo, T. Nakajima, T. Niizato, K. Aoki and M. Kumazawa: "The Horonobe Underground Research Laboratory Project – Outline and progress of development of remote monitoring system (ACROSS)", Abstr. Jpn. Geosci. Union Meet. 2006, Chiba, Japan, 14-18 May 2006, O106-P009 (2006).

271) R. Tsukui, T. Niizato, K. Aoki, and T. Fukushima: "Developing remote monitoring system using ACROSS in Horonobe Underground Research Laboratory", Proc. 1st Int. Workshop 'Active Monitoring in the Solid Earth Geophysics (IWAM04)', Mizunami, Japan, 30 Jun. – 2 Jul. 2004,

S1-P02 (2004).

272) Japan Nuclear Cycle Development Institute: “Horonobe Underground Research Laboratory Project Investigation Report for the 2002 Fiscal Year”, JNC TN5400 2003-001 (2003). (in Japanese)

273) T. Kunitomo and M. Kumazawa: “Active monitoring of the earth’s structure by the seismic ACROSS – Transmitting and receiving technologies of the seismic ACROSS”, Chikyu Monthly Symp., No. 47, pp. 44-52 (2004). (in Japanese)

274) S. Niunoya, Y. Mito, K. Aoki and H. Matsui: “Basic study on the measurements of AE behavior in Neogene siliceous rocks”, Proc. Tunnel Eng., JSCE, 15, pp. 411-416 (2005). (in Japanese)

5. Development of engineering technologies for the deep geological environment

One of the key issues of the Horonobe URL project is the development of engineering techniques for the deep geological environment. The aims of this include developing, for soft sedimentary rock, advanced systematic techniques for planning the design and construction of underground facilities and to gain experience with the actual design and construction of the underground facilities, based on information on the geological environment obtained from surface-based investigations, and demonstrating the safety of construction and operation of the underground facilities. The experience accumulated in the design, construction and maintenance of the underground facilities in the geological environment in situ will be used as input for investigations using the underground facilities subsequent to the detailed investigation stage in the actual disposal project.

This chapter describes the specifications and layout of the underground facilities developed in Phase I of the Horonobe URL project and the procedure for planning the design and construction of the underground facilities in sedimentary rock, as well as the results of the development work described above. The results of the assessment of engineering techniques for the EBS and disposal facility are described in a separate volume on “Geological Disposal Research”.

5.1 Background of URL construction

5.1.1 Major requirements for the URL

In the Horonobe URL project, the depth of the tunnels was specified to be around 500 m (see Chapter 3 for details), considering the assumptions made in the H12 report[1)] for disposal in soft rocks. The sedimentary rock of interest has low rock strength and high ground pressure and contains flammable gases (mainly CH_4), as described in Chapters 3 and 4. For the construction of underground facilities under these conditions, a tunnel stability analysis and disaster prevention measures are required as part of the design and construction project to ensure safety during construction and operation.

5.1.2 Topography and characteristics of the geological environment at the URL site

At the URL site selected in the Hokushin district, around 3.5 km northeast of the central Horonobe, surface preparations started in 2003 and were completed in 2005. The area purchased by JAEA was approximately 191,000 m^2 (19.1 ha). The total area for construction of the surface facilities, including the administration building, and the areas for the underground facilities was approximately 68,000 m^2 (6.8 ha).

The selected URL site is located in a basin with gently dipping formations at the Soya Hill, with smooth undulation influenced by periglacial process, where the Koetoi Formation, composed of diatomaceous mudstone, is overlain by Quaternary periglacial brecciated sediments. The altitude of the surrounding hills is about 100 m elevation, while that of the URL site is about 60 m elevation.

The soft sedimentary rocks at the URL site (the Wakkanai and Koetoi Formations) have high porosity, low unit mass, low strength, low permeability, low swelling properties because of the low content of swelling clay minerals and medium to high rock slake resistance (Table 5.1.2-1). These characteristics of the geological environment are basically within the range of properties specified in the dataset for soft rock for the assessment of the geological disposal system in the H12 report[1)], except that the in situ stress in the horizontal plane is anisotropic. Environmental conditions unique to the URL area were also identified, including the presence of saline groundwater, natural gas and toxic heavy metals contained in the rock.

Table 5.1.2-1 Petrophysical properties and representative environmental conditions

		Wakkanai Formation	Koetoi Formation
Porosity	[%]	40–50	60–65
Unit weight	[kN m^{-3}]	15–19	14–16
Uniaxial compressive strength	[MPa]	5–30	3–5
Hydraulic conductivity	[m s^{-1}]	10^{-11}–10^{-6}	10^{-9}–10^{-8}
Swelling factor	[%]	<0.03	<0.04
Durability factor (Id_2)	[%]	>95	>90
Dominant dissolved gas		CH_4	CH_4
Groundwater		Saline	Saline

5.2 Planning of URL construction

5.2.1 Basic strategy

In Phase I, the specifications and layout of the tunnels were developed based on information on the geological environment obtained in the surface-based investigations, the investigation programme planned for the underground facilities and currently available construction techniques. The design and construction plan was formulated based on considerations of construction measures for ensuring safety and of maintenance of an appropriate in-tunnel environment in view of the various phenomena that may occur in the deep subsurface environment during the construction and operation of the facilities. When formulating the plan, emphasis was placed on efficient and cost-effective designs, subject to the major premise that the underground facilities are safely constructed and maintained.

When comparing the preliminary design and construction plan for the underground facilities in the Horonobe URL project with the actual repository design concept outlined in the H12 report[1)], it should be borne in mind that constraints on the actual operation of the repository and restrictions on the temperature of the waste and buffer material will be determined based on future investigations and have not been factored into the URL project. Both plans have in common that tunnel stability is taken into account in the tunnel design. This programme considers constraints associated with the implementation of the project, such as the construction period and cost, as well as requirements ensuring safety and environmental preservation.

5.2.2 Conceptual design and layout of the URL

The shafts will be sunk to a depth of about 500 m and horizontal drifts (circular-profile experiment drifts and connecting drifts) will be located at a several depths along the length of the shafts. The layout of tunnels in the underground facilities, drawn at the end of Phase I, is shown in Figure 5.2.2-1.

(1) Access

A comparison was made of two systems, i.e. a shaft and a spiral tunnel, in terms of volume of construction work, area requirements, the investigation programme, tour group facilities, safety of the environment, construction period, cost etc. The shaft system, which proved to be better in terms of construction period and cost, was eventually selected.

(2) Cross-section of shafts and horizontal drifts

The shape and dimensions of the cross-section of the shafts were determined based on full-face sinking, taking into account space occupied by temporary construction installations such as kibbles, lifts and air ducts, transport infrastructure for investigation materials and apparatus for use in the horizontal drifts, transport of construction machinery for excavation of the horizontal drifts and past experience in shaft and tunnel excavation. Considering the minimum cross-section that can accommodate the materials and equipment mentioned above, the cross-sections of the East, West and Ventilation Shafts were determined to have a circular cross-section with diameters of 6.5 m, 6.5 m and 4.5 m respectively (Figure 5.2.2-1).

The cross-section of the horizontal drifts was designed to be a horseshoe shape with no corners; this has mechanical advantages considering the low rock strength at the site and workability. The standard cross-section width was set at 4 m in order to provide a space in which borehole investigations can be conducted at given locations in the drift (work space with (w) 3 m × (h) 3 m; Figure 5.2.2-1). For areas where large-scale borehole investigations are planned, the cross-section was expanded to a width of 7 m.

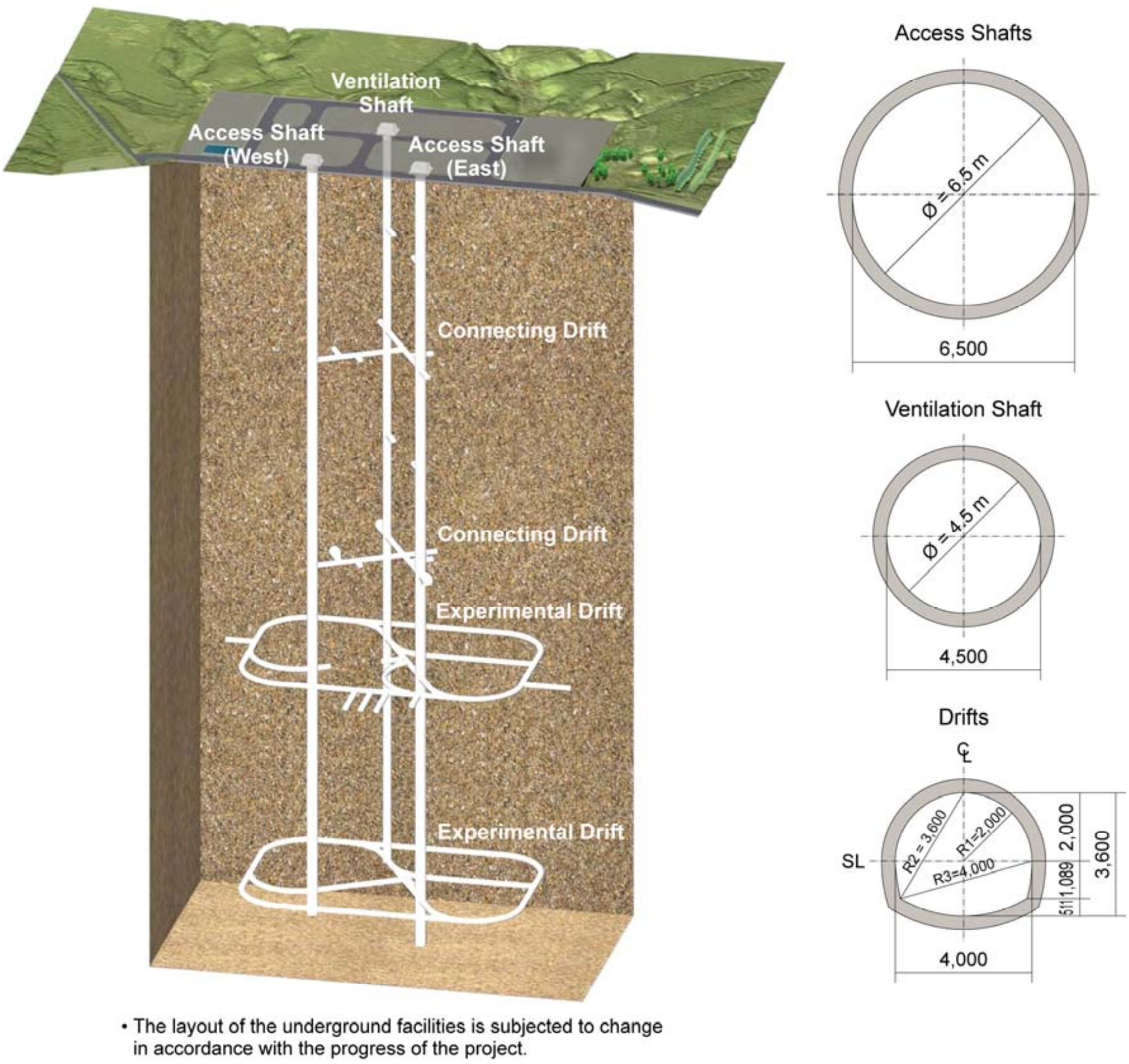

Figure 5.2.2-1 Layout and cross-sections of shafts and drifts

(3) Layout of shafts

Based on fundamental concepts for disaster prevention in underground facilities, fire was selected as the accident most likely to cause a serious disaster. Given the potential for CH_4 blowout, preventing fire in the tunnels was identified as the most important measure against disaster in the underground facilities in the Horonobe URL project. The basic strategy was to develop a disaster prevention system that is capable of securing a safe zone by means of ventilation control in the event that an accident such as fire occurs at any location, ensuring that personnel in the tunnels are able to evacuate safely to the ground surface. Based on this concept, an evaluation was made of evacuation routes based on the rough ventilation network diagram in the case of fire. As a result, two shafts alone were found to be inadequate for implementing the basic disaster prevention concept (e.g. in the case of fire occurring in a downcast shaft). Provision of three shafts, including two downcast shafts and one upcast shaft was therefore decided. The centre to centre distance between the adjacent shafts was determined to be 70 m to ensure that operations can be carried out safely and effectively, including the installation of temporary surface facilities such as the shaft tower, transport of material and machinery and removal of excavated rock (muck). A large fan will be installed in the Ventilation Shaft to provide the required amount of air in the tunnels at the time of ventilation. Considering safety in the event that a gas explosion occurs (measures against fan breakage), the fans will be installed in dedicated tunnels branching off from the Ventilation Shaft.

(4) Layout of horizontal drifts

The depths for constructing the circular experiment drifts, where major investigations will be conducted, will be decided based on the results of borehole investigations conducted in the vicinity of the URL site, considering the requirements of the Phase II investigation programme and information obtained during the construction of the underground facilities. Several connecting drifts will be also constructed at intermediate to provide space for preliminary testing and to improve working conditions during construction.

The circular experiment drifts were designed as horizontal drifts with a minimum length to allow them to encircle the shaft, while maintaining a distance between drifts which ensures that there is no effect owing to excavation of adjacent drifts (the centre to centre distance between adjacent drifts was three times greater than the diameter of the drifts) and a minimum radius that ensures workability (machine excavation and rail construction method) during the construction of the underground facilities. For experiments on the EDZ and gas migration, drifts extending outwards from the circular drifts, turnout area and pump stations were also installed. Considering mechanical stability requirements, the longitudinal direction of the circular drifts was aligned with the direction of the maximum principal stress (E-W direction) determined by the hydraulic fracturing tests during the borehole investigations as described in Subsection 4.4.3. The connecting drifts that connect the shafts have a turnout area, drilling station and pump station as necessary.

5.2.3 URL construction plan

(1) Excavation of the underground facilities

Excavation of the Ventilation and East Shafts started in March and August 2006 respectively. Excavation of the West Shaft is scheduled to start in 2009. Investigations scheduled for the Phase II programme will be conducted concurrently with shaft sinking with aims of checking the reliability of the results obtained in Phase I and conducting long-term in situ tests, monitoring of excavation damage around the underground facilities and investigation of excavation damage at the shaft.

Since tunnel ventilation is required at an early stage, considerations of cost-effectiveness indicate that the Ventilation Shaft should first be sunk to the final depth, while, at the depth where horizontal drifts are planned, excavating only the minimum length required for the excavation of subsequent horizontal drift. Meanwhile, the East Shaft will be sunk to the depth of a horizontal drift, where a connecting drift to the Ventilation Shaft will be excavated. The procedure will be repeated for each of the connecting drifts. The West Shaft will be sunk to the final depth while excavating the connecting drifts that connect the West Shaft with the already excavated horizontal drifts.

Tunnel ventilation is planned to start after the Ventilation Shaft has been sunk to the final depth and the horizontal drift extending from the East Shaft is connected with the Ventilation Shaft.

(2) Excavation methods and support measures

Shaft sinking will be conducted using the full-face excavation method. Mechanical methods are used in order to restrict the effects on the surrounding rock mass, since the rock at the predetermined excavation depth of 500 m has a uniaxial compressive strength of less than 30 MPa (see also Subsection 4.4.3). However, the East Shaft will be excavated by blasting in order to identify the difference in the EDZ generated by different types of excavation. The standard method used for shaft sinking was the irregular short-step method in which excavation of 1 m is conducted twice before emplacing the concrete lining. Figure 5.2.3-1 shows a diagram of the shaft sinking procedure.

Excavation of the horizontal drifts will basically be by mechanical excavation using part-face tunnelling machines and breakers. Excavation of the circular drifts will be based on the rail method which is advantageous in terms of ventilation, movement of excavated rock and preventing explosions. Excavated rock will be removed by a muck car to the intersection with the shaft, where it will be transferred to a kibble and then taken out of the tunnel. Considering that the rock competence factor is lower than two in most of the areas in the drifts, using shotcrete at an early stage of excavation was selected as the standard procedure for tunnel support along the entire section of the drift in order to prevent deformation. Figure 5.2.3-2 shows a diagram of the excavation procedure of the horizontal drifts.

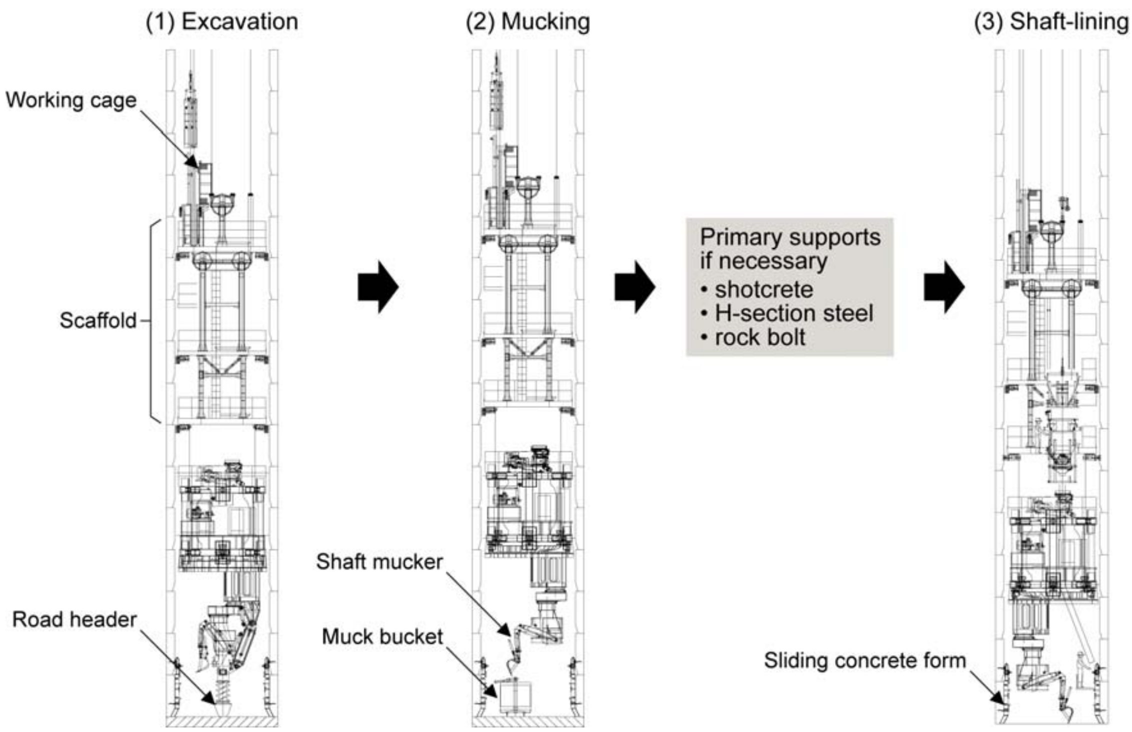

Figure 5.2.3-1 Construction plan for shafts (mechanical method)

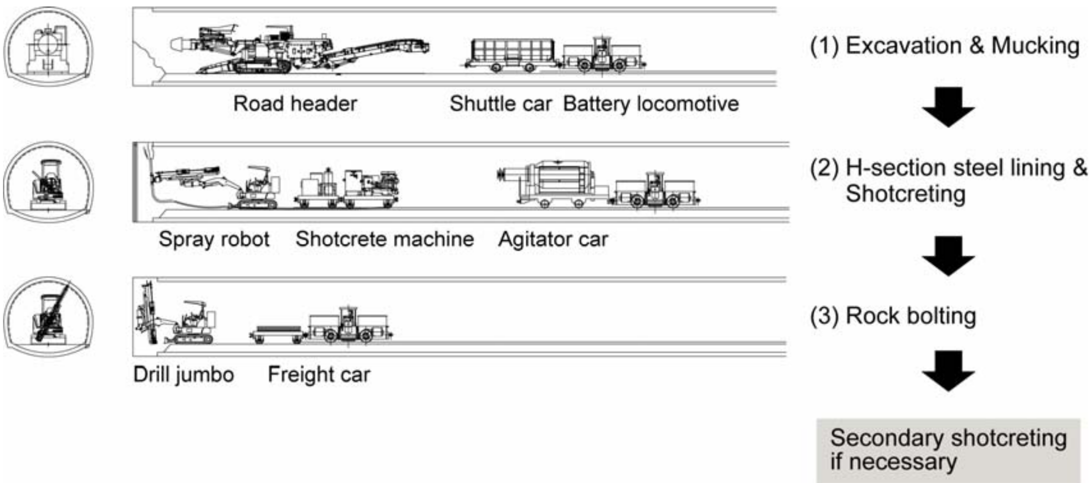

Figure 5.2.3-2 Construction plan for drifts (using road header)

(3) Excavated rock (muck) processing

Cores from boreholes HDB-3 and HDB-6, located near the underground facilities, were checked for hazardous materials using the criteria defined in the Soil Contamination Countermeasures Law (Law no.53 of 2002; referred to as the Soil Law in this chapter).

The excavated rock from the underground facilities will not be subject to provisions of the Soil Law because the specified toxic substances contained in the excavated rock are derived from natural sources. However, in view of the potential impact on the surrounding environment when excavated material is used, for example, as an embankment and as a result of consultation with relevant authorities, measures compliant with the Soil Law will be taken. Evaluating the contamination level of the soil based on the content and dissolution of specified toxic substances, the Soil Law sets standards for implementing measures such as removal of contaminants, depending on the type and concentration of the toxic substance in question. With regard to dissolution in particular, the primary and the secondary dissolution criteria are stipulated and appropriate countermeasures are proposed.

Laboratory tests on content and dissolution indicate that there are no toxic substances with a content that exceeds the specified criteria. However, the dissolution of specified toxic substances such as As, B, Cd, F and Se was found to exceed the primary criteria. The dissolution of these elements, however, does not exceed the secondary criteria. A structure conforming to the seepage control requirements specified in the Soil Law will therefore be used to store the excavated rock generated by the construction of the underground facilities.

The muck storage location is planned to be about 700 m distant from the URL site. Its structure is an embankment on the downstream side to be filled on the inside with excavated material. Double liner sheets will be used for sealing at the bottom and non-woven fabric is sandwiched between the sheets for their protection. After the storage facility is filled with muck, it will be covered with the liner sheets and then with soil to prevent infiltration of rain from through the top surface, thus preventing seepage of toxic substances to off-site locations.

Analyses of the content and dissolution of toxic substances in the excavated rock and water chemistry surveys of seepage water from the stored rock will be carried out on a regular basis. Monitoring holes will also be drilled around the storage site for continuous monitoring of potential leakage of toxic substances.

(4) Drainage water treatment programme

Saline groundwater is found deep subsurface where the underground facilities will be constructed. Geophysical logging covering depths from 50 to 590 m in boreholes HDB-3 and HDB-6 indicates that the Cl concentrations in the groundwater are in the range of 2,102–14,071 mg l^{-1}. The Cl concentrations in the drainage water from the underground facilities were calculated based on the relationship between the depth profile of Cl concentrations obtained by logging and the seepage at each depth and dilution by the drainage water from construction to be maximum of 4,600 mg l^{-1} (approximately 1/4 that of seawater), which may be higher than that of river water around the facilities. Although no specific guidelines regarding Cl concentrations in drainage water are contained in the Water Pollution Control Law (Law no.33 of 2005; referred to as the Water Law in this chapter), which regulates the waste water chemistry from industrial fields released to public water areas, an evaluation was made of the waste water processing method considering the potential impact on the surrounding environment.

There are two approaches for diluting Cl: removal of Cl and mixing with freshwater. The latter was selected since the former involved high operating costs and problems of residual salt. Since a large volume of water is required to sufficiently dilute the drainage water from the underground facilities, drainage will be through a pipeline into the Teshio River located about 8 km south of the underground facilities; this will avoid increases in river flow rate and changes in the Cl concentrations. The result of an investigation of the flow regime indicates that the Teshio River, to which drainage will be discharged, is sufficiently wide and has a sufficiently high flow rate to ensure dilution. The brackish environment around the discharge point, where seawater runs in to form a poorly mixed saline wedge, will also minimise the impact on the surrounding environment.

The groundwater chemistry derived from the analysis conducted in advance revealed that specific toxic substances (B and ammoniacal-N) are already present in amounts that exceed the drainage criteria stipulated by the Water Law. All of these specified toxic substances in the groundwater are of natural origin. The drainage water will be treated to remove B and ammoniacal-N before being discharged into the river to ensure that the concentrations will not exceed the criteria specified in the Water Law and criteria specified on the basis of consultation with relevant organisations. Water chemistry of drainage water from the underground facilities and drainage water after processing will thus be monitored and checked to make sure levels are in line with the Water Law and its relevant regulations. The chemistry of the Teshio River water will be monitored in accordance with the measurement items, survey points and survey frequency decided on the basis of consultation with responsible organisations.

5.2.4 Tunnel stability analysis

A tunnel stability analysis was carried out with a view to designing the tunnel supports prior to the excavation of the underground facilities; the analysis conditions were set based on rock mechanical investigation results from boreholes HDB-3 and HDB-6 up to 2003[2)] (see Subsection 4.4.3).

(1) Classification of rock mass and specifying the rock parameters for analysis

It is clear that deformation of the rocks around the underground facilities is likely to result in crack formation[2)], although classified as soft rock, by the borehole loading test conducted in the vicinity (Figure 5.2.4-1). The results of core logging also indicate that fractures caused by drying or changes in external loading (hairline cracks) are distributed widely in the rock. An analysis of shear planes in the specimens used for the uniaxial compressive strength tests on cores revealed that numerous shear planes were generated along the hairline cracks observed prior to the tests[2)] (Figure 5.2.4-2). The rock strength and elasticity coefficient of cores with hairline cracks are lower than those of the cores without cracks (Figure 5.2.4-3).

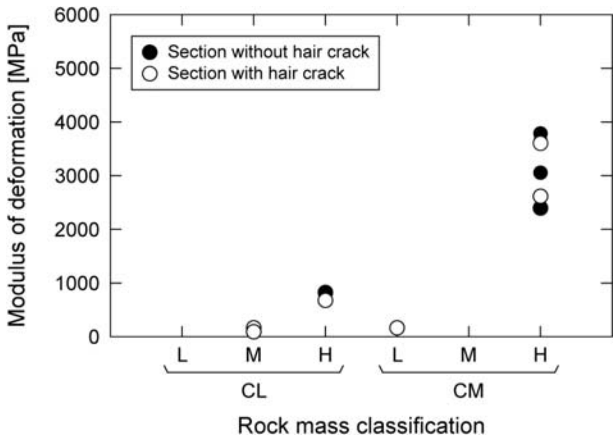

Figure 5.2.4-1 Results of borehole loading test
Rock mass classification presented in Table 5.2.4-1

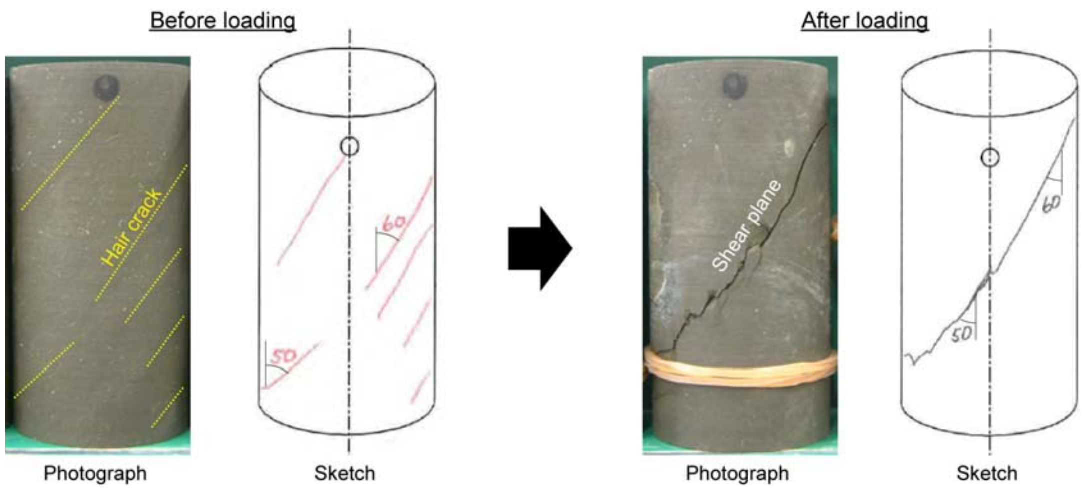

Figure 5.2.4-2 Generation of shear plane by unconfined compression

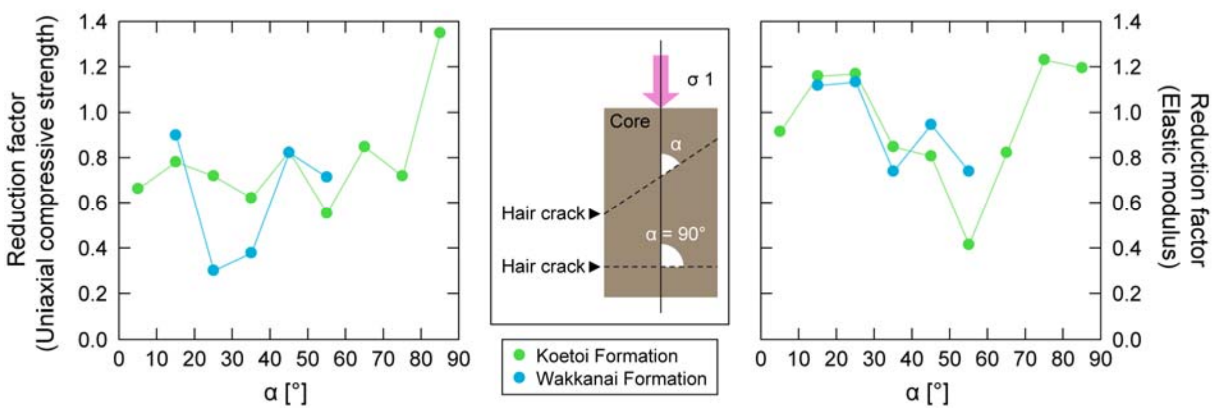

Figure 5.2.4-3 Effects of hairline cracks on mechanical properties

Based on these findings, when setting the rock parameters to be used in predicting behaviour at the time of tunnel excavation, rocks have to be considered in terms of a possible reduction in strength and elasticity coefficient owing to hairline cracks; they also have to be evaluated as a jointed rock mass considering the influence of fractures. The rock mass classification to be used in the tunnel stability analysis for the underground facilities is based on the results of core logging in accordance with the rock mass classification illustrated in Table 5.2.4-1, focussing on hardness, fracturing and hairline cracks that are considered to have a significant influence on mechanical properties (strength and deformation characteristics). In the rock mass classification, it was determined whether the percentage of sections with cracks in a 10 m interval of core exceeds 10%. If so, the interval is assumed to be affected by the cracks.

The mechanical properties for analysis were defined in the following order:

a) initially assume such properties of rock without fractures or hairline cracks as a reference;
b) specify reduction factors for each of the rock properties derived from the influence of fractures or hairline cracks based on the results of tests and in situ experiments;
c) calculate the properties for each rock mass classification by multiplying the reference value by the reduction factors (Table 5.2.4-2).

Here, when no fractures or hairline cracks were present, the average values for the Wakkanai and Koetoi Formations obtained from triaxial compression tests (CD test) using samples without fractures or cracks were used as the strength values. When setting the reduction factor owing to the influence of fractures, the ratio of the deformation modulus with and without fractures obtained from borehole loading tests (Figure 5.2.4-1) was used as the reduction factor for the elasticity coefficient for each rock classification. The reduction factor for rock strength was assumed to be identical to that of the elasticity coefficient. To obtain the strength value, cohesion was multiplied by the reduction factor, while the angle of internal friction remained fixed, since the effect of the cohesion is generally dominant in mudstone.

The reduction factor owing to the influence of hairline cracks was set as follows:

- The average uniaxial compressive strength and elasticity modulus for each rock mass classification was set to one based on the results of uniaxial compression tests using samples with no fractures or cracks. The generation frequency of shear planes along a hairline cracks was then defined as a ratio of the average value of each intersection angle. Thus, the reduction factor for rock mass classification with low fracture frequency (H class) was determined for each lithofacies.
- Considering the anisotropy of reduction factors observed in the Wakkanai Formation with respect to the intersection angle between the loading direction and hairline cracks (Figure 5.2.4-2), local stress conditions around the tunnels at the time of excavation were considered to be complex. However, since quantitative modelling of these conditions was not possible, the variations in strength owing to differences in the loading directions were all assumed to be the minimum reduction factor of 0.3, thus setting strength as an isotropic property.
- It should be noted that the reduction factor for rock mass with a higher fracture frequency (L class) was set to 1.0, while that for rock mass with medium fracture frequency (M class) was set at the mean value between the H and L classes because the influence of hairline cracks varies depending on the frequency of existing fractures.

Table 5.2.4-1 Rock mass classification from core

<table>
<tr><th>Formation</th><th>Class</th><th>Crack*</th><th>Hair crack**</th><th>Characteristics</th></tr>
<tr><td rowspan="4">Koetoi Formation</td><td>D</td><td></td><td>–</td><td>Soft; scratched to >2 mm depth by a utility knife; breccias, debris and clayey materials</td></tr>
<tr><td rowspan="3">CL</td><td>L</td><td>–</td><td>Scratched about to 1 mm depth by a utility knife; breccias and debris</td></tr>
<tr><td>M</td><td>+-</td><td>Scratched about to 1 mm depth by a utility knife; <10 cm long columnar cores</td></tr>
<tr><td>H</td><td>+-</td><td>Scratched about to 1 mm depth by a utility knife; >10 cm long core sticks</td></tr>
<tr><td rowspan="3">Wakkanai Formation</td><td rowspan="3">CM</td><td>L</td><td>–</td><td>Scratched only on the surface by a utility knife; breccias and debris</td></tr>
<tr><td>M</td><td>+-</td><td>Scratched only on the surface by a utility knife; <10 cm long columnar cores</td></tr>
<tr><td>H</td><td>+-</td><td>Scratched only on the surface by a utility knife; >10 cm long core sticks</td></tr>
</table>

* Crack: Separated plane identified by core logging

** Hair crack: Latent crack in columnar core, becoming visible when dried or externally loaded; exist (+) or not exist (-)

Table 5.2.4-2 Mechanical properties and reduction factor of rock mass

<table>
<tr><th rowspan="2">Formation</th><th rowspan="2">Classification (+: Hair crack)</th><th rowspan="2">Unit weight γ [kN m⁻³]</th><th rowspan="2">Poisson's ratio ν</th><th rowspan="2">Elastic modulus E [MPa]</th><th rowspan="2">Cohesion c [MPa]</th><th rowspan="2">Friction angle ø [°]</th><th colspan="2">Reduction factor</th></tr>
<tr><th>E</th><th>c</th></tr>
<tr><td rowspan="7">Koetoi Formation</td><td>D</td><td>14.8</td><td>0.300</td><td>8.3</td><td>0.1</td><td>24.1</td><td>–</td><td>–</td></tr>
<tr><td>CL-L</td><td rowspan="6">15.1</td><td rowspan="6">0.164</td><td>300</td><td>0.5</td><td rowspan="6">15</td><td>0.23</td><td>–</td></tr>
<tr><td>CL-L +</td><td>300</td><td>0.5</td><td>1.00</td><td>1.00</td></tr>
<tr><td>CL-M</td><td>500</td><td>0.8</td><td>0.38</td><td>–</td></tr>
<tr><td>CL-M +</td><td>450</td><td>0.6</td><td>0.90</td><td>0.80</td></tr>
<tr><td>CL-H</td><td>1,300</td><td>2.2</td><td>1.00</td><td>–</td></tr>
<tr><td>CL-H +</td><td>1,040</td><td>1.5</td><td>0.80</td><td>0.70</td></tr>
<tr><td rowspan="6">Wakkanai Formation</td><td>CM-L</td><td rowspan="6">18.5</td><td rowspan="6">0.186</td><td>500</td><td>1.0</td><td rowspan="6">25</td><td>0.20</td><td>–</td></tr>
<tr><td>CM-L +</td><td>500</td><td>1.0</td><td>1.00</td><td>1.00</td></tr>
<tr><td>CM-M</td><td>1,500</td><td>3.1</td><td>0.60</td><td>–</td></tr>
<tr><td>CM-M +</td><td>1,350</td><td>1.6</td><td>0.90</td><td>0.50</td></tr>
<tr><td>CM-H</td><td>2,500</td><td>5.2</td><td>1.00</td><td>–</td></tr>
<tr><td>CM-H +</td><td>2,000</td><td>1.6</td><td>0.80</td><td>0.30</td></tr>
</table>

The initial host rock pressures used for the predictive analysis were determined as follows:

- The pressure in the vertical direction was assumed to be equivalent to the overburden pressure, while the pressure in the horizontal plane was obtained by normalising the results of hydraulic fracturing tests conducted in a nearby borehole (10 depths, see also Subsection 4.4.3) with the overburden pressure.
- The average of the resulting normalised values was obtained for each of the principal stresses. The maximum principal stress in the horizontal plane, the minimum principal stress in the horizontal plane and the vertical principal stress were set to 1.3, 0.9 and 1.0 respectively.
- The unit weight and Poisson's ratio were set to the averages of the results obtained from each lithofacies in the laboratory tests on core samples.

(2) Properties of support measures

The long-term allowable compressive stress of lining concrete and shotcrete was determined in compliance with the standards for non-reinforced concrete specified by the Japan Society of Civil Engineers (JSCE)[3)], as shown in Table 5.2.4-3. The short-term allowable compressive stress of primary shotcrete support was determined in accordance with the construction guidelines specified by the Japan Railway Construction Corporation (JRCC)[4].

Since the short-step method is a standard technique for lining the shaft, the properties of early-age concrete immediately after placement should be assumed. In this evaluation, the material properties for the predictive analysis were obtained by calculating the age-dependent strength and Young's modulus taking the construction cycle time into account[5]. The Young's modulus of shotcrete was set based on the JRCC guideline[4] and on existing literature[6], as presented in Table 5.2.4-4. Two types of settings were specified for steel supports, viz. normal and high (high-tensile steel) standards. The allowable stress for the steel supports for the predictive analysis was determined in compliance with the standards for steels defined by the JSCE [7] (Table 5.2.4-3) and Young's modulus was set to 210 GPa.

Table 5.2.4-3 Mechanical properties of support materials

Material		Design strength f'_{ck} [MPa]	Allowable stress [MPa]	
			Short-term	Long-term
Concrete (Compressive)	Lining concrete	24	–	6.0 ($f'_{ck}/4$)
		40	–	10.0 ($f'_{ck}/4$)
		60	–	15.0 ($f'_{ck}/4$)
	Shotcrete	18	13.8 ($f'_{ck}/1.3$)	4.5 ($f'_{ck}/4$)
		36	27.7 ($f'_{ck}/1.3$)	9.0 ($f'_{ck}/4$)
Steel (Tensile)	SS-400 (Standard)	–	400	160
	HT-590 (High tension)	–	590	236

Table 5.2.4-4 Mechanical properties of early-age concrete

	Design strength f'_{ck} [MPa]	Young's modulus [MPa]			Compressive strength [MPa]		
		V-Shaft	E-Shaft	W-Shaft	V-Shaft	E-Shaft	W-Shaft
Lining concrete* (For shafts)	24	8,700	8,300	8,800	6.4	5.8	6.6
		9,600	9,100	9,800	7.8	7.0	8.2
	40	11,200	10,600	11,400	10.7	9.6	11.1
		12,400	11,700	12,700	13.0	11.7	13.6
	60	11,800	11,100	12,000	11.8	10.5	12.2
		13,100	12,400	13,500	14.6	13.0	15.4
Shotcrete (For shafts and drifts)	18	3,400			–		
	36	6,000			–		

*Upper values for standard support; Lower values for multiple-layer support

(3) Methods and models for predictive analysis of behaviour

A 2D FEM analysis with an elastic-plastic model was used for the predictive analysis in the tunnel and the Mohr-Coulomb failure criterion applied. As the cross-sections of the tunnels are symmetrical, 1/4 of the shaft cross-section and 1/2 of the horizontal drift cross-section were used for modelling. The analysis domain was set at five times larger than the excavation diameter. Rock and concrete were modelled by using the plane strain element. The steel supports were converted into a number of supports per unit length. The total strength of the equivalent number of supports was then modelled with the use of the beam element. It should be noted that concrete was treated as an elastic body.

In order to consider the 3D rock stress conditions that vary with the advance of the working face, a sequential excavation analysis was conducted, in which the effect of stress release (owing to excavation) is applied in a stepwise manner in accordance with the actual excavation procedure. The occurrence rate of deformations of the tunnel wall as a function of distance from the working face was calculated based on the result of a 3D elastic FEM analysis (axisymmetrical model) conducted for a case where a circular tunnel is excavated without support. This occurrence rate was used to determine the stress release rate owing to excavation in accordance with the advance of the working face. It should be noted that the stress release rate immediately after excavation in the shaft was set at 70% based on the above.

(4) Support design

Focussing on the plastic zone calculated in the predictive behaviour analysis, the supports were designed such that the thickness of the plastic zone would remain within the range of the length of a standard rock bolt. A 2D FEM analysis using an elastic-plastic model as the constitutive equation was adopted for the predictive analysis and the Mohr-Coulomb failure criterion applied. The stress of the support members was checked based on the allowable stress design. When designing supports for the shafts and horizontal drifts, a tentative support system was drawn up based on the past construction practices in accordance with the above rock mass classification and the stress exerted on the support installations was then calculated by an analysis taking into account the in situ stress at each depth and the rock properties according to the rock mass classification. When the calculated stress exceeds the allowable limit, the grade of the support measure or the construction method was reviewed.

As described above, construction of the underground facilities in the Horonobe URL project often involves construction under low competence factor conditions and the load on the support installations therefore significantly increases. The support (concrete lining) used in standard short-step methods would require an extremely thick lining to ensure safety in terms of excavation and maintenance of the tunnels. A design based on double-layer support structure that conforms to the NATM design concept was thus adopted[2).]

In designing the double-layer support structure for the shafts, the specifications of the primary support, consisting mainly of shotcrete, were determined first such that stress generated immediately after the excavation of the working face becomes stable with respect to the short-term allowable stress and the integrity of the secondary support to be emplaced after installation of the primary support was then checked. The load to be borne by the secondary support was determined as follows:

- calculate the equivalent stress release rate based on the difference in tunnel face deformation without support;
- calculate the stress placed on the primary support;
- allocate the value obtained by subtracting the long-term allowable stress from the stress on the primary support to the secondary support.

The specifications of the support members were determined such that the stress imposed on the double-layer support structure (primary + secondary support) as a whole remains within the long-term allowable stress. In other words, tunnel stability shortly after excavation was ensured by installing primary support immediately after the excavation of the working face and some stress was then allocated to the secondary support (concrete lining), making full use of the strength of the primary support and the rocks. This results in an efficient design which reduces the required thickness of concrete lining.

The shafts and horizontal drifts designed based on the concept described above used the double-layer support structure over about 50% of the total length of the experiment drifts. Figure 5.2.4-4 shows an example of the support system for the sections with the double-layer support structure. The distribution of plastic zones calculated by the predictive analysis is shown in Figure 5.2.4-5. The result of the analysis indicates that the thickness of the plastic zone associated with tunnel excavation is up to about 3.4 m in the shafts and about 1.8 m in the horizontal drifts.

For typical connecting/intersecting points between the tunnels, a 3D FEM analysis taking the tunnel shape into account was conducted and the resulting maximum shear strain on the tunnel wall was compared with the results of the 2D FEM analysis carried out for the standard parts to calculate the influence coefficient. The supports were designed based on values obtained by multiplying the stress on the support member in the standard areas by the influence coefficient.

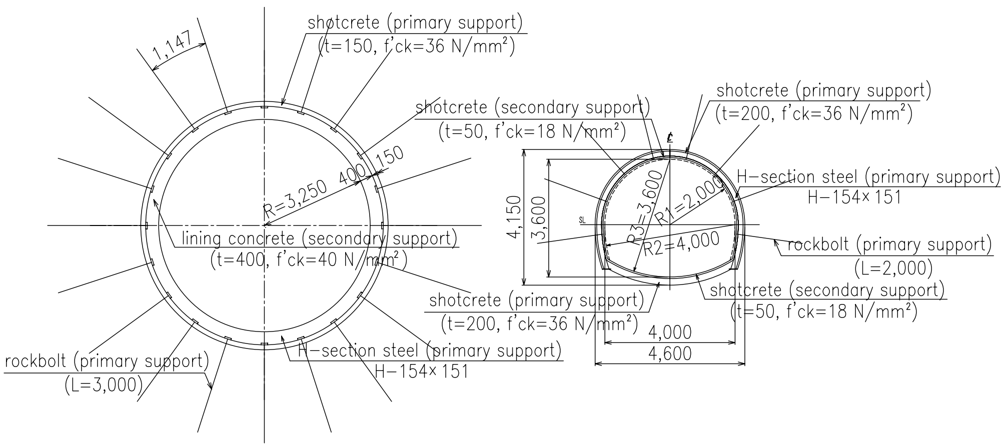

Figure 5.2.4-4 Typical support system (Multiple-layer support)

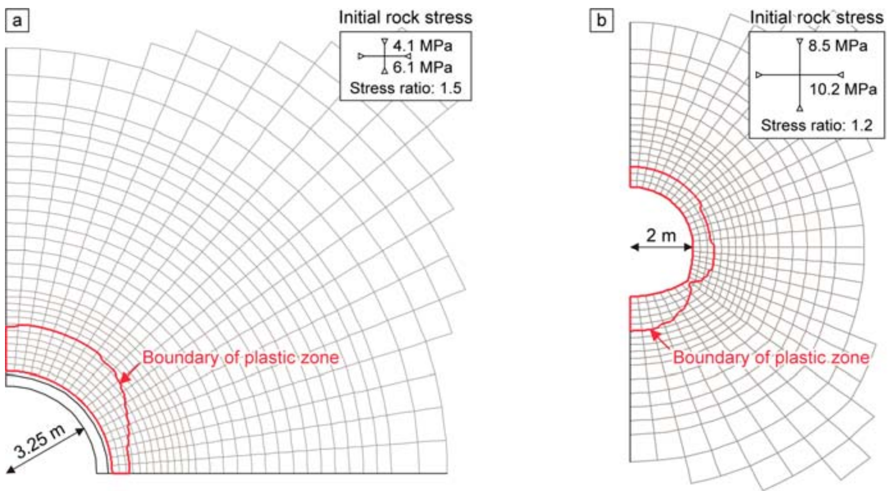

Figure 5.2.4-5 Plastic zone by numerical analysis (FEM)

a: Access Shaft (Depth: 340 m), *b*: Drift (Depth: 400 m)

(5) Checking seismic stability

The underground facilities in the Horonobe URL project are located in soft rock with relatively low strength and a high overburden pressure (thickness around 500 m) and the facilities consist of complex and partly unique structures including shafts. Some typical structures were therefore checked for their stability against seismic events such as earthquakes[8].

1) Analytical conditions and models

Non-reinforced concrete, which is the main support material used in the underground facilities, cannot be expected to be ductile like reinforced concrete and hence it would undergo brittle destruction. The point when compression failure occurs was thus defined as the final state in the analysis. The seismic resistance of the structures was analysed under the assumption that, when the stress imposed on the concrete is lower than the ultimate strength, the underground facilities would withstand earthquake motion. The seismic ground motion level applied in the analysis was Level 2 (ground motion with extremely low probability which occurs several times during the lifetime of the structure), which is relatively large seismic force[9)].

The maximum acceleration for the design ground motion was set to 230 gal, which is the maximum acceleration for the deep subsurface of the Horonobe area determined by examining records of historical earthquakes in the northwest region of Hokkaido[10)] and estimates based on the results of investigations of active faults[11)-13)]. Since the fault rupture mechanism in this area was not fully understood, the input seismic ground motion was formulated by a method that adjusts the amplitude of marine type ground motion proposed by JSCE[9)] among empirical approaches, which is expected to cause the most severe influence on the tunnel in the ground response analysis. Figure 5.2.4-6 shows the comparison of the response spectrum of the input seismic ground motion formulated as outlined above.

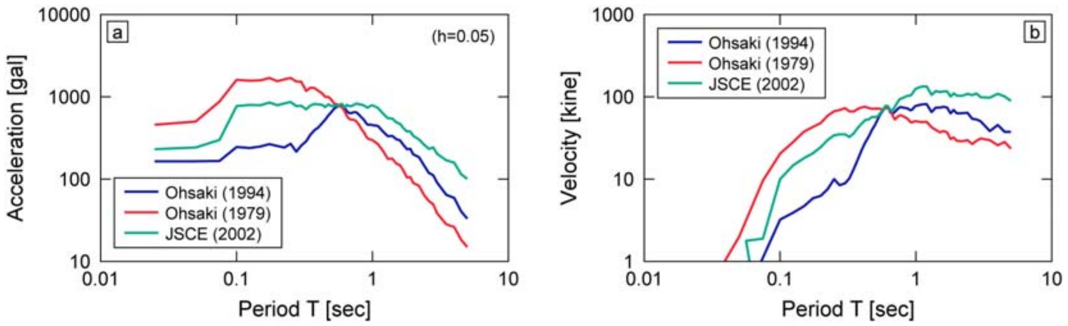

Figure 5.2.4-6 Response spectrum of input earthquake ground motion

a: Acceleration response spectrum, *b*: Velocity response spectrum

The analysis was carried out for the East Shaft, the horizontal drifts, the intersections in the horizontal drifts (at angles of 30° and 90°) and the connection between the shaft and a horizontal drift. The East Shaft was modelled in 3D and the horizontal drifts in 2D. The intersections and connections were modelled locally in 3D and the conditions of intersection and connection in the facilities were simulated by changing the direction of the input seismic waveform. Any analysis model involves the ground and tunnels and analysis was in principle according to the ground response acceleration method which applies the seismic ground motion to the entire model. Meshes used for the shaft and intersection (90°) in the analysis are shown in Figure 5.2.4-7.

The inertial force and other parameters used in the ground response acceleration method were calculated using a 1D layer ground analysis software SHAKE. The dynamic rock properties were evaluated based on the velocity logging conducted in the borehole and the rock mass classification and the unit weight were the same as those used in the excavation analysis. Table 5.2.4-5 shows the properties of the rock mass used in the analysis. It should be noted that non-linearity was taken into account in the analysis for rocks in the near-surface zone down to a depth of 25 m; rocks deeper than 25 m were considered to be elastic. The ultimate strength of the concrete supports was determined in compliance with the standards proposed by JSCE[9)], applying material factors etc. to the specified design-based strength.

The result of the dynamic analysis for the shaft model indicates that a shear strain of around 0.6% is generated at a depth of 25 m (Figure 5.2.4-8). For the analysis of the ground inertia force, the equivalent seismic coefficient which represents the maximum shear strain distribution was used in the East Shaft, while the distribution of seismic intensity at the time when the shear strain reached a maximum was used for the horizontal drifts, intersections and connections.

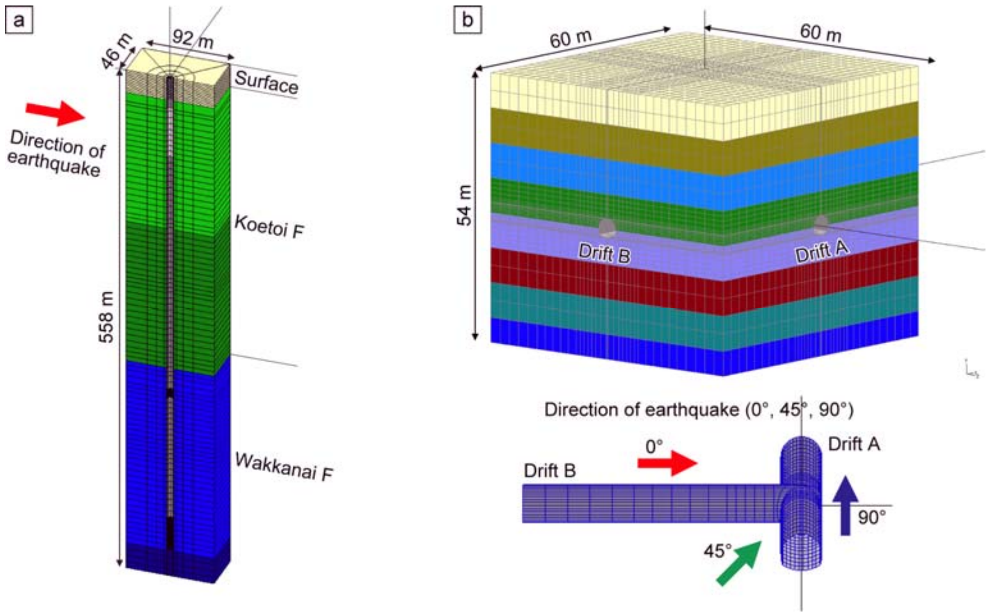

Figure 5.2.4-7 Seismic analysis model

a: Access Shaft model, *b*: Intersection model (90°)

Table 5.2.4-5 Mechanical properties for seismic analysis

Layer (Depth [mbgl])	P-wave velocity [m s^{-1}]	S-wave velocity [m s^{-1}]	Unit weight [kg m^{-3}]
Surface (0–25)	1,330	170	1480
Koetoi F (25–160)	1,330	510	1510
(160–326)	1,660	590	1510
Wakkanai F (326–530)	2,000	900	1850
(530–604)	2,120	1,070	1850

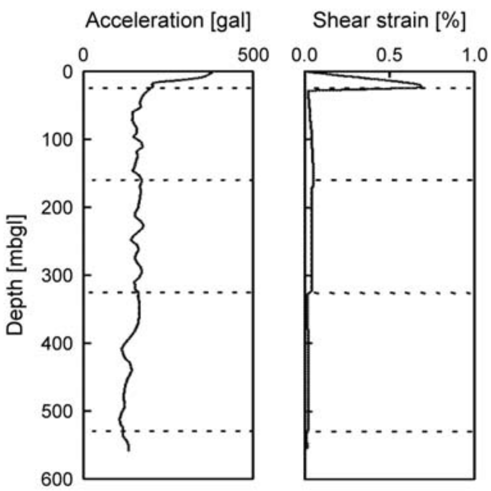

Figure 5.2.4-8 Result of seismic analysis (Access Shaft model)

2) Confirmation of seismic resistance

In order to confirm the stress intensity in the concrete members (lining and shotcrete), it was determined whether or not the coseismic increment in the stress intensity was lower than the difference between the ultimate strength and the normal allowable stress intensity. In parts where there is some margin for stress intensity, it was confirmed if the stress was within the allowable coseismic increment limit in stress intensity (difference between the ultimate strength and normal allowable stress intensity). The test was conducted on the inner side where the stress develops without being affected by the restraint from rocks.

Figure 5.2.4-9 shows the depth profile of the increase in the maximum principal stress generated on the concrete lining in the shaft. The result of the analysis indicates that the stress level is generally lower than the allowable stress intensity, thus satisfying the stability requirement, except for the part around a depth of 25 m, which is the boundary between the surface and the Koetoi Formation. The stability of the part at a depth of 25 m during an earthquake was improved by increasing the design strength f'_{ck} of the concrete lining determined by the excavation analysis from 24 MPa to 40 MPa. It was also confirmed that the stresses generated in the horizontal drifts and in all of the intersections and connections are lower than the allowable coseismic increment in stress intensity.

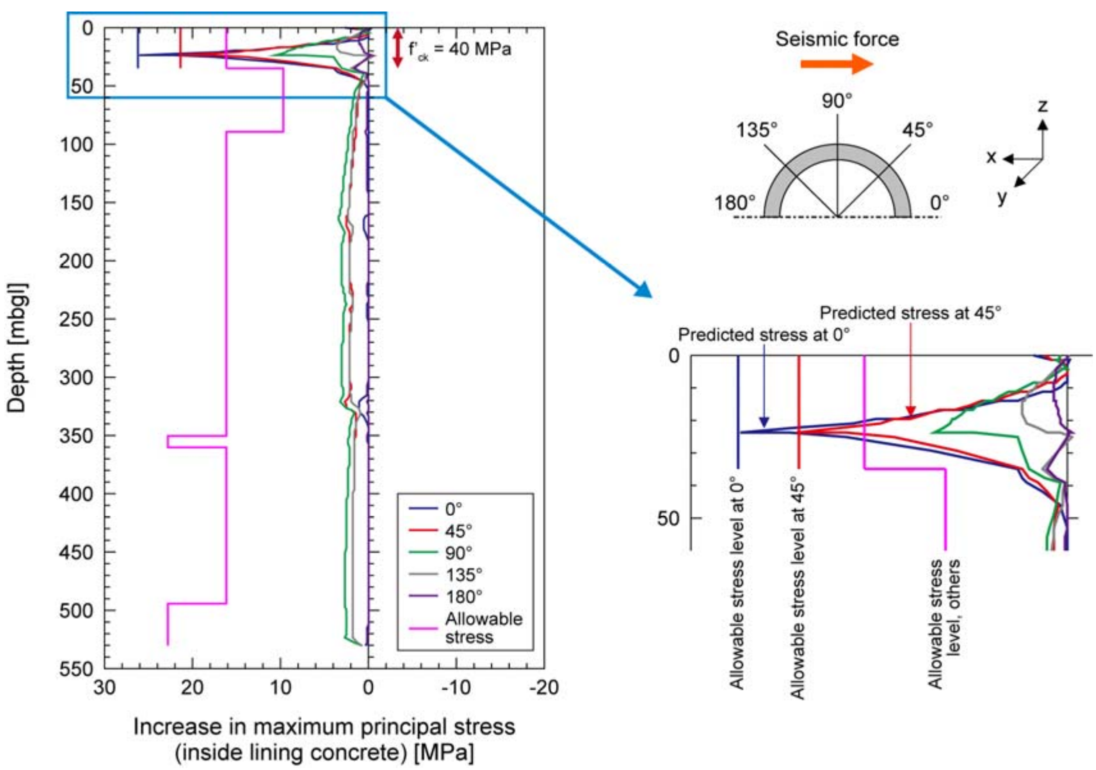

Figure 5.2.4-9 Relationship between increase in maximum principal stress and allowable stress level

5.2.5 Disaster prevention measures

It is expected that flammable gases will be generated in the tunnels. In order to ensure safety of the environment for investigations and operations and of personnel in the tunnels, appropriate measures and an in-tunnel information management system were considered.

(1) Measures against flammable gas

Past accidents were reviewed to identify the causes of gas-related fires and measures that needed to be taken in the underground facilities were studied based on the results of flammable gas blowout analyses. The exhaust ventilation system is used mainly to keep the atmosphere in the tunnels under negative pressure to improve the discharge of flammable gases under normal ventilation conditions and to suppress any flammable gas blowout when the fans are not operating. An exhaust ventilation fan was installed at the mouth of each shaft when the Connecting Drifts between the shafts were not completed; after the Connecting Drifts were linked, an exhaust ventilation fan was installed at the mouth of the Ventilation Shaft. A small forced ventilation fan was also used together with the exhaust ventilation fan to maintain a clean environment at the tunnel working face during excavation.

Factors that need to be evaluated to determine the required air flow rate include dust concentration, wind velocity limit, controlled gas concentration, gas concentration after blasting and inhalation of workers. The capacity of the ventilation system was determined based on the flow rate required to achieve the wind velocity limit (wind velocity of 0.5 m s^{-1} or higher will be required to prevent the formation of a gas layer). Although there is no risk that the gas content in the air will reach the explosion limit provided there is sufficient ventilation in the tunnels, the gas content may increase locally around the working face. Ventilation fans, the in-tunnel communication system and electrical and safety equipment such as gas sensors used within 30 m of the working face were therefore provided with explosion protection.

For the management of flammable gas, stationary flammable gas sensors will be installed in the tunnels serving as the main ventilation pathways and at the working face for continuous monitoring. A power shutdown system is also planned so that, when gas content is higher than 1.5% is detected, the system will automatically turn off all electrical apparatus located within the range of the gas effects, except for intrinsically safe apparatus such as sensors and communication devices. In order to check for flammable gases in front of the working face, an advance borehole will also be drilled once every excavation cycle.

(2) Measures for securing an appropriate in-tunnel operating environment

In order to provide an appropriate in-tunnel environment in terms of temperature, humidity, wind velocity and airflow rate in a complex tunnel layout, an analysis of the thermal environment was conducted taking heat generation by equipment and systems and the geothermal gradient into account. It was verified that the in-tunnel environment satisfies the requirements specified in the Ordinance on Industrial Safety and Health. During winter, icicles and frost may cause failure of equipment and systems, impacts on the working environment and hazards to workers. The temperature in the tunnels will therefore be kept higher than 0°C by installing heating systems at the mouth of the tunnels.

(3) Measures against fire

Fire sources, combustible materials and the causes of fire expected for the different installations in the underground facilities were reviewed and, assuming that fire may occur anywhere where combustible material is present, appropriate countermeasures were formulated. In this formulation, predictions of the area that will be affected by fire in the case of an in-tunnel accident and the ventilation control method used for the evacuation to the ground surface were verified based on a ventilation network analysis. As a result, it was confirmed that the dispersion range of smoke from fires in the tunnels can be reduced to a minimum, thus securing the safety zone for evacuating to the surface, by providing adequate ventilation control for each construction step of the underground facilities. It was also confirmed that the safety zone for evacuation can be secured even in tunnels under excavation.

Considering the evacuation procedure in the case of a disaster such as fire in the tunnels, measures for preventing disorder resulting from the arbitrary actions of individuals in the tunnels as well as prioritisation in the event of shortage in the capacity of evacuation means such as passenger kibbles and lifts should be established. Temporary emergency shelters should be provided in the horizontal drifts to help achieve smooth evacuation to the surface and should provide information required for the evacuation and identification of personnel in the tunnels. The basic concept for disaster prevention cannot be fully implemented at working faces in the shafts and horizontal drifts during excavation because they are dead-ends. It is therefore advisable to provide temporary shelter at the working face with adequate ventilation so that evacuation can proceed once the safety of the evacuation route has been confirmed.

(4) Ventilation behaviour model

With the aim of improving the reliability of the disaster prevention measures in the underground facilities, a test was carried out using a model combining shafts and horizontal drifts to provide an understanding of the complex behaviour of ventilation air during a fire in the tunnels. A laboratory model simulating the underground facilities is shown in Figure 5.2.5-1 and an example of the test result is shown in Figure 5.2.5-2. The test on ventilation air behaviour was conducted using smoke from an incense stick as a tracer. The behaviour of the smoke in the heated model was observed by laser. The distribution of airflow, temperature and gas concentration in the model was also measured.

The findings of the test include an inversion phenomenon of the main airflow owing to buoyancy generated by the fire and ventilation air behaviour occurring when the air door of horizontal drift is opened/closed. Based on the findings, a ventilation air behaviour model will be developed and the suitability of the current ventilation system verified by the time the shaft excavation reaches deep subsurface and tunnel ventilation starts.

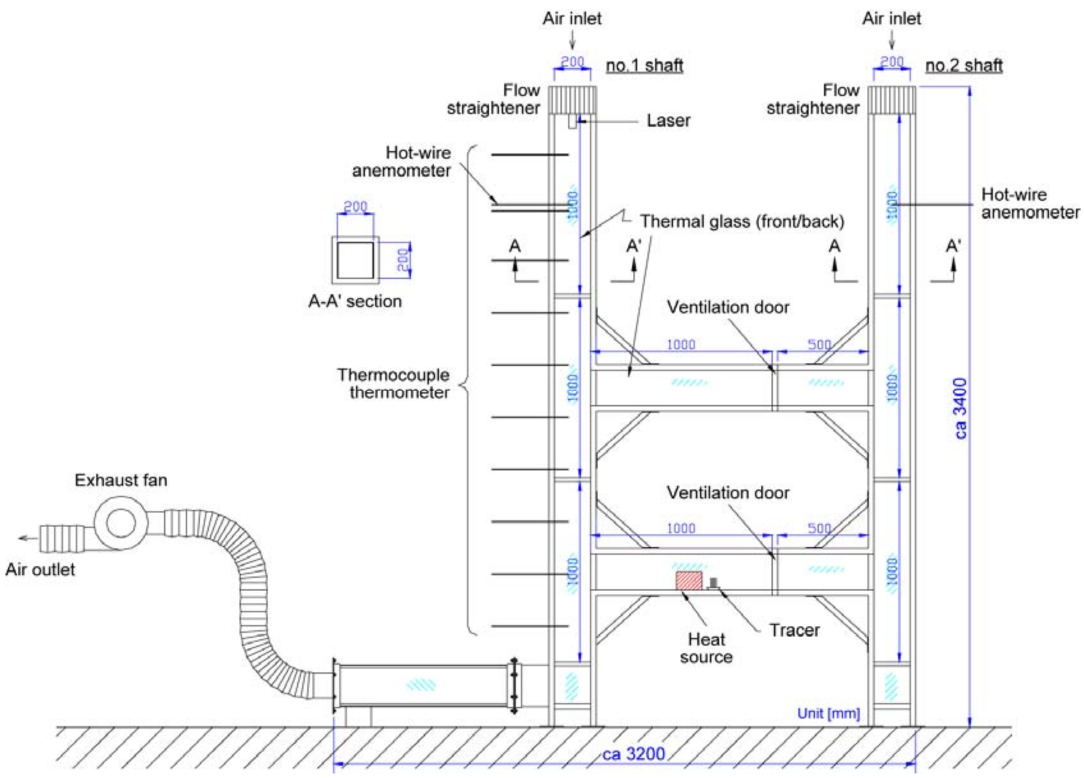

Figure 5.2.5-1 Layout of the laboratory model

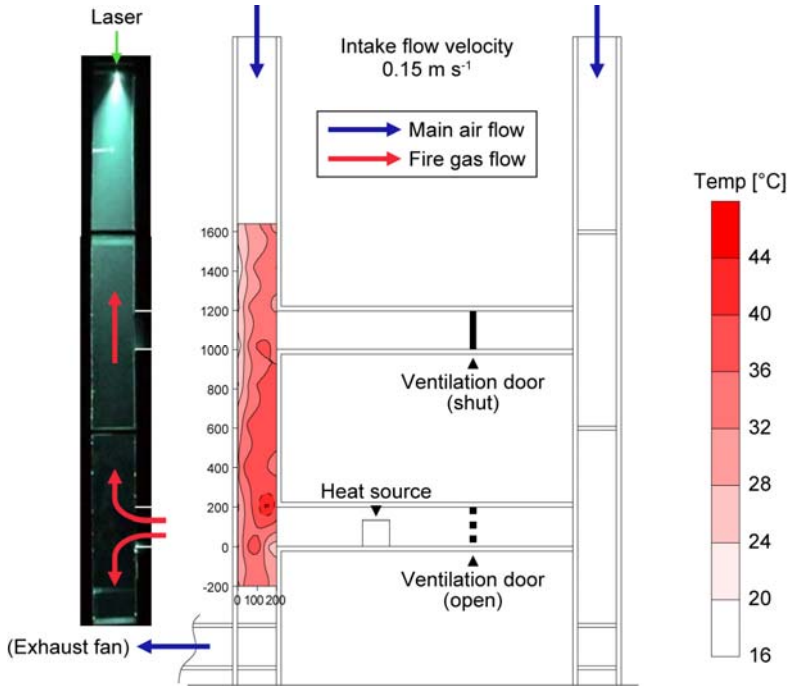

Figure 5.2.5-2 Example of the experimental result

This result showing the upward airflow from fire against the intake flow in the shaft

5.3 Summary

5.3.1 Achievements of Phase I work

The development of engineering techniques for the deep geological environment in Phase I involved, based on information from the surface-based investigations, preparation of the investigation and test programme to be conducted in the underground facilities, defining the specifications and layout of the tunnels, examining construction techniques and construction management methods required to ensure safety and an appropriate in-tunnel environment in view of the various phenomena likely to occur during construction and operation of the facilities and formulation of design and construction plans for the underground facilities. More specifically, for the preliminary design of the underground facilities, a method for determining the rock mass classification and mechanical properties of rocks with hairline cracks was proposed in order to take into account potential rock behaviour resulting from discontinuity planes in soft sedimentary rocks. For excavation under conditions with low rock competence, the concept of a double-layer support structure was assumed in order to achieve effective support by sharing the released stress (owing to excavation) between the rock and the supports and maintaining the tunnel stability immediately after the excavation. Stability in the event of an earthquake was analysed for typical structures in the underground facilities in order to establish a method for evaluating the seismic resistance of the underground facilities.

In the design planning technology, a plan to excavate a deep vertical shaft using a part-face tunnelling machine, which would be the first trial at Horonobe, was formulated. Methods for treating specified toxic substances in the excavated rock (muck) and groundwater were formulated in view of the impact on the surrounding environment, in accordance with various laws and regulations and based on consultation with the responsible authorities. To ensure safety in the underground facilities, countermeasures against flammable gases, measures for maintaining an appropriate in-tunnel environment, measures against fire and an in-tunnel information management system were developed. The inversion of the main airflow owing to buoyancy generated fire and ventilation air when the air door of a horizontal tunnel is open or closed were confirmed through laboratory experiments.

5.3.2 Remaining key issues and Phase II work

The applicability of the preliminary design methods and construction techniques evaluated in Phase I will be checked by applying them during actual construction in Phase II, which will enhance systematising stepwise engineering technology for the deep geological environment. Investigations in Phase II will also be aimed at developing advanced techniques for planning the design and construction of tunnels, construction measures and securing safety. More specifically, techniques for computer-controlled construction, which would allow prompt and accurate feedback of measured data obtained during excavation into the design and construction work, will be developed systematically based on actual construction. The deep vertical shaft sinking method using a part-face tunnelling machine will be developed with the aim of refining it to become an established construction technique by making technical improvements during actual construction. The advantages and disadvantages of both blasting and mechanical excavation will be identified by analysing their differences in the EDZ generated.

Construction of the URL is a project that will attract a great deal of social attention. For the project to be successful, risks related to safety, construction costs and the impact on the surrounding environment have to be evaluated and adequate measures provided. In the Horonobe URL project, a risk analysis method (decision-making basis) will be established through experience with the actual construction of the underground facilities; for the various risks that may be encountered during construction, the associated impact will be quantified in advance and priorities will be set for countermeasures taking into consideration the effect on the overall project.

The achievements made in development of engineering techniques in Phase II will be combined with the results of investigations on disposal technology being conducted concurrently as part of R&D on geological disposal technology. The project aims to establish design and construction techniques for the underground facilities, taking into account the restrictions assumed for operation of the actual repository.

5.3.3 Lessons learnt from Phase I work

The technical findings obtained through the investigations conducted as part of the development of engineering techniques for the deep geological environment in Phase I are summarised below. It should be noted again that the findings described below are presented here on the premise that their applicability will be checked through application in actual excavation work conducted in Phase II.

The sedimentary rock of interest for the investigations in the Horonobe URL project is classified as soft rock in terms of rock strength, but the strength and deformation characteristics of the rock are influenced by the presence of fractures and hairline cracks. In the preliminary design of the underground facilities, the rock properties should therefore be characterised taking the influence of these discontinuities into account. For the design of tunnel support in an environment with a low competence factor, effective support structures can be designed by sharing the released stress (owing to excavation) between the rock and the support system, while maintaining tunnel stability immediately after excavation, based on the concept of a double-layer support structure.

For efforts to reduce the impact on the surrounding environment, laboratory tests using rock samples and groundwater chemistry analyses should be conducted and processing methods for excavated rock (muck) and groundwater optimised through consultation of various laws and regulations and discussions with responsible bodies should be used. Since the inversion phenomenon of the main airflow owing to buoyancy generated by tunnel fire and the complex air ventilation behaviour occurring when the air lock of a horizontal tunnel is open have been confirmed by laboratory experiments, implementation of measures against these phenomena is crucial for securing safety in the underground facilities.

References

1) Japan Nuclear Cycle Development Institute: “H12: Project to Establish the Scientific and Technical Basis for HLW Disposal in Japan”, Project Overview Report, JNC TN1410 2000-001 (2000).
2) H. Morioka, G. Orukawa, S. Murakawa, K. Sugawara and T. Kobayashi: “Support design for underground research shafts and drifts of Horonobe Underground Research Laboratory Project”, Proc. 35th Symp. Rock Mech., Tokyo, Japan, 12-13 Jan. 2006, pp. 69-74 (2006). (in Japanese with English abstract)
3) Japan Society of Civil Engineers: “Standard Specifications for Concrete Structures -2002”, Structural Performance Verification, JSCE Guidelines for Concrete, No. 3 (2002).
4) Japan Railway Construction Public Corporation: “A Guide to Design and Construction of Tunnels by NATM” (1996). (in Japanese)
5) Japan Society of Civil Engineers: “Standard Specifications for Concrete Structures -2002”, Materials and Construction”, JSCE Guidelines for Concrete, No. 6 (2002).
6) T. Kobayashi, T. Teramoto, T. Kokado, M. Shinohara: “Challenge to higher standardization of tunnel timbering – Aiming at application of large-section tunnel”, Tunnels Underground, 29, pp. 49-56 (1998). (in Japanese)
7) Japan Society of Civil Engineers: “Standard Specifications for Tunneling -1996”, Shield Tunnels, pp. 28-29 (1996).
8) G. Orukawa, H. Morioka and S. Nishiyama: “Seismic performance verification of support for underground research shafts and drifts of Horonobe Underground Research Laboratory Project”, Proc. 41st Jpn. Natl. Conf. Geotech. Eng., Kagoshima, Japan, 12-14 Jul. 2006, pp. 1739-1740 (2006). (in Japanese)
9) Japan Society of Civil Engineers: “Standard Specifications for Concrete Structures -2002”, Seismic Performance Verification, JSCE Guidelines for Concrete, No. 5 (2002). (in Japanese)
10) T. Usami: “Materials for Comprehensive List of Destructive Earthquakes in Japan, [416]-2001”, Latest Edition, Univ. Tokyo Press (2003). (in Japanese)
11) Earthquake Research Committee Headquarters for Earthquake Research Promotion Prime Minister’s Office, Government of Japan: “Long-term Evaluation of Earthquakes in the Eastern Margin of the Japan Sea”, <http://www.jishin.go.jp/main/chousa/03jun_nihonkai/> (accessed on 11th Jun. 2008). (in Japanese)
12) Research Group for Active Faults of Japan: “Active Faults in Japan: Sheet Maps and Inventories”, Revised Edition, Univ. Tokyo Press (1991). (in Japanese)
13) T. Nakata and T. Imaizumi (Eds.): “Digital Active Fault Map of Japan”, Univ. Tokyo Press (2002). (in Japanese)

6. Assessment of the environmental impact of URL construction

The construction scale of the Horonobe URL project is smaller than that subject to the provisions of the Environmental Impact Assessment Law (Law no.81 of 1997) and the Hokkaido Environmental Impact Assessment Ordinance (Ordinance no.42 of 1998). Nevertheless, environmental investigations covering the URL area were conducted voluntarily in order to identify impacts associated with surface-based investigations and surface preparations for construction of the URL and to minimise these impacts. Impacts on the subsurface environment in the surrounding areas associated with the construction of the underground facilities were also investigated. This chapter describes the environmental investigations conducted in Phase I.

6.1 Basic strategy and procedures

As described in Subsection 3.3.5, flora and fauna and water usage were investigated prior to the selection of the URL area, i.e. in 2001, focussing on the potential URL areas (areas A, B1, B2 and C, except for the Teshio Experimental Forest of Hokkaido University). Investigation routes and points are shown in Figure 6.1-1 and investigation items and methods in Table 6.1-1. Following the selection of the URL area, investigations of flora and fauna, noise and vibration and water chemistry were conducted within the URL area in the summer, autumn and winter of 2002 and spring of 2003. Considering various environmental compartments, viz. river vegetation, windbreak, scrub and wetland vegetation, in the URL area, investigation routes and points were selected to cover all compartments. Investigation routes and points are shown in Figure 6.1-2 and investigation items and methods in Table 6.1-2.

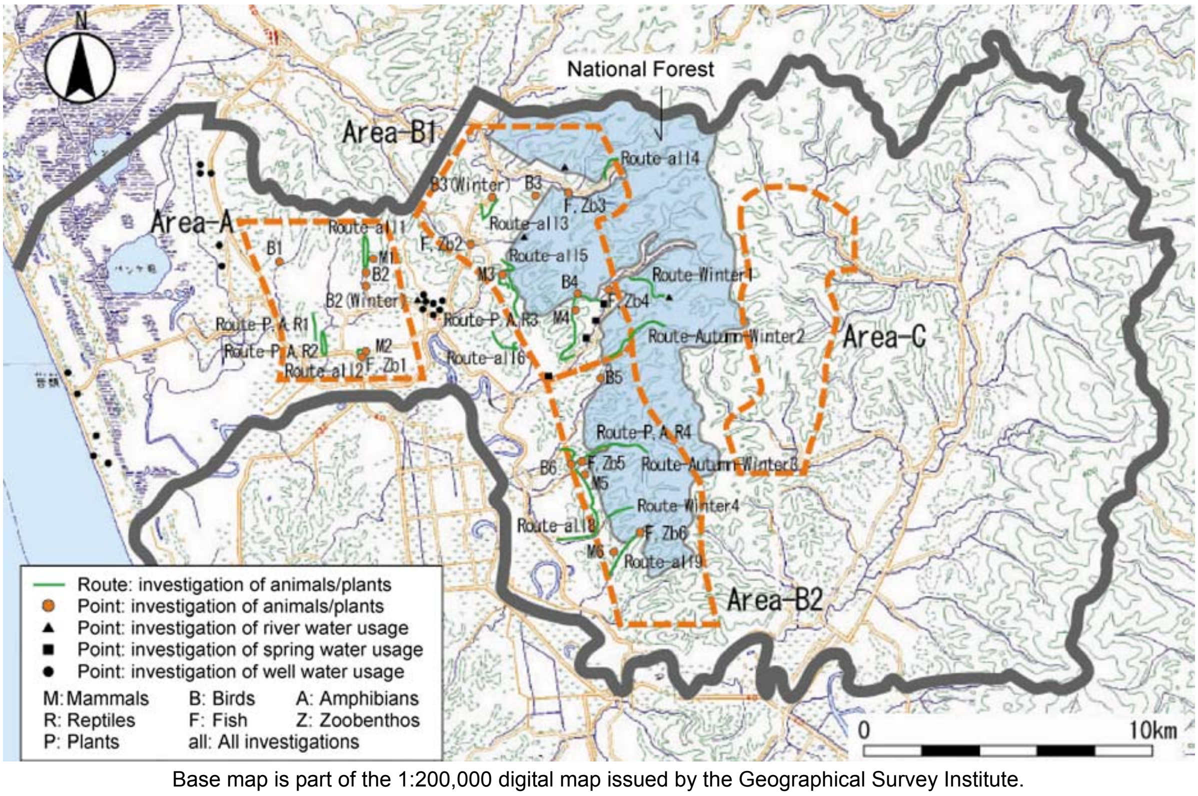

Base map is part of the 1:200,000 digital map issued by the Geographical Survey Institute.

Figure 6.1-1 Locations of environmental investigations in the potential URL areas in 2001

Table 6.1-1 Items and methods of environmental investigations in the potential URL areas in 2001

Items		Timing	Methods
Animals	Mammals	Summer – Autumn 2001	Harvest, Field sign
	Birds	Summer – Autumn – Winter 2001	Direct observation, Field sign, Fixed-point census (daytime/night-time)
	Amphibians/Reptiles	Summer 2001	Direct observation
	Fish	Summer – Autumn 2001	Direct observation, Harvest
	Insects	Summer 2001	Direct observation, Collection
	Zoobenthos	Summer – Autumn 2001	Direct observation, Collection
Plants	Flora/Plant community	Summer – Autumn 2001	Direct observation
River/well water usage		Summer – Autumn 2001	Interview, River flow/level measurement, Well water flow/level measurement

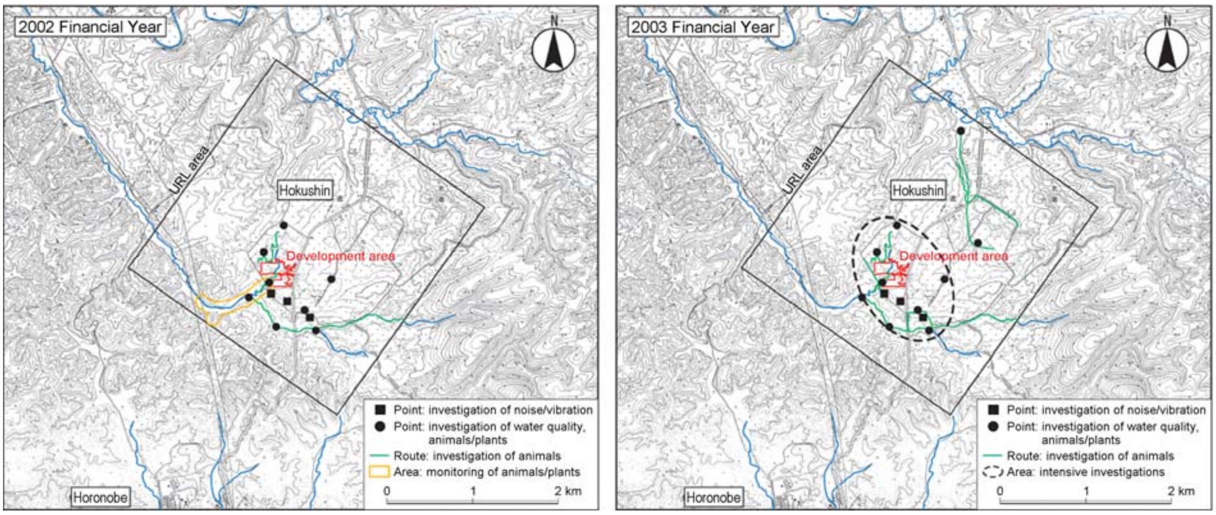

Base map is part of the 1:25,000 topographical map (Horonobe, Honryu) published by the Geographical Survey Institute.

Figure 6.1-2 Locations of environmental investigations in the URL area in 2002–2003

Table 6.1-2 Items and methods of environmental investigations in the URL area in 2002–2003

Items		Timing	Methods
Animals	Mammals	Summer – Autumn – Winter 2002, Spring 2003	Direct observation, Harvest, Field sign
	Birds	Summer – Autumn – Winter 2002, Spring 2003	Field sign, Fixed-point census Line census
	Amphibians/Reptiles	Summer 2002, Spring 2003	Direct observation
	Fish	Summer – Autumn 2002, Spring 2003	Direct observation, Harvest
	Insects	Summer – Autumn 2002, Spring 2003	Direct observation, Collection
	Zoobenthos	Autumn 2002, Spring 2003	Direct observation, Collection
Plants	Flora/Plant community	Summer 2002	Direct observation, Quadrat
Noise		Autumn 2002	In accordance with 'Regulatory Standards for Noise Emitted from Specified Construction Work' (Public Notice of the Ministry of Welfare and Ministry of Construction no.1 of 1968) and Environment Agency[1]
Vibration		Autumn 2002	In accordance with 'Ordinance for Enforcement of the Vibration Regulation Law' (Ordinance of the Prime Minister's Office no.58 of 1976)
Water chemistry		Summer – Autumn 2002, Spring 2003	In accordance with 'Environmental Quality Standards for Water Pollution' (Environment Agency Notification no.59 of 1971)

Based on the results of these investigations, animals and plants, the effectiveness of conservation measures, noise and vibration and water chemistry were monitored after the start of surface preparations for construction of the URL in the summer of 2003. The monitoring areas and points are shown in Figure 6.1-3. Preliminary investigations focussing on groundwater were conducted to evaluate the regional impact associated with the construction of the underground facilities. For the hydrochemical characterisation of surface water, a chemical analysis was carried out on precipitation and sampled river water in combination with the shallow subsurface hydrological investigations conducted on a regular basis throughout the year. Surface water was also collected from the entire Horonobe Town area to determine the distribution of the H and O isotopic ratios. In addition, water pressure and temperature were also continuously monitored using the long-term monitoring systems installed in the boreholes.

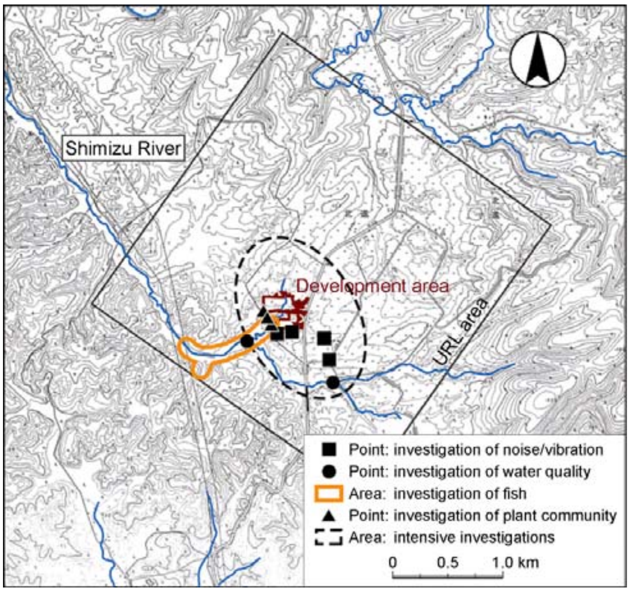

Base map is part of the 1:25,000 topographical map (Horonobe, Honryu) published by the Geographical Survey Institute.

Figure 6.1-3 Locations of monitoring in and around the URL site in 2003–2005

6.2 Environmental assessment 2001 – 2003

(1) Animals and plants

In the regional investigation of animals and plants conducted in 2001, a total of 36 species were identified as key species (Table 6.2-1). Of these species, the endangered or vulnerable species identified are listed in Table 6.2-2. It should be noted that species for which habitats could not be identified are not included in this table, even though they might be listed as key species in the literature[2), 3)]. The number of key species identified in each area was essentially the same, i.e. 17 species in area A, 16 species in area B1 and 17 species in area B2. Looking at the investigation items in detail, the number of zoobenthos that inhabit stagnant water is high and birds that prey on fish in reservoirs and migratory birds such as geese were observed mainly in area A, while areas B1 and B2 are characterised by fish that inhabit small rivers, resident birds and key species related to mountainous land.

Investigations in the URL area in the summer, autumn and winter of 2002 identified a total of 19 key species and those in spring 2003 identified also a total of 19 key species, as shown in Table 6.2-1. Of the animals and plants identified above, those specified as threatened species by law and the list published by the Ministry of the Environment are identified as key species, as shown in Table 6.2-3.

Table 6.2-1 Key species identified through the environmental investigations

Taxon	Investigation year	Investigation area	Total number of identified orders/families/species	Number of key species
Mammals	2001	Potential URL areas	6/9/17	4
	2002	URL area	4/5/10	0
	2003	URL area	5/6/6	0
Birds	2001	Potential URL areas	15/32/76	13
	2002	URL area	7/18/42	5
	2003	URL area	8/17/33	3
Amphibians/Reptiles	2001	Potential URL areas	4/4/4	1
	2002	URL area	2/2/2	1
	2003	URL area	2/2/2	1
Fish	2001	Potential URL areas	6/7/16	6
	2002	URL area	4/5/8	5
	2003	URL area	5/5/7	5
Insects	2001	Potential URL areas	12/100/325	5
	2002	URL area	10/64/255	2
	2003	URL area	6/20/43	2
Zoobenthos	2001	Potential URL areas	18/54/86	5
	2002	URL area	11/19/21	1
	2003	URL area	12/23/27	2
Plants	2001	Potential URL areas	- /78/318	2
	2002	URL area	- /56/171	5
	2003	URL area	- /58/214	6

Table 6.2-1 Endangered or vulnerable species identified in the potential URL areas in 2001

Taxon	Scientific name (English name)	Basis of selection						
		a	b	c	d	e	f	g
Birds	*Accipiter gentilis* (Northern Goshawk)		+		VU	Vu		
	Haliaeetus pelagicus (Steller's Sea Eagle)	+	+		VU	En		
	Haliaeetus albicilla (White-tailed Eagle)	+	+		EN	En		
	Circus spilonotus (Eastern Marsh Harrier)				VU	En		
	Accipiter nisus (Sparrowhawk)				NT	Vu		
	Anser fabalis (Bean Goose)	+			VU	R		
	Pandion haliaetus (Osprey)				NT	Vu		
Fish	*Lefua nikkonis* (Hokkaido's Eight-barbell Loach)				VU	R		
	Lethenteron reissneri (Far Eastern Brook Lamprey)				VU			
Zoobenthos	*Margaritifera laevis* (Freshwater Pearl Mussel)				VU			
	Radix auricularia japonica (Japanese Big-ear Radix)				VU			
Plants	*Viola kamtschadalorum* ('Kamchatka/Sakhalin native Viola')							VU

a: Law for the Protection of Cultural Properties (Law no.214 of 1950); +: Natural monument

b: Law for the Conservation of Endangered Species of Wild Fauna and Flora (Law no.75 of 1992); +: National Endangered Species of Wild Fauna and Flora

c: Environment Agency (Ed.)[4]; EX: Extinct, EW: Extinct in the Wild, CR: Critically Endangered, EN: Endangered, VU: Vulnerable, NT: Near Threatened, DD: Data Deficient, LP: Locally Threatened Population

d: Environment Agency[5–7]; EX: Extinct, EW: Extinct in the Wild, CR: Critically Endangered, EN: Endangered, VU: Vulnerable, NT: Near Threatened, DD: Data Deficient, LP: Locally Threatened Population

e: Hokkaido Prefectural Government[8]; Ex: Extinct, Ew: Extinct in the Wild, Cr: Critically Endangered, En: Endangered, Vu: Vulnerable, R: Rare, LP: Locally Threatened Population, N: Noteworthy

f: Fisheries Agency (Ed.)[9]; E: Endangered, V: Vulnerable, R: Rare, D: Decreased

g: Environment Agency (Ed.)[10]; EX: Extinct, EW: Extinct in the Wild, CR: Critically Endangered, EN: Endangered, VU: Vulnerable, NT: Near Threatened, DD: Data Deficient, LP: Locally Threatened Population

Table 6.2-3 Threatened species identified in the URL area in 2002–2003

Taxon	Scientific name (English name)	Basis of selection						
		a	b	c	d	e	f	g
Birds	*Anser fabalis* (Bean Goose)	+		VU	R			
	Haliaeetus albicilla (White-tailed Eagle)	+	+	EN	En		M	R
	Accipiter gentilis (Northern Goshawk)		+	VU	Vu			R
	Accipiter nisus (Sparrowhawk)			NT	Vu		M	
	Circus spilonotus (Eastern Marsh Harrier)			VU	Vu			R
	Gallinago hardwickii (Japanese Snipe)			NT	R		M	
Amphibians	*Hynobius retardatus* (Hokkaido's Salamander)				N		M	I
Insects	*Aphrophora brevis* ('Species of Froghoppers')				R			
	Damaster gehinii gehinii (Hokkaido's Damaster Ground Beetle)						M	S
	Gyrinus japonicas (Japanese Whirligig Beetle)				R			
Fish	*Lethenteron reissneri* (Far Eastern Brook Lamprey)			VU		R		
	Oncorhynchus masou masou (Seema)				N	D		
	Lefua nikkonis (Hokkaido's Eight-barbell Loach)			VU	En			
	Pungitius tymensis (Short-spined Ninespine Stickleback)			NT	R			R
	Cottus nozawae (Wrinklehead Sculpin)				N			
Zoobenthos	*Margaritifera laevis* (Freshwater Pearl Mussel)			VU				
	Somatochlora japonica ('Species of Japanese Dragonflies')						E	
Plants	*Rumex longifolius* (Dooryard Dock)			VU				
	Stellaria radians ('Species of Hokkaido's Chickweed')						V	
	Viola kamtschadalorum ('Kamchatka/Sakhalin native Viola')			VU				
	Veronica americana (American Brooklime)						V	
	Torreyochloa viridis ('Species of Manna Grass')				R			
	Sparganium glomeratum (Clustered Bur-reed)			VU				
	Platanthera chorisiana (Chimissso's Orchid)			VU				

a: Law for the Protection of Cultural Properties (Law no.214 of 1950); +: Natural monument

b: Law for the Conservation of Endangered Species of Wild Fauna and Flora (Law no.75 of 1992); +: National endangered species of wild fauna and flora

c: Environment Agency (Ed.)[4), 7), 10)], Ministry of the Environment (Ed.)[11)–13)]; EX: Extinct, EW: Extinct in the wild, CR: Critically endangered, EN: Endangered, VU: Vulnerable, NT: Near Threatened, DD: Data deficient, LP: Locally threatened population

d: Hokkaido Prefectural Government[8)]; Ex: Extinct, Ew: Extinct in the wild, Cr: Critically endangered, En: Endangered, Vu: Vulnerable, R: Rare, LP: Locally threatened population, N: Noteworthy

e: Fisheries Agency (Ed.)[9)]; E: Endangered, V: Vulnerable, R: Rare, D: Decreased

f: Environment Agency[14)]; M: Main wild animals, V: Valuable plants, E: Excellent nature

g: Environment Agency[15)]; R: Rare species, I: Investigated species, S: Specified insects

The passage of birds such as the Sparrowhawk, Eastern Marsh Harrier, White-tailed Eagle and Northern Goshawk was confirmed, while the inhabitation of amphibian/reptile such as Hokkaido's Salamander, fish such as Seema and Short-spined Ninespine Stickleback, zoobenthos such as Freshwater Pearl Mussel and insects such as *Aphrophora brevis* ('species of Froghoppers'), Hokkaido's Damaster Ground Beetle and Japanese Whirligig Beetle was confirmed. In addition, plants such as Dooryard Dock and *Torreyochloa viridis* ('species of Manna Grass') were identified.

Based on the results of the investigations prior to the start of surface preparations for construction of the URL, animals and plants that are likely to be affected in the surrounding environment and their habitats were selected for providing conservation measures aimed at mitigating these impacts. Considering that their presence was confirmed in areas where an impact of construction can be expected and taking into account the opinions of experts, conservation measures were taken for two species, viz. the Hokkaido's Salamander and *Torreyochloa viridis* ('species of Manna Grass').

For the salamander, in order to reduce the impact on its habitat resulting from the changes in the quantity of water, egg masses were collected and relocated to a natural spawning site similar to the original habitat in early May 2003. For *Torreyochloa viridis*, in order to compensate for loss of habitat owing to partial reclamation of rivers, it was moved to a habitat with a similar environment to that of the original one in early October 2003 prior to its dormant period. These conservation measures will be confirmed by periodical monitoring.

The conclusion of the investigations and interviews with experts were that the environment around the area to be developed (i.e. the URL site) had already undergone artificial alteration; no unique species were identified which cannot inhabit other areas and the impacts associated with the surface-based investigations and surface preparations on the environment was negligible, although conservation measures may be necessary in some areas.

(2) Noise and vibration

Noise and vibration were measured at three points around the URL site in 2002 in order to obtain data to serve as a baseline level before the start of the construction work. The measurement points are shown in Figure 6.1-2. The noise and vibration levels were about 40–50 dB and 30–40 dB respectively.

(3) Surface water chemistry

Investigation of water usage in Horonobe Town conducted in 2001 found that groundwater is used as a public water source, in private homes and offices in coastal areas (in the Shimonuma, Hamasato, Azahoronobe and central Horonobe districts; see Appendix 2), and surface water is used as a public water source in mountain areas (in the Hokushin, Kamihoronobe, Kaishin, Yukou, Toikanbetsu, Nakatoikan and Kamitoikan districts). No groundwater (well water) is used in the Yukou, Toikanbetsu, Nakatoikan and Kamitoikan districts, based on interviews with staff in the Horonobe Town office.

In order to acquire baseline data, river water was sampled in 2002 and 2003 from two points, i.e. upstream and downstream, in the Shimizu River (Figure 6.1-2), into which precipitation drained from the proposed URL site will be released, and river water chemistry was determined. The major analytical items include pH, suspended solid (SS), dissolved oxygen (DO) and biochemical oxygen demand (BOD). The results were pH = 6.7–6.9, SS = 2–10 mg l^{-1}, DO = 8.4–10.4 mg l^{-1} and BOD = 0.6–0.9.

For hydrochemical characterisation of surface water in the region, a chemical analysis was made of precipitation and sampled river water since 2002 in combination with the shallow subsurface hydrological investigations conducted regularly throughout the year (see Subsection 4.2.3). River water chemistry at point P-3 located downstream of the Shimizu River shows a periodic seasonal variation in which the concentration of dissolved ions in the river water increases in winter and decreases in summer (Figure 6.2-1). This trend is due to the fact that the amount of precipitation flowing into the river decreases because of snow cover and freezing in winter and hence the relative concentration of the dissolved ions increases. In addition, the concentration of dissolved ions such as Na^+ and Cl^- may increase with the effect of salt particles brought by wind blowing from the Japan Sea to inland, which is the prevailing wind direction in winter owing to monsoon activity. Another reason might be the seasonal temperature change observed in this area, because the concentration of dissolved ions depends on the solubility of the solute in question. These factors will be analysed through surface hydrochemical investigations. For the river water chemistry in this area, the background data was obtained because no notable changes in the concentration of dissolved ions that span two years were observed in spite of seasonal variation.

Monitoring will be continued to confirm that the construction of the underground facilities will not affect the chemistry of river water and groundwater in and around the URL site.

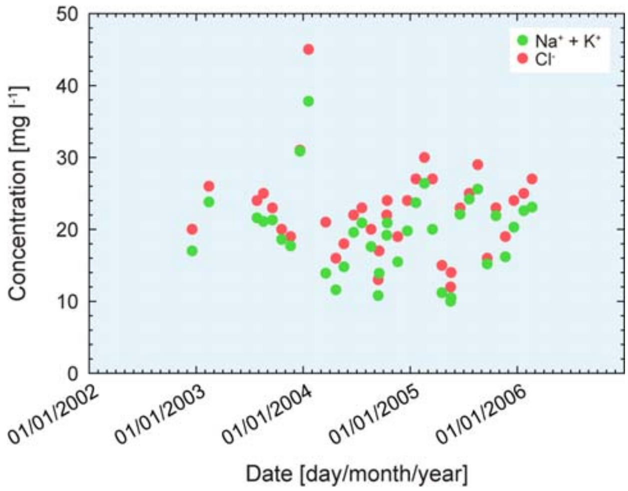

Figure 6.2-1 River water chemistry at point P-3 of the Shimizu River

(4) Groundwater level and pressure

Water pressure and temperature have been continuously monitored with long-term monitoring systems installed in boreholes to determine any hydraulic changes associated with the construction of the underground facilities (see Subsection 4.2.3). Water level and soil moisture in the shallow subsurface, which are assumed to be correlated with vegetation, have also been monitored (see Subsection 4.2.2).

Long-term monitoring systems are installed in boreholes HDB-1 to HDB-11 except HDB-4 and HDB-5 to monitor the water pressure prior to the construction of the underground facilities. Figure 6.2-2 shows the result of monitoring water pressure in borehole HDB-7. Although the start of the monitoring differs depending on the borehole, stable values are observed in most of the monitoring intervals over about half a year. However, long-term variations in the water pressure were observed in some monitoring intervals. Long-term monitoring of the water pressure conducted to date prior to the construction of the underground facilities showed no evidence demonstrating that specific external factors, for example, human activities such as borehole investigations and natural phenomena such as earthquakes, had caused impacts on the water pressure in the monitoring interval. Monitoring will be continued in the boreholes to confirm the impact on the groundwater regime around the URL site.

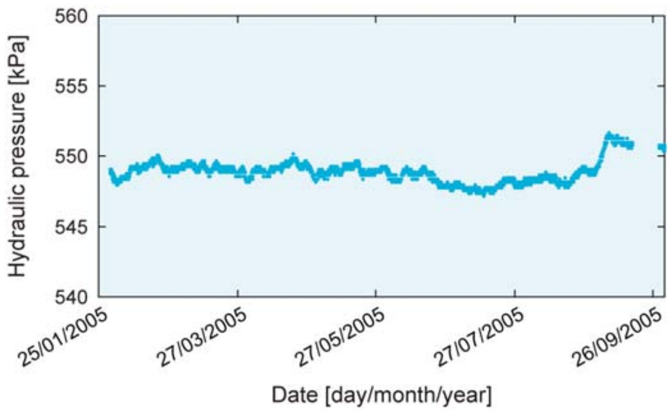

Figure 6.2-2 Hydraulic pressure monitored at 45.55 mbgl in borehole HDB-7

6.3 Environmental monitoring 2003 – 2005

Since summer 2003, after the start of the construction work at the URL site, monitoring of animals and plants, effectiveness of conservation measures, noise and vibration and water chemistry has continued (Figure 6.1-3). The results of the monitoring from the start of surface preparations until the start of the construction of the underground facilities (in early November 2005) are described below.

(1) Animals and plants

Seven species of fish were identified from the monitoring conducted in 2005. Of these, those listed by law as threatened species[8),9)13)–15)] are shown as key species in Table 6.3-1. It is concluded from these results that the habitats of the fish are preserved even after the start of the construction work.

Table 6.3-1 Confirmed threatened wildlife (fish) in and around the URL site in 2004

Scientific name (English name)	Basis of selection						
	a	b	c	d	e	f	g
Lethenteron reissneri (Far Eastern Brook Lamprey)			VU		R		
Oncorhynchus masou masou (Seema)				N*	D**		+
Tribolodon ezoe (Hokkaido's Rosyface Dace)				N		+	
Pungitius tymensis (Short-spined Ninespine Stickleback)			NT	R			+
Cottus nozawae (Wrinklehead Sculpin)				N		+	

a: Law for the Protection of Cultural Properties (Law no.214 of 1950); +: Natural monument

b: Law for the Conservation of Endangered Species of Wild Fauna and Flora (Law no.75 of 1992); +: National endangered species of wild fauna and flora

c: Ministry of the Environment (Ed.)[13)]; EX: Extinct, EW: Extinct in the wild, CR: Critically endangered, EN: Endangered, VU: Vulnerable, NT: Near Threatened, DD: Data deficient, LP: Locally threatened population

d: Hokkaido Prefectural Government[8)]; Ex: Extinct, Ew: Extinct in the wild, Cr: Critically endangered, En: Endangered, Vu: Vulnerable, R: Rare, LP: Locally threatened population, N: Noteworthy

e: Fisheries Agency (Ed.)[9)]; E: Endangered, V: Vulnerable, R: Rare, D: Decreased

f: Environment Agency[14)]; +: Investigated species

g: Environment Agency[15)]; +: Investigated species

*Fresh-water Seema only, **Cherry Salmon only

Regarding plant communities, the composition of species was almost unchanged compared to that prior to the start of surface preparations for construction of the URL. It was concluded from these results that there was no impact on plants, including alteration of habitats, and the vegetation environment prior to the start of construction work will be preserved on the basis of advice from experts.

Concerning the vegetation state of *Torreyochloa viridis* that is subject to conservation measures, planting in the transplanted area and similar growth to native plants in the habitat after transplantation were confirmed. A number of flowering species were also identified. The selected transplantation area thus proved to be suitable. In addition, a follow-up survey conducted after transplantation in 2003 confirmed that the eggs of the Hokkaido Salamander had hatched without any problems. Overall, the conservation measures were therefore appropriate. Monitoring will be continued in the URL area on a regular basis.

(2) Noise and vibration

The noise monitored in the URL site after the start of the construction work was lower than the criteria (85 dB) specified in the "Regulatory Standards for Noise Emitted from Specified Construction Work" (Public Notice of the Ministry of Welfare and Ministry of Construction no.1 of 1968), which is used as a reference for percentile noise level. The equivalent continuous A-weighted sound pressure level was also lower than the criteria (daytime 60 dB and night-time 50 dB in area C; daytime 65 dB and night-time 55 dB in area C facing a road with one or more lanes) defined in the “Environmental Quality Standards for Noise” (Environment Agency Notification no.64 of 1998).

The vibration monitored at the boundary of the URL site and the vibration level by the roadside were lower than the criteria (75 dB at the boundary; daytime 70 dB and night-time 65 dB by the roadside) defined in the “Ordinance for Enforcement of the Vibration Regulation Law” (Ordinance of the Prime Minister’s Office no.58 of 1976).

These results show that the measures taken have been to date appropriate for minimising the impact on the environment in terms of noise and vibration during construction in the URL area. The measurement of noise and vibration in the URL area will be continued on a regular basis.

(3) Surface water chemistry

Some seasonal changes in pH, SS, DO and BOD were observed, but no rapid drastic changes in water chemistry that could be attributed to the construction work in the URL area were identified. This demonstrates that the measures taken have been to date appropriate for minimising the impact on river environments during construction in the URL area. The measurement of river water chemistry will be continued for the Shimizu River on a regular basis.

6.4 Summary

In the Horonobe URL project, environmental investigations prior to the start of surface preparations for construction of the URL and continuous monitoring after the start of the construction of the underground facilities were conducted over the entire URL area to identify and minimise any impacts on the surface and subsurface environment.

The investigations before the start of the construction work provided baseline information on animals and plants, vibration and noise, surface water chemistry and groundwater level and pressure. Animal and plant species likely to be affected (Hokkaido’s Salamander and *Torreyochloa viridis*) were identified for a programme of conservation measures aiming at mitigating the impact.

Monitoring after the start of construction of the underground facilities indicated that no animals and plants, noise and vibration or surface water chemistry had been affected by the construction until the year 2005. This means that appropriate measures have been taken to minimise the impact on the surrounding environment. The conservation measures taken for animals and plants are also considered to be appropriate because both flora and fauna were confirmed to be in excellent condition.

The monitoring of animals and plants, noise and vibration and surface water chemistry in the URL area will continue on a regular basis with input from academic experts. The monitoring of chemistry, level and pressure of groundwater will also continue to identify any impact on the groundwater regime associated with the construction of the underground facilities.

References

1) Environment Agency: "Evaluation Manual for Environmental Quality Standards for Noise" (1999). (in Japanese)
2) Environment Agency: "The 3rd National Survey on the Natural Environment" (1988). (in Japanese)
3) Environment Agency: "The 4th National Survey on the Natural Environment" (1993). (in Japanese)
4) Environment Agency (Ed.): "Threatened Wildlife of Japan – Red Data Book", 2nd Edition, Volume 3: Reptilia/amphibia, Jpn. Wildl. Res. Ctr. (2000). (in Japanese with English summary)
5) Environment Agency: "Revision of the Red List of Mammals and Birds", Announcement Environ. Agency, 12th Jun. 1998 (1998). (in Japanese)
6) Environment Agency: "Revision of the Red List of Brackish and Fresh Water Fish" Announcement Environ. Agency, 18th Feb. 1999 (1999). (in Japanese)
7) Environment Agency: "Revision of the Red List of Invertebrates (Insects, Shellfish, Spiders, Crustaceans and others)", Announcement Environ. Agency, 12th Apr. 2000 (2000). (in Japanese)
8) Hokkaido Prefectural Government: "Threatened Wildlife of Hokkaido – Red Data Book of HOKKAIDO", Hokkaido Inst. Environ. Sci. (2001). (in Japanese)
9) Fisheries Agency (Ed.): "Data Book of Rare Aquatic Wildlife of Japan", Jpn. Fish. Resour. Conserv. Assoc. (1998). (in Japanese)
10) Environment Agency (Ed.): "Threatened Wildlife of Japan – Red Data Book", 2nd Edition, Volume 8: Vascular plants, Jpn. Wildl. Res. Ctr. (2000). (in Japanese with English summary)
11) Ministry of the Environment (Ed.): "Threatened Wildlife of Japan – Red Data Book", 2nd Edition, Volume 1: Mammalia, Jpn. Wildl. Res. Ctr. (2002). (in Japanese with English summary)
12) Ministry of the Environment (Ed.): "Threatened Wildlife of Japan – Red Data Book", 2nd Edition, Volume 2: Aves, Jpn. Wildl. Res. Ctr. (2002). (in Japanese with English summary)
13) Ministry of the Environment (Ed.): "Threatened Wildlife of Japan – Red Data Book", 2nd Edition, Volume 4: Pisces – Brackish and fresh water fishes, Jpn. Wildl. Res. Ctr. (2003). (in Japanese with English summary)
14) Environment Agency: "Green Census: Report of National Survey on the Natural Environment" (1976). (in Japanese)
15) Environmental Agency: "The Second Green Census: Report of National Survey on the Natural Environment" (1983). (in Japanese)

7. Conclusions and future perspectives

The Horonobe URL project was initiated in March 2001 and is one of two deep URL projects defined in the Long-Term Program on Research, Development and Utilization of Nuclear Energy and the Framework for Nuclear Energy Policy in Japan. It is a comprehensive R&D project aimed at studying the deep geological environment within a sedimentary formation. The primary aims of the R&D programme are to enhance understanding of the deep geological environment and to establish a sound basis for techniques for systematically characterising the deep geological environment and engineering technologies for use in the deep subsurface. This is done by applying various technologies relevant to geological disposal to an actual geological environment, based on a stepwise investigation approach. In July 2002, the URL area where the surface-based investigations were to be focussed was selected in the Hokushin district in Horonobe Town. In March 2003, the site within the URL area for constructing the underground and surface facilities was acquired. The Phase I surface-based investigations were conducted in and around the URL area and were completed at the end of March 2006.

This report presents the achievements of the surface-based investigations carried out over around five years as part of the geoscientific research in Phase I of the Horonobe URL project. The main accomplishments and lessons learnt from conducting the geoscientific research in Phase I and recommendations for the Phase II programme are summarised below.

(1) Selection process for the URL area and site

The selection of the URL area and site in Horonobe Town was a practical example of a stepwise selection process first of an investigation area and then of a site within this area for URL construction. In this project, the potential URL areas were first selected based on an evaluation of existing information and, from these areas, the candidate URL area was then selected based on the results of aerial and ground reconnaissance surveys conducted at the regional scale. For the selection of the URL area, requirements relating to geological environment criteria (i.e. the presence of a suitable rock formation and groundwater) and safety factors for construction of the URL were taken into account. The URL site was selected based on the results of borehole investigations and the social and environmental conditions (e.g. land use, infrastructure and regulatory procedures).

For the screening and selection of investigation areas in a stepwise manner, the basic strategy and resulting requirements in each stage had to be clearly defined, as the basis for drawing up specific investigation programmes commensurate with the progress in the selection process. In addition to technical requirements, social and environmental constraints and/or requirements to be considered were listed in a comprehensive manner and priorities for comparing and evaluating candidate areas were clearly stated. From the viewpoint of ease of execution of surface-based investigations and construction of the underground facilities, topography and social and environmental conditions such as land use and infrastructure were taken into account.

(2) Characterisation of the geological environment from the surface

Starting with existing information, ground exploration and borehole investigations were carried out focussing on the Neogene sedimentary formations and saline groundwater, in the region of Horonobe Town in two investigation stages: investigations covering the whole area of Horonobe Town and investigations in and around the URL area. Most of the properties of the geological environment and processes involved (e.g. distribution of discontinuities, groundwater flow, erosion/sedimentation and mechanical/thermal properties) which would be of relevance for geological disposal could be generally understood through interpretation of the individual investigation results and an integrating conceptualisation and associated modelling of the geological environment. Systematic techniques were developed stepwise for investigations from the surface focussed on three key aspects for the assessment of the safety of the geological disposal system: solute transport/retardation, future evolution of the geological environment and perturbations induced by construction of the underground facilities. Issues such as limited information and level of QC in some of the investigations were addressed.

Since the sedimentary rocks of interest for the investigations contain oil and natural gas, in addition to saline groundwater, expertise relating to the applicability of key investigation techniques for these conditions was accumulated. At the same time, the applicability of long-term monitoring equipment was also evaluated in such geological conditions.

For more effective understanding of the deep geological environment, properties and processes which need to be investigated and evaluated should be specified and prioritised and, based on this prioritisation, investigation programmes should be formulated. For effective implementation of the investigation programmes, it is of particular importance to implement an effective organisational scheme and build-up the respective teams and to develop an appropriate QA system which is applicable to all aspects of the investigation process.

(3) Development of engineering techniques for application deep underground

Taking into account that the rocks of interest have a low competence factor and contain flammable gases, specifications and layouts were determined and the design and construction plans for the underground facilities were formulated for ensuring safe construction and maintenance of the underground facilities, as well as providing a suitable in-tunnel environment for investigations. In particular, disaster prevention measures required in the underground facilities were examined from various standpoints (e.g. measures against flammable gases and fire and development of an in-tunnel information management system). For excavated rock and groundwater, appropriate treatment and processing methods were established considering the impact on the surrounding environment.

The design and construction programme for the underground facilities in gas-bearing sedimentary formations (soft rock) can be based on current, applied engineering techniques. However, the applicability of new preliminary design techniques for the underground facilities (e.g. effective design of tunnel supports and a method for seismic resistance analysis of the underground facilities) need to be checked during actual construction of the underground facilities in Phase II.

(4) Assessment of the impact of URL construction on the surrounding environment

Although there was no legal requirement, it was decided to conduct regional environmental investigations voluntarily in parallel with the selection of the URL area. After the URL area had been selected, environmental impact assessments were also carried out within the URL area itself to determine the impact on the surface and subsurface environment associated with the URL construction and to define measures required to reduce this impact. Since no impact resulting from the construction work at the URL site or from construction of the underground facilities was observed on the environment, animals and plants at the end of March 2006, the measures that were taken to minimise the impact on the surrounding environment were considered to be appropriate.

The two goals for Phase I, viz. i) development of conceptual models of the geological environment and enhancing understanding of the undisturbed deep geological environment before tunnel excavation and ii) detailed design of the underground facilities and formulation of a construction plan, were successfully achieved. Various issues, however, still remain, ranging from further improving the reliability of techniques and interpretation of data to optimising approaches/strategies and management methods for surface-based investigations as a whole. Of these, further enhancing the reliability of systematic characterisation techniques from the surface and understanding of groundwater flow and chemistry and solute transport in the environment at the saline – fresh water interface are of particular technical significance. It is important to refine the methodologies through iteration for understanding the geological environment in accordance with the stepwise progress of the project, at the same time integrating know-how and experience (including failures) accumulated during the course of the project as a knowledge database. In addition, based on the achievements from other research organisations, surface-based investigation techniques can be further improved to reinforce the technical basis for implementation and the formulation of safety regulations. Characterisation of the coastal geological environment was one of the subjects assigned at the beginning of the Horonobe URL project and since the development of systematic characterisation techniques for the coastal zone is indispensable in Japan's geological disposal programme, efforts should be made to accomplish this task in future investigations of the project.

Phase II of the project, which involves carrying out investigations during tunnel excavation (construction of the underground facilities), was started in 2005 and, at the time of writing (March 2007), excavation had reached the upper part of the sedimentary formation to be characterised in both the East Shaft (about 40 m depth) and the Ventilation Shaft (about 50 m depth). In parallel with constructing the underground facilities and considering safety and environmental preservation, basic strategies and detailed programmes for the investigations in Phase II will be formulated as soon as possible, to allow the geoscientific research and R&D on geological disposal technologies to be closely coordinated and driven efficiently. The issues that remained unresolved in Phase I will be addressed in the course of the Phase II programme. Based on information obtained during tunnel excavation, the depth of understanding of the properties of the geological environment and the processes involved, which are relevant for geological disposal will be increased, and confidence in the geological environment models and the predicted evolution of geological environment based on the Phase I investigations will be enhanced, allowing the reliability of the systematic techniques for characterising the geological environment from the surface to be checked. With regard to development of engineering technologies for use in the deep underground, the applicability of the design methods and construction techniques from Phase I will be confirmed through the actual construction of underground facilities in Phase II. Development of advanced techniques for formulating the design and construction plans for the underground facilities, construction measures and measures for ensuring safety will also be promoted. The results of these investigations will be integrated to form the technical basis that supports both repository implementation and the formulation of safety regulations, with a view to the selection of detailed investigation areas scheduled in the mid 2010s.

As a core R&D organisation, JAEA will implement the two deep URL projects at Horonobe and Mizunami, as well as key R&D using experimental facilities (ENTRY and QUALITY) at Tokai. The results of R&D will be published widely, facilities will be open to the public and JAEA will collaborate in R&D activities of relevant organisations and universities both domestically and internationally in a bid to contribute to the success of Japan's geological disposal programme and to promote public understanding of geological disposal.

The achievements presented in this report have been made possible by support from Hokkaido Prefecture and Horonobe Town, as well as from many domestic and international researchers and research organisations. In particular, the Swiss National Cooperative for the Disposal of Radioactive Waste (Nagra) has provided useful technical input to this project and reviews and suggestions for improving this report. JAEA would like to thank all those involved for their assistance and to ask for their continuous support and guidance.

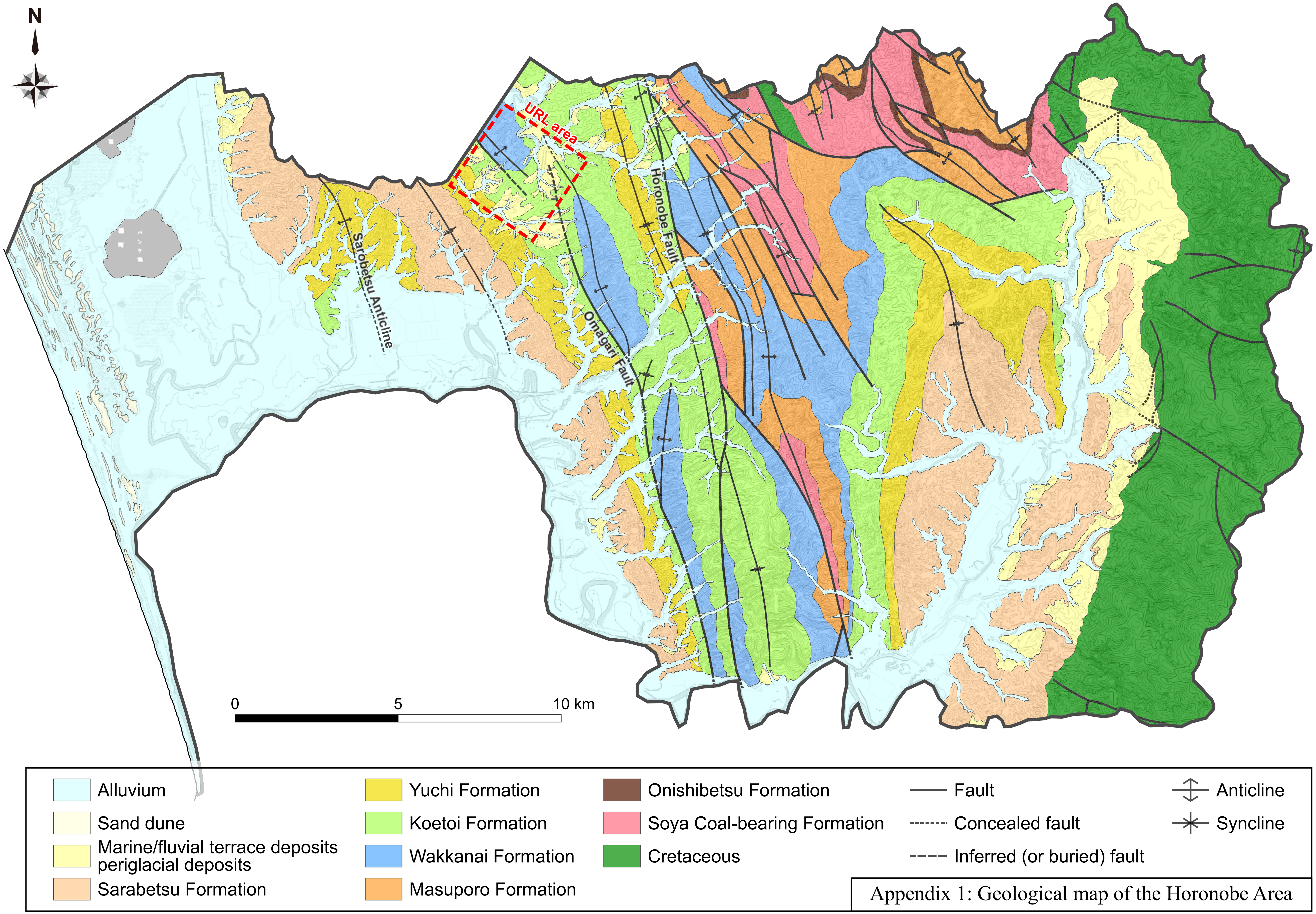

Appendix 1: Geological map of the Horonobe Area

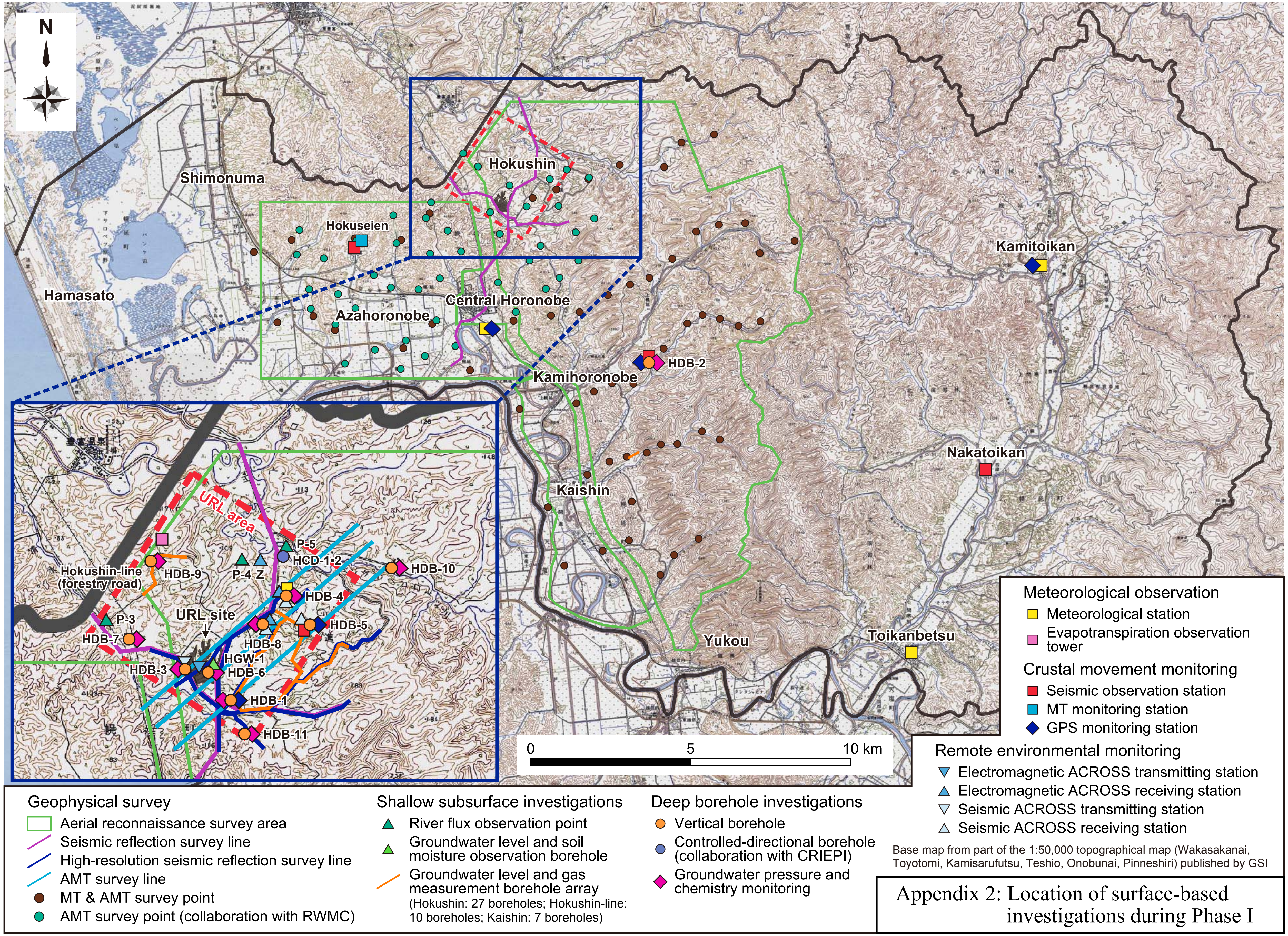

Appendix 2: Location of surface-based investigations during Phase I

Methods		Period	Main aims	Contents/Overview	Results
Aerial geo-physical surveys	Electromagnetic survey	Jun 2001	Confirmation of the distribution and extent of rock formations and of geological structures covering the whole area of Horonobe Town, which were estimated on the basis of existing information	Survey covering areas A, B1 and B2 except for the Teshio Experimental Forest of Hokkaido University, using a helicopter-towed EM sensor	The survey results supported the understanding of the distribution of rock formations based on existing information. Additional information about the distribution of the Horonobe and Omagari Faults was not obtained.
	Magnetic survey	Jun 2001		Survey covering areas A, B1 and B2 except for the Teshio Experimental Forest of Hokkaido University, using a helicopter-towed magnetometer	
	Radiometric survey	Jun 2001		Survey covering areas A, B1 and B2 except for the Teshio Experimental Forest of Hokkaido University, using an NaI detector on helicopter	
Ground geophysical surveys	MT survey	Jul – Oct 2001	Characterisation of the distribution and extent of rock formations and of geological structures covering the whole area of Horonobe Town	Survey down to about 3,000 m depth in the Horonobe Town	The survey results supported the understanding of the distribution of rock formations based on existing information. Additional information about the distribution of the Horonobe and Omagari Faults was not obtained.
	Reflection seismic survey	Aug 2002	Characterisation of the distribution (location) and geometry of the Omagari Fault in and around the URL area	Survey down to about 2,000 m depth in and around the URL area	The location of the Omagari Fault was not identified as most reflectors were ambiguous.
	AMT survey	Sep – Oct 2003	Characterisation of the distribution (location) and geometry of the Omagari Fault in and around the URL area	Survey down to about 1,000 m depth around the estimated location of the Omagari Fault	Higher resistivity zones showing a flower structure were identified, indicating the distribution and geometry of the Omagari Fault.
	Multi-offset VSP survey	Nov 2004	Checking of the feasibility and applicability of the VSP technique for characterising moderately to steeply dipping sedimentary formations in and around the URL area	Survey conducted in boreholes HDB-6 and HDB-8	The VSP results were not consistent with those obtained by the reflection seismic survey in the CDP mapping, suggesting that the VSP technique would not be applicable to sedimentary formations with varying dip angles.
	High resolution reflection seismic survey	Dec 2004	Checking of the feasibility and applicability of the high resolution reflection seismic technique for identifying changes in the petrophysical properties of sedimentary formations in and around the URL area	Survey down to about 1,000 m depth around the estimated location of the Omagari Fault with an increase in the density of shot/receiver points compared with the reflection seismic survey conducted in 2002	The continuity of reflectors and the resolution were not enhanced considerably, suggesting the difficulty in applying the reflection seismic technique in an area with homogeneous petrophysical properties.
	Gravity survey	Dec 2004	Characterisation of the distribution (location) and geometry of the Omagari Fault in and around the URL area	Survey around the estimated location of the Omagari Fault	An anomaly of gravity was observed at the estimated location of the Omagari Fault.
	Electrical survey	Jun 2005	Checking of the feasibility and applicability of the electrical technique for estimating the infiltration of meteoric water in and around the URL area	Survey down to about 250 m depth around the estimated location of the Omagari Fault	Resistivity was found to increase with depth around the estimated location of the Omagari Fault, suggesting the infiltration of meteoric water to depth.
	Ground penetrating radar survey	Oct 2005	Characterisation of the distribution (location) and geometry of the Omagari Fault in and around the URL area	Survey of the terrace deposits around the estimated location of the Omagari Fault	A structure concordant with the strike direction of the fault associated with the Omagari Fault was observed.
Geological surveys	Geological mapping	Jul – Aug 2001	Characterisation of the distribution and extent of rock formations and of geological structures covering the whole area of Horonobe Town	Field survey in the Horonobe Town with the associated laboratory programme (analyses of mineral and whole rock chemical compositions, microfossils and palaeomagnetism and FT dating)	The survey results were consistent with existing information. Additional information about the distribution of the Horonobe and Omagari Faults was not obtained.
		Oct 2002 Oct – Nov 2003 Oct – Nov 2004	Characterisation of the distribution and extent of rock formations in and around the URL area	Field survey involving shallow borehole investigations in and around the URL area with the associated laboratory programme (analyses of mineral compositions and microfossils and porosity determination)	The survey results (particularly on the distribution of Masuporo, Wakkanai, Koetoi, Yuchi and Sarabetsu Formations) were consistent with those obtained in 2001.
	Geological observation of the Omagari Fault outcrop	Oct 2004	Characterisation of the geometry and geological properties of the Omagari Fault in and around the URL area	Description of the geometry and geological properties of the Omagari Fault	A fault plane along the boundary between the Wakkanai and Koetoi Formations and minor faults around the fault plane with 120 m wide were observed.
	Geological observation of stripped horizontal outcrop	Jun 2005	Characterisation of the distribution, geometry and geological properties of minor faults	Description of the distribution, geometry and geological properties of minor faults	Fault zones were found to be formed by the distribution of minor faults at a high angle to the bedding plane densely together en echelon.
	Gas measurement	Nov 2002 ~ ongoing	Identification of the location of the Omagari Fault	Measurement of CH_4 and CO_2 concentrations immediately above the groundwater surface in shallow boreholes around the estimated location of the Omagari Fault	CO_2 concentrations near the estimated location of the Omagari Fault (> a few thousand ppm) were found to be much higher than those in the area away from the estimated fault location (< a few hundred ppm).
Shallow subsurface hydrological/hydrochemical investigations	River flux measurement	Oct 2002 ~ ongoing	Acquisition of river flux data for calculating a groundwater recharge rate by the hydrological balance method	Automatic monitoring of river water levels using a pressure gauge or manual measurement of river flux using a current meter at three points in the URL area	The height of runoff was calculated for the P-1, P-2 and P-3 drainage basins in the period of Aug 2003 to Jul 2004 (about 970 mm, 1,220 mm and 860 mm respectively) and for the P-3, P-4 and P-5 drainage basins in the period of Dec 2004 to Nov 2005 (about 810 mm, 800 mm and 1,070 mm respectively).
	River water chemistry measurement	Jul 2003 ~ ongoing	Characterisation of the baseline chemistry of river water	River water sampling once a month at three points in the URL area	The seasonal changes of river water chemistry were observed almost every year, suggesting that the baseline chemistry of river water was understood.
	Precipitation measurement	Aug 2003 ~ ongoing	Acquisition of precipitation data for calculating a groundwater recharge rate by the hydrological balance method	Monitoring of precipitation at four meteorological stations in Horonobe Town	The annual precipitation was determined for the periods of Aug 2003 to Jul 2004 (about 1,620 mm) and of Dec 2004 to Nov 2005 (about 1,375 mm).
	Estimation of evapotranspiration	Aug 2003 ~ ongoing	Acquisition of evapotranspiration data for calculating a groundwater recharge rate by the hydrological balance method	Meteorological observation at the Hokushin meteorological station and the Hokushin evapotranspiration observation tower	The annual evapotranspiration was estimated for the periods of Aug 2003 to Jul 2004 (about 420 mm) and of Dec 2004 to Nov 2005 (about 260 mm).
	Groundwater level measurement	Dec 2003 ~ ongoing	Characterisation of the distribution of groundwater level (as one of the boundary conditions of groundwater flow analysis)	Manual measurement or automatic monitoring of groundwater levels at 48 boreholes in and around the URL site	The annual and rainfall-induced short-term fluctuations of groundwater level were observed, the ranges of which depend on the monitoring location. In addition, the topographical watershed was found to be different from the groundwater divide.
	Soil moisture measurement	Dec 2004 ~ ongoing	Acquisition of soil moisture data for calculating a groundwater recharge rate by the hydraulic engineering method	Monitoring of soil moisture by the amplitude domain reflectometry (ADR) method at four depths in the URL site with the associated laboratory programme (prediction of relative permeability curves)	The recharge rate was not estimated based on the unsaturated nature and depth distribution of soil moisture as the ground at the measurement point has a higher content of fine grains than expected and the soil is less permeable.

Appendix 3: Overview of surface-based investigations during Phase I (Aerial/ground geophysical surveys geological surveys, shallow subsurface hydrological/hydrochemical investigations)

Methods/Location		Period	Main aims	Contents/Overview*	Results
Deep borehole investigations	HDB-1	3 Sep 2001 ~ 31 Jul 2002	• Confirmation of the geological structures predicted based on existing information and the results of aerial/ground geophysical surveys • Characterisation of the geological environment within sedimentary formations for selecting the URL area • Establishment of borehole drilling techniques for sedimentary formations	• Core/geophysical/fluid logging, hydraulic packer tests, groundwater sampling/analysis, rock mechanical tests etc. down to 720 m depth (1, 4, 6–9, 11–13, 15, 16[a], 18–21, 27) • Mineralogical/microfossil analyses, porewater squeezing/analysis, hydraulic tests, uniaxial tests etc. on core materials in the laboratory (3, 14, 18, 21–26)	The geological structures predicted based on existing information and the results of aerial/ground geophysical surveys were identified in the borehole investigations. It was found that the properties of the geological environment characterised in both boreholes met the technical requirements for a URL area, although the amount of dissolved gas in the groundwater in HDB-2 was greater than that of HDB-1. In addition, drilling with fresh water caused extensive enlargement of the borehole.
	HDB-2	11 Sep 2001 ~ 31 Jul 2002			
	HDB-3	3 Sep 2002 ~ 14 Mar 2003	• Characterisation of the distribution and geometry of, and the geological environment within, sedimentary formations on both sides of the Omagari Fault for selecting the URL area and the URL site in area B1 • Checking of the applicability of use of fresh water and bentonite mud for borehole drilling in sedimentary formations • Development of hydraulic testing techniques applicable in a borehole drilled with bentonite mud in gas-bearing sedimentary formations	• Core/geophysical/fluid logging (calliper logging after every 50 m of drilling), hydraulic packer tests (applying the improved testing procedure and surface/downhole equipment), groundwater sampling/analysis, rock mechanical tests etc. down to 520 m depth, (1, 2, 4, 6–9, 11–13, 15, 16[b], 18–21, 27) • Mineralogical/microfossil analyses, porewater squeezing/analysis, hydraulic tests, uniaxial tests etc. on core materials in the laboratory (3, 18, 21–25, 26[c])	The geological structures predicted based on existing information and the results of aerial/ground geophysical surveys were identified in the borehole investigations. Particularly, the boundary between the Wakkanai and Koetoi Formations on the east side of the Omagari Fault is shallower than that on the west side. Large loss of circulation occurred during drilling of HDB-4 and HDB-5, suggesting the existence of water-conducting features. In addition, the effectiveness of the hydraulic testing procedure and equipment was finally confirmed.
	HDB-4	3 Sep 2002 ~ 14 Mar 2003			
	HDB-5	3 Sep 2002 ~ 14 Mar 2003			
	HDB-6	26 Jun 2003 ~ 12 Mar 2004	Characterisation of the hydraulic and rock mechanical properties of the host sedimentary formations for designing the underground facilities	• Core/geophysical/fluid logging, hydraulic packer tests, groundwater sampling/analysis, intensive rock mechanical tests etc. down to 620 m depth (1, 2, 4–13, 15, 17–21, 27, 28) • Mineralogical/microfossil analyses, porewater squeezing/analysis, hydraulic tests, uniaxial tests etc. on core materials in the laboratory (3, 18, 21–26)	It was found that the rock strength is sufficient for construction of the underground facility and that water-conducting features occur in the host sedimentary formations.
	HDB-7	26 Jun 2003 ~ 12 Mar 2004	Characterisation of the hydraulic properties of the Yuchi Formation for groundwater flow analysis	• Core/geophysical/fluid logging, hydraulic packer tests, groundwater sampling/analysis, rock mechanical tests etc. down to 520 m depth in HDB-7 and HDB-9, 470 m in HDB-8 and 550 m in HDB-10 (1, 2, 4, 5[d], 6–13, 15, 18, 19–21[e], 27[f]) • Mineralogical/microfossil analyses, porewater squeezing/analysis, hydraulic tests, uniaxial tests etc. on core materials in the laboratory (3, 14[f], 18[g], 21, 22[e], 23[e], 24, 25, 26[h])	It was found that the Yuchi Formation is composed mainly of soft sandy mudstone and has low hydraulic conductivities (10^{-10}–10^{-9} m s^{-1}).
	HDB-8	26 Jun 2003 ~ 12 Mar 2004	Characterisation of the geological properties of the Omagari Fault		Although the borehole was drilled near the estimated location of the Omagari Fault, the Omagari Fault did not occur in the drilled section.
	HDB-9	26 Jul 2004 ~ 11 Mar 2005	Characterisation of the geological properties of the Omagari Fault and of the geological environment on the north-west side of the URL area for establishing the boundary conditions for geological environment models		The occurrence of fractures associated with the Omagari Fault was identified and the distribution of porewater pressure was defined.
	HDB-10	26 Jul 2004 ~ 11 Mar 2005	Characterisation of the geological environment on the east side of the URL area for establishing the boundary conditions for geological environment models		The distribution of porewater pressure was defined.
	HDB-11	5 Aug 2004 ~ 10 Mar 2006	• Characterisation of the geological environment on the south side of the URL area for establishing the boundary conditions for geological environment models and down to 1,000 m depth for updating the models • Development of techniques for measuring in situ physico-chemical parameters at greater depths	• Core/geophysical/fluid logging, hydraulic packer tests, groundwater sampling/analysis with in situ physico-chemical parameter monitoring, rock mechanical tests etc. down to 1,020 m depth (1, 2, 4–13, 15, 17–21, 27) • Mineralogical/microfossil analyses, porewater squeezing/analysis, hydraulic tests, uniaxial tests etc. on core materials in the laboratory (3, 14, 18, 21–25)	The distribution of porewater pressure was defined. A variety of data on the properties of the geological environment, including in situ physico-chemical parameters of groundwater, down to 1,000 m depth was acquired.

*Numbers in parentheses representing investigations conducted; 1: Core observation/description, 2: Core scanning, 3: Petrological/mineralogical/microfossil analyses, 4: Electro Micro Imaging (EMI™) logging, 5: Borehole televiewer (BHTV) logging, 6: Calliper logging, 7: Electrical resistivity logging, 8: Density logging, 9: Neutron – gamma-ray logging, 10: Spectral gamma-ray logging, 11: Temperature logging, 12: Velocity logging, 13: Cement bond logging, 14: Magnetic susceptibility/resistivity tests, 15: Electromagnetic flowmeter logging, 16: Spinner flowmeter logging, 17: Flowing fluid electrical conductivity logging, 18: Hydraulic test, 19: Pumping test, 20: Physico-chemical parameter monitoring, 21: Water sampling/analysis, 22: Organics/microbes analyses, 23: Gas analysis, 24: Rock mechanical test, 25: Rock physical test, 26: Rock thermal test, 27: Hydraulic fracturing test, 28: Borehole load test

[a]HDB-1 only, [b]HDB-5 only, [c]HDB-3 only, [d]HDB-9/10, [e]HDB-8/9/10, [f]HDB-9 only, [g]HDB-7 only, [h]HDB-7/8

Methods		Period	Main aims	Contents/Overview	Results
Joint research programmes	Controlled directional drilling (HCD-1•2) (collaboration with CRIEPI[†])	Nov 2003 ~ May 2006	Development of controlled directional drilling techniques and checking of the applicability of a variety of downhole logging and testing techniques in such a borehole	Controlled directional drilling down to 706 mabh in the URL area and geophysical and flowmeter logging during and after drilling	It was confirmed that the controlled directional drilling techniques as well as downhole geophysical and flowmeter logging techniques are feasible in soft sedimentary formations.
	Groundwater dating (collaboration with CRIEPI)	2004 ~ ongoing	Estimation of the residence time of groundwater in low permeability sedimentary rocks	Chemical/isotopic analyses of groundwaters and porewaters and of rock samples collected from the deep boreholes	An appropriate methodology for ^{4}He and $^{36}Cl/Cl$ groundwater dating for low permeability sedimentary rocks was established. The residence time of deep groundwater was estimated to be over 1 million years in the Horonobe area.
	3D AMT survey (collaboration with RWMC[‡])	Oct – Nov 2005	Demonstration of the feasibility of a technique for 3D interpretation of MT/AMT data	Survey in an area of about 3 km × 2 km in the Hokushin district and 3D interpretation of the AMT data	The accuracy of 3D interpretation of geological structures was improved compared with that of a 2D technique. Consistency between the distribution of resistivity and that of groundwater salinity was found, suggesting that the 3D AMT technique would be used as an effective alternative to characterise groundwater chemistry.
	Microbiological investigations (collaboration with IRI[§])	Nov – Dec 2005	In situ characterisation of microbial activity	Drilling of a 52.2 m deep borehole (H17-1-01) and in situ groundwater sampling	The applicability of methodologies for detecting and quantifying microbial species and for measuring microbial metabolism was confirmed.

[†]CRIEPI: Central Research Institute of Electric Power Industry, [‡]RWMC: Radioactive Waste Management Funding and Research Center, [§]IRI: Institute Research and Innovation (dissolved in September 2007)

Appendix 3: Overview of surface-based investigations during Phase I (Deep borehole investigations, joint research programmes)

Methods/Location			Period	Main aims	Contents/Overview	Results
Long-term monitoring	HDB-1		Aug 2003 ~ ongoing	• Monitoring of hydraulic changes in the geological environment associated with construction of the underground facilities and with borehole drilling • Checking of the applicability of the long-term monitoring system	Monitoring of groundwater pressure in four packed-off intervals using the MP system	The groundwater pressures have been gradually increasing, suggesting that the recovery of hydraulic condition to the initial state would be very slow owing to the very low permeable nature of the sections. No hydraulic responses were observed during drilling of other boreholes.
	HDB-2		Mar 2003 ~ ongoing	• Characterisation of the distribution and long-term variation of groundwater pressure (abnormally higher at depth) • Checking of the applicability of a different long-term monitoring system from the MP system	Monitoring of groundwater pressure in seven packed-off intervals using the SPMP system	The hydraulic pressure increases with depth, indicating that groundwater is distributed in the range from hydrostatic to highly artesian conditions.
	HDB-3		Nov 2003 ~ ongoing	Monitoring of hydraulic changes, associated with construction of the underground facilities, in the geological environment in the URL site	Monitoring of groundwater pressure in six packed-off intervals using the MP system	The groundwater pressures have been reached stable, indicating the initial hydraulic conditions before starting construction of the underground facilities.
	HDB-4		Nov 2003 ~ ongoing	Monitoring of the seasonal and URL construction related changes in groundwater chemistry	Groundwater sampling several times a year in two packed-off intervals using the MP system	No seasonal changes were identified in the groundwater chemistry, but its evolution most likely resulted from the reaction with the cement used to fix the casing pipes was observed.
	HDB-6		Mar 2005 ~ ongoing	Monitoring of hydraulic changes, associated with construction of the underground facilities, in the geological environment in the URL site	Monitoring of groundwater pressure in 11 packed-off intervals using the MP system	The groundwater pressures have been reached stable, indicating the initial hydraulic conditions before starting construction of the underground facilities.
	HDB-7		Jan 2005 ~ ongoing	• Monitoring of hydraulic changes, associated with construction of the underground facilities, in the geological environment at the west boundary of the URL area • Characterisation of the distribution of groundwater pressure in the Yuchi Formation	Monitoring of groundwater pressure in nine packed-off intervals using the MP system	The groundwater pressures have been reached stable, indicating the initial hydraulic conditions in the Koetoi and Yuchi Formations before starting construction of the underground facilities.
	HDB-8		Mar 2005 ~ ongoing	Monitoring of hydraulic changes in the geological environment associated with construction of the underground facilities	Monitoring of groundwater pressure in nine packed-off intervals using the MP system	The groundwater pressures have been reached stable, indicating the initial hydraulic conditions before starting construction of the underground facilities.
	HDB-9		Oct 2005 ~ ongoing	• Monitoring of hydraulic changes, associated with construction of the underground facilities, in the geological environment near the boundary of Horonobe Town • Characterisation of the distribution of groundwater pressure at the high elevations of the URL area	Monitoring of groundwater pressure in nine packed-off intervals using the MP system	The groundwater pressures have been reached stable, indicating the initial hydraulic conditions before starting construction of the underground facilities. Here groundwater occurs in unconfined conditions.
	HDB-10		Mar 2006 ~ ongoing	• Characterisation of the distribution of groundwater pressure near the east boundary of the URL area • Checking of the applicability of the long-term monitoring system developed for simultaneous groundwater sampling and groundwater pressure monitoring	Monitoring of groundwater pressure in 11 packed-off intervals using the PIEZO system	Although the groundwater pressures have not been reached stable by Jan 2007, it was confirmed that the PIEZO system monitored the groundwater pressures without any troubles.
	HDB-11		(Feb 2007 ~ ongoing)	Characterisation of the distribution of groundwater pressure near the south boundary of the URL area	Monitoring of groundwater pressure in 15 packed-off intervals using the MP system	(Groundwater pressure monitoring was commenced in Feb 2007)
Crustal movement monitoring	Seismic observation	Kamihoronobe station Hokushin station Hokuseien station Nakatoikan station	Dec 2002 ~ ongoing Sep 2003 ~ ongoing Sep 2003 ~ ongoing Mar 2004 ~ ongoing	Determination of the distribution of hypocentres and estimation of the subsurface structures for understanding neotectonics of the Horonobe area	Acquisition of seismic data using a surface seismometer (about 1.5 mbgl) and a deep seismometer (about 138 mbgl) in the borehole at Kamihoronobe and determination of the distribution of hypocentres using JAEA and Hi-net data	It was shown that the relocated hypocentre distributions become deeper toward the west and are aligned in an N-S or NNE-SSW direction. This feature is consistent with the N-S trending geological structures in northern Hokkaido.
	GPS observation	HDB-1 station	Jan 2003 ~ ongoing	Evaluation of the amount and rate of crustal movement for understanding neotectonics of the Horonobe area	GPS monitoring and estimation of the horizontal crustal strain rates (from baseline lengths) using JAEA data and the GPS data obtained at 12 GEONET and 4 IGS stations	The results of the estimation of the horizontal crustal strain rates and deformation based on tectonics in northern Hokkaido showed that the trend and rate of crustal movement changed before and after the occurrence of Tokachioki earthquake (on 26th September 2003).
		Kamihoronobe station Hokushin station Central Horonobe station Kamitoikan station	Jul 2004 ~ ongoing Feb 2004 ~ ongoing Sep 2004 ~ ongoing Aug 2004 ~ ongoing		GPS observation using a portable GPS logger system at temporal observation stations	
Remote environmental monitoring	Seismic ACROSS: HDB-3 transmitting station and HDB-4, HDB-5 and HDB-8 receiving stations		Dec 2005 ~ ongoing	Establishment of the ACROSS techniques for identifying changes in the geological environment (with a high resolution) occurring before, during and after construction of the underground facilities	Test monitoring using both the seismic and the electromagnetic ACROSS, involving constantly transmitting seismic and electromagnetic waves and receiving their signals.	The results of the test monitoring showed that it was possible to obtain seismic and electromagnetic data with high S/N ratios.
	Electromagnetic ACROSS: transmitting station in the URL site and HDB-4, HDB-5 and Z receiving stations		Dec 2004 ~ ongoing (Started in Mar 2005 at HDB-8)			

Appendix 3: Overview of surface-based investigations during Phase I (Long-term monitoring, crustal movement monitoring, remote environmental monitoring)

Number	Location (WGS84, Zone54N)	Length	Rationale behind the locations and depths	Method/Diameter	Drilling fluid
HDB-1	Latitude (X): 45°02'24.0283" N (4,987,758.417 m) Longitude (Y): 141°51'52.8339" E (568,102.258 m) Elevation (Z): 69.102 m	720.00 m	• The locations were selected considering the land use, the ease of formalities and the degree of development of infrastructure (specifically access to main roads). • The depth (excluding 20 m overbreak) was determined so as to define the thickness of the target formations and to obtain information on the geological environment below the planned URL depth (500 m depth) for groundwater flow analysis.	6¼" wireline, triple-tube, core drilling (Ø 86mm core) from 4.40 to 720.00 mbgl	Fresh water from 4.40 to 275.50 mbgl Bentonite fluid from 275.50 to 720.00 mbgl
HDB-2	Latitude (X): 44°59'48.3752" N (4,983,002.942 m) Longitude (Y): 141°55'10.3830" E (572,478.747 m) Elevation (Z): 42.529 m	720.00 m		6¼" wireline, triple-tube, core drilling (Ø 86mm core) from 4.40 to 720.00 mbgl	Fresh water from 4.40 to 404.90 mbgl Bentonite fluid from 404.90 to 720.00 mbgl
HDB-3	Latitude (X): 45°02'39.5035" N (4,988,229.854 m) Longitude (Y): 141°51'26.6447" E (567,524.238 m) Elevation (Z): 58.192 m	520.00 m	• The locations were selected so as to obtain information on the geological environment on both sides of the Omagari Fault (i.e. HDB-3 on the west side; HDB-4/5 on the east side) and to define the continuity of the sedimentary formations along the strike, considering the land use, the ease of formalities and the degree of development of infrastructure (specifically access to main roads). • The depth (excluding 20 m overbreak) was determined so as to obtain information on the geological environment down to the planned URL depth (500 m depth).	6¼" wireline, triple-tube, core drilling (Ø 86mm core) from 4.40 to 520.00 mbgl	Fresh water from 4.40 to 157.00 mbgl Bentonite fluid from 157.00 to 520.00 mbgl
HDB-4	Latitude (X): 45°03'16.3510" N (4,989,381.786 m) Longitude (Y): 141°52'30.2881" E (568,904.226 m) Elevation (Z): 63.610m	520.00 m		6¼" wireline, triple-tube, core drilling (Ø 86mm core) from 4.10 to 520.00 mbgl	Fresh water from 4.10 to 162.20 mbgl Bentonite fluid from 162.20 to 520.00 mbgl
HDB-5	Latitude (X): 45°02'57.7507" N (4,988,811.807 m) Longitude (Y): 141°51'38.6432" E (569278.059 m) Elevation (Z): 78.768 m	520.00 m		6¼" wireline, triple-tube, core drilling (Ø 86mm core) from 4.10 to 520.00 mbgl	Fresh water from 4.10 to 54.00 mbgl Bentonite fluid from 54.00 to 520.00 mbgl
HDB-6	Latitude (X): 45°02'39.0934" N (4,988,219.987 m) Longitude (Y): 141°51'38.6432" E (567,786.853 m) Elevation (Z): 60.212 m	620.00 m	• The borehole was located in the URL site so as to obtain information on the geological environment necessary for designing the underground facility. • The depth (excluding 20 m overbreak) was determined so as to more precisely characterise groundwater flow in and around the URL site.	6¼" wireline, triple-tube, core drilling (Ø 86mm core) from 4.20 to 620.00 mbgl	Bentonite fluid from 4.20 to 620.00 mbgl
HDB-7	Latitude (X): 45°02'51.3035" N (4,988,583.098 m) Longitude (Y): 141°50'39.3235" E (566,485.228 m) Elevation (Z): 43.752 m	520.00 m	• The location was selected so as to characterise the Yuchi Formation (specifically hydraulic properties) and of the upper part of the Koetoi Formation, considering the land use, the ease of formalities and the degree of development of infrastructure (specifically access to main roads). • The depth (excluding 20 m overbreak) was determined so as to obtain information on the geological environment down to the planned URL depth (500 m depth).	6¼" wireline, triple-tube, core drilling (Ø 86mm core) from 11.69 to 520.00 mbgl	Bentonite fluid from 11.69 to 520.00 mbgl
HDB-8	Latitude (X): 45°03'00.0458" N (4,988,873.700 m) Longitude (Y): 141°52'09.3122" E (568,450.835 m) Elevation (Z): 70.051 m	470.00 m	• The location was selected around the estimated location of the Omagari Fault so as to characterise the fault, considering the ease of formalities and the degree of development of infrastructure (specifically access to main roads). • The depth (excluding 20 m overbreak) was determined so as to confirm the geological structures (specifically the distribution of the Omagari Fault) estimated on the basis of the HDB-3/4/5 investigation results.	6¼" wireline, triple-tube, core drilling (Ø 86mm core) from 4.20 to 470.00 mbgl	Bentonite fluid from 4.20 to 470.00 mbgl
HDB-9	Latitude (X): 45°03'36.1962" N (4,989,973.229 m) Longitude (Y): 141°51'00.4532" E (566,932.893 m) Elevation (Z): 97.188 m	520.00 m	• The location was selected around the estimated location of the Omagari Fault near the north-west boundary of the URL area so as to characterise the fault and to obtain information on the geological environment as the boundary conditions for geological environment models. The land use, the ease of formalities and the degree of development of infrastructure (specifically access to main roads) were considered for the final decision. • The depth (excluding 20 m overbreak) was determined so as to obtain information on the geological environment down to the planned URL depth (500 m depth).	6¼" wireline, triple-tube, core drilling (Ø 86mm core) from 26.50 to 520.00 mbgl	Bentonite fluid from 26.50 to 520.00 mbgl
HDB-10	Latitude (X): 45°03'31.9231" N (4,989,878.519 m) Longitude (Y): 141°53'38.1125" E (570,382.397 m) Elevation (Z): 50.829 m	550.00 m	• The borehole was located near the east boundary of the URL area so as to obtain information on the geological environment as the boundary conditions for geological environment models. The land use, the ease of formalities and the degree of development of infrastructure (specifically access to main roads) were considered for the final decision. • The depth of 500 m was determined so as to obtain information on the geological environment down to the planned URL depth. An additional 50 m was drilled so as to test the borehole stability and groundwater chemistry without casing pipes and cement.	6¼" wireline, triple-tube, core drilling (Ø 86mm core) from 26.00 to 500.00 mbgl HQ wireline, triple-tube, core drilling (Ø 65mm core) from 500.00 to 550.00 mbgl	Bentonite fluid from 26.00 to 550.00 mbgl
HDB-11	Latitude (X): 45°02'08.7169" N (4,987,289.753 m) Longitude (Y): 141°52'09.1032" E (568,463.269 m) Elevation (Z): 66.848 m	1,020.00 m	• The borehole was located near the south boundary of the URL area so as to obtain information on the geological environment as the boundary conditions for geological environment models. The land use, the ease of formalities and the degree of development of infrastructure (specifically access to main roads) were considered for the final decision. • The depth (excluding 20 m overbreak) was determined so as to obtain information on the geological environment for checking the results of groundwater flow analysis.	6¼" wireline, triple-tube, core drilling (Ø 86mm core) from 23.00 to 1,020.00 mbgl	Bentonite fluid from 23.00 to 1,020.00 mbgl

Appendix 4: Overview of deep borehole drilling

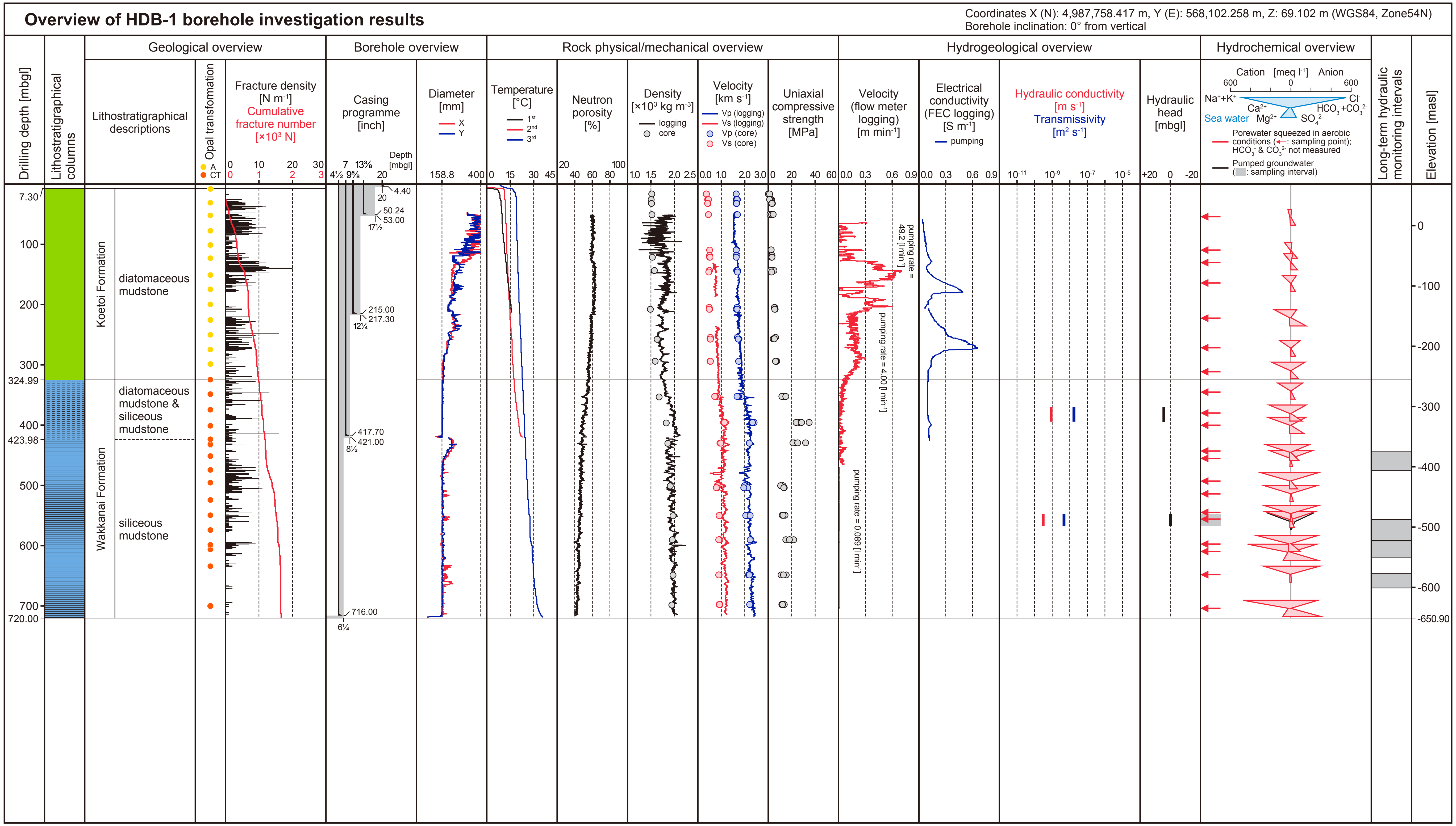

Appendix 5: Overview of deep borehole investigation results (HDB-1)

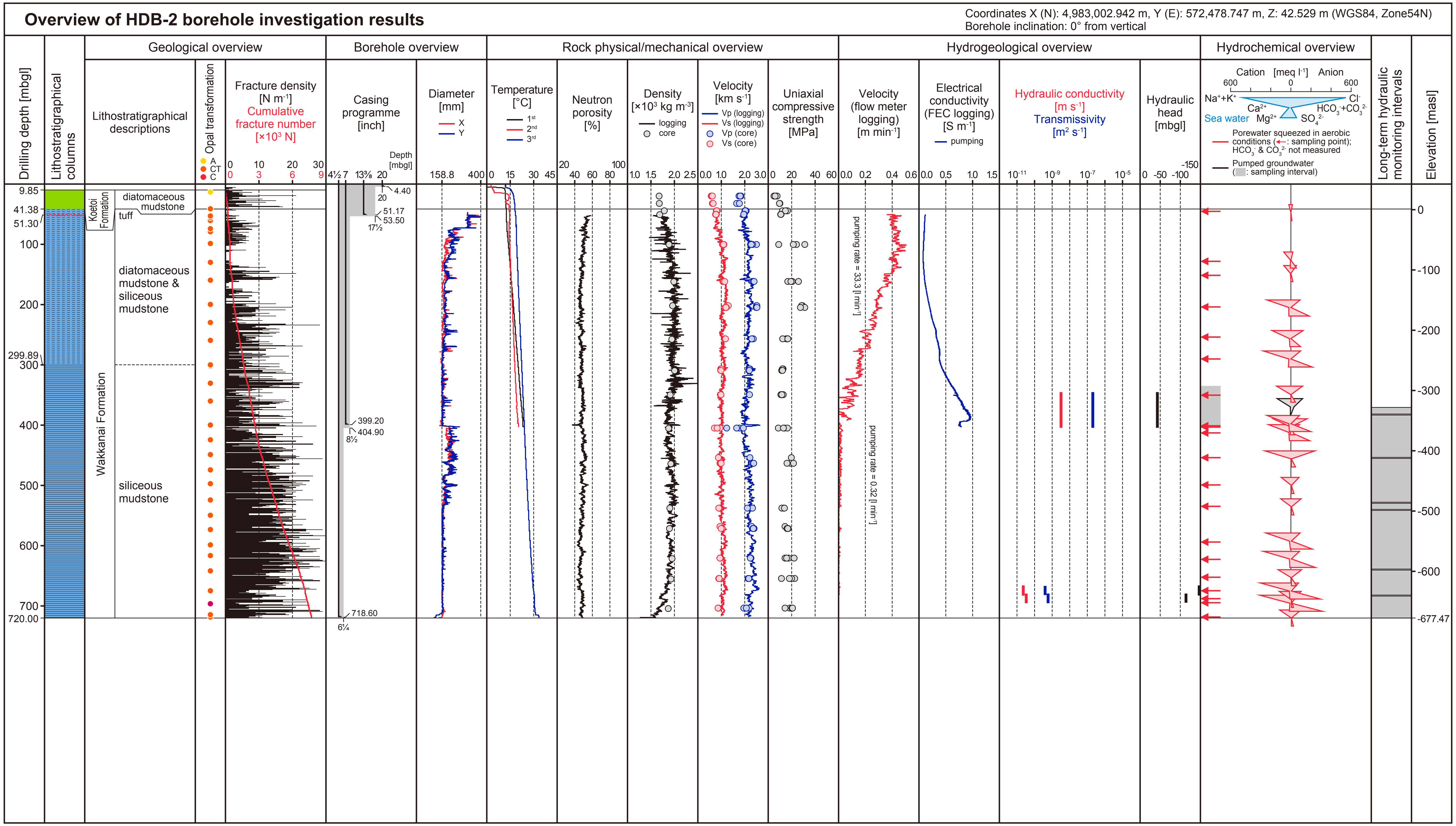

Appendix 5: Overview of deep borehole investigation results (HDB-2)

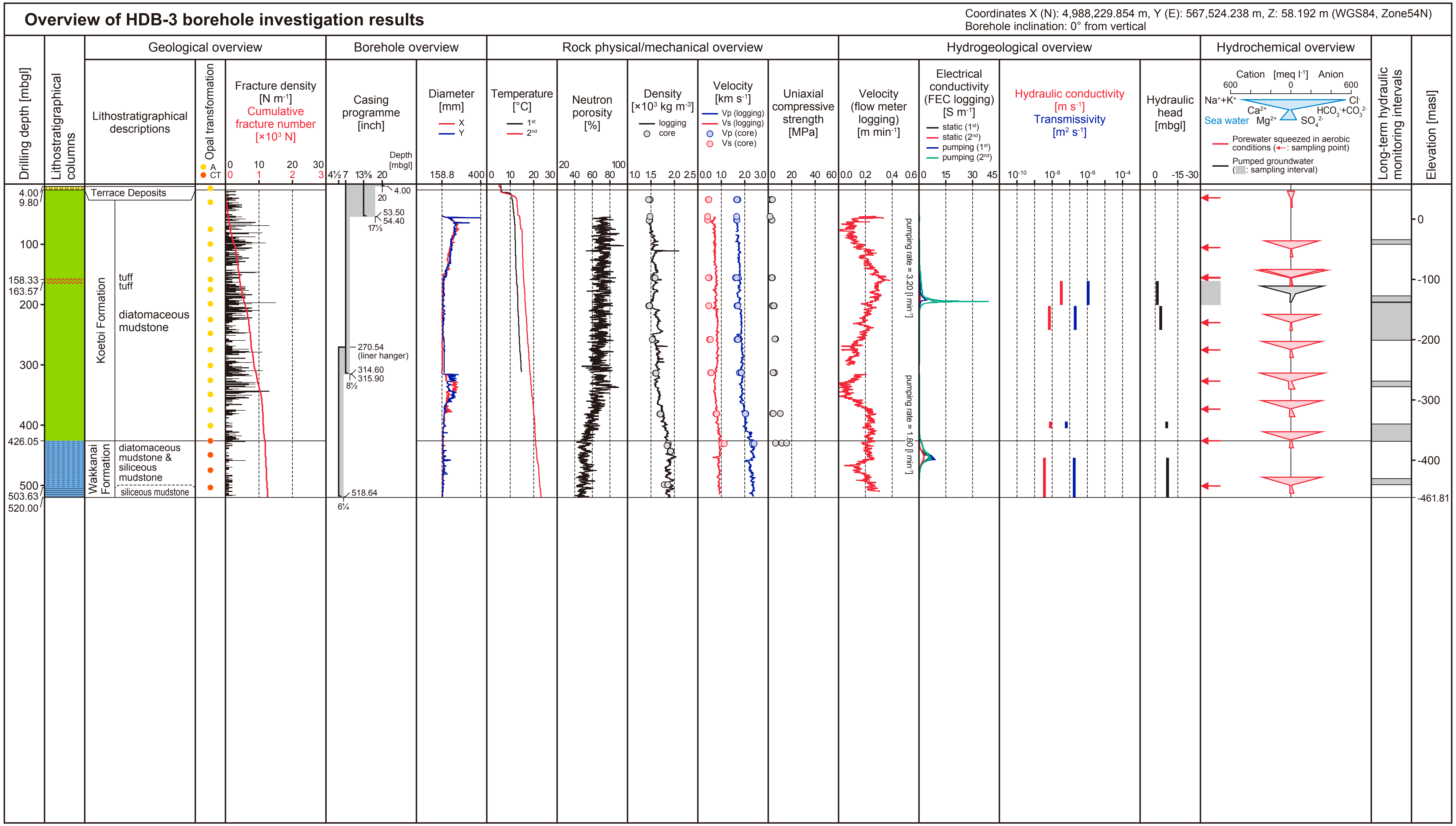

Appendix 5: Overview of deep borehole investigation results (HDB-3)

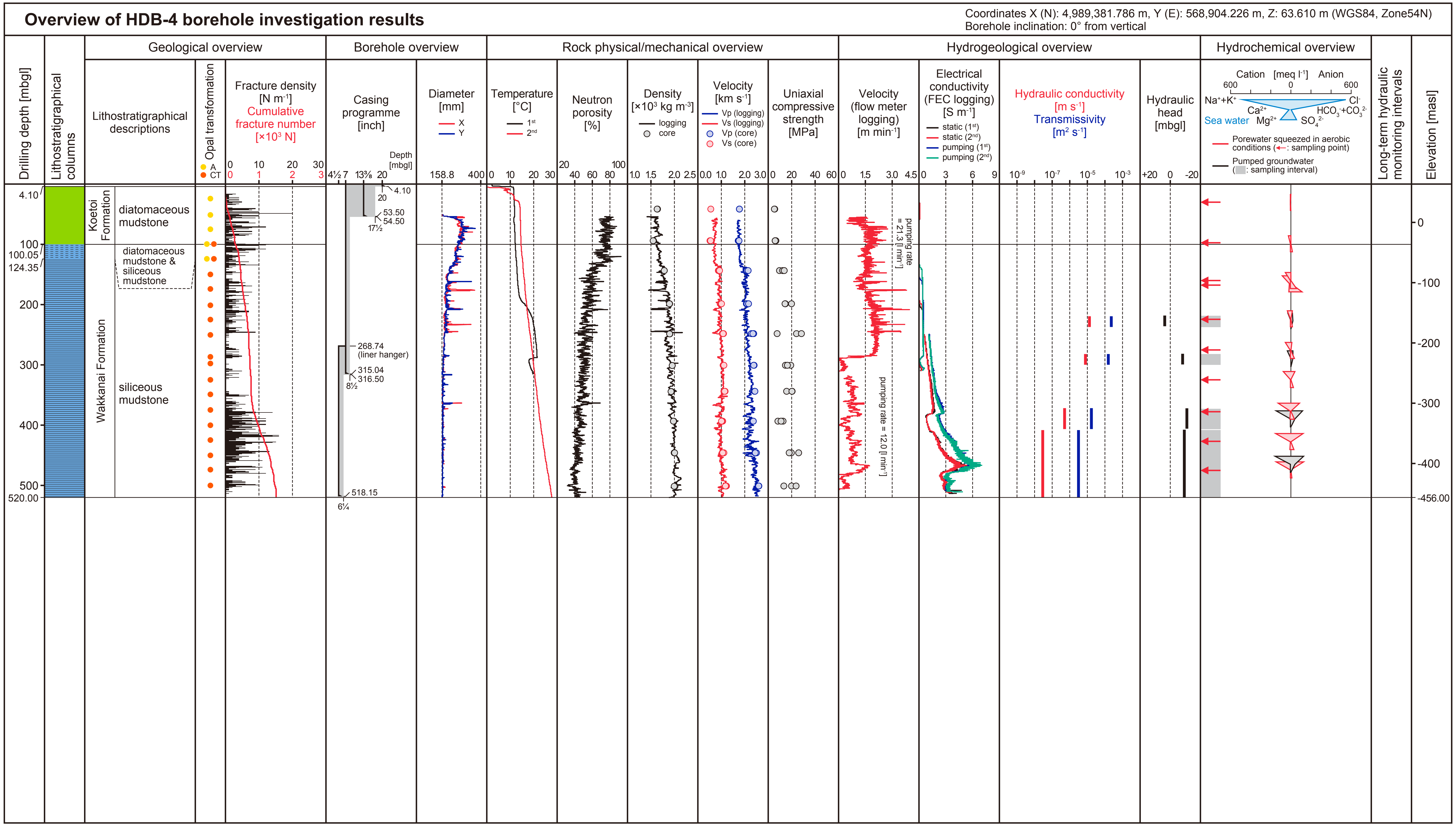

Appendix 5: Overview of deep borehole investigation results (HDB-4)

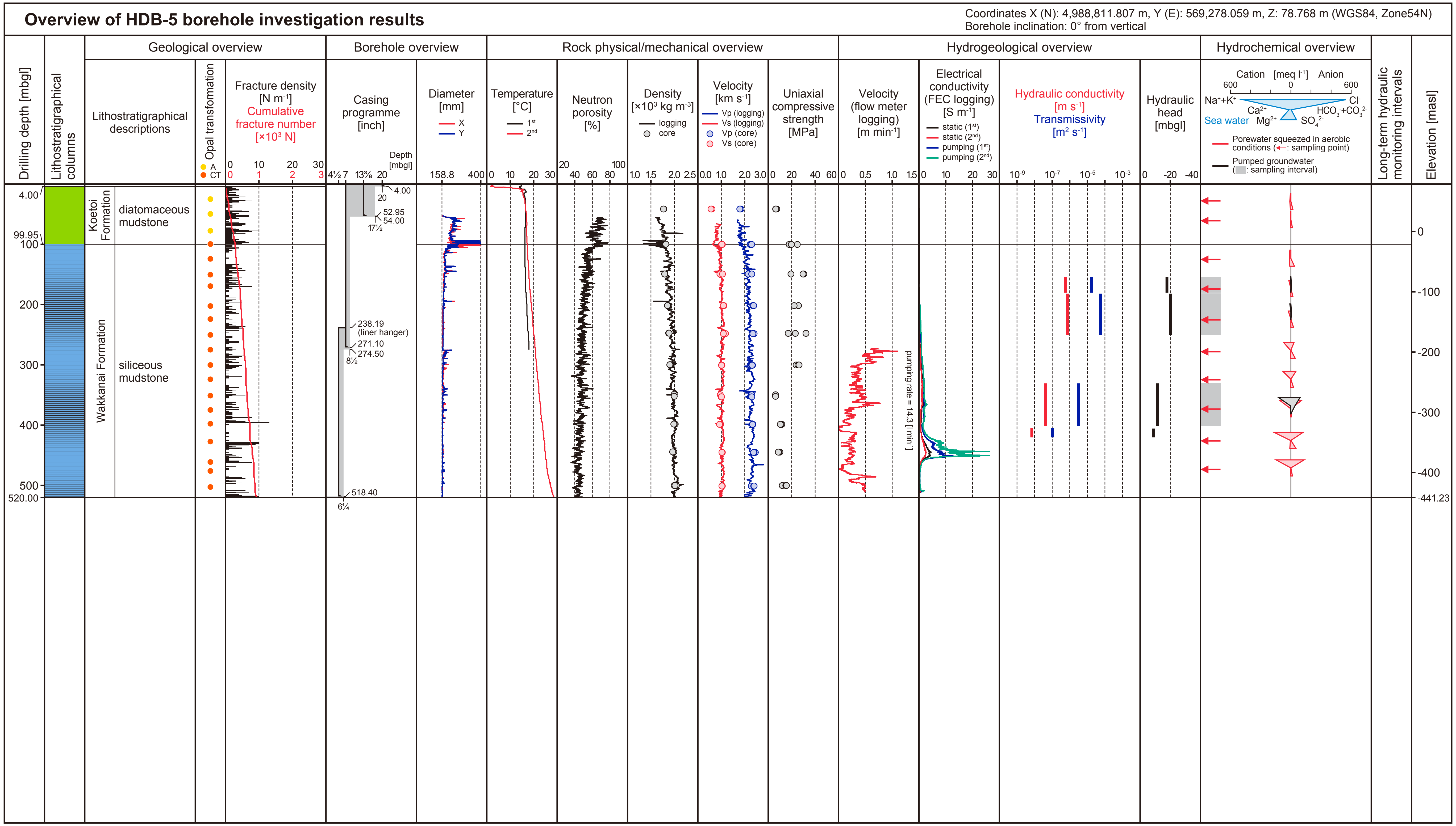

Appendix 5: Overview of deep borehole investigation results (HDB-5)

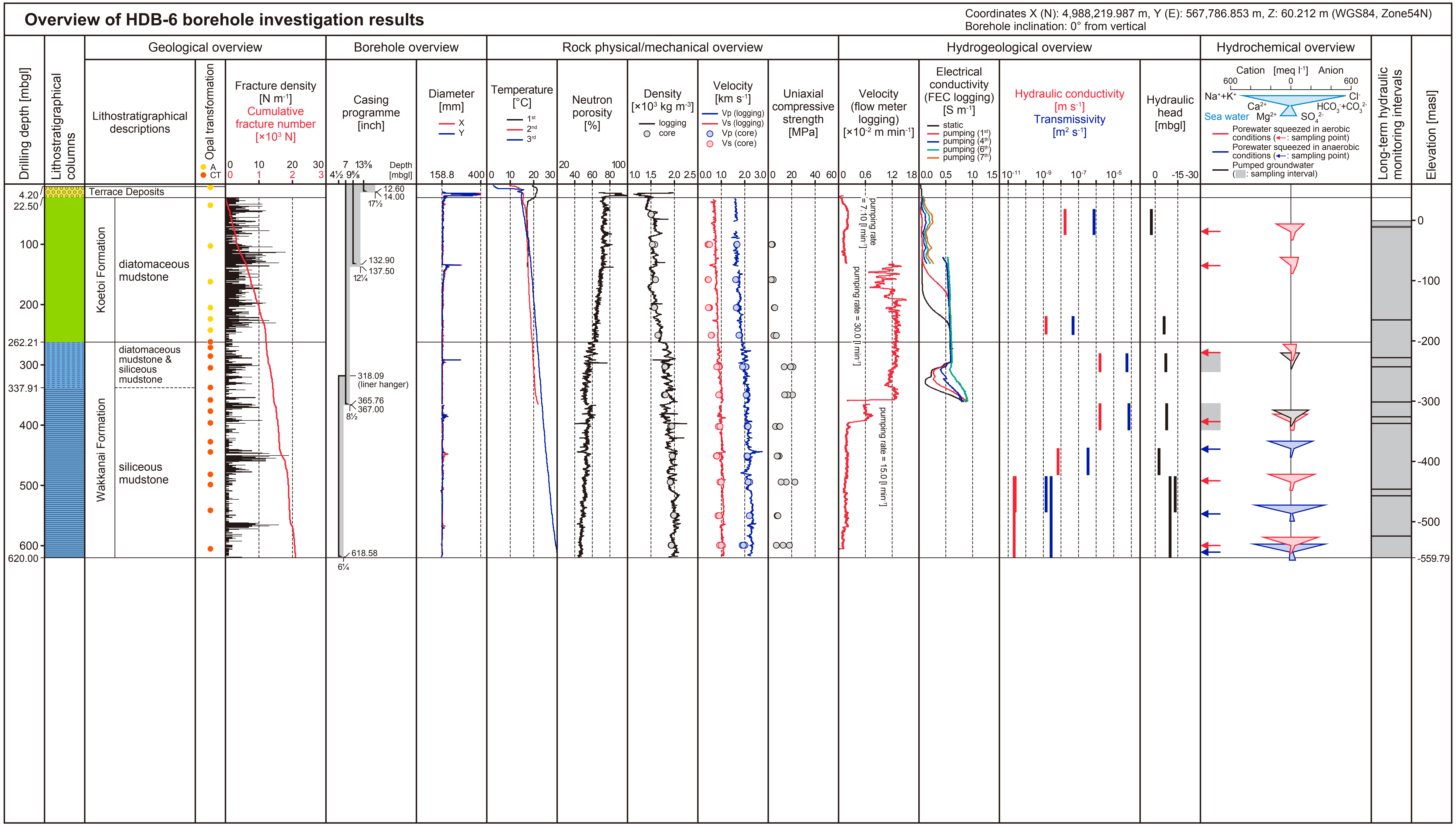

Appendix 5: Overview of deep borehole investigation results (HDB-6)

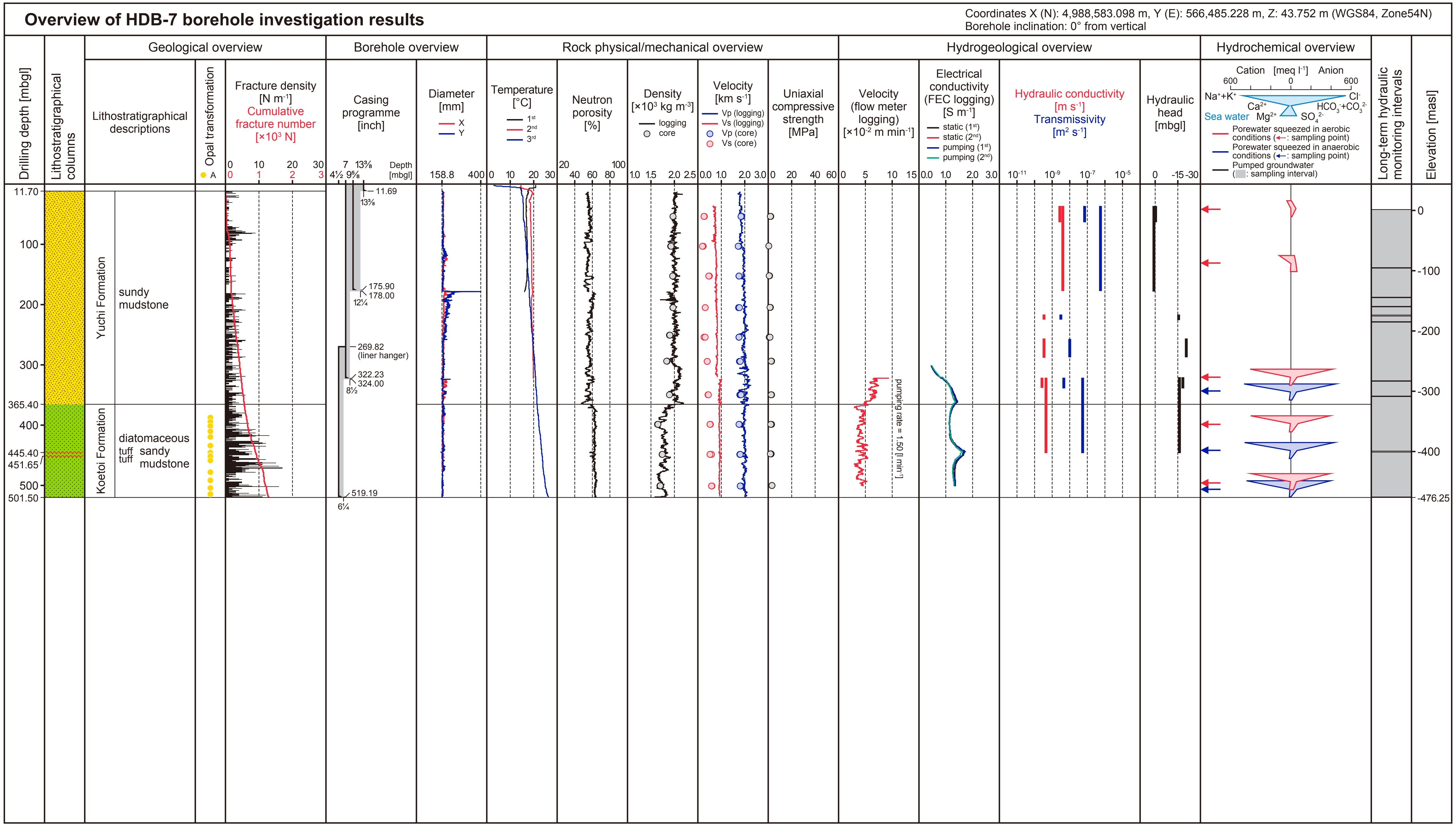

Appendix 5: Overview of deep borehole investigation results (HDB-7)

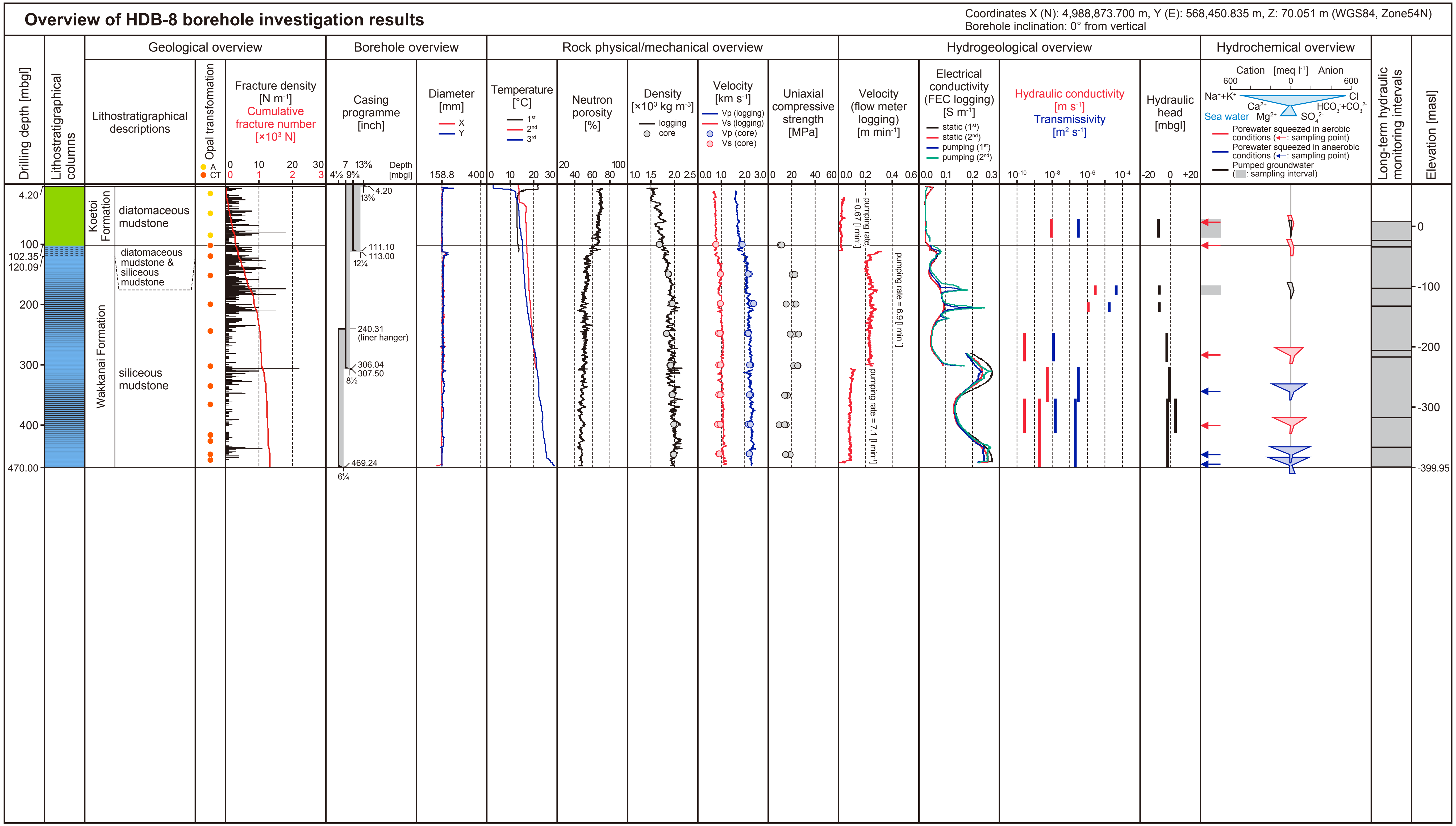

Appendix 5: Overview of deep borehole investigation results (HDB-8)

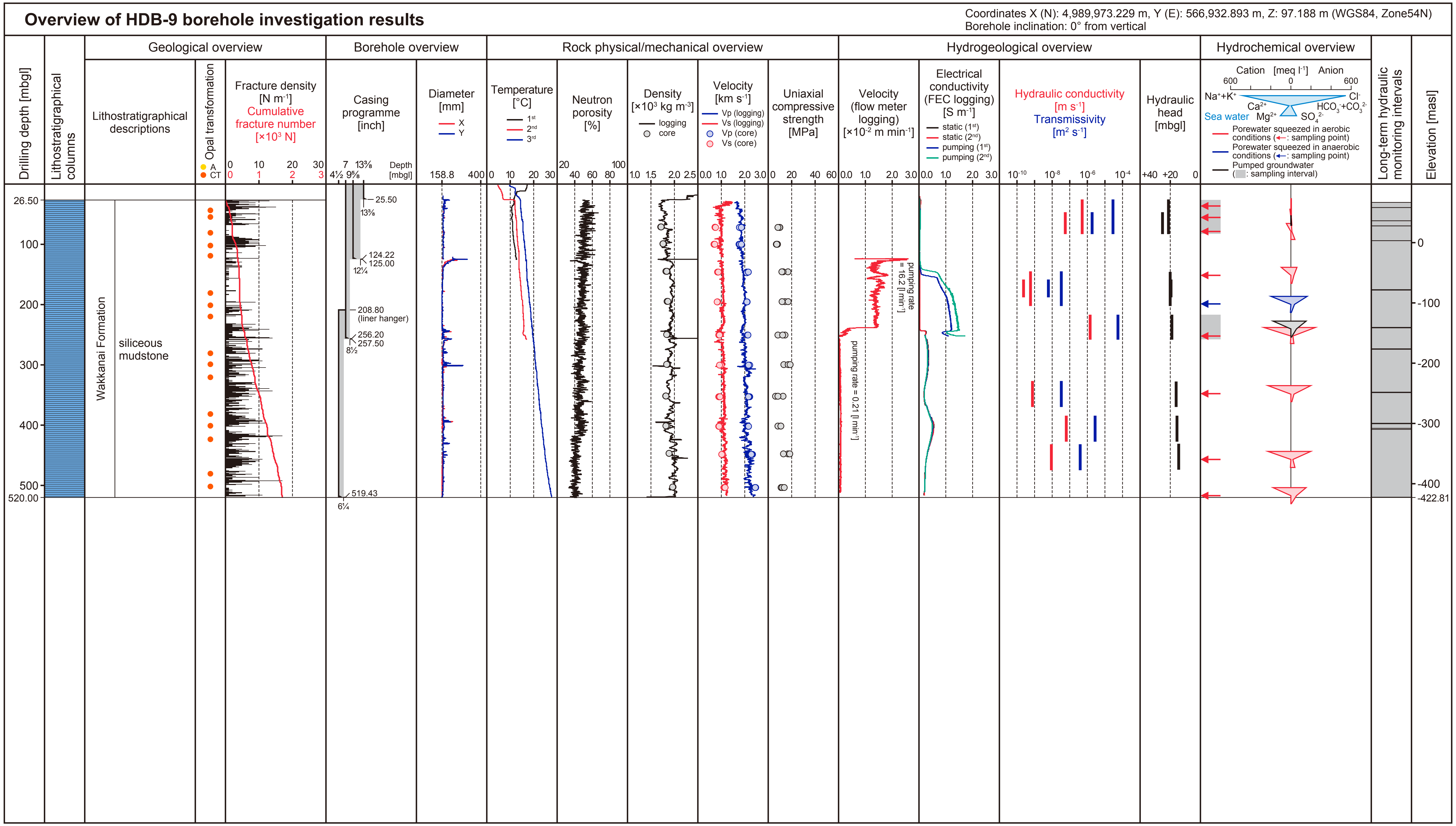

Appendix 5: Overview of deep borehole investigation results (HDB-9)

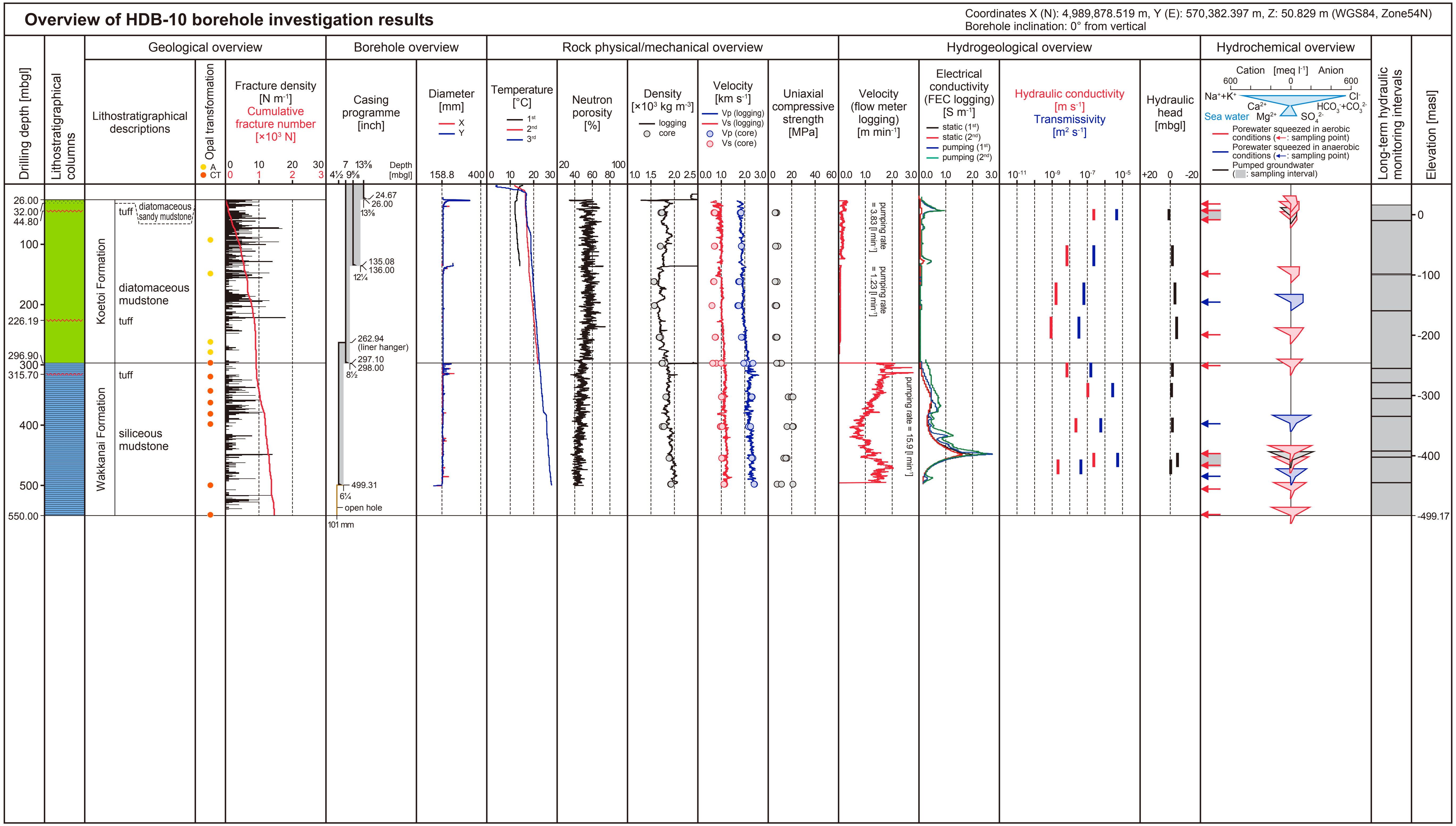

Appendix 5: Overview of deep borehole investigation results (HDB-10)

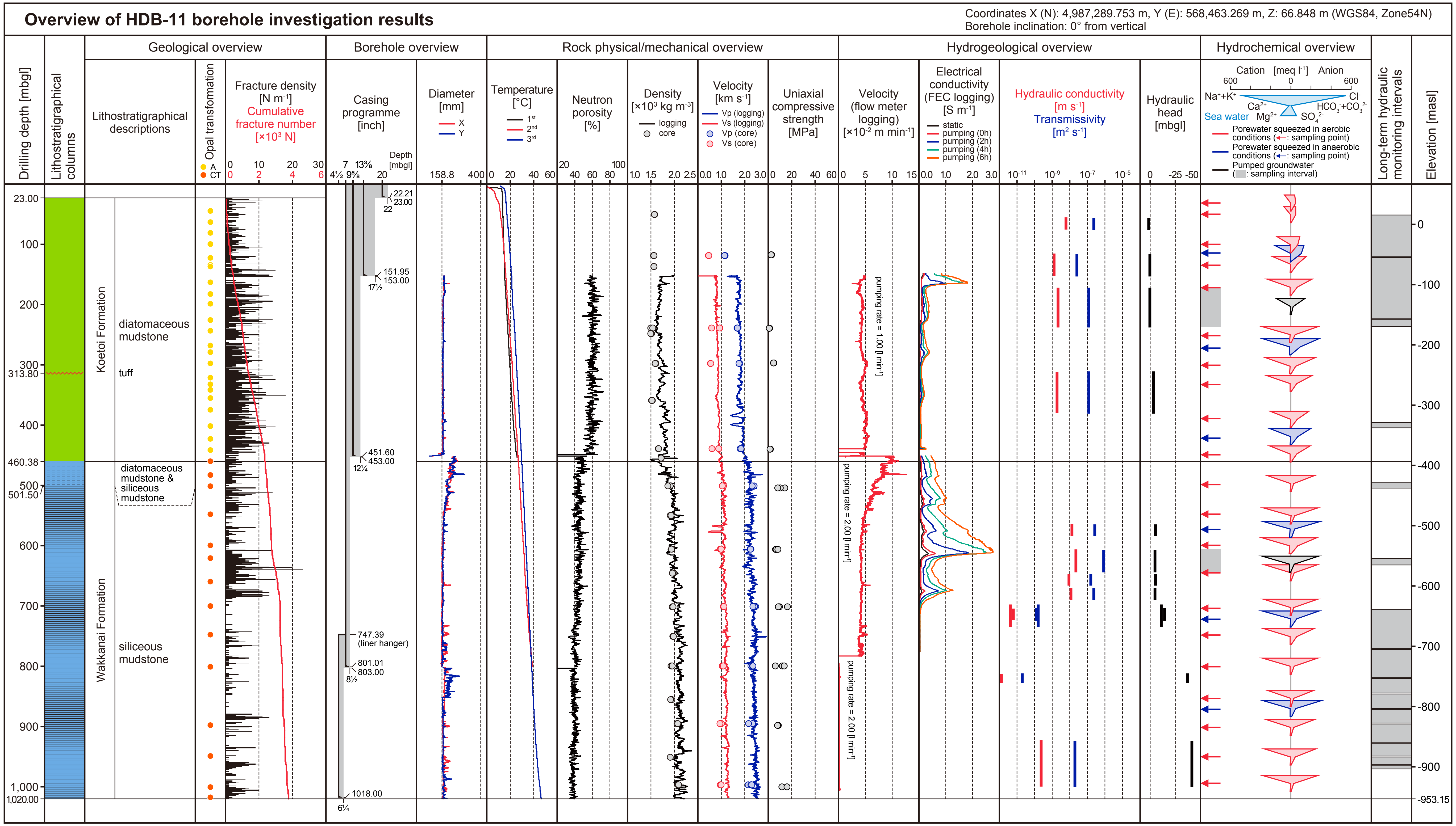

Appendix 5: Overview of deep borehole investigation results (HDB-11)

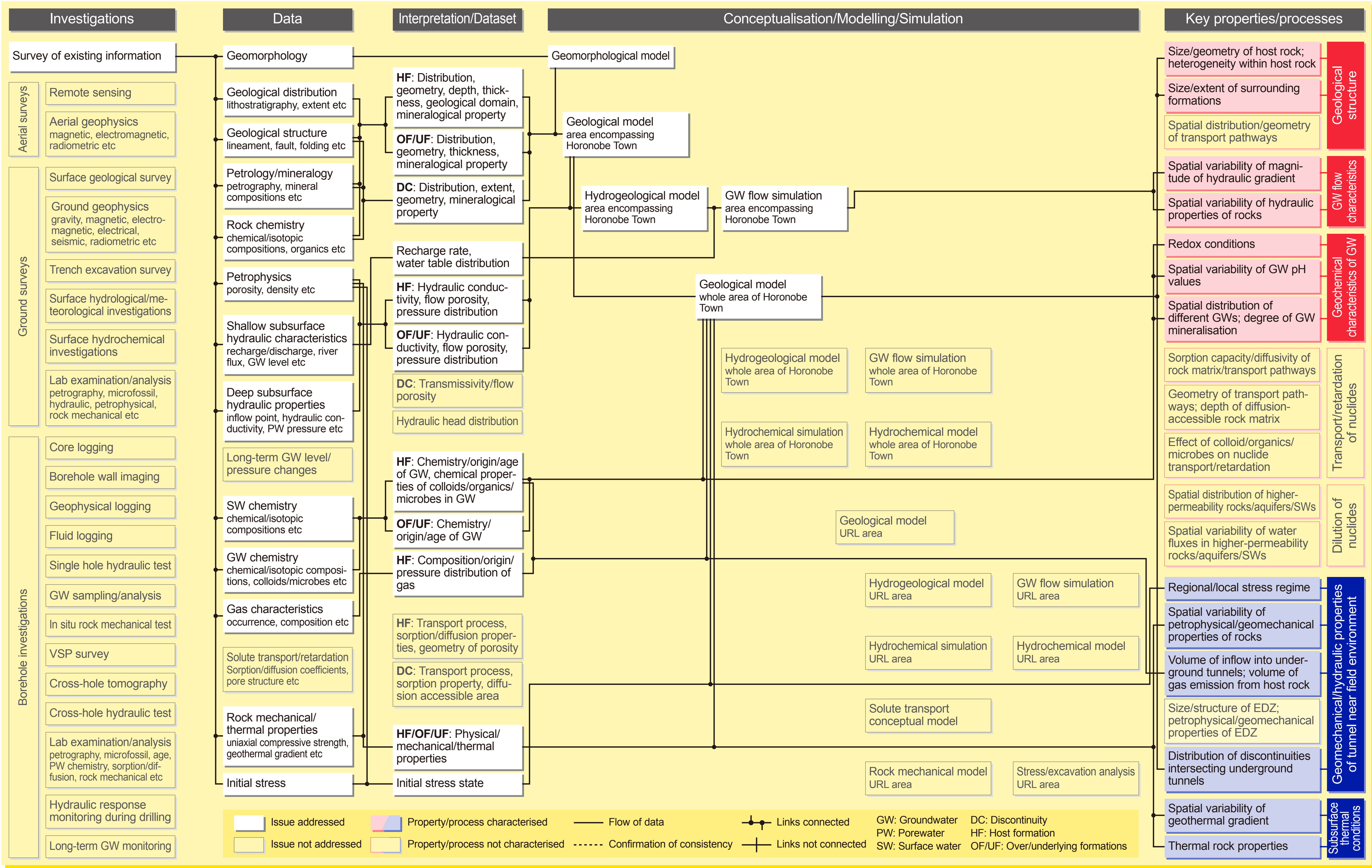

Appendix 6: Geosynthesis Data Flow Diagram (Surface-based investigations covering the whole Horonobe Town: Survey of existing infromation)

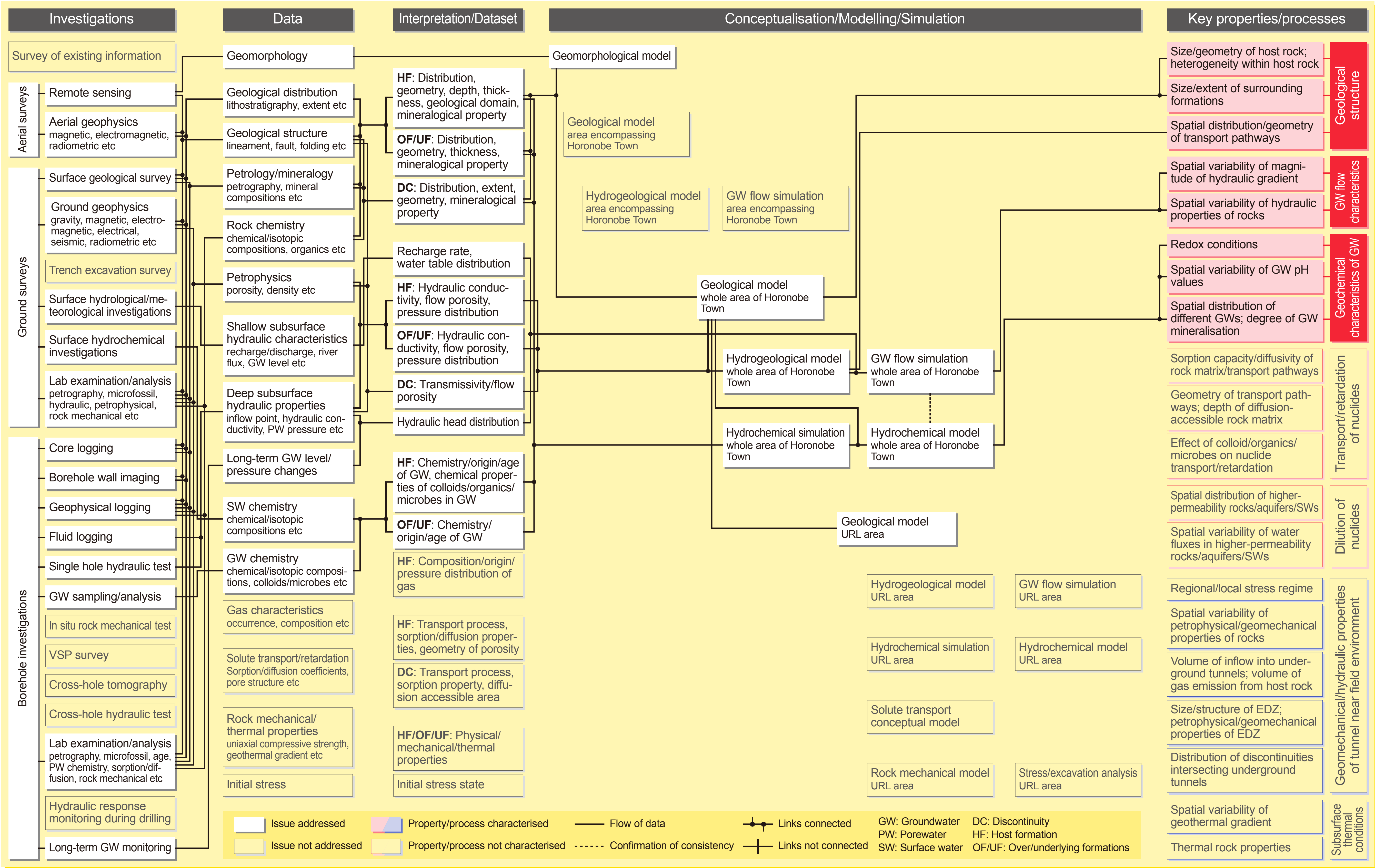

Appendix 6: Geosynthesis Data Flow Diagram (Surface-based investigations covering the whole Horonobe Town: Aerial/ground reconnaissance surveys and borehole investigations)

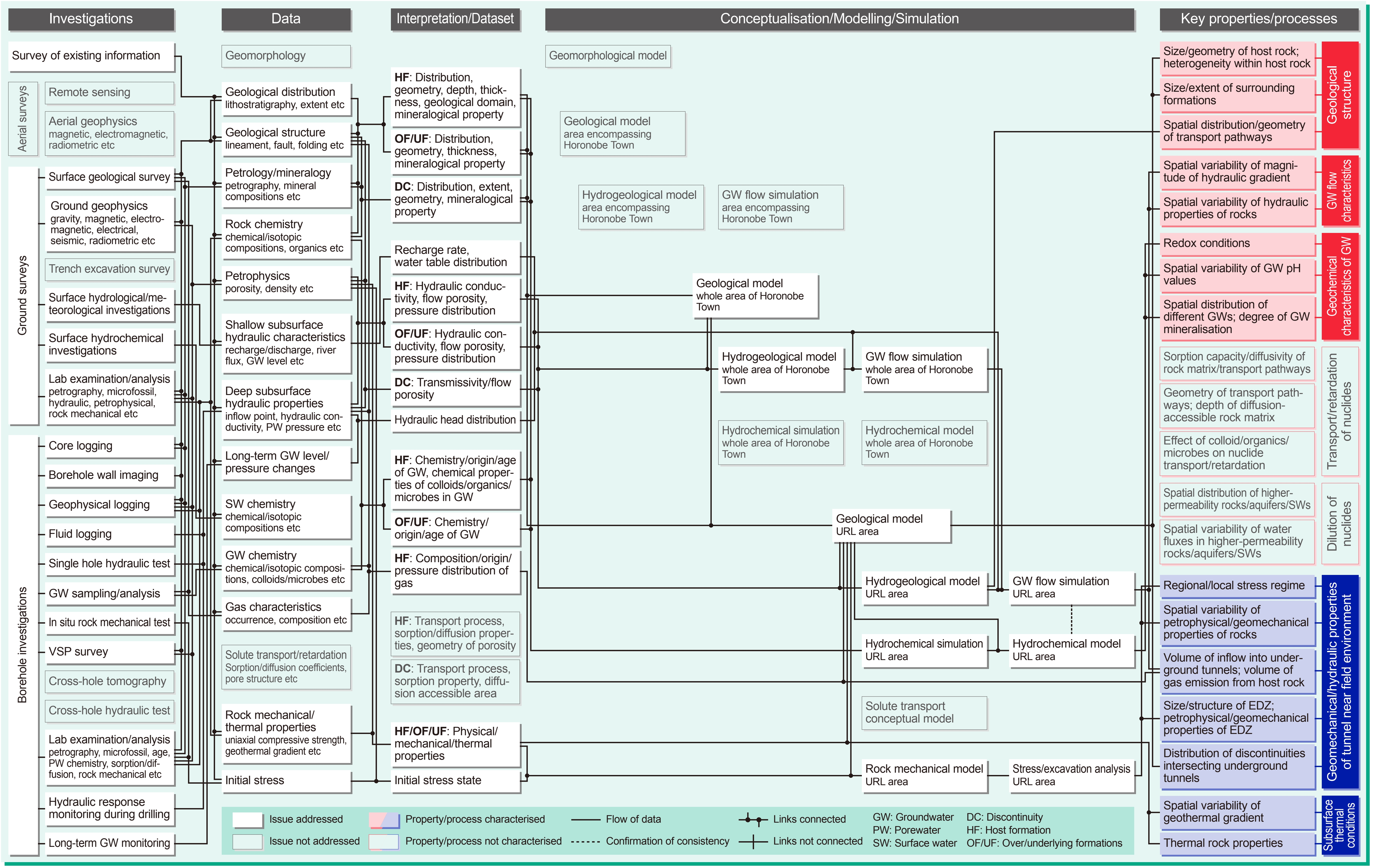

Appendix 6: Geosynthesis Data Flow Diagram (Surface-based investigations in/around the URL area: Survey of existing information, ground reconnaissance surveys and borehole investigations)

国際単位系（SI）

表１．SI 基本単位

基本量	SI 基本単位	
	名称	記号
長さ	メートル	m
質量	キログラム	kg
時間	秒	s
電流	アンペア	A
熱力学温度	ケルビン	K
物質量	モル	mol
光度	カンデラ	cd

表２．基本単位を用いて表されるSI組立単位の例

組立量	SI 基本単位	
	名称	記号
面積	平方メートル	m^2
体積	立法メートル	m^3
速さ，速度	メートル毎秒	m/s
加速度	メートル毎秒毎秒	m/s^2
波数	毎メートル	m^{-1}
密度，質量密度	キログラム毎立方メートル	kg/m^3
面積密度	キログラム毎平方メートル	kg/m^2
比体積	立方メートル毎キログラム	m^3/kg
電流密度	アンペア毎平方メートル	A/m^2
磁界の強さ	アンペア毎メートル	A/m
量濃度 (a)，濃度	モル毎立方メートル	mol/m^3
質量濃度	キログラム毎立法メートル	kg/m^3
輝度	カンデラ毎平方メートル	cd/m^2
屈折率 (b)	（数字の） 1	1
比透磁率 (b)	（数字の） 1	1

(a) 量濃度（amount concentration）は臨床化学の分野では物質濃度（substance concentration）ともよばれる。
(b) これらは無次元量あるいは次元１をもつ量であるが、そのことを表す単位記号である数字の１は通常は表記しない。

表３．固有の名称と記号で表されるSI組立単位

組立量	SI 組立単位			
	名称	記号	他のSI単位による表し方	SI基本単位による表し方
平面角	ラジアン(b)	rad	1 (b)	m/m
立体角	ステラジアン(b)	sr(c)	1 (b)	m^2/m^2
周波数	ヘルツ (d)	Hz		s^{-1}
力	ニュートン	N		$m\ kg\ s^{-2}$
圧力，応力	パスカル	Pa	N/m^2	$m^{-1}\ kg\ s^{-2}$
エネルギー，仕事，熱量	ジュール	J	N m	$m^2\ kg\ s^{-2}$
仕事率，工率，放射束	ワット	W	J/s	$m^2\ kg\ s^{-3}$
電荷，電気量	クーロン	C		s A
電位差（電圧），起電力	ボルト	V	W/A	$m^2\ kg\ s^{-3}\ A^{-1}$
静電容量	ファラド	F	C/V	$m^{-2}\ kg^{-1}\ s^4\ A^2$
電気抵抗	オーム	Ω	V/A	$m^2\ kg\ s^{-3}\ A^{-2}$
コンダクタンス	ジーメンス	S	A/V	$m^{-2}\ kg^{-1}\ s^3\ A^2$
磁束	ウエーバ	Wb	Vs	$m^2\ kg\ s^{-2}\ A^{-1}$
磁束密度	テスラ	T	Wb/m^2	$kg\ s^{-2}\ A^{-1}$
インダクタンス	ヘンリー	H	Wb/A	$m^2\ kg\ s^{-2}\ A^{-2}$
セルシウス温度	セルシウス度(e)	℃		K
光束	ルーメン	lm	cd sr(c)	cd
照度	ルクス	lx	lm/m^2	$m^{-2}\ cd$
放射性核種の放射能 (f)	ベクレル (d)	Bq		s^{-1}
吸収線量, 比エネルギー分与, カーマ	グレイ	Gy	J/kg	$m^2\ s^{-2}$
線量当量, 周辺線量当量, 方向性線量当量, 個人線量当量	シーベルト (g)	Sv	J/kg	$m^2\ s^{-2}$
酸素活性	カタール	kat		$s^{-1}\ mol$

(a)SI接頭語は固有の名称と記号を持つ組立単位と組み合わせても使用できる。しかし接頭語を付した単位はもはやコヒーレントではない。
(b)ラジアンとステラジアンは数字の１に対する単位の特別な名称で、量についての情報をつたえるために使われる。実際には、使用する時には記号rad及びsrが用いられるが、習慣として組立単位としての記号である数字の１は明示されない。
(c)測光学ではステラジアンという名称と記号srを単位の表し方の中に、そのまま維持している。
(d)ヘルツは周期現象についてのみ、ベクレルは放射性核種の統計的過程についてのみ使用される。
(e)セルシウス度はケルビンの特別な名称で、セルシウス温度を表すために使用される。セルシウス度とケルビンの単位の大きさは同一である。したがって、温度差や温度間隔を表す数値はどちらの単位で表しても同じである。
(f)放射性核種の放射能（activity referred to a radionuclide）は、しばしば誤った用語で"radioactivity"と記される。
(g)単位シーベルト（PV,2002,70,205）についてはCIPM勧告2（CI-2002）を参照。

表４．単位の中に固有の名称と記号を含むSI組立単位の例

組立量	SI 組立単位		
	名称	記号	SI 基本単位による表し方
粘度	パスカル秒	Pa s	$m^{-1}\ kg\ s^{-1}$
力のモーメント	ニュートンメートル	N m	$m^2\ kg\ s^{-2}$
表面張力	ニュートン毎メートル	N/m	$kg\ s^{-2}$
角速度	ラジアン毎秒	rad/s	$m\ m^{-1}\ s^{-1}=s^{-1}$
角加速度	ラジアン毎秒毎秒	rad/s^2	$m\ m^{-1}\ s^{-2}=s^{-2}$
熱流密度，放射照度	ワット毎平方メートル	W/m^2	$kg\ s^{-3}$
熱容量，エントロピー	ジュール毎ケルビン	J/K	$m^2\ kg\ s^{-2}\ K^{-1}$
比熱容量，比エントロピー	ジュール毎キログラム毎ケルビン	J/(kg K)	$m^2\ s^{-2}\ K^{-1}$
比エネルギー	ジュール毎キログラム	J/kg	$m^2\ s^{-2}$
熱伝導率	ワット毎メートル毎ケルビン	W/(m K)	$m\ kg\ s^{-3}\ K^{-1}$
体積エネルギー	ジュール毎立方メートル	J/m^3	$m^{-1}\ kg\ s^{-2}$
電界の強さ	ボルト毎メートル	V/m	$m\ kg\ s^{-3}\ A^{-1}$
電荷密度	クーロン毎立方メートル	C/m^3	$m^{-3}\ sA$
表面電荷	クーロン毎平方メートル	C/m^2	$m^{-2}\ sA$
電束密度，電気変位	クーロン毎平方メートル	C/m^2	$m^{-2}\ sA$
誘電率	ファラド毎メートル	F/m	$m^{-3}\ kg^{-1}\ s^4\ A^2$
透磁率	ヘンリー毎メートル	H/m	$m\ kg\ s^{-2}\ A^{-2}$
モルエネルギー	ジュール毎モル	J/mol	$m^2\ kg\ s^{-2}\ mol^{-1}$
モルエントロピー, モル熱容量	ジュール毎モル毎ケルビン	J/(mol K)	$m^2\ kg\ s^{-2}\ K^{-1}\ mol^{-1}$
照射線量（Ｘ線及びγ線）	クーロン毎キログラム	C/kg	$kg^{-1}\ sA$
吸収線量率	グレイ毎秒	Gy/s	$m^2\ s^{-3}$
放射強度	ワット毎ステラジアン	W/sr	$m^4\ m^{-2}\ kg\ s^{-3}=m^2\ kg\ s^{-3}$
放射輝度	ワット毎平方メートル毎ステラジアン	$W/(m^2\ sr)$	$m^2\ m^{-2}\ kg\ s^{-3}=kg\ s^{-3}$
酵素活性濃度	カタール毎立方メートル	kat/m^3	$m^{-3}\ s^{-1}\ mol$

表５．SI 接頭語

乗数	接頭語	記号	乗数	接頭語	記号
10^{24}	ヨタ	Y	10^{-1}	デシ	d
10^{21}	ゼタ	Z	10^{-2}	センチ	c
10^{18}	エクサ	E	10^{-3}	ミリ	m
10^{15}	ペタ	P	10^{-6}	マイクロ	µ
10^{12}	テラ	T	10^{-9}	ナノ	n
10^{9}	ギガ	G	10^{-12}	ピコ	p
10^{6}	メガ	M	10^{-15}	フェムト	f
10^{3}	キロ	k	10^{-18}	アト	a
10^{2}	ヘクト	h	10^{-21}	ゼプト	z
10^{1}	デカ	da	10^{-24}	ヨクト	y

表６．SIに属さないが、SIと併用される単位

名称	記号	SI 単位による値
分	min	1 min=60s
時	h	1h =60 min=3600 s
日	d	1 d=24 h=86 400 s
度	°	1°=(π/180) rad
分	’	1’=(1/60)°=(π/10800) rad
秒	”	1”=(1/60)’=(π/648000) rad
ヘクタール	ha	$1ha=1hm^2=10^4m^2$
リットル	L，l	$1L=11=1dm^3=10^3cm^3=10^{-3}m^3$
トン	t	$1t=10^3$ kg

表７．SIに属さないが、SIと併用される単位で、SI単位で表される数値が実験的に得られるもの

名称	記号	SI 単位で表される数値
電子ボルト	eV	$1eV=1.602\ 176\ 53(14)\times10^{-19}J$
ダルトン	Da	$1Da=1.660\ 538\ 86(28)\times10^{-27}kg$
統一原子質量単位	u	1u=1 Da
天文単位	ua	$1ua=1.495\ 978\ 706\ 91(6)\times10^{11}m$

表８．SIに属さないが、SIと併用されるその他の単位

名称	記号	SI 単位で表される数値
バール	bar	$1\ bar=0.1MPa=100kPa=10^5Pa$
水銀柱ミリメートル	mmHg	1mmHg=133.322Pa
オングストローム	Å	$1\ Å=0.1nm=100pm=10^{-10}m$
海里	M	1 M=1852m
バーン	b	$1\ b=100fm^2=(10^{-12}cm)2=10^{-28}m^2$
ノット	kn	1 kn=(1852/3600)m/s
ネーパ	Np	SI単位との数値的な関係は、対数量の定義に依存。
ベル	B	
デジベル	dB	

表９．固有の名称をもつCGS組立単位

名称	記号	SI 単位で表される数値
エルグ	erg	$1\ erg=10^{-7}\ J$
ダイン	dyn	$1\ dyn=10^{-5}N$
ポアズ	P	$1\ P=1\ dyn\ s\ cm^{-2}=0.1Pa\ s$
ストークス	St	$1\ St\ =1cm^2\ s^{-1}=10^{-4}m^2\ s^{-1}$
スチルブ	sb	$1\ sb\ =1cd\ cm^{-2}=10^4cd\ m^{-2}$
フォト	ph	$1\ ph=1cd\ sr\ cm^{-2}\ 10^4lx$
ガル	Gal	$1\ Gal\ =1cm\ s^{-2}=10^{-2}ms^{-2}$
マクスウェル	Mx	$1\ Mx = 1G\ cm^2=10^{-8}Wb$
ガウス	G	$1\ G\ =1Mx\ cm^{-2}\ =10^{-4}T$
エルステッド (c)	Oe	$1\ Oe ≙ (10^3/4\pi)A\ m^{-1}$

(c) ３元系のCGS単位系とSIでは直接比較できないため、等号「 ≙ 」は対応関係を示すものである。

表10．SIに属さないその他の単位の例

名称	記号	SI 単位で表される数値
キュリー	Ci	$1\ Ci=3.7\times10^{10}Bq$
レントゲン	R	$1\ R = 2.58\times10^{-4}C/kg$
ラド	rad	$1\ rad=1cGy=10^{-2}Gy$
レム	rem	$1\ rem=1\ cSv=10^{-2}Sv$
ガンマ	γ	1γ=1 nT=10-9T
フェルミ		1フェルミ=1 fm=10-15m
メートル系カラット		1メートル系カラット = 200 mg = 2×10-4kg
トル	Torr	1 Torr = (101 325/760) Pa
標準大気圧	atm	1 atm = 101 325 Pa
カロリー	cal	1cal=4.1858J（「15℃」カロリー），4.1868J（「IT」カロリー）4.184J（「熱化学」カロリー）
ミクロン	µ	$1\ \mu=1\mu m=10^{-6}m$

（第8版，2006年改訂）

この印刷物は再生紙を使用しています